Topics in Current Chemistry Collections

Xiao-Feng Wu · Matthias Beller *Editors*

Chemical Transformations of Carbon Dioxide

Springer

Topics in Current Chemistry Collections

Journal Editors

Massimo Olivucci, Siena, Italy and Bowling Green, USA
Wai-Yeung Wong, Hong Kong

Series Editors

Hagan Bayley, Oxford, UK
Kendall N. Houk, Los Angeles, USA
Greg Hughes, Codexis Inc, USA
Christopher A. Hunter, Cambridge, UK
Seong-Ju Hwang, Seoul, South Korea
Kazuaki Ishihara, Nagoya, Japan
Barbara Kirchner, Bonn, Germany
Michael J. Krische, Austin, USA
Delmar Larsen, Davis, USA
Jean-Marie Lehn, Strasbourg, France
Rafael Luque, Córdoba, Spain
Jay S. Siegel, Tianjin, China
Joachim Thiem, Hamburg, Germany
Margherita Venturi, Bologna, Italy
Chi-Huey Wong, Taipei, Taiwan
Henry N.C. Wong, Hong Kong
Vivian Wing-Wah Yam, Hong Kong
Chunhua Yan, Beijing, China
Shu-Li You, Shanghai, China

Aims and Scope

The series *Topics in Current Chemistry Collections* presents critical reviews from the journal *Topics in Current Chemistry* organized in topical volumes. The scope of coverage is all areas of chemical science including the interfaces with related disciplines such as biology, medicine and materials science.

The goal of each thematic volume is to give the non-specialist reader, whether in academia or industry, a comprehensive insight into an area where new research is emerging which is of interest to a larger scientific audience.

Each review within the volume critically surveys one aspect of that topic and places it within the context of the volume as a whole. The most significant developments of the last 5 to 10 years are presented using selected examples to illustrate the principles discussed. The coverage is not intended to be an exhaustive summary of the field or include large quantities of data, but should rather be conceptual, concentrating on the methodological thinking that will allow the non-specialist reader to understand the information presented.

Contributions also offer an outlook on potential future developments in the field.

More information about this series at http://www.springer.com/series/14181

Xiao-Feng Wu • Matthias Beller
Editors

Chemical Transformations of Carbon Dioxide

With contributions from

Matthias Beller • Hendrik Büttner • Kuiling Ding • Kaiwu Dong
Liang-Nian He • Yuya Hu • Tharun Jose • Henrik Junge
Nicole Kindermann • Arjan W. Kleij • Yuehui Li • Xi Liu
Lars Longwitz • Rauf Razzaq • Alonso Rosas-Hernández
Johannes Steinbauer • Christoph Steinlechner • Hua Wang
Thomas Werner • Xiao-Feng Wu • Christoph Wulf • Zhuo Xin
Feng Zheng

Springer

Editors
Xiao-Feng Wu
Leibniz-Institut für Katalyse
Universität Rostock
Rostock, Germany

Matthias Beller
Leibniz-Institut für Katalyse
Universität Rostock
Rostock, Germany

Partly previously published in Top Curr Chem (Z) Volume 375 (2017); Top Curr Chem (Z) Volume 376 (2018).

ISSN 2367-4067
Topics in Current Chemistry Collections
ISBN 978-3-319-77756-6

Library of Congress Control Number: 2018938094

© Springer International Publishing AG, part of Springer Nature 2018
This work is subject to copyright. All rights are reserved by the Publisher, whether the whole or part of the material is concerned, specifically the rights of translation, reprinting, reuse of illustrations, recitation, broadcasting, reproduction on microfilms or in any other physical way, and transmission or information storage and retrieval, electronic adaptation, computer software, or by similar or dissimilar methodology now known or hereafter developed.
The use of general descriptive names, registered names, trademarks, service marks, etc. in this publication does not imply, even in the absence of a specific statement, that such names are exempt from the relevant protective laws and regulations and therefore free for general use.
The publisher, the authors and the editors are safe to assume that the advice and information in this book are believed to be true and accurate at the date of publication. Neither the publisher nor the authors or the editors give a warranty, express or implied, with respect to the material contained herein or for any errors or omissions that may have been made. The publisher remains neutral with regard to jurisdictional claims in published maps and institutional affiliations.

Printed on acid-free paper

This Springer imprint is published by the registered company Springer International Publishing AG part of Springer Nature.
The registered company address is: Gewerbestrasse 11, 6330 Cham, Switzerland

Contents

Preface

Since the beginning of the industrial revolution and the concomitant use of fossil resources, the concentration of carbon dioxide significantly increased in the atmosphere. This growth is generally considered to be the main reason for global warming. It is clear that the chemical use of carbon dioxide cannot solve this problem; however, it's utilization in synthesis offers interesting opportunities for the chemical industry and organic synthesis. In general, carbon dioxide is a favorable C1 feedstock due to its abundance, availability and low toxicity. As shown in this collection recent advances in organometallic catalysis provide effective means for several chemical transformations of carbon dioxide and its incorporation into interesting building blocks such as carbonates. In addition, advancements of academic and industrial investigations provide the basis for efficient catalytic reductions of carbon dioxide. In this respect the production of formic acid derivatives but also methanol are worth mentioning. Finally, also more basic topics for carbon dioxide valorization are covered. Here, the photocatalytic reduction of CO_2 is an example, which currently creates lots of attention in basic research. We sincerely hope the readers will be inspired by the different articles and benefit from the described concepts and ideas for their own research.

We would like to take this chance to thank the editorial staff of *Topics in Current Chemistry* and the editorial board for choosing us to help assemble this collection. Special acknowledgements should go to Na Xu and Dr. Charlotte Hollingworth for their great assistances.

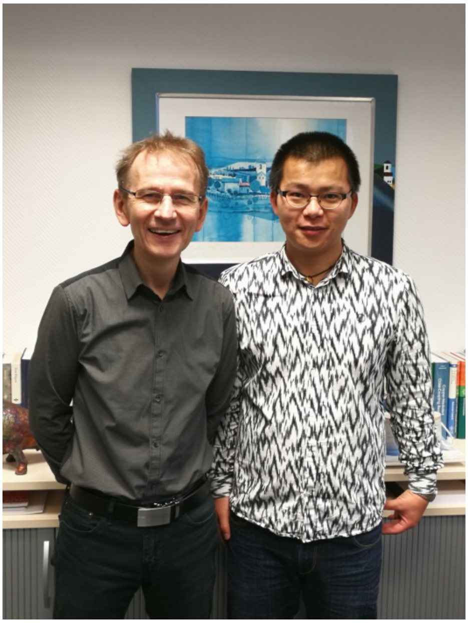

Top Curr Chem (Z) (2017) 375:4
DOI 10.1007/s41061-016-0091-6

REVIEW

Synthesis of Carboxylic Acids and Esters from CO_2

Xiao-Feng Wu[1,3] · **Feng Zheng**[2]

Received: 17 October 2016 / Accepted: 23 November 2016 / Published online: 12 December 2016
© Springer International Publishing Switzerland 2016

Abstract The achievements in the synthesis of carboxylic acids and esters from CO_2 have been summarized and discussed.

Keywords Carboxylic acid · Carbon dioxide · C–C bond formation · Carboxylation · Organic halides

1 Introduction

Carboxylic acids and derivatives are one of the most important structural units that are frequently found in a vast array of natural products, and they are highly versatile starting materials for the preparation of biologically active compounds and other fine chemicals [1–3]. There are well-established protocols for the preparation of carboxylic acids [4, 5], such as the oxidation of alcohols or aldehydes and the hydrolysis of nitriles and related derivatives. Despite the efficiency of these conventional procedures, however, the most straightforward method for accessing

---

Chapter 1 was originally published as Wu, X-F. & Zheng, F. Top Curr Chem (Z) (2017) 375: 4. DOI 10.1007/s41061-016-0091-6.

✉ Xiao-Feng Wu
xiao-feng.wu@catalysis.de

✉ Feng Zheng
gavinzheng@mail.ipc.ac.cn

[1] Department of Chemistry, Zhejiang Sci-Tech University, Xiasha Campus, Hangzhou 310018, People's Republic of China

[2] Hangzhou Branch of Technical Institute of Physics and Chemistry, Chinese Academy of Sciences, 600 No. 21 Street, Hangzhou, China

[3] Leibniz-Institut für Katalyse e.V. an der Universität Rostock, Albert-Einstein-Straße 29a, 18059 Rostock, Germany

carboxylic acids is the direct carboxylation of carbon nucleophiles using CO_2, the simplest alternative feedstock, as the electrophilic partner. Therefore, novel carboxylation methodologies have been developed to induce the inert CO_2 molecule to undergo chemical transformations [6–17]. Employment of high-energy starting materials, including alkenes/allenes/alkynes, aromatic compounds, and organometallic reagents, is common choice for fixation of inactive CO_2 to construct carboxylic acid derivatives [18–25]. Transition-metal complexes are well known to catalyze the formation of carboxylic acids from carbon dioxide and various nucleophilic reagents [26–36]. Recently, transition-metal-catalyzed reductive carboxylation of organic (pseudo)halides with CO_2 and direct insertion of CO_2 into C–H bond become powerful alternatives to classic methodologies for preparing carboxylic acids [37]. Additionally, CO_2 transformations driven by external energy input, such as light (photo irradiation) or electricity (electrolysis) [38], as well as biocatalytic carboxylation [39, 40], were also well developed for incorporation of CO_2 into organic substrates to furnish the corresponding carboxylic acids.

2 Addition of CO_2 to Unsaturated Hydrocarbons

2.1 Coupling of CO_2 and Olefins

Since the first discovery of the reactions of metal complexes with carbon dioxide and olefins in the late 1970s, [41] a plethora of reports have been published in oxidative coupling of CO_2. The group of Hoberg performed seminal research in the field of CO_2 activation. They prepared and isolated the stable nickelalactone, formed from ethene and CO_2 at a Ni complex in the presence of DBU [42]. The Nickelalactone complex exhibits properties characteristic for an organometallic compound (Scheme 1). Thus, as expected, hydrolysis yields propionic acid (85%, identified as the methyl ester). The Ni–C bond is available for insertion reactions with systems containing C=C double bonds; the products obtained after acid hydrolysis are shown in Scheme 1. Insertion of CO_2 into the Ni–C bond afforded succinic anhydride in 80% yield [43]. Analogously, (α,β-unsaturated)zirconacycles

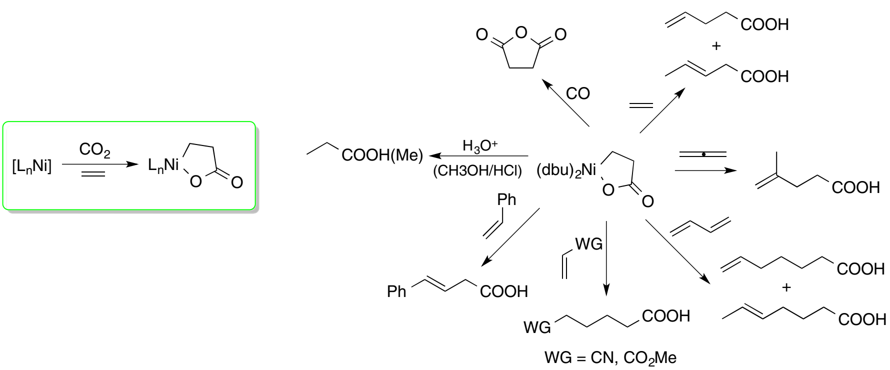

Scheme 1 Reactions of nickelalactone with various electrophiles

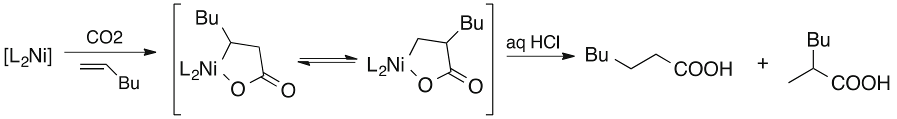

Scheme 2 Carboxylation of monosubstituted olefins

Scheme 3 Hydrocarboxylation of electron-poor styrene derivatives

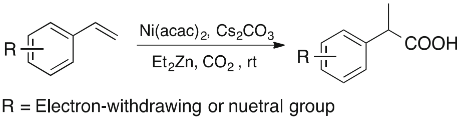

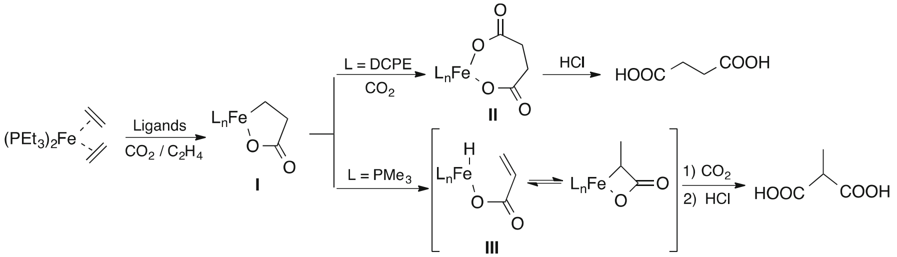

Scheme 4 Iron complex-mediated double carboxylation of ethene

were found to react with various electrophiles just as those employed in the coupling reactions of nickelalactone to give the corresponding carboxylic acids [44].

Cycloolefins are also ideal substrates for CO_2 coupling reactions with nickel(0) systems [45, 46]. In the case of cyclopentene, by variation of the ligands and additives, it is possible by successive application of carbon dioxide or carbon monoxide to prepare a highly selective series of cyclopentane- and cyclopentene-carboxylic acids, cyclopentanedicarboxylic acids or 2-hydroxycyclopentane carboxylic acid in good yields. The C5-skeleton is retained in the products.

The nickel-mediated stoichiometric fixation of carbon dioxide with monosubstituted olefins was also developed by Hoberg's group originally (Scheme 2) [47]. The regioselectivity of the C–C bond formation was largely dependent on temperature and ligands. The branched thermodynamical product was further favored for the branched/linear ratio of products raised from 4/1 to 25/1 as the temperature increased from 25 to 60 °C.

Inspired by the work of Hoberg's, Rovis demonstrated a reductive carboxylation of electron-deficient and -neutral styrene derivatives in the presence of substoichiometric nickel^{II} catalyst together with Et_2Zn as reducing [H] source, yielding the single α-carboxylated products regioselectively [48] (see Scheme 3).

Hoberg's group further extended their investigations to the reactions of ethene on iron(0) complexes. Surprisingly, no monocarboxylic acids but exclusively dicarboxylic acids, namely succinic acid and the isomeric methylmalonic acid, are formed (Scheme 4). Apparently, the iron carboxylates **II** and **III** derived from a common intermediate, the oxaferracyclopentanone **I**, which was influenced significantly by the ligands on the course of the C–C coupling reaction [49].

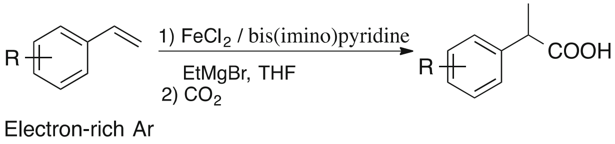

Scheme 5 Iron-catalyzed hydrocarboxylation of electron-rich styrene derivatives

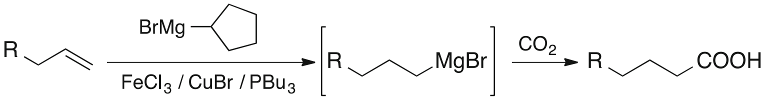

Scheme 6 Cooperative iron–copper catalyzed hydrocarboxylation of terminal alkenes

Recently, the iron-catalyzed hydrocarboxylation of electron-rich aryl alkenes had been developed by Thomas's group using a highly active bench-stable iron^{II} precatalyst to give α-aryl carboxylic acids in excellent yields and with near-perfect regioselectivity (Scheme 5) [50], which was a good complement to Rovis's carboxylation of electron-deficient styrene.

Furthermore, Hayashi and Shirakawa reported a cooperative iron–copper catalyzed hydromagnesiation of terminal alkenes by alkene-Grignard exchange (Scheme 6). The resulting alkyl Grignard reagents could react with carbon dioxide to afford the corresponding carboxylic acid in good yield after acidic workup [51].

2.2 Acrylic Acid Synthesis from Ethene and CO_2

Acrylic acid is an important basic chemical for the synthesis of polyacrylates, which find use as special plastics and superabsorbers. It is, therefore, of great interest to develop a cost-efficient route to acrylic acid under mild conditions. The synthesis of acrylic acid from the cheap starting materials ethylene and CO_2 is particularly attractive via β-H elimination of the metallactone. However, the rigid five-membered metallactone ring did not undergo β-H elimination readily in most cases (Scheme 7), likely due to kinetic barriers and unfavorable free energy of the overall coupling reaction [52]. Hence, the matellactones are in most cases quite stable, and cleavage of the M–C or the M–O bond would not occur without decomposing the metalcomplex.

Scheme 7 Proposed catalytic cycle for acrylic acid synthesis

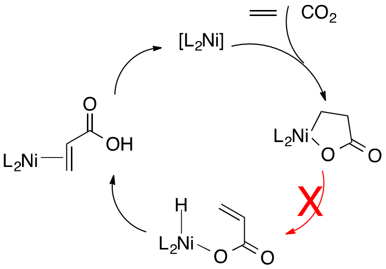

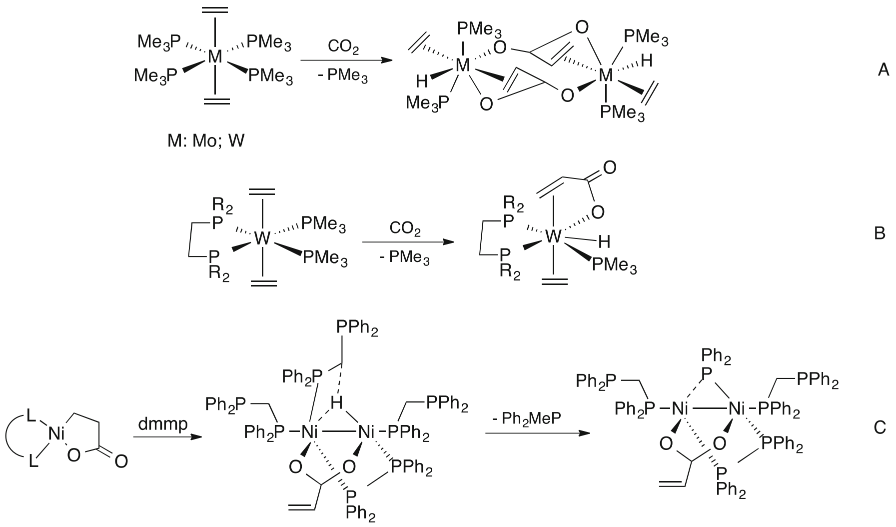

Scheme 8 Preparation of hydrido-acrylate metal complexes

Challenged by this perception, extensive investigations were conducted to catalytic synthesis of acrylic acid based on transition metal systems. It was found that Mo and W complexes [53–55] readily coupled with ethene and CO_2, yielding hydrido-acrylate complexes that were not able to eliminate acrylic acid (Scheme 8a, b). Later, nickel metallacycles were also converted into hydrido-acrylates upon treatment with bis(diphenylphosphino)methane (dppm) [56], which then evolved to give dimeric phosphido Ni complexes bearing a bridging acrylate (Scheme 8c), although no evidence for the release of acrylic acid was obtained either.

The research group of Pápai examined the mechanism of metal-assisted CO_2/C_2H_4 coupling reactions by means of density functional calculations [57, 58] and revealed that although the formation of acrylic acid from ethene and CO_2 is thermodynamically allowed, the high bond-dissociation energies of the M–H and M–O moieties in the hydrido-acrylate intermediates present substantial kinetic barriers to the elimination of acrylic acid. A preformed Pd–COOMe moiety was used as a model system to investigate the insertion of an olefin into the Pd–C bond and subsequent acrylate elimination (Scheme 9) [59]. The experimental findings demonstrated that the esterification of the carboxylic moiety prevented the formation of O–M bond and facilitated the release of acrylate moiety from the metal center. Rieger and coworkers further confirmed this discovery [60] and showed that β-H elimination could be induced by a splitting of the M–O bond and in situ methylation of nickelalactone. However, the reaction was not catalytic, and acrylic acid was obtained in a low yield, probably due to the decomposition of the complex to elemental nickel in a significant degree. Later, it was found that when using bidentate ligands, the conversion of nickelalactones into acrylates upon treatment with CH_3I was largely dependent on the size of the ligand (Scheme 10) [61]. The ring-opened intermediate could not undergo β-H elimination if too bulky ligand was employed.

Scheme 9 Pd–COOMe model system for acrylate elimination

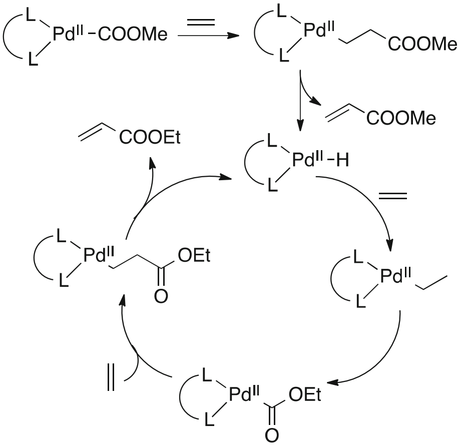

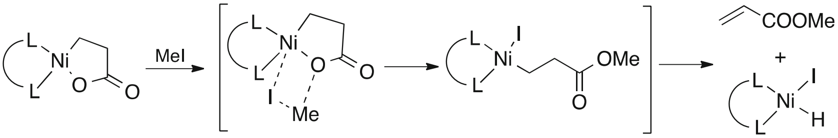

Scheme 10 Synthesis of methyl acrylate via methylation of metallacycles

Alternatively, catalytic coupling of ethylene and CO_2 to form acrylate salt in the presence of a base is a reaction of high interest. Schaub described the palladium- or nickel-catalyzed synthesis of sodium acrylate from ethylene and CO_2 using *t*BuONa [62] or sodium phenolates [63, 64] as bases. Lithium acrylate was obtained via nickel-catalyzed carboxylation of ethylene with CO_2 employing stoichiometric amounts of LiI, NEt_3, and Zn [65]. However, the yield and TON observed was quite low.

2.3 Carboxylation of 1,3-Dienes

Apart from monoenes, the reaction of 1,3-dienes with CO_2 mediated by metal complex were also studied. Hoberg and Schaefer prepared sorbic acid from {Ni(cod)$_2$}, dcpe or bipy as ligands, 1,3-pentadiene, and 1 bar CO_2 in THF [66]. It was found that the coupling of 1,3-dienes with CO_2 at nickel(0) gives allyl carboxylate complex predominantly [66, 67], which could react with maleic anhydride or be protonated to release the CO_2-containing product (Scheme 11). Wakther et al. synthesized two air-stable nickel^{II} allyl carboxylate complexes [68], which showed an η-3-allyl- and a monodentate carboxylate group at the ends of the chain in X-ray analyses.

Hoberg also demonstrated that further exposure of nickel^{II}(TMEDA) allyl monocarboxylate complex **I** to CO_2 for another 24 h (or for 5 days after adding extra pyridine) led to the formation of nickel dicarboxylate complex **II**, which treated with MeOH/HCl provided the corresponding *cis*-diester (Scheme 12a) [69].

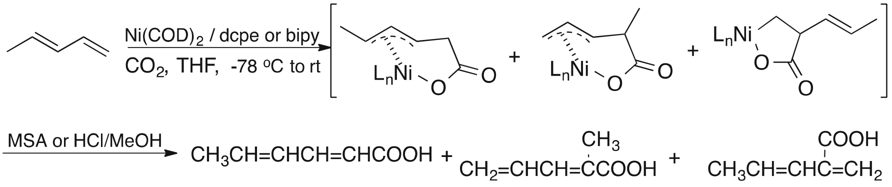

Scheme 11 Ni-prompted carboxylation of 1,3-dienes

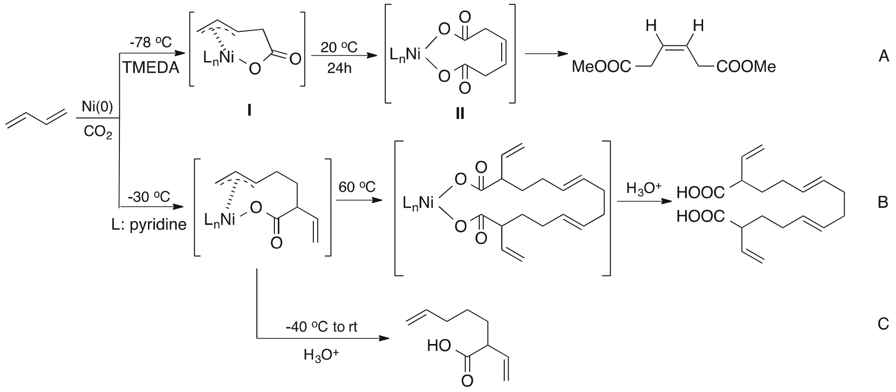

Scheme 12 Diverse products obtained from nickel-mediated coupling of 1,3-dienes and CO_2 under different conditions

Not long afterwards, Hoberg et al. found that in the presence of a pyridinenickel(0) system, 1,3-butadiene coupled with carbon dioxide to form C9-mono- or C18-dicarboxylic acids depending on the temperature (Scheme 12c, b) [70]. It is also found that linear C13-acids with three or four C=C double bonds and terminal carboxylic groups can be prepared by reaction of 1,3-butadiene and carbon dioxide under similar fluorinated pyridine/nickel(0)-mediated conditions [71].

The first catalytic telomerization of butadiene and incorporation of CO_2 by using nickel complexes was reported in 1987 [72], which gave an olefin-functionalized cyclopentane carboxylic acid in a conversion of 95% (Scheme 13). Interestingly, a very similar structure of the bicyclic six-membered nickelalactone intermediate was determined by X-ray as early as in 1978 [73], which provided good insight into the catalytic cycle. However, despite this finding, further investigations on the tautomerization of butadiene and the insertion of CO_2 catalyzed by nickel complex mostly failed. It seems that the only way to obtain the products of nickel-mediated conversions of dienes and CO_2 is by the hydrolysis of the relatively stable nickel^{II} carboxylate complexes [74, 75].

Recently, Mori and coworkers systematically developed the concept of nickelacycle cleavage using oxophilic reagents [76] and combined it with the earlier work of Hoberg and Walther. They used dimethyl- or arylzinc reagents to cleave intermediates generated from the coupling of 1,3-dienes and CO_2 promoted by nickel(0) complexes (Scheme 14a) [77]. The transmetalation affords a [Ni^{II}R’]

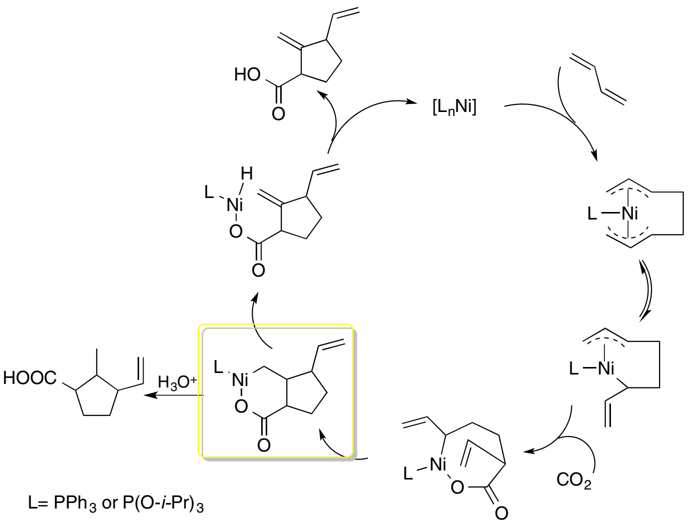

Scheme 13 Ni-catalyzed tautomerization of butadiene and incorporation of CO_2

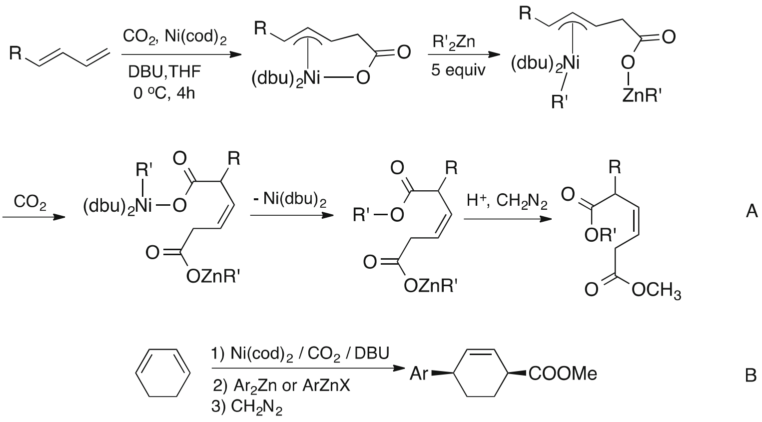

Scheme 14 Nickelacycle cleavage using organozinc reagents

species, which readily undergoes reductive elimination, thereby releasing the products from dicarboxylation or arylative carboxylation and reforming the nickel(0) complexes. The reaction had the potential of being carried out with catalytic amounts of nickel(0), which could be recovered without decomposition. Interestingly, when arylzinc instead of alkylzinc reagents were employed, arylative carboxylation rather than dicarboxylation occurred, affording the corresponding 1,4-addition products in good yield (Scheme 14b).

Soon after, the nickel-catalyzed ring-closing carboxylation of bis-1,3-diene and CO_2 utilizing organozinc compounds as supplemental reagents was realized (Scheme 15) [78, 79]. A remarkable feature of this reaction is the role of ZnR_2 not only as a transmetalation agent but also as a reduction medium, thus allowing

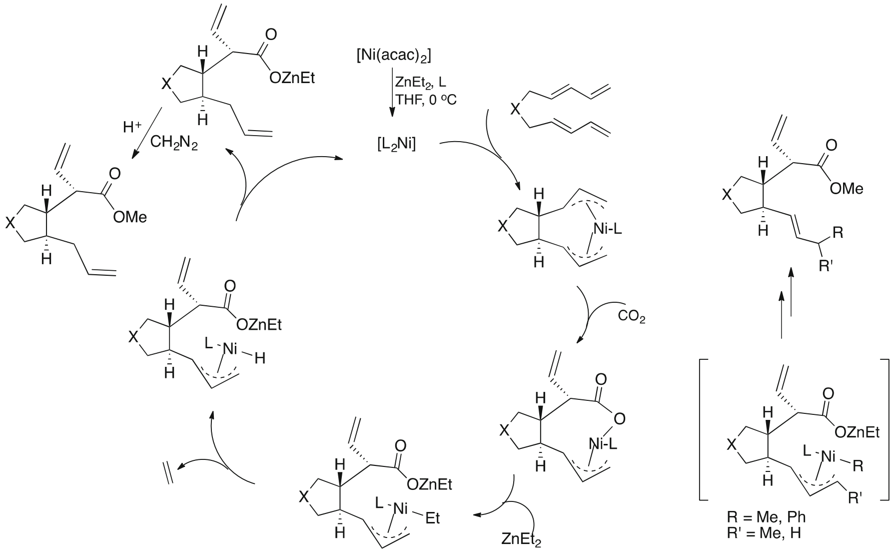

Scheme 15 Ni-catalyzed ring-closing carboxylation of bis-1,3-diene and CO_2

the use of air stable [Ni(acac)$_2$] as a precatalyst. Furthermore, Mori and coworkers upgraded this reaction to an asymmetric level [79], which afford cyclic carboxylic acids in good yields and with high enantioselectivities.

Besides nickel(0) complexes, iron(0) complexes also mediate the coupling reaction of diene and CO_2 (Scheme 16). Starting from [Fe(η^4-butadiene)(PMe$_3$)$_3$] [80], iron^{II} η^3-allyl carboxylate complex **I** was prepared, which exhibits a dynamic equilibrium in solution. Acid hydrolysis in methanol (−30 °C) affords the methyl esters of the two carboxylic acids **II**$_a$ and **II**$_b$ in a molar ratio 10/1. As expected, **I** could further react with CO_2 (90 °C, 5 bar) with preferential insertion in the terminal Fe–C δ-bond of **I**$_a$ and not in that of **I**$_b$. After hydrolysis, only 1,4-dicarboxylicacids (**III**$_a$/**III**$_b$ = 27/1) were isolated. More interestingly, upon treatment of **I** with FeCl$_3$, the symmetrical, linear α, ω-dicarboxylic acid **V** was obtained in good yield after acidic workup, the formation of which could be explained in terms of an intermolecular C–C coupling of the allyl ligands of two molecules of **I**$_a$. When PEt$_3$ was used as ligand instead of PMe$_3$ [81], the relative amount of compound **II**$_b$ increased in direct hydrolysis; and the 1,2-diacid **IV**$_b$ appeared as the main product in the further reaction of the Iron^{II} η^3-allyl carboxylate complex with CO_2.

The catalytic formation of carboxylation compounds from 1,3-butadiene and CO_2 has been achieved on palladium complexes (Scheme 17), and attracted a considerable interest since its discovery by Inoue et al. [82, 83]. Many studies have been aimed at gaining a better understanding of the factors governing the selectivity of the reaction. Thus, Musco [84, 85] studied catalysts of the type Pd(PR$_3$)$_n$ (n = 2, 3) and found that lactone is preferentially formed with the more basic phosphines [e.g., PCy$_3$, P(i-Pr)$_3$], whereas mainly open esters are formed with ligands less basic than P(t-Bu)$_2$Ph. Behr and coworkers improved the original

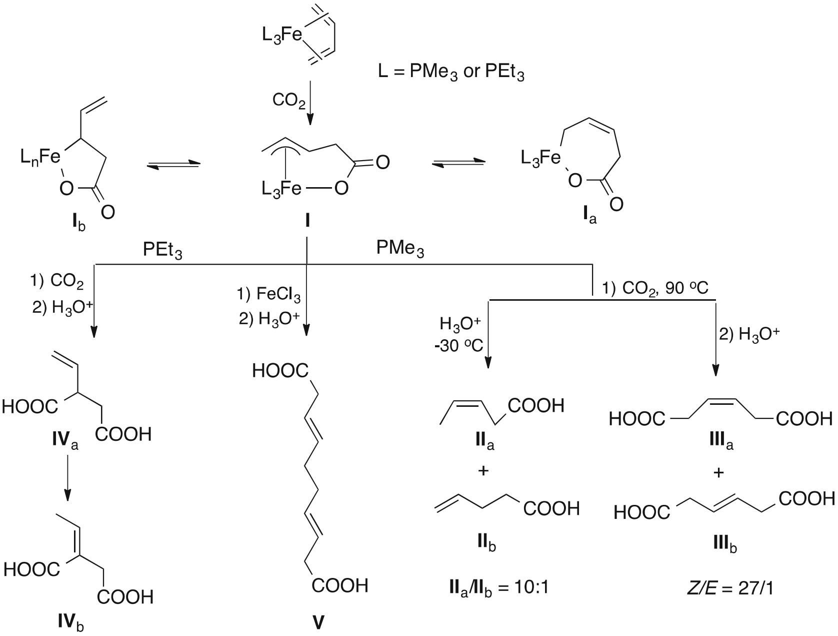

Scheme 16 Iron-mediated coupling reaction of diene and CO_2

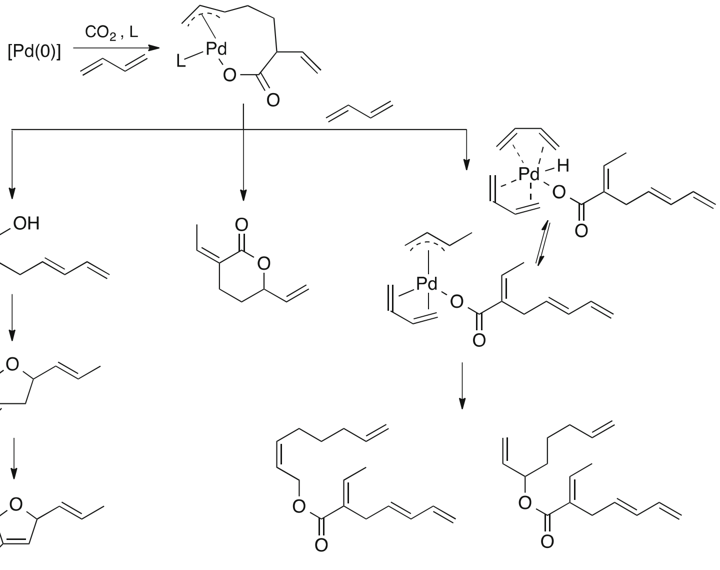

Scheme 17 Product distribution in the palladium(II)-catalyzed reaction of 1,3-butadiene and CO_2

synthetic procedures of Inoue and Musco by using palladium^{II} acetate or acetylacetonate complexes and phosphines in acetonitrile as the solvent, which led to a significant increase in the yield of the lactones [86]. The use of phosphine ligands of high basicity and large cone angle proved necessary in order to optimize yield and selectivity [87, 88]. In general, it was found that six major products may be obtained with palladium catalysts system [89–93].

Rhodium and ruthenium catalysts were also tested. In the rhodium-catalyzed reaction of butadiene and carbon dioxide, besides the C9-lactones generated as in the case of palladium catalysts system, a new C13 γ-lactone-2-ethyl-2,4,9-undecatrien-4-olide is formed in a novel combination of three molecules of butadiene with one of CO_2 [94]. Unfortunately, ruthenium catalysts were found to be quite ineffective. The total yield of the products from tautomerization of butadiene and insertion of CO_2 is in less than 7% [90].

2.4 Carboxylation of Allenes

As early as 1980, Döhring and Jolly probed the co-oligomerization of allenes and CO_2 with catalytic amounts of $[Pd(\eta^3\text{-allyl})_2]$ and mono- or bisphosphines in toluene, and obtained a mixture of six-membered lactones, esters, and oligomeric and polymeric materials (Scheme 18) [95]. Later, an analogous result was obtained using $[Rh(dppe)(\eta\text{-}BPh_4)]$ as catalyst in this reaction [96].

Later, a palladium-catalyzed cycloaddition of methoxyallene with CO_2 was studied by Tsuda et al. [97], which afforded the hetero-D-A-like [2 + 2 + 2] product in relatively high yield stereospecifically (Scheme 19). The methoxy functional group plays an important role, as it enriched the electron density on allene, which facilitated the cycloaddition of methoxyallene with the electron-deficient CO_2.

In 1984, Hoberg investigated the nickel-mediated coupling of terminal allene and CO_2 with basic chelate ligands (Scheme 20) [98]. The supposed five-membered nickelalactone is reminiscent of those formed in the reaction of CO_2 with alkenes. Acidic workup with CH_3OH/HCl affords the ester whose *exO–M*ethyl group is arranged to the α-position of carbonyl group as the only product regioselectively. Recently, well-designed electron-donating bidentate amidines were applied to this nickel-mediated reaction as ligands [99], and as expected, the 1,2-addition products was prepared in good yield with high regioselectivity.

Interestingly, Mori et al. showed that nickel-mediated sequential addition of CO_2 and aryl aldehydes into terminal allenes gave the "opposite" 2,3-addition products mainly (Scheme 21) [100]. This can be attributed to the sterically bulky ligands coordinated to the nickel center, which keeps aryl aldehydes away from the α-carbon, forcing the electrophile attacking at the γ-position.

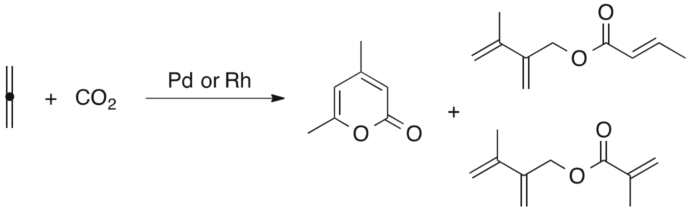

Scheme 18 Pd- or Rh-catalyzed coupling reaction of allene and CO_2

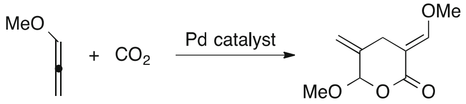

Scheme 19 Palladium-catalyzed cycloaddition of methoxyallene with CO_2

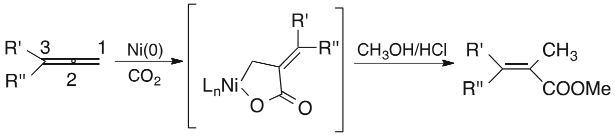

Scheme 20 Nickel-mediated coupling of terminal allene and CO_2

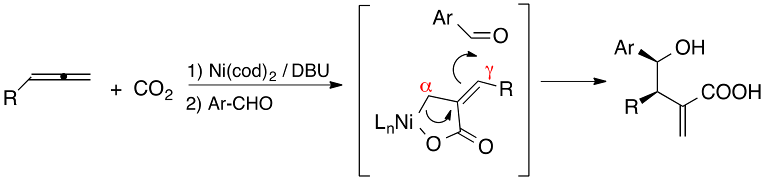

Scheme 21 Nickel-mediated cascade addition of CO_2 and aryl aldehyde to terminal allene

Not long afterwards, Nickel-mediated regio- and stereoselective carboxylation of trimethylsilylallene was also achieved [101, 102], using $PhMe_2SiH$ or R_2Zn as the reducing agent (Scheme 22). Allyl silane mono- or di-esters were produced in medium yield depending on the equivalent of CO_2 employed.

In 2008, Iwasawa's group reported an approach to catalytic CO_2-fixation through σ-allyl palladium species generated from hydropalladation of allenes [103]. The tridentate silyl pincer-type palladium precatalyst was triggered by appropriate reducing agents, like Et_3Al or Et_2Zn, forming the active [Pd-H] species, which drove the catalytic cycle efficiently (Scheme 23). The proposed allyl palladium intermediates in the catalytic cycle as well as several off-cycle species were isolated, identified, and characterized [104]. All of these complexes were found to be kinetically competent catalysts, which thus further supported the mechanism proposed by Iwasawa and coworkers.

Sato and coworkers described a nickel(0)-promoted carboxylation of allenamides with carbon dioxide proceeding via a nickelalactone intermediate, affording β-amino acid derivatives in good yield. (Scheme 24) [105]. The regioselectivity was largely dependent on the substituent *R′* on the allene moiety. When R′=H, (*Z*)-α,β-dehydro-β-amino acids were obtained, while more bulky group, such as Me, *t*-Bu, presented at the allene end, α,β′-unsaturated-β-amino acids were delivered. Inspired by this work, Hou further developed a methodology for catalytic alkylative carboxylation of allenamide with CO_2 in the presence of NHC-Cu complex and using dialkylzinc reagents as coupling partners [106]. The resulting alkyl-attached (*Z*)-α,β-dehydro-β-amino acid derivatives were obtained in good yield with high regio- and stereoselectivtiy.

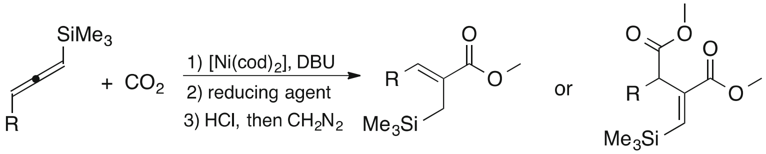

Scheme 22 Nickel-mediated carboxylation of trimethylsilylallene

Scheme 23 Regioselective carboxylation of allenes catalyzed by palladium complexes

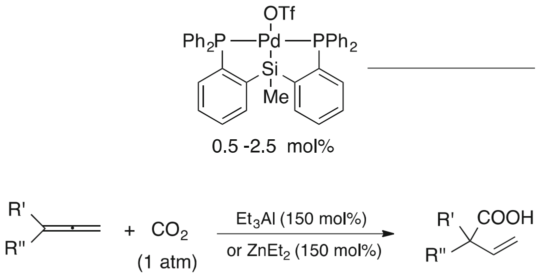

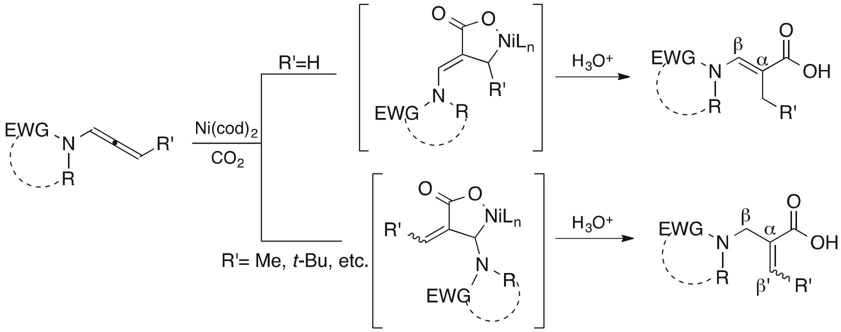

Scheme 24 Nickel-promoted carboxylation of allenamides

2.5 Carboxylation of Alkynes via Cyclization

The first nickel-catalyzed cycloaddition of CO_2 to terminal alkyne was observed by Inoue in 1977 [107], giving 4,6-dibutyl-2-pyrone together with 1-hexyne oligomers. However, the yield and selectivity of this reaction were quite low. The same reaction was also carried out using cobalt complex as catalyst, which provided pyrone in an even lower yield. Later, Inoue expanded the substrate scope to 3-hexyne [108] and 4-octyn [109], and found that the main product pyrone was given in much better yield along with several by-products (Scheme 25). Analogously, Complex $[(dppe)Rh][BPh_4]$ was applied to the oligomerization of methylacetylene and CO_2, which gave a mixture of dimeric, trimeric, and aromatic products [110].

Inoue et al. firstly suggested a mechanism involving the formation of nickelacyclopentadiene from the nickel catalyst and two equivalents of alkyne, followed by subsequent insertion of CO_2 to afford the pyrone (Scheme 26a)

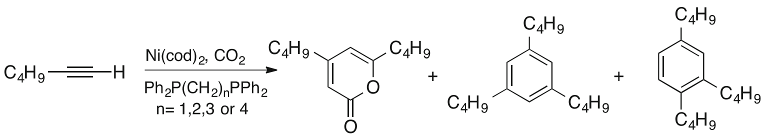

Scheme 25 Nickel-catalyzed cycloaddition of CO_2 to 3-hexyne

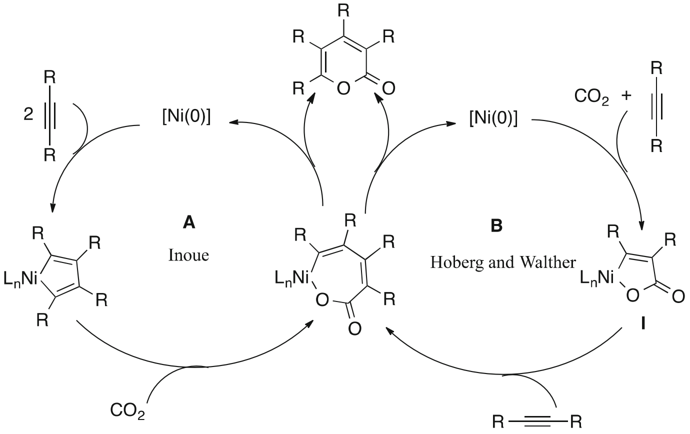

Scheme 26 Proposed mechanism routes to formation of pyrone from alkyne and CO_2

[107, 109]. Soon afterwards, oxanickelacyclopentene generated from carbon dioxide, one equivalent of alkynes and nickel(0) complex was also proposed to be the potential intermediate in pyrone preparation (Scheme 26b) [111–113], and which was confirmed by Walther et al., who performed the IR-investigations of the catalytic formation of tetraethyl-2-pyrone from hex-3-yne and CO_2 at Ni(0) centers, and determined the structure of tetraethyl-oxanickelacyclopentene complex **I** by *X*-ray [114]. Walther and coworkers also studied the influence of the nature of the phosphine ligands on the product distribution, and found that the yield of pyrone could increase up to 96% when phosphanes of high basicity and small cone angle were employed [115]. On the basis of DFT calculations, Buntine and coworkers suggested that, in analogy to the reaction of CO_2 and olefins at nickel(0) complexes, oxidative coupling of one alkyne and CO_2 with nickel complex results in a thermodynamically stable oxanickelacyclopentene complex [116].

Oxanickelacyclopentene derivatives were shown to be versatile synthones (Scheme 27) [47, 111–113]. Protonolysis of complex **I** led to 2-methylcrotonic acid, and incorporation of carbon monoxide into complex **I** gave dimethylmaleic anhydride [113]. Furthermore, coupling of two equivalents of complex **I** with geminal dihalides afforded cyclic anhydride [112]. Insertion of a second alkyne into Complex **I** delivered oxanickelacycloheptadienones **II**, which could undergo reductive elimination forming pyrone. Hydrolysis of Complex **II** gave (*Z, Z*)- 2,4-dienyl carboxylic acid (R=CF_3). Interestingly, when R=CO_2Me, the originally formed dienyl carboxylic acid further underwent intramolecular 1,4-addition

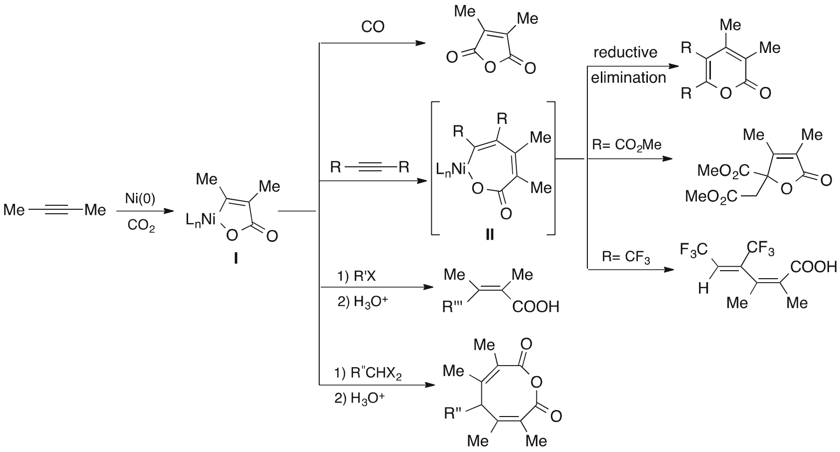

Scheme 27 Reactions of oxanickelacyclopentene with various electrophiles

leading to the five-membered lactone [111, 112]. Recently, five- or six-membered nickelacyclic carboxylates [117], analogous to Complex **I**, was found to be quite active to couple with α-haloketones, forming α,β-unsaturated δ-ketocarboxylic acids in good yield, which were easily converted into pyranones or isocoumarins.

Diynes were also found to be good substrates in cycloaddition with CO_2. Upon treatment with equimolar [118] or catalytic [119, 120] amounts of $[Ni(cod)_2]$ and several bisphosphines, diynes coupled with CO_2 to give bicyclic α-pyrones in moderate to good yield (Scheme 28a). Recently, Louie et al. developed an efficient approach to catalytic formation of bicyclic α-pyrones from diynes and CO_2 in the presence of Ni-NHC complex under mild conditions (Scheme 28b) [121, 122]. It is suggested that the steric bulk of the NHC ligand shields the Ni(0) complex from an unproductive coupling with the diyne, leading to a high selectivity of oxanickelacyclopentene formation. Subsequent insertion of the second pendant alkynyl unit followed by a carbon–oxygen bond-forming reductive elimination then released the pyrone product in good yield. Similarly, Sato et al. investigated the nickel-mediated carboxylation of α, ω-enyne [123, 124], and the corresponding cyclic carboxylic acids were obtained in moderate yield though with a little bit low selectivity.

In 1999, Saito et al. reported on the nickel-mediated *syn*-hydrocarboxylation of terminal alkynes that resulted in α,β-unsaturated carboxylic acids regio- and chemoselectively (Scheme 29) [125]. Indirect evidence for the formation of the nickelacycle intermediate was obtained by using a deuterated acid as the quenching reagent. The deuterium atom was introduced at the vinyl position (96% atom % D), indicating the existence of a Ni–C bond in intermediate. They also expanded the substrate scope to conjugated enynes and diynes (Scheme 29), and found that hydrocarboxylation occurred only at the alkynyl unit, and CO_2 was incorporated at the end carbon with less steric substituent. Analogously, Iwasawa et al. developed a nickel/bidentate amidines system for coupling of alkynes and CO_2 [99], which offered α,β-unsaturated carboxylic acids with lower regioselectivity. Besides the nickel system, titanium complexes generated from $Ti(O\mathit{i}Pr)_4$ and C_5H_9MgCl, were

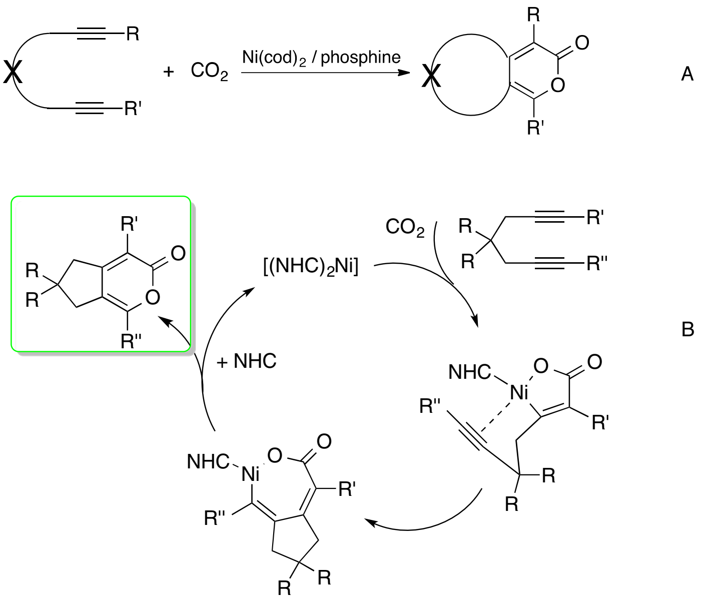

Scheme 28 Ni-mediated or catalyzed cycloaddition of diynes and CO_2 to form bicyclic α-pyrones

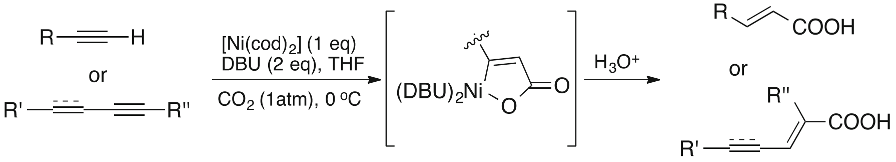

Scheme 29 Nickel-mediated *syn*-hydrocarboxylation of alkynes

also employed for the synthesis of vinylcarboxylic acids and butenolides via *syn*-hydrocarboxylation and hydroxyalkyl-carboxylation of alkynes, respectively [126].

Later, nickel-promoted *syn*- alkylative or arylative carboxylation of terminal alkynes, using organozinc reagents as the alkyl/aryl source, was performed under CO_2 atmosphere [127], providing β,β′-disubstituted, α,β-unsaturated carboxylic acids regio- and stereoselectively (Scheme 30a). The α,β-unsaturated carboxylic acids could further be trapped by an intramolecular proximity-nucleophile (-OH, -NHR) to give heterocyclic compounds in good yield (Scheme 30b) [128]. Not long afterwards, the *syn*-addition of alkyl group and CO_2 to silylated alkyne was also achieved via a similar method using catalytic amount of Ni complex, and the regioselectivity was largely dependent on the steric and electronic nature of the substituent [129]. Analogously, *syn*- arylative carboxylation of disubstituted alkynes delivered tetrasubstituted alkene in high yield and, however, with a relatively low regioselectivity [130].

More recently, several research groups revisited the hydrocarboxylation of alkynes with CO_2 and focused on carrying out the reactions at low transition-metal

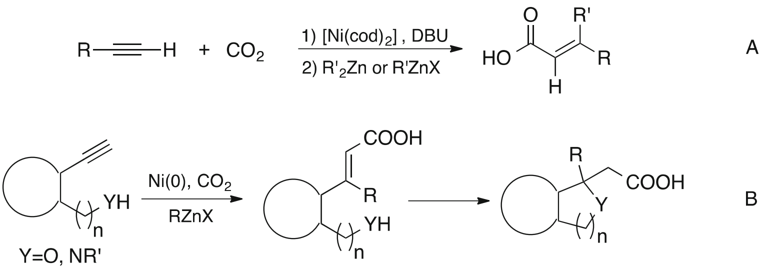

Scheme 30 Nickel-promoted *syn*-alkylative or arylative carboxylation of terminal alkynes

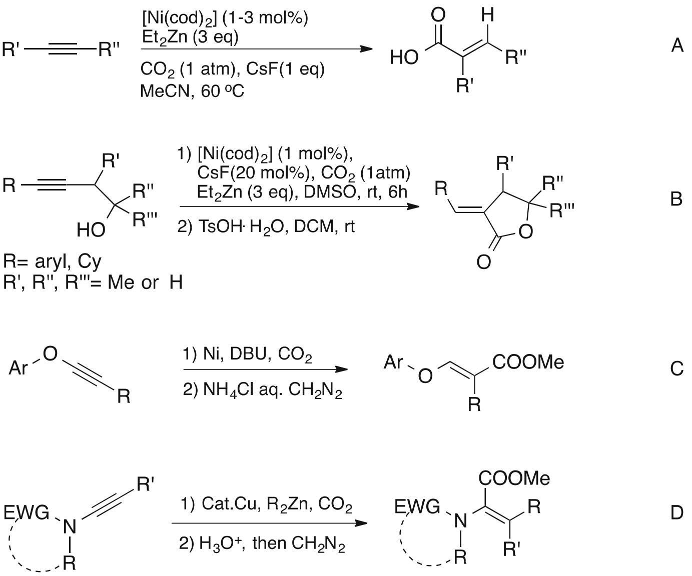

Scheme 31 Hydro-, alkyl-, or aryl-carboxylation of alkynes in the presence of Ni or Cu complexes

catalyst loadings under mild conditions with expanding substrate scope of alkynes. Ma and coworkers reported on a concise synthetic route to 2-alkenoic acids via nickel-catalyzed coupling of alkynes and CO_2 using diethyl zinc as the [H] reservoir with high regio- and stereoselectivity (Scheme 31a) [131]. Further, Ma et al. employed this method to the preparation of α-alkylidene-γ-butyrolactones via hydrocarboxylation of homopropargylic alcohols and subsequent intramolecular esterification (Scheme 31b) [132]. Almost at the same time, Tsuji et al. investigated the copper-catalyzed CO_2-fixation with alkynes in the presence of hydrosilanes as reducing reagents [133]. Both the internal and terminal (symmetrical or unsymmetrical) alkynes were hydrocarboxylated in moderate to good yield. Hou described an analogously hydro- or methylative carboxylation of both terminal and inter alkynes with high regioselectivity using cascade (hydro-) methylative alumination and NHC-Cu catalyzed carboxylation in one pot [134]. However, the inter alkynes was narrowly limited to those possessing a tethered directing ether group.

Additionally, it was found that nickel(0)-mediated carboxylation of aryl ynol ether proceeded in a highly regioselective manner to give α-substituted-β-aryloxyacrylic acid derivatives (Scheme 31c) [105]. Furthermore, in 2016, Hou demonstrated a NHC-Cu-catalyzed alkylative carboxylation of ynamides (Scheme 31d), both cyclic and acyclic, in simple one-pot procedure, affording the corresponding α-amide-α,β-unsaturated carboxylic acids with high regio- and stereoselectivity [135].

Sakaki and Tsuji [136] reported a nickel-catalyzed double carboxylation of internal alkynes with CO_2 (Scheme 32) employing Zn powder as reducing reagent, and $MgBr_2$ as an indispensable additive for its key role in the second CO_2 incorporation, which was disclosed and supported by DFT calculations. A wide range of maleic anhydrides were prepared in good to high yield.

In 2012, Ma and coworkers unveiled the first copper-catalyzed *anti*-nucleometallation–carboxylation of 2-alkynylanilines with carbon dioxide in the presence of dimethylzinc and cesium fluoride (CsF) for the effective synthesis of indolyl-3-carboxylic acids and indolodi- hydropyran-2-one (Scheme 33) [137]. They suggested that all the three metals Cu, Cs and Zn created a synergetic environment for the smooth conversion to the *anti*-amino carboxylation products, which was further facilitated by fluoride ion for its CO_2-activation through FCO_2^- intermediate. In the same year, Inamoto et al. reported another example of *anti*-amino(oxo) carboxylation [138], and found that in the absence of transition metal catalysts, *o*-(1-alkynyl)anilines could be transformed into indolyl-3-carboxylic acids using 10 equivalents of K_2CO_3 with CO_2 at 10 atm.

Along with the heterocarboxylation of alkynes mentioned above, the more challenging catalytic silacarboxylation [139] and boracarboxylation [140] were also accomplished (Scheme 33). Such novel conversions would lead to the addition of both a silyl or bory unit and a carboxylate group to the C–C triple bond, and the resulting products α,β-unsaturated β-(sila)boralactone derivatives could serve as versatile building blocks for further construction of multifunctionalized alkenes. Inspired by the work of stoichiometric silylcupration of 1-hexyne [141, 142], Tsuji and coworkers developed the first catalytic silacarboxylation of internal alkynes employing CO_2 and silylborane in the presence of a copper catalyst [L-Cu-Cl], affording silalactones regioselectively in good to excellent yields (Scheme 33a) [139]. Analogously, Hou et al. demonstrated the first catalytic boracarboxylation of alkynes with bis(pinacolato)diboron and CO_2 using an *N*-heterocyclic carbene (NHC) copper catalyst, giving β-boralactone derivatives regio- and stereoselectively (Scheme 33b). The isolation and structural characterization of β-boryl alkenyl copper complex, β-boryl alkenyl carboxylate copper salt and the lithium–copper transmetalation intermediate provided key insight into the mechanistic aspects of the catalytic cycle (Schemes 33c, 34) [140].

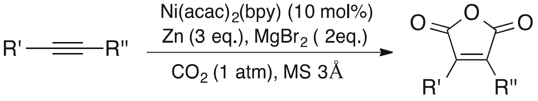

Scheme 32 Nickel-catalyzed double carboxylation of internal alkynes with CO_2

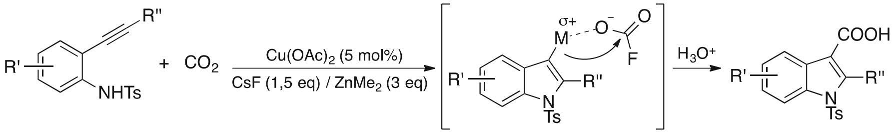

Scheme 33 Copper-catalyzed *anti*-nucleometallation-carboxylation of 2-alkynylanilines

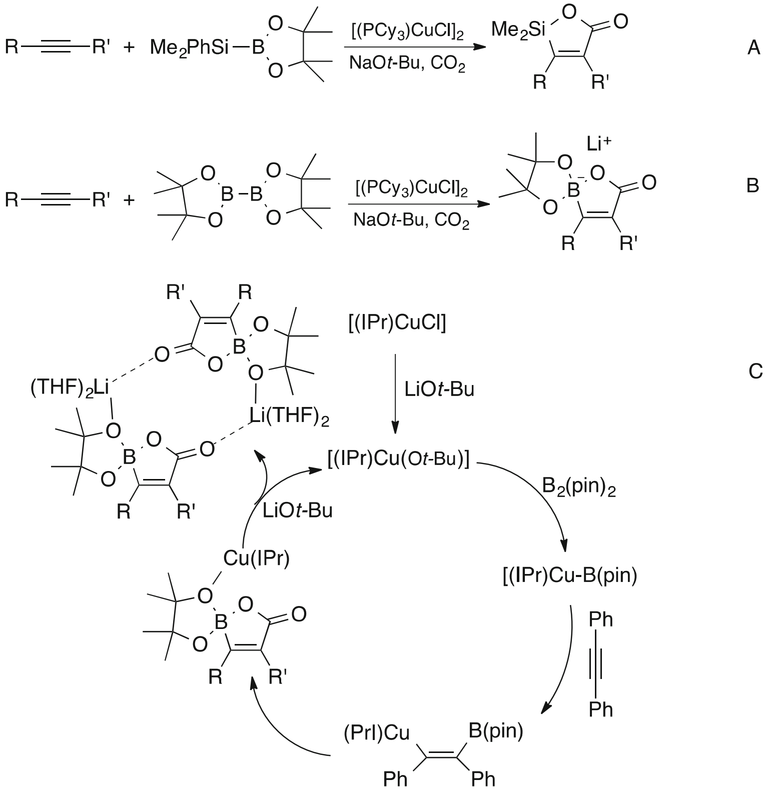

Scheme 34 Copper-catalyzed silacarboxylation and boracarboxylation

3 Insertion of CO_2 into Organometallic Reagents

As a long-known reaction, insertion of CO_2 molecule into the M–C bond of a organometallic compound afforded carboxylate species straightforwardly. Originally, organometallic compounds of group I and II were employed to investigate this kind of CO_2-fixation. The use of organomagnesium compounds in carboxylic acid synthesis could be traced back to the beginning of the "Grignard reagents" legacy around 1900. Due to its strong nucleophilicity and basicity, the addition of Grignard reagents to CO_2 delivered the corresponding carboxylic acid efficiently (Scheme 35a) [143–146]. Interestingly, treatment of CO_2 with allylic magnesium reagent resulted in γ-carboxylation (Scheme 35b1), whereas α-carboxylation

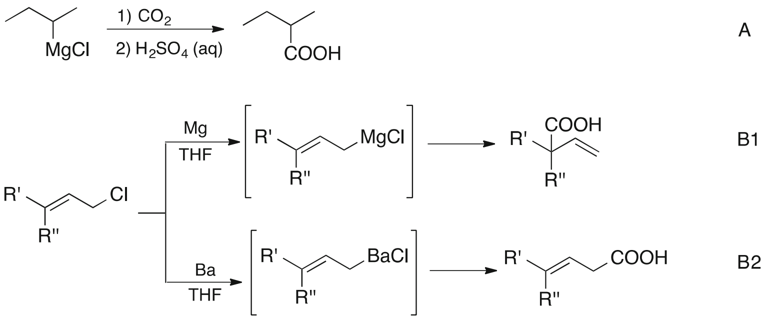

Scheme 35 Reaction of organomagnesium(barium) compounds with CO_2

occurred with allylic barium reagent (Scheme 35b2) [147]. The regioselectivity of γ-carboxylation of allyl-magnesium might attribute to the aggregation of magnesiated species. The double bond geometry of allylbarium was completely retained.

Magnesium amides (alkyl magnesium amides) [148–151], especially $Mg(N\textit{i}Pr_2)_2$, $BuMgN\textit{i}Pr_2$, and $(TMP)_2Mg$ (TMP: 2,2,6,6-tetramethylpiperidino), are a kind of new bases for stoichiometric, position-selective deprotonation/magnesiation of weakly acidic CH, such as cyclopropyl-CH cyclobutyl-CH and cubyl-CH, in particular those activated by an adjacent amide group. The resulting amido-stabilized magnesium spices could be trapped by CO_2 smoothly, affording the corresponding carboxylic acids with high regio- and stereoselectivity and in moderate to good yield (Scheme 36).

Organolithium reagents came into the synthetic use for carboxylic acid somewhat later, but are very important for the low-cost preparation of carboxylic acids [152–156]. For example, aryl lithium intermediate generated from Br/Li exchange smoothly coupled with CO_2 to give lithium benzoates, which underwent lactonization after acidic workup spontaneously (Scheme 37) [157].

However, Grignard and organolithium reagents are quite restricted in the types of functional groups that can be present in either organometallic compounds or reactants due to their high reactivity, and thus is of limited use in organic synthesis.

The organometallic compounds of group III elements, especially the organoboron reagents, had their wide application in coupling reactions, and of course were found to react efficiently with CO_2. In 1960, Ziegler and coworkers demonstrated that the addition of triethylaluminum to CO_2 offered the compound $Et_2Al(OOC\text{-}Et)$, which can—depending on the stoichiometry—further react with $AlEt_3$, leading to a mixture of carboxylic acids and alcohol after subsequent hydrolysis [158]. The research groups of Zweifel and Eisch reported that *ate* vinylalane complexes underwent a smooth conversion to the corresponding alkenoic acids upon treatment with CO_2 in the presence [159, 160] or absence [161] of organolithium reagents (Scheme 38A). Recently, Hou and coworkers [162] found that when treatment with CO_2 in the presence of NHC-Cu catalyst, arylaluminum species generated in situ by deprotonative *ortho*-alumination of aromatic compounds bearing a directing group could be transformed into the corresponding aryl carboxylic acid with moderate to high yield (Scheme 38b).

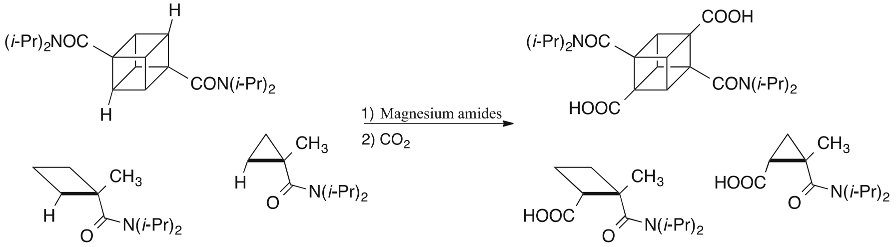

Scheme 36 Magnesium amides-mediated deprotonation/magnesiation for CO_2 incorporation

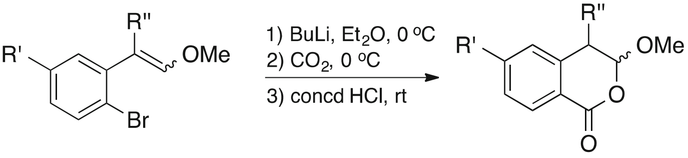

Scheme 37 Synthetic use of organolithium reagents for the preparation of carboxylic acid derivatives

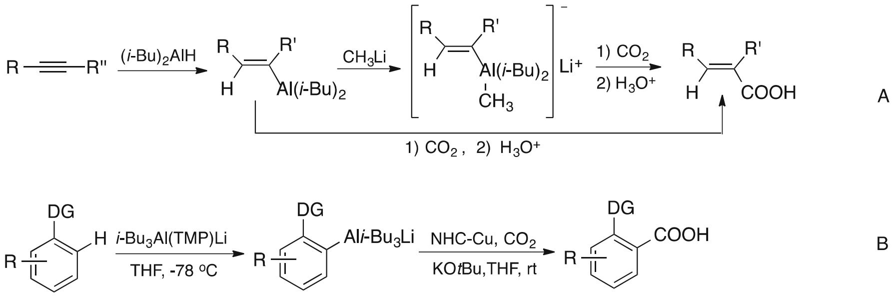

Scheme 38 Conversion of organoaluminium to carboxylic acid with CO_2

One of the early attempts to activate CO_2 by utilizing less polarized boron–carbon bonds was reported in 2006 by Iwasawa and coworkers [163]. In this report, rhodium catalysts were employed to conduct carboxylations of aryl- and alkenylboronic esters under an atmospheric pressure of CO_2 (Scheme 39). However, it was observed that the boronic esters bearing bromo, nitro, alkynyl, and vinyl substituents were entirely inert under otherwise identical Rh(I)-catalyzed carboxylation conditions. Some of these drawbacks have been circumvented later by the research groups of Hou [164] and Iwasawa [165] who independently introduced the less-expensive and readily available copper catalysts to perform the carboxylation of such boron-type compounds (Scheme 39). In accordance with the findings, the copper–catalyst system showed a broader substrate scope than the rhodium-catalyzed methods and allowed for the synthesis of a wide range of functionalized carboxylic acids. DFT studies on the Cu^I-catalyzed carboxylation of arylboronate esters suggested a basic catalytic cycle including transmetalation, CO_2 insertion and carboxylate displacement [166]. Analogously, a simple $silver^I$/phosphine system was also found to enable the catalytic conversion of arylboronic esters to the

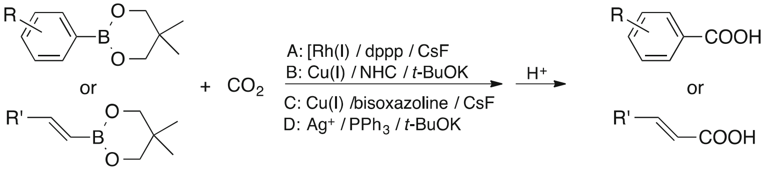

Scheme 39 Transition-metal-catalyzed carboxylation of aryl- and alkenylboronic esters

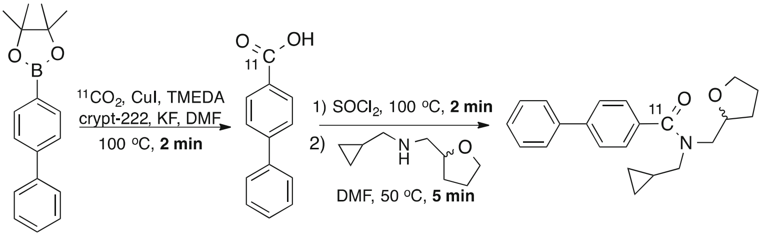

Scheme 40 Radiotracer synthesis of ^{11}C-labeled carboxylic acid via Cu^{I}-catalyzed carboxylation of arylboronate esters

corresponding carboxylic acid with wide functional group compatibility as well as good yield [167].

Recently, a pH-controlled monophasic/biphasic switchable Cu-NHC catalyst system was developed for carboxylation of organoboronic esters and benzoxazole with carbon dioxide [168]. The tertiary amine-functionalized catalysts could be recycled and used for at least four times with a slight loss of activity.

The approach of Cu^{I}-catalyzed carboxylation of arylboronate esters further found its application in radiotracer synthesis of ^{11}C-labeled carboxylic acids [169]. In this way, a ^{11}C-labeled oxytocin receptor ligand was prepared in one pot for less than 10 min (Scheme 40). HPLC gave [^{11}C]-X in 20% RCY at 43 min from radionuclide production with a radiochemical purity of >98% and a specific radioactivity of 1.5 Ci μmol^{-1}.

Allylborons as well as allylstannanes were carboxylated using (η3 -allyl)Pd^{II}(-L)(carboxylate) (L=PR$_3$ or NHC) or allyl-bridged Pd(I) dimers (η^3-allyl)$_2$Pd$_2$/NHC as active catalysts in high efficiency (Scheme 41a) [170–174]. However, substrates possessing substituent(s) at α or γ position(s) were not fit in this Pd-catalyzed coupling reaction. The substrate scope was extended to more substituted allylborons by employing a well-studied NHC-Cu/*t*BuOK catalyst system in Duong's group (Scheme 41b) [175]. A diverse array of substituted β, γ-unsaturated carboxylic acids were prepared via this method with high regioselectivity, including that featuring all-carbon quaternary centers.

Alkylboron compounds, generated from hydroboration of terminal alkenes with 9-borabicyclo-[3.3.1]nonane, were also successfully used as substrates for carboxylation with CO$_2$ in the presence of a copper (I) complex [176, 177], which showed high functional group compatibility (Scheme 42). A stoichiometric amount of base, such as MeOLi or *t*-BuOK, played an important role in promotion of the coupling.

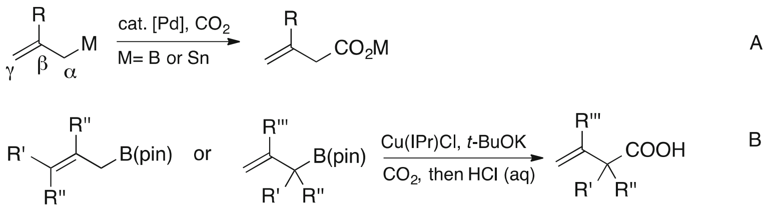

Scheme 41 Pd- and Cu-catalyzed carboxylation of allylborons

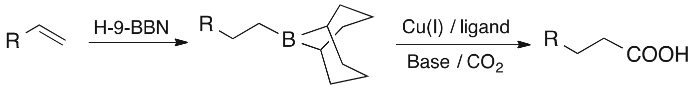

Scheme 42 Cu-catalyzed carboxylation of alkylborons

In 1997, Shi and Nicholas reported the oxidative addition of $[Pd^0(PR_3)_4]$ to allylstannanes, followed by insertion of CO_2 into the palladium–allyl bond, thereby created a carboxylate ligand, which is cleaved from the palladium center by the oxophilic R'_3Sn species (Scheme 43) [178]. The resulting organotin carboxylates, especially diorganotin esters, have a wide range of commercial applications in industry as stabilizers for polymers and copolymers made from vinyl chlorides. Later, the research group of Wendt [179] revisited the work of Shi and Nicholas, and found that carboxylation of allylstannanes with CO_2 occurred in the presence of palladium pincer catalysts, which afforded the organotin carboxylates in good yield. Recently, just as mentioned above, Hazari and coworkers developed another two efficient $(\eta^3\text{-allyl})_2Pd$/NHC and $(\eta^3\text{-allyl})_2Pd_2$/NHC catalyst systems for the CO_2-fixation with allylstannanes or with allylborons [170–174].

Based on the work of Pd-catalyzed carboxylation of allylstannanes, Nicholas and coworkers [180] further studied a tentative three-component carboxylative coupling reaction between allyl halides, allylstannanes and CO_2, using Pd or Pt phosphine complexes as catalysts, which gave a mixture of four allyl esters in moderate to good yield (Scheme 44a). The low selectivity probably resulted from the reversible carboxylative procedure and the unfavorable reductive elimination equilibrium to form ester and regenerate Pd(0) species. Similarly, Bao et al. [181] performed the carboxylative coupling of allyltributylstannan with benzyl chlorides and CO_2 to produce benzyl but-3-enoates in satisfactory to good yields in the presence of catalytic palladium nanoparticles (Scheme 44b).

Interestingly, other than the allylstannanes, *N*-Boc-α-amido stannanes and α-acetoxy stannanes were also transformed into the corresponding α-amino acids and mandelic acid derivatives, respectively, using CO_2 as C1 source, which were promoted by CsF in the absence of any transition-metal catalyst (Scheme 45a) [182–184]. In addition, the configuration of the α-carbon was inverted up to 90% when chiral N-protected α-amido stannanes (*ee* > 99%) were employed in this reaction. Alternatively, α-amido stannanes could undergo facile Sn–Li exchange for in situ generation of lithiated amide, which could be trapped with CO_2 to form α-amino acids derivatives in good yields (Scheme 45, b) [185].

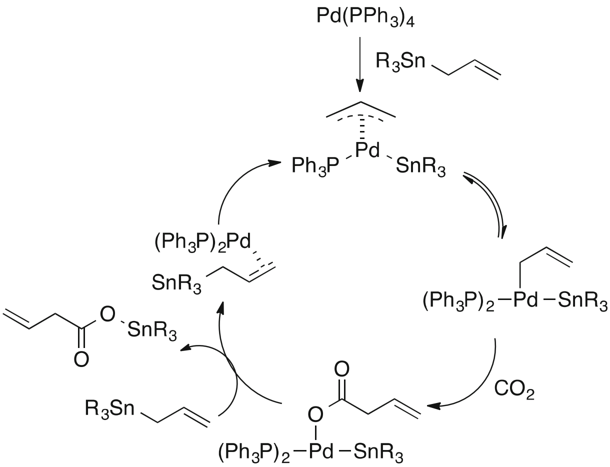

Scheme 43 Pd-catalyzed carboxylation of allylstannanes

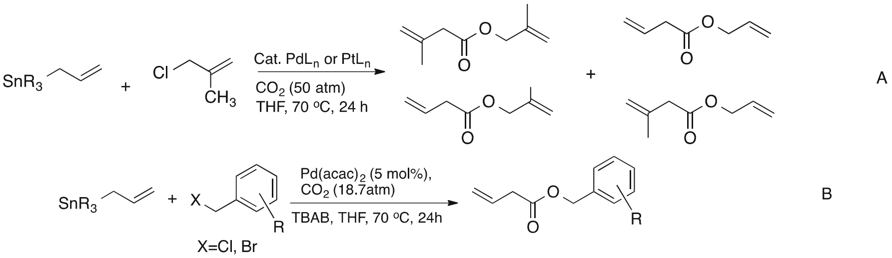

Scheme 44 Pd-catalyzed carboxylative coupling between allyl halides, allylstannanes, and CO_2

Scheme 45 Carboxylation of *N*-Boc-α-amido stannanes and α-acetoxy stannanes

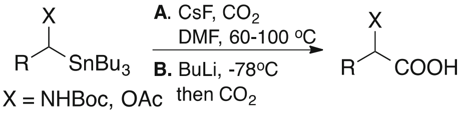

Silicon is similar in electronegativity to carbon and the carbon-silicon bond is quite strong (~75 kcal/mol). Most of the valuable synthetic procedures base on organosilanes involves either alkenyl (aryl) or allylic silicon substituents. Carboxylation of aryl- and allylsilanes were first realized with the aid of aluminum-based Lewis acids, giving aromatic and β,γ-unsaturated carboxylic acids respectively with relatively low yield (Scheme 46a, b) [186]. Later, a more efficient CsF-mediated desily-carboxylation method, just as that used for activation of organostannanes, was developed [187]. Various electron-deficient aryltriethylsilanes were coupled with CO_2 smoothly, affording the corresponding desily-carboxylated products in high yield. On the other hand, desily-carboxylation of electron-rich aryltriethylsilanes did not proceed at all. Furthermore, in combined use of CsF-mediated desily-carboxylation and Ag^{I}-catalyzed cyclization [188], numerous trimethyl(2-methylenebut-3-yn-1-yl)- silane derivatives were transformed into

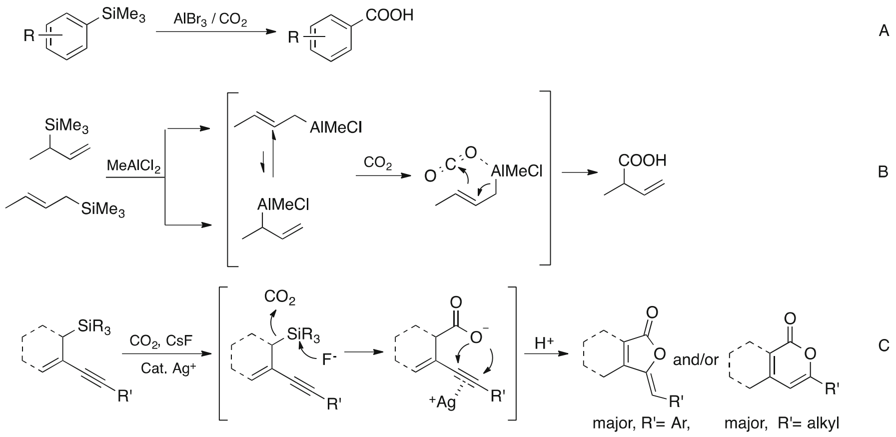

Scheme 46 Carboxylation of aryl- and allylsilanes prompted by aluminum-based Lewis acids or CsF

2-furanone or 2-pyrone derivatives depending on the substituent *R′* at the alkyne-motif (Scheme 46c).

Later, Mita and Sato successfully expanded the substrate scope of CsF-mediated desily-carboxylation to α-hetero (O, N) silanes. α-Siloxy silanes were carboxylated efficiently through a key intramolecular Brook rearrangement intermediate (Scheme 47a) [189], while carboxylation of α-amino silanes proceeded smoothly via direct intermolecular activation of silanes with fluoride (Scheme 47b) [190]. Furthermore, domino reactions including successive ammonium salt formation, CsF-mediated desily-carboxylation, esterification, and 2,3- or 1,2-Stevens rearrangement were applied to a kind of structure-limited α-amino silanes for one-pot synthesis of α-amino acids via ammonium ylide intermediates (Scheme 47c) [191].

Organozinc reagents have become one of the most useful of organometallics in terms of synthesis since they tolerate a broad range of functional groups. The reactivity patterns of organozinc compounds are similar to derivatives of Group IA and IIA metals. However, the carbon-zinc bond has more covalent character, and thus the organozinc reagents are considerably less reactive towards electrophiles. Many of the synthetic applications of these organometallics derived from zinc are based on this attenuated reactivity and involve the use of a specific catalyst or addictive to promote reaction. As in case of CO_2-fixation, the research groups of Dong [192] and Oshima [193] almost simultaneously published their findings of the coupling between alkyl- and arylzinc halides with CO_2 promoted by in situ formed Aresta complex [194] $[(Cy_3P)\ _2M(\eta^2\text{-}CO_2)]$ (Dong: M=Ni, Pd; Oshima: M=Ni;), which enables carboxylation of functional group compatible both aliphatic and aromatic nucleophiles (Scheme 48).

Later, an efficient process for the carboxylation of functionalized organozinc reagents with CO_2 under transition-metal-free conditions was investigated by employing LiCl as promoter in different solvents (Scheme 49a) [195], results of which suggested that the polarity and donor numbers of solvent may affect the coupling reaction significantly, and DMF was found to be the best one in this

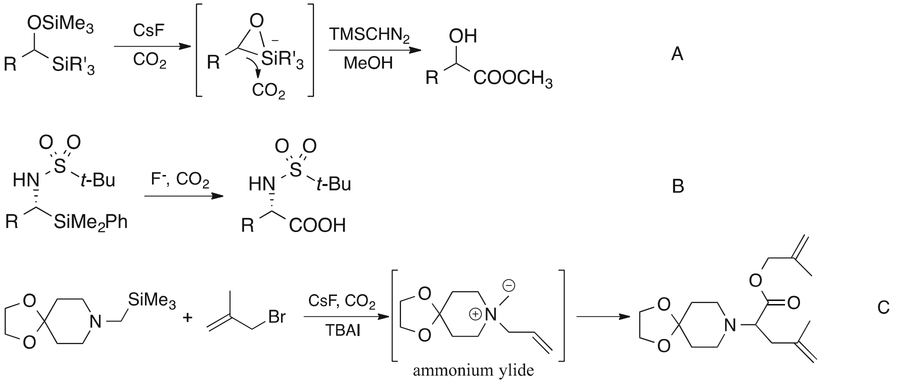

Scheme 47 Fluoride prompted desily-carboxylation of α-hetero (O, N) silanes

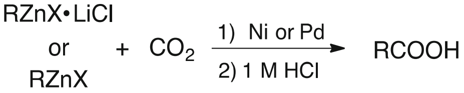

Scheme 48 Ni- or Pd-catalyzed carboxylation of organozinc reagents

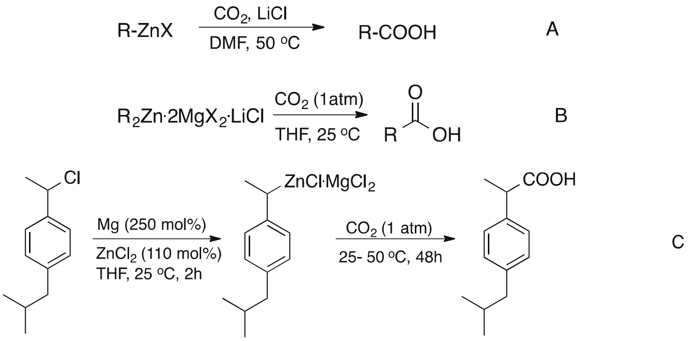

Scheme 49 LiCl or MgCl2 prompted carboxylation of organozinc reagents

reaction. Analogously, $MgCl_2$-accelerated addition of functionalized organozinc reagents to carbon dioxide was also achieved under mild conditions (Scheme 49b) [196, 197]. By this method, ibuprofen was prepared in a short four-step route (Scheme 49c).

The insertion of CO_2 into the metal-C bond of organo transition-metal compounds [198–203], such as organo scandium [204], titanium [205], zirconium [205–209], nickel [210–213], iron [214], copper [215–219], tungsten, [220, 221], palladium [207, 222–224], iridium [225], ruthenium [226–228], and rhodium [225, 229–231] complexes, also had been widely investigated, and in most cases, carboxylation of the C-ligand(s) occurred efficiently, affording the corresponding functionalized metal carboxylate products (Scheme 50). Experimental and computational studies showed

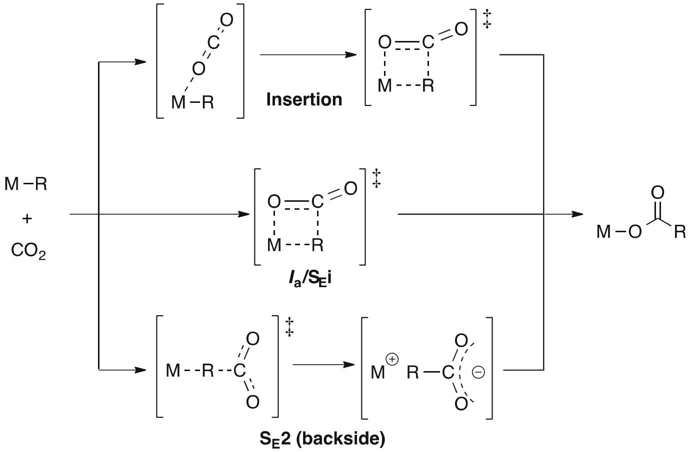

Scheme 50 Mechanism routes for insertion of CO_2 into the transition-metal M–C bond

that the carboxylation of zirconium and other d^0 metal as well as ruthenium alkyls species likely proceed via *coordination-migratory insertion* mechanisms. On the other hand, carboxylation of group 10 metal complexes (M=Pd, Ni) occurs by direct S_E2 backside attack of CO_2 on the M–R group to generate a $M^+ \, ^- O_2CR$ ion pair that collapses to the product. For the most thoroughly studied carboxylation of group 6 metal complexes, a concerted I_a (associative interchange)/S_Ei (internal electrophilic substitution) mechanism was proposed. Similar I_a/S_Ei mechanisms had been implicated for the incorporation of CO_2 into Ru, Rh, and Cu complexes too.

4 Insertion of CO_2 into C–X Bond

Taking into consideration that stoichiometric organometallic species are frequently prepared from organic halides, an ideal strategy within the carboxylation filed would be the use of organic (pseudo)halides as coupling partners, thus avoiding the need for well-defined and stoichiometric organometallic reagents [37]. As evident from the wealth of literature data reported in recent years, the metal-catalyzed reductive carboxylation of organic (pseudo)halides has reached remarkable levels of sophistication, representing powerful alternatives for preparing carboxylic acids from simple precursors.

In 2009, a novel protocol for the Pd-catalyzed coupling of carbon dioxide with aryl halides directly without pre-synthesis of organometallic reagents was presented by Arkaitz Correa and Rubén Martín, using $ZnEt_2$ as reducing agent (Scheme 51) [232]. It was proposed that, instead of coupling with organozinc species that are often formed by halogen-metal exchange between Et_2Zn and aryl iodides, the insertion of carbon dioxide into the Pd-aryl bond followed by transmetalation with Et_2Zn is the key step for this catalytic transformation. Analogously, Daugulis described a Cu/TMEDA system for catalytic carboxylation of aryl iodides using Et_2Zn as reducing agent [233]. Good functional group tolerance is observed, and

Scheme 51 Pd-catalyzed coupling of carbon dioxide with aryl bromides

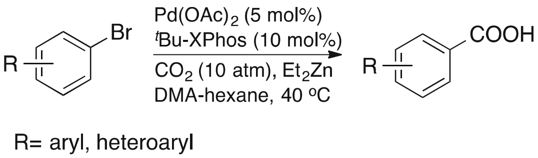

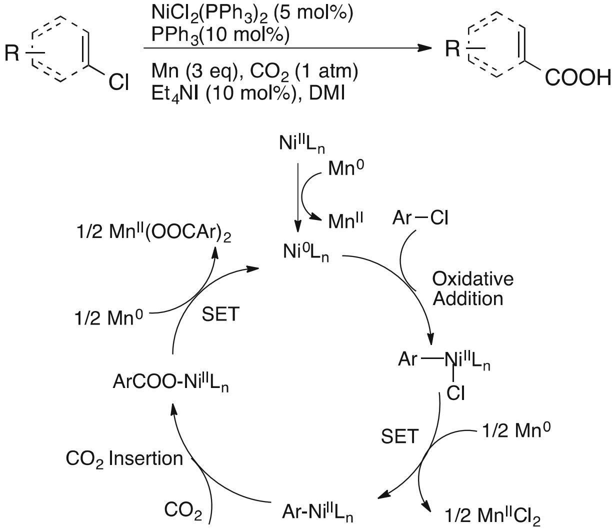

Scheme 52 Ni-catalyzed coupling of carbon dioxide with aryl- or vinyl- chlorides via SET processes

additionally, hindered aryl iodides such as iodomesitylene could also be carboxylated.

Apart from the regular Et$_2$Zn, manganese with the aid of Et$_4$NI could work as efficient reducing agent in nickel-catalyzed carboxylation of aryl- and vinyl-chlorides with CO$_2$ (Scheme 52) [234]. Various aryl- and vinyl- chlorides were successfully converted to the corresponding carboxylic acid in good to high yield. The proposed mechanism suggested that a key aryl–Ni(I) intermediate was generated upon single-electron transfer (SET) mediated by Mn, probably facilitated by Et$_4$NI. Subsequent insertion of CO$_2$ into the C(sp2)–Ni(I) bond followed by a second SET process would regenerate the LnNi(0) species while forming the targeted carboxylic acid upon final hydrolytic workup.

Later, Rubén Martín and coworkers extended this kind of reaction further to the development of Ni-catalyzed direct carboxylation of benzyl halides with CO$_2$ using zinc as reducing partner for assembling phenylacetic acids (Scheme 53) [235]. All the primary, secondary, and tertiary benzyl halides were coupled with CO$_2$ efficiently via benzylic C(sp^3)–halide activation under mild reaction conditions with an excellent chemoselectivity profile. A similar key benzyl–Ni(I) intermediate generated upon SET reduction mediated by Zn was also proposed. DFT calculations [236] revealed the crucial roles of MgCl$_2$ as a non-innocent additive for either stabilizing a Ni(I)-CO$_2$ complex prior CO$_2$ insertion, or facilitating SET-type

Scheme 53 Ni-catalyzed carboxylation of benzyl halides

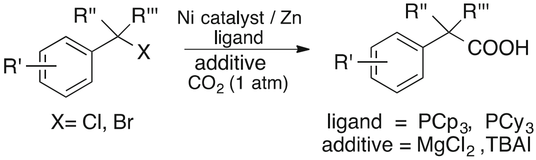

processes. Alternatively, reductive carboxylation of primary benzyl halides employing Pd catalysts and Mn as reductant was developed by He et al. [237]. Again, $MgCl_2$ was found to be essential for stabilizing Pd/benzylhalide adduct and thus CO_2 insertion.

The carboxylation of unactivated alkyl halides possessing β-hydrogens were also achieved by utilizing Ni precatalysts and bidentate nitrogen-containing ligands, particularly 1,10-phenanthroline backbones, together with Mn as reducing agent (Scheme 54) [238, 239]. Despite the reluctance to undergo oxidative addition and the proclivity of the in situ generated alkyl-Ni species towards destructive β-hydride elimination or homodimerization, the coupling between unactivated alkyl halides and CO_2 proceeded smoothly, delivering the corresponding carboxylic acids with excellent functional group compatibility as well as moderate to good yield. Interestingly, it was found that the inclusion of orthosubstituents adjacent to the nitrogen atom of the 1,10-phenanthroline backbone was critical for success. With a combination of *n*-butyl *N*-orthosubstituted 1,10-phenanthroline and additive *n*-Bu_4NBr (TBAB), nickel-catalyzed carboxylation of unactivated primary, secondary and even tertiary alkyl chlorides occurred with an exquisite chemoselectivity profile at atmospheric pressure of CO_2 (Scheme 54b). This methodology was further adapted in iterative cross-coupling scenarios of polyhalogenated backbones for its feasibility on promoting intermolecular cross electrophile coupling reactions (Scheme 54c).

Specifically, based on extensive studies and experimental finds, Rubén Martín reported a mild and user-friendly cascade reductive cyclization/carboxylation of unactivated alkyl halides with CO_2 route to elusive tetrasubstituted carboxylated olefins with five- or even six-membered ring substituents upon treatment with the well-developed Ni^{II}/1,10-phenanthroline/Mn system [240], in which CO_2 insertion took place at a distal reaction site rather than the initial site (Scheme 55). Alkyl halides possessing alkyne motifs at an appropriate position within an alkyl side-chain were converted to the desired tetrasubstituted vinyl carboxylic acid with excellent chemoselectivity and divergent *syn/anti* selectivity. The observed anti-selectivity might be attributed to a preferential recombination of the Ni^{I} center to the less steric side of the vinyl radical during SET-type processes, which was supported by indirect evidence that only a single *anti* carboxylic acid was obtained when upon exposure of iodo(2-methoxycyclopentylidene)methyl benzene (E:Z = 2:1) under the typical reaction conditions.

Very recently, Ni-catalyzed reductive carboxylation of secondary organic halides was developed [241] employing bromocyclopropane derivatives due to ring strain and sp2-like orbital rehybridization of cyclopropyl rings, which facilitated the carboxylation to some extent as aromatic rings did (Scheme 56). Interestingly,

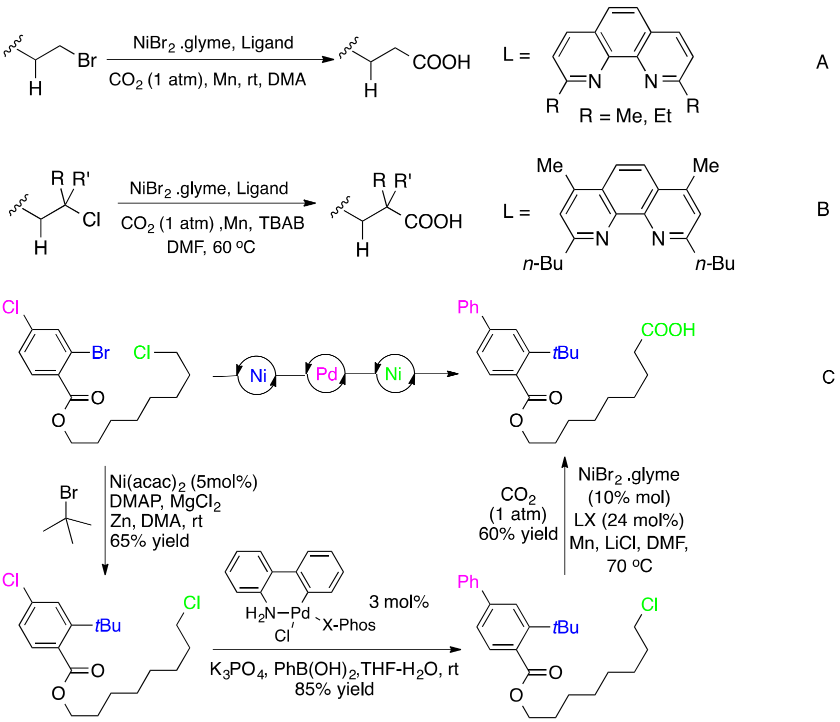

Scheme 54 Ni-catalyzed carboxylation of unactivated alkyl halides

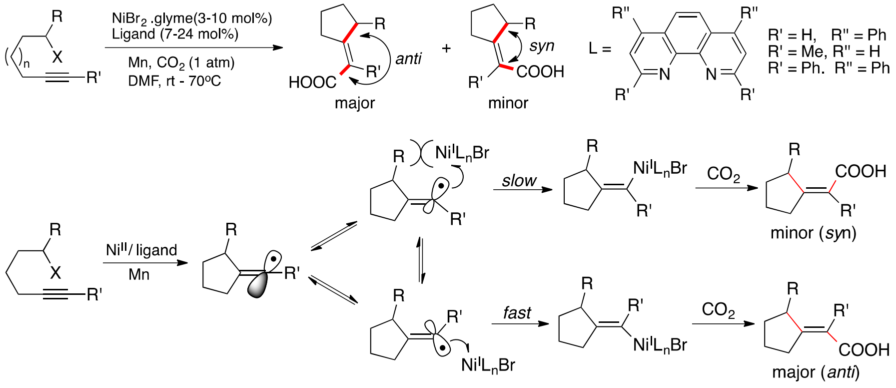

Scheme 55 Ni-catalyzed reductive cyclization/carboxylation of unactivated alkyl halides

cis/trans ratios were invariably observed for unsymmetrically substituted substrates, regardless whether diastereomerically pure *trans*- or *cis*-cyclopropyl bromides were utilized, thus suggesting the intermediacy of SET-processes via Ni(I) reaction intermediates. There was no competitive ring-opened products obtained through a radical intermediate was suggested as a key role played in catalytic cycle.

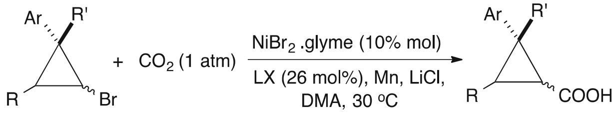

Scheme 56 Ni-catalyzed reductive carboxylation of bromocyclopropane

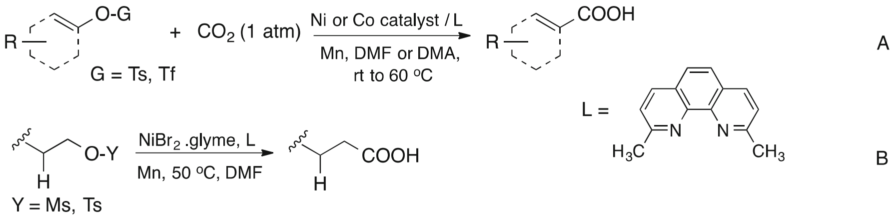

Scheme 57 Ni- or Co-catalyzed carboxylation of tosylates, triflates, and mesylates

Inspired by the success of cross-coupling reactions of organic halides with CO_2, simple C–O electrophiles have recently emerged as powerful alternatives to organic halides in cross-coupling reactions due to their low toxicity, ready availability and natural abundance of alcohols. The first example of a catalytic CO_2 insertion into C–O bonds was reported by Tsuji and Fujihara using aryl tosylates and triflates under similar conditions to those employed for the carboxylation of aryl chlorides with a system based on $NiCl_2(PPh_3)_2/Et_4NI$ and Mn as reductant (Scheme 57a) [234]. Later, Tsuji and Fujihara further extended the scope of these reactions by utilizing either Co^{II} or Ni^{II} catalysts (Scheme 57a) [242]. Alkenyl as well as sterically hindered aryl triflates was converted to the corresponding carboxylic acids smoothly via this approach. Analogously, by employing $NiBr_2(bpy)$ as catalyst in the absence of halogenated additives, a wide variety of electron-rich or electron-poor aryl tosylates including ortho-substituted substrates were found to be quite active to couple with CO_2 under moderate temperatures and atmospheric pressure [243]. Carboxylation of unactivated primary alkyl mesylates or tosylates were also achieved by Rubén Martín and coworkers under similar conditions as those utilized for the carboxylation of unactivated aryl bromides (Scheme 57b) [238].

The powerful Ni^{II}/Mn system was employed further for the efficient carboxylation of either aryl or benzyl ester derivatives via activation of traditionally considered inert C(sp2)- and C(sp3)-O bonds (Scheme 58) [244]. However, most C–O bond-cleavage remained limited to π-extended systems. This limitation could be partially overcome by the use of hemilabile directing groups on the ester motif.

In 2014, Tsuji and Fujihara described the cobalt-catalyzed carboxylation of propargyl acetates with CO_2 again using Mn as reducing agent (Scheme 59a). The incorporation of CO_2 into the C–O bond of various secondary or tertiary propargyl acetates with bulky substituent on the alkyne terminus proceeded smoothly, affording the corresponding carboxylic acids in good to high yields [245]. There is no allenyl carboxylic acid observed, which could be one of the main products in traditional Zn-mediated coupling of propargyl bromides with CO_2 [246]. In late 2014, Rubén Martín et al. reported on catalyst-controlled regiodivergent reductive

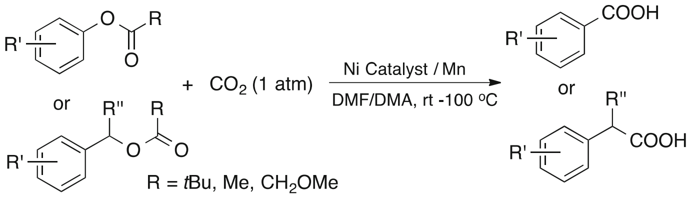

Scheme 58 Ni-catalyzed carboxylation of aryl and benzyl ester

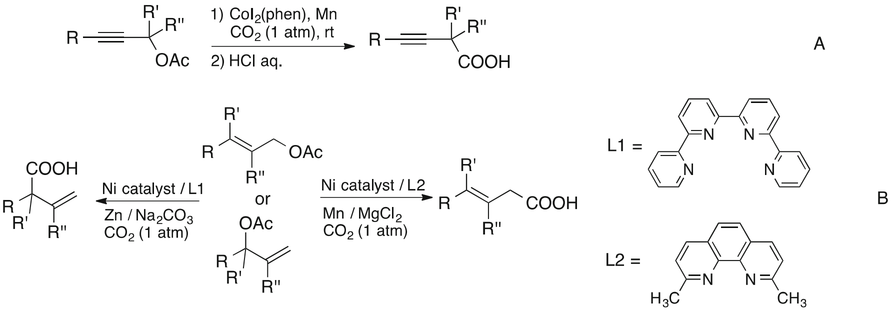

Scheme 59 Co- or Ni-catalyzed carboxylation of propargyl acetates and allyl acetates

carboxylation of allyl acetates, which was capable of introducing the carboxylic acid function selectively at either site of the allyl terminus (Scheme 59b) [247]. The ligand as well additives and reducing agent exerted non-negligible influence on reactivity and thus determination of the selectivity. Specifically, a protocol based on L2 with Mn/$MgCl_2$ resulted in linear carboxylic acids, whereas a selectivity switch was observed when operating with L1 and Zn/Na_2CO_3, obtaining α-branched carboxylic acids.

Recently, the group of Mita and Sato described the Pd-catalyzed carboxylation of allylic alcohols via formal activation of C–OH bonds using the classic Et_2Zn as reducing agent (Scheme 60a) [248]. In all cases analyzed, α-branched carboxylic acids were exclusively obtained regardless of whether linear or α-branched allyl alcohols were utilized. Very recently, Zhu and coworkers described the direct conversion of 4-hydroxybenzoic acid that derived from lignin-based vanillic acid and syringic acid to terephthalic acid by activation of phenolic C(sp2)-OH bond using PdNiOx supported on activated carbon as catalyst precursor in a fixed reactor (Scheme 60b) [249].

Additionally, a catalytic carboxylation of air-, thermally stable and highly crystalline ammonium salts via benzylic C(sp3)–N cleavage was developed in Rubén Martín's group [250] under almost the same conditions as those used for coupling of benzyl halides with CO_2 (Scheme 61). Various phenyl acetic acid derivatives were prepared with moderate to high yield including those possessing α-alkyl chains.

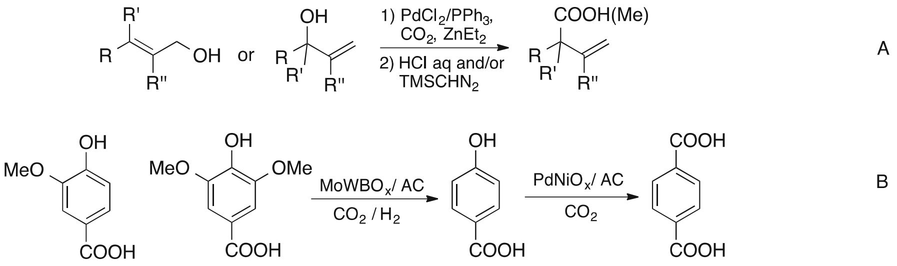

Scheme 60 Pd-catalyzed carboxylation of allylic alcohols and 4-hydroxybenzoic acid

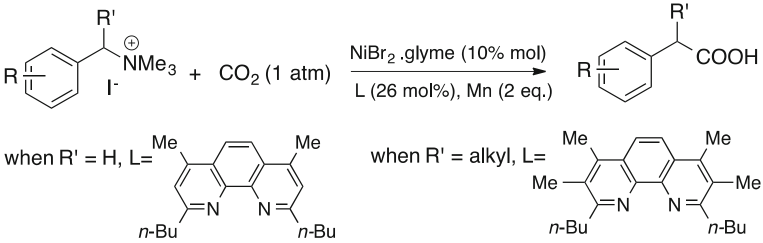

Scheme 61 Ni-catalyzed carboxylation of benzylic C–N bonds

5 Insertion of CO_2 into C–H Bond

The development of efficient catalytic systems for direct C–H bond functionalization is a long-desired goal of chemists because these protocols provide environmental friendly and waste-reducing alternatives to classical methodologies for C–C and C–heteroatom bond formation. During the past decade, remarkable progress in organometallic chemistry has set the stage for the development of increasingly viable metal catalysts for C–H bond activation reactions.

Undoubtedly, as one of the rapidly emerging areas for C–H bond functionalization, direct and catalytic carboxylation of saturated as well as aromatic, olefinic, and acetylenic hydrocarbons is of considerable interest to chemical researchers and remains a challenge to chemists.

5.1 Carboxylation of C(sp)–H Bonds

In noncatalytic processes, the direct carboxylation of terminal alkyne can be achieved by insertion of CO_2 into alkynyl–metal species [251], obtained by deprotonation of alkynes with strong bases such as alkali metal hydrides or organometallic reagents [252–255]. In these transformations, however, the benefit of using chemically inert CO_2 is more than offset by the requirement of using such energy-rich substrates. Recently, Zhang et al. reported on the carboxylations of particularly C–H acidic alkynes by only employing mild Cs_2CO_3 as the base under relatively forcing conditions (120 °C and 2.5 bar of CO_2) [256]. Using this method, after treatment with acid after the reaction, various propiolic acids were synthesized in good to excellent yields with a wide substrate scope (see Scheme 62).

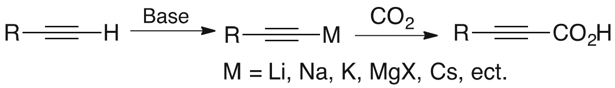

Scheme 62 Insertion of CO_2 into alkynyl–metal species

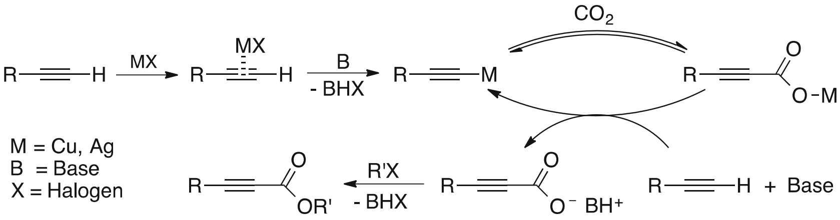

Scheme 63 Transition-metal-mediated carboxylation of phenylacetylene

In 1974, Saegusa et al. demonstrated the first transition-metal mediated carboxylation of phenylacetylene with CO_2 gas at atmospheric pressure in the presence of stoichiometric amounts of Cu(I) or Ag(I) salts (Scheme 63) [257]. Alkylation of the in situ intermediately formed Cu(I)- or Ag(I)-propiolate complexes with methyl iodide drove the carboxylation/decarboxylation equilibrium toward the desired products, giving the corresponding propiolic esters in moderate yield. In the absence of an alkylating agent, the Cu(I)-phenylpropiolate complexes extrude CO_2 readily at 35 °C with regeneration of copper phenylacetylide species.

About 20 years later, Inoue et al. reported the first example of catalytic carboxylation of terminal alkynes with C–H functionalization in the presence of copper or silver salts (Scheme 64) [258]. The Cu- or Ag- propiolates formed intermediately were once again removed from the equilibrium by in situ alkylation with 1-bromohexane. This way, various hexyl alkynyl esters with aliphatic and aromatic substituents were prepared in moderate to good yields. Recently, Lu et al. developed a new version of this transformation using (IPr)Cu^ICl as catalyst and K_2CO_3 as base [259]. They found that under an elevated CO_2 pressure of 15 bar, various propiolic esters were synthesized via coupling of terminal alkynes, CO_2 and allyl-, benzyl-, or similarly reactive organochlorides in good to excellent yields, and the (IPr)Cu^ICl catalyst could be easily recovered without any loss in activity. Similarly, Kondo et al. discovered that alkyl propiolic esters could be accessed at ambient CO_2 pressure utilizing a copper/phosphine catalyst system in the presence of Cs_2CO_3 and alkyl halides (R′-Br or R′-I) [260].

Building on the work of carboxylative esterification of terminal alkynes, a new approach was investigated [261] for the synthesis of arylnaphthalene lignan lactones that are valuable natural products with promising anticancer and antiviral properties. One-pot multicomponent coupling between phenylacetylene, carbon dioxide, and

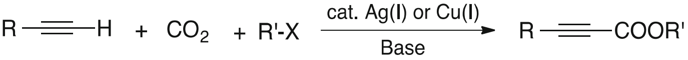

Scheme 64 Ag^I- or Cu^I-catalyzed carboxylative esterification of terminal alkynes

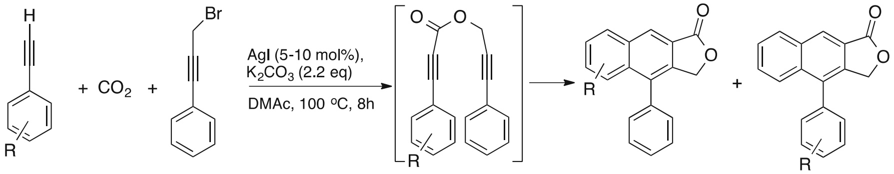

Scheme 65 Synthesis of arylnaphthalene lignan lactones via carboxylative esterification of terminal alkynes

$$R-\equiv-H + CO_2 \xrightarrow[Cs_2CO_3]{Cu(I)/\ phenanthroline} R-\equiv-COOH$$

Scheme 66 Preparation of propiolic acids by Cu^{I}-catalyzed carboxylation of terminal alkynes

3-bromo-1-phenyl-1-propyne afforded the corresponding 1,6-diyne in situ, which further underwent [2 + 2 + 2] cycloaddition, forming the naphthalene core efficiently (Scheme 65). This methodology could be used to generate a broad range of arylnaphthalene lactones and closely related analogues, both naturally occurring and otherwise, in a parallel or high-throughput fashion [262]. Via a similar 1,6-diyne propargyl propiolate intermediate, Müller and coworkers [263] developed a sequentially four-component copper-catalyzed alkyne carboxylation–propargylation-azide cycloaddition process furnishing 1,2,3-triazolylmethyl arylpropiolates, which could be further expanded to a five-component synthesis of 1,2,3-triazolylmethyl 3-amino arylacrylates by a concluding Michael addition in the same pot.

Following the principle of microscopic reversibility, Gooßen and coworkers found that copper(I)-phenanthroline systems, which are known for their high activity in catalytic decarboxylations, could also shift the carboxylation/decarboxylation equilibrium toward the carboxylated products at a lowered temperature [264]. By this way, for the first time, propiolic acids can thus be synthesized in excellent yields from alkynes and carbon dioxide in the presence of the mild base cesium carbonate (Scheme 66).

Soon later, Zhang et al. disclosed an alternative CuCl-TMEDA system for the carboxylation of terminal alkynes at room temperature and atmospheric CO_2 pressure in DMF [265]. However, electron-deficient aryl alkynes could not be converted using this method just as that happened in Gooßen's work. To overcome this limitation, Zhang et al. developed a CuCl-poly-NHC catalytic system with substantially improved activity, with which even (4-nitrophenyl)acetylene and similarly electron-deficient derivatives were carboxylated at room temperature and ambient CO_2 pressure (Scheme 67).

In continuation of the pioneering studies by Saegusa and Inoue, several research groups investigated the use of silver catalysts in carboxylation of terminal alkynes. In 2011, Lu and coworkers reported AgI salt catalyzed direct carboxylation of terminal alkynes under ligand-free conditions [266]. This catalytic system showed a substrate scope similar to the copper-based catalysts, although the yields were somewhat lower. Later, Gooßen and coworkers discovered that low loadings of silver(I)/DMSO

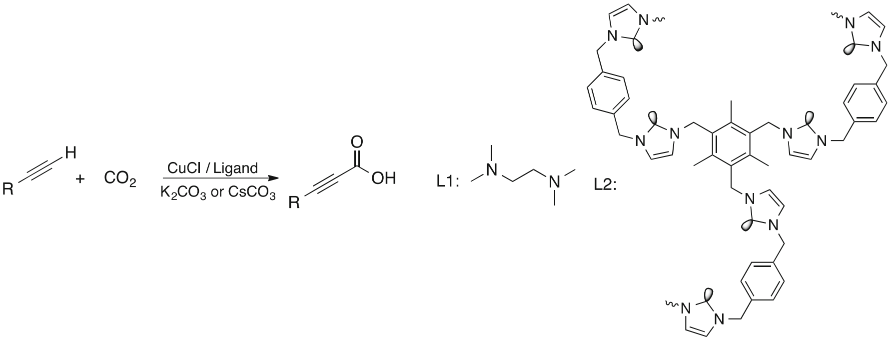

Scheme 67 Catalytic carboxylation of electron-deficient terminal alkynes using CuCl-poly-NHC

catalysts in ppm-quantities effectively promote the carboxylation of terminal alkynes at 50° C and ambient CO_2 pressure [267]. Almost simultaneously, Zhang et al. extended their Cu(I)-NHC approach to sliver catalysts, and prepared silver nanoparticles that deposited on the poly-NHC ligand material to facilitate the coupling reaction of terminal alkynes and CO_2 [268]. A high catalytic activity is reached that allows the conversion even of electron-deficient aryl-substituted alkynes. The key advantages of this approach are the recyclability of the heterogeneous catalyst and the negligible silver leaching. In all three cases, Cs_2CO_3 was once again critical for reaching high yields with low catalyst loadings (see Scheme 68).

Very recently, several new catalytic systems, such as ferrocenyl diphosphines Cu(I) complexes [269], bridged bis(amidate) rare-earth metal amides [270] and metal–organic framework MIL-101 supported bimetallic Pd–Cu Nanocrystals [271], were developed for efficient coupling of terminal alkynes and CO_2 at ambient pressure. It was also found that bifunctional silver tungstate salt (Ag_2WO_4) could activate alkyne with Ag^+ and CO_2 with WO_4^- synergistically [272], which allows the coupling reaction to perform smoothly at room temperature and under atmospheric pressure of CO_2 without extra addition of ligand (Scheme 69).

Some other aspects of this kind of carboxylation were also investigated. For example, it was found that ethylene carbonate could be used as superior solvent for carboxylation of terminal alkynes, since its ability to reduce the energy barrier for CO_2 insertion, which was revealed by DFT calculations [273]. The Cu^I salts could be incorporated into ionic liquid, which showed no loss of catalytic activity towards the carboxylative reaction [274]. Supercritical CO_2 was also employed as both a reactant and solvent in the reaction, giving the functionalized propiolic acids in excellent yields [275]. All of these investigations resulted in a more extended substrate scope and a better yield.

5.2 Carboxylation of C(sp2)–H Bonds

5.2.1 Friedel–Crafts Carboxylation of Aromatics

The most desirable route to the synthesis of arylcarboxylic acids would be the direct use of carbon dioxide via Friedel–Crafts chemistry. Friedel and Crafts themselves

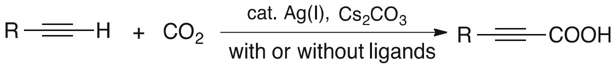

Scheme 68 Ag^I-catalyzed carboxylation of terminal alkynes

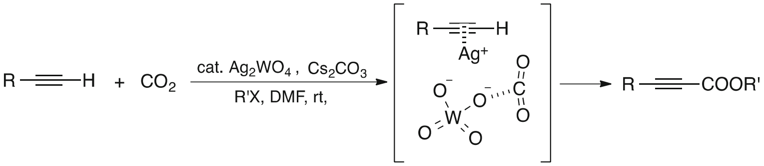

Scheme 69 Carboxylation of terminal alkynes catalyzed by bifunctional silver tungstate salt

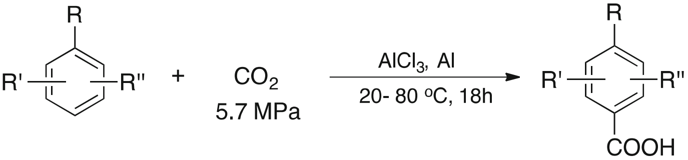

Scheme 70 Al_2Cl_6/Al promoted carboxylation of aromatic compounds

observed that a minor amount of benzoic acid was formed when carbon dioxide was bubbled through a mixture of aluminum chloride and benzene heated to the boiling point of the latter [276]. Many attempts to make this reaction practical had failed [277–282], and arylcarboxylic acids are generally obtained in poor yields because of the low electrophilicity of CO_2 and/or side reactions caused by the strong Lewis acidity of aluminum-based species which promoted the formation of secondary products such as benzophenones and diphenylmethanes in major amounts.

In 2002, the research group of Olah and Prakash reported the first efficient and chemoselective preparation of aromatic carboxylic acids with a carbon dioxide-Al_2Cl_6/Al system (Scheme 70) [283]. Aluminum served as a scavenger for the disturbing HCl liberated from the reaction to generate the high active $AlCl_3$ species in situ, which initiated the substitution further. Later, alkyl or arylsilyl chlorides were also found to be an efficient promoter for the Lewis acid AlBr3-mediated direct carboxylation of aromatics [284]. Using this method, alkylbenzenes as well as polycyclic arenes are carboxylated regioselectively with CO_2 of 3.0 Mpa at room temperature.

In 2010, Munshi and coworkers showed that Al_2Cl_6 can perform as a catalyst in Friedel–Crafts carboxylation of toluene with CO_2 under the combined influence of fluorinated solvent and base, forming *p*-toluic acid with a turnover number of 7.87, which may set a stage for further improvement in catalytic Friedel–Crafts carboxylation [285].

Friedel–Crafts carboxylation with CO_2 could also be applied to 1-substituted indoles and pyrroles. Dialkylaluminum chlorides instead of aluminum trihalides were employed as the CO_2-activator, with the aid of which, indole-3-carboxylic acids and pyrrole-2-carboxylic acids were prepared regioselectively in moderate to

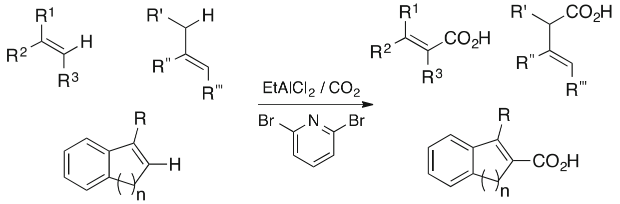

Scheme 71 EtAlCl$_2$ promoted carboxylation of α-arylalkenes and trialkyl-substituted alkenes

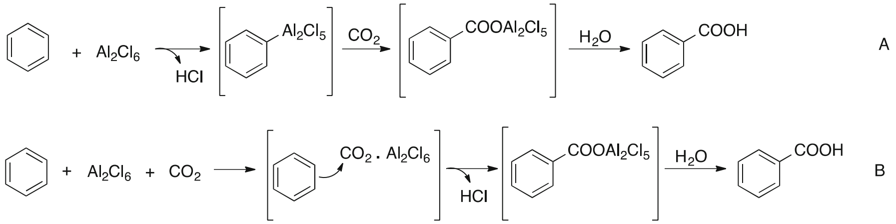

Scheme 72 Proposed mechanistic pathways for Friedel–Crafts carboxylation

good yield [286]. Furthermore, Lewis-acid EtAlCl$_2$ was found to be a good initiator for the carboxylation of α-arylalkenes and trialkyl-substituted alkenes with CO$_2$ by combined use of 2,6-dibromopyridine to afford α,β- and/or β/γ-unsaturated carboxylic acids through a Friedel–Crafts-like process (Scheme 71) [287].

On the basis of experimental findings, there are two most possible mechanistic pathways for Friedel–Crafts carboxylation (Scheme 72) [283]. One possible pathway involves an initial complex between benzene and Al$_2$Cl$_6$, with subsequent formation of organoaluminum intermediates, which was first suggested by Friedel and Crafts (Scheme 72a) [276]. The other proceeds through the formation of various complexes of CO$_2$ with aluminum chloride, followed by a typical electrophilic aromatic substitution (Scheme 72b). According to the experimental data and DFT theoretical calculations, the most feasible reaction mechanism proposed involves super electrophilic aluminum chloride-activated carbon dioxide reacting with the aromatics in a typical electrophilic substitution.

To learn more about the carboxylation of aromatics and to find optimized conditions, Olah and Prakash tested a wide range of solid and liquid Lewis and Brønsted acids and found that except for aluminum halides none of the other acids (TiCl$_4$, FeCl$_3$, FeBr$_3$, GaCl$_3$, Ga(OTf)$_3$, CF$_3$SO$_3$H, K-10, Nafion-H) were able to promote the effective carboxylation reaction. Interestingly, this limitation was partly overcome just by changing the addition order of reactants [288]. Incubation of Lewis acid and CO$_2$ for 1 h prior to the addition of toluene led carboxylation to occur with a few other Lewis acids other than Al$_2$Cl$_6$ in the usual way. Spectacularly, CuBr$_2$ produced *p*-toluic acid as major product when preincubated with CO$_2$, whereas bromotoluene is a major product when added with toluene and then pressurized with CO$_2$ at the same temperature and pressure. Later, a kinetic study involving stoichiometry, order of reaction, rate constants (*k*), and rate laws

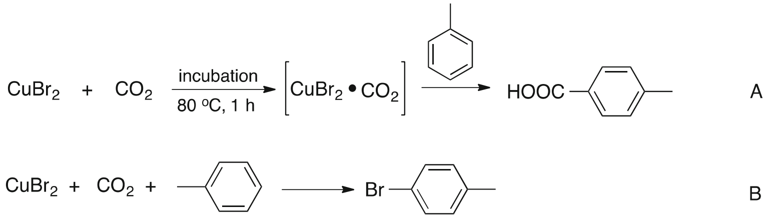

Scheme 73 Effect of incubation on the course of reaction showing an example for $CuBr_2$. **a** Incubation -> carboxylation; **b** no incubation -> bromination

performed on carboxylation of toluene by CO_2 further demonstrated that addition of $[CO_2{\cdot}Al_2Cl_6]$ complex generated from preincubation of CO_2 with Al_2Cl_6 for 1 h to toluene with subsequent elimination of $[H^+]$ was much faster than the typical Friedel–Crafts reaction [289] (see Scheme 73).

5.2.2 Kolbe-Schmidt Carboxylation of Phenols

The preparation of hydroxyl benzoic acid from carbon dioxide and alkali metal phenoxides is generally known as Kolbe-Schmidt synthesis [290, 291]. It is a subject of novel experimental [292–301] and theoretical investigations [302–307], by which hydroxyl benzoic acid was industrially produced as one of few chemicals from CO_2. It was observed that the yield of the reaction and distribution of products were highly dependent on the experimental conditions. It is interesting that sodium phenolate always leads to the formation of ortho-hydroxyl benzoic acid, i.e., salicylic acid (Scheme 74a), whereas potassium phenolate often results in the production of *para*-hydroxyl benzoic acid (Scheme 74b). Even though the mechanism is not quite clear, it is possible that sodium phenolate exists as contact ion pairs, of which sodium cation coordinates with one oxygen of CO_2 that prefers the formation of salicylic acid; in contrast, potassium phenolate forms dissociated ion pairs and thus attacks CO_2 through the *para*-position. Although in most cases this reaction is feasible only with highly electron-rich phenols, phenols with electron-withdrawing groups such as CF_3 could also undergo this reaction under certain conditions [292], and such a reaction even occurs for 3-hydroxy pyridine [293] (Scheme 74b) and hydroxyl-2(1H)-pyridinone [308].

Modification of the Kolbe-Schmitt process for the synthesis of *p*-aminosalicylic acid was also investigated [309–312], and the yields claimed in most instances are modest. Boric acid was found to be a proper promoter to increases the yield of PAS presumably by chelation and removal of the PAS formed in situ from the equilibrium, thus leading to a greater conversion of *m*-aminophenol to PAS [313].

5.2.3 Transition-Metal-Catalyzed Carboxylation of C(sp2)–H Bond

One of the first reports on the promoted or catalyzed conversion of CO_2 by insertion of sp2 C–H bond was published by Fujiwara and coworkers in 1984 [314]. Treatment of simple palladium^{II} salts with aromatic compounds led to activation of

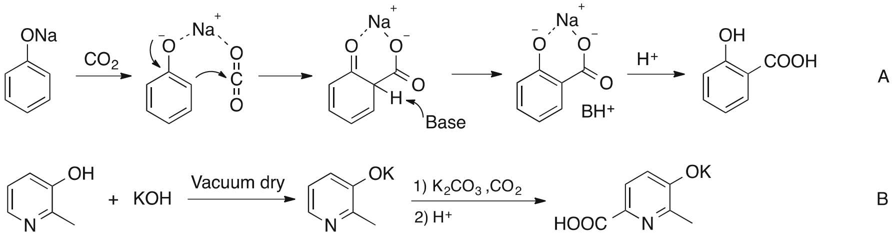

Scheme 74 Kolbe-Schmidt carboxylation of phenols

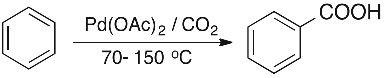

Scheme 75 Pd-catalyzed carboxylation of aromatic C(sp2)-H bond

the Ar–H bond to yield [Ar–Pd–H] species. Subsequent coupling with CO_2 at 1–30 bar gave aromatic carboxylic acids in yields between 2 and 66% (Scheme 75). However, the authors also observed, not unusual for palladium complexes, biphenyl self-cross coupling products in yields of up to 60%.

Since then, this area kept in silence for almost three decades until recently, in 2011, when Iwasawa et al. reported on a novel Rh(I)-catalyzed carboxylation of aromatic compounds directly via chelation-assisted *ortho* C–H bond activation (Scheme 76) [315]. Variously substituted and functionalized 2-arylpyridines and 1-arylpyrazoles underwent carboxylation in the presence of the rhodium catalyst and a stoichiometric methylating reagent, $AlMe_2$ (OMe), to give carboxylated products in good yields. Later, insertion of CO_2 into the C–H bond of simple arenes was also achieved using rhodium(I)-catalyst without the assistance of a directing group. Various arenes such as benzene, toluene, xylene, and other electron-rich or electron-deficient benzene derivatives, and heteroaromatics are directly carboxylated with high TONs [316]. However, despite the wide generality, the regioselectivity is not as high for this reaction, and a mixture of regioisomers was always obtained.

Very recently, Ma and coworkers applied the Rh(I)/phosphine/$AlMe_2$(OMe) catalytic system to the direct carboxylation of heterogeneous solid-state aryl C–H bonds of dcppy backbones that constructed UiO metal–organic framework (MOF) as organic linkers to generate free carboxylate groups for the first time (Scheme 77) [317].

For direct carboxylation of C–H acidic (hetero)arenes [318], Boogaerts and Nolan developed a novel approach [319] on the basis of the Gold(I)-mediated C–H activation [320, 321]. They discovered that gold complex [Au(IPr)OH] enabled efficient, direct carboxylation of (hetero)arenes at ambient temperature, provided that KOH is present as a stoichiometric base. Soon later, Hou and coworkers [322], as well as Cazin, Nolan, and coworkers [323] independently found that inexpensive copper NHC-copper complexes could serve as excellent catalysts for the direct carboxylation of aromatic heterocyclic C–H bonds with CO_2 (Scheme 78).

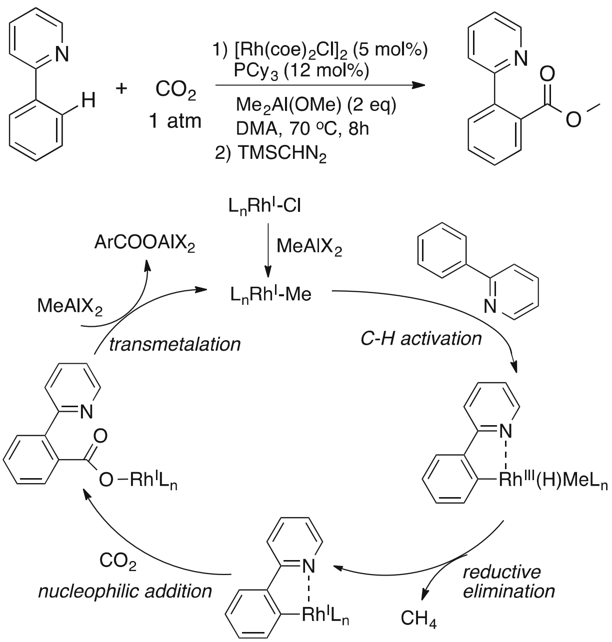

Scheme 76 Rh-catalyzed carboxylation of aromatic C(sp2)–H bond adjacent to a nitrogen-directing group

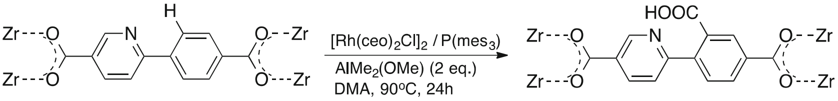

Scheme 77 Rh-catalyzed direct carboxylation of heterogeneous solid-state aryl C–H bond

Interestingly, both isolated complex [Cu(IPr)Cl] as well as the in situ-generated NHC/copper complexes proved to be viable catalytic system in the presence of a strong base, such as K*t*-OBu [324]. Key to the success was the remarkably high basicity of *N*-heterocyclic carbene (NHC) gold complex 1 (pK_{aDMSO} of 30.3) and NHC-copper complex 2 (pK_{aDMSO} of 27.7), which allowed the functionalization of heteroarenes and arenes bearing moderately acidic C–H bonds with pK_a values of less than 32.3 {with complex [Au(I*t*Bu)OH]} and less than 27.7. Later, a new kind of NHC-Cu catalyst (*tz*NHC-CuCl) using 1,2,3-triazol-5-ylidene as ligand was employed for the direct C–H carboxylation of benzoxazole and benzothiazole derivatives [325], which showed better catalytic efficiency than that of the [Cu(IPr)Cl] complex, giving the corresponding carboxylic esters after treatment with methyl iodide in high yields.

As the initial C–H activation proceeds through a simple protonolysis mechanism [326–329], simple base, such as LiO*t*Bu [330, 331], Cs_2CO_3 [332], could be used as an effective reagent for direct carboxylation of aromatic heterocycles such as

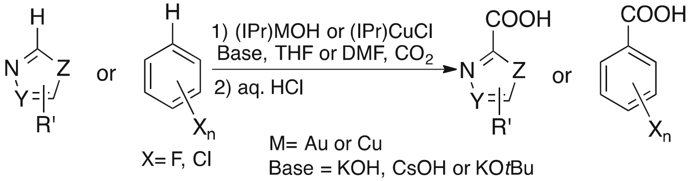

Scheme 78 Au^{I}- or Cu^{I}-catalyzed carboxylation of (hetero)arenes

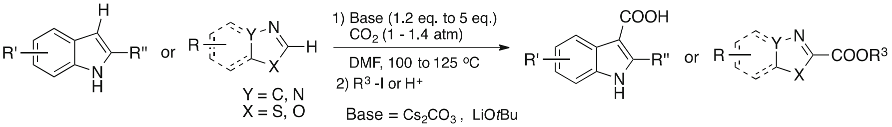

Scheme 79 Simple base-mediated direct carboxylation of aromatic heterocycles

indoles, oxazoles, thiazoles, and oxadiazoles without any transition-metal catalyst, though, under a little harsher conditions (Scheme 79).

5.3 Carboxylation of C(sp3)–H Bonds

Additional challenges are represented by direct carboxylation of less active Csp3–H bonds, as well as the employment of mild reaction conditions. An early and familiar example for a base-mediated insertion of CO_2 into C(sp3)–H bond was shown by the carboxylation of various acidic methylene compounds [333–336], such as ketones, fluorene, indene, acetonitrile derivatives, etc. Using this method, a sequential carboxylation/intramolecular cyclization reaction of *o*-alkynyl acetophenone with CO_2 was developed recently for the preparation of 1(3*H*)-isobenzofuranylidene acetic acids and esters in good yield and with high selectivity toward 5-exo oxygen cyclization at room temperature (Scheme 80) [337].

Recently, DBU as a mild base has attracted more attention in this area. Stoichiometric DBU was utilized as an efficient promoter for the synthesis of *β*-hydroxycarboxylic acids from ketones via carboxylation with CO_2 and sequential asymmetric hydrogenation (Scheme 81a) [338]. Interestingly, DBU could be immobilized on methylhydrosiloxane support and reacted with CO_2 to form a reversible CO_2 carrier (RCC), which could transfer the ketones to *β*-ketoester under ambient CO_2 pressure and temperature (Scheme 81b) [339]. This RCC is found to be recyclable and shows retention of activity in five recycles.

The carboxylation of acidic C(sp3)–H bonds of acetylacetone could also be realized using carbon dioxide at zinc sulfide with deposited ruthenium nanoparticles photo catalytically (Scheme 82). The reaction encompasses ruthenium-mediated one-electron reduction of CO_2 to $CO_2^{\cdot-}$ with electrons from the conduction band of ZnS and one-hole oxidation of acetylacetone to the relevant radical. Coupling of photo-generated radicals leads to the formation of carboxylic acids [340].

Besides the acidic C(sp3)–H bonds of ketones(acetylacetones), the direct carboxylation of active benzylic or allylic C–H bonds were also achieved. In

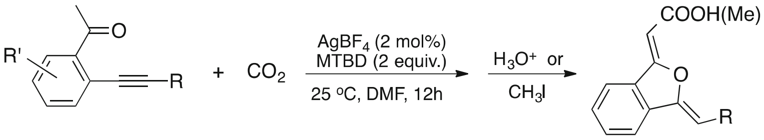

Scheme 80 Preparation of 1(3*H*)-isobenzofuranylidene acetic acids (esters) via sequential carboxylation/intramolecular cyclization

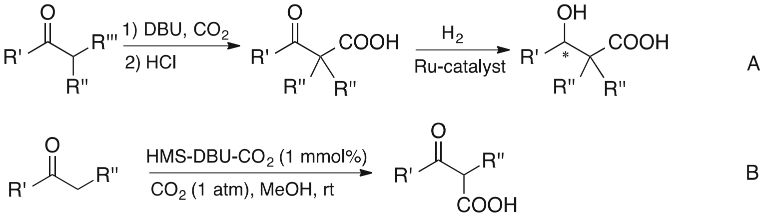

Scheme 81 DBU-mediated carboxylation of acidic C(sp3)–H bonds of ketones

Scheme 82 Photocatalytic carboxylation of acidic C(sp3)–H bonds of acetylacetone

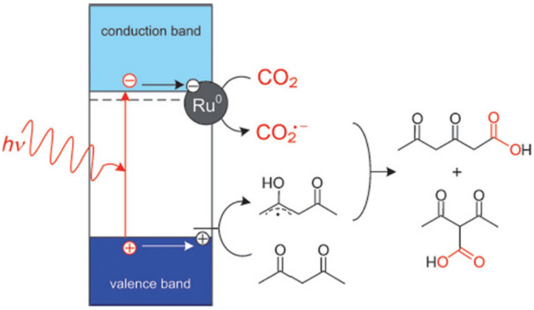

2012, Sato and coworkers developed a sequential protocol for insertion of CO_2 into the benzylic C(sp3)–H bond by combined operation of nitrogen-directed, Ru(0)- or Ir(I)- assisted, catalytic C–H silylation and fluoride-mediated desily-carboxylation (Scheme 83) [341]. The main drawback of this approach is that despite the high conversion efficiency of the C–H silylation, the undesired protodesilylation occurred in the next key step of desily-carboxylation, resulting in generation of a small amount of C(sp2)-silylated byproducts.

Later, light-driven carboxylation of *o*-alkylphenyl ketones was devised by Murakami and coworkers [342]. Photoirradiation of *o*-alkylphenyl ketones induces photoenolization to generate the highly reactive *o*-quinodimethanes, which was captured by CO_2 and underwent a [4 + 2] cycloaddition to afford the six-membered cycloadduct. Subsequent ring-opening gave the desired *o*-acylphenylacetic acids with moderate to good yield (Scheme 84a). Very recently, using a similar light/ketone/copper system, Murakami and coworkers developed a new method for photo-assisted direct carboxylation of allylic C(sp3)–H bond (Scheme 84b) [343]. The mechanism studies suggested that photo-excited ketone firstly grabbed an allylic hydrogen atom from a simple alkene, and then coupled with the resulting

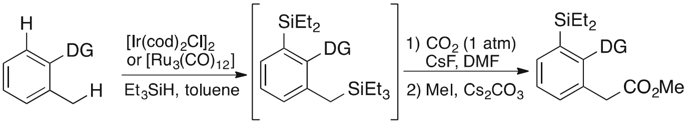

Scheme 83 Carboxylation of benzylic C–H bonds via sequential C–H silylation and fluoride-mediated desily-carboxylation

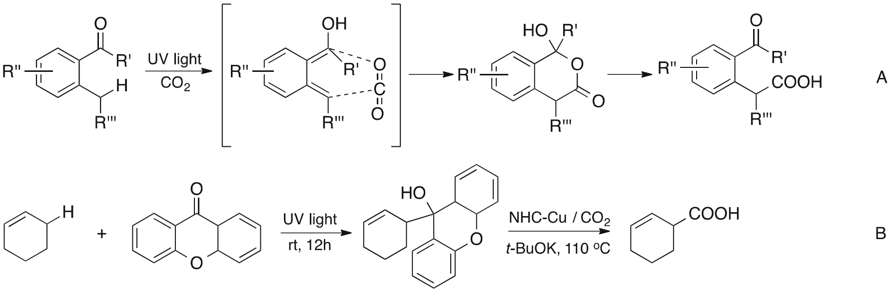

Scheme 84 Photo-assisted carboxylation of benzylic and allylic C(sp3)–H bonds

allylic radical species to form homoallyl alcohol intermediates, which underwent a NHC-copper catalyzed migration of allyl group upon treatment with CO_2.

6 Hydrogenation of Carbon Dioxide

The hydrogenation of carbon dioxide to formic acid by insertion of CO_2 into the metal–hydrogen bond of the catalyst is one of the best-studied catalytic reactions of CO_2 [16, 28, 38, 344–347]. The synthesis of formic acid by hydrogenation of CO_2 was first discovered by Farlow and Adkins in 1935 using Raney nickel as the catalyst [348]. The first homogeneously catalyzed example was reported by Inoue et al. [349]. To date, the most active homogeneous catalysts used so far for this reaction are complexes of rhodium [350–359], ruthenium [358–368], and iridium [358, 359, 367, 369–373], usually with halide(s) or hydride(s) as anionic ligands and phosphines, NHCs or pyridines as neutral ligands. In general, the production of formic acid is promoted by a base, such as triethylamine, KOH, NaOH, present in the reaction medium, which converts the acid into formate salts. The formation of formate salts improved the thermodynamics and drove the equilibrium towards the desired product side. The catalytic hydrogenation of CO_2 could be carried out in organic solvents, water or ionic liquids, or else directly in supercritical CO_2.

In 2009, Nozaki and coworkers [371] studied the catalytic activity of iridium hydride complexes bearing PNP pincer ligands towards the hydrogenation of CO_2 in aqueous media in the presence of KOH (Scheme 85). This water-soluble iridium complex exhibits both a remarkable TOF (73,000 h^{-1}) and TON (3,500,000) at 120 °C, which are the highest values for this reaction reported to date. Later, Hazari and coworkers established a simple model for predicting the thermodynamic

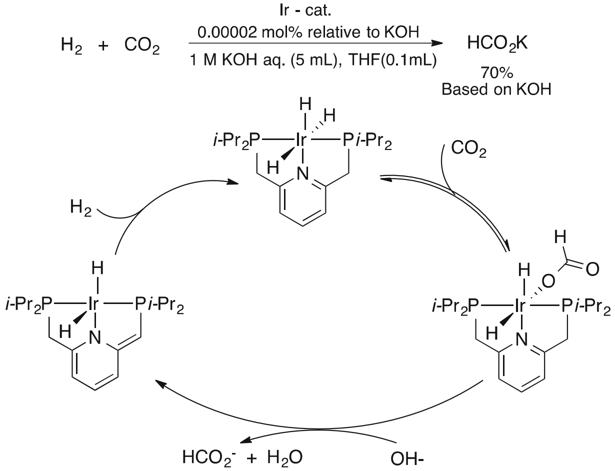

Scheme 85 Active iridium hydride complexes catalyzed hydrogenation of CO_2

favorability of CO_2 insertion into Ir^{III} hydrides, and developed a new Ir^{III} trihydride complex that has a basic structure similar to Nozaki's catalyst with an additional hydrogen bond donor in the secondary coordination sphere (Scheme 86). The CO_2-inserted Ir^{III} formate complex X is one of the most active water-soluble catalysts for CO_2 hydrogenation.

Recently, along with the classic Ru [374–378], Rh [376, 379], and Ir [380–386] catalysts, other transition–metal complexes [387–394] were also investigated for the synthesis of formic acid/formate from CO_2 and H_2, in particular the inexpensive iron [395–404] and copper [322, 405–407] complexes.

Remarkably, Marino and coworkers demonstrated that an artificial carbonic anhydrase enzyme in which the native zinc cation had been replaced with a Rh(I) could catalyze the conversion of CO_2 to HCOOH efficiently by direct hydrogenation (Scheme 87) [379].

In 2010, Beller and coworkers reported the first iron-catalyzed preparation of methyl formate from CO_2/H_2 in MeOH in the presence of amines (Scheme 88, left) [395]. Later, the same group developed a well-defined second-generation of iron catalysts for improved hydrogenation of carbon dioxide and bicarbonate (Scheme 88, right) [396]. The achieved turnover numbers are at least 1 order of magnitude higher in comparison with any previously reported iron system, which is comparable to the known Ru, Ir, and Rh systems.

Very recently, Christopher et al. demonstrated that copper(I) complex $LCu(MeCN)PF_6$ could be used as an active catalyst for CO_2 hydrogenation in the presence of a suitable base DBU (Scheme 89). Mechanism studies revealed that the relatively weak base DBU which could strongly coordinated to copper played important and unusual roles in pushing the catalytic cycle forward [406]. Coordination of the base to Cu^I is essential for promoting H_2 activation and displacing formate from the inactive formate complex, and most importantly, (re)generating the active hydride intermediate LCuH from the less active $[(LCu)_2H]^+$ [405].

Scheme 86 Design and synthesis of novel iridium hydride complexes for hydrogenation of CO_2

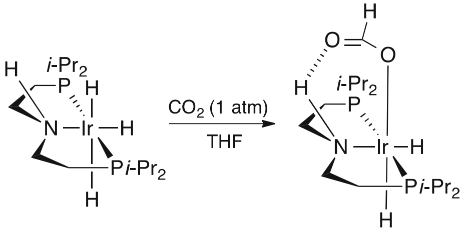

Scheme 87 Artificial carbonic anhydrase enzyme catalyzed conversion of CO_2 to HCOOH

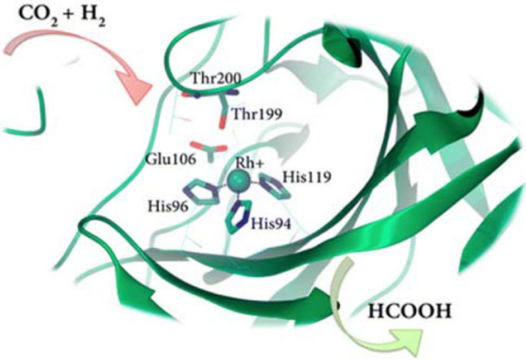

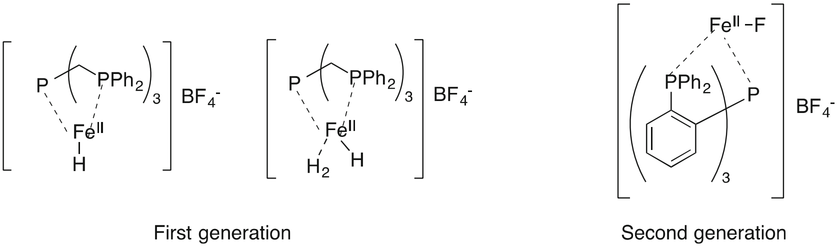

Scheme 88 Well-defined iron catalysts for CO_2 hydrogenation

Based on the wonderful works of transition metal-catalyzed CO_2 hydrogenation, a Ru–Rh bimetallic catalyst system was developed for the synthesis of acetic acid via methanol hydrocarboxylation with CO_2 and H_2 using imidazole as ligand and LiI as additive in 1,3-dimethyl-2-imidazolidinone (DMI) solvent (Scheme 90) [376]. The acetic acid can be generated in large amount at 180 °C and above, and the TON still exceeds 1000 after five cycles. The mechanism studies suggested that the ligand imidazole played a key role in stabilizing catalyst and improving catalytic activity due to its good coordination capability to the active metal center. It was also found that imidazole could suppress the reduction of CO_2 to CO, which led to a high selectivity of acetic acid production. The additive LiI was indispensable too in this transformation. Without LiI, the Ru–Rh complex was liable to decompose and no acetic acid was formed.

Scheme 89 CO_2 hydrogenation driven by Cu^I-DBU catalyst system

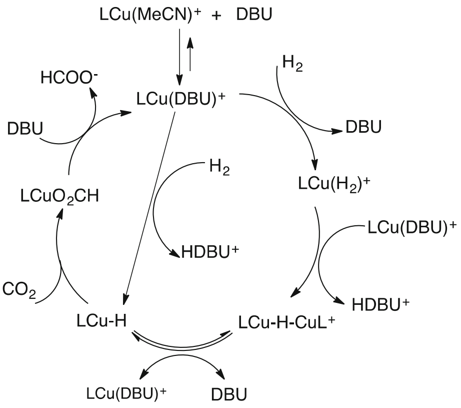

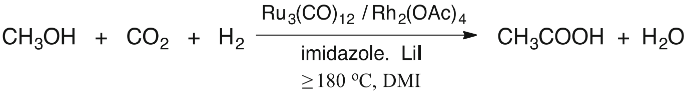

$$CH_3OH + CO_2 + H_2 \xrightarrow[\substack{\text{imidazole. LiI} \\ \geq 180\ ^{\circ}C,\ DMI}]{Ru_3(CO)_{12}\,/\,Rh_2(OAc)_4} CH_3COOH + H_2O$$

Scheme 90 Synthesis of acetic acid via methanol hydrocarboxylation on Ru–Rh bimetallic catalyst

Alternatively, apart from transition metal catalyst, intramolecular N/B frustrated Lewis pairs were employed as metal-free promoter for CO_2 hydrogenation (Scheme 91) [408]. Activation of H_2 on weakly Lewis acidic boron centers together with the concurrent interaction of NH and BH fragments with CO_2 facilitated the reaction between CO_2 and H_2, affording formate mainly as well as a small amount of acetal and methoxy derivatives.

7 Electrochemical Carboxylation

The electrochemical carboxylation of organic substrates with carbon dioxide is an interesting method of synthesis of carboxylic acids, which could be performed with or without transition-metal catalysts. By this approach, carboxylic groups are introduced into organic halides [409–420], alkenes [421–425], alkynes [426–432], vinyl triflates [433–435], ketones [436–438], etc. For example, electrocatalytic carboxylation of 2-amino-5-bromopyridine afforded the corresponding benzyl 6-aminonicotinic carboxylate in good yield after treatment with BnBr (Scheme 92a); [439] while pentafluoroethylarenes was transformed into 2-aryltetrafluoropropanoic acids under similar electrochemical conditions (Scheme 92b) [440]. Direct electrochemical carboxylation of electron-deficient benzyl alcohols was also realized [441], giving the corresponding phenylacetic acids in moderate yield together with a small amount of reductive byproducts, toluene derivatives (Scheme 92c). A similar electrochemical procedure was applied to the synthesis of biologically interesting flavanone-2-carboxylic acids with high regioselectivity and moderate to good yield (Scheme 92d) [442, 443].

Scheme 91 Intramolecular N/B frustrated Lewis pairs promoted CO_2 hydrogenation

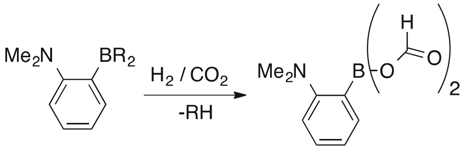

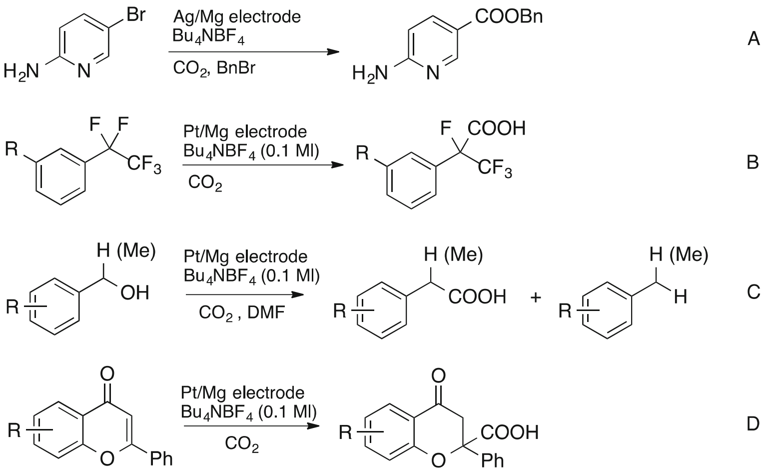

Scheme 92 Electrochemical fixation of CO_2

8 Biocatalytic Carboxylation

In parallel to recent advances in the chemical CO_2-fixation, enzymatic (biocatalytic) carboxylation is currently being investigated at an increased pace [40, 444, 445]. To date, four major pathways of biological CO_2-fixation are known: [446, 447].

1. Calvin–Benson–BasshaM–Cycle [448, 449],

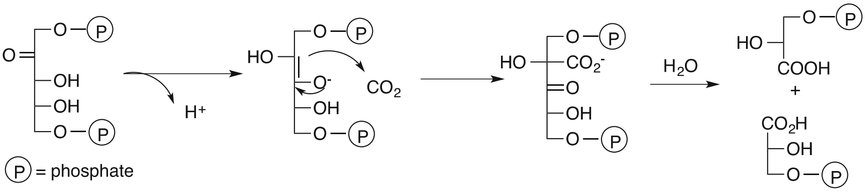

2. reductive TCA (Arnon–Buchanan) cycle [450],

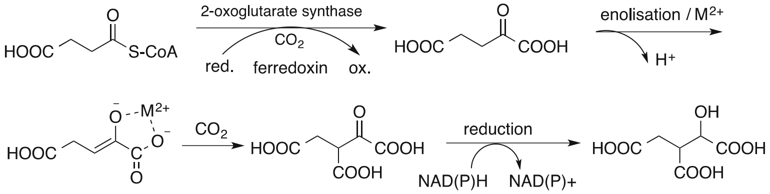

3. reductive Acetyl-CoA (Wood–Ljungdahl) pathway [451–453],

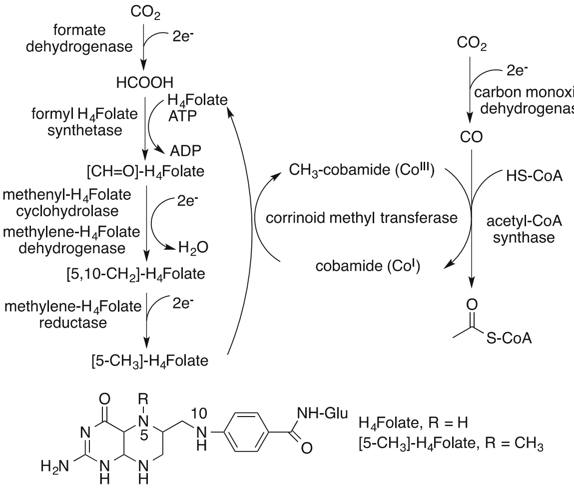

4. acyl-CoA carboxylase pathways: 3-hydroxypropionate/malonyl-CoA cycle [454, 455], 3-hydroxy-propionate/4-hydroxybutyrate cycle [456], dicarboxylate/4-hydroxybutyrate pathway [457], and the ethylmalonyl-CoA pathway [458].

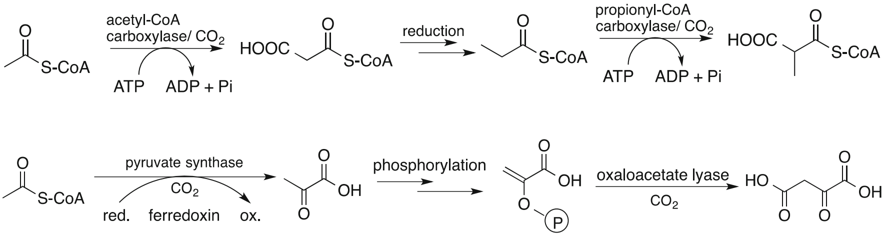

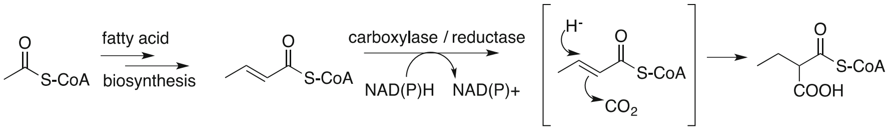

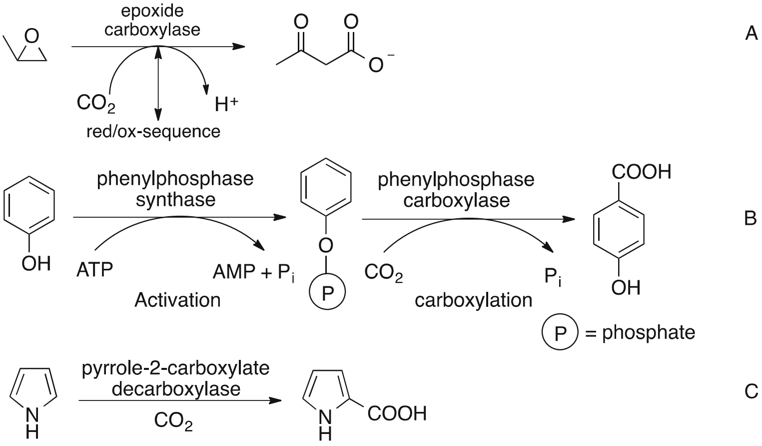

Scheme 93 Biocatalytic carboxylation of epoxides (**a**), phenol (**b**) and pyrrole (**c**)

However, due to the high substrate specificity of these biosynthetic pathways, it is unlikely that these pathways might be exploited to convert non-natural substrate surrogates.

On the other hand, several unspecific CO_2-fixation reactions occur in catabolic (biodegradation) pathways. Carboxylases or decarboxylases involved in biodegradation usually possess relaxed substrate specificities, which enable the regioselective carboxylation of various types of substrates, in particular epoxides (Scheme 93a) [459–461], phenolic compounds (Scheme 93b) [445, 462–468] or electron-rich heteroaromatics (Scheme 93c) [469–476]. In summary, it appears that the enzymatic fixation of CO_2 to produce well-defined carboxylic acids in a broadest sense seems feasible.

9 Conclusions and Outlook

In conclusion, the preparative aspects of using CO_2 in carboxylic acid and ester synthesis as C1 source undoubtedly represent a key strategy for the development of greener chemical processes. In recent years, substantial advances in the field of CO_2-based carboxylic acid (ester) preparation, have allowed the use of relatively less-reactive coupling partners, such as unactivated organic (pseudo)halides, (hetero)aromatics, and allylic/benzylic compounds. These methods are distinguished by their wide scope and functional group tolerance and therefore may importantly emerge as competitive and convenient protocols for the synthesis of carboxylic acid derivatives.

Despite the recent advances realized, the use of superstoichiometric amounts of reducing agents is still a remaining issue. In this regard, more environmentally benign reducing agents or the implementation of photocatalytic techniques using clean solar energy would be a considerable step-forward. Additionally, although some progress had been made in direct carboxylation of C–H bonds, the means to functionalization of unactivated C(sp3)-H with CO_2 is still rare. Moreover, catalytic asymmetric carboxylation of organic compounds for the synthesis of enantioenriched carboxylic acids is virtually absent in the literature. In this regard, development of elegant catalyst systems with robustness and long-term stability, which could exhibit high selectivity in bond-breaking and bond-forming transformations would be the key matter in this area. Alternatively, biotechnologies would provide highly specific biosynthetic pathways for CO_2-fixation and carboxylic acid production. Overall, It is certainly speculated that a continued growth and impressive advances in this promising area of research have yet to come.

References

1. Patai S (1992) The chemistry of acid derivatives. Wiley, New York
2. Gooßen LJ, Rodríguez N, Gooßen K (2008) Angew Chem Int Ed 47:3100–3120
3. Maag H (2007) Prodrugs of carboxylic acids. Springer, USA
4. Bew SP (2005) In comprehensive organic functional groups transformation II. Elsevier, Oxford
5. Franklin AS (1998) J Chem Soc Perkin Trans 1:2451–2466
6. Sakakura T, Choi J-C, Yasuda H (2007) Chem Rev 107:2365–2387
7. Aresta M, Dibenedetto A (2007) Dalton Trans 2975–2992
8. Mikkelsen M, Jorgensen M, Krebs FC (2010) Energy Environ Sci 3:43–81
9. Riduan SN, Zhang Y (2010) Dalton Trans 39:3347–3357
10. Zhang W, Lü X (2012) Chin J Catal 33:745–756
11. Cai X, Xie B (2013) Synthesis 45:3305–3324
12. Dibenedetto A, Angelini A, Stufano P (2013) J Chem Technol Biotechnol 89:334–353
13. Maeda C, Miyazaki Y, Ema T (2014) Catal Sci Technol 4:1482–1497
14. Liu A-H, Yu B, He L-N (2015) Greenh Gas Sci Technol 5:17–33
15. Saptal VB, Bhanage BM (2016) Chem Sus Chem 9:1980–1985
16. Boddien A, Gärtner F, Federsel C, Piras I, Junge H, Jackstell R, Beller M, Laurenczy G, Shi M (2012) Organic chemistry—breakthroughs and perspectives. Wiley, Weinheim, pp 685–724
17. Aresta M, Dibenedetto A, Angelini A (2014) Chem Rev 114:1709–1742
18. Zhang Y, Riduan SN (2011) Angew Chem Int Ed 50:6210–6212
19. North M (2009) Angew Chem Int Ed 48:4104–4105
20. Yu B, Diao ZF, Guo CX, He LN (2013) J CO_2 Util 1, 60–68
21. Mori M (2007) Eur J Org Chem 2007:4981–4993
22. Wang Z (2010) Comprehensive organic name reactions and reagents. Wiley, Weinheim
23. Gibson DH (1999) Coord Chem Rev 185–186:335–355
24. Correa A, Martín R (2009) Angew Chem Int Ed 48:6201–6204
25. Manjolinho F, Arndt M, Gooßen K, Gooßen LJ (2012) ACS Catal 2:2014–2021
26. Tsuji Y, Fujihara T (2012) Chem Commun 48:9956–9964
27. Louie J (2005) Curr Org Chem 9:605–623
28. Cokoja M, Bruckmeier C, Rieger B, Herrmann WA, Kühn FE (2011) Angew Chem Int Ed 50:8510–8537
29. Huang K, Sun C-L, Shi Z-J (2011) Chem Soc Rev 40:2435–2452

30. Martín R, Kleij AW (2011) ChemSusChem 4:1259–1263
31. Wang S, Du G, Xi C (2016) Org Biomol Chem 14:3666–3676
32. Omae I (2012) Coord Chem Rev 256:1384–1405
33. Zhang L, Hou Z (2013) Chem Sci 4:3395–3403
34. Iwao O (2016) Curr Org Chem 20:953–962
35. Mori M, Takimoto M (2005) Modern organonickel chemistry. Wiley, Weinheim, pp 205–223
36. Pinaka A, Vougioukalakis GC (2015) Coord Chem Rev 288:69–97
37. Börjesson M, Moragas T, Gallego D, Martin R (2016) ACS Catal 6:6739–6749
38. Wang W-H, Himeda Y, Muckerman JT, Manbeck GF, Fujita E (2015) Chem Rev 115:12936–12973
39. Glueck SM, Gümüs ATS, On leave from Middle East Technical University, Fabian WMF, Faber K (2009) Chem Soc Rev 39, 313–328
40. Shi J, Jiang Y, Jiang Z, Wang X, Wang X, Zhang S, Han P, Yang C (2015) Chem Soc Rev 44:5981–6000
41. Lapidus AL, Pirozhkov SD, Koryakin AA (1978) Russ Chem Bull 27:2513–2515
42. Hoberg H, Peres Y, Krüger C, Tsay Y-H (1987) Angew Chem Int Ed Engl 26:771–773
43. Hoberg H, Schaefer D (1983) J Organomet Chem 251:c51–c53
44. Yamashita K, Chatani N (2005) Synlett 2005:0919–0922
45. Hoberg H, Ballesteros A, Sigan A, Jegat C, Milchereit A (1991) Synthesis 1991:395–398
46. Hoberg H, Schaefer D (1982) J Organomet Chem 236:C28–C30
47. Hoberg H, Schaefer D, Burkhart G, Krüger C, Romao MJ (1984) J Organomet Chem 266:203–224
48. Williams CM, Johnson JB, Rovis T (2008) J Am Chem Soc 130:14936–14937
49. Hoberg H, Jenni K, Angermund K, Krüger C (1987) Angew Chem Int Ed Engl 26:153–155
50. Greenhalgh MD, Thomas SP (2012) J Am Chem Soc 134:11900–11903
51. Shirakawa E, Ikeda D, Masui S, Yoshida M, Hayashi T (2012) J Am Chem Soc 134:272–279
52. Graham DC, Mitchell C, Bruce MI, Metha GF, Bowie JH, Buntine MA (2007) Organometallics 26:6784–6792
53. Alvarez R, Carmona E, Cole-Hamilton DJ, Galindo A, Gutierrez-Puebla E, Monge A, Poveda ML, Ruiz C (1985) J Am Chem Soc 107:5529–5531
54. Galindo A, Pastor A, Perez PJ, Carmona E (1993) Organometallics 12:4443–4451
55. Bernskoetter WH, Tyler BT (2011) Organometallics 30:520–527
56. Fischer R, Langer J, Malassa A, Walther D, Gorls H, Vaughan G (2006) Chem Commun 2510–2512
57. Schubert G, Pápai I (2003) J Am Chem Soc 125:14847–14858
58. Pápai I, Schubert G, Mayer I, Besenyei G, Aresta M (2004) Organometallics 23:5252–5259
59. Aresta M, Pastore C, Giannoccaro P, Kovács G, Dibenedetto A, Pápai I (2007) Chem A Eur J 13:9028–9034
60. Bruckmeier C, Lehenmeier MW, Reichardt R, Vagin S, Rieger B (2010) Organometallics 29:2199–2202
61. Lee SYT, Cokoja M, Drees M, Li Y, Mink J, Herrmann WA, Kühn FE (2011) ChemSusChem 4:1275–1279
62. Lejkowski ML, Lindner R, Kageyama T, Bódizs GÉ, Plessow PN, Müller IB, Schäfer A, Rominger F, Hofmann P, Futter C, Schunk SA, Limbach M (2012) Chem Euro J 18:14017–14025
63. Huguet N, Jevtovikj I, Gordillo A, Lejkowski ML, Lindner R, Bru M, Khalimon AY, Rominger F, Schunk SA, Hofmann P, Limbach M (2014) Chem Euro J 20:16858–16862
64. Manzini S, Huguet N, Trapp O, Schaub T (2015) Eur J Org Chem 2015:7122–7130
65. Hendriksen C, Pidko EA, Yang G, Schäffner B, Vogt D (2014) Chem Euro J 20:12037–12040
66. Hoberg H, Schaefer D (1983) J Organomet Chem 255:C15–C17
67. Hoberg H, Schaefer D, Oster BW (1984) J Organomet Chem 266:313–320
68. Walther D, Dinjus E, Görls H, Sieler J, Lindqvist O, Andersen L (1985) J Organomet Chem 286:103–114
69. Hoberg H, Apotecher B (1984) J Organomet Chem 270:c15–c17
70. Hoberg H, Peres Y, Milchereit A, Gross S (1988) J Organomet Chem 345:C17–C19
71. Hoberg H, Bärhausen D (1989) J Organomet Chem 379:C7–C11
72. Hoberg H, Gross S, Milchereit A (1987) Angew Chem Int Ed Engl 26:571–572
73. Jolly PW, Stobbe S, Wilke G, Goddard R, Krüger C, Sekutowski JC, Tsay Y-H (1978) Angew Chem Int Ed Engl 17:124–125
74. Behr A, Kanne U (1986) J Organomet Chem 317:C41–C44
75. Langer J, Walther D, Görls H (2006) J Organomet Chem 691:4874–4881
76. Sato Y, Takanashi T, Mori M (1999) Organometallics 18:4891–4893

77. Takimoto M, Mori M (2001) J Am Chem Soc 123:2895–2896
78. Takimoto M, Mori M (2002) J Am Chem Soc 124:10008–10009
79. Takimoto M, Nakamura Y, Kimura K, Mori M (2004) J Am Chem Soc 126:5956–5957
80. Hoberg H, Jenni K, Krüger C, Raabe E (1986) Angew Chem Int Ed Engl 25:810–811
81. Hoberg H, Jenni K (1987) J Organomet Chem 322:193–201
82. Sasaki Y, Inoue Y, Hashimoto H (1976) J Chem Soc Chem Commun 605–606
83. Inoue Y, Sasaki Y, Hashimoto H (1978) Bull Chem Soc Jpn 51:2375–2378
84. Musco A (1980) J Chem Soc Perkin Trans 1:693–698
85. Musco A, Perego C, Tartiari V (1978) Inorg Chim Acta 28:L147–L148
86. Behr A, Juszak KD, Keim W (1983) Synthesis 1983:574
87. Behr A, Juszak K-D (1983) J Organomet Chem 255:263–268
88. Dinjus E, Leitner W (1995) Appl Organomet Chem 9:43–50
89. Braunstein P, Matt D, Nobel D (1988) J Am Chem Soc 110:3207–3212
90. Behr A, He R, Juszak K-D, Krüger C, Tsay Y-H (1986) Chem Ber 119:991–1015
91. Behr A, Becker M, Beckmann T, Johnen L, Leschinski J, Reyer S (2009) Angew Chem Int Ed 48:3598–3614
92. Behr A, Henze G (2011) Green Chem 13:25–39
93. Behr A, Bahke P, Klinger B, Becker M (2007) J Mol Catal A: Chem 267:149–156
94. Behr A, He R (1984) J Organomet Chem 276:c69–c72
95. Döhring A, Jolly PW (1980) Tetrahedron Lett 21:3021–3024
96. Aresta M, Quaranta E, Ciccarese A (1985) C1 Mol Chem 1:283–284
97. Tsuda T, Yamamoto T, Saegusa T (1992) J Organomet Chem 429:C46–C48
98. Hoberg H, Oster BW (1984) J Organomet Chem 266:321–326
99. Aoki M, Kaneko M, Izumi S, Ukai K, Iwasawa N (2004) Chem Commun 2568–2569
100. Takimoto M, Kawamura M, Mori M (2003) Org Lett 5:2599–2601
101. Takimoto M, Kawamura M, Mori M (2004) Synthesis 2004:791–795
102. Takimoto M, Kawamura M, Mori M, Sato Y (2005) Synlett 2005:2019–2022
103. Takaya J, Iwasawa N (2008) J Am Chem Soc 130:15254–15255
104. Suh H-W, Guard LM, Hazari N (2014) Chem Sci 5:3859–3872
105. Saito N, Sun Z, Sato Y (2015) Chem Asian J 10:1170–1176
106. Gholap SS, Takimoto M, Hou Z (2016) Chem Euro J 22:8547–8552
107. Inoue Y, Itoh Y, Hashimoto H (1977) Chem Lett 6:855–856
108. Inoue Y, Itoh Y, Hashimoto H (1978) Chem Lett 7:633–634
109. Inoue Y, Itoh Y, Kazama H, Hashimoto H (1980) Bull Chem Soc Jpn 53:3329–3333
110. Albano P, Aresta M (1980) J Organomet Chem 190:243–246
111. Hoberg H, Schaefer D (1982) J Organomet Chem 238:383–387
112. Hoberg H, Schaefer D, Burkhart G (1982) J Organomet Chem 228:C21–C24
113. Burkhart G, Hoberg H (1982) Angew Chem Int Ed Engl 21:76
114. Walther D, Bräunlich G, Kempe R, Sieler J (1992) J Organomet Chem 436:109–119
115. Walther D, Schönberg H, Dinjus E, Sieler J (1987) J Organomet Chem 334:377–388
116. Graham DC, Bruce MI, Metha GF, Bowie JH, Buntine MA (2008) J Organomet Chem 693:2703–2710
117. Langer J, Gärtner M, Görls H, Walther D (2006) Synthesis 2006:2697–2706
118. Tsuda T, Sumiya R, Saegusa T (1987) Synth Commun 17:147–154
119. Tsuda T, Morikawa S, Sumiya R, Saegusa T (1988) J Org Chem 53:3140–3145
120. Tsuda T, Morikawa S, Hasegawa N, Saegusa T (1990) J Org Chem 55:2978–2981
121. Louie J, Gibby JE, Farnworth MV, Tekavec TN (2002) J Am Chem Soc 124:15188–15189
122. Tekavec TN, Arif AM, Louie J (2004) Tetrahedron 60:7431–7437
123. Takimoto M, Mizuno T, Mori M, Sato Y (2006) Tetrahedron 62:7589–7597
124. Takimoto M, Mizuno T, Sato Y, Mori M (2005) Tetrahedron Lett 46:5173–5176
125. Saito S, Nakagawa S, Koizumi T, Hirayama K, Yamamoto Y (1999) J Org Chem 64:3975–3978
126. Six Y (2003) Eur J Org Chem 2003:1157–1171
127. Takimoto M, Shimizu K, Mori M (2001) Org Lett 3:3345–3347
128. Shimizu K, Takimoto M, Mori M (2003) Org Lett 5:2323–2325
129. Shimizu K, Takimoto M, Sato Y, Mori M (2005) Org Lett 7:195–197
130. Shimizu K, Takimoto M, Mori M, Sato Y (2006) Synlett 2006:3182–3184
131. Li S, Yuan W, Ma S (2011) Angew Chem Int Ed 50:2578–2582
132. Li S, Ma S (2012) Chem Asian J 7:2411–2418

133. Fujihara T, Xu T, Semba K, Terao J, Tsuji Y (2011) Angew Chem Int Ed 50:523–527
134. Takimoto M, Hou Z (2013) Chem Euro J 19:11439–11445
135. Takimoto M, Gholap SS, Hou Z (2015) Chem Euro J 21:15218–15223
136. Fujihara T, Horimoto Y, Mizoe T, Sayyed FB, Tani Y, Terao J, Sakaki S, Tsuji Y (2014) Org Lett 16:4960–4963
137. Li S, Ma S (2012) Adv Synth Catal 354:2387–2394
138. Inamoto K, Asano N, Nakamura Y, Yonemoto M, Kondo Y (2012) Org Lett 14:2622–2625
139. Fujihara T, Tani Y, Semba K, Terao J, Tsuji Y (2012) Angew Chem Int Ed 51:11487–11490
140. Zhang L, Cheng J, Carry B, Hou Z (2012) J Am Chem Soc 134:14314–14317
141. Fleming I, Newton TW, Roessler F (1981) J Chem Soc Perkin Trans 1:2527–2532
142. Fleming I, Roessler F (1980) J Chem Soc Chem Commun 276–277
143. Gilman H, Kirby RH (1925) Org Synth 5:75
144. Marvel CS, Blomquist AT, Vaughn LE (1928) J Am Chem Soc 50:2810–2812
145. Bowen DM (1941) Org Synth 21:77
146. Carey FA, Sundberg RJ (2007) Advanced organic chemistry, 5th edn. Springer, New York, pp 619–667
147. Yanagisawa A, Yasue K, Yamamoto H (1992) Synlett 1992:593–594
148. Eaton PE, Lee CH, Xiong Y (1989) J Am Chem Soc 111:8016–8018
149. Zhang M-X, Eaton PE (2002) Angew Chem Int Ed 41:2169–2171
150. Eaton PE, Lukin KA (1993) J Am Chem Soc 115:11370–11375
151. Eaton PE, Zhang M-X, Komiya N, Yang C-G, Steele I, Gilardi R (2003) Synlett 2003:1275–1278
152. Venkatraman S, Tweedie S, McLaws M, Lathbury D (2014) Managing Hazardous reactions and compounds in process chemistry, vol 1181. American Chemical Society, USA, pp 441–453
153. Tanoury GJ, Chen M, Dong Y, Forslund R, Jurkauskas V, Jones AD, Belmont D (2014) Org Process Res Dev 18:1234–1244
154. Nagaki A, Takahashi Y, Yoshida J-I (2014) Chem Euro J 20:7931–7934
155. Schlosser M (2007) Synlett 2007:3096–3102
156. Hickey MR, Allwein SP, Nelson TD, Kress MH, Sudah OS, Moment AJ, Rodgers SD, Kaba M, Fernandez P (2005) Org Process Res Dev 9:764–767
157. Kobayashi K, Nagaoka T, Shirai Y, Miyatani W, Yokoi Y, Konishi H (2012) Helv Chim Acta 95:191–196
158. Ziegler K, Krupp F, Weyer K, Larbig W, Liebigs J (1960) Ann Chem 629:251–256
159. Zweifel G, Steele RB (1967) J Am Chem Soc 89:2754–2755
160. Zweifel G, Steele RB (1967) J Am Chem Soc 89:5085–5086
161. Eisch JJ, Foxton MW (1968) J Organomet Chem 11:P7–P8
162. Ueno A, Takimoto M, Nishiura M, Ikariya T, Hou Z (2015) Chem Asian J 10:1010–1016
163. Ukai K, Aoki M, Takaya J, Iwasawa N (2006) J Am Chem Soc 128:8706–8707
164. Ohishi T, Nishiura M, Hou Z (2008) Angew Chem Int Ed 47:5792–5795
165. Takaya J, Tadami S, Ukai K, Iwasawa N (2008) Org Lett 10:2697–2700
166. Dang L, Lin Z, Marder TB (2010) Organometallics 29:917–927
167. Zhang X, Zhang W-Z, Shi L-L, Guo C-X, Zhang L-L, Lu X-B (2012) Chem Commun 48:6292–6294
168. Wang W, Zhang G, Lang R, Xia C, Li F (2013) Green Chem 15:635–640
169. Riss PJ, Lu S, Telu S, Aigbirhio FI, Pike VW (2012) Angew Chem Int Ed 51:2698–2702
170. Wu J, Hazari N (2011) Chem Commun 47:1069–1071
171. Hazari N, Hruszkewycz DP, Wu J (2011) Synlett 2011:1793–1797
172. Hruszkewycz DP, Wu J, Hazari N, Incarvito CD (2011) J Am Chem Soc 133:3280–3283
173. Hruszkewycz DP, Wu J, Green JC, Hazari N, Schmeier TJ (2012) Organometallics 31:470–485
174. Wu J, Green JC, Hazari N, Hruszkewycz DP, Incarvito CD, Schmeier TJ (2010) Organometallics 29:6369–6376
175. Duong HA, Huleatt PB, Tan Q-W, Shuying EL (2013) Org Lett 15:4034–4037
176. Ohishi T, Zhang L, Nishiura M, Hou Z (2011) Angew Chem Int Ed 50:8114–8117
177. Ohmiya H, Tanabe M, Sawamura M (2011) Org Lett 13:1086–1088
178. Shi M, Nicholas KM (1997) J Am Chem Soc 119:5057–5058
179. Johansson R, Wendt OF (2007) Dalton Trans 488–492
180. Franks RJ, Nicholas KM (2000) Organometallics 19:1458–1460
181. Feng X, Sun A, Zhang S, Yu X, Bao M (2013) Org Lett 15:108–111
182. Mita T, Sugawara M, Hasegawa H, Sato Y (2012) J Org Chem 77:2159–2168

183. Mita T, Chen J, Sugawara M, Sato Y (2011) Angew Chem Int Ed 50:1393–1396
184. Mita T, Higuchi Y, Sato Y (2011) Org Lett 13:2354–2357
185. Xu B, Arndtsen BA (2014) ACS Catal 4:843–846
186. Hattori T, Suzuki Y, Miyano S (2003) Chem Lett 32:454–455
187. Mita T, Tanaka H, Michigami K, Sato Y (2014) Synlett 25:1291–1294
188. Sekine K, Sadamitsu Y, Yamada T (2015) Org Lett 17:5706–5709
189. Mita T, Higuchi Y, Sato Y (2014) Org Lett 16:14–17
190. Mita T, Sugawara M, Saito K, Sato Y (2014) Org Lett 16:3028–3031
191. Mita T, Sugawara M, Sato Y (2016) J Org Chem 81:5236–5243
192. Yeung CS, Dong VM (2008) J Am Chem Soc 130:7826–7827
193. Ochiai H, Jang M, Hirano K, Yorimitsu H, Oshima K (2008) Org Lett 10:2681–2683
194. Aresta M, Nobile CF, Albano VG, Forni E, Manassero M (1975) J Chem Soc Chem Commun 636–637
195. Kobayashi K, Kondo Y (2009) Org Lett 11:2035–2037
196. Metzger A, Bernhardt S, Manolikakes G, Knochel P (2010) Angew Chem Int Ed 49:4665–4668
197. Bernhardt S, Metzger A, Knochel P (2010) Synthesis 2010:3802–3810
198. Palmer DA, Van Eldik R (1983) Chem Rev 83:651–731
199. Braunstein P, Matt D, Nobel D (1988) Chem Rev 88:747–764
200. Gibson DH (1996) Chem Rev 96:2063–2096
201. Leitner W (1996) Coord Chem Rev 153:257–284
202. Walther D (1987) Coord Chem Rev 79:135–174
203. Yin X, Moss JR (1999) Coord Chem Rev 181:27–59
204. LeBlanc FA, Berkefeld A, Piers WE, Parvez M (2012) Organometallics 31:810–818
205. Zucchini U, Albizzati E, Giannini U (1971) J Organomet Chem 26:357–372
206. Wang S, Shao P, Chen C, Xi C (2015) Org Lett 17:5112–5115
207. Lau K-C, Petro BJ, Bontemps S, Jordan RF (2013) Organometallics 32:6895–6898
208. Hill M, Wendt OF (2005) Organometallics 24:5772–5775
209. Kloppenburg L, Petersen JL (1996) Organometallics 15:7–9
210. Osakada K, Sato R, Yamamoto T (1994) Organometallics 13:4645–4647
211. Schmeier TJ, Hazari N, Incarvito CD, Raskatov JA (2011) Chem Commun 47:1824–1826
212. Schmeier TJ, Nova A, Hazari N, Maseras F (2012) Chem Euro J 18:6915–6927
213. Jonasson KJ, Wendt OF (2014) Chem Euro J 20:11894–11902
214. Lau KC, Jordan RF (2016) Organometallics 35:3658–3666
215. Mankad NP, Gray TG, Laitar DS, Sadighi JP (2004) Organometallics 23:1191–1193
216. Ebert GW, Juda WL, Kosakowski RH, Ma B, Dong L, Cummings KE, Phelps MVB, Mostafa AE, Luo J (2005) J Org Chem 70:4314–4317
217. Miyasuta A, Yamamoto A (1976) J Organomet Chem 113:187–199
218. Marsich N, Camus A, Nardin G (1982) J Organomet Chem 239:429–437
219. Ikariya T, Yamamoto A (1974) J Organomet Chem 72:145–151
220. Darensbourg DJ, Grotsch G (1985) J Am Chem Soc 107:7473–7476
221. Darensbourg DJ, Hanckel RK, Bauch CG, Pala M, Simmons D, White JN (1985) J Am Chem Soc 107:7463–7473
222. Johnson MT, Johansson R, Kondrashov MV, Steyl G, Ahlquist MSG, Roodt A, Wendt OF (2010) Organometallics 29:3521–3529
223. Johnson MT, Wendt OF (2014) J Organomet Chem 751:213–220
224. Johansson R, Jarenmark M, Wendt OF (2005) Organometallics 24:4500–4502
225. English AD, Herskovitz T (1977) J Am Chem Soc 99:1648–1649
226. Allen OR, Dalgarno SJ, Field LD, Jensen P, Willis AC (2009) Organometallics 28:2385–2390
227. Darensbourg DJ, Kyran SJ, Yeung AD, Bengali AA (2013) Eur J Inorg Chem 2013:4024–4031
228. Janes T, Osten KM, Pantaleo A, Yan E, Yang Y, Song D (2016) Chem Commun 52:4148–4151
229. Darensbourg DJ, Groetsch G, Wiegreffe P, Rheingold AL (1987) Inorg Chem 26:3827–3830
230. Hartwig JF, Bergman RG, Andersen RA (1991) J Am Chem Soc 113:6499–6508
231. Ostapowicz TG, Hölscher M, Leitner W (2011) Chem Euro J 17:10329–10338
232. Correa A, Martín R (2009) J Am Chem Soc 131:15974–15975
233. Tran-Vu H, Daugulis O (2013) ACS Catal 3:2417–2420
234. Fujihara T, Nogi K, Xu T, Terao J, Tsuji Y (2012) J Am Chem Soc 134:9106–9109
235. León T, Correa A, Martin R (2013) J Am Chem Soc 135:1221–1224
236. Sayyed FB, Sakaki S (2014) Chem Commun 50:13026–13029

237. Zhang S, Chen W-Q, Yu A, He L-N (2015) ChemCatChem 7:3972–3977
238. Liu Y, Cornella J, Martin R (2014) J Am Chem Soc 136:11212–11215
239. Börjesson M, Moragas T, Martin R (2016) J Am Chem Soc 138:7504–7507
240. Wang X, Liu Y, Martin R (2015) J Am Chem Soc 137:6476–6479
241. Moragas T, Martin R (2016) Synthesis 48:2816–2822
242. Nogi K, Fujihara T, Terao J, Tsuji Y (2014) J Org Chem 80:11618–11623
243. Rebih F, Andreini M, Moncomble A, Harrison-Marchand A, Maddaluno J, Durandetti M (2016) Chem Euro J 22:3758–3763
244. Correa A, León T, Martin R (2014) J Am Chem Soc 136:1062–1069
245. Nogi K, Fujihara T, Terao J, Tsuji Y (2014) Chem Commun 50:13052–13055
246. Miao B, Li G, Ma S (2015) Chem Euro J 21:17224–17228
247. Moragas T, Cornella J, Martin R (2014) J Am Chem Soc 136:17702–17705
248. Mita T, Higuchi Y, Sato Y (2015) Chem Euro J 21:16391–16394
249. Bai Z, Phuan WC, Ding J, Heng TH, Luo J, Zhu Y (2016) ACS Catal 6:6141–6145
250. Moragas T, Gaydou M, Martin R (2016) Angew Chem Int Ed 55:5053–5057
251. Brandsma L (1988) Studies in organic chemistry: preparative acetylenic chemistry, vol 34. Elsevier, Amsterdam, pp 97–111
252. Braga AL, Comasseto JV, Petragnani N (1984) Synthesis 1984:240–243
253. Yokoo K, Kijima Y, Fujiwara Y, Taniguchi H (1984) Chem Lett 13:1321–1322
254. Oppolzer W, Siles S, Snowden RL, Bakker BH, Petrzilka M (1985) Tetrahedron 41:3497–3509
255. Wang Y, Zhang W-X, Wang Z, Xi Z (2011) Angew Chem Int Ed 50:8122–8126
256. Dingyi Y, Yugen Z (2011) Green Chem 13:1275–1279
257. Tsuda T, Ueda K, Saegusa T (1974) J Chem Soc Chem Commun 380–381
258. Fukue Y, Oi S, Inoue Y (1994) J Chem Soc Chem Commun 2091–2091
259. Zhang W-Z, Li W-J, Zhang X, Zhou H, Lu X-B (2010) Org Lett 12:4748–4751
260. Inamoto K, Asano N, Kobayashi K, Yonemoto M, Kondo Y (2012) Org Biomol Chem 10:1514–1516
261. Eghbali N, Eddy J, Anastas PT (2008) J Org Chem 73:6932–6935
262. Foley P, Eghbali N, Anastas PT (2010) J Nat Prod 73:811–813
263. Schreiner E, Wilcke T, Müller TJJ (2016) Synlett 27:379–382
264. Gooßen LJ, Rodríguez N, Manjolinho F, Lange PP (2010) Adv Synth Catal 352:2913–2917
265. Yu D, Zhang Y (2010) Proc Natl Acad Sci 107:20184–20189
266. Zhang X, Zhang W-Z, Ren X, Zhang L-L, Lu X-B (2011) Org Lett 13:2402–2405
267. Arndt M, Risto E, Krause T, Gooßen LJ (2012) ChemCatChem 4:484–487
268. Yu D, Tan MX, Zhang Y (2012) Adv Synth Catal 354:969–974
269. Trivedi M, Singh G, Kumar A, Rath NP (2015) Dalton Trans 44:20874–20882
270. Cheng H, Zhao B, Yao Y, Lu C (2015) Green Chem 17:1675–1682
271. Trivedi M, Kumar A, Singh G, Kumar A, Rath NP (2016) New J Chem 40:3109–3118
272. Guo C-X, Yu B, Xie J-N, He L-N (2015) Green Chem 17:474–479
273. Yu B, Diao Z-F, Guo C-X, Zhong C-L, He L-N, Zhao Y-N, Song Q-W, Liu A-H, Wang J-Q (2013) Green Chem 15:2401–2407
274. Xie J-N, Yu B, Zhou Z-H, Fu H-C, Wang N, He L-N (2015) Tetrahedron Lett 56:7059–7062
275. Li F-W, Suo Q-L, Hong H-L, Zhu N, Wang Y-Q, Han L-M (2014) Tetrahedron Lett 55:3878–3880
276. Friedel C, Crafts JM (1878) Compt. Rend. 86:1368
277. Norris JF, Wood JE (1940) J Am Chem Soc 62:1428–1432
278. Fumasoni S, Collepardi M (1964) Ann Chim 54:1122
279. Ito T, Sugahara N, Kindaichi Y, Takami Y (1976) Nippon Kagaku Kaishi 353–355
280. Lebedev BL, Pastukhova IV, Éidus YT (1972) Russ Chem Bull 21:929–931
281. Kinney CR, Ward OW (1933) J Am Chem Soc 55:3796–3798
282. Suzuki Y, Hattori T, Okuzawa T, Miyano S (2002) Chem Lett 31:102–103
283. Olah GA, Török B, Joschek JP, Bucsi I, Esteves PM, Rasul G, Surya GK (2002) Prakash. J Am Chem Soc 124:11379–11391
284. Nemoto K, Yoshida H, Egusa N, Morohashi N, Hattori T (2010) J Org Chem 75:7855–7862
285. Munshi P, Beckman EJ, Padmanabhan S (2010) Ind Eng Chem Res 49:6678–6682
286. Nemoto K, Onozawa S, Egusa N, Morohashi N, Hattori T (2009) Tetrahedron Lett 50:4512–4514
287. Tanaka S, Watanabe K, Tanaka Y, Hattori T (2016) Org Lett 18:2576–2579
288. Munshi P, Beckman EJ (2008) Ind Eng Chem Res 48:1059–1062
289. Sarve AN, Ganeshpure PA, Munshi P (2012) Ind Eng Chem Res 51:5174–5180

290. Kolbe H (1860) Ann 113:125
291. Schmidt R (1885) J Prakt Chem 31:397
292. Hauptschein M, Nodiff EA, Saggiomo AJ (1051) J Am Chem Soc 1954:76
293. Rapoport H, Volcheck EJ (1956) J Am Chem Soc 78:2451
294. Meek WH, Fuchsman CH (1969) J Chem Eng Data 14:388–391
295. Gu M, Cheng Z (2014) Ind Eng Chem Res 53:9992–9998
296. Wuensch C, Gross J, Steinkellner G, Lyskowski A, Gruber K, Glueck SM, Faber K (2014) RSC Adv 4:9673–9679
297. Wang Y, Gevorgyan V (2015) Angew Chem 127:2283–2287
298. Krtschil U, Hessel V, Kost HJ, Reinhard D (2013) Chem Eng Technol 36:1010–1016
299. Luo J, Preciado S, Xie P, Larrosa I (2016) Chem Euro J 22:6798–6802
300. Rahim MA, Matsui Y, Matsuyama T, Kosugi Y (2003) Bull Chem Soc Jpn 76:2191–2195
301. Sclafani A, Palmisano L, Farneti G (1997) Chem Commun 529–530
302. Hales JL, Jones JI, Lindsey AS (1954) J Chem Soc 3145–3151
303. Marković Z, Marković S, Manojlović N, Predojević-Simović J (2007) J Chem Inf Model 47:1520–1525
304. Marković Z, Marković S (2008) J Chem Inf Model 48:143–147
305. Kosugi Y, Imaoka Y, Gotoh F, Rahim MA, Matsui Y, Sakanishi K (2003) Org Biomol Chem 1:817–821
306. Markovic S, Markovic Z, Begovic N, Manojlovic N (2007) Russ J Phys Chem A 81:1392–1397
307. Stanescu I, Gupta RR, Achenie LEK (2006) Mol Simul 32:279–290
308. Gorden AEV, Xu JD, Raymond KN, Durbin P (2003) Chem Rev 103:4207
309. Sheehan JT (1948) J Am Chem Soc 70:1665
310. Erlenmeyer H, Prijs B, Sorkin E, Suter E (1948) Heh Chinz Acta 31:988
311. Drain DJ, Martin DD, Mitchell BW, Seymour DE, Spring FS (1949) J Chem Soc 1489–1503
312. Wesseley F, Benedict K, Benger H (1948) Monatsh 79:185
313. Doub L, Schaefer JA, Stevenson OL, Walker CT, Vandenbelt JM (1958) J Org Chem 23:1422–1424
314. Sugimoto H, Kawata I, Taniguchi H, Fujiwara Y (1984) J Organomet Chem 266:c44–c46
315. Mizuno H, Takaya J, Iwasawa N (2010) J Am Chem Soc 133:1251–1253
316. Suga T, Mizuno H, Takaya J, Iwasawa N (2014) Chem Commun 50:14360–14363
317. Gao W-Y, Wu H, Leng K, Sun Y, Ma S (2016) Angew Chem Int Ed 55:5472–5476
318. Ackermann L (2011) Angew Chem Int Ed 50:3842–3844
319. Boogaerts IIF, Nolan SP (2010) J Am Chem Soc 132:8858–8859
320. Gaillard S, Slawin AMZ, Nolan SP (2010) Chem Commun 46:2742–2744
321. Lu P, Boorman TC, Slawin AMZ, Larrosa I (2010) J Am Chem Soc 132:5580–5581
322. Zhang L, Cheng J, Ohishi T, Hou Z (2010) Angew Chem Int Ed 49:8670–8673
323. Boogaerts IIF, Fortman GC, Furst MRL, Cazin CSJ, Nolan SP (2010) Angew Chem 122:8856–8859
324. Zhang L, Cheng J, Ohishi T, Hou Z (2010) Angew Chem 122:8852–8855
325. Inomata H, Ogata K, Fukuzawa SI, Hou Z (2013) Org Lett 14:3986–3989
326. Sun ZM, Zhang J, Manan RS, Zhao P (2010) J Am Chem Soc 132:6935–6937
327. Meier SK, Young KJH, Ess DH, Tenn WJ, Oxgaard J, Goddard WA, Periana RA (2009) Organometallics 28:5293–5304
328. Bercaw JE, Hazari N, Labinger JA, Oblad PF (2008) Angew Chem 120:10089–10091
329. Cundari TR, Grimes TV, Gunnoe TB (2007) J Am Chem Soc 129:13172–13182
330. Yoo WJ, Capdevila MG, Du X, Kobayashi S (2012) Org Lett 14:5326–5329
331. Fenner S, Ackermann L (2016) Green Chem 18:3804–3807
332. Vechorkin O, Hirt N, Hu X (2010) Org Lett 12:3567–3569
333. Haruki E, Arakawa M, Matsumura N, Otsuji Y, Imoto E (1974) Chem Lett 3:427–428
334. Chiba K, Tagaya H, Miura S, Karasu M (1992) Chem Lett 21:923–926
335. Chiba K, Tagaya H, Karasu M, Ishizuka M, Sugo T (1994) Bull Chem Soc Jpn 67:452–454
336. Abe H, Inoue S (1994) J Chem Soc Chem Commun 1197–1198
337. Zhang W-Z, Shi L-L, Liu C, Yang X-T, Wang Y-B, Luo Y, Lu X-B (2014) Org Chem Front 1:275–283
338. Flowers BJ, Gautreau-Service R, Jessop PG (2008) Adv Synth Catal 350:2947–2958
339. Beckman EJ, Munshi P (2011) Green Chem 13:376–383
340. Baran T, Dibenedetto A, Aresta M, Kruczała K, Macyk W (2014) ChemPlusChem 79:708–715
341. Mita T, Michigami K, Sato Y (2012) Org Lett 14:3462–3465
342. Masuda Y, Ishida N, Murakami M (2015) J Am Chem Soc 137:14063–14066

343. Ishida N, Masuda Y, Uemoto S, Murakami M (2016) Chem Euro J 22:6524–6527
344. Jessop PG, Joó F, Tai CC (2004) Coord Chem Rev 248:2425–2442
345. Leitner W (1995) Angew Chem Int Ed Engl 34:2207–2221
346. Jessop PG, Ikariya T, Noyori R (1995) Chem Rev 95:259–272
347. Klankermayer J, Wesselbaum S, Beydoun K, Leitner W (2016) Angew Chem Int Ed 55:7296–7343
348. Farlow MW, Adkins H (1935) J Am Chem Soc 57:2222–2223
349. Inoue Y, Izumida H, Sasaki Y, Hashimoto H (1976) Chem Lett 5:863–864
350. Burgemeister T, Kastner F, Leitner W (1993) Angew Chem Int Ed Engl 32:739–741
351. Leitner W, Dinjus E, Gaßner F (1994) J Organomet Chem 475:257–266
352. Graf E, Leitner W (1992) J Chem Soc Chem Commun 623–624
353. Tsai JC, Nicholas KM (1992) J Am Chem Soc 114:5117–5124
354. Fornika R, Gorls H, Seemann B, Leitner W (1995) J Chem Soc Chem Commun 1479–1481
355. Angermund K, Baumann W, Dinjus E, Fornika R, Görls H, Kessler M, Krüger C, Leitner W, Lutz F (1997) Chem Euro J 3:755–764
356. Gassner F, Leitner W (1993) J Chem Soc Chem Commun 1465–1466
357. Joo F, Joo F, Nadasdi L, Elek J, Laurenczy G, Nadasdi L (1999) Chem Commun 971–972
358. Himeda Y, Onozawa-Komatsuzaki N, Sugihara H, Arakawa H, Kasuga K (2004) Organometallics 23:1480–1483
359. Kröcher O, Köppel RA, Fröba M, Baiker A (1998) J Catal 178:284–298
360. Lau CP, Chen YZ (1995) J Mol Catal A: Chem 101:33–36
361. Jessop PG, Hsiao Y, Ikariya T, Noyori R (1996) J Am Chem Soc 118:344–355
362. Munshi P, Main AD, Linehan JC, Tai C-C, Jessop PG (2002) J Am Chem Soc 124:7963–7971
363. Jessop PG, Ikariya T, Noyori R (1994) Nature 368:231–233
364. Kovács G, Schubert G, Joó F, Pápai I (2006) Catal Today 115:53–60
365. Elek J, Nádasdi L, Papp G, Laurenczy G, Joó F (2003) Appl Catal A 255:59–67
366. Federsel C, Jackstell R, Boddien A, Laurenczy G, Beller M (2010) ChemSusChem 3:1048–1050
367. Sanz S, Azua A, Peris E (2010) Dalton Trans 39:6339–6343
368. Kathó Á, Opre Z, Laurenczy G, Joó F (2003) J Mol Catal A: Chem 204–205:143–148
369. Himeda Y, Onozawa-Komatsuzaki N, Sugihara H, Kasuga K (2007) Organometallics 26:702–712
370. Federsel C, Jackstell R, Beller M (2010) Angew Chem Int Ed 49:6254–6257
371. Tanaka R, Yamashita M, Nozaki K (2009) J Am Chem Soc 131:14168–14169
372. Erlandsson M, Landaeta VR, Gonsalvi L, Peruzzini M, Phillips AD, Dyson PJ, Laurenczy G (2008) Eur J Inorg Chem 2008:620–627
373. Schmeier TJ, Dobereiner GE, Crabtree RH, Hazari N (2011) J Am Chem Soc 133:9274–9277
374. Zhang P, Ni S-F, Dang L (2016) Chem Asian J 11:2528–2536
375. Ramakrishnan S, Waldie KM, Warnke I, De Crisci AG, Batista VS, Waymouth RM, Chidsey CED (2016) Inorg Chem 55:1623–1632
376. Qian Q, Zhang J, Cui M, Han B (2016) Nat Commun 7:11481
377. Kothandaraman J, Czaun M, Goeppert A, Haiges R, Jones J-P, May RB, Prakash GKS, Olah GA (2015) ChemSusChem 8:1442–1451
378. Filonenko GA, Smykowski D, Szyja BM, Li G, Szczygieł J, Hensen EJM, Pidko EA (2015) ACS Catal 5:1145–1154
379. Piazzetta P, Marino T, Russo N, Salahub DR (2015) ACS Catal 5:5397–5409
380. Osadchuk I, Tamm T, Ahlquist MSG (2016) ACS Catal 6:3834–3839
381. Oldenhof S, van der Vlugt JI, Reek JNH (2016) Catal Sci Technol 6:404–408
382. Lu S-M, Wang Z, Li J, Xiao J, Li C (2016) Green Chem 18:4553–4558
383. Aoki W, Wattanavinin N, Kusumoto S, Nozaki K (2016) Bull Chem Soc Jpn 89:113–124
384. Osadchuk I, Tamm T, Ahlquist MSG (2015) Organometallics 34:4932–4940
385. Onishi N, Xu S, Manaka Y, Suna Y, Wang W-H, Muckerman JT, Fujita E, Himeda Y (2015) Inorg Chem 54:5114–5123
386. Liu C, Xie J-H, Tian G-L, Li W, Zhou Q-L (2015) Chem Sci 6:2928–2931
387. Zhang Y, Williard PG, Bernskoetter WH (2016) Organometallics 35:860–865
388. Spentzos AZ, Barnes CL, Bernskoetter WH (2016) Inorg Chem 55:8225–8233
389. Wu C, Zhang Z, Zhu Q, Han H, Yang Y, Han B (2015) Green Chem 17:1467–1472
390. Jeletic MS, Helm ML, Hulley EB, Mock MT, Appel AM, Linehan JC (2014) ACS Catal 4:3755–3762
391. Zhang Y, Hanna BS, Dineen A, Williard PG, Bernskoetter WH (2013) Organometallics 32:3969–3979

392. González-Sebastián L, Flores-Alamo M, Garcia JJ (2013) Organometallics 32:7186–7194
393. Badiei YM, Wang W-H, Hull JF, Szalda DJ, Muckerman JT, Himeda Y, Fujita E (2013) Inorg Chem 52:12576–12586
394. Suh H-W, Schmeier TJ, Hazari N, Kemp RA, Takase MK (2012) Organometallics 31:8225–8236
395. Federsel C, Boddien A, Jackstell R, Jennerjahn R, Dyson PJ, Scopelliti R, Laurenczy G, Beller M (2010) Angew Chem Int Ed 49:9777–9780
396. Ziebart C, Federsel C, Anbarasan P, Jackstell R, Baumann W, Spannenberg A, Beller M (2012) J Am Chem Soc 134:20701–20704
397. Zell T, Langer R (2016) Recycl. Catal. 2:87–109
398. Ge H, Chen X, Yang X (2016) Chem Commun 52:12422–12425
399. Bertini F, Gorgas N, Stöger B, Peruzzini M, Veiros LF, Kirchner K, Gonsalvi L (2016) ACS Catal 6:2889–2893
400. Zhu F, Zhu-Ge L, Yang G, Zhou S (2015) ChemSusChem 8:609–612
401. Zhang Y, MacIntosh AD, Wong JL, Bielinski EA, Williard PG, Mercado BQ, Hazari N, Bernskoetter WH (2015) Chem Sci 6:4291–4299
402. Yang X (2015) Chem Commun 51:13098–13101
403. Rivada-Wheelaghan O, Dauth A, Leitus G, Diskin-Posner Y, Milstein D (2015) Inorg Chem 54:4526–4538
404. Fong H, Peters JC (2015) Inorg Chem 54:5124–5135
405. Zall CM, Linehan JC, Appel AM (2016) J Am Chem Soc 138:9968–9977
406. Zall CM, Linehan JC, Appel AM (2015) ACS Catal 5:5301–5305
407. Watari R, Kayaki Y, Hirano S-I, Matsumoto N, Ikariya T (2015) Adv Synth Catal 357:1369–1373
408. Courtemanche M-A, Pulis AP, Rochette E, Legare M-A, Stephan DW, Fontaine F-G (2015) Chem Commun 51:9797–9800
409. Pokhodenko VD, Koshechko VG, Titov VE, Lopushanskaja VA (1995) Tetrahedron Lett 36:3277–3278
410. Silvestri G, Gambino S, Filardo G, Gulotta A (1984) Angew Chem 96:978–979
411. Folest J-C, Duprilot J-M, Perichon J, Robin Y, Devynck J (1985) Tetrahedron Lett 26:2633–2636
412. Barba F, Guirado A, Zapata A (1982) Electrochim Acta 27:1335–1337
413. Wang H-M, Sui G-J, Wu D, Feng Q, Wang H, Lu J-X (2016) Tetrahedron 72:968–972
414. Niu D-F, Xiao L-P, Zhang A-J, Zhang G-R, Tan Q-Y, Lu J-X (2008) Tetrahedron 64:10517–10520
415. Damodar J, KrishnaMohan S, KhajaLateef SK, JayaramaReddy S (2005) Synth Commun 35:1143–1150
416. Isse AA, Gennaro A, Vianello E (1996) J Chem Soc Dalton Trans 1613–1618
417. Yamauchi Y, Hara S, Senboku H (2010) Tetrahedron 66:473–479
418. Tokuda M, Yoshikawa A, Suginome H, Senboku H (1997) Synthesis 1997:1143–1145
419. Feroci M, Inesi A, Orsini M, Palombi L (2002) Org Lett 4:2617–2620
420. Feroci M, Orsini M, Palombi L, Sotgiu G, Colapietro M, Inesi A (2004) J Org Chem 69:487–494
421. Senboku H, Komatsu H, Fujimura Y, Tokuda M (2001) Synlett 2001:0418–0420
422. Chowdhury MA, Senboku H, Tokuda M (2004) Tetrahedron 60:475–481
423. Matthessen R, Fransaer J, Binnemans K, Devos DE (2015) ChemElectroChem 2:73–76
424. Orsini M, Feroci M, Sotgiu G, Inesi A (2005) Org Biomol Chem 3:1202–1208
425. Wang H, Zhang K, Liu Y-Z, Lin M-Y, Lu J-X (2008) Tetrahedron 64:314–318
426. Duñach E, Périchon J (1988) J Organomet Chem 352:239–246
427. Derien S, Dunach E, Perichon J (1991) J Am Chem Soc 113:8447–8454
428. Labbé E, Duñach E, Périchon J (1988) J Organomet Chem 353:C51–C56
429. Katayama A, Senboku H, Hara S (2016) Tetrahedron 72:4626–4636
430. Derien S, Clinet JC, Dunach E, Perichon J (1991) J Chem Soc Chem Commun 549–550
431. Dérien S, Duñach E, Périchon J (1990) J Organomet Chem 385:C43–C46
432. Derien S, Clinet JC, Dunach E, Perichon J (1993) J Org Chem 58:2578–2588
433. Jutand A, Négri S (1997) Synlett 1997:719–721
434. Kamekawa H, Senboku H, Tokuda M (1998) Tetrahedron Lett 39:1591–1594
435. Senboku H, Kanaya H, Tokuda M (2002) Synlett 2002:0140–0142
436. Zhang K, Wang H, Zhao SF, Niu DF, Lu JX (2009) J Electroanal Chem 630:35–41
437. Damodar J, Mohan SRK, Reddy SRJ (2002) Synthesis 2002:0399–0402
438. Zhang K, Wang H, Wu L, Zhang J, Lu J (2010) Chin J Chem 28:509–513
439. Feng Q, Huang K, Liu S, Wang X (2010) Electrochim Acta 55:5741–5745
440. Yamauchi Y, Sakai K, Fukuhara T, Hara S, Senboku H (2009) Synthesis 2009:3375–3377

441. Senboku H, Yoneda K, Hara S (2015) Tetrahedron Lett 56:6772–6776
442. Senboku H, Yamauchi Y, Kobayashi N, Fukui A, Hara S (2011) Electrochemistry 79:862–864
443. Senboku H, Yamauchi Y, Kobayashi N, Fukui A, Hara S (2012) Electrochim Acta 82:450–456
444. Glueck SM, Gumus S, Fabian WMF, Faber K (2010) Chem Soc Rev 39:313–328
445. Aresta M, Dibenedetto A (2002) Rev Mol Biotechnol 90:113–128
446. Hügler M, Huber H, Stetter KO, Fuchs G (2003) Arch Microbiol 179:160–173
447. Thauer RK (2007) Science 318:1732–1733
448. Calvin M (1961) Nature 192:799
449. Hartman FC, Harpel MR (1994) Annu Rev Biochem 63:197–232
450. Evans MC, Buchanan BB, Arnon DI (1966) Proc Natl Acad Sci USA 55:928–934
451. Drake HL, Gößner AS, Daniel SL (2008) Ann N Y Acad Sci 1125:100–128
452. Ragsdale SW (2008) Ann N Y Acad Sci 1125:129–136
453. Ragsdale SW, Pierce E (2008) Biochim Biophys Acta 1784:1873–1898
454. Herter S, Fuchs G, Bacher A, Eisenreich W (2002) J Biol Chem 277:20277–20283
455. Alber B, Olinger M, Rieder A, Kockelkorn D, Jobst B, Hügler M, Fuchs G (2006) J Bacteriol 188:8551–8559
456. Berg IA, Kockelkorn D, Buckel W, Fuchs G (2007) Science 318:1782–1786
457. Huber H, Gallenberger M, Jahn U, Eylert E, Berg IA, Kockelkorn D, Eisenreich W, Fuchs G (2008) Proc Natl Acad Sci USA 105:7851–7856
458. Erb TJ, Berg IA, Brecht V, Müller M, Fuchs G, Alber BE (2007) Proc Natl Acad Sci USA 104:10631–10636
459. Allen JR, Ensign SA (1996) J Bacteriol 178:1469–1472
460. Small FJ, Ensign SA (1995) J Bacteriol 177:6170–6175
461. Allen JR, Ensign SA (1999) Biochemistry 38:247–256
462. Aresta M, Quaranta E, Liberio R, Dileo C, Tommasi I (1998) Tetrahedron 54:8841–8846
463. Boll M, Fuchs G (2005) Biol Chem 386:989
464. Lupa B, Lyon D, Shaw LN, Sieprawska-Lupa M, Wiegel J (2008) Can J Microbiol 54:75–81
465. Ding B, Schmeling S, Fuchs G (2008) J Bacteriol 190:1620–1630
466. Dibenedetto A, Lo Noce R, Pastore C, Aresta M, Fragale C (2006) Environ Chem Lett 3:145–148
467. Ren J, Yao P, Yu S, Dong W, Chen Q, Feng J, Wu Q, Zhu D (2016) ACS Catal 6:564–567
468. Pesci L, Glueck SM, Gurikov P, Smirnova I, Faber K, Liese A (2015) FEBS J 282:1334–1345
469. Yoshida T, Nagasawa T (2000) J Biosci Bioeng 89:111–118
470. Wieser M, Yoshida T, Nagasawa T (2001) J Mol Catal B Enzym 11:179–184
471. Wieser M, Yoshida T, Nagasawa T (1998) Tetrahedron Lett 39:4309–4310
472. Matsuda T, Ohashi Y, Harada T, Yanagihara R, Nagasawa T, Nakamura K (2001) Chem Commun 2194–2195
473. Matsuda T, Harada T, Nakamura K (2004) Green Chem 6:440–444
474. Wieser M, Fujii N, Yoshida T, Nagasawa T (1998) Eur J Biochem 257:495–499
475. Omura H, Wieser M, Nagasawa T (1998) Eur J Biochem 253:480–484
476. Matsuda T, Marukado R, Koguchi S, Nagasawa T, Mukouyama M, Harada T, Nakamura K (2008) Tetrahedron Lett 49:6019–6020

Top Curr Chem (Z) (2017) 375:15
DOI 10.1007/s41061-016-0101-8

REVIEW

Synthesis of Carbonates from Alcohols and CO_2

Nicole Kindermann[1] · **Tharun Jose**[1] ·
Arjan W. Kleij[1,2]

Received: 18 October 2016 / Accepted: 22 December 2016 / Published online: 18 January 2017
© Springer International Publishing Switzerland 2017

Abstract Alcohols are ubiquitous compounds in nature that offer modular building blocks for synthetic chemistry. Here we discuss the most recent development of different classes of alcohols and their coupling chemistry with carbon dioxide as to afford linear and cyclic carbonates, the challenges associated with their formation, and the potential of this chemistry to revive a waste carbon feed stock.

Keywords Carbon dioxide · Carboxylative cyclization · Cyclic carbonates · Diols · Heterogeneous catalysis · Homoallylic alcohols · Homogeneous catalysis · Linear carbonates · Propargylic alcohols

1 Synthesis of Acyclic Organic Carbonates

1.1 The Importance of the Formation of Acyclic Carbonates from Alcohols

Among various organic molecules which can in principle be derived from CO_2 and alcohols, acyclic carbonates such as dimethyl carbonate (DMC), diethyl carbonate (DEC), and diphenyl carbonate (DPC) have attracted considerable attention over the past decades [1, 2]. Especially DMC has been a focus of active recent research in the field, since it represents a multifunctional molecule that can be applied as an

---

Chapter 2 was originally published as Kindermann, N., Jose, T. & Kleij, A. W. Top Curr Chem (Z) (2017) 375: 15. DOI 10.1007/s41061-016-0101-8.

✉ Arjan W. Kleij
akleij@iciq.es

[1] The Barcelona Institute of Science and Technology, Institute of Chemical Research of Catalonia (ICIQ), Av. Països Catalans 16, 43007 Tarragona, Spain

[2] Catalan Institute of Research and Advanced Studies (ICREA), Pg. Lluis Companys 23, 08010 Barcelona, Spain

apolar solvent, a fuel additive, or as an organic reagent in the production of higher carbonates including polycarbonates, polyurethanes, and isocyanates [3–5].

Conventionally, DMC has been produced either from oxidative carbonylation of methanol or through a reaction between methanol and phosgene (Scheme 1) [4]. Neither process can be regarded as sustainable or environmentally benign, since they use highly toxic and corrosive reagents, and require expensive catalysts in the case of the oxidative carbonylation or disposal of hydrogen chloride when using phosgene. A much more attractive way to produce DMC (and related acyclic carbonates) would be the direct reaction between CO_2 and methanol, as shown in Scheme 1. The sole byproduct of this process is water, and its atom economy is comparable to that of the oxidative carbonylation of methanol.

One major drawback of this reaction, however, is its equilibrium limitation (thermodynamics), providing only (very) low yields in DMC. High pressures of CO_2 might help to partially overcome these limitations [6] but at the cost of a high energy demand accompanying this pressurization. Removal of the water formed in the DMC synthesis is another way to shift the equilibrium towards the desired product DMC. Accordingly, the development of efficient catalysts and in combination with a dehydrating agent has become one major focus in the synthesis of acyclic carbonates [7]. Besides DMC, DEC and DPC also have relevance in industrial processes [8, 9]. DPC has already found wide application in polycarbonate synthesis being efficiently used for transesterification of Bisphenol A (BPA). The derived polycarbonate is a thermoplastic polymer used on a large scale as a material for numerous applications (including electrical insulation) with a production of more than a billion tons per year; apart from the DPC route, the major process towards BPA-based polycarbonates still relies on the direct reaction of BPA with phosgene. DPC synthesis from phosgene or through oxidative carbonylation, comparable to DMC synthesis, has technical and logistic disadvantages. Transesterification of DMC with phenol is an attractive alternative to the conventional synthesis methods, however, in order to make the overall process "greener", DMC needs to be produced in a sustainable way.

For the direct synthesis of DMC from methanol and CO_2, efficient removal of water—besides the adequate choice of a catalyst—seems to be crucial in order to

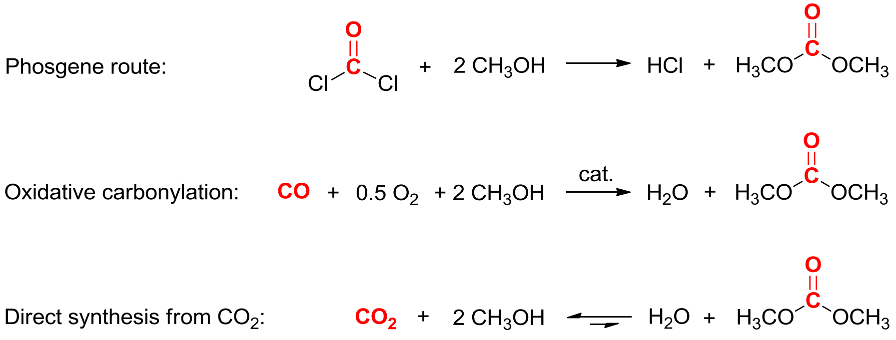

Scheme 1 Different routes for the synthesis of dimethyl carbonate (DMC)

achieve an improvement of this promising methodology and to increase its relevance in industrial synthesis. Thus, the following sections will concentrate on organic and inorganic promoters for DMC formation, and the importance of dehydrating agents.

1.2 Organic Promoters

One approach to address the equilibrium limitation is based on organic molecules acting as promoters for DMC formation. Activation of CO_2 or water capture might both be performed by the same organic molecule [10–12]. Especially in the latter scenario, a stoichiometric use of the promoter is required, since water is usually bound irreversibly. For instance, Aresta and coworkers established the use of dicyclohexylcarbodiimide (DCC; Scheme 2) for the direct synthesis of DMC from CO_2 and methanol under mild conditions (e.g., 80 °C and 5.0 MPa of CO_2). Based on the use of DCC, they reported yields of up to 62% for DMC after only 6 h, but the protocol could also be successfully employed in the conversion of ethanol or allyl alcohol substrates, thereby giving access to other dialkyl carbonates. Mechanistic and computational studies led to a putative mechanism, with an isourea/hemi-carbonate adduct as the proposed key intermediate (Scheme 2).

A different synthetic route towards DMC synthesis, which gives access to symmetric and asymmetric acyclic carbonates, is based on Mitsunobu's reagent. This methodology, developed by Chaturvedi et al. [11], can furthermore be successfully employed to convert primary, secondary, and even tertiary alcohols in a one-pot reaction with good to high yields (70–98%) in all reported cases. Recently, the successful application of DBU for the synthesis of acyclic carbonates was demonstrated by Jang and coworkers [12]. The scope comprised the synthesis of various cyclic and acyclic organic carbonates, including DMC, which could be obtained in 48% yield under comparatively mild reaction conditions (70 °C, 10 bar CO_2).

1.3 Metal-Based Homogeneous Catalysis

Among the homogeneous metal catalysts considered, metal alkoxides have been intensively studied in DMC synthesis since they have been shown to absorb CO_2 to form organic carbonates [13, 14]. Besides titanium, zirconium, and niobium

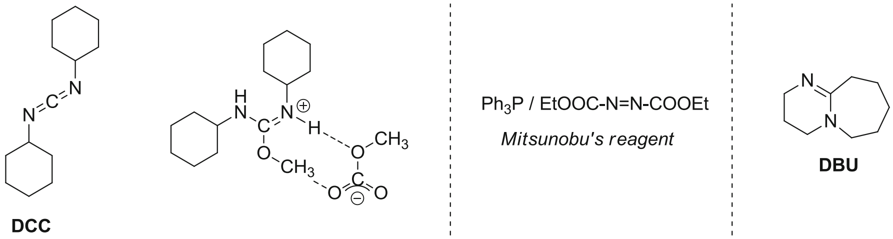

Scheme 2 Organic promotors for the direct formation of DMC from alcohols and CO_2

compounds [14–18], tin(IV) complexes have been investigated in detail with respect to DMC formation from methanol and carbon dioxide. Tetraalkoxy [$Sn(OR)_4$] as well as dialkoxydialkyl [$R^1_2Sn(OR^2)_2$] tin compounds are classes of organometallics both active in DMC formation, even though the efficiency of the reported systems remains rather low [18–20]. Significant improvements of the methodology were made by Sakakura et al. by investigating the effect of different drying agents on the DMC formation catalyzed by organometallic tin compounds. Initially starting with orthoesters, DMC yields of 48% (based on the orthoester reagent) and a selectivity of 85% (DMC) were found under high pressures of CO_2 (300 atm) and reaction temperatures of 180 °C, using [$Bu_2Sn(OMe)_2$] as catalyst [21]. Notably, a substantial enhancement of the catalyst performance by the addition of onium salts was observed. One drawback of this approach, however, was the required stoichiometric use of orthoesters. As shown in Scheme 3, they can capture water under the release of an alcohol and an ester, but recycling of the desiccant is not feasible.

By contrast, drying agents such as acetals promised to be more sustainable, since they feature recovery potential from the formed ketone that upon reaction with alcohols can regenerate the acetal [22]. In comparison to the orthoester system, a combination of tin compound and acetal performed slightly better with a DMC yield of 58% based on the acetal. Even though in this case onium salts do not lead to improved catalyst performance, more recently it has been shown that acidic co-catalysts have a pronounced influence on the efficiency in DMC formation, and for instance the presence of small amounts of co-catalytic Ph_2NH_2OTf accelerated the reaction substantially [15].

Besides organic desiccants, also inorganic versions such as molecular sieves have been successfully employed in the dehydration process [6]. Even though zeolites are not considered to be very efficient under high reaction temperature conditions, yields up to 45% based on MeOH were reported [6]. Mechanistic proposals are based on early structural findings [23], as depicted in Scheme 4. After CO_2 insertion into the metal methoxide moiety, the bridging alkoxide reacts with the hemicarbonate anion with subsequent DMC release. The active species can be reestablished from the corresponding oxide or hydroxide by reacting with methanol under the release of water [24]. Recent reinvestigations and density functional theory (DFT) calculation, though, suggest that the actual active intermediates might be stannoxane dimers (Scheme 4) [25, 26].

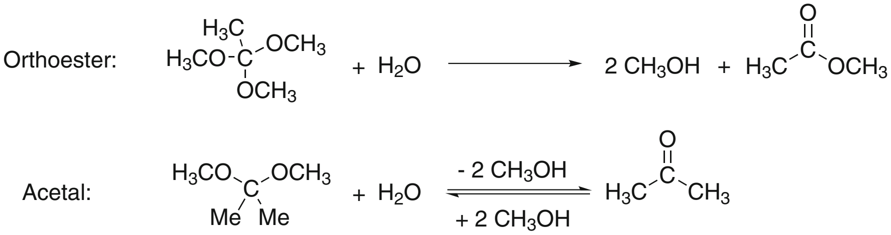

Scheme 3 Organic desiccants that have been employed as water-capturing agents

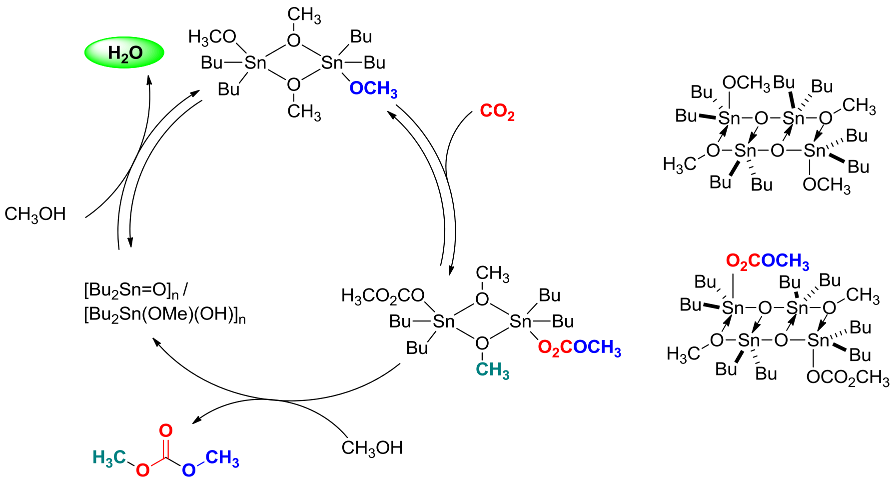

Scheme 4 Mechanistic proposal based on structural findings (*left*); reactive intermediates suggested by computational and experimental studies

1.4 Metal-Based Heterogeneous Catalysis

The use of heterogeneous catalysts in the synthesis of chemical compounds has several key benefits if compared with homogenous catalysis. Separation of the catalyst from the products is usually straightforward, e.g., by a simple filtration. At the same time, the ease of separation is advantageous when it comes to recyclability of the catalyst. This makes heterogeneous catalysts an interesting choice for industry, especially when similar selectivities and activities as in the case of homogenous catalysts can be achieved. For DMC synthesis, the use of metal oxides has had a considerable impact on the field. Beside main group metal oxides such as Mg–Al hydrotalcites [27, 28], mainly transition metal oxides have been employed. Among these are vanadium oxides, doped with Brønsted acids [29] or copper/nickel [30], but the most widely studied systems consist of zirconium and cerium oxides.

Early work by Tomishige and Fujimoto revealed the great potential of the amphoteric materials ZrO_2 and CeO_2 (or solid solution mixtures) [31–35], being mainly attributed to synergistic effects between their acidic and basic sites [31]. However, for the simple metal oxides the equilibrium restriction did not allow for yields exceeding 2% [34] even under high CO_2 pressures of 6 MPa and temperatures around 127 °C. Doping of the metal oxides with Brønsted acidic sites using H_3PO_4 or $H_3W_{12}O_{40}$ led to slightly improved yields or shorter reaction times under comparable conditions [36–38].

Major breakthroughs were only achieved, though, if dehydrating agents were added. In contrast to orthoesters or acetals, which were formerly used by Sakakura, Tomishige, and coworker suggested the use of nitriles in 2009 [39, 40]. Water capture with nitriles leads to amides, which can later be converted back to the corresponding nitrile and enable the regeneration of the dehydrating species. The elegance of this synthetic route is based on the simultaneous conversion of CO_2 and methanol to DMC and the nitrile hydration to the corresponding amide by CeO_2. If using acetonitrile as desiccant at 0.5 MPa CO_2 pressure and 150 °C, the yield of DMC after 48 h reached about 9% but with only a mediocre selectivity for DMC of 65%. Also the selectivity of amide formation upon water capture remained an issue, especially in the light of recyclability of the dehydrating agent. Benzonitrile proved to be a much better choice not only with respect to selective amide formation, but its use also increased the DMC yield to a remarkable 47% (1 MPa, 150 °C, 86 h), with a significantly improved chemo-selectivity of 75% [41].

As suggested by the authors, the reason for this improved reactivity/selectivity behavior might be suppression of competitive alcoholysis of the formed amide, if compared to acetamide that is in situ produced from acetonitrile. A systematic screening for suitable nitrile-based dehydrating agents [42, 43], which are efficiently hydrated by CeO_2, finally led to the use of 2-cyanopyridine as the preferred nitrile in combination with a cerium oxide catalyst. With this system (5 MPa, 120 °C, 12 h), yield of *and* selectivity for DMC were extraordinarily high, reaching levels of 94 and 96%, respectively. The recycling of the formed amide was also addressed, and the dehydration of 2-picolinamide by Na_2O/SiO_2 was shown to be feasible even though the overall efficiency should be improved. The scope is not only limited to the formation of DMC, but also ethanol or branched alcohols could be converted in a similar way albeit with a drop in yield of the corresponding carbonate product.

In order to provide a lead for further improvement of the catalytic system, mechanistic insights are inevitable. Tomishige et al. [44] proposed a reaction cycle based on kinetic, spectroscopic, and computational studies, leading to an overall mechanism as depicted in Scheme 5. It resembles the mechanism suggested by Bell et al. for the zirconium oxide catalyzed formation of DMC from methanol and CO_2 [45]. A molecule of CO_2 inserts into the Ce-OCH_3 bond of surface bound methanol to yield a Ce-methyl carbonate species. For the next step the authors suggested a nucleophilic attack of another surface bound methoxy group to give DMC. The formed hydroxide species on the cerium oxide surface can subsequently react with 2-cyanopyridine and result in the formation of 2-picolinamide [46, 47]. Other authors, however, claim the attack of gas-phase methanol [48], or the formation of a carbomethoxide intermediate on the cerium oxide surface [49]. Therefore, the exact mechanism concerning the cerium oxide mediated formation of DMC remains subject of ongoing debate in the literature.

Its superb performance regarding yield and selectivity towards DMC formation makes the combination of cerium(IV) oxide and 2-cyanopyridine a promising candidate for further commercial applications. This is reflected in the development of the first continuous flow process using fixed bed reactors [50], as well as intensified research concerning the reusability of the cerium oxide catalyst, which eventually suffers from deactivation by adsorption of the formed amide [44, 51]. Interestingly, the scope of this system is not limited to the formation of simple acyclic carbonates, but can also be employed to cyclic carbonates (see “Cyclic Organic Carbonates from Saturated Alcohols” and “Formation of Six-membered Cyclic Carbonates” sections of this review) [52], as well as cyclic and acyclic carbamates and urea derivatives [53–55]. Very recently, cerium oxide and 2-cyanopyridine was furthermore used to synthesize polymeric materials from

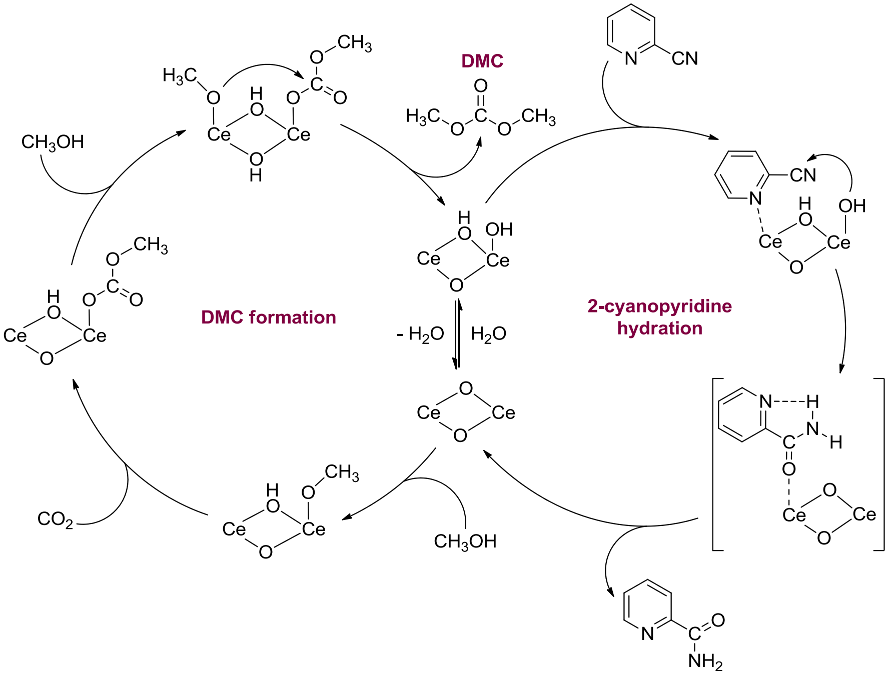

Scheme 5 Mechanism of cerium oxide catalyzed simultaneous formation of DMC and 2-picolinamide formation from MeOH/CO_2 and 2-cyanopyridine, respectively

CO_2 and diols, as depicted in Scheme 6 [56]. Despite the low molecular weight of the produced materials, this represents the first exciting example of a direct copolymerization between CO_2 and diols.

1.5 Prospects of Acyclic Carbonate Formation

Over the last two decades, huge progress has been made regarding the yield and chemo-selectivity in the production of DMC from methanol and carbon dioxide. Homogeneous and heterogeneous catalyst systems have been improved continuously, going hand in hand with the development of efficient dehydrating systems to shift the reaction equilibrium towards the formation of DMC. Various studies were dedicated to homogeneous metal alkoxide compounds, with tin(IV) complexes leading the way. In combination with different water-removing agents, good yields

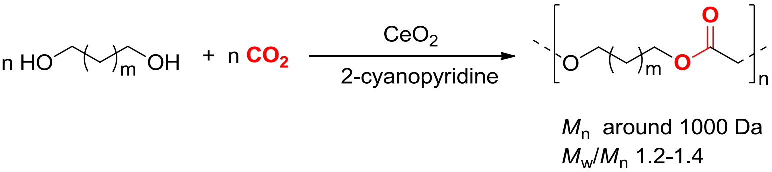

Scheme 6 Direct polycarbonate formation from diols and carbon dioxide

and selectivities for the formation of acyclic carbonates were obtained. Even better performances were achieved using heterogeneous, amphoteric metal oxides such as zirconium oxide and cerium oxide, with the latter giving excellent yields and selectivities towards DMC when combined with 2-cyanopyridine as desiccant. Although product separation and recyclability of catalyst and dehydrating agent have been clearly demonstrated, recovery of the nitrile from 2-picolinamide remains problematic for further applications and is at the same time crucial to optimize the cost-benefit ratio as well as to design a truly sustainable, atom-economical route for the preparation of acyclic organic carbonates. New reactor technologies such as the use of flow chemistry with a clever use of recycle streams may at some point in time allow to efficiently run DMC and related synthesis in continuous mode at low conversion of the alcohol without the need for a dehydrating agent.

2 Cyclic Organic Carbonates from Saturated Alcohols

2.1 Synthesis of Five-Membered Cyclic Carbonates

2.1.1 Metal-Based Catalysts

From an industrial point of view, the transformation of ethylene glycol (**EG**) and propylene glycol (**PG**) is of high interest. Both **EG** and **PG** are byproducts obtained in the transesterification of ethylene carbonate (**EC**) and propylene carbonate (**PC**), respectively, using MeOH as a reagent and with the aim to produce DMC. Thus, recycling of the **EG** or **PG** by reaction with CO_2 has the potential to lift the overall sustainability of DMC synthesis from **EC** or **PC** (Scheme 7) [57].

Tomishige reported the first attempt for this transformation using a calcined CeO_2-ZrO_2 catalyst system in the presence of acetonitrile [58, 59]. Conversions of 0.7 and 1.6% were obtained under optimal reaction conditions using 0.36 mmol (total amount of Ce and Zr) of catalyst weight, 200 mmol of CO_2, 120 mmol acetonitrile, a reaction temperature of 150 °C for 2 h: these conditions led to the synthesis of **EC** and **PC** from **EG** and **PG**, respectively. Interestingly, the **EC** and **PC** amount increased when the calcination temperature of the catalyst system was increased, which resulted in lowering the amount of acid/base sites and the surface area. As in the formation of linear carbonates, the reaction mediated by the CeO_2–ZrO_2 catalyst system is thermodynamically limited with a maximum conversion of 2%; removal of H_2O would be crucial to maximize the conversion/yield of the carbonate product.

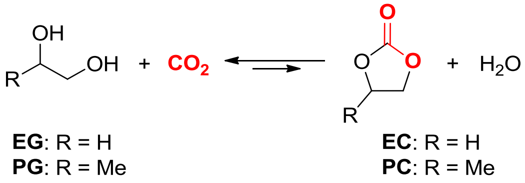

Scheme 7 Synthesis of cyclic carbonates from CO_2 and the glycols **EG** and **PG**

Subsequently, He et al. reported two different catalyst systems such as dibutyltin oxide/dibutyltin dimethoxide and low toxic magnesium and its oxide for the synthesis of **PC** from **PG** and CO_2 under supercritical conditions using *N*,*N*,-dimethylformamide (DMF) as solvent [60, 61]. In both cases, the maximum conversion obtained for **PG** was <4% with 100% chemo-selectivity. Also, alkali carbonates were used to catalyze the **PC** synthesis from **PG** and CO_2 with a relative high yield of 10.5% under supercritical conditions in the presence of ammonium carbonate and acetonitrile [62]. Acetonitrile did not only act as a solvent here but also as the dehydrating agent to eliminate the water produced during the reaction thereby shifting the equilibrium towards the formation of **PC**. However, the hydrolysis of acetonitrile may generate acetamide and can subsequently react with water to form acetic acid and ammonia. Acetic acid can react with **PG** to produce propylene glycol-2-acetate, lowering the overall selectivity towards **PC**. Therefore, introduction of ammonium carbonate into the reaction system inhibited the hydrolysis of acetamide and improved the chemo-selectivity toward **PC**.

The combination of its bio-based origin and wide reactivity has made glycerol carbonate (**GC**) a versatile and renewable building block for organic chemistry. The direct carboxylation of glycerol (**Gly**) and CO_2 is a very interesting though challenging route that would convert two waste materials from the chemical industry into a valuable product (Scheme 8). Mouloungui et al. attempted to prepare **GC** under supercritical conditions but the reaction did not occur [63]. Later on, Dibenedetto employed tin-based catalyst systems [n-$Bu_2Sn(OMe)_2$] and [n-Bu_2SnO] under solvent-free conditions using 6 mol% of catalyst [n-$Bu_2Sn(OMe)_2$], 5 MPa of CO_2 pressure, a reaction temperature of 180 °C for 15 h to obtain a maximum conversion of 6.7% [64]. Molecular sieves were introduced into the reactor to reduce the water content in the homogeneous phase to favor the equilibrium towards the formation of **GC**.

Hereafter, Dibenedetto applied mixed oxide catalysts (CeO_2/Al_2O_3 and CeO_2/Nb_2O_5) under the same reaction condition mentioned above in a biphasic system using tetra(ethylene glycol) dimethyl ether (TEGDME) as solvent to obtain a maximum **Gly** conversion of 2.5%. The catalyst was recyclable at least 3 times without any observable loss of activity [65]. Munshi et al. showed that addition of methanol to the Dibendetto's n-Bu_2SnO-based catalyst system enhanced the catalytic activity and as a result 30% yield for **GC** in 4 h at 80 °C and 3.5 MPa CO_2 pressure using 1 mol% of catalyst could be attained [66]. The reaction with diglyme, an inert aprotic solvent, instead of methanol did not improve the yield of **GC** and also the use of other alcohols such as ethanol, propanol and butanol slowed down the reaction rate. These combined results indicated that the role of methanol is not just acting as a solvent but it is likely also chemically involved. The proposed mechanism presumes the activation of n-Bu_2SnO by methanol to give n-

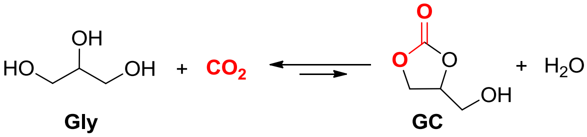

Scheme 8 Synthesis of **GC** from **Gly** and CO_2

$Bu_2Sn(OMe)_2$ which in turn reacts with **Gly** forming *n*-Bu_2Sn(glycerol-2H) and undergoes CO_2 insertion, leading eventually to **GC** via a Sn(glycerolcarbonate) complex. The catalytic cycle is completed by ligand exchange in the presence of methanol followed by ring-closing, release of the **GC** product and the reformation of the $Sn(OMe)_2$ complex species as shown in Scheme 9. During the process, the monomeric species (*n*-Bu_2Sn(glycerol-2H)) can either incorporate CO_2 or oligomerize causing catalyst deactivation. The addition of methanol prevents the formation of an oligomeric species as it is actively involved in the formation of **GC** whereas the water formed during reaction is removed continuously from the system.

Similar to Tomishige's work [58] using acetonitrile as a medium that helps to overcome the thermodynamic limitation of the process, Sun and coworkers used acetonitrile as a sacrificial coupling agent in the presence of a $La_2O_2CO_3$–ZnO catalyst system for the transformation of CO_2 and **Gly** into **GC** [67]. The highest **Gly** conversion (30.3%) with a **GC** yield of 14.3% was reported at 4 MPa of CO_2 pressure, a reaction temperature of 170 °C after 12 h when the catalyst system was calcined at 500 °C. The envisioned mechanism involves the activation of **Gly** by Lewis acidic sites (Zn^{2+}) forming a glyceroxide anion, and subsequently the oxygen atom of the adjacent hydroxyl group attacks the zinc cation resulting in zinc-glycerolate species along with the formation of a molecule of water which is converted to an amide reacting with acetonitrile.

The uncalcined catalyst produces only a low yield of **GC** due to the higher content of crystal lattice water, which favors the hydrolysis of acetonitrile (*cf.*, amide formation) and results in more byproducts. With the introduction of $La_2O_2CO_3$, the amount of lattice oxygens (La–O pairs) increases on the surface and leads to an increase of moderately basic sites, which in turn enhance the activation of glycerol and CO_2 and thereby exhibit higher catalytic activity than pure ZnO.

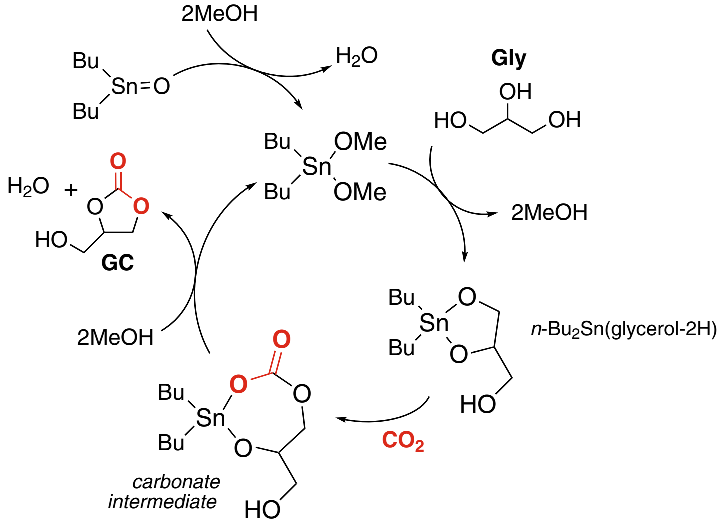

Scheme 9 Proposed reaction path towards GC formation [66]

Likewise, various other catalysts systems such as Cu/La_2O_3 and Cu-supported catalysts, Zn/Al/La and Zn/Al/La/M (M=Li, Mg and Zr) hydrotalcites, and Zn/Al/La/X (X=F, Cl, Br) catalysts were also successfully employed for the direct carbonylation of **Gly** to obtain maximum conversions of the substrate of <36% under typically harsh, supercritical reaction conditions in the presence of acetonitrile [68–70].

Very recently, He and coworkers obtained **GC** from the carbonylation of **Gly** and CO_2 over CeO_2 catalysts with the hydrolysis of 2-cyanopyridine as the sacrificial dehydrating agent [71]. Calcined CeO_2 with three different morphologies pertinent to nanoparticles, nano-rods and sponge-like nanomaterials were prepared corresponding to three different types of methods being precipitation, hydrothermal treatment and sol–gel methodology, respectively. All three samples showed excellent catalytic performance obtaining **GC** yields between 20 and 34% under relatively mild reaction conditions (150 °C, 4 MPa, 5 h) with an activity order of nanorod catalyst > catalytic nanoparticles > sponge-like catalyst. The CeO_2 nanorod type catalyst with the most abundant basic sites and oxygen vacancies gave the highest yield of **GC**, and sponge-like CeO_2 with medium amount of basic sites and the least defects gave the lowest, indicating that the oxygen vacancies play an important role in the catalytic system. Among various dehydrating agents used, 2-cyanopyridine showed the best performance ascribed to the relatively strong alkalinity and the formation of intramolecular hydrogen bonding in the produced amide when the nitrile reacts with water. By optimizing the reaction conditions, the **GC** yield could be increased to as high as 78.9% and the used catalyst could be easily regenerated through the calcination process at 400 °C for 5 h, and was recycled five times successfully.

2.1.2 Organocatalysts

Jang and coworkers introduced a metal-free carbonylation reaction in which alcohols are converted into their corresponding cyclic carbonates in the presence of an organic base and dibromomethane (CH_2Br_2) as the solvent [11]. The organic base, 1,8-diazabicyclo[5.4.0]undec-7-ene (DBU), is assumed to deprotonate the OH unit of ethylene glycol (**EG**), which would render it more nucleophilic. DBU is also known to form an adduct with CO_2, and can in this way increase the nucleophilic character of CO_2 favoring reaction with **EG**. In the presence of 2 equivalents of DBU at 0.5 M of CH_2Br_2 and at 0.5 MPa/70 °C, **EG** (0.5 mmol) was converted into **EC** (24% after 18 h). In the presence of an ionic liquid (IL: bmimPF_6), the **EC**-yield was enhanced to 54% and under higher CO_2 pressure (1 MPa) it was further improved to 74%.

ILs are well known to increase the solubility of CO_2 in the reaction media. Under the optimized reaction conditions, various other alcohols were also tested as substrates and it was found that **Gly** underwent good conversion obtaining a **GC** yield of 86%. Similarly, other methyl- and phenyl-substituted ethylene diols underwent smooth conversion to their cyclic carbonates to afford yields of 67–79%. A cyclic diol was also tested and displayed an excellent yield of 73%. A set of additional experiments was performed to understand the operating mechanism in these diol/CO_2 coupling reactions. First, an ^{18}O-labeling experiment was conducted with mono-^{18}O-labeled styrene glycol and a 70% yield of the styrene carbonate was achieved, where the ^{18}O label did not exchange with ^{16}O during the reaction, *i.e.* the cyclic carbonate had the ^{18}O-labeled atom incorporated. Second, the use of optically active (*S*)-styrene glycol was examined, and the resultant styrene carbonate was analyzed by HPLC showing full retention of the initial configuration.

The mechanism of the aforementioned reaction is shown in Scheme 10 in which the primary alcohol first attacks the DBU-CO_2 adduct to form the carbonate intermediate **I**, which then reacts with CH_2Br_2 to form reactive carbonate **II**. Then the intermolecular attack of the (pre-activated) secondary alcohol unit onto the carbonate followed by the elimination of $HOCH_2Br$ affords the styrene carbonate product. The intramolecular addition of the carbonate nucleophile in intermediate **III** likely is not competitive under these conditions as supported by the experimental result obtained using (*S*)-styrene glycol.

3 Formation of Six-Membered Cyclic Carbonates

3.1 Metal-Based Catalysts

The pioneering group of Tomishige has successfully performed various carbonylation reactions of diols and CO_2 to afford their cyclic carbonates. Recently, they employed the privileged CeO_2 catalyst in combination with 2-cyanopyridine as dehydrating agent to yield various five- and six-membered cyclic carbonates from CO_2 and diols [52]. From a series of different metal oxides combined with 2-cyanopyridine for the synthesis of **PC** from **PG** and CO_2, CeO_2 was shown to be more active by 2 orders of magnitude compared with other metal oxides. 2-Cyanopyridine was preselected as nitrile for its exceptional reactivity towards hydration forming 2-picolinamide. Without the addition of 2-cyanopyridine, the **PC** yield was as low as 0.3% due to the unfavorable thermodynamics. Addition of 100 mmol of 2-cyanopyridine provided an excellent **PC** yield of >99% (chemo-

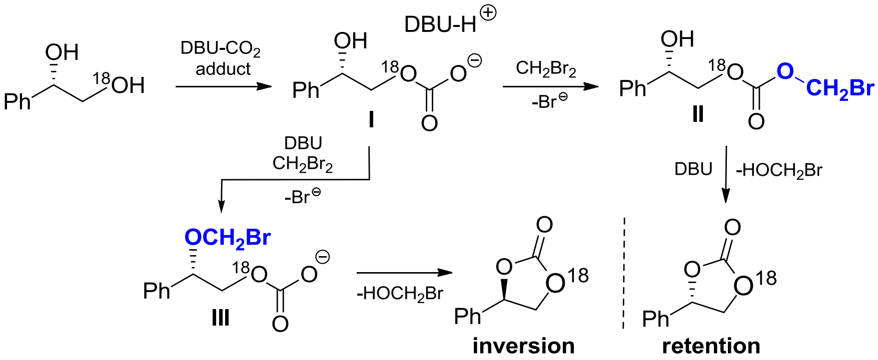

Scheme 10 Plausible mechanism for cyclic carbonate formation from styrene glycol and CO_2

selectivity >99%) in just 1 h using 20 mol% catalyst (CeO_2), at 130 °C/5 MPa CO_2 and this is the highest yield of **PC** from CO_2 and **PG** to date.

To extend the synthetic potential of this catalyst system, synthesis of six-membered ring carbonates was carried out by employing various 1,3-diols with monoalkyl-, dialkyl-, and phenyl-substitutions and generally the corresponding cyclic carbonates were obtained in high yields of 62–97% with good to excellent chemo-selectivity (77–99%). The ester that is formed by reaction of the diol starting material with 2-picolinamide in situ produced was spotted as the major byproduct. Syntheses of six-membered ring carbonates, especially those having multiple substituents, are difficult to realize using any methodology, despite the fact that they represent useful chemicals and intermediates for, *inter alia*, biodegradable polymers for drug delivery systems. The results obtained for this Ce-based catalyst system mediating the synthesis of various six-membered carbonates are highly attractive compared to other methodologies reported to date, except for the non-substituted trimethylene carbonate derived from oxetane and CO_2, for which Kleij et al. [72] reported a very high yield (95%) using a simple though highly reactive Al-catalyst based on amino-triphenolate ligands.

After the reaction, the CeO_2 catalyst was removed from the reaction mixture and the filtrate was analyzed by inductively coupled plasma atomic emission spectroscopy (ICP-AES), which indicated that no Ce species had leached into the filtrate (<0.1 ppm). The catalyst was therefore successfully reused for three times without any loss of its high selectivity and yield; the BET surface area and X-ray diffraction pattern of the CeO_2 material before and after the reaction remained virtually unchanged and thus indicated that the CeO_2 catalyst is highly stable under the experimental conditions. The mechanistic details are similar to the ones already discussed for the formation of acyclic carbonates in "Synthesis of Acyclic Organic Carbonates" section. Overall, this catalyst system shows the best yields for cyclic carbonate synthesis (five- and six-membered ones) from diols and CO_2 reported to date.

3.2 Organocatalysts

Buchard and coworkers [73] performed the synthesis of six-membered cyclic carbonates directly from various 1,3-diols and CO_2 at room temperature, 0.1 MPa of CO_2 using standard reagents. First, the selective mono-insertion of CO_2 into one of the O–H bonds of 1,3-butanediol in various solvents was examined in the presence of DBU as catalyst. After the selective formation of the mono-carbonate intermediate at low concentration, 1 equivalent of tosyl chloride/triethylamine was added to the reaction mixture and stirred at room temperature. The pure targeted product was isolated in an appreciable yield of 44%, which was increased to 68% when a higher concentration of diol (going from 0.1 to 1.7 M) was applied. Investigation into the scope of diol substrates revealed that various 1,3-diols were good reaction partners in this organocatalytic approach, and the corresponding six-membered cyclic carbonates were isolated in low to good yields (11–70%). After initial insertion of CO_2, into one of the O–H bonds, tosylation of the carbonate species or the remaining alcohol function can be envisaged. Hereafter, the cyclization proceeds via either an addition/elimination sequence or an S_N2 pathway, leading to retention or inversion of stereochemistry, respectively.

However, the exclusive formation and isolation of the (*R*,*R*)-configured cyclic carbonate from (*R*,*R*)-2-4-pentanediol (yield: 53%) as well as the optical activities of the cyclic carbonates obtained from enantiopure (*R*)- and (*S*)-1,3-butanediol, clearly indicated a preference for the addition/elimination pathway (Scheme 11), with no observable racemization or inversion of stereochemistry, which was further supported by DFT calculations.

4 Cyclic Carbonates Derived from Unsaturated Alcohols

4.1 Metal-Based Catalysts

Reaction of CO_2 with propargylic alcohols typically affords α-alkylidene cyclic carbonates through a carboxylative cyclization process (Scheme 12), which is also a promising and green route to convert CO_2. Moreover, α-alkylidene cyclic carbonates possess a wide range of applications in organic synthesis being for instance building blocks in the formation of α-hydroxy ketones and 5-methylene-oxazolidin-2-one derivatives.

Inoue et al. [74] performed the Pd(0)-catalyzed [$Pd(PPh_3)_4$] carboxylative cyclization reaction of CO_2 (1 MPa) with sodium 2-methyl-3-butyn-2-olate (prepared from the corresponding alcohol and a slight excess of NaH) and iodobenzene in THF as solvent at 100 °C and obtained the cyclic vinylidene carbonate in 68% yield. Alternatively, the use of copper catalysis proved to be highly beneficial to further develop this type of reaction. For instance, a cationic copper complex derived from 2,5,19,22-tetraaza[6](1,1′)ferrocenophane-1,5-diene was an effective catalyst operating under 3.8 MPa of CO_2 and 100 °C affording good yields of the cyclic carbonates (>90%) using various substituted propargylic alcohols under neat conditions [75]. Similarly, CuCl in the presence of the IL [BMIm][$PhSO_3$] yielded the α-alkylidene cyclic carbonate in 97% yield under a milder CO_2 pressure of 1 MPa at 120 °C [76].

Substantial improvement in activity was reported for metal-based catalyst systems when Mizuno et al. communicated a tungstate-based complex (i.e., $TBA_2[WO_4]$, TBA = tetrabutylammonium) as an efficient homogeneous catalyst

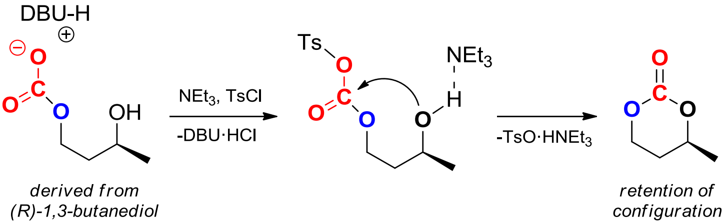

Scheme 11 Preferred pathway for the conversion of (*R*)-1,3-butanediol into its six-membered carbonate [73]

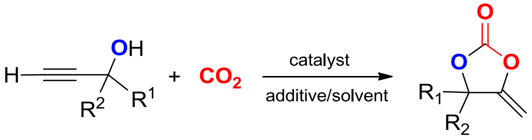

Scheme 12 Conversion of CO_2 into an α-alkylidene cyclic carbonate with an *exo*-cyclic double bond using propargylic alcohols

for conversion of CO_2 with propargylic alcohols to give the corresponding cyclic carbonates under mild reaction conditions [77]. DFT calculations allowed optimizing the tungstate structure and the basicities of oxygen atoms in various polyoxometalates (POMs) were compared with the natural bond orbital (NBO) charges; the simple $[WO_4]^{2-}$ tungstate was found to be the most basic among the series. Under only 0.1 MPa of CO_2 pressure and at a relatively low temperature of 60 °C, propargylic alcohol (2-methylbut-3-yn-2-ol) was coupled with CO_2 in acetonitrile to give the corresponding carbonate structure in 76% yield. Upon lowering the catalyst loading while increasing the CO_2 pressure (2 MPa) and reaction time, the total turnover number could be enhanced to a significant 473 with a yield of 95%. In a similar way, more lethargic substrates such as propargylic alcohols with internal triple bonds (*cf.*, 1-ethynylcyclohexan-1-ol) were also effectively transformed to their cyclic carbonates in excellent yield of up to 95%.

Having witnessed the enhancement in activity brought about by the $[WO_4]^{2-}$ anion in carbonate formation under much milder conditions, Song and coworkers [78] employed a Ag_2WO_4/Ph_3P dual catalyst system for the conversion of CO_2 and propargylic alcohols to provide the α-alkylidene carbonates under solvent-free conditions. In this dual catalyst system, the $[WO_4]^{2-}$ anion was envisioned to activate both CO_2 and the propargylic alcohol generating a carboxylate intermediate which could then be intercepted by Ag-activated C≡C triple bond to afford the product (Scheme 13).

Using this system at 1 mol% of catalyst loading, 25 °C and 0.1 MPa of CO_2 pressure an optimum yield of 96% was obtained. Subsequently, other substrates were examined with this dual catalyst and propargylic alcohols with alkyl and aryl substituents at the propargylic position were also effective substrates to give the corresponding cyclic carbonates in good to excellent yields. The method was, however, not effective for 1-isopropyl and 1,1-cyclopentylene substituted substrates which showed (very) low conversions due to a combination of steric hindrance and

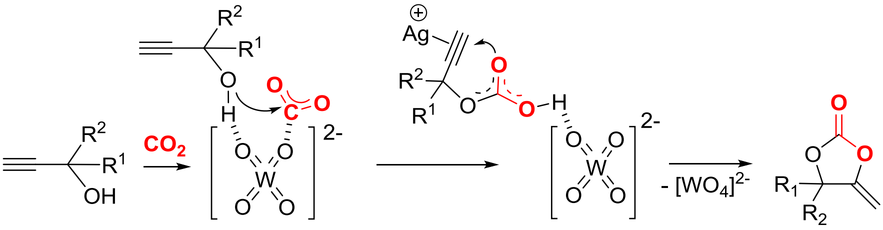

Scheme 13 Chemical fixation of CO_2 through the dual activation pathway [78]

ring strain. Secondary propargylic alcohols failed to form the carbonate product, while the internal propargylic substrate 2-methyl-4-phenylbut-3-yn-2-ol required both higher CO_2 pressure (1 MPa) and temperature (80 °C) to afford the corresponding cyclic carbonate in good yield (82%) using longer reaction times (36 h). This catalyst system was easily separated by extraction with hexane and after drying the catalyst could be successfully recycled four times without observable loss of activity.

At room temperature and CO_2 pressures <2 MPa, AgOAc/DBU [79] and F-MOP-3-Ag/DBU catalyst systems (F-MOPs = fluorinated microporous organic polymers having Ag(I) sites incorporated) [80] in toluene gave good results. Notably, both catalyst systems were successful in converting various terminal and bulky internal propargylic alcohols to their corresponding cyclic carbonates in good yields. Heterogeneous metal systems have also been reported as effective catalysts for α-alkylidene carbonate formation. Important limitations for these supported catalyst systems, though, were primarily the required supercritical conditions and high catalyst loadings and, moreover, a limited substrate scope allowing only the conversion of terminal propargylic alcohols [81, 82]. Significant improvement of activity and reusability features of heterogeneous metal catalysts was reported by Liu and coworkers [83] who used porous organic polymers (POPs) as a solid support. This material allows the introduction of various CO_2-philic functional species inside its structure to obtain a more active, functional and reusable catalyst. Specifically, the authors prepared porous poly(triphenylphosphine) with azo (R–N=N–R) functionalities (i.e., a poly(PPh_3)-azo material) with the Ag sites being coordinated by the phosphine ligands. This system was efficiently used for CO_2 transformations taking advantage of cooperative effects between the functional porous polymer and the metal species. The poly(PPh_3)-azo-Ag/DBU catalyst converted at room temperature and a CO_2 pressure of 1 MPa the benchmark propargylic alcohol 2-methylbut-3-yn-2-ol to its corresponding cyclic carbonate with a yield of 56% in 3 h; a higher yield was achieved by further increasing the reaction time to 18 h (>99%) with a remarkable total TON of 1563. The presence of a high local concentration of PPh_3 ligands and azo functionalities in the polymer (PPh_3/Ag = 200:1, azo/Ag = 300:1) facilitated cooperative effects towards the formation of α-alkylidene compounds. Moreover, the catalyst system was also shown to be recyclable at least five times without loss of activity. After several uses, transmission electron microscopic (TEM) analysis of the catalytic material indicated that the metallic Ag particles were still highly dispersed without changes in particle size after recycling. In order to establish possible leaching, the catalyst was separated through centrifugation after the reaction performed for 1 h, and the filtrate was analyzed by ICP-AES which demonstrated that there was no observable leaching of Ag species (<10 ppb). Then, various terminal propargylic alcohols with both alkyl and aryl substituents were examined as substrates and these reacted efficiently with CO_2, though substrates comprising bulky isopropyl groups or small rings required longer reaction times to obtain good yields presumably due to steric effects.

The proposed mechanism for the formation of α-alkylidene cyclic carbonates mediated by the poly(PPh_3)-azo-Ag catalyst system is shown in Scheme 14 [83].

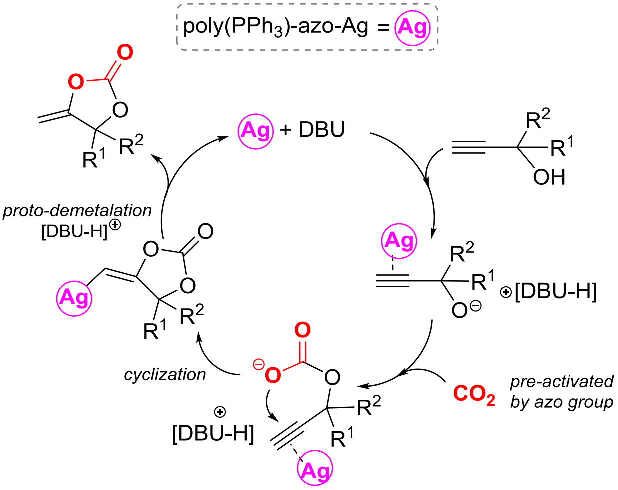

Scheme 14 Proposed mechanism for the coupling reaction of propargylic alcohols with CO_2 catalyzed by poly(PPh_3)-azo-Ag/DBU [83]

First, the propargylic alcohol, activated by DBU, reacts with pre-activated CO_2 to generate a carbonate intermediate. An intramolecular ring-closing step is then followed by proto-demetalation to afford the corresponding cyclic carbonate with the regeneration of the active Ag species and DBU.

Similarly, He et al. [84] used $[(PPh_3)_2Ag]_2CO_3$ (in situ formed from Ag_2CO_3 and PPh_3) as a robust and highly efficient single-component bifunctional catalyst for the coupling of propargylic alcohols and CO_2 at room temperature and atmospheric pressure. After only 2 h, 2-methylbut-3-yn-2-ol and CO_2 were converted to the cyclic carbonate in 93% yield under neat conditions using the in situ prepared catalyst. The recovered precipitate after the reaction could be reused in a subsequent carboxylative cyclization cycle.

Ag nanoparticles (NPs) have been immobilized to other solid supports such as sulfonated macro-reticular resins (SMRs) forming an active AgNPs/SMR catalyst [85]. Alternatively, Ag halides were supported on a porous carbon material (AgX@C, X=Cl, Br and I) [86] and the resultant catalyst was effective at room temperature and atmospheric pressure in the carboxylative cyclization of the propargylic alcohol 2-methylbut-3-yn-2-ol and CO_2 in the presence of DBU as co-promoter. The use of the AgNPs/SMR catalyst gave a 91% yield of the cyclic carbonate after 10 h in DMF, and the catalyst was shown to be recyclable at least five times. The AgI@C catalyst furnished the product in 99% yield within 4 h in acetonitrile, and was used in a total of 10 cycles without any significant loss in activity.

Interestingly, a zinc salt (ZnI_2) in combination with triethylamine (NEt_3) was recently proposed as a catalyst system in this area and showed excellent synergistic effects to promote the solvent-free reaction of CO_2 and 2-methylbut-3-yn-2-ol under a CO_2 pressure of 1 MPa and at 30 °C to obtain 4,4-dimethyl-5-methylene-1,3-

dioxolan-2-one in 95% yield after 10 h [87]. These results are promising to devise new catalyst systems based on earth-abundant and cheap metals such as Zn.

4.2 Organocatalysts

As CO_2 prevalently behaves as an electrophile, strong Lewis bases based on nitrogen heterocycles have the potential to activate CO_2 affording zwitterionic adducts. Thus, such organocatalytic promotors can be utilized as convenient and cheap CO_2 transformers to accomplish its conversion by increasing its nucleophilic character. N-heterocyclic carbenes (NHCs) incorporating electron-donating heteroatoms have a strong basic character and this enables strong σ-donor ability of the NHC useful for CO_2 activation. Imidazolium-2-carboxylates (with the integrated CO_2 molecule in an activated state) have been spectroscopically and structurally identified as NHC–CO_2 adducts. Ikariya and coworkers [88] prepared NHCs (1,3-dialkylidazol-2-ylidenes) and their corresponding CO_2 adducts (1,3-dialkylimidazolium-2-carboxylates), and employed them as efficient catalysts for cyclic carbonate synthesis using propargylic alcohols and CO_2.

The NHC–CO_2 adducts showed comparatively superior activity under milder conditions than the NHCs themselves, which required supercritical conditions to obtain good results for the conversion of 2-methyl-3propyn-2-ol in the carboxylative cyclization with CO_2 to form the corresponding cyclic carbonate. Under solvent-free conditions at 4.5 MPa CO_2 and 60 °C, various NHC–CO_2 adducts, prepared by variation of the N-substituents (di-isopropyl, di-*tert*-butyl, diaryl) were tested for their catalytic activity. The NHC–CO_2 adduct 1,3-di-*tert*-butylimidazolium-2-carboxylate gave the best yield (99%) for the cyclic carbonate product among the adducts tested. If the catalyst loading, CO_2 pressure and/or temperature were lowered, a significant amount of an acyclic product (1,1-dimethyl-2-oxopropyl-1′,1′-dimethyl-2′-propynyl carbonate) was obtained along with the desired cyclic carbonate. The carboxylative cyclization affording the cyclic carbonate and the subsequent addition of another propargylic alcohol to the product is thought to lead to this 2:1 coupling product of both substrates.

Various five-membered cyclic carbonates were prepared in good yields from different propargylic substrates having disubstituted alkyne groups using the NHC–CO_2 catalyst. The presence of electron-withdrawing groups conjugated to the triple bond in the substrate led to the targeted products in faster rates and at lower reaction temperatures. The NHC-based catalyst also tolerates propargylic substrates equipped with heterocycles such as pyridine and thiophene, whereas *allylic* compounds such as 2-methyl-3-buten-2-ol and 2-methyl-4-phenyl-3-buten-2-ol did not give any cyclization product. In each product, the C=C double bond was found to have a (*Z*)-configuration, indicating that the addition of the NHC–carboxylate to the alkyne fragment proceeded predominantly in an *anti* fashion. The postulated mechanism for the NHC–CO_2 mediated carboxylative cyclization of propargylic alcohols and CO_2 involves the nucleophilic addition of the imidazolium-2-carboxylate to the C$\equiv$C triple bond and subsequent intramolecular cyclization of the alkoxide intermediate (Scheme 15). A significant positive effect of electron-donating *N*-alkyl substituents present in the NHC structure implies that the

Scheme 15 Mechanism of the carboxylative cyclization catalyzed by a NHC–CO_2 adduct [88]

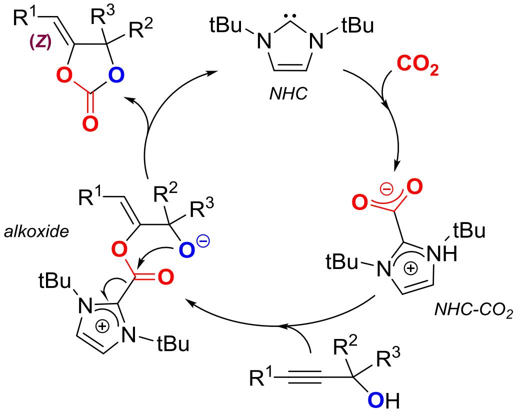

intramolecular nucleophilic attack of the CO_2 moiety, once bound to the NHC, onto the substrates may be rate-limiting step in this catalytic cycle.

N-heterocyclic *olefins* (NH**O**s) are compounds that are capable of further stabilizing the positive charge that arises upon activation of CO_2 due to aromatization of the heterocyclic ring thereby making the terminal carbon atom of the initial olefin group more electronegative and susceptible towards the activation of electrophilic reaction partners. Recently, Lu et al. [89] prepared various NH**O**–CO_2 adducts and employed them as catalysts for coupling of propargylic alcohols and CO_2 to yield α-alkylidene carbonates. For comparative reasons, NH**C**–CO_2 adducts were also prepared and in situ decarboxylation experiments monitored by IR spectroscopy in CH_2Cl_2 at 40 °C revealed that decarboxylation of the NH**O** systems occurred within 2 h, whereas only small amounts of NH**C** adducts decomposed under similar conditions. This demonstrates that the decarboxylation of NH**O**–CO_2 adducts is relatively easy and therefore of more practical use for cyclic carbonate synthesis. The relatively poor thermal stability of NH**O**–CO_2 adducts therefore offers an opportunity to use these compounds as active catalysts for CO_2 transformations at low temperature. In the catalyst activity screening phase, 2-methyl-4-phenylbut-3-yn-2-ol was chosen as a model substrate and reacted with CO_2 at 2 MPa pressure and 60 °C for 12 h. Among the various NH**O**–CO_2 adducts, the isopropyl-substituted NH**O**–CO_2 adduct showed the best results leading to a 93% isolated yield of the cyclic carbonate. The difference in catalytic activity observed for the NH**O**–CO_2 adduct in comparison with its corresponding NH**C**–CO_2 was established for various propargylic substrates, and typically the NH**O** adducts are about 10–100 times more active than their NH**C** analogues. Various terminal and internal propargylic alcohols smoothly underwent the carboxylative cyclization reaction and were converted into their corresponding α-alkylidene cyclic carbonates in moderate to excellent yields. Apparently only a slight structural difference exists between the NH**O** and NH**C** adducts; the much higher reactivity for the NH**O**–CO_2 adducts was tentatively ascribed to the lower stability of the $C_{carboxylate}$–C_{NHO} bond.

The proposed mechanistic manifold begins with the zwitterionic compound NH**O**–CO_2 that adds to the triple bond of propargylic substrate through nucleophilic attack. Meanwhile, hydrogen transfer of alcohol generates the new zwitterion **Ia** (Scheme 16, path A), and then the alkoxide anion attacks the carboxylate carbon to release the desired product and regenerating the NH**O**, which rapidly captures free CO_2 to form the NH**O**–CO_2 adduct to induce further turnover. The higher thermal instability of the NH**O**–CO_2 adducts favorably adds to the overall kinetics of the reaction, thus creating higher turnover at lower temperatures as compared with the reactivity of analogous NH**C**–CO_2 adducts. The NH**O** with increased electronegativity at the terminal carbon atom can also act as a Brønsted base able to abstract a proton from the propargylic alcohol to form the intermediate **IIa** (path B) which subsequently reacts with CO_2 to give intermediate **IIb** (Scheme 16, path B). Subsequently, the intermediate **IIc** is obtained by intramolecular ring-closure within intermediate **IIb**, which abstracts a proton from the 2-methyl imidazolium cation to release the desired product. The obvious difference between both pathways A and B is that the hydrogen at the alkenyl position of cyclic carbonate originates exclusively from the propargylic substrate (path A) or both substrate and catalyst (path B): this aspect may be elucidated by a proper labeling of the NH**O** and/or propargylic substrate.

The same group also prepared various CO_2 adducts of alkoxide-functionalized imidazolium betaines (abbreviated as AFIBs) and explored the AFIB–CO_2 adducts as effective organocatalysts within the context of carboxylative cyclization of propargylic alcohols with CO_2 [90]. The best result (97% yield) for the AFIB–CO_2 mediated formation of the cyclic carbonate product was obtained under 2 MPa pressure at 60 °C using 2-methylbut-3-yn-2-ol as substrate. The catalyst system

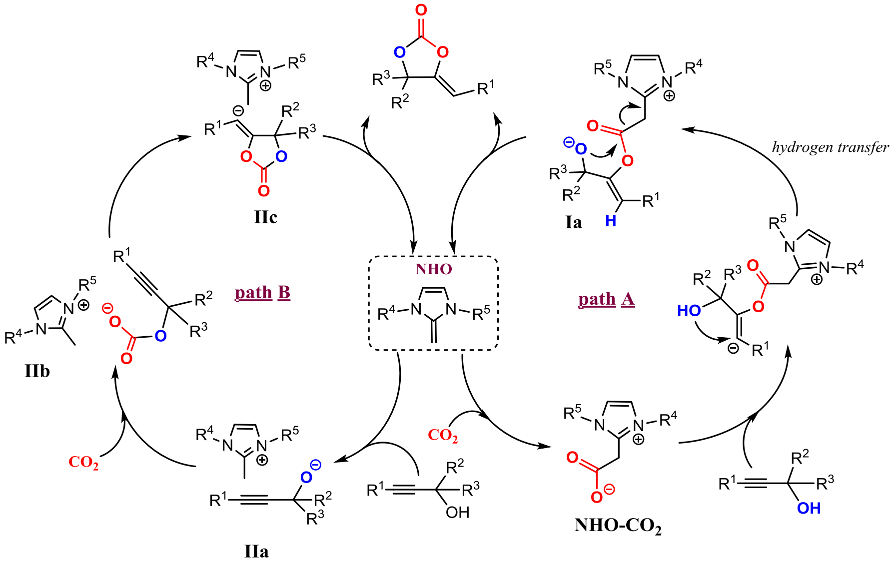

Scheme 16 Proposed mechanism of the carboxylation reaction catalyzed by the NHO–CO_2 adduct [89]

proved to be more effective for the carboxylative cyclization of terminal rather than internal propargylic substrates.

Minakata et al. [91] treated various allylic alcohols with stoichiometric *t*BuOI under 0.1 MPa of CO_2 pressure and low reaction temperature resulting in the synthesis of five-membered cyclic carbonates containing a potentially useful alkyliodide group. The reagent, *t*BuOI, can be readily prepared in situ from commercially available *tert*-butyl hypochlorite (*t*BuOCl) and sodium iodide (NaI), and serves to iodinate an elusive and rather unstable alkyl carbonic acid that is first generated from CO_2 and an unsaturated alcohol. The introduction of the iodine atom radically changes the position of the equilibrium of the initial CO_2-trapping reaction (Scheme 17). The use of tetrahydrofuran (THF) as solvent and a reaction temperature of −20 °C resulted in the conversion of prop-2-en-1-ol into the corresponding cyclic carbonate in 92% yield. To further investigate the efficacy of *t*BuOI, other iodinating reagents such as bis(pyridine)iodine tetrafluoroborate (IPy_2BF_4), *N*-iodosuccinimide (NIS), I_2 and a combination of I_2 and triethylamine were tested, but all these reagents failed to provide the desired product.

The main reason for *t*BuOI being the most appropriate iodinating reagent is related to the liberation of a relatively weak acid (*i.e.*, *t*BuOH) during the reaction of allyl-carbonic acid and *t*BuOI. *β*-Branched allylic alcohols also could be smoothly transformed into their corresponding cyclic carbonates in good yields. Both (*E*)- and (*Z*)-allylic alcohols were transformed into their corresponding cyclic carbonates. Allyl alcohols containing rigid cyclic olefins, hydroxyl, ester or silyl groups, and homo-allylic alcohols allowing the formation of six-membered cyclic carbonates were also compatible with this CO_2 conversion reaction. Similarly, various internal propargylic alcohols reacted with CO_2 under similar conditions and permitted the synthesis of the corresponding iodoalkyl derived carbonates in good yields.

Recently, an efficient carboxylation/alkene functionalization reaction of homoallylic alcohols was reported by Johnston et al. [92] to produce chiral cyclic carbonates (Scheme 18) using an approach similar to the one reported by Minakata (vide supra). At low temperatures and ambient pressure, a toluene solution of 3-phenylbut-3-en-1-ol was treated with CO_2/*N*-iodosuccinimide in the presence of various bases including NaH, DBU, TBD, DMAP as well as hydrogen bond donors such as TFA and thiourea but these conditions failed to deliver the desired carbonate product or gave only rise to low yields. A Brønsted acid/base combination was then explored to promote the reaction and the use of a chiral pyrrolidine-substituted

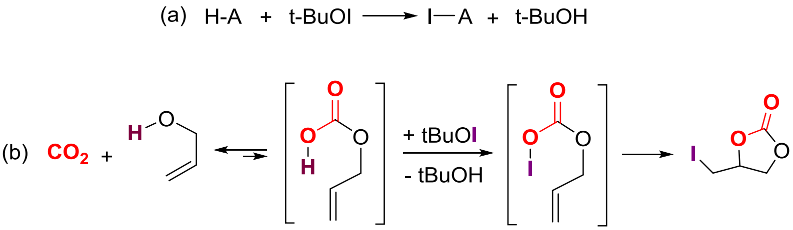

Scheme 17 **a** Reaction of *tert*-butyl hypoiodite with weak acids. **b** Strategy for trapping carbonic acids with *tert*-butyl hypoiodite [91]

Scheme 18 An enantioselective method for the synthesis of cyclic carbonates from homoallylic alcohols and CO_2 using a chiral StilbPBAM organocatalyst [92]

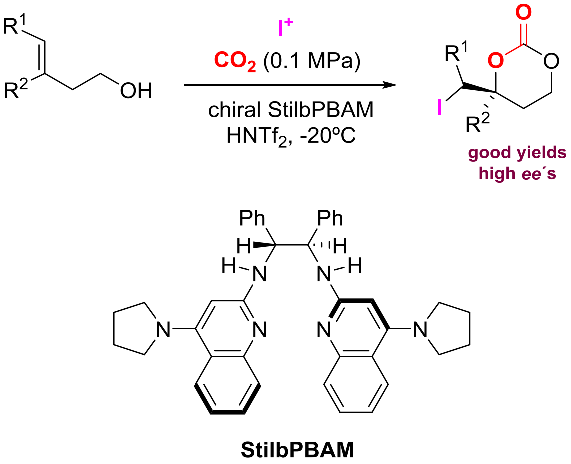

bis(amidine) gave a promising 18% yield of the iodinated cyclic carbonate in 39% *ee*. An analogous catalyst incorporating *trans*-stilbene diamine (StilbPBAM; Scheme 18) instead of *trans*-cyclohexane diamine provided the product in 33% yield and 36% *ee*. Exploration of strong Brønsted acid additives ($HNTf_2$) (1 equiv) combined with the StilbPBAM organocatalyst enhanced the activity to provide a 95% yield (91% *ee*) in the presence of molecular sieves (4 Å). Combined, the results suggest an important role for hydrogen-bonding in the key selectivity-determining step, and a unique reactivity associated with the proper mutual positioning of the Brønsted acid and base in the relevant transition state that controls the asymmetric induction. Various other substituted styrene homoallylic alcohols were also tested: *β*-naphthyl substituted anisole derivatives (*meta*- and *para*-substituted), and halogen substituted substrates were all converted into their six-membered carbonates with excellent enantioselectivity and in good yields, whereas substitution near the alkene moiety was not tolerated and no conversion was noted in these cases.

5 Cyclic Carbonates from Halo-Alcohols

Another approach for the preparation of cyclic carbonates from CO_2 could be the use of halohydrins (haloalcohols) as potential starting substrate in presence of a base. The obvious drawback of this approach is the stoichiometric amount of halide waste that is produced alongside, but in certain cases it may provide an alternative if other methods fail to deliver the desired organic carbonate structure.

Using PEG-400 as an environmentally friendly solvent and K_2CO_3 as an easily accessible base, various cyclic carbonates (yield 72–100%) were prepared by the group of Wu starting from vicinal halohydrins such as chlorohydrin, bromohydrin, and phenyl and alkyl-substituted halohydrins at low CO_2 pressure (2 MPa) and temperature (50 °C) [93]. The choice of PEG-400 as a reaction medium is beneficial in terms of solvation of the potassium cation to increase the basicity of K_2CO_3, an increase in CO_2 concentration in this specific medium accelerating the reaction, and the ease of product separation. Similarly, Zhang and coworkers [94] reported on the utilization of 1.1 equiv. of Cs_2CO_3 as base, obtaining both five- and six-membered cyclic carbonates in good to excellent yield under relatively mild conditions (40 °C under 0.1 MPa CO_2, Scheme 19). By variation of different solvents and bases, the optimal conditions were determined (Cs_2CO_3, DMF) and the haloalcohol substrate 3-chloro-1-propanol reacted efficiently with CO_2 giving 95% yield of trimethylene carbonate (TMC). One advantage of this method, which seems a general approach if the haloalcohol is readily available, is the easy formation of larger-ring size cyclic carbonates which remains a synthetic challenge in the area of organic carbonates. The mechanism of this reaction is pretty straightforward with the Cs_2CO_3 first deprotonating the alcohol resulting in the formation of a cesium alkoxide. The latter in turn reacts with CO_2 to form a carbonate intermediate which in the final step undergoes an intramolecular ring closing reaction affording CsCl as a byproduct and TMC.

Even more recently, Buchard and coworkers developed a related protocol for the formation of six-membered cyclic carbonates starting from 1,3-diols at low (0.1 MPa) CO_2 pressure and using DBU [73]. The procedure involves the activation of both the alcohol functions of the substrate by tosyl chloride and DBU allowing the in situ formation of a *pseudo* haloalcohol. This intermediate is then easily converted in the presence of NEt_3 to the desired cyclic carbonate. DFT analysis revealed that the mechanism most likely goes through an addition/elimination sequence with intermediate formation of a tosylated carbonate species, and subsequent attack of the other activated alcohol (by NEt_3) onto this carbonate fragment releasing the product with retention of configuration as was indeed experimentally observed for various chiral substrates. As for the aforementioned methodologies, stoichiometric amounts of DBU-HCl and $TsOHNEt_3$ are produced, and some optimization regarding the atom-economy will still be required.

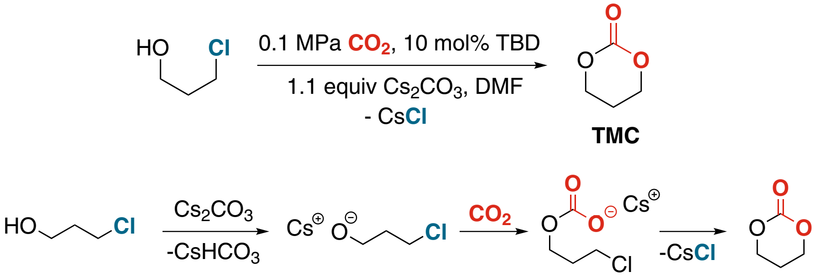

Scheme 19 Reaction manifold for the formation of TMC using 3-chloro-1-propanol as the starting material and Cs_2CO_3 as base [94]

6 Conclusions and Outlook

This overview of the latest developments in the area of cyclic carbonate synthesis from alcohol substrates and CO_2 shows several advances made over the last 5–10 years with a major focus on the more recent achievements. Since the direct conversion of alcohols in the presence of CO_2 is thermodynamically limited and only low equilibrium yields can be attained, several catalytic processes have been developed to circumvent this issue by using dehydrating agents. This approach has resulted in the high-yield synthesis of both cyclic as well as acyclic carbonates in good yields, though a crucial feature to optimize remains the regeneration of the dehydrating species. If this agent can be efficiently recycled then such a process would be extremely useful for larger scale preparation of carbonates, and commercial exploitation. Apart from bypassing the thermodynamic limitations, other approaches that use more functional substrates such as propargylic alcohols have also been proven to be effective, and the carboxylative cyclization reaction is now a valuable tool in organic synthesis. Similar types of activation protocols where the initial alcohol function can first react with CO_2 to form a linear carbonate followed by intramolecular attack onto a pre-activated alkyne fragment would be welcome in order to design new conversions and amplify the role of mono- and polyalcohols as suitable platform molecules in organic synthesis. Several useful protocols towards five- and six-membered carbonate synthesis in the presence of stoichiometric amounts of often simple and cheap reagents have already been developed. However, to answer the ever-growing need for more sustainable manufacturing of bulk and fine chemicals, new catalysis protocols are warranted to address this feature more effectively. Thus it seems that the combination of (poly)alcohols and CO_2 as reaction partners will continue to inspire scientists to work on greener and more sustainable catalytic methods for the production of carbonated compounds that will find use in areas diverse as bulk, polymer and pharmaceutical chemistry.

Acknowledgements Funding was provided by ICREA, the CERCA Program/Generalitat de Catalunya and MINECO (Grant Nos. CTQ-2014-60419-R, SEV-2013-0319).

References

1. Huang S, Yan B, Wang S, Ma X (2015) Recent advances in dialkyl carbonates synthesis and applications. Chem Soc Rev 44:3079–3116
2. Aresta M, Dibenedetto A, Dutta A (2017) Energy issues in the utilization of CO_2 in the synthesis of chemicals: the case of the direct carboxylation of alcohols to dialkyl-carbonates. Catal Today in press. 281(2):345–351. doi: 10.1016/j.cattod.2016.02.046
3. Tundo P, Selva M (2002) The chemistry of dimethyl carbonate. Acc Chem Res 35:706–716
4. Pacheco MA, Marshall CL (1997) Review of dimethyl carbonate (DMC) manufacture and its characteristics as a fuel additive. Energy Fuels 11:2–29
5. Shaikh A-AG (1996) Organic carbonates. Chem Rev 96:951–976
6. Choi J-C, He L-N, Yasuda H, Sakakura T (2002) Selective and high-yield synthesis of dimethyl carbonate directly from carbon dioxide and methanol. Green Chem 4:230–234
7. Honda M, Tamura M, Nakagawa Y, Tomishige K (2014) Catalytic CO_2 conversion to organic carbonates with alcohols in combination with dehydration system. Catal Sci Technol 4:2830–2845

8. Shukla K, Srivastava VC (2016) Diethyl carbonate: critical review of synthesis routes, catalysts used and engineering aspects. RSC Adv 6:32624–32645
9. Gong J, Ma X, Wang S (2007) Phosgene-free approaches to catalytic synthesis of diphenyl carbonate and its intermediates. Appl Catal A General 316:1–21
10. Aresta M, Dibenedetto A, Fracchiolla E, Giannoccaro P, Pastore C, Pápai I, Schubert G (2005) Mechanism of formation of organic carbonates from aliphatic alcohols and carbon dioxide under mild conditions promoted by carbodiimides. DFT calculation and experimental study. J Org Chem 70:6177–6186
11. Chaturvedi D, Mishra N, Mishra V (2007) A high yielding, one-pot synthesis of dialkyl carbonates from alcohols using Mitsunobu's reagent. Tetrahedron Lett 48:5043–5045
12. Lim YN, Lee C, Jang H-Y (2014) Metal-free synthesis of cyclic and acyclic carbonates from CO_2 and alcohols. Eur J Org Chem 2014:1823–1826
13. Bloodworth BAJ, Davies AG, Vasishtha SC (1967) Organometallic reactions. Part VII. Further addition reactions of tributyltin methoxide and of bistributyltin oxide. J Chem Soc C 1309–1313
14. Hidai M, Hikita T, Uchida Y (1972) Reactions of carbon dioxide with transition metal alkoxides. Chem Lett 1:521–522
15. Choi J-C, Kohno K, Ohshima Y, Yasuda H, Sakakura T (2008) Tin- or titanium-catalyzed dimethyl carbonate synthesis from carbon dioxide and methanol: large promotion by a small amount of triflate salts. Catal Commun 9:1630–1633
16. Kohno K, Choi J-C, Ohshima Y, Yasuda H, Sakakura T (2008) Synthesis of dimethyl carbonate from carbon dioxide catalyzed by titanium alkoxides with polyether-type ligands. ChemSusChem 1:186–188
17. Aresta M, Dibenedetto A, Pastore C (2003) Synthesis and characterization of $Nb(OR)_4[OC(O)OR]$ (R=Me, Et, Allyl) and their reaction with the parent alcohol to afford organic carbonates. Inorg Chem 42:3256–3261
18. Kizlink J, Pastucha I (1995) Preparation of dimethyl carbonate from methanol and carbon dioxide in the presence of Sn(IV) and Ti(IV) alkoxides and metal acetates. Collect Czechoslov Chem Commun 60:687–692
19. Kizlink J (1993) Synthesis of dimethyl carbonate from carbon dioxide and methanol in the presence of organotin compounds. Collect Czechoslov Chem Commun 58:1399–1402
20. Kizlink J, Pastucha I (1994) Preparation of dimethyl carbonate from methanol and carbon dioxide in the presence of organotin compounds. Collect Czechoslov Chem Commun 59:2116–2118
21. Sakakura T, Saito Y, Okano M, Choi J-C, Sako T (1998) Selective conversion of carbon dioxide to dimethyl carbonate by molecular. J Org Chem 63:7095–7096
22. Sakakura T, Choi J, Saito Y, Masuda T, Sako T, Oriyama T (1999) Metal-catalyzed dimethyl carbonate synthesis from carbon dioxide and acetals. J Org Chem 64:4506–4508
23. Choi J-C, Sakakura T, Sako T (1999) Reaction of dialkyltin methoxide with carbon dioxide relevant to the mechanism of catalytic carbonate synthesis. J Am Chem Soc 121:3793–3794
24. Sakakura T, Choi J-C, Saito Y, Sako T (2000) Synthesis of dimethyl carbonate from carbon dioxide: catalysis and mechanism. Polyhedron 19:573–576
25. Kohno K, Choi J-C, Ohshima Y, Yili A, Yasuda H, Sakakura T (2008) Reaction of dibutyltin oxide with methanol under CO_2 pressure relevant to catalytic dimethyl carbonate synthesis. J Organomet Chem 693:1389–1392
26. Wakamatsu K, Orita A, Otera J (2010) DFT Study on activation of carbon dioxide by dimethytin dimethoxide for synthesis of dimethyl carbonate. Organometallics 29:1290–1295
27. Stoian DC, Taboada E, Llorca J, Molins E, Medina F, Segarra AM (2013) Boosted CO_2 reaction with methanol to yield dimethyl carbonate over Mg–Al hydrotalcite-silica lyogels. Chem Commun 49:5489–5491
28. Kumar S, Khatri OP, Cordier S, Boukherroub R, Jain SL (2015) Graphene oxide supported molybdenum cluster: first heterogenized homogeneous catalyst for the synthesis of dimethylcarbonate from CO_2 and methanol. Chem Eur J 21:3488–3494
29. Wu XL, Xiao M, Meng YZ, Lu YX (2005) Direct synthesis of dimethyl carbonate on H_3PO_4 modified V_2O_5. J Mol Catal A Chem 238:158–162
30. Wu XL, Meng YZ, Xiao M, Lu YX (2006) Direct synthesis of dimethyl carbonate (DMC) using Cu–Ni/VSO as catalyst. J Mol Catal A Chem 249:93–97
31. Tomishige K, Sakaihori T, Ikeda Y, Fujimoto K (1999) A novel method of direct synthesis of dimethyl carbonate from methanol and carbon dioxide catalyzed by zirconia. Catal Lett 58:225–229

32. Ikeda Y, Sakaihori T, Tomishige K, Fujimoto K (2000) Promoting effect of phosphoric acid on zirconia catalysts in selective synthesis of dimethyl carbonate from methanol and carbon dioxide. Catal Lett 66:59–62
33. Tomishige K, Ikeda Y, Sakaihori T, Fujimoto K (2000) Catalytic properties and structure of zirconia catalysts for direct synthesis of dimethyl carbonate from methanol and carbon dioxide. J Catal 192:355–362
34. Tomishige K, Furusawa Y, Ikeda Y, Asadullah M, Fujimoto K (2001) CeO_2–ZrO_2 solid solution catalyst for selective synthesis of dimethyl carbonate from methanol and carbon dioxide. Catal Letters 76:71–74
35. Yoshida Y, Arai Y, Kado S, Kunimori K, Tomishige K (2006) Direct synthesis of organic carbonates from the reaction of CO_2 with methanol and ethanol over CeO_2 catalysts. Catal Today 115:95–101
36. Ikeda Y, Asadullah M, Fujimoto K, Tomishige K (2001) Structure of the active sites on H_3PO_4/ZrO_2 catalysts for dimethyl carbonate synthesis from methanol and carbon dioxide. J Phys Chem B 105:10653–10658
37. Lee HJ, Joe W, Song IK (2011) Direct synthesis of dimethyl carbonate from methanol and carbon dioxide over transition metal oxide/$Ce_{0.6}Zr_{0.4}O_2$ catalysts: effect of acidity and basicity of the catalysts. Korean J Chem Eng 29:317–322
38. Jiang C, Guo Y, Wang C, Hu C, Wu Y, Wang E (2003) Synthesis of dimethyl carbonate from methanol and carbon dioxide in the presence of polyoxometalates under mild conditions. Appl Catal A Gen 256:203–212
39. Honda M, Suzuki A, Noorjahan B, Fujimoto K, Suzuki K, Tomishige K (2009) Low pressure CO_2 to dimethyl carbonate by the reaction with methanol promoted by acetonitrile hydration. Chem Commun 4596–4598
40. Honda M, Kuno S, Begum N, Fujimoto K, Suzuki K, Nakagawa Y, Tomishige K (2010) Catalytic synthesis of dialkyl carbonate from low pressure CO_2 and alcohols combined with acetonitrile hydration catalyzed by CeO_2. Appl Catal A 384:165–170
41. Honda M, Kuno S, Sonehara S, Fujimoto K, Suzuki K, Nakagawa Y, Tomishige K (2011) Tandem carboxylation-hydration reaction system from methanol, CO_2 and benzonitrile to dimethyl carbonate and benzamide catalyzed by CeO_2. ChemCatChem 3:365–370
42. Tamura M, Wakasugi H, Shimizu K, Satsuma A (2011) Efficient and substrate-specific hydration of nitriles to amides in water by using a CeO_2 catalyst. Chem Eur J 17:11428–11431
43. Honda M, Tamura M, Nakagawa Y, Sonehara S, Suzuki K, Fujimoto K, Tomishige K (2013) Ceria-catalyzed conversion of carbon dioxide into dimethyl carbonate with 2-cyanopyridine. ChemSusChem 6:1341–1344
44. Honda M, Tamura M, Nakagawa Y, Nakao K, Suzuki K, Tomishige K (2014) Organic carbonate synthesis from CO_2 and alcohol over CeO_2 with 2-cyanopyridine: scope and mechanistic studies. J Catal 318:95–107
45. Jung KT, Bell AT (2002) Effects of catalyst phase structure on the elementary processes involved in the synthesis of dimethyl carbonate from methanol and carbon dioxide over zirconia. Top Catal 20:97–105
46. Tamura M, Kishi R, Nakagawa Y, Tomishige K (2015) Self-assembled hybrid metal oxide base catalysts prepared by simply mixing with organic modifier. Nat Commun 6:8580
47. Tamura M, Sawabe K, Tomishige K, Satsuma A, Shimizu K (2015) Substrate-specific heterogeneous catalysis of CeO_2 by entropic effects via multiple interactions. ACS Catal 5:20–26
48. Aresta M, Dibenedetto A, Pastore C, Angelini A, Aresta B, Pápai I (2010) Influence of Al_2O_3 on the performance of CeO_2 used as catalyst in the direct carboxylation of methanol to dimethylcarbonate and the elucidation of the reaction mechanism. J Catal 269:44–52
49. Chen L, Wang S, Zhou J, Shen Y, Zhao Y, Ma X (2014) Dimethyl carbonate synthesis from carbon dioxide and methanol over CeO_2 versus over ZrO_2: comparison of mechanisms. RSC Adv 4:30968–30975
50. Bansode A, Urakawa A (2014) Continuous DMC synthesis from CO_2 and methanol over a CeO_2 catalyst in a fixed bed reactor in the presence of a dehydrating agent. ACS Catal 4:3877–3880
51. Stoian D, Bansode A, Medina F, Urakawa A (2017) Catalysis under microscope: unraveling the mechanism of catalyst de- and re-activation in the continuous dimethyl carbonate synthesis from CO_2 and methanol in the presence of a dehydrating agent. Catal Today in press. 283:2–10. doi: 10.1016/j.cattod.2016.03.038

52. Honda M, Tamura M, Nakao K, Suzuki K, Nakagawa Y, Tomishige K (2014) Direct cyclic carbonate synthesis from CO_2 and diol over carboxylation/hydration cascade catalyst of CeO_2 with 2-cyanopyridine. ACS Catal 4:1893–1896
53. Honda M, Sonehara S, Yasuda H, Nakagawa Y, Tomishige K (2011) Heterogeneous CeO_2 catalyst for the one-pot synthesis of organic carbamates from amines, CO_2 and alcohols. Green Chem 13:3406–3413
54. Tamura M, Honda M, Noro K, Nakagawa Y, Tomishige K (2013) Heterogeneous CeO_2-catalyzed selective synthesis of cyclic carbamates from CO_2 and aminoalcohols in acetonitrile solvent. J Catal 305:191–203
55. Tamura M, Noro K, Honda M, Nakagawa Y, Tomishige K (2013) Highly efficient synthesis of cyclic ureas from CO_2 and diamines by a pure CeO_2 catalyst using a 2-propanol solvent. Green Chem 15:1567–1577
56. Tamura M, Ito K, Honda M, Nakagawa Y, Sugimoto H, Tomishige K (2016) Direct copolymerization of CO_2 and diols. Sci Rep 6:24038
57. Tamura M, Honda M, Nakagawa Y, Tomishige K (2014) Direct conversion of CO_2 with diols, aminoalcohols and diamines to cyclic carbonates, cyclic carbamates and cyclic ureas using heterogeneous catalysts. J Chem Technol Biotechnol 89:19–33
58. Tomishige K, Yasuda H, Yoshida Y, Nurunnabi M, Li B, Kunimori K (2004) Catalytic performance and properties of ceria-based catalysts for cyclic carbonate synthesis from glycol and carbon dioxide. Green Chem 6:206–214
59. Tomishige K, Yasuda H, Yoshida Y, Nurunnabi M, Li B, Kunimori K (2004) Novel route to propylene carbonate: selective synthesis from propylene glycol and carbon dioxide. Catal Letters 95:45–49
60. Du Y, He L-N, Kong D-L (2008) Magnesium-catalyzed synthesis of organic carbonate from 1,2-diol/alcohol and carbon dioxide. Catal Commun 9:1754–1758
61. Du Y, Kong D-L, Wang H-Y, Cai F, Tian J-S, Wang J-Q, He L-N (2005) Sn-catalyzed synthesis of propylene carbonate from propylene glycol and CO_2 under supercritical conditions. J Mol Catal A Chem 241:233–237
62. Huang S, Liu S, Li J, Zhao N, Wei W, Sun Y (2006) Effective synthesis of propylene carbonate from propylene glycol and carbon dioxide by alkali carbonates. Catal Letters 112:187–191
63. Vieville C, Yoo JW, Pelet S, Mouloungui Z (1998) Synthesis of glycerol carbonate by direct carbonatation of glycerol in supercritical CO_2 in the presence of zeolites and ion exchange resins. Catal Lett 56:245–247
64. Aresta M, Dibenedetto A, Nocito F, Pastore C (2006) A study on the carboxylation of glycerol to glycerol carbonate with carbon dioxide: the role of the catalyst, solvent and reaction conditions. J Mol Catal A Chem 257:149–153
65. Dibenedetto A, Angelini A, Aresta M, Ethiraj J, Fragale C, Nocito F (2011) Converting wastes into added value products: from glycerol to glycerol carbonate, glycidol and epichlorohydrin using environmentally friendly synthetic routes. Tetrahedron 67:1308–1313
66. George J, Patel Y, Pillai SM, Munshi P (2009) Methanol-assisted selective formation of 1,2-glycerol carbonate from glycerol and carbon dioxide using nBu_2SnO as a catalyst. J Mol Catal A Chem 304:1–7
67. Li H, Gao D, Gao P, Wang F, Zhao N, Xiao F, Wei W, Sun Y (2013) The synthesis of glycerol carbonate from glycerol and CO_2 over $La_2O_2CO_3$–ZnO catalysts. Catal Sci Technol 3:2801–2809
68. Zhang J, He D (2014) Surface properties of Cu/La_2O_3 and its catalytic performance in the synthesis of glycerol carbonate and monoacetin from glycerol and carbon dioxide. J Colloid Interface Sci 419:31–38
69. Zhang J, He D (2015) Synthesis of glycerol carbonate and monoacetin from glycerol and carbon dioxide over Cu catalysts: the role of supports. J Chem Technol Biotechnol 90:1077–1085
70. Li H, Jiao X, Li L, Zhao N, Xiao F, Wei W, Sun Y, Zhang B (2015) Synthesis of glycerol carbonate by direct carbonylation of glycerol with CO_2 over solid catalysts derived from Zn/Al/La and Zn/Al/La/M (M=Li, Mg and Zr) hydrotalcites. Catal Sci Technol 5:989–1005
71. Liu J, Li Y, Zhang J, He D (2016) Glycerol carbonylation with CO_2 to glycerol carbonate over CeO_2 catalyst and the influence of CeO_2 preparation methods and reaction parameters. Appl Catal A Gen 513:9–18
72. Whiteoak CJ, Kielland N, Laserna V, Escudero-Adan EC, Martin E, Kleij AW (2013) A powerful aluminium catalyst for the synthesis of highly functional organic carbonates. J Am Chem Soc 135:1228–1231

73. Gregory GL, Ulmann M, Buchard A (2015) Synthesis of 6-membered cyclic carbonates from 1,3-diols and low CO_2 pressure: a novel mild strategy to replace phosgene reagents. RSC Adv 5:39404–39408
74. Inoue Y, Itoh Y, Yen IF, Imaizumi S (1990) Palladium(0)-catalyzed carboxylative cyclized coupling of propargylic alcohol with aryl halides. J Mol Catal 60:L1–L3
75. Kim H-S, Kim J-W, Kwon S-C, Shim S-C, Kim T-J (1997) Catalytic formation of carbamates and cyclic carbonates by copper complex of 2,5,19,22-tetraaza[6](1,1′)ferrocenophane-1,5-diene X-ray crystal structure of $[Cu(1)]PF_6$. J Organomet Chem 545–546:337–344
76. Gu Y, Shi F, Deng Y (2004) Ionic liquid as an efficient promoting medium for fixation of CO_2: clean synthesis of α-methylene cyclic carbonates from CO_2 and propargyl alcohols catalyzed by metal salts under mild conditions. J Org Chem 69:391–394
77. Kimura T, Kamata K, Mizuno N (2012) A bifunctional tungstate catalyst for chemical fixation of CO_2 at atmospheric pressure. Angew Chem Int Ed 51:6700–6703
78. Song Q-W, Yu B, Li X-D, Ma R, Diao Z-F, Li R-G, Li W, He L-N (2014) Efficient chemical fixation of CO_2 promoted by a bifunctional Ag_2WO_4/Ph_3P system. Green Chem 16:1633–1638
79. Yamada W, Sugawara Y, Hau MC, Ikeno T, Yamada T (2007) Silver-catalyzed incorporation of carbon dioxide into propargylic alcohols. Eur J Org Chem 2007:2604–2607
80. Yang Z-Z, Zhao Y, Zhang H, Yu B, Ma Z, Ji G, Liu Z (2014) Fluorinated microporous organic polymers: design and applications in CO_2 adsorption and conversion. Chem Commun 50:13910–13913
81. Jiang HF, Wang AZ, Liu HL, Qi CR (2008) Reusable polymer-supported amine-copper catalyst for the formation of α-alkylidene cyclic carbonates in supercritical carbon dioxide. Eur J Org Chem 2008:2309–2312
82. Tang X, Qi C, He H, Jiang H, Ren Y, Yuan G (2013) Polystyrene-supported N-heterocyclic carbene-silver complexes as robust and efficient catalysts for the reaction of carbon dioxide and propargylic alcohols. Adv Synth Catal 355:2019–2028
83. Yang Z, Yu B, Zhang H, Zhao Y, Chen Y, Ma Z, Ji G, Gao X, Han B, Liu Z (2016) Metalated mesoporous poly(triphenylphosphine) with Azo functionality: efficient catalysts for CO_2 conversion. ACS Catal 6:1268–1273
84. Song QW, Chen WQ, Ma R, Yu A, Li QY, Chang Y, He LN (2015) Bifunctional silver(I) complex-catalyzed CO_2 conversion at ambient conditions: synthesis of α-methylene cyclic carbonates and derivatives. ChemSusChem 8:821–827
85. Cui M, Qian Q, He Z, Ma J, Kang X, Hu J, Liu Z, Han B (2015) Synthesizing Ag nanoparticles of small size on a hierarchical porosity support for the carboxylative cyclization of propargyl alcohols with CO_2 under ambient conditions. Chem Eur J 21:15924–15928
86. Qiu J, Zhao Y, Wang H, Cui G, Wang J (2016) AgX@carbon (X=Br and I) as robust and efficient catalysts for the reaction of propargylic alcohols and CO_2 to carbonates under ambient conditions. RSC Adv 6:54020–54026
87. Hu J, Ma J, Zhu Q, Qian Q, Han H, Mei Q, Han B (2016) Zinc(II)-catalyzed reactions of carbon dioxide and propargylic alcohols to carbonates at room temperature. Green Chem 18:382–385
88. Kayaki Y, Yamamoto M, Ikariya T (2009) N-heterocyclic carbenes as efficient organocatalysts for CO_2 fixation reactions. Angew Chem Int Ed 48:4194–4197
89. Wang Y-B, Wang Y-M, Zhang WZ, Lu X-B (2013) Fast CO_2 sequestration, activation, and catalytic transformation using N-heterocyclic olefins. J Am Chem Soc 135:11996–12003
90. Wang Y-B, Sun D-S, Zhou H, Zhang W-Z, Lu X-B (2014) Alkoxide-functionalized imidazolium betaines for CO_2 activation and catalytic transformation. Green Chem 16:2266–2272
91. Minakata S, Sasaki I, Ide T (2010) Atmospheric CO_2 fixation by unsaturated alcohols using tBuOI under neutral conditions. Angew Chem Int Ed 49:1309–1311
92. Vara BA, Struble TJ, Wang W, Dobish MC, Johnston JN (2015) Enantioselective small molecule synthesis by carbon dioxide fixation using a dual Brønsted acid/base organocatalyst. J Am Chem Soc 137:7302–7305
93. Wang JL, He LN, Dou XY, Wu F (2009) Poly(ethylene glycol): an alternative solvent for the synthesis of cyclic carbonate from vicinal halohydrin and carbon dioxide. Aust J Chem 62:917–920
94. Reithofer MR, Sum YN, Zhang Y (2013) Synthesis of cyclic carbonates with carbon dioxide and cesium carbonate. Green Chem 15:2086–2090

Top Curr Chem (Z) (2017) 375:50
DOI 10.1007/s41061-017-0136-5

REVIEW

Recent Developments in the Synthesis of Cyclic Carbonates from Epoxides and CO_2

Hendrik Büttner[1] · Lars Longwitz[1] · Johannes Steinbauer[1] · Christoph Wulf[1] · Thomas Werner[1]

Received: 13 December 2016 / Accepted: 27 March 2017 / Published online: 24 April 2017
© Springer International Publishing Switzerland 2017

Abstract The use of CO_2 as a C1 building block will be of essential importance in the future. In this context the synthesis of cyclic carbonates from epoxides and CO_2 gained great attention recently. These products are valuable compounds in a variety of chemical fields. The development of new catalysts and catalytic systems for this atom-economic, scalable, and industrially relevant reaction is a highly active research field. Over the past 17 years great advances have been made in this area of research. This chapter covers the survey of the important known classes of homogeneous catalysts for the addition of CO_2 to epoxides. Besides pioneering work, recent developments and procedures that allow this transformation under mild reaction conditions (reaction temperatures of $\leq$100 °C and/or CO_2 pressures of 0.1 MPa) are especially emphasized.

Keywords CO_2 · Carbon dioxide · Cyclic carbonates · 1,3-Dioxolan-2-one · Catalysis · Homogeneous catalysis · Organocatalysis · Transition metal catalysis · Onium salts · Ionic liquids · Green chemistry · Main group metal catalysis · Epoxide

1 Introduction

Until now, the availability of raw materials and their origin, i.e. fossil resources, were not a major concern. However, this is changing due to an increasing awareness of the public with respect to sustainability, as well as economic constraints. In this respect, establishing an economy based on methanol and carbon dioxide as a

---

Chapter 3 was originally published as Büttner, H., Longwitz, L., Steinbauer, J., Wulf, C. & Werner, T. Top Curr Chem (Z) (2017) 375: 50. DOI 10.1007/s41061-017-0136-5.

✉ Thomas Werner
thomas.werner@catalysis.de

[1] Leibniz Institute for Catalysis, Albert-Einstein-Str. 29a, 18059 Rostock, Germany

feedstock is a long-standing challenge, as well as a fascinating vision [1–4]. In addition, part of global warming is attributed to increasing carbon dioxide levels in the atmosphere, which is mainly caused by the thermal use of fossil fuels [5]. On 9 May, 2013, the daily average concentration of CO_2 in the atmosphere at Mauna Loa Observatory (Hawaii) surpassed 400 parts per million for the first time in human history [6]. In recent years these concerns resulted in several strategies to reduce the atmospheric CO_2 concentration. Besides the prevention of CO_2 emissions, which is the most reasonable long-term approach, the use of CO_2 as a readily available, non-toxic, and cost efficient C1 source received considerable interest as an alternative feedstock for the chemical industry [7–10]. In particular, the addition of CO_2 to epoxides is a frequently studied reaction, which is used even on an industrial scale for the synthesis of cyclic carbonates and polycarbonates (Scheme 1) [11–13]. The synthesis of cyclic carbonate is of particular interest due the wide range of possible applications, e.g. as solvents, electrolytes, monomers for polymer synthesis, synthetic building blocks, fine chemicals, and industrial lubricants [14–18].

Various other approaches have been reported for the synthesis of cyclic carbonates (Scheme 2). As early as 1883, the reaction of highly toxic phosgene and ethylene glycol to produce ethylene carbonate was reported by Nemirowsky [19]. Besides phosgene, various other C1 building blocks such as dimethyl carbonate [20, 21], urea [22–24], CO [25–27], and CO_2 [28–30] have been converted with diols to yield cyclic carbonates. Moreover, halohydrins [31, 32], propargyl alcohols [33–35], and even alkenes have been used as starting materials [36–38]. For the conversion of alkenes the substrate is either epoxidized or converted to a halohydrin in the first step and subsequently converted with CO_2.

However, the most attractive route, especially with respect to green and sustainable chemistry, is the atom-economic and redox neutral addition of CO_2 to epoxides [39, 40]. This reaction is currently intensively investigated and great advances have been made over the past 17 years. The interest in this up to date and highly active research area can be illustrated by the dramatic increase of the number of publications concerning the synthesis of cyclic carbonates since 2000 (Fig. 1).

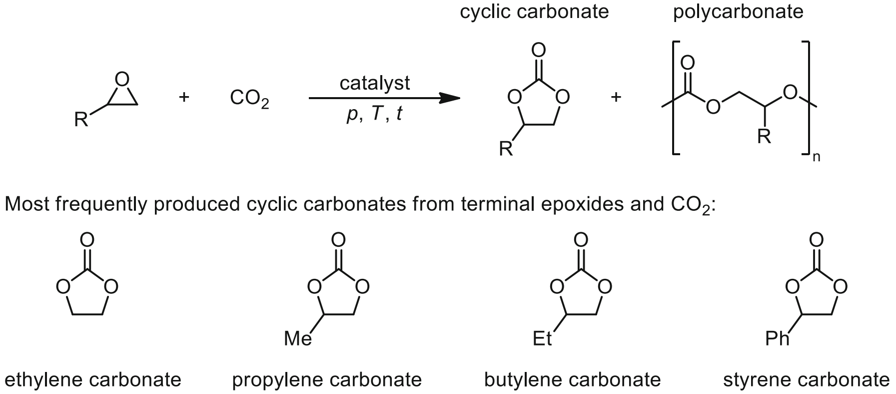

Scheme 1 Cycloaddition of CO_2 to epoxides yielding cyclic carbonates and/or polycarbonates

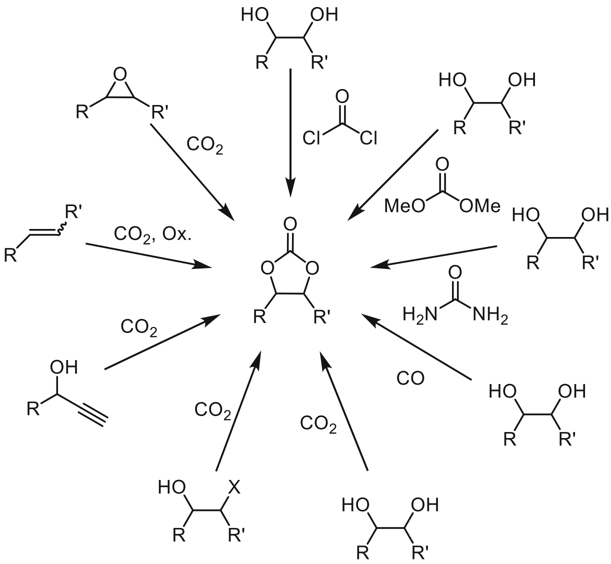

Scheme 2 Synthetic routes for the formation of cyclic carbonates

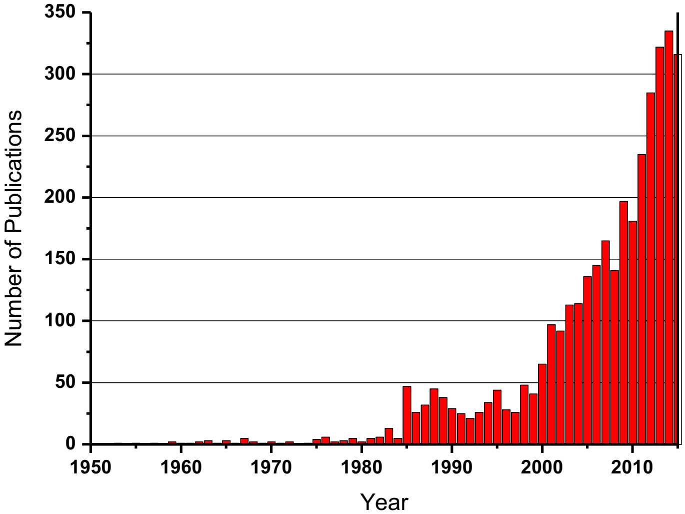

Fig. 1 Number of publications between 1950 and 2015 for a structural search (synthesis of a 1,3-dioxolan-2-one substructure) in Scifinder®

During this time, several excellent general reviews [12, 14, 41–44] on different aspects, as well as surveys on catalysts and catalytic systems including organocatalysts [45, 46], ionic liquids [47–51], metal organic frameworks [52, 53], and homogeneous metal-based catalysts [54–57] for this transformation have been reported. This review covers the most important classes of homogeneous catalysts and catalytic systems for the conversion of epoxides and CO_2. Besides highlighting pioneering work, recent developments and procedures that allow this transformation under mild reaction conditions (reaction temperatures of $\leq$100 °C and/or CO_2 pressures of 0.1 MPa) are especially emphasized. Thereby, this review is divided into three main sections based on the catalyst category: organocatalysts including ionic liquids, privileged metal complex catalysts, and miscellaneous catalytic systems based on transition metals and main group elements.

2 Organocatalysts

2.1 Ammonium Salt Catalysts

In 1956, Lichtenwalter and Cooper reported that quarternary ammonium halides were active catalysts for the synthesis of cyclic carbonates [58]. They described tetrabutylammonium bromide (TBAB) and tetraethylammonium bromide as easily accessible and most active in the synthesis of ethylene carbonate starting from ethylene oxide (EO) and CO_2 (Table 1, entry 1). Notably, this catalyst showed higher activity and stability compared to other systems known at that time [59, 60]. Subsequently, numerous organo- and metal catalyst systems based on quaternary ammonium salts have been reported. In general, tetrabutylammonium salts can be considered the most frequently used (co-)catalysts in the addition of CO_2 to epoxides.

In 2002 Caló et al. reported the use of tetrabutylammonium halides as solvents and catalysts in the synthesis of cyclic carbonates [61]. A mixture of TBAB and tetrabutylammonium iodide (TBAI) in a ratio of 1:1 w/w allowed full conversion of epoxides, e.g. styrene oxide (SO) into cyclic carbonates. Remarkably, TBAI catalyzed the reaction even at low CO_2 pressure (0.1 MPa) and a reaction temperature of 60 °C (entry 2). Recently, Crousse studied hydrofluoroethers as solvents in combination with TBAI [62]. The reactions were realized under mild conditions at 80 °C and atmospheric pressure or 0.5 MPa. The hydrofluoroethers allowed the enhanced delivery of CO_2 towards the reagents and facilitated the reaction, in comparison to classical organic solvents. In particular, **1** was an excellent solvent for the synthesis of cyclic carbonates (entry 3). Endo et al. described simple hydro iodides of secondary and primary amines as effective catalysts even under mild conditions [63]. Detailed investigations revealed that the activity was highly affected by the nature of the counter anion. The catalytic activity increased with increasing bulkiness of the substituents on the ammonium nitrogen atom, as well as with increasing basicity of the parent amine. Dicyclohexyl ammonium iodide (**2**) was the best catalyst among the ammonium salts investigated

Table 1 Selected homogeneous ammonium salt-based catalytic systems

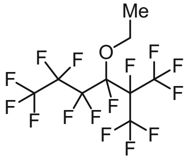

1

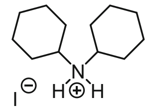

2

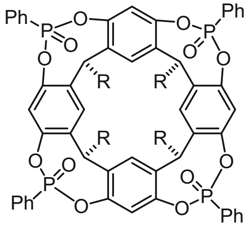

3

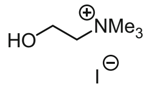

4

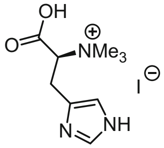

5

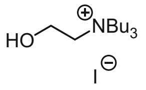

6

Entry	Cat. (mol%)	Sub. (mmol)	*T* (°C)	*p* (MPa)	*t* (h)	Yield (%)	References
1	TBAB (1)	EO	200	3.4[a]	0.5	97	[58]
2	TBAI (10)[b]	SO (250)	60	0.1	22	80	[61]
3[c]	TBAI (5)	SO (1)	80	0.5	6	91	[62]
4[d]	**2** (5)	SO (1)	45	0.1	24	84	[63]
5[e]	BnBr (1)	SO (5)	120	0.1	4	86	[64]
6	$[Bu_4N]OH$ (1)	SO (10)	120	1	24	88	[65]
7[f]	$[Me_4N]I$ (1)	SO (5)	100	0.1	24	92	[67]
8[g]	**4** (6)	SO (14.3)	85	1	6	99	[68]
9	**5** (0.28)	SO (35.5)	120	0.1	6	95	[69]
10	**6** (5)	SO (16)	45	1	18	89	[70]

[a] Initial CO_2 pressure at 40 °C before heating to 200 °C

[b] Amount given in wt%

[c] Hydrofluoroether **1** was used as solvent

[d] NMP was used as solvent

[e] 500 mol% DMF were employed

[f] 1 mol% cavitand **3**

[g] EtOH was used as solvent

(entry 4). Notably, for some examples excellent yields were obtained even at 24 °C even though only 20% yield was obtained at this temperature for styrene carbonate.

The use of benzylbromide (1 mol%) in combination with DMF (500 mol%) as a very simple catalyst system at low CO_2 pressure (0.1 MPa) has also been reported (entry 5) [64]. However, high reaction temperatures >100 °C were required. Interestingly, Ema and co-workers recently reported quaternary ammonium hydroxide as metal-free and halogen-free catalyst for the synthesis of cyclic carbonate (entry 6) [65]. Tetrabutylammonium hydroxide was converted into the bicarbonate which was the catalytic active species. DFT calculations revealed the lowest-energy process in which the rate determining step is the initial ring-opening reaction by the bicarbonate and subsequent CO_2 addition. Remarkably, the tetrabutylammonium cation carries the positive charges on the hydrogen atoms, but not on the central nitrogen atom. The positively charged hydrogen atoms form an anion-binding site are capable of stabilizing various anionic transition states and intermediates.

Tetramethylammonium halides have never shown any activity in the coupling of CO_2 and epoxides even under harsh reaction conditions [66]. Remarkably, Mirabaud et al. reported the use of host–guest systems consisting of tetramethylammonium halides and cavitand **3** [67]. Interestingly, the usually unreactive salts $[Me_4N]X$ could efficiently be activated through host–guest chemistry. In this system $[Me_4N]I$ showed the highest activity even at low CO_2 pressure (0.1 MPa) and low catalyst loading (1 mol%) (entry 7).

Functionalized ammonium salts bearing a hydrogen donor group in the side chain have been studied as catalysts. In this respect, choline iodide (**4**) has been reported as an efficient bifunctional catalyst in ethanol as solvent (entry 8) [68]. Park and co-workers described the microwave-assisted one pot-synthesis of amino acid based ionic liquids in water [69]. These compounds, e.g. **5** exhibit good activities for the conversion of styrene oxide even at low CO_2 pressure (0.1 MPa, entry 9). Previously the same group reported the use of amino acids with water as additive as a metal- and halide-free catalyst system [71]. More recently, Büttner et al. reported the use of bifunctional ammonium salt **6** as efficient catalyst for the addition of CO_2 to epoxides achieving turnover numbers (TONs) up to 693 and initial turnover frequencies (TOFs) of up to 392 h^{-1} [70]. At higher catalyst loading (5 mol%) this catalyst gave good conversion and yields even at 45 °C (entry 10). Based on the obtained results and in accordance with previous reports the authors proposed the dual activation of the epoxide as shown in Scheme 3 [45, 46].

The epoxide is activated by hydrogen bonding of the catalyst. A nucleophilic substitution reaction of the iodide forms an alkoxide. Subsequent addition of CO_2 and intramolecular nucleophilic substitution forms the cyclic carbonate and liberates catalyst **6**.

Concurrent to the development of homogeneous catalytic systems, the immobilization of catalysts on organic and inorganic supports has been intensively studied over the past decades. The majority of those systems operates under drastic conditions (reaction temperatures $\geq$100 °C and/or at CO_2 pressures >0.1 MPa). For example He and co-workers used soluble polyethylene glycols (PEGs), e.g. PEG6000 for the immobilization of quaternary ammonium salts which proved to be efficient and recyclable catalysts under supercritical conditions [72]. In the presence of 0.5 mol% **7** propylene oxide (PO) was converted with CO_2 to yield 98% propylene carbonate (Table 2, entry 1).

However, systems that operate efficiently under milder conditions are comparatively rare. In 1993 Nishikubo and co-workers reported insoluble polystyrene supported quaternary onium salts as recyclable catalysts for the addition of CO_2 to epoxides [76]. In further investigations they observed that the activation energy for

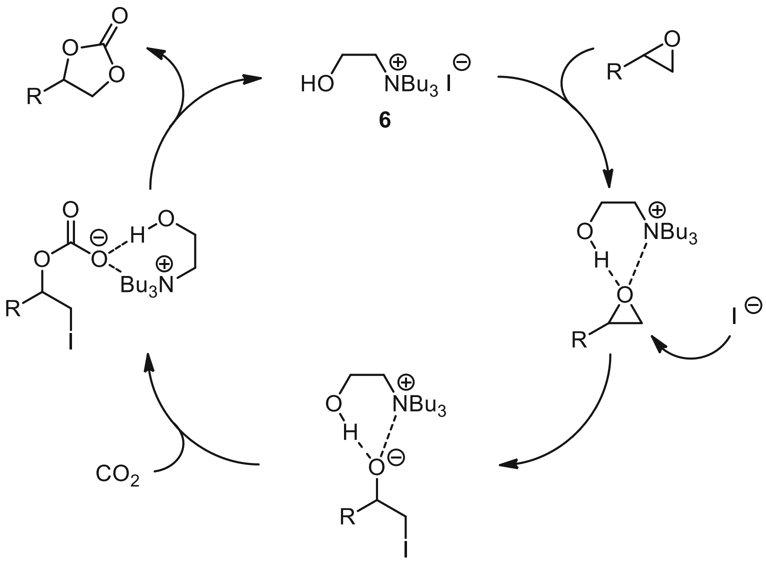

Scheme 3 Proposed mechanism for the conversion of epoxides with CO_2 in the presence of bifunctional ammonium salt **6** [70]

Table 2 Selected immobilized ammonium salts as catalysts

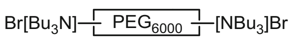

7

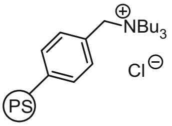

8

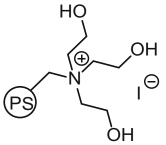

9

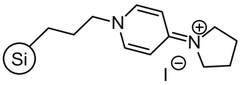

10

Entry	Cat. (mol%)	Sub. (mmol)	*T* (°C)	*p* (MPa)	*t* (h)	Yield (%)	References
1	**7** (0.5)	PO (28.6)	120	8	6	98	[72]
2[a]	**8** (1)	PGE[b] (4)	90	0.1	5	92	[73]
3	**9** (2)	SO	90	1	4	93	[74]
4	**10** (0.9)	SO (4.4)	100	0.1	20.5	89	[75]

[a] Dimethylacetamide was used as solvent

[b] Phenyl glycidyl ether

soluble supported catalysts is significantly lower compared to their insoluble counterpart [73]. Thus, soluble catalyst **8** gave excellent yield on phenylglycidyl carbonate with low catalyst loading (1 mol%) and low pressure (0.1 MPa) of CO_2 at 90 °C (entry 2). More recently, Kohrt et al. reported polystyrene and silica supported bifunctional ammonium salts as efficient catalysts for the conversion of various epoxides under mild conditions. Notably, the polystyrene supported catalyst **9** was more active but showed partial decomposition during recycling experiments (entry 3) [74]. In contrast the respective silica supported catalyst was stable over 13

Table 3 Selected homogeneous phosphonium salt-based catalytic systems

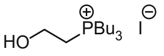

11

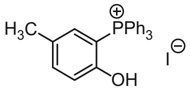

12

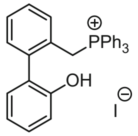

13

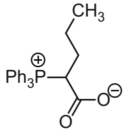

14

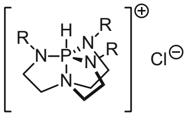

15a, R= -CH$_2$-*t*Bu

Entry	Cat. (mol%)	Sub. (mmol)	*T* (°C)	*p* (MPa)	*t* (h)	Yield (%)	References
1	[Ph_3PEt]I (0.1)	EO (400)	221	8.3	4	91	[77]
2[a]	[Ph_3PBu]I (0.5)	PO (200)	125	2	1	95	[78]
3[b]	[Ph_3PMe]I (5)	PGE (1)	25	0.1	24	99	[79]
4	**11** (2)	PO (34.4)	90	1	3	99	[80]
5[c]	**12** (15)	SO (0.2)	120	0.1	12	91	[81]
6	**13** (1)	SO (10)	60	0.1	24	92	[82]
7	**14** (5)	PO (10)	25	0.1	6	90	[83]
8	**15a** (1)	SO (5.0)	100	0.1	7	50	[84]

[a] Water (33.5 mol%) was used as co-catalyst/solvent

[b] 1-Methoxy-2-propanol was used as solvent

[c] Chlorobenzene was used as solvent

cycles. The use of silica supports has also been reported, e.g. silica supported aminopyridinium iodide **10** catalyzed the conversion of styrene oxide with CO_2 under atmospheric pressure (entry 4) [75].

2.2 Phosphonium Salt Catalysts

Already in the early 1960s simple phosphonium salts were used for the synthesis of ethylene carbonate (Table 3, entry 1) [77]. Zhang and co-workers showed that the presence of water remarkably improved the activity of various onium salts [78]. The activity order of cations was $PPh_3Bu^+ > Bu_4N^+ \approx [Bmim]^+ > K^+ > Na^+$. The activity of anions varies in the order $I^- > Br^- > Cl^- > PF_6^- > BF_4^-$ under protic conditions (presence of water) while it was $Br^- > Cl^- > I^- > PF_6^- \approx BF_4^-$ without water. Thus, [Ph_3PBu]I proved to be the most active catalyst in the presence of water (entry 2). The turnover frequency of the reaction in water (194 h^{-1}) was about four times higher compared to the reaction without water (48 h^{-1}).

More recently, several phosphonium-based catalysts have been reported, which show excellent activity below 100 °C and/or low CO_2 pressure. In 2013 Endo and co-workers reported phosphonium iodides as efficient catalysts for the synthesis of phenyl glycidyl carbonate (PGC) even at low CO_2 pressure (0.1 MPa) and ambient temperature (entry 3) [79]. It was observed that the nature of the solvent had a significant effect on the catalyst performance. Protic solvents such as 1-methoxy-2-propanol proved to be most suitable, which was attributed to the activation of the epoxide by hydrogen bonding. Furthermore, the impact of the counter ions was studied. If no nucleophile was present the formation of the desired cyclic carbonates

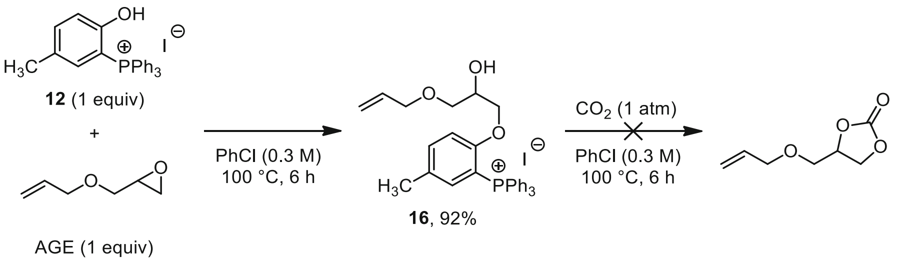

Scheme 4 Formation of adduct **16** from **12**, as well as the attempt to convert **16** with CO_2 [81]

was not observed. The activity for counter ions under protic polar conditions was identical to the reported results by Zhang and co-workers [78]. Werner and co-workers reported a bifunctional phosphonium salt catalyst **11** (entry 4) [80, 85]. The introduction of the alcohol group as a hydrogen bond donor functionality in the catalyst structure significantly increased the activity of the catalyst compared to simple tetrabutyl phosphonium halides. This is attributed to epoxide activation by hydrogen bonding in line with the respective bifunctional ammonium catalyst **6** (Scheme 3). Even at low reaction temperatures of 45 °C the reaction operates smoothly and the catalyst can simply be recovered by organic solvent nanofiltration [86].

Most recently, Toda and Suga used phenolic phosphonium salts in cyclic carbonate formation from epoxides and CO_2 (entry 5) [81]. In the presence of 15 mol% **12** at 120 °C and atmospheric CO_2 pressure, styrene carbonate was produced in 91% yield. Interestingly, adduct **16** was observed after trying to recycle the phenolic phosphonium catalyst **12** (Scheme 4). This adduct could be prepared by converting allyl glycidyl ether (AGE) with **12**. Even though **16** does not form the desired cyclic carbonate with CO_2, it is assumed that this adduct generated in situ can catalyze the overall process of cyclic carbonate formation. Werner and co-workers reported bifunctional catalysts based on a phosphonium salts bearing a simple phenolic moiety for the synthesis of oleochemical carbonates from CO_2 and renewables [87].

Recently, Shirakawa and co-workers reported a bifunctional arylic phosphonium salt catalyst **13** (entry 6) [82]. A distinct trend regarding the position of the alcohol moiety and the yield was observed (the yield decreased in the order *ortho* > *para* > *meta*). If the alcohol moiety was protected by a methyl group the yield decreased significantly from 80 to 16% emphasizing the crucial involvement of the acidic phenol moiety. In addition, chiral bifunctional binaphthyl catalysts were developed and tested in kinetic resolution reactions. However, an enantiomeric excess of 13% was not exceeded.

Zhou and Lu developed a halide-free organocatalyst based on phosphorus ylides such as **14** (entry 7) [83]. In contrast to the organocatalysts **11–13**, the catalytic reaction of an epoxide and CO_2 in the presence of the P-ylide-CO_2-adduct **14** involves the direct activation of CO_2. Mechanistic in situ FTIR experiments revealed that in the absence of a CO_2 atmosphere the formation of cyclic carbonate

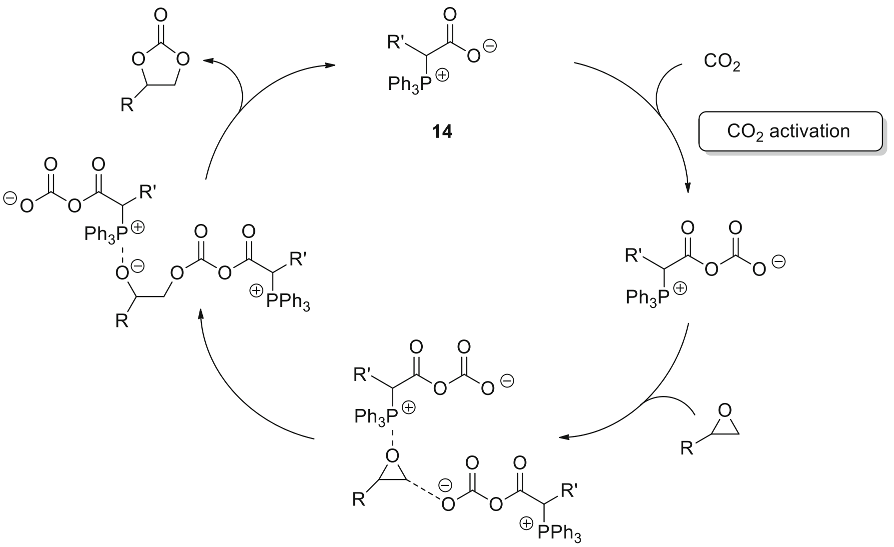

Scheme 5 Proposed dual activation of CO$_2$ and epoxides by **14** in the synthesis of cyclic carbonates. [83]

did not occur. However, as soon as CO$_2$ was introduced to the reaction system the specific PC band at $\lambda^{-1} = 1800\ \mathrm{cm}^{-1}$ increased gradually. The authors attributed this fact to a direct activation of CO$_2$ by the P-ylide-CO$_2$-adduct **14**. Moreover, kinetic studies were performed to clarify the reaction mechanism. These experiments revealed a second order dependence on catalyst concentration indicating a dual activation by the phosphonium and carboxylate moieties (Scheme 5).

In addition, if enantiopure epoxides were employed retention of the stereochemistry was observed and enantiomeric excesses >99% for cyclic carbonates were obtained.

Dufaud and Martinez studied azaphosphatrane **15a** as catalyst for the cycloaddition of epoxides and CO$_2$ at ambient pressure (entry 8) [84]. Mechanistic studies revealed first order dependence on CO$_2$, styrene oxide, and catalyst **15a** concentrations. The rate-determining step of this reaction is the activation of CO$_2$. Carbon dioxide inserts into the P–N bond forming a tricyclic phosphoryl–carbamate structure which is highly reactive and sensitive to hydrolysis. The epoxide can be activated by the hydrogen of the P–H center. Overall, a dual activation of CO$_2$ and epoxide is reported. Interestingly, the stability and activity increases with the bulkiness of the substituents at the nitrogen center. These bulky groups act as protecting groups and prevent degradation of the activated phosphoryl–carbamate structure. Among the tested catalysts, neo-pentyl substituents in **15a** led to an active and stable catalyst which achieved a turnover number of >1000 after 4 days for the conversion of epichlorohydrin. Further investigations were carried out to evaluate the effect of increasing the bulkiness of the R groups in catalyst **15** [84, 88, 89]. A molecular cavity of the azaphosphatranes was anticipated which plays a crucial role for epoxide activation of the P–H center.

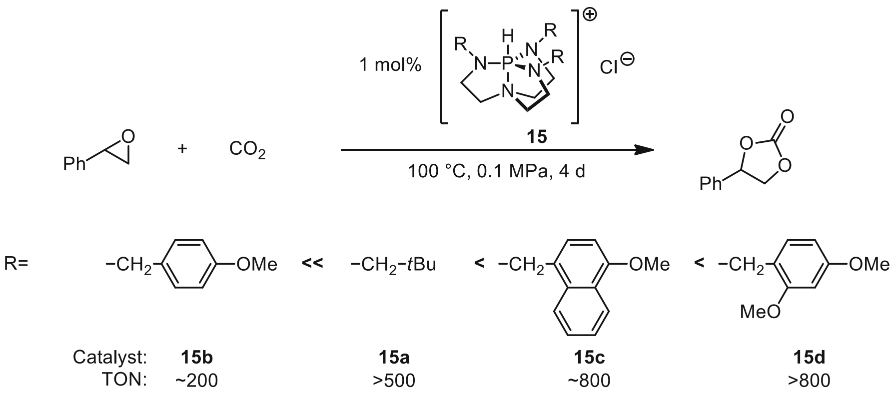

Scheme 6 TONs for the azaphosphatranes in the reaction of SO and CO_2 at 100 °C, 0.1 MPa, and 4 days using 1 mol% catalyst **15** [84, 88, 89]

High catalytic activity was obtained if the substituents at the nitrogen atoms in **15b** were replaced by the napthyl analogues –CH_2–*p*OMe-naphtyl (**15c**, Scheme 6).

The catalytic activity increased due to changes in the local substitution of the aromatics. This was attributed to the tailor-made cavity for epoxide activation by the P–H center and is related rather to available space around the catalytic center than to electronic properties. The catalyst **15d** reached a TON of 800 after 4 days, which was four times higher than obtained for **15b**.

2.3 Imidazolium Salt Catalysts

In the early 2000s, epoxides were converted with CO_2 in the presence of imidazolium salts and imidazolium-based ionic liquids (ILs) [90, 91]. Notably, this was achieved even under halide-free conditions and temperatures below 100 °C, even though in those cases only low conversions were achieved [90]. In the presence of **17** a TOF of up to 515 h^{-1} was obtained under supercritical conditions (Table 4, entry 1) [91].

In 2008 Zhang and co-workers were the first to report the use of hydroxyl-functionalized imidazolium-based ILs as catalyst for this reaction [92]. Among the investigated salts compound **18** was the most active (entry 2). The superior activity of the hydroxyl-functionalized IL was addressed to the activation of the epoxide through hydrogen bonding which facilitates the nucleophilic attack of the halide anion (Scheme 7). More recently, Denizalti reported hydroxyl-functionalized imidazolium iodide **19** as highly efficient catalyst even at moderate reaction temperatures of 60 °C (entry 3) [93].

Interestingly, Cokoja and co-workers showed that simple imidazolium bromides can catalyze the addition of CO_2 to epoxides even under mild reaction conditions [94]. The acidic C_2 proton of the imidazolium salt activates the epoxide by hydrogen interaction which was observed in FTIR studies [96].

Table 4 Selected imidazolium salts as homogeneous catalysts

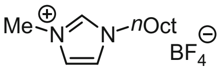

17

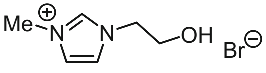

18

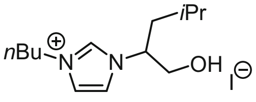

19

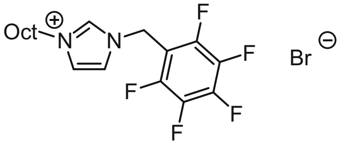

20

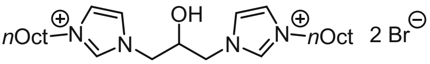

21

Entry	Cat. (mol%)	Sub. (mmol)	*T* (°C)	*p* (MPa)	*t* (h)	Yield (%)	References
1	**17** (1.7)	PO (30)	100	14	0.08	98	[91]
2	**18** (1.6)	PO (200)	125	2	1	99	[92]
3	**19** (2)	PO (10)	60	0.5	8	>99	[93]
4	**20** (10)	PO (10)	70	0.4	22	91[a]	[94]
5	**21** (5)	PO (10)	70	0.4	16	95[a]	[95]

[a] The conversion is given ($\geq$99% selectivity)

Consequently, increasing the acidity of imidazolium proton by introducing electron withdrawing substituents to the nitrogen atoms further increased the activity. Thus, catalyst **20** showed higher activity compared to the respective non-fluorinated salt which gave only 73% conversion under the same conditions as described in entry 4. Subsequently, the same group introduced hydroxyl-functionalized bisimidazolium salt **21** which showed even higher activity under the same conditions (entry 5) [95]. DFT calculations showed that intermediate A is approximately 13 kcal mol^{-1} lower in energy compared to intermediate B of the unfunctionalized catalyst (Fig. 2).

2.4 Amidine-Based Catalysts

1,8-Diazabicyclo[5.4.0]undec-7-ene (DBU, **22**) is a frequently employed (co-)catalyst in CO_2 fixation reactions. He and co-workers studied Lewis basic ionic liquids as catalysts for the conversion of propylene oxide with CO_2 [97]. Both the cation and the anion had a strong impact on the catalytic activity. $HDBU^+$ in combination with Cl^- showed excellent results at low catalyst loading (1 mol%), but high reaction temperatures (140 °C) while DBU alone was found to be inactive. The tertiary nitrogen in the cation has the potential to form a carbamate species with CO_2 , which can be considered an activated form of CO_2 [98, 99]. Moreover, the epoxide might be activated by a hydrogen bond formed between the oxygen of the epoxide and the proton attached to the ammonium nitrogen. In 2012 Endo et al.

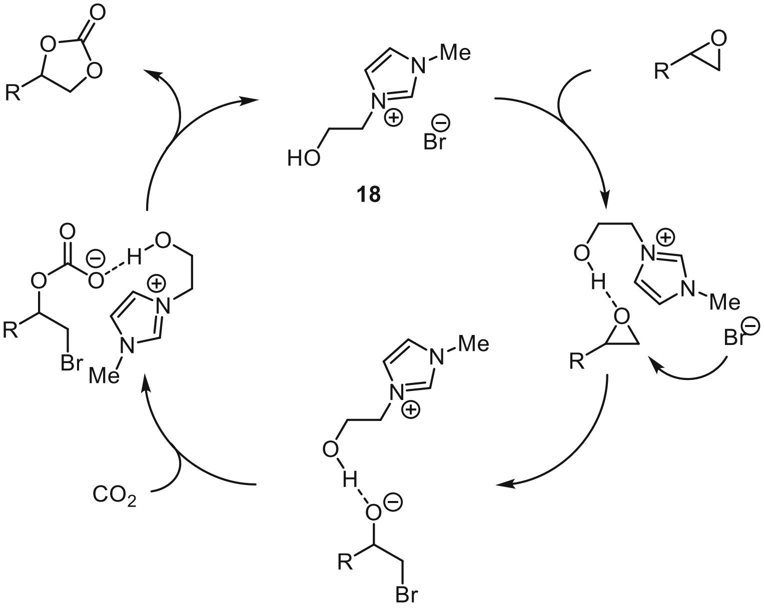

Scheme 7 Proposed mechanism according to Zhang et al., for the conversion of epoxides with CO_2 in the presence of bifunctional imidazolium salt **18** [92]

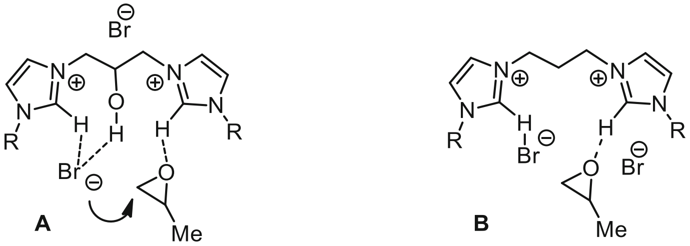

Fig. 2 Activation of the epoxide via hydrogen bonding by catalyst with hydroxyl group (**a** *left*) and without hydroxyl group in the bridge (**b** *right*) [95]

reported adduct **23** as an efficient catalyst for the synthesis of cyclic carbonates at room temperature and atmospheric pressure of CO_2 (Table 5, entry 1) [100].

Coulembier et al. described the iodine DBU adduct **22**·I_2 as a dual catalyst (entry 2) [101]. Most recently, Hirose and co-workers reported DBU in combination with benzyl bromide to catalyze the addition of CO_2 to various epoxides under similar conditions. The initial step is the in situ formation of the catalytic active species **24** (entry 3) [102]. Weiss and co-workers employed amidinium iodide **25** as catalyst in the synthesis of cyclic carbonates in amidinium carbamate **26** as reaction media (entry 4) [103]. Compound **26** is a reversible, room temperature ionic liquid and easily prepared by exposing a 1:1 mixture of the respective amidine and primary

Table 5 Selected amidine-based catalytic systems

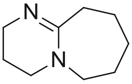

22

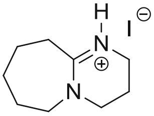

23

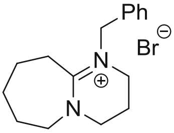

24

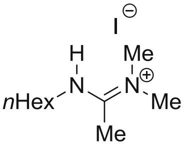

25

Entry	Cat. (mol%)	Sub. (mmol)	T (°C)	p (MPa)	t (h)	Yield (%)	References
1	**23** (5)	SO	25	0.1	24	64	[100]
2	**22**·I_2 (5)	BO	65	0.1	4.75	96[a]	[101]
3	**24** (5)	SO (6)	65	0.1	22	82	[102]
4[b]	**25** (2)	PGE (0.7)	50	2.5	8	99	[103]

[a] The conversion is given

[b] Room temperature ionic liquid **26** was used as solvent

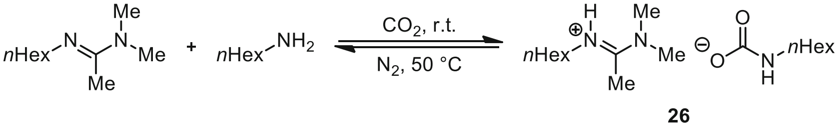

Scheme 8 Synthesis of reversible, room temperature ionic liquid **26** [103]

amine to CO_2 gas (Scheme 8). Notably, no reaction was observed in the absence of a catalyst **25**.

2.5 Carbene-Based Catalysts

In 2008 Lu and co-workers studied the thermal stability and catalytic activity of CO_2 *N*-heterocyclic carbene (NHC-CO_2) adducts [104]. They observed that in the presence of free CO_2 the decomposition of NHC-CO_2 adducts can be significantly inhibited. However, upon addition of PO the formation of propylene carbonate was detected. Notably, adduct **27** proved to be an efficient organocatalyst for the addition of CO_2 to propylene oxide, as well as other epoxides (Table 6, entry 1). Subsequently, the same group reported the immobilization of **27** on MCM-41. Even though longer reaction times are required, the immobilized catalyst gave comparable yields and was recovered by simple filtration [105]. The authors proposed the in situ activation of CO_2 and subsequent addition to the epoxide followed by the ring-closing, which liberates the product and the carbene catalyst **27** (pathway A, Scheme 9). This is one of the rare examples of direct organocatalyzed CO_2 activation in this reaction and subsequent conversion with epoxides which operates even under halogen- and solvent-free conditions. Furthermore, Ajitha et al. studied various pathways for NHC-catalyzed addition of CO_2 to epoxides by means of DFT calculations [106]. They suggest that the favored pathway B proceeds via a S_N2 anti-attack of the carbene to the least-substituted carbon of a CO_2-epoxide complex.

Table 6 Selected carbene-based catalytic systems

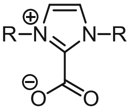

27

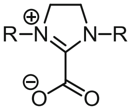

28

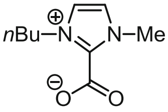

29

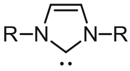

30

R= 2,6-diisopropylphenyl

Entry	Cat. (mol%)	Co-cat. (mol%)	Sub. (mmol)	*T* (°C)	*p* (MPa)	*t* (h)	Yield (%)	References
1[a]	**27** (0.5)	–	PO (50)	120	2.0	24	100	[104]
2	**28** (2)[b]	$ZnBr_2$ (2)	SO (17.5)	80	0.1[c]	24	88	[107]
3	**29** (3)[d]	$ZnBr_2$ (3)	SO (5)	r.t.	0.1	2	98	[108]
4	**30** (1)	KI/18C6 (1)[e]	BO (25)	90	1.0	24	91	[109]

[a] CH_2Cl_2 was used as solvent

[b] In situ generation from *N,N'*-(2,6-diisopropylphenyl)dihydro-imidazolium chloride and K_2CO_3 (1:1). DMSO was used as solvent

[c] Argon/CO_2 = 1:1

[d] In situ generation from [BMIM]Br and 3 mol% K_2CO_3. [Bmim]Br was used as solvent

[e] KI:18-crown-6 ether (18C6) = 1:1

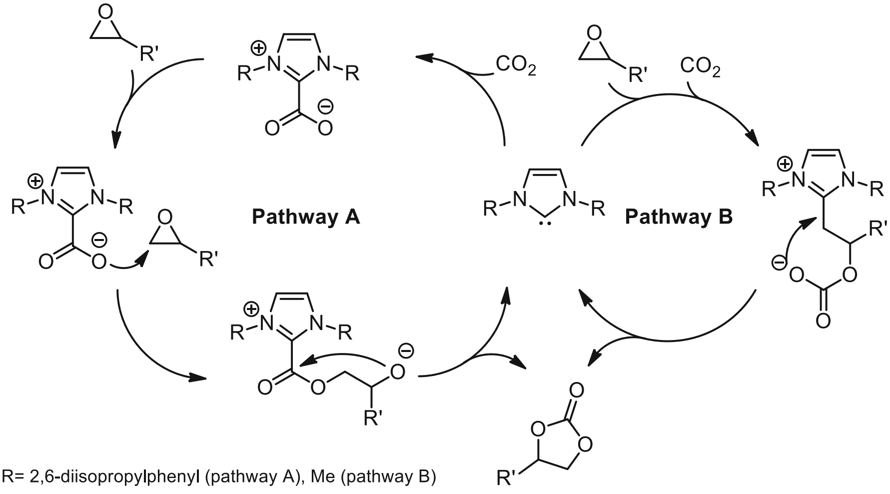

R= 2,6-diisopropylphenyl (pathway A), Me (pathway B)

Scheme 9 Possible mechanism for the NHC catalyzed addition of CO_2 to epoxides adapted from Lu and Ajitha [104, 106]

The group of Cao and Shi reported the in situ formation of **28** from the respective imidazolinium chloride and equimolar amounts of K_2CO_3 as a base (Table 6, entry 2) [107]. In the presence of $ZnBr_2$ as co-catalyst, this system was active under low CO_2 pressure (0.05 MPa) and concentration (50 vol.%). Hence, SO could be converted to the respective carbonate in 88% yield. The authors propose a similar mechanism as shown in Scheme 9 (pathway A). Additionally, the activation of the epoxide by the Lewis-acidic metal center, as well as the nucleophilic ring-opening by the bromide is taken into account. Most recently, they reported a similar system utilizing *n*-butyl methyl imidazolium bromide ([Bmim]Br) as solvent and precursor for the in situ formation of catalytic amounts of the respective NHC [108]. If the corresponding CO_2-Adduct **29** is employed in combination with 3 mol% $ZnBr_2$ in [Bmim]Br, an excellent yield on styrene carbonate were obtained at room temperature and 0.1 MPa CO_2 (entry 3). Werner and co-workers reported a catalytic system for the simultaneous activation of CO_2 by **30** and the epoxide by KI/18-crown-6 complex. Utilizing this system TONs up to 403 and TOFs up to 228 h^{-1} could be achieved. Butylene oxide (BO) was used as test substrate which could be converted to the respective carbonate in excellent yield at 90 °C under solvent-free conditions (entry 4) [109].

2.6 Hydrogen Bond Donor-Based Catalytic Systems

Organocatalytic systems based on phenol derivatives are frequently used for epoxide activation by hydrogen bonding enabling the conversion with CO_2 under mild conditions. Thus, they can be considered a privileged class of organocatalysts. In 2003 Shi and co-workers reported the use of phenols as catalysts in combination with different amine bases as co-catalyst. Several active systems for the synthesis of propylene carbonate have been identified. The combination of 4-dimethyl aminopyridine (DMAP) and *p*-methoxyphenol (**31**) proved to be the most efficient representing the most active catalytic phenol/base system under otherwise the same conditions (Table 7, entry 1) [110]. To elucidate the mode of activation, *trans*-deuteriohexylene oxide (**37**) was prepared and used as substrate in the DMAP and phenol co-catalyzed reaction with CO_2 (Scheme 10). Only *trans*-**38** was observed which suggests that this reaction system proceeds via pathway A. In this case the epoxy ring is activated by phenol through hydrogen bonding. Subsequently, the epoxide is first opened by DMAP and reacts with CO_2 to form *trans*-**38**. If the reaction would proceed via pathway B carbonate *cis*-**38** would be expected having the opposite configuration at the carbon center bearing the deuterium atom. In an extension of their work Shi et al. reported the use of Schiff bases in combination with DMAP as catalyst system under comparable reaction conditions [111].

Kleij and co-workers developed a binary catalytic system comprising commercially available phenolic compounds in combination with TBAI as a co-catalyst [112]. In a wide screening, pyrogallol (**32**) showed high activity even at low reaction temperatures of 45 °C (entry 2). Notably, this system is also active at room temperature (23 °C) leading to 63% yield of propylene carbonate under otherwise the same conditions. The mechanism for the carbonate formation was studied by DFT calculations. The computational studies revealed that besides the activation of the epoxide the key role of the hydroxyl groups in **32** is to stabilize intermediates and transition states by inter- and intramolecular hydrogen bonding. The same group recently reported a one-component bifunctional catalytic system based on polystyrene supported pyrogallol **33** [113]. The catalyst was prepared by two

Table 7 Selected catalytic systems based on phenol derivatives as hydrogen bond donors

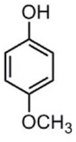

31

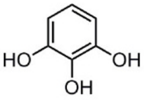

32

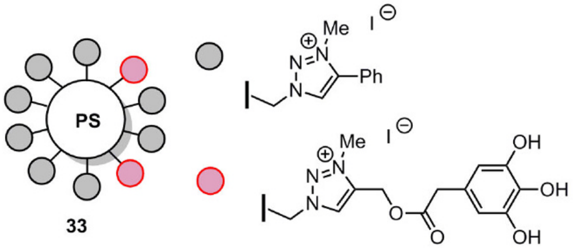

33

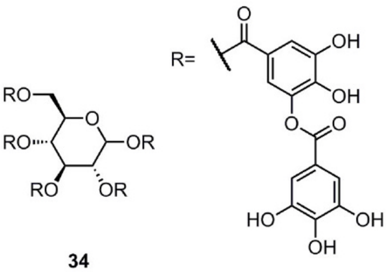

34

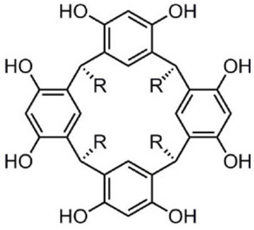

35, R= C_9H_{19}

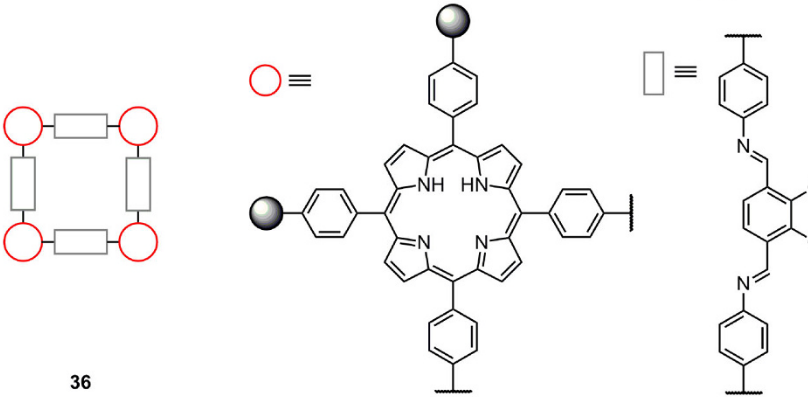

36

Entry	Cat. (mol%)	Co-cat. (mol%)	Sub. (mmol)	*T* (°C)	*p* (MPa)	*t* (h)	Yield (%)	References
1[a]	**31** (4)	DMAP (4)	PO (4.5)	120	3.57	48	100	[110]
2[b]	**32** (5)	TBAI (5)	PO (0.002)	45	1	18	83	[112]
3	**33** (8)	–	PO (10)	45	1	18	96	[113]
4[b]	**34** (0.5)	TBAI (5)	SO (2)	80	1	18	76	[114]
5[b]	**35** (1.5)	TBAI (5)	SO (1)	50	1	18	93	[115]
6	**36** (0.2)	TBAI (0.5)	SO (10)	110	0.1	12	94	[116]

[a] CH_2Cl_2 was used as solvent

[b] MEK was used as solvent

sequential copper-catalyzed alkyne azide cycloaddition reactions and final treatment with methyl iodide. The 1,2,3-trihydroxybenzene moieties and the phenyltriazolium unit existed in a 1:4 ratio.

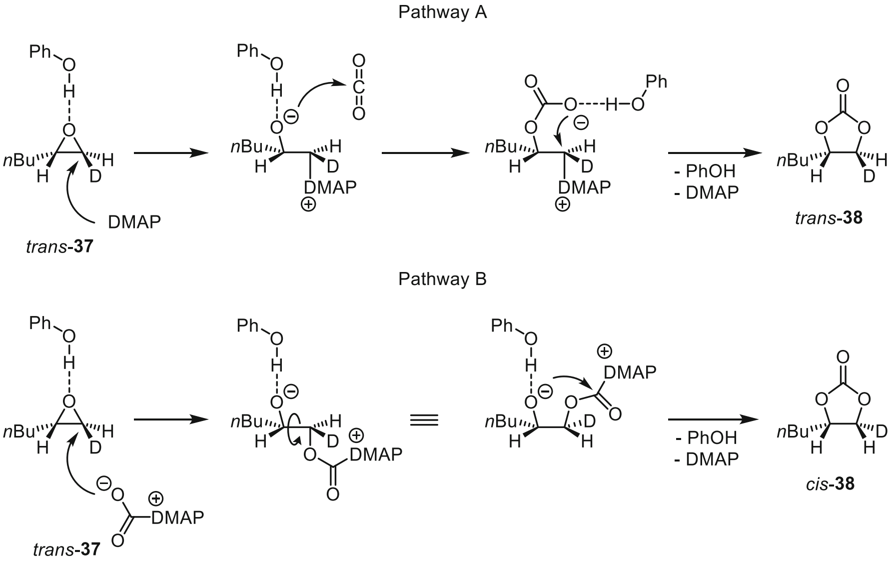

Scheme 10 Possible reaction pathways for the synthesis of **38** in the presence of phenol as hydrogen bond donor and DMAP as nucleophilic co-catalyst [110]

Even at low temperatures (45 °C) catalyst **33** showed high activity in the coupling of epoxides with CO_2 (entry 3). This catalyst could be recycled and reused for various substrates, but had to be reactivated with MeI after five runs to regain the initial catalytic activity.

Subsequently, the same group showed that increasing the local concentration of phenolic sites is beneficial for catalytic turnover [114]. Tannic acid (**34**) is a naturally occurring plant polyphenol which is inexpensive and readily available [115]. It contains multiple phenol fragments and proved to be a highly active catalyst in combination with TBAI as co-catalyst (entry 4). Notably, initial turnover frequencies up to 236 h^{-1} were achieved. Most recently, cavitand-based polyphenols were also reported as highly active organocatalysts. Resorcin [4] arene-based catalyst **35** showed a broad substrate scope with low catalyst loading (1.5 mol%) and low reaction temperature (50 °C, entry 5). At elevated temperature, high initial turnover frequencies up to 488 h^{-1} were observed which are among the highest reported to date for organocatalysts. Saptal et al. described the synthesis of catechol porphyrin-based covalent organic framework **36** [116]. This catalyst is also used in combination with TBAI as co-catalyst, but is active even at low CO_2 pressures (0.1 MPa) and solvent-free conditions (entry 6). This catalyst **36** has a high surface area ($\sim 10^3$ m^2 g^{-1}) and is thermally stable up to 250–300 °C.

Besides the phenol systems, several other hydroxyl functionalized compounds have been studied as hydrogen bond donor catalysts for the conversion of epoxides with CO_2 under mild conditions (Table 8). Also, in those cases the activation of the epoxide and stabilization of formed intermediates via hydrogen bonding is the accepted mode of activation. Jerome and Tassaing used 2.5 mol% fluorinated

Table 8 Selected catalytic systems based on hydroxyl functionalized organocatalysts except phenol-based systems

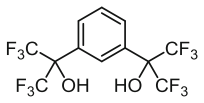

39

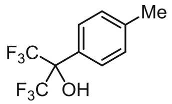

40

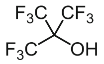

41

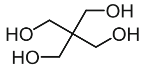

42

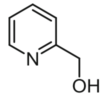

43

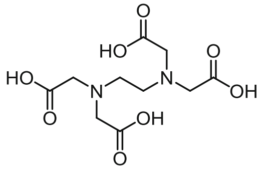

44

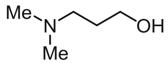

45

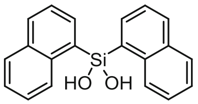

46

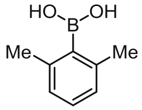

47

Entry	Cat. (mol%)	Co-cat. (mol%)	Sub. (mmol)	*T* (°C)	*p* (MPa)	*t* (h)	Yield (%)	References
1	**39** (2.5)	TBAI (2.5)	ED[a]	80	8.0	0.5	>98[b]	[117]
2	**39** (3.0)	TBAB (3.0)	PO	60	2.0	2	>99	[117]
3	**40** (3.0)	TBAB (3.0)	PO	60	2.0	2.5	100[b]	[118]
4	**41** (2.2)	TBAB (2.2)	ELSO[c]	120	5.0	10	>99[b]	[119]
5	**42** (5)	TBAI (5)	PO (10)	70	0.4	16	96[b]	[120]
6	**43** (8)	TBAI (8)	PO (6)	25	0.1	20	86	[121]
7	**44** (5)	TBAB (5)	PO (5)	70	0.5	18	99	[122]
8	**45** (0.8)	–	PO (42.8)	120	1.0	3	91	[123]
9	**46** (10)	TBAI (10)	SO (0.9)	23	0.1	18	93	[124]
10[d]	**47** (10)	TBAI (5)	PO (2000)	50	1.0	7	98	[125]

[a] 1,2-Epoxydodecane

[b] Conversion is given

[c] Epoxidized linseed oil

[d] Water was used as solvent

alcohol **39** in combination with 2.5 mol% TBAI as catalytic system (Table 8, entry 1) [117]. Kinetic investigations revealed a significant improvement of the reaction rate in the presence of **39** as activator of the epoxide. For the model reaction, the conversion of CO_2 and 1,2-epoxydodecane (ED) at 80 °C and 8.0 MPa, the rate constant k' increased from 0.0005 min^{-1} when TBAI is used alone to 0.1200 min^{-1} for TBAI combined with **39**. It should be noted that the non-fluorinated equivalent of **39** lead to rather low reaction rate constant of 0.017 min^{-1} , which confirms the positive impact of CF_3-substitution of the catalyst. Moreover, **39** (3 mol%) was tested in combination with TBAB (3 mol%) to produce propylene carbonate (PC) at 60 °C, 2.0 MPa (entry 2). The increase of the rate was attributed to synergistic effect between TBAB and the fluorinated hydrogen bond donor. A comparison of **39** and pyrogallol (**32**, Table 7, Entry 2) in combination with TBAB revealed that both catalysts showed a superior catalytic activity compared to TBAB (0.0058 min^{-1})

alone; however, the constant for pyrogallol (0.0162 min^{-1}) was lower than for **39** (0.0270 min^{-1}).

Further investigations were carried out to test several commercially available fluorinated alcohols as activators [118]. Accordingly, **40** also proved to be an efficient activator of PO for the formation of propylene carbonate (entry 3). However, the determined reaction rate constants for **40** (1.59 h^{-1}) was slightly lower than for **39** (2.24 h^{-1}) in the cycloaddition of PO and CO_2 at 60 °C, 2.0 MPa (3 mol% TBAB). Eventually, DFT calculations were carried out and demonstrated that the substitution of alcohols with trifluoromethyl groups significantly increases the stabilization of intermediates and transition states within the catalytic cycle. Moreover, the decrease of Gibbs energy of each step in the catalytic cycle was determined in the presence of fluorinated alcohols compared to non-fluorinated [126]. Finally, fluorinated hydrogen bond donor catalysts in combination with TBAB were introduced in an organocatalytic approach for the synthesis of carbonated linseed oil from the respective epoxide and CO_2 (entry 4) [119]. Quantitative conversion for this challenging substrate was observed in the presence of 2.2 mol% TBAB, 2.2 mol% perfluoro-*tert*-butanol (**41**) after 10 h at 120 °C and 5.0 MPa.

Hou and co-workers reported pentaerythritol (PETT, **42**) in combination with KI as binary catalytic system for the synthesis of cyclic carbonates [127]. However, harsh reaction conditions were required even for the conversion of terminal epoxides. Cokoja and co-workers developed a catalyst system also based on PETT (**42**), in which the nucleophile was provided by TBAI co-catalyst [120]. Excellent results were obtained at 70 °C, 0.4 MPa after 16 h reaction time, e.g. yielding 96% of propylene carbonate (entry 5). In eight catalytic cycles high yields $\geq$90% of PC were obtained, proving the high recyclability of this system.

Hirose and co-workers developed a binary catalyst system composed of 2-pyridine-methanol (**43**) and TBAI which efficiently catalyzes the conversion of epoxides with CO_2 even at room temperature and 0.1 MPa CO_2 pressure (entry 6) [121]. ^{1}H NMR investigations revealed hydrogen bond donation of the catalyst to the epoxide, which was indicated by a significant upfield shift of the OH proton signal from $\delta = 6.50$ to 5.49 ppm. Interestingly, if benzyl alcohol was used as catalyst, the yield decreased significantly revealing the crucial influence of the pyridine moiety. He and co-workers used ethylenediaminetetraacetic acid (EDTA, **44**) as hydrogen bond donor (entry 7) [122]. Also, in this system a nucleophile is necessary and provided by TBAB. Under optimized reaction conditions of 5 mol% **44** and 5 mol% TBAB after 18 h at 70 °C and 0.5 MPa an excellent yield of PC of 99% was obtained.

Alkanol amines are produced in great amounts and employed as CO_2 scrubber for flue gas. Park and co-workers reported alkanol amine CO_2 scrubbers as catalysts for the synthesis of PC from PO and CO_2 (entry 8) [123]. Among the tested alkanol amines, *N*,*N*-dimethylpropanolamine **45** proved to be the most active catalyst. Notably, under the given reaction no co-catalyst or solvent was required.

Mattson and co-workers used dinaphthylsilanediol (**46**) and TBAI to produce styrene carbonate at 23 °C (entry 9) [124]. Titrations experiments of **46** with either TBAI or SO were monitored by ^{1}H NMR and gave evidence for hydrogen bond interaction of the silanediol with both the halide and the epoxide. Most recently, Zhang and co-worker tested several boronic acids as hydrogen bond donor catalysts in combination with tetrabutylammonium salts in the synthesis of cyclic carbonates [125]. Excellent yield of 98% of PC was obtained in the presence of 10 mol% (2,6-dimethylphenyl)boronic acid (**47**) and 5 mol% TBAI at 50 °C, 1.0 MPa after 7 h (entry 10). It was found that the two *ortho* substituents play a crucial role for catalytic activity. Moreover, several solvents were tested and water proved to be a unique reaction medium for this binary catalytic system. Boronic acids tend to form dimers or trimers in neat or non-coordinating solvents. Thus, when triphenylboroxine was tested as catalyst no reaction was observed in THF while in water 53% of cyclic carbonate was obtained.

3 Privileged Metal Complex Catalysts

3.1 Metal Complexes Based on Porphyrins

Inoue and co-workers reported as early as 1978 the trapping of CO_2 by tetraphenyl-porphinato-aluminium methoxide (Al(TPP)OMe, **48a**) and the conversion of propylene oxide with CO_2 even at room temperature and low CO_2 pressure of 0.1 MPa (Table 9, entry 1) [128]. Notably, this system operates under halide-free conditions. Ahmadi et al. reported $Sn(TPP)(OTf)_2$ **48b** as efficient catalyst in the presence of stoichiometric amounts of tetrabutylphosphonium bromide (TBPB) in DMF at 50 °C (entry 2) [129]. Subsequently, chromium(III) porphyrinate **49** was also found to be a good catalyst in combination with DMAP as co-catalyst (entry 3). The tetra-*p*-tolyl derivative **49** showed better solubility and thus was a more effective catalyst than the tetraphenyl analogue [130]. Jing and co-workers studied several biomimetic metalloporphyrin complexes based on main group metals [Mg(II), Al(III), Sn(II), and Sn(IV)] [131]. They observed a direct correlation between the Lewis acidity of the metal center and the catalytic activity of the metalloporphyrin complex. They also studied the influence of various co-catalysts. As a result two catalytic systems Mg(TPP) **48c**/TBAI and Al(TPP)Cl **48d**/ phenyltrimethyl ammonium tribromide (PTAT) have been identified as the most active systems to catalyze the addition of CO_2 to epoxides at room temperature (entries 4 and 5).

Ema et al. studied several onium salt-functionalized porphyrin catalysts for this reaction [132]. Based on their initial studies they designed catalyst **50** which showed very high catalytic activity (TON of 138,000 and TOF of 19,000 h^{-1}) for the conversion of epoxyhexane at 120 °C (entry 6). Mechanistic studies with ^{18}O-labeled CO_2 and D-labeled epoxide suggested that the catalytic cycle involved initial nucleophilic attack of Br^- on the less hindered side of the epoxide to generate an oxyanion (Scheme 11). The insertion of CO_2 and subsequent intramolecular ring-closure forms the cyclic carbonate and regenerates the catalyst. DFT calculations supported the experimental results revealing that the quaternary ammonium cation underwent conformational changes which stabilize various anionic species generated during the catalytic cycle [133].

Table 9 Porphyrin-based catalysts and catalytic systems

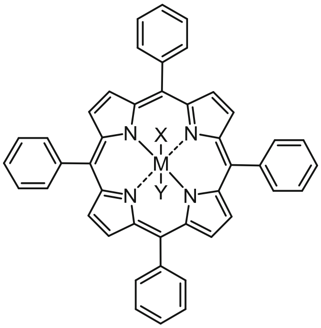

48a, M= Al, X= OMe, Y= –
48b, M= Sn, X=Y= OTf
48c, M= Mg, X=Y= –
48d, M= Al, X= Cl, Y= –

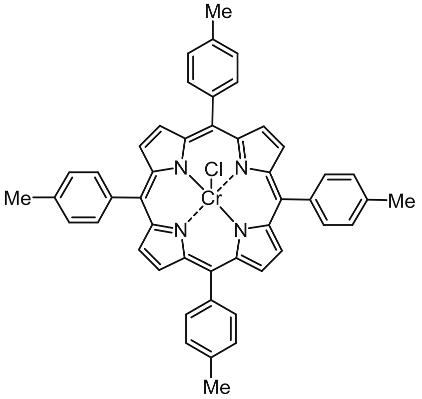

49

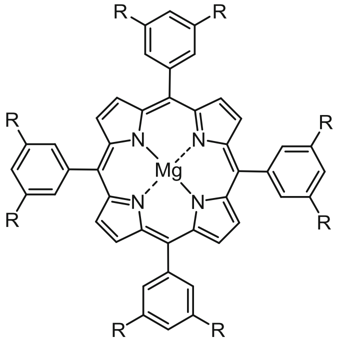

50, R= –[O(CH$_2$)$_6$NBu$_3$]Br

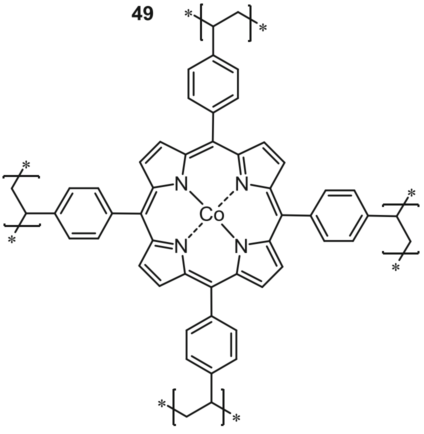

51

Entry	Cat. (mol%)	Co-cat. (mol%)	Sub. (mmol)	T (°C)	p (MPa)	t (h)	Yield (%)	References
1	**48a** (0.18)	NMI[a] (0.29)	PO (140)	20	0.1	96	8	[128]
2[b]	**48b** (2)	TBPB (100)	SO (1)	50	0.1	20	98	[129]
3	**49** (0.014)	DMAP (0.088)	PO (159)	60	5.4	40	>99	[130]
4	**48c** (0.05)	TBAI (0.2)	PO (100)	25	1.4	24	99	[131]
5	**48d** (0.1)	PTAT (0.2)	PO (50)	25	1.0	5	99	[131]
6	**50** (0.0005)	–	EH (10)	120	1.7	24	69	[132]
7	**51** (0.22)	TBAB (7.2)	PO (12.5)	29	0.1	24	96[c]	[134]

[a] 1-Methylimidazole

[b] DMF was used as solvent

[c] The conversion is given (99% selectivity)

[d] 1,2-Epoxyhexane

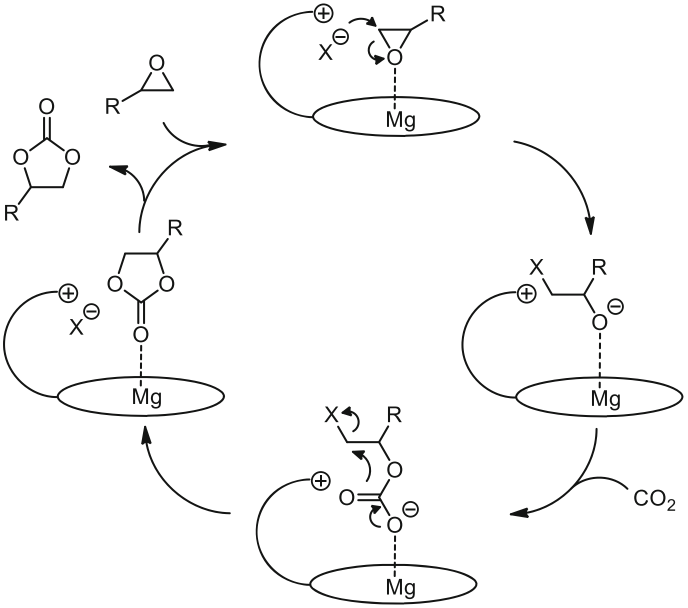

Scheme 11 Proposed catalytic cycle for the ammonium-functionalized catalyst **50** [132, 133]

Dai et al. prepared a porous organic tetrastyryl porphyrine polymer by solvothermal polymerization of the tetrastyryl porphyrine monomer [134]. Subsequently, the polymer was metalated with Co(III), Zn(II), and Mg(II), respectively, and used as heterogeneous catalysts for the coupling of CO_2 with epoxides. Immobilized Co-catalyst **51** gave the best results at 29 °C and 0.1 MPa CO_2 pressure (entry 7) Notably, the catalytic activity at low CO_2 concentration (0.1 MPa, 15 vol.% CO_2 and 85 vol.% N_2) was similar to the respective homogeneous Co(TPP) catalyst.

3.2 Cr(III)(salen) and Co(III)(salen) and Related Metal Complexes

In contrast to many other ligand systems, salen, salophen, and related ligands offer several advantages: (1) They can be easily and efficiently synthesized usually in high yields, and (2) the modular construction from diamines and salicylaldehydes enables easy tuning the steric and electronic properties of the catalyst [54, 135]. Thus, salen ligands are widely employed and can be considered as a privileged class of ligands in transition metal catalysis. Hence, it is no surprise that complexes based on those ligands have also been employed in the coupling of CO_2 with epoxides. In 2001 Nguyen and co-workers reported the use of chromium salen complex **52** in combination with DMAP as efficient binary catalyst system for this reaction [136]. Notably, in the presence of this system PO is quantitatively converted to the cyclic carbonate at 75 °C and 0.34 MPa CO_2 (Table 10, entry 1). At higher temperatures (100 °C) and pressure (0.69 MPa) a turnover frequency of 916 h^{-1} was obtained. The groups of Lu and Sun reported the synthesis of chrome complexes bearing the

Table 10 Selected examples for Cr(III) and Co(III) complexes as catalysts

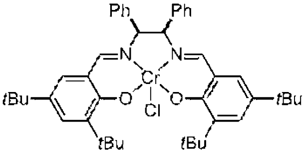

52

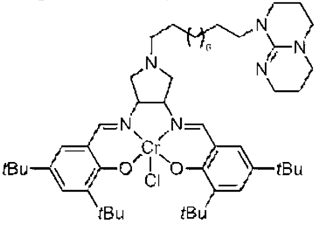

53

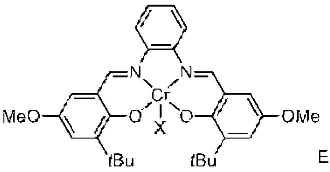

54a, X= Br

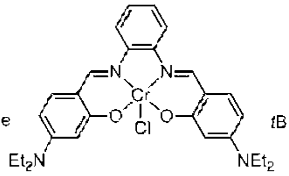

55

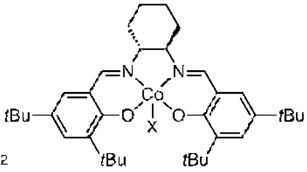

56a, X= Cl
56b, X= O_2CCCl_3
56c, X= OAc

Entry	Cat. (mol%)	Co-cat. (mol%)	Sub. (mmol)	*T* (°C)	*p* (MPa)	*t* (h)	Yield (%)	References
1[a]	**52** (1)	DMAP (1)	PO (3.81)	75	0.35	1.5	100	[136]
2	**53** (0.02)	–	PO (200)	80	2.0	8	97	[137]
3	**54a** (2.5)	TBAB (2.5)	SO (1.66)	25	0.1	24	92	[138]
4	**55** (1.5)	TBAB (1.5)	SO (1.66)	25	0.1	24	84	[139]
5[a]	**56a** (1.0)	DMAP (2)	PO (14.3)	100	2.07	1.5	100	[140]
6	**56b** (0.1)	TBAB (0.1)	PO (500)	25	1.2	2.0	49[b]	[141]
7	**56c** (0.1)	[TBA]Ala (0.1)[c]	PO (100)	0	0.69	20	10[d]	[142]

[a] CH_2Cl_2 was used as solvent

[b] Conversion is given, 50.5% *ee*

[c] [TBA]Ala = tetrabutylammonium L-alaninate

[d] Under the given reaction conditions an *ee%* of 85.2 was obtained

nucleophilic co-catalysts covalently bound to the ligand backbone [137]. The catalyst **53** proved to be the most active. The initial turnover frequency (after 1 h) for the conversion of PO was reported to be 1936 h^{-1}. However, 8 h were required to obtain the desired propylene carbonate in an excellent yield of 97% which corresponds to a TOF of 609 h^{-1} (entry 2). Remarkably, **53** was active even at lower temperature (25 °C) and CO_2 pressure (0.5 MPa). Interestingly, the analogue binary system composed of Cr(salen) complex with *N*-benzyl-pyrrolidine backbone and 7-methyl-1,5,7-triazabicyclo[4.4.0]dec-5-ene (MTBD) as co-catalyst was completely inactive at 25 °C.

Most recently, North et al. reported the synthesis and use of various chromium salophen complexes in combination with TBAB as a binary catalytic system [138]. Complex **54a** proved to be the best catalyst allowing the conversion of terminal

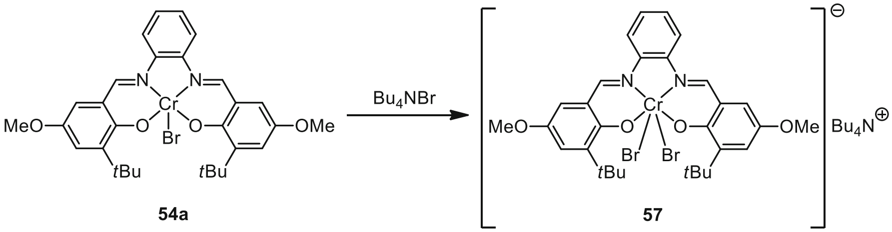

Scheme 12 Proposed in situ formation of catalytically active species **57** from **54a** and TBAB [138]

epoxides, e.g. styrene oxide at ambient temperature and 0.1 MPa carbon dioxide pressure (entry 3). The authors showed that neither the metal complex **54a** nor TBAB displayed significant activity when used alone.

The catalytic activity of both the catalyst and co-catalyst strongly depend on the nature of the counterion. The conversion in the presence of tetrabutylammonium salts as co-catalysts decreased in the order $Br^- \approx I^- > Cl^- > F^-$ in combination with **52**. The catalytic activity of the metal complex **54** showed the trend $X = Br^- > Cl^- > AcO^- > I^- > TsO^-$. Kinetic studies indicate that both catalyst components interact to form complex **57**, which is considered to be the catalytically active species (Scheme 12). Most recently, North and co-workers reported chromium-based catalyst **55**, which gave similar results to **54a** (entry 3 vs. 4) [139].

Nguyen and co-workers reported chiral cobalt salen complex **56a** in combination with DMAP as binary catalytic system for the conversion of terminal epoxides with CO_2 reaching TOFs up to 1200 h^{-1} (entry 5) [140]. The conversion of propylene oxide gave the respective carbonate in quantitative yield after 1.5 h at 100 °C in CH_2Cl_2 and 2 MPa CO_2 pressure. The use of chiral catalysts offers the possibility to perform kinetic resolutions by selective addition of CO_2 to one enantiomer of a racemic mixture of an epoxide. Lu et al. studied the kinetic resolution of racemic propylene oxide at 25 °C using **56b** in combination with TBAB as co-catalysts (entry 6) [141]. In the presence of this catalyst system, a turnover frequency up to 245 h^{-1} and 50.5% *ee* was achieved. Under similar conditions the enantiomeric excess could be improved up to 70.2% using tetrabutylammonium chloride as co-catalyst. Under comparable conditions Jing et al. reported an enantiomeric excess of up to 85.2 and 10% yield for propylene carbonate using catalyst **56c** in combination with amino acid-based chiral ionic liquids (entry 7) [142].

3.3 Zn(II)(salen) and Related Metal Complexes

Zinc salen and salphen complexes are frequently studied catalysts for the addition of CO_2 to epoxides. In this context, Kleij and co-workers studied various zinc salphen complexes in combination with TBAI as binary catalyst system [143]. In an initial screening complex, **58** showed the highest activity even at a low reaction temperature of 45 °C. Under optimized reaction conditions propylene carbonate was obtained in 90% yield (Table 11, entry 1). If the reaction is performed under supercritical conditions the solvent can be omitted and the reaction time is

Table 11 Zinc(II) salphen, salen and related complexes as catalysts

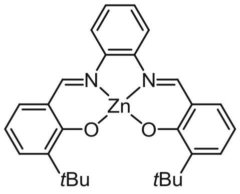

58

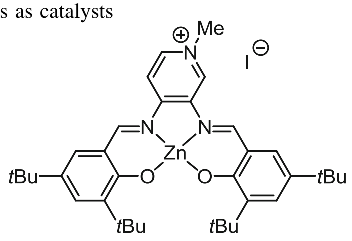

59

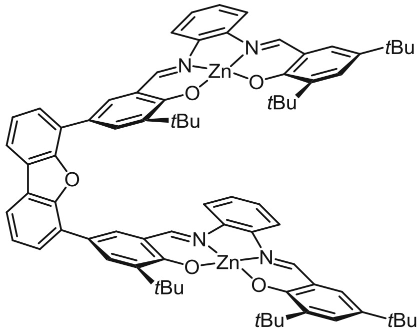

60

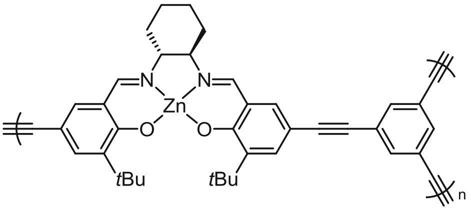

61

Entry	Cat. (mol%)	Co-cat. (mol%)	Sub. (mmol)	T (°C)	p (MPa)	t (h)	Yield (%)	References
1[a]	**58** (2.5)	TBAI (2.5)	PO (2)	45	1.0	18	90	[143]
2[b]	**58** (2.5)	TBAI (2.5)	PO (2)	25	0.2	18	73	[145]
3	**59** (0.5)	–	SO (10)	80	1.0	18	88	[147]
4	**60** (0.01)	TBAI (0.5)	PO (42.9)	85	1.0	2	86[c]	[148]
5	**61** (0.2)	TBAB (1.8)	PO (50)	25	0.1	48	76	[149]

[a] CH_2Cl_2 was used as solvent

[b] 2-Butanone (MEK) was used as solvent

[c] The conversion is given

significantly decreased [144]. Previous to this report, Kleij and co-workers published a study on the influence of the ligand structure, metal center and solvent on the reaction outcome [145]. Notably, the reaction can be performed under much milder conditions by choosing the right solvent. If the reaction is performed in MEK as solvent at 25 °C and 0.2 MPa CO_2 propylene carbonate was isolated in 73% after 18 h (entry 2). Subsequently Kleij, Bo and co-workers reported a detailed DFT study on the cycloaddition of CO_2 to propylene oxide in the presence of catalyst **58** and TBAI [146]. The coordination of the zinc salphen complex to the epoxide polarizes the C–O bond, which facilitates the ring-opening step by nucleophilic attack of the iodide (Scheme 13). The study revealed that the nucleophilic attack to the methylene carbon is predominantly controlled by steric factors. In contrast, the nucleophilic attack to the methine carbon is influenced by electronic factors, which are more dominant.

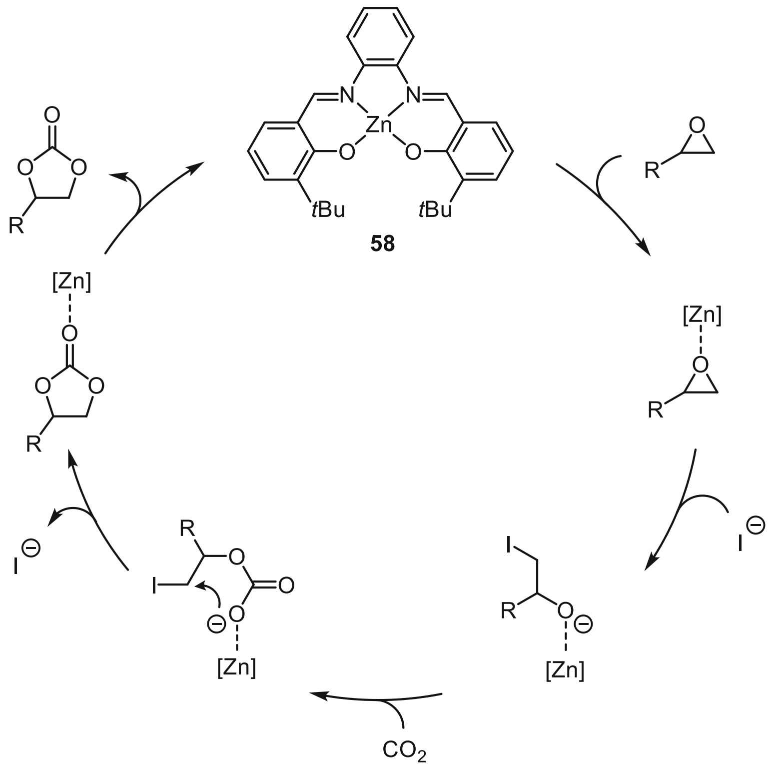

Scheme 13 Proposed catalytic cycle for the synthesis of cyclic carbonates in the presence of Zn(salphen) complex **58** [143]

Recently, the synthesis of bifunctional catalyst **59** has been reported [147]. Instead of salphen, a salpyr ligand was used and alkylated with MeI at the *N*-pyridyl atom. Thus, the catalyst **59** provides the nucleophile which makes the addition of a co-catalyst unnecessary (entry 3). Chan and co-workers reported catalyst **60** as highly active catalyst [148]. In the presence of 0.01 mol% **60** and TBAI as the co-catalyst a conversion of 86% of propylene oxide was achieved after 2 h at 85 °C (entry 4).

The turnover frequency for this reaction was 4300 h^{-1} per zinc center. Even higher TOF values were achieved in the conversion of 1,2-epoxyhexane. At 95 °C and low catalyst loading of 0.0025 mol% an initial turn TOF of 7400 h^{-1} per zinc center was determined. The groups of Zou and Deng reported the preparation of salen-based zinc-coordinated conjugated microporous polymer **61** by linking Zn(salen) **62** with 1,3,5-triethynylbenzene (Scheme 14) [149]. Catalyst **61** in combination with TBAB as co-catalyst exhibits extraordinary activities with initial turnover frequencies up to 11,600 h^{-1} at 120 °C. Notably, the catalyst was even active under ambient conditions even though longer reaction times (48 h) are required (Table 11, entry 5).

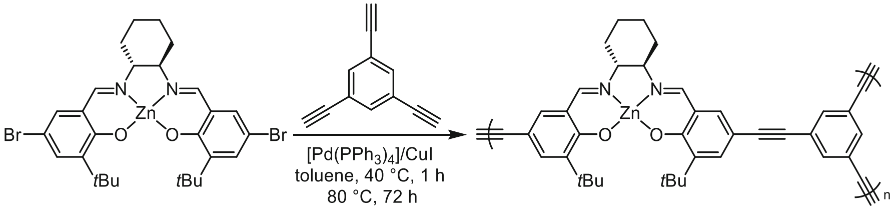

62

61

Scheme 14 Preparation of zinc-coordinated conjugated microporous polymer **62** [149]

3.4 Al(III)(salen) and Related Metal Complexes

Aluminum salen and related complexes are extensively studied as catalysts for the coupling for epoxides with CO_2. In 2004 Lu et al. studied, based on their previous work [150], the use of the monometallic aluminum salen complex **63a** in combination with various tetrabutylammonium salts as binary catalytic systems for this reaction [150, 151]. Catalyst **63a** showed the highest activity in combination with TBAI as co-catalyst. Notably, a turnover frequency of 61.5 h^{-1} was achieved in the conversion of propylene oxide with CO_2 at room temperature (Table 12, entry 1). Alternatively potassium iodide 18-crown-6 complex can be used as nucleophilic co-catalyst leading to comparable results [152]. Recently, the groups of Ren and Lu studied bifunctional catalyst **64** the conversion of both epoxides, as well as aziridines with CO_2 [153]. In the conversion of propylene oxide with CO_2 catalyst **64** showed superior activity reaching a turnover frequency of 3100 h^{-1} at 120 °C (entry 2). In contrast the respective binary catalytic system comprising aluminum salen complex **63b** and 2 equiv TBAB reached a TOF of only 245 h^{-1} under the same conditions (entry 3). Catalyst **64** was even active at 80 °C with an initial TOF of 2210 h^{-1} (entry 4).

Cuesta-Aluja et al. reported an aluminum salabza catalyst **65** (entry 5) [154]. This monometallic catalyst system reached a TOF of 901 h^{-1} for the conversion of PO and a maximum TOF of 3434 h^{-1} for epichlorohydrin conversion. Interestingly, the provided nucleophile has a crucial influence on the selectivity of the epoxide CO_2 coupling reaction. If $(Ph_3P{=}N{=}PPh_3)Cl$ (PPNCl) was used as co-catalyst instead of TBAB for the reaction of cyclohexene oxide (CHO) with CO_2, poly(cyclohexene carbonate) is the main product. Styring and co-workers used a non-symmetric aluminum salenac complex **66** for the addition of CO_2 to SO (entry 6) [155]. However, to obtain SC in reasonable yields of 90% the reaction needs to be carried out at 0.1 MPa and 110 °C for 48 h employing CH_2Cl_2 as solvent and TBAB as co-catalyst. Notably, under these conditions TBAB alone gave comparable conversion of SO (70%) to **66** alone (73%).

Ji and co-workers reported monometallic aluminum salen complex **67** with covalently bound imidazolium-based ionic liquids (entry 7) [156]. Polyether chains were attached to the imidazolium moieties in order to increase the "CO_2 capture". It is suggested that the oxygen of the polyether side chains interacts weakly with CO_2 exhibiting higher activities compared to non-PEG functionalized catalyst.

Table 12 Monometalic Al(III)(salen) and related complexes as catalysts

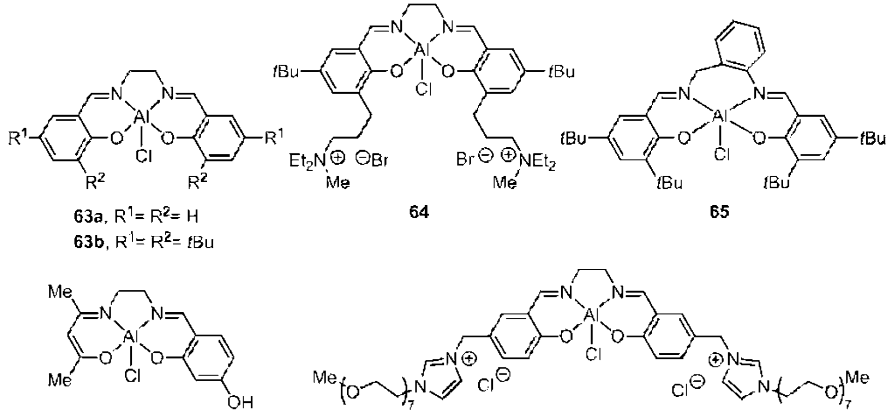

63a, $R^1 = R^2 = H$
63b, $R^1 = R^2 = tBu$
64
65
66
67

Entry	Cat. (mol%)	Co-cat. (mol%)	Sub. (mmol)	*T* (°C)	*p* (MPa)	*t* (h)	Yield (%)	References
1	**63a** (0.125)	TBAI (0.125)	PO (192)	25	0.6	8	62	[151]
2	**64** (0.004)	–	PO (100)	120	2.5	8	99	[153]
3	**63b** (0.004)	TBAB (0.008)	PO (100)	120	2.5	8	8	[153]
4	**64** (0.01)	–	PO (100)	80	2.5	1	22	[153]
5	**65** (0.05)	TBAB (0.25)	PO (42.9)	80	1.0	0.5	23	[154]
6[a]	**66** (1.0)	TBAB (1.0)	SO (2)	110	0.1	48	90[b]	[155]
7	**67** (0.5)	–	AGE[c]	100	1.0	2.5	95	[156]

[a] CH_2Cl_2 was used as solvent

[b] Conversion is given

[c] Allyl glycidyl ether

Moreover, recycling experiments with 6 runs without the loss of selectivity and excellent conversion were performed.

3.5 Bimetallic Al(III)(salen) and Related Metal Complexes

In 2007, North and co-workers reported bimetallic aluminum salen complex for the synthesis of cyclic carbonates at ambient temperature and pressure [157]. Bimetallic aluminum salen complex **68** proved to be remarkably active, catalyzing the synthesis of cyclic carbonates at ambient temperature and pressure (Fig. 3; Table 13, entry 1) [157, 158].

In the presence of 2.5 mol% **68** and 2.5 mol% TBAB as co-catalyst, 98% conversion of styrene oxide was observed at 25 °C and 0.1 MPa CO_2 pressure after 24 h (Table 13, entry 1). Remarkably, even at 0 °C propylene carbonate could be isolated in 77% yield after 3 h. Further investigations of this binary catalyst system revealed first-order kinetics of CO_2, epoxide, catalyst **68** but a second-order dependence for TBAB (Eq. 1).

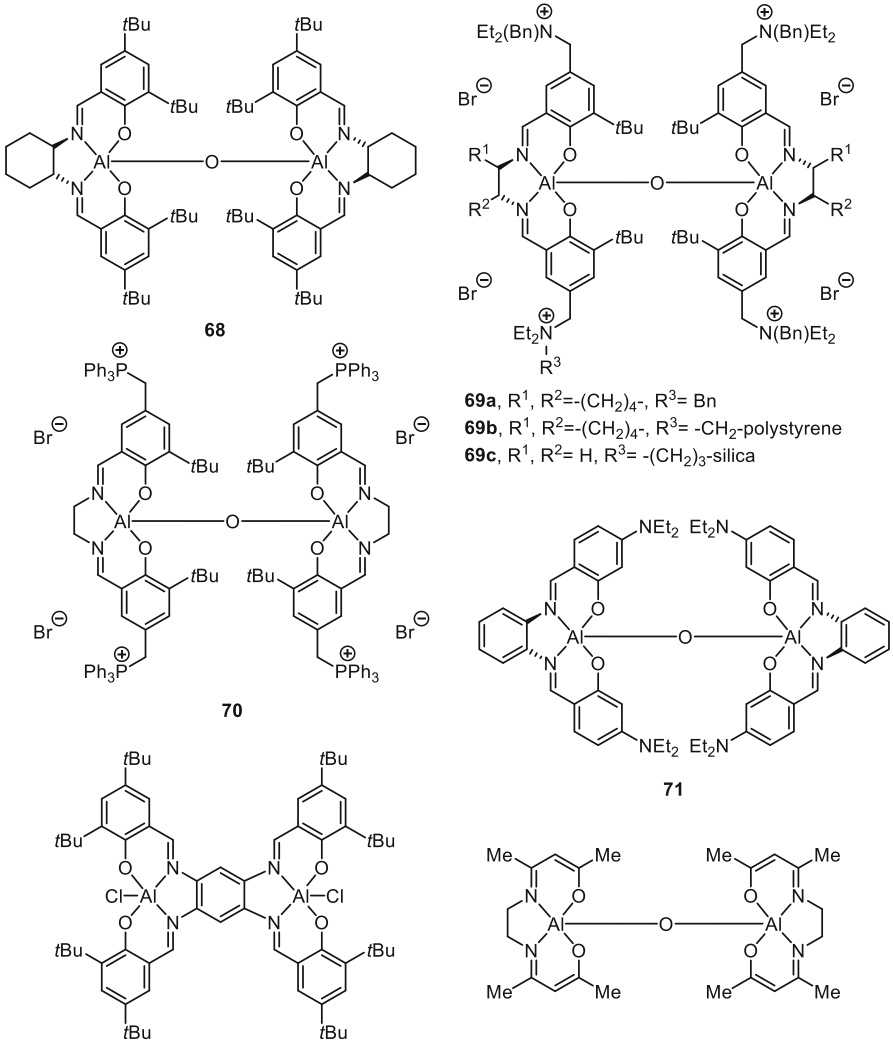

68

69a, R^1, R^2=-$(CH_2)_4$-, R^3= Bn
69b, R^1, R^2=-$(CH_2)_4$-, R^3= -CH_2-polystyrene
69c, R^1, R^2= H, R^3= -$(CH_2)_3$-silica

70

71

72

73

Fig. 3 Catalysts discussed in this section (for details see Table 13)

$$\text{rate} = k[\text{epoxide}]^1[\text{CO}_2]^1[68]^1[\text{Bu}_4\text{NBr}]^2. \tag{1}$$

Based on these studies a mechanism was proposed that takes the observed second-order dependence of the reaction rate of TBAB concentration and the identification of tributylamine in the reaction mixture into consideration (Scheme 15) [165, 166]. North et al. reported the decomposition of TBAB to tributylamine (Bu_3N) and 1-bromobutane (BuBr) to play a crucial role in the catalytic cycle. The amine activates CO_2 in situ forming the corresponding carbamate salt A which is supposed to coordinate more readily to the Al(salen)

Table 13 Bimetallic Al(III)(salen) and related complexes as catalysts

Entry	Cat. (mol%)	Co-cat. (mol%)	Sub. (mmol)	*T* (°C)	*p* (MPa)	*t* (h)	Yield (%)	References
1	**68** (2.5)	TBAB (2.5)	SO (2)	25	0.1	24	98[a]	[157]
2	**69a** (2.5)	–	SO (1.66)	26	0.1	6	89	[159]
3[b]	**69b** (2.5)	–	SO (1.66)	26	0.1	20	79[a]	[160]
4	**69c** (2.5)	–	SO (1.66)	26	0.1	24	86[a]	[160]
5	**70** (2.5)	–	SO	27	0.1	24	99[a]	[161]
6	**71** (1.5)	TBAB (1.5)	SO (1.66)	25	0.1	24	83	[139]
7	**72** (0.25)	TBAB (0.5)	SO (1.66)	50	1.0	24	85	[162]
8	**73** (2.5)	TBAB (2.5)	SO (1.66)	26	0.1	24	93[a]	[163]
9	**68** (0.5)	–	PO	50	5.0	24	50	[164]

[a] The conversion is given

[b] Propylene carbonate was used as solvent

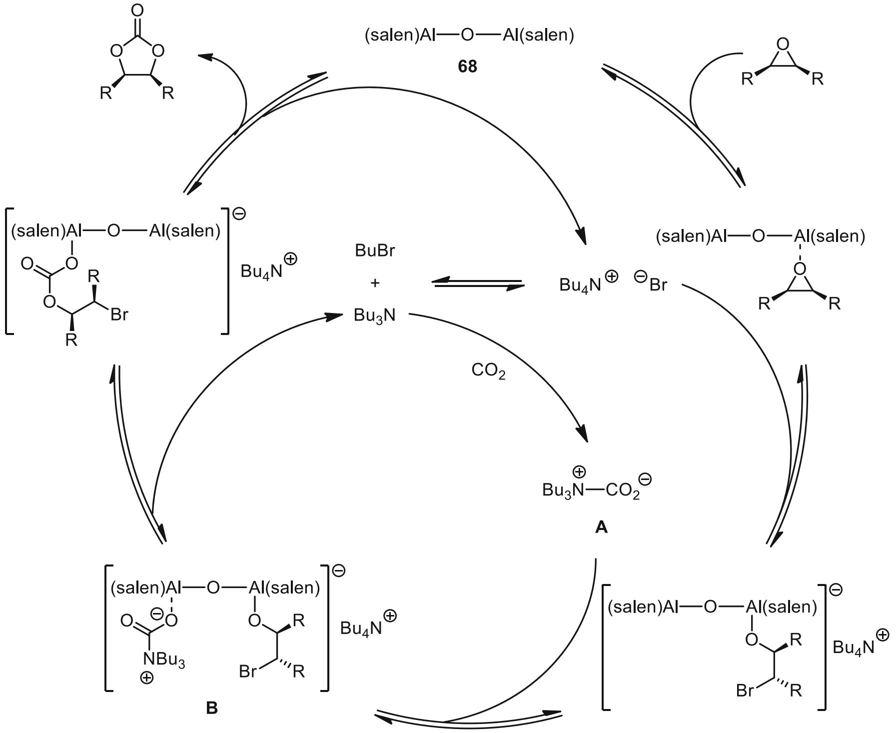

Scheme 15 Catalytic cycle for the cyclic carbonate synthesis using **68** and TBAB [165, 166]

complex **68** than CO_2. Experiments in presence of added Bu_3N imply that the rate-determining step is the formation of B. Notably, complex **68** was stable over 60 reactions, though the TBAB decomposed in situ and had to be regularly replaced during the recycling experiments. In addition, a one-component catalyst **69a** with an ammonium salts covalently bound to the catalyst was prepared (Table 13, entry 2) [159, 160, 167].

Moreover, polystyrene and silica supported derivatives **69b** and **69c** were synthesized, which gave comparable results to **69a** (Table 13, entry 2 vs. entries 3 and 4). Furthermore, **69c** was used in a gas phase flow reactor and allows even the conversion of flue gas with styrene oxide to produce styrene carbonate [160, 168]. Even though catalyst deactivation was observed over time, this effect was reversible by requarternization of the deactivated catalyst. Following to the concept of binding the co-catalyst to the ligand backbone, one-component catalysts **70** with covalently attached quaternary phosphonium groups onto the salen ligand was prepared. This catalyst showed comparable results to **69a** (entry 5) [161]. Furthermore, amine functionalized Al(salphen) complex **71** was synthesized, which exhibits even higher activity than **68** since under the same reaction conditions of **68** only 1.5 mol% catalyst amount were necessary to obtain similar results (entry 1 vs. 6) [139].

Contrary to the bimetallic μ-oxo-bridged aluminum salphen complexes **68–71**, a phenyl bridged bimetallic complex **72** was reported [162]. Even though this catalyst proved to be active at lower catalyst/co-catalyst loadings elevated reaction temperature of 50 °C and a pressure of 1.0 MPa were necessary to obtain styrene carbonate in 85% after 24 h (entry 7). Notably, this catalyst proved to be efficient for the conversion of several internal epoxides into the corresponding cyclic carbonates. Furthermore, North et al. reported the synthesis of bimetallic aluminum acen complexes, e.g. **73** [158, 163]. Catalyst **73** was highly active even at 0 °C in the presence of TBAB as co-catalyst (entry 8). Catalysts **68–73** have in common that they require the presence of a nucleophilic organocatalysts. Thus, either TBAB was used as co-catalyst or in case of **69** and **70** ammonium or phosphonium bromides were covalently bound to the ligand of the aluminum complexes to enable the formation of cyclic carbonate. However, further studies revealed that under suitable reaction conditions (high CO_2 pressure) **68** can catalyze the addition of CO_2 to epoxides even in the absence of any co-catalyst (entry 9) [164]. This suggests a change in the reaction pathway. In this context, mechanistic investigations and density functional theory calculations revealed carbonato-bridged bis-aluminum salen complex **74** to be a key intermediate in this halide-free reaction (Scheme 16) [169]. This complex is formed by CO_2 insertion into the bridging metal–oxygen-metal bond of complex **68** and was characterized by ^{1}H NMR, infrared spectroscopy and mass spectrometry.

3.6 Metal Complexes Based on Amino Phenolate Ligands

Amino triphenolate ligands are readily accessible and easy to modify. Thus, they have emerged as an interesting ligand scaffold [170]. During the past 5 years metal complexes based on this ligand type have been established as a privileged class of catalyst for the synthesis of cyclic carbonates from epoxides and CO_2 under mild reaction conditions. In 2012 Kleij and co-workers reported iron(III) amino triphenolate complex **75** as an efficient catalyst for this reaction [171]. The combination of iron complex **75** and TBAI as co-catalyst leads to an active system

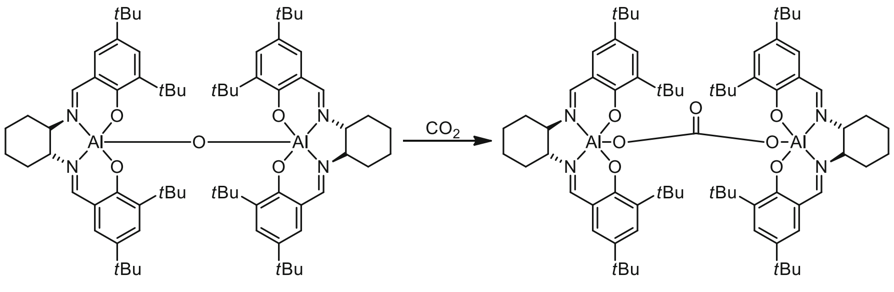

68 **74**

Scheme 16 Insertion of CO_2 into the μ-oxo-bridge of **68** forming μ-carbonato-bridged bis-aluminum salen complex **74** [169]

giving good to excellent yields of cyclic carbonates even at 25 °C and 0.2 MPa CO_2 pressure in MEK e.g. propylene carbonate was obtained in 74% yield (Table 14, entry 1). Neither the catalyst **75** nor the co-catalyst TBAI showed catalytic activity when used alone.

Mechanistic investigations suggest that the dimeric complex **75** dissociates in the presence of propylene oxide into a more reactive monomeric species **81** (Scheme 17). Internal epoxides and even oxetanes were converted; however, the reaction temperature had to be increased to 85 °C. Interestingly, the stereochemistry can be controlled by the catalyst/co-catalyst ratio which relates to two possible reaction pathways leading either to the *cis*- or *trans*-product [177].

Kleij and co-workers also reported aluminium complex **76** as catalyst, which showed extraordinary high initial turnover frequencies up to 36,000 h^{-1} [172]. At catalyst loadings of 0.05 mol% **76** and a loading of TBAI of 0.25 mol% high conversion of epoxyhexane (EH) was achieved at 90 °C (Table 14, entry 2). Moreover, a variety of functionalized terminal internal epoxides, as well as oxetanes could be converted. Notably, catalyst **76** was used for selective formation of a wide range of *cis*-carbonates, which were subsequently hydrolyzed yielding the respective *cis*-diols in high selectivities and yields [178]. Further studies revealed that lower catalytic activities were obtained when the Cl substituents are changed to Me, *t*Bu or H [179]. Kinetic studies and DFT calculations indicated the monometallic mechanism is operative, with the insertion of CO_2 as rate-limiting step. Interestingly, the initial coordination of the epoxide to the Lewis-acidic metal center is around 15 kcal mol^{-1} lower compared to a zinc salphen **58**/TBAI binary catalytic system. The higher catalytic activity is mainly addressed to the lower energetic span and the potential of complex **76** to form a less energy-demanding hexacoordinated transition state. Complex **76** also catalyzed the challenging coupling of highly substituted terpene oxides with CO_2 into bio-based cyclic carbonates [180].

Most recently the groups of Yuan and Yao reported the application of rare earth metal catalysts for this reaction [173]. Catalyst **77** in combination with TBAB proved to be an active binary catalytic system (entry 3). Interestingly, this complex also catalyzed the reaction of epoxides with CO_2 and anilines yielding cyclic

Table 14 Selected examples for metal complexes based on amino phenolate ligands

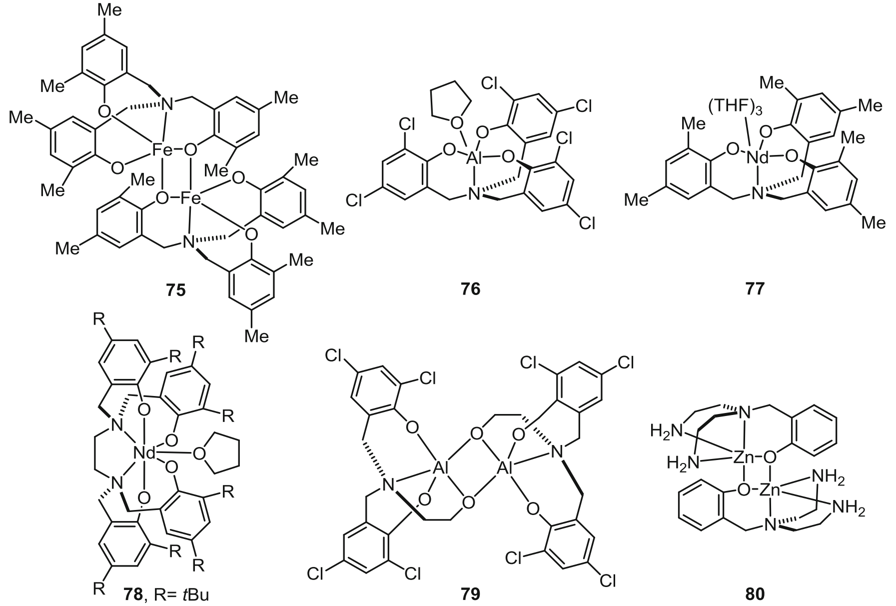

75 **76** **77**

78, R= *t*Bu **79** **80**

Entry	Cat. (mol%)	Co-cat. (mol%)	Sub. (mmol)	*T* (°C)	*p* (MPa)	*t* (h)	Yield (%)	References
1[a]	**75** (0.5)	TBAI (5)	PO (2)	25	0.2	18	74	[171]
2	**76** (0.05)	TBAI (0.25)	EH (10)	90	1	2	96[b]	[172]
3	**77** (0.1)	TBAB (0.6)	SO (29.5)	85	0.1	24	83	[173]
4	**78** (0.2)	TBAI (0.8)	SO (2.5)	85	0.1	24	93	[174]
5	**79** (0.3)	TBAB (0.9)	SO (16.63)	85	0.1	24	91	[175]
6	**80** (0.16)	TBAB (1.8)	SO (2.5)	100	0.1	6	79	[176]

[a] MEK was used as solvent

[b] Conversion is given (>99% selectivity)

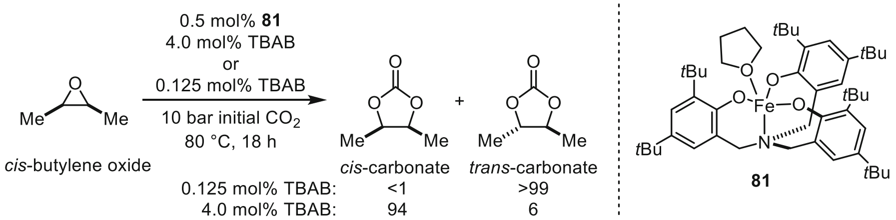

Scheme 17 Conversion of *cis*-butylene oxide to the *cis*- or *trans*-carbonate depending on the **81**/TBAB ration [177]

carbamates. The authors suggest the initial formation of the cyclic carbonate and subsequent reaction with the aniline as one possible reaction pathway. Previously, the same group reported neodymium complex **78** containing a bridged poly(phenolate) ligand and its use as catalyst for the cycloaddition of epoxides and CO_2 [174]. In the presence of TBAI as a co-catalyst a turnover frequency of up to 4000 h^{-1} was achieved for complex **78**. Styrene oxide was converted under atmospheric pressure at 85 °C in 24 h yielding 93% of the respective carbonate (entry 4). The synthesis and utilization of bimetallic aluminum complexes based on amino triphenolate ligands has also been reported [175]. In the presence of catalyst **79** various terminal carbonates, e.g. styrene carbonate (entry 5), as well as internal carbonates were obtained in good to excellent yields from the respective epoxides.

The group of Sun reported dinuclear Zn, Cu, and Cd complexes bearing NH_2-functionalized phenolate ligands [176]. These complexes were successfully applied to the addition of CO_2 to epoxides. The authors described catalyst **80** as the most active of the investigated catalysts. Styrene oxide was converted in the presence of 0.16 mol% **80** and 1.8 mol% TBAB (entry 6). Even though a low CO_2 pressure of 0.1 MPa was sufficient to obtain styrene carbonate in 79% yield a relatively high reaction temperature of 100 °C was required. The conversion of enantiomerically pure (*R*)- or (*S*)-styrene oxide (>99% *ee*) led to the respective carbonates in only 80 and 81% *ee*. Besides a stereospecific S_N2 pathway leading to retention of configuration at the stereocenter, an alternative S_N1 pathway leading to partial racemization was considered. Moreover, the role of the NH_2-groups of the ligand in the catalytic process was investigated. The improved activity of the catalyst compared to complexes bearing tertiary amine groups is addressed to the Lewis-basic activation of CO_2 by the NH_2-groups.

4 Miscellaneous Catalysts Based on Transition Metals and Main Group Elements

4.1 Alkali and Alkaline Earth Metal-Based Catalytic Systems

In 1984 Kuran and co-workers reported a detailed study on the use of alkali metal salts in combination with various phase transfer catalysts [181]. Potassium iodide in combination with 18-crown-6 **82a** as phase transfer catalyst proved to be a very efficient system (Table 15, entry 1). It was found that various other alkali metal salts such as K_2CO_3 and potassium phenolate as well as other phase transfer agents such as polyglyme, PEG, and even DABCO and TMEDA facilitate the reaction under drastic conditions (120 °C, 4 MPa, 24 h). More recently, Werner and co-workers used poly(dibenzo)-18-crown-6 (**82b**) in combination with potassium iodide as recyclable catalyst system. They showed that this system can be used for the conversion of a various terminal epoxides even at 80 °C, e.g. propylene carbonate was obtained in 93% yield after 14 h (entry 2) [182]. Jing and co-worker prepared aza-crown ether based ionic liquid **83**, which showed in combination with KI cooperative catalytic activity in the addition of CO_2 to propylene oxide (entry 3) [183]. Desens and Werner utilized the KI/18C6 system reported by Kuran et al. [181]. in combination with *N*-heterocyclic carbenes for the convergent activation of CO_2 and the epoxide (Table 6, entry 4) [109].

Table 15 Selected alkali and alkaline earth metal-based catalytic systems

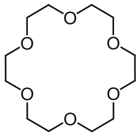
82a

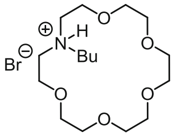
83

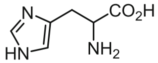
84

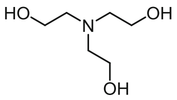
85

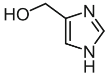
86

Entry	Cat. (mol%)	Co-cat. (mol%)	Sub. (mmol)	*T* (°C)	*p* (MPa)	*t* (h)	Yield (%)	References
1	KI (0.67)	**82a** (0.2)	PO (180)	120	4	4	90	[181]
2	KI (2)	**82b** (2)[a]	PO (25)	80	1	14	93	[182]
3	KBr (1)	**83** (1)	PO (100)	100	1.2	15	97	[183]
4[b]	LiBr (5)	–	PGE (2)	100	0.1	3	87	[185]
5	LiBr (0.1)	DMAP (0.1)	PO (68)	130	2	3	86	[187]
6	KI (1.6)	HCO_2H (15)	PO (18.6)	MWI[c]	0.96	0.25	59	[189]
7	KI (0.2)	**84** (0.2)	PO (42.8)	120	1	3	98	[190]
8	KI (2)	**85** (2)	PO (25)	90	1	2	95	[192]
9	KI (1)	**86** (1)	BO (25)	60	1	24	97	[194]
10	$MgBr_2$ (5)	Ph_3P (10)	PO (10)	r.t.	3.5	12	91	[195]
11[d]	$CaBr_2$ (5)	DBU (5)	SO (5)	100	0.1	12	90	[196]

[a] Poly(dibenzo)-18-crown-6 ether (**82b**)

[b] NMP was used as solvent

[c] Microwave irradiation (200 W)

[d] DMF was used as solvent

Endo and co-workers studied the conversion of phenyl glycidyl ether [184] and other epoxides [185] with CO_2 under atmospheric pressure in the presence of 5 mol% of various alkali metal salts. LiBr proved to be the most active catalyst in *N*-methylpyrrolidinone (NMP) as solvent (entry 4). Notably, only halide salts showed high catalytic activity. The order of intrinsic activity was found to depend on the nature of the halide ($Cl^- > Br^- > I^-$), which is the order of nucleophilicity of the anion in polar aprotic solvents. Furthermore, the order of the activity for the cation is in accordance with the Lewis acidity and was found to be lithium salt > sodium salt > ammonium salt. However, LiCl, which presumably should be the best catalyst, showed only low conversion due to its low solubility in the reaction mixture. Moreover, a kinetic analysis showed that the CO_2 pressure showed no effect on the reaction rate. Wu and co-workers performed DFT calculations for the addition of CO_2 to epoxides catalyzed by LiBr [186]. Based on the determined free energies of activation, they identified the ring-opening of the epoxide or the ring-closing to form the cyclic carbonate as possible rate-determining steps depending on the reaction conditions.

Ghosh and co-workers studied alkali metal salts in combination with Lewis basic co-catalysts [187]. Lithium bromide in combination with DMAP proved to be active even below 100 °C. A turnover frequency of 295 h^{-1} was obtained at 130 °C and 2 MPa CO_2 pressure (entry 5). Notably, in the absence of DMAP, the turnover frequency dropped to 8.2 h^{-1}. Sun et al. reported the increased catalytic activities of alkali metal salts in the presence of water [78]. Also in this study the intrinsic activity of the salts depended on the nature of the anion. However, in water as protic solvent the activity increased in the order $Cl^- < Br^- < I^-$. Han and co-workers performed DFT calculations to elucidate the catalytic mechanism of KI in the presence of hydroxyl substances as co-catalysts [188]. It was demonstrated that the introduction of hydrogen bond donors as co-catalyst allowed the activation of the epoxide, as well as the stabilization of the transition states via hydrogen bonding. Park et al. reported the microwave-assisted synthesis of cyclic carbonates catalyzed by formic acid as hydrogen bond donor in combination with KI. The reaction progresses rapidly (15 min) using 200 W microwave power even at low CO_2 pressure <1 MPa (entry 6) [189]. The calculated transition state energy for the rate-determining step (ring-opening) shows a significant energy difference of 31.29 kJ mol^{-1} compared to H_2O/KI. Natural occurring amino acids in combination with KI have also been reported [190, 191].

Park et al. showed that the histidine (**84**)/KI system gave a turnover number of 535 for propylene oxide in 3 h (entry 7) [190]. The use of co-catalyst with alcohol moieties as hydrogen bond donors, e.g. triethanol amine (**85**) in combination with KI has also been reported [192, 193]. Werner and co-workers reported that this system was active even at reaction temperatures <100 °C (entry 8) [192]. Similar results could be obtained in the presence of hydroxyl functionalized imidazole **86** (entry 9) [194]. Notably, in the presence of **86** as co-catalyst the yields could be improved for several examples compared to the triethanol amine catalyst system. Both systems also gave good results at 60 °C even though longer reaction times were required.

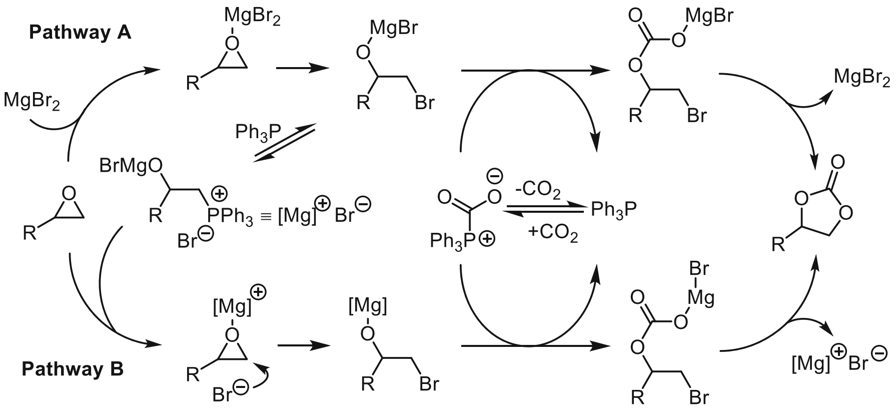

Scheme 18 Proposed mechanism for the $MgBr_2/Ph_3P$ catalyzed conversion of epoxides with CO_2 according to Shim and co-workers [195]

It should be noted that alkali metal salts have been extensively studied in combination with various organic supports, e.g. catalytic systems based on biomass derived hydrogen bond donors such as β-cyclodextrin [197], cellulose [198, 199], lignin [200], sugarcane bagasse [201], as well as lecithin [202], organic polymers [203, 204]. However, these systems usually require reaction temperatures $\geq$100 °C and carbon dioxide pressure well above 0.1 MPa. A detailed discussion would go beyond the scope of this chapter.

In contrast to alkali metal-based systems, alkaline earth metal salts have been much less frequently used as catalysts. However, Ren and co-workers recently reported a Mg(II)-based catalyst system which operates at room temperature [195]. The most active system was the combination of $MgBr_2$ and triphenylphosphane (entry 10). In this case, the reaction time can be reduced to 1 h if the reaction is performed at 60 °C. The authors propose two pathways for the addition of CO_2 to the epoxide (Scheme 18). In pathway A the epoxide is activated by the Lewis-acidic $MgBr_2$ while in pathway B activation occurs by an in situ formed phosphonium salt. In both pathways CO_2 activation by the Lewis-basic phosphane is suggested.

Most recently, He et al. reported calcium halides in combination with DBU as a cooperative catalytic system [196]. The halide activity increased in the order $F^- < Cl^- < Br^- \approx I^-$. The reaction proceeds smoothly at atmospheric CO_2 pressure (entry 11). Notably, in the absence of the $CaBr_2$ the yield dropped to 41%. In the absence of DBU the yield was <10%. The authors proposed an dual activation model involving the epoxide ring opening by either a DBU–CO_2 adduct or bromide in combination with the Lewis-acidic activation of the epoxide by Ca^{2+}.

4.2 Boron and Carbon Group-Based Catalytic Systems

Several boron group catalysts have been discussed in previous sections, e.g. Zhang and co-workers reported boronic acid catalyst **47** in combination with tetrabutylammonium salts as co-catalysts in the synthesis of cyclic carbonates (see

Table 16 Selected boron and carbon group-based catalytic systems

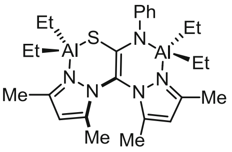

87

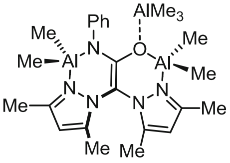

88

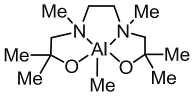

89

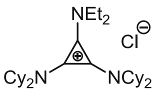

90

Entry	Cat. (mol%)	Co-cat. (mol%)	Sub. (mmol)	*T* (°C)	*p* (MPa)	*t* (h)	Yield (%)	References
1	**87** (5)	TBAB (5)	SO (1.7)	r.t.	1	24	83	[205]
2	**88** (5)	TBAB (5)	SO (1.7)	18	0.1	24	89	[206]
3	**89** (0.1)	PPNCl (0.1)	PO (10)	100	1	12	87[a]	[208]
4	$InBr_3$ (5)	Ph_3P (10)	PO (10)	r.t.	0.1	5	82	[210]
5	**90** (2.5)	–	SO (8.8)	75	0.1	20	90	[211]
6	$SnCl_4$ (0.05)	DBU (0.25)	PO (200)	50	0.2	3	>99	[212]
7	Bu_3SnI (2)	TBPI[b] (2)	PO (50)	40	4.9	1	100	[213]

[a] Conversion is given (selectivity >99%)

[b] Tetrabutylphosphonium iodide

Chapter 2.6) [125]. Moreover, aluminum-based systems were discussed in the privileged metal complex section (Chapter 3). Besides those systems, recently several other aluminum-based catalytic systems have been described which facilitate the efficient conversion of epoxides with CO_2 under mild reaction conditions. In 2012 Castro-Osma et al. reported bimetallic aluminum complex **87** in combination with TBAB as co-catalyst operating at room temperature (Table 16, entry 1) [205]. Notably, this complex displayed significantly higher catalytic activity than the corresponding monometallic complex. Subsequently, this catalytic system was further evaluated [206, 207]. A parallel screening of various catalysts was performed including 19 different aluminum complexes based on **87** as lead structure. As a result of this screening, trimetallic complex **88** was identified as the best catalyst allowing the reaction to be performed even at 0.1 MPa CO_2 pressure (entry 2) [206]. Kim, Lee, and co-workers studied mono- and dinuclear aluminum complexes based on multidentate aliphatic amino alcohols [208, 209]. ^{27}Al NMR revealed that the dinuclear complexes remain dimeric in solution regardless of the presence of a co-catalyst and/or epoxide [209]. Aluminum complex **89** showed the highest activity in combination with PPNCl (entry 3) [208]. Shibata et al. reported an efficient and very simple catalytic system comprising $InBr_3$ as catalyst and triphenylphosphane as additive [210]. Notably, this binary catalytic system allowed the conversion of several terminal epoxides, e.g. propylene oxide at room temperature and 0.1 MPa CO_2 pressure (entry 4).

Systems based on Si, Ge, Sn, and Pb are far less studied. However, a silanol-based catalyst **46** has been discussed in Chapter 2.6 and tin porphyrine complex **48b** was introduced in Chapter 3.1. Usually group 15 onium compounds, namely ammonium and phosphonium salts, are frequently employed as catalysts and co-catalysts in the addition of CO_2 to epoxides. Recently, Lambert and co-workers used a cyclopropenium salt **90** as a metal-free one component organocatalyst for this reaction (entry 5) [211]. Even though only four cyclic carbonates were prepared from the respective epoxides, **90** exhibits an easily modifiable structure and thus is a promising new class of onium salt catalysts. Jing and Nguyen reported the use of simple $SnCl_4$ in combination with different amine bases as catalyst. In the presence of DMAP initial turnover frequencies up to 1388 h^{-1} could be achieved [212]. A binary catalytic system based on $SnCl_4$ in combination with DBU allowed the conversion of propylene oxide with CO_2 even at 50 °C and low CO_2 pressure of 0.2 MPa (entry 6). In situ ^{119}Sn NMR spectra indicated 8 different tin species. The Lewis-acidic metal center is coordinated by propylene oxide, chloride and/or DBU. Another simple Sn-based system which operates under mild conditions has already been reported in 1987 by Baba and co-workers (entry 7) [213].

4.3 Transition Metal-Based Catalytic Systems

In this chapter transition metal-based catalytic systems are discussed. However, transition metal complexes comprising privileged ligands namely porphyrines, salen, and related ligands as well as amino phenolate ligands have been discussed in chapter 3. D'Elia and co-workers recently gave an excellent overview about group III–V transition metal complexes as catalysts for the addition of CO_2 to epoxides [56]. Only very few of the early transition metal systems catalyze this reaction under mild conditions.

Eddaoudi and co-workers reported the use of readily available YCl_3 in combination with TBAB as a catalytic system for the conversion of propylene oxide under ambient conditions (Table 17, entry 1) [214]. The direct capture and conversion of CO_2 from flue gas emitted by a point source, e.g. industrial flue gas might maximize the benefits of CO_2 use. Barthel et al. studied various early transition metal salts in combination with TBAB as catalyst system for the synthesis of cyclic carbonates [215]. YCl_3 proved to be a feasible catalyst leading to 98% CO_2 conversion and 37% yield of propylene carbonate even under a stream of CO_2 with a total gas flow (50 vol.% CO_2 with Ar) of 59.44×10^{-7} mol s^{-1}. If oxygen was used instead of argon slightly lower catalytic efficiency was observed. The presence of water, which is also a component of flue gas, led also to a reduction of the reaction rate. However, the authors could finally show that this catalytic system is active even if real flue gas (10.2 vol.% CO_2 content) was used, reaching CO_2 conversions of up to 73% based on propylene carbonate yield.

Go et al. reported a series of new half-sandwich titanocenes and their application in the synthesis of propylene carbonate. A titanium complex **91** based on a mono anionic bidentate tetrazole in combination with TBAI provides a conversion of propylene oxide of 86% at a temperature below 100 °C (entry 2) [216]. Kim et al. reported a dinuclear zirconium complex **92** as catalyst for this reaction [217]. Notably, this was the first study on zirconocene catalysts for the addition of CO_2 to epoxides. TBPB proved to be the best co-catalyst for the conversion of PO at a moderate reaction temperature of 75 °C (entry 3). Lee and co-workers studied various simple transition metal salts MX_n in combination with onium salt co-

Table 17 Selected group III–V-based catalytic systems for the conversion of CO_2 with epoxides

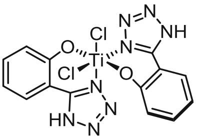

91

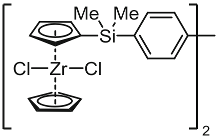

92

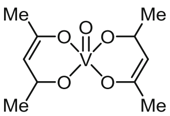

93

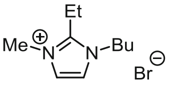

94

Entry	Cat. (mol%)	Co-cat. (mol%)	Sub. (mmol)	*T* (°C)	*p* (MPa)	*t* (h)	Yield (%)	References
1	YCl_3 (1)	TBAB (2)	PO (100)	25	0.1	4	75[a]	[214]
2	**91** (0.1)	TBAI (0.1)	PO (28.5)	75	2.2	4.5	86[a]	[216]
3	**92** (0.2)	TBPB (0.2)	PO (10)	75	1	7	92	[217]
4	VCl_3 (0.33)	$[Bu_4N]OAc$ (0.33)	PO (100)	90	1.5	4	98	[218]
5	**93** (2.5)	TBAI (5)	EH (2)	25	0.2	18	91	[219]
6	$NbCl_5$ (0.5)	TBAB (1)	PO (100)	25	0.05	14	99[a]	[220]
7	$NbCl_5$ (1)	**94** (2)	PO (10)	r.t.	0.4	2	93	[221]

[a] Conversion is given

catalysts. Vanadium(III) and iron(III)chloride showed the highest activity. Subsequently, different onium salts were studied as co-catalysts. Most interestingly, non-nucleophilic tetrabutyl-ammonium acetate was highly active. The order of activity for the tetrabutyl-ammonium salts in combination with $FeCl_3$ was $AcO^- > Cl^- > Br^- > I^-$. Hence, in the presence of 0.33 mol% of VCl_3 and 0.33 mol% $[Bu_4N]OAc$ a conversion of 98% of PO was achieved at 90 °C and a pressure of 1.5 MPa CO_2. (entry 4) [218]. Coletti et al. evaluated a series of different substituted salen and salphen vanadyl complexes as well as commercially available $VO(acac)_2$ **93** with TBAI as co-catalyst. Interestingly, **93** proved to be the most active catalyst allowing the conversion of various epoxides, e.g. epoxyhexane at 25 °C and low CO_2 pressure of 0.2 MPa (entry 5) [219].

In an initial study Monassier et al. explored group IV–VI transition metal halides and oxychlorides in combination with DMAP for the conversion of propylene oxide with CO_2 under mild conditions (50 °C, 0.5 MPa, 12 h) [220]. $NbCl_5$/DMAP formed an active catalyst system leading to high conversion up to 96% and turnover frequencies up to 67.2 h^{-1}. A screening of different nucleophiles resulted in a system which showed even better performance. The combination of $NbCl_5$ and TBAB allowed the conversion of propylene oxide even at room temperature and $p(CO_2) = 0.05$ MPa (entry 6). Furthermore, it has been reported that the catalytic activity of the Nb halides decreased in the order $NbCl_5 > NbBr_5 \gg NbF_5$ [222]. Subsequently, mechanistic studies on the synthesis of propylene carbonate from PO and CO_2 for both systems ($NbCl_5$/DMAP and $NbCl_5$/TBAB) have been reported [223]. The potential energy surface profile calculated by Zhang et al. showed a barrier for the ring-opening of PO by TBAB of 28.2 kcal mol^{-1} [224]. This relatively high activation barrier prevents the reaction to occur at ambient conditions in the absence

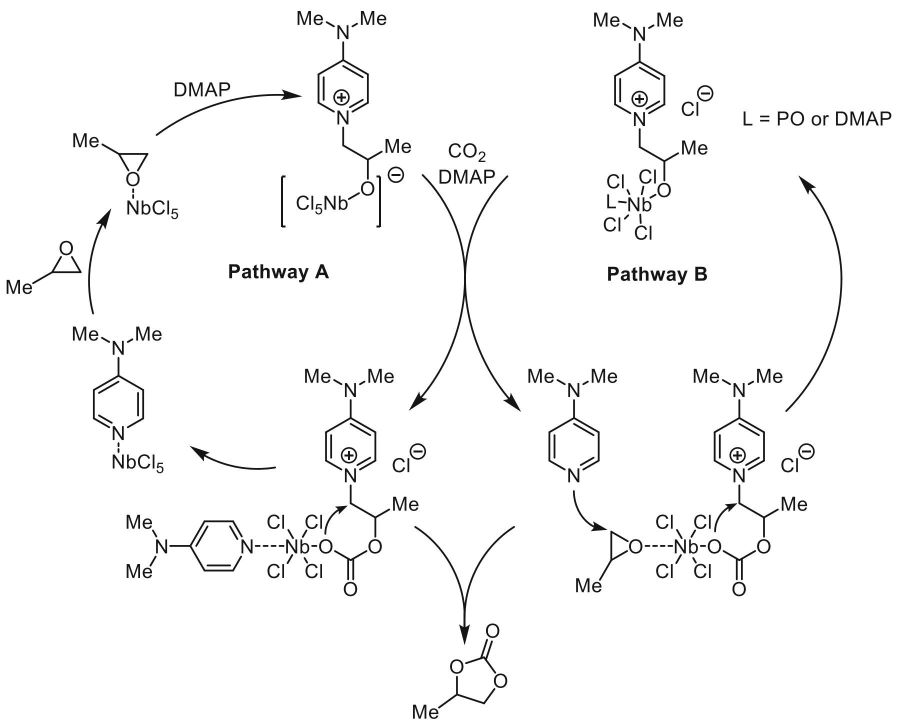

Scheme 19 Proposed mechanistic pathways for the addition of CO_2 to PO catalyzed by $NbCl_5$ and DMAP [223]

of $NbCl_5$. In contrast, in the presence of DMAP-$NbCl_5$ the barrier for the ring-opening step at the less substituted carbon atom is lowered to 3.2 kcal mol^{-1}. For the $NbCl_5$/TBAB the ring-opening is barrierless reaction at the sterically less hindered carbon center assisted by the Lewis acid [223]. Another interesting aspect for the $NbCl_5$/DMAP system has been revealed by a combination of kinetic investigations and in situ spectroscopy which suggested the involvement of a second DMAP molecule in the rate-determining step (the ring-closing). DMAP facilitates this step after the dissociation of a chloride ligand from the niobium center. This may take place through direct nucleophilic attack of DMAP at the hemicarbonate species (pathway A, Scheme 19) or ring opening of an activated epoxide molecule (pathway B). The same groups also reported the use of imidazolium bromides as co-catalysts for this reaction [221]. In wide screening of 31 different salts compound **94** proved to be the most efficient co-catalyst allowing complete conversion of PO within 2 h at room temperature and low CO_2 pressure (entry 7).

In the early 1980s, Kisch and Ratzenhofer reported that $MoCl_5$, $FeCl_3$, and $CoCl_2$ catalyzed the addition of CO_2 to propylene oxide at room temperature and low CO_2 pressure (0.1 MPa) in the presence of triphenylphosphane. Even though long reaction times of 7 days were required the respective carbonate was obtained in yields $\geq 75\%$. The best catalytic system was the combination of $MoCl_5$ and triphenyl-phosphane (5:1) yielding propylene carbonate in 78% (Table 18, entry 1) [225].

Group VII- and VIII-based systems able to catalyze the addition of CO_2 to epoxides under mild conditions have also been reported. Wong et al. reported tricarbonyl rhenium (I) complex **95** with a pyrrolidinium bromide moiety as catalyst for the addition of CO_2 and epoxides, e.g. styrene oxide in a pyrollidinium-based ionic liquid as solvent (entry 2) [226]. Bu et al. used ruthenium complex **96** for the synthesis of propylene carbonate. At low catalyst loading (0.024 mol%) the desired product was obtained in 97% yield in the presence of cetyltrimethylammonium chloride (CTAC) as co-catalyst (entry 3) [227]. The same group also reported *trans*-dichlorotetrapyridine-ruthenium(II) as a catalyst [228]. Under slightly more drastic conditions (80 °C, 3.0 MPa, 4 h) 99% yield was achieved. Buonerba et al. reported the synthesis of an air stable dinuclear iron(III) thioether-triphenolate complex **97** and its application in the addition of CO_2 to epoxides (entry 4) [229]. Fuchs et al. used iron(III) catalyst **98** without co-catalyst for the synthesis of cyclic carbonates from epoxides and CO_2 [230]. High conversions were obtained for several terminal epoxides, e.g. 96% for styrene oxide at 80 °C (entry 5).

Dinuclear cobalt complex **99** has been reported by Tang and co-workers as catalyst for cyclic carbonate synthesis [231]. In combination with phenyltrimethylammonium tribromide this catalyst facilitates the reaction at ambient temperature (entry 6). Zevaco and co-workers reported a series of differently substituted *N,N*-bis(2-pyridinecarboxamide)-1,2-benzene ligands [232]. Cobalt, chromium, and iron complexes based on these ligands were prepared and tested as catalysts in the coupling of CO_2 with epoxides to produce polycarbonates and cyclic carbonates, respectively. In the presence of catalyst **100** propylene carbonate was obtained at 80 °C and 3.5 MPa CO_2 pressure in 78% yield (entry 7). Notably, this ionic complex bearing a tetraethyl ammonium counterion does not require any additional co-catalyst.

Most recently, Rulev and co-workers reported chiral cobalt(III) complex **101**, which offers Brønsted acid as well as Lewis base properties [233]. The authors propose the ligand acting as a hydrogen bond donor activating the epoxide. In the presence of **101** various epoxides, e.g. styrene oxide could be converted to the respective carbonates without the addition of a co-catalyst (entry 8).

Unfortunately, no kinetic resolution was observed when terminal epoxides were used as substrates. However, if chalcone oxide was converted kinetic resolution did occur. At 60% conversion the enantiomeric purity of the remaining epoxide was 55%.

Since the pioneering work of Inoue and co-workers [234], catalysts based on zinc are probably the most frequently studied metal containing catalytic systems for the synthesis of cyclic carbonates and polycarbonates from carbon dioxide and epoxides. Thus, several privileged zinc complexes have been already discussed in chapter 3. However, numerous other systems based on zinc complexes or simple zinc salts have been studied that catalyze the addition of CO_2 to epoxides under mild conditions.

In 2014 Zevaco and co-workers reported the synthesis of **102a** as catalyst for the synthesis of propylene carbonate (Table 19, entry 1) [235]. In the presence of 0.2 mol% TBAI as co-catalyst the desired product was obtained in a yield of 88% after 20 h at 40 °C and 0.2 MPa. Initial turnover frequencies of up to 744 h^{-1} were

Table 18 Selected group VI–IX-based catalytic systems for the conversion of CO_2 with epoxides

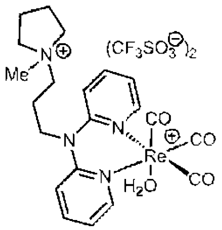

95

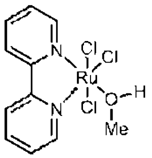

96

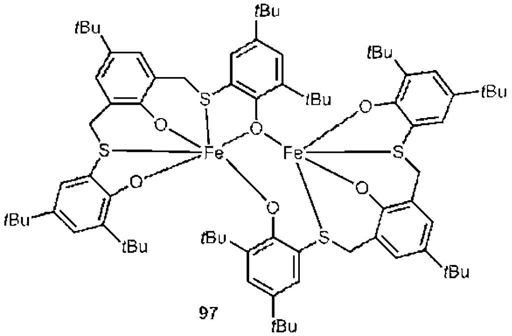

97

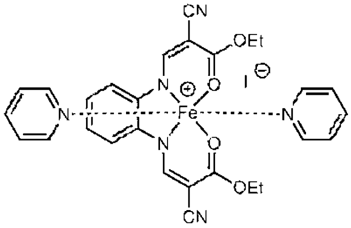

98

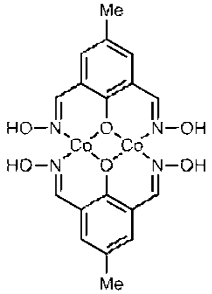

99

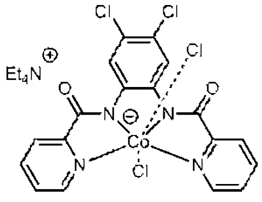

100

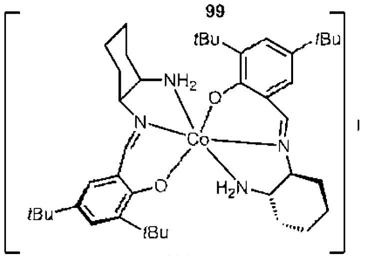

101

Entry	Cat. (mol%)	Co-cat. (mol%)	Sub. (mmol)	*T* (°C)	*p* (MPa)	*t* (h)	Yield (%)	References
1	$MoCl_5$ (1)	PPh_3 (5)	PO (143)	r.t.	0.1	168	78	[225]
2[a]	**95** (0.8)	–	SO (2.5)	80	1.5	2	94	[226]
3	**96** (0.024)	CTAT (0.024)	PO (210)	75	3.0	4	97	[227]
4	**97** (0.25)	TBAB (0.5)	PO	60	2.0	6	99[b]	[229]
5	**98** (0.2)	TBAB (0.2)	SO	80	5.0	20	96	[230]
6	**99** (0.1)	PTAT (0.4)	PO (100)	r.t.	0.69	3	91.2	[231]
7	**100** (0.2)	–	PO (143)	80	3.5	20	78	[232]
8	**101** (2)	–	SO	50	5.0	24	95[b]	[233]

[a] The ionic liquid *N,N*-methyl ethyl pyrrolidinium bromide was used as solvent

[b] Conversion is given

determined in the presence of only 0.1 mol% **102a** at 80 °C after 1 h. Moreover, under adjusted reaction conditions Zn-catalyst **102a** was also able to produce poly(cyclohexene carbonate) (PCHC) from CHO and CO_2. Additionally, different co-catalysts were tested in the reaction of CHO and CO_2. In terms of selectivity, using TBAB and TBAI lead rather to cyclohexene carbonate (CHC) as the main product while tetrabutylammonium chloride and PPNCl lead to the formation of pure PCHC. Hence, it was considered that soft Lewis bases like Br^- and I^- promote the reaction of CHC and a harder Lewis base will give PCHC. Further investigations were conducted with special emphasis on the ligand structure of the Zn–N_2O_2 catalyst system [236]. In total, 19 ligands were tested. Under the given reaction conditions the TOF and yield of PC of catalyst **102a** was further increased by substitution of electron withdrawing groups CN to CO_2Et and Cl substituents at the phenyl backbone (**102b**, entry 2). Regarding the mechanism, Zevaco and co-workers proposed the formation of an ionic complex bearing tetrabutylammonium counterion (similar to cobalt complex **100**) to play a crucial role within the catalytic cycle. The same group reported zinc bispyridylamide complexes for the catalytic formation of cyclic carbonates [237].

In the model reaction catalyst 0.1 mol% **103** and 0.1 mol% TBAI co-catalyst produced PC in 92% yield after 20 h at 80 °C and 3.5 MPa (entry 3). PPNCl or DMAP proved to be inappropriate co-catalyst. In the case of DMAP, poor reactivity was observed, which was attributed to the formation of a stable **103**/DMAP complex.

He and co-workers reported a Zn-complex **104** for the formation of cyclic carbonates using 1-hydroxy-2-pyridone as ligand (entry 4) [238]. In the presence of 0.15 mol% **104** and 0.5 mol% TBAI PC was obtained after 6 h at 80 °C and 1.0 MPa. The maximum TOF for this catalyst was 22,000 h^{-1} at 120 °C and 3.0 MPa CO_2 (0.0025 mol% **104**, 0.9 mol% TBAI, 1 h, yield = 55%). However, high catalytic activity was only observed when both **104** and TBAI were employed. In recycling experiments, five runs were performed. FT-IR spectra of fresh **104** and recovered catalyst **104**/TBAI after the 5th run displayed overlapping bands for ν(NO) at 1185 cm^{-1} and ν(CO) at 1624 cm^{-1} , indicating good stability of **104**.

Mashima and co-workers developed a zinc cluster system **105** operating under ambient reaction conditions (entry 5) [239]. However, to yield propylene carbonate in 99% at 25 °C and atmospheric CO_2 pressure comparably high catalyst loadings of 2 mol% **105** and 4 mol% TBAI were required. In order to investigate the applicability of this catalytic system several gas impurities in the ratio of $\nu(CO_2)/\nu(X) = 95/5$ (X = Ar, Air, O_2, CO, NO_2, SO_2) were investigated yielding similar rates of conversion to pure CO_2 regardless from the type of impurity.

Claver, Godard, and co-workers reported a monometallic zinc complex **106** as catalyst for the addition of CO_2 to epoxides (entry 6) [240]. A maximum TOF of 480 h^{-1} was calculated after a conversion of 24% (1,2-epoxyhexane with CO_2) in the presence of 0.05 mol% **106**. IR, NMR, and XRD investigations revealed a rapid exchange of the Zn-species of the “ligand arms” at room temperature. The catalyst system **106**/TBAI was recycled five times, yielding 98% PC after the first run and 88% after the fifth run.

Table 19 Selected examples of zinc-based complexes as catalysts for the addition of CO_2 to epoxides under mild conditions

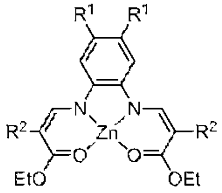

102a, R^1= H, R^2= CN
102b, R^1= Cl, R^2= CO_2Et

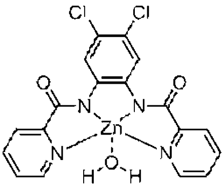

103

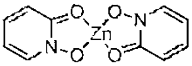

104

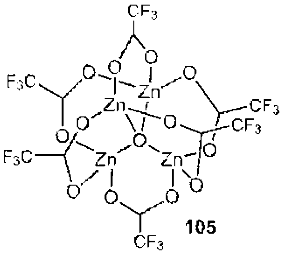

105

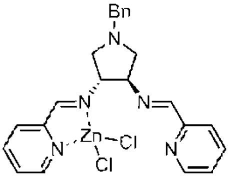

106

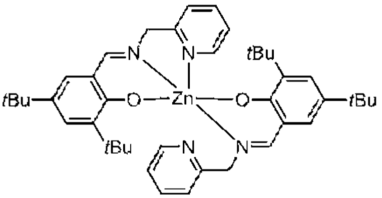

107

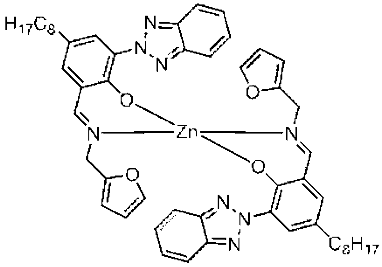

108

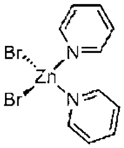

109

Entry	Cat. (mol%)	Co-cat. (mol%)	Sub. (mmol)	T (°C)	p (MPa)	t (h)	Yield (%)	References
1	**102a** (0.2)	TBAI (0.2)	PO	40	0.2	20	88	[235]
2	**102b** (0.2)	TBAI (0.2)	PO	40	0.2	20	97	[236]
3	**103** (0.1)	TBAI (0.1)	PO (143)	80	3.5	20	92[a]	[237]
4	**104** (0.15)	TBAI (0.5)	PO (5)	80	1.0	6	99	[238]
5	**105** (2.0)	TBAI (4.0)	PO (20.0)	25	0.1	6	99	[239]
6	**106** (0.05)	TBAI (0.1)	PO (42.9)	80	3.0	16	89	[240]
7	**107** (0.14)	TBAB (0.2)	PO (43.8)	80	5.0	24	82[a]	[241]
8	**108** (1.0)	TBAB (5.0)	PO (71.5)	50	1.0	24	98[a]	[242]
9	**109** (0.1)	–	EO	100	3.4	1	83	[243]

[a] Conversion is given

Masedu-Bultó and Aghmiz reported a tridentate NN’O-donor Schiff base ligand forming a mononuclear Zn(II) complex **107** for the cycloaddition of CO_2 and epoxides (entry 7) [241]. DFT studies in order to compare the stability of tetra-, penta-, or hexacoordinated species were carried out. Although hexacoordinated is the major species, in solution penta- and hexacoordinated species coexist due to only small energy differences between both species. However, X-ray diffraction crystallography of the isolated **107** revealed a penta-coordinated complex. Under supercritical conditions at 100 MPa, 100 °C and only 0.5 h employing 0.005 mol% **107** and 0.0005 mol% TBAI a maximum TOF of 3733 h^{-1} was observed.

Chen et al. reported a zinc complex **108** bearing imine-benzotriazole phenoxide ligands (entry 8) [242]. At 50 °C and 1.0 MPa a yield of 98% SC was obtained in the presence of 1.0 mol% **108**. However, the use of 5.0 mol% TBAB was required. Kim and Kang reported **109** as catalyst for the formation of cyclic carbonates from epoxides and CO_2 (entry 9) [243]. The complex **109** was treated with 10 equiv of epoxide to give **110** suitable for XRD analysis (Scheme 20).

In the proposed mechanism **110** is considered to be a key intermediate in the catalytic cycle (Scheme 20). NMR investigations were performed introducing labeled $^{13}CO_2$ into an NMR tube with **110** to give a new set of broad resonances in the ^1H NMR, as well as a specific carbonate resonance at $\delta = 170$ ppm in the ^{13}C NMR spectra. A maximum TOF of 851 h^{-1} was determined in the presence of **109**. Moreover, in further studies polystyrene pyridine was used to form an immobilized $ZnBr_2$ complex of type **109** [244].

Even very simple catalytic systems comprising zinc salts and onium salt co-catalysts facilitate the conversion of CO_2 with epoxides even under mild conditions. Already in 1986 Kisch and co-workers employed several MCl_x salts in combination with onium co-catalysts (Table 20, entry 1) [245]. In the presence of 0.2 mol% $ZnCl_2$ and 0.8 mol% TBAI propylene carbonate was obtained in 98% yield after 24 h at room temperature and atmospheric CO_2 pressure. Interestingly, if PC was used as solvent, $ZnCl_2$ (0.7 mol%) and KI (1.4 mol%) proved to be also a feasible catalyst system under ambient reaction conditions (r.t., atmospheric pressure, 21 h). However, $ZnCl_2$/TBAI was only suitable for the conversion of terminal epoxides. Internal epoxides like CHO and 2,3-epoxybutane could not be converted to the corresponding cyclic carbonates under these conditions. In 2005, Fujita and co-workers reported a similar catalyst system composed of $ZnBr_2$ and TBAI (entry 2) [246]. At elevated reaction temperature of 90 °C and a short reaction time of 0.5 h an excellent yield of 98% SC was obtained. The pressure had a crucial impact on the reaction outcome. The optimum was found to be 8.0 MPa, thus reaction occurs in $scCO_2$. A maximum TOF of 996 h^{-1} was determined with 0.05 mol% $ZnBr_2$ and 0.2 mol% TBAI after 0.5 h at 80 °C and 8.0 MPa. Notably, a distinct trend regarding the yield was effect by the counterions of the employed zinc salts with decreasing yield in the order of $ZnBr_2 \gg ZnI_2 > ZnCl_2$.

Yin, Au, and co-workers reported $ZnBr_2$ as a suitable catalyst in combination with $[Ph_4P]I$ as co-catalyst (entry 3) [247]. At elevated reaction temperatures it is possible to achieve excellent TOF of 6272 h^{-1} in the synthesis of PC, which was obtained in 90% yield after 1 h at 120 °C and 2.5 MPa. However, the presence of even trace amounts of water decreased the yield significantly. Hence, epoxides

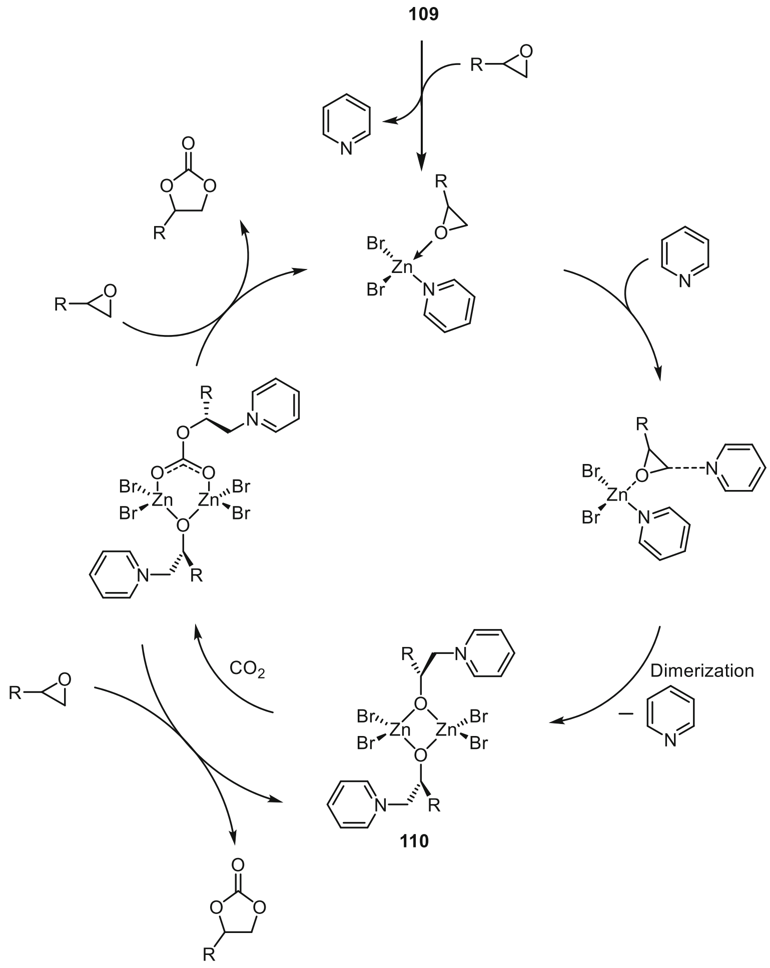

Scheme 20 Proposed mechanism for the formation of cyclic carbonate in the presence of **109** [243]

needed to be dried prior use to obtain reproducible results, as well as high yields. In contrast, Qiao and Yokohama reported zinc phenosulfonate octahydrate and TBAB for the synthesis of PC (entry 4) [248]. The use of microwave irradiation (TOF = 6989 h^{-1}) compared to conventional heating (TOF = 6383 h^{-1}) accelerated the catalytic reaction significantly applying 3 MPa CO_2 and 100 °C or 300 W MW irradiation for 0.25 h. Remarkably, TOFs of up to 20,371 h^{-1} could be obtained at 120 °C using only 0.01 mol% Zinc catalyst after 0.25 h to yield 51% of PC. In consideration of CO_2 to be in an excessive amount in the system Arrhenius law was used to determine the catalytic constant for the pseudo-first order reaction in $v = k$ [PO]. In respect to those assumptions, for MW irradiation a catalytic constant $10^4k = 8.44\ s^{-1}$ and for oil bath heating $10^4k = 7.59\ s^{-1}$ were determined at 100 °C, 3 MPa, 0.25 h.

Table 20 Selected catalytic systems based on simple zinc and onium salts

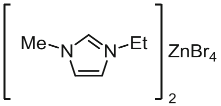

111

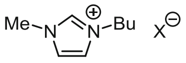

112a, X= Cl
112b, X= Br

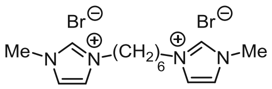

113

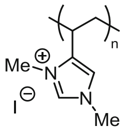

114

Entry	Cat. (mol%)	Co-cat. (mol%)	Sub. (mmol)	*T* (°C)	*p* (MPa)	*t* (h)	Yield (%)	References
1	$ZnCl_2$ (0.2)	TBAI (0.8)	PO (1000)	23	0.1	24	98	[245]
2	$ZnBr_2$ (0.3)	TBAI (0.6)	SO (35)	90	8.0	0.5	98	[246]
3	$ZnBr_2$ (0.015)	$[Ph_4P]I$ (0.09)	PO (105)	120	2.5	1	90	[247]
4	$Zn(PhSO_3)_2 \cdot 8H_2O$ (0.04)	TBAB (2.2)	PO (29.9)	100[a]	3.0	0.25	76	[248]
5	**111** (0.02)	–	EO	100	3.5	1	72	[249]
6	$ZnBr_2$ (0.4)	**112a** (0.8)	SO (35)	80	14	2	100	[250]
7	$ZnCl_2$ (0.02)	**112b** (0.11)	PO (285)	100	1.5	1	95	[251]
8	ZnI_2 (0.3)	**113** (0.14)	PO (34.5)	110	1.5	2	96	[252]
9	$ZnBr_2$ (1)	**114** (1), DBU (2)	SO (5)	80	0.1	10	94	[253]

[a] Under microwave irradiation of 300 W

Even though often reaction temperatures $\geq$100 °C are required it has to be mentioned that zinc salts in combination with imidazolium salts have been frequently studied and represent a privileged class of catalytic systems, too. In 2003 Kim et al. reported the synthesis of ionic liquid-derived zinc tetrahalide complexes, which are obtained by reacting 1-alkyl-3-methylimidazolium with zinc halides [249, 254]. The catalytic activity of imidazolium zinc tetrahalide in the coupling of ethylene and propylene oxide with CO_2 was greatly influenced by the nature of halide groups bonded to the zinc center. The catalytic activity increased in the order $[ZnBr_4]^{2-} > [ZnBr_2Cl_2]^{2-} \gg [ZnCl_4]^{2-}$. High TOFs up to 3588 h^{-1} (ethylene oxide) and 1846 h^{-1} (propylene oxide) were achieved with catalyst **111** for the coupling reactions at 100 °C and 3.5 MPa (entry 5). The obtained TOFs were considerably higher compared to simple imidazolium-based ionic liquids. Arai et al. studied the catalytic activity of various metal salts in the presence of 1-butyl-3-methylimidazolium chloride (**112a**) for the conversion of styrene oxide [250]. The nature of the metal cation had a significant impact. The catalytic activity decreased in the order $Zn^{2+} > Fe^{3+} > Fe^{2+} > Mg^{2+} > Li^{+} > Na^{+}$, which is in accordance with the Lewis acidity of the metal cations. Quantitative yield on SC was achieved for the catalyst system $ZnBr_2$/**112a** at a reaction temperature of 80 °C (entry 6). Xia et al. showed that turn over frequencies up to 5410 h^{-1} could be achieved with $ZnCl_2$ in combination with [BMim]Br (entry 7) [251]. An even higher TOF of 5580 h^{-1} was obtained when $ZnBr_2$ was employed. More recently, Sun and co-workers reported dicationic ionic liquids, e.g. **113** in combination with zinc iodide (entry 8) [252]. For the best catalyst system, excellent yields on various cyclic carbonates could be obtained even though reaction temperatures of 110 °C were required. Notably, zinc salts have also been studied with ionic liquids immobilized on various supports. Chung and co-workers reported a polyimidazolium-based tertiary catalytic system. The imidazolium-based polymer originates from histamine as precursor. In the presence of **114** styrene carbonate was obtained in 94% yield (entry 9) [253].

5 Summary and Future Trends

The reaction of carbon dioxide with epoxides to produce cyclic carbonates has gained considerable attention over the past 17 years. Notably, the synthesis of ethylene and propylene carbonates has already been industrialized. In this chapter we have summarized recent progress in cyclic carbonate synthesis starting from CO_2 and epoxides. Especially emphasized were homogeneous catalysts and catalytic systems which allow this transformation at reaction temperatures $\leq$100 °C and/or carbon dioxide pressures $\leq$0.1 MPa. With respect to the employed catalyst types it can be stated that organocatalysts in contrast to metal complex catalysts are often commercially available and/or easily accessible, e.g. ammonium and imidazolium salts. The nature of these catalysts includes often a modular synthesis, which allows easy modification and thus comparably simple optimization of the catalyst structure. However, metal complexes show considerable higher activity and thus can be employed in considerable smaller amounts (1–2 magnitudes) compared to the organocatalysts. Although metal-based systems usually require the use of onium salts as co-catalysts.

The reaction of terminal epoxides with carbon dioxide is well established and can be performed at room temperature and low CO_2 pressure. In contrast the conversion of internal epoxides under mild conditions remains challenging. In several cases the experimental work was nicely complemented by theoretical calculations. The gained knowledge and insights into the interaction between the catalytic species and substrate helped to rationalize the experimental results and might allow the design of new catalysts and processes. The development of catalysts which are able to facilitate the conversion of epoxides at low CO_2 concentrations and pressure (preferably at 0.1 MPa) namely simple air would be a significant progress. The control of the *cis*/*trans* selectivity in the conversion of internal epoxides as well as kinetic resolutions of racemic epoxides are still open challenges. The direct access of cyclic carbonates from olefins has been investigated, but so far no efficient catalytic method has been developed which is generally applicable. The increasing number of publications since 2000 on the synthesis and application of cyclic carbonates reveals the major interest in this field of research to the chemical community. The authors hope that this review is a valuable contribution for scientists interested in the field and might stimulate further developments.

References

1. Olah GA (2013) Angew Chem Int Ed 52:104
2. Olah GA, Prakash GKS, Goeppert A (2011) J Am Chem Soc 133:12881
3. Olah GA, Goeppert A, Prakash GKS (eds) (2009) The “methanol economy”: general aspects. Wiley, Weinheim
4. Bertau M, Offermanns H, Plass L, Schmidt F, Wernicke H-J (eds) (2014) Methanol: the basic chemical and energy feedstock of the future. Springer, Heidelberg
5. Pachauri RK, Meyer LA (eds) (2014) IPCC, Climate Change 2014: synthesis report. Intergovernmental Panel on Climate Change, Geneva
6. Mauna Loa Observatory (Hawaii), U.S. Department of Commerce, National Oceanic & Atmospheric Administration (NOAA). http://www.esrl.noaa.gov/news/2013/CO2400.html. Accessed 28 Nov 2016
7. Klankermayer J, Wesselbaum S, Beydoun K, Leitner W (2016) Angew Chem Int Ed 55:7296
8. Liu Q, Wu L, Jackstell R, Beller M (2015) Nat Commun 6:5933
9. Aresta M, Dibenedetto A, Angelini A (2014) Chem Rev 114:1709
10. Otto A, Grube T, Schiebahn S, Stolten D (2015) Energy Environ Sci 8:3283
11. Sakakura T, Choi J-C, Yasuda H (2007) Chem Rev 107:2365
12. Besse V, Camara F, Voirin C, Auvergne R, Caillol S, Boutevin B (2013) Polym Chem 4:4545
13. Pescarmona PP, Taherimehr M (2012) Catal Sci Technol 2:2169
14. Schäffner B, Schäffner F, Verevkin SP, Börner A (2010) Chem Rev 110:4554
15. Shaikh A-AG, Sivaram S (1996) Chem Rev 96:951
16. Alder CM, Hayler JD, Henderson RK, Redman AM, Shukla L, Shuster LE, Sneddon HF (2016) Green Chem 18:3879
17. Philipp M, Bhandary R, Groche FJ, Schönhoff M, Rieger B (2015) Electrochim Acta 173:687
18. Sonnati MO, Amigoni S, Taffin de Givenchy EP, Darmanin T, Choulet O, Guittard F (2013) Green Chem 15:283
19. Nemirowsky J (1883) J Prakt Chem 28:439
20. Selva M, Caretto A, Noè M, Perosa A (2014) Org Biomol Chem 12:4143

21. Khusnutdinov RI, Shchadneva NA, Mayakova YY (2014) Russ J Org Chem 50:948
22. Indran VP, Haji Saud AS, Maniam GP, Yusoff MM, Taufiq-Yap YH, Ab. Rahim MH (2016) RSC Adv 6:34877
23. Kuznetsov VA, Pervova MG, Pestov AV (2013) Russ J Org Chem 49:1859
24. Peña-López M, Neumann H, Beller M (2016) Eur J Org Chem 2016:3721
25. Doro F, Winnertz P, Leitner W, Prokofieva A, Müller TE (2011) Green Chem 13:292
26. Gabriele B, Mancuso R, Salerno G, Veltri L, Costa M, Dibenedetto A (2011) ChemSusChem 4:1778
27. Pearson DM, Conley NR, Waymouth RM (2011) Adv Synth Catal 353:3007
28. Bobbink FD, Gruszka W, Hulla M, Das S, Dyson PJ (2016) Chem Commun 52:10787
29. Honda M, Tamura M, Nakao K, Suzuki K, Nakagawa Y, Tomishige K (2014) ACS Catal 4:1893
30. Lim YN, Lee C, Jang H-Y (2014) Eur J Org Chem 2014:1823
31. Reithofer MR, Sum YN, Zhang Y (2013) Green Chem 15:2086
32. Hirose T, Shimizu S, Qu S, Shitara H, Kodama K, Wang L (2016) RSC Adv 6:69040
33. Chen K, Shi G, Dao R, Mei K, Zhou X, Li H, Wang C (2016) Chem Commun 52:7830
34. Hu J, Ma J, Zhu Q, Qian Q, Han H, Mei Q, Han B (2016) Green Chem 18:382
35. Kayaki Y, Yamamoto M, Ikariya T (2009) Angew Chem Int Ed 48:4194
36. Wu J, Kozak JA, Simeon F, Hatton TA, Jamison TF (2014) Chem Sci 5:1227
37. Rocha CC, Onfroy T, Launay F (2015) C R Chimie 18:270
38. Kumar S, Singhal N, Singh RK, Gupta P, Singh R, Jain SL (2015) Dalton Trans 44:11860
39. Poliakoff M, Leitner W, Streng ES (2015) Faraday Discuss 183:9
40. Anastas P, Eghbali N (2010) Chem Soc Rev 39:301
41. Zhang H, Liu H-B, Yue J-M (2014) Chem Rev 114:883
42. North M, Pasquale R, Young C (2010) Green Chem 12:1514
43. Sakakura T, Kohno K (2009) Chem Commun 45:1312
44. Martín C, Fiorani G, Kleij AW (2015) ACS Catal 5:1353
45. Fiorani G, Guo WS, Kleij AW (2015) Green Chem 17:1375
46. Cokoja M, Wilhelm ME, Anthofer MH, Herrmann WA, Kühn FE (2015) ChemSusChem 8:2436
47. Bobbink FD, Dyson PJ (2016) J Catal 343:52
48. Xu B-H, Wang J-Q, Sun J, Huang Y, Zhang J-P, Zhang X-P, Zhang S-J (2015) Green Chem 17:108
49. Cheng W, Su Q, Wang J, Sun J, Ng F (2013) Catalysts 3:878
50. Sun J, Fujita S-i, Arai M (2005) J Organomet Chem 690:3490
51. He Q, O'Brien JW, Kitselman KA, Tompkins LE, Curtis GCT, Kerton FM (2014) Catal Sci Technol 4:1513
52. Beyzavi MH, Stephenson CJ, Liu Y, Karagiaridi O, Hupp JT, Farha OK (2015) Front Energy Res 2:1
53. Kathalikkattil AC, Babu R, Tharun J, Roshan R, Park D-W (2015) Catal Surv Asia 19:223
54. Decortes A, Castilla AM, Kleij AW (2010) Angew Chem Int Ed 49:9822
55. Wu X, Castro-Osma J, North M (2016) Symmetry 8:4
56. D'Elia V, Pelletier JDA, Basset J-M (2015) ChemCatChem 7:1906
57. Comerford JW, Ingram IDV, North M, Wu X (2015) Green Chem 17:1966
58. Cooper JF, Lichtenwalter M (1956) US Patent 2,773,070, 4 Sep 1956
59. Peppel WJ (1958) Ind Eng Chem 50:767
60. Springmann H (1971) Fette, Seifen, Anstrichmittel 73:396
61. Caló V, Nacci A, Monopoli A, Fanizzi A (2002) Org Lett 4:2561
62. Mamone M, Milcent T, Crousse B (2015) Chem Commun 51:12736
63. Aoyagi N, Furusho Y, Endo T (2013) J Polym Sci A Polym Chem 51:1230
64. Wang L, Lin L, Zhang G, Kodama K, Yasutake M, Hirose T (2014) Chem Commun 50:14813
65. Ema T, Fukuhara K, Sakai T, Ohbo M, Bai F-Q, J-y Hasegawa (2015) Catal Sci Technol 5:2314
66. Shim JJ, Kim D, Ra CS (2006) Bull Korean Chem Soc 27:744
67. Mirabaud A, Mulatier J-C, Martinez A, Dutasta J-P, Dufaud V (2015) ACS Catal 5:6748
68. Amaral AJR, Coelho JFJ, Serra AC (2013) Tetrahedron Lett 54:5518
69. Roshan KR, Jose T, Kim D, Cherian KA, Park DW (2014) Catal Sci Technol 4:963
70. Büttner H, Lau K, Spannenberg A, Werner T (2015) ChemCatChem 7:459
71. Tharun J, Roshan KR, Kathalikkattil AC, Kang D-H, Ryu H-M, Park D-W (2014) RSC Adv 4:41266
72. Du Y, Wang J-Q, Chen J-Y, Cai F, Tian J-S, Kong D-L, He L-N (2006) Tetrahedron Lett 47:1271

73. Nishikubo T, Kameyama A, Yamashita J, Fukumitsu T, Maejima C, Tomoi M (1995) J Polym Sci Polym Chem 33:1011
74. Kohrt C, Werner T (2015) ChemSusChem 8:2031
75. Motokura K, Itagaki S, Iwasawa Y, Miyaji A, Baba T (2009) Green Chem 11:1876
76. Nishikubo T, Kameyama A, Yamashita J, Tomoi M, Fukuda W (1993) J Polym Sci Polym Chem 31:939
77. Crosby GW, Millikan AF (1961) The Pure Oil Company US 2994705
78. Sun J, Ren J, Zhang S, Cheng W (2009) Tetrahedron Lett 50:423
79. Aoyagi N, Furusho Y, Endo T (2013) Tetrahedron Lett 54:7031
80. Werner T, Büttner H (2014) ChemSusChem 7:3268
81. Toda Y, Komiyama Y, Kikuchi A, Suga H (2016) ACS Catal 6:6906
82. Liu S, Suematsu N, Maruoka K, Shirakawa S (2016) Green Chem 18:4611
83. Zhou H, Wang G-X, Zhang W-Z, Lu X-B (2015) ACS Catal 5:6773
84. Chatelet B, Joucla L, Dutasta J-P, Martinez A, Szeto KC, Dufaud V (2013) J Am Chem Soc 135:5348
85. Büttner H, Steinbauer J, Werner T (2015) ChemSusChem 8:2655
86. Großeheilmann J, Büttner H, Kohrt C, Kragl U, Werner T (2015) ACS Sustainable Chem Eng 3:2817
87. Büttner H, Steinbauer J, Wulf C, Dindaroglu M, Schmalz H-G, Werner T (2016) ChemSusChem 10:1076
88. Chatelet B, Joucla L, Dutasta J-P, Martinez A, Dufaud V (2014) Chem Eur J 20:8571
89. Chatelet B, Jeanneau E, Dutasta J-P, Robert V, Martinez A, Dufaud V (2014) Catal Commun 52:26
90. Peng J, Deng Y (2001) New J Chem 25:639
91. Kawanami H, Sasaki A, Matsui K, Ikushima Y (2003) Chem Commun 39:896
92. Sun J, Zhang S, Cheng W, Ren J (2008) Tetrahedron Lett 49:3588
93. Denizalti S (2015) RSC Adv 5:45454
94. Anthofer MH, Wilhelm ME, Cokoja M, Markovits IIE, Pothig A, Mink J, Herrmann WA, Kühn FE (2014) Catal Sci Technol 4:1749
95. Anthofer MH, Wilhelm ME, Cokoja M, Drees M, Herrmann WA, Kühn FE (2015) ChemCatChem 7:94
96. Girard A-L, Simon N, Zanatta M, Marmitt S, Goncalves P, Dupont J (2014) Green Chem 16:2815
97. Yang Z-Z, He L-N, Miao C-X, Chanfreau S (2010) Adv Synth Catal 352:2233
98. Pérez ER, Santos RHA, Gambardella MTP, de Macedo LGM, Rodrigues-Filho UP, Launay J-C, Franco DW (2004) J Org Chem 69:8005
99. Heldebrant DJ, Jessop PG, Thomas CA, Eckert CA, Liotta CL (2005) J Org Chem 70:5335
100. Aoyagi N, Furusho Y, Endo T (2012) Chem Lett 41:240
101. Coulembier O, Moins S, Lemaur V, Lazzaroni R, Dubois P (2015) J CO2 Util 10:7
102. Wang L, Kodama K, Hirose T (2016) Catal Sci Technol 6:3872
103. Yu T, Weiss RG (2012) Green Chem 14:209
104. Zhou H, Zhang W-Z, Liu C-H, Qu J-P, Lu X-B (2008) J Org Chem 73:8039
105. Zhou H, Wang Y-M, Zhang W-Z, Qu J-P, Lu X-B (2011) Green Chem 13:644
106. Ajitha MJ, Suresh CH (2011) Tetrahedron Lett 52:5403
107. Liu X, Cao C, Li Y, Guan P, Yang L, Shi Y (2012) Synlett 23:1343
108. Zhang H, Kong X, Cao C, Pang G, Shi Y (2016) J CO2 Util 14:76
109. Desens W, Werner T (2016) Adv Synth Catal 358:622
110. Shen Y-M, Duan W-L, Shi M (2003) Adv Synth Catal 345:337
111. Shen Y-M, Duan W-L, Shi M (2004) Eur J Org Chem 2004:3080
112. Whiteoak CJ, Nova A, Maseras F, Kleij AW (2012) ChemSusChem 5:2032
113. Whiteoak CJ, Henseler AH, Ayats C, Kleij AW, Pericas MA (2014) Green Chem 16:1552
114. Sopeña S, Fiorani G, Martín C, Kleij AW (2015) ChemSusChem 8:3248
115. Martínez-Rodríguez L, Otalora Garmilla J, Kleij AW (2016) ChemSusChem 9:749
116. Saptal V, Shinde DB, Banerjee R, Bhanage BM (2016) Catal Sci Technol 6:6152
117. Gennen S, Alves M, Mereau R, Tassaing T, Gilbert B, Detrembleur C, Jerome C, Grignard B (2015) ChemSusChem 8:1845
118. Alves M, Grignard B, Gennen S, Mereau R, Detrembleur C, Jerome C, Tassaing T (2015) Catal Sci Technol 5:4636
119. Alves M, Grignard B, Gennen S, Detrembleur C, Jerome C, Tassaing T (2015) RSC Adv 5:53629

120. Wilhelm ME, Anthofer MH, Cokoja M, Markovits IIE, Herrmann WA, Kühn FE (2014) ChemSusChem 7:1357
121. Wang L, Zhang G, Kodama K, Hirose T (2016) Green Chem 18:1229
122. Liu X-F, Song Q-W, Zhang S, He L-N (2016) Catal Today 263:69
123. Roshan KR, Kim BM, Kathalikkattil AC, Tharun J, Won YS, Park DW (2014) Chem Commun 50:13664
124. Hardman-Baldwin AM, Mattson AE (2014) ChemSusChem 7:3275
125. Wang J, Zhang Y (2016) ACS Catal 6:4871
126. Alves M, Mereau R, Grignard B, Detrembleur C, Jerome C, Tassaing T (2016) RSC Adv 6:36327
127. Zhou L, Liu Y, He Z, Luo Y, Zhou F, Yu E, Hou Z, Eli W (2013) J Chem Res 37:102
128. Takeda N, Inoue S (1978) Bull Chem Soc Jpn 51:3564
129. Ahmadi F, Tangestaninejad S, Moghadam M, Mirkhani V, Mohammadpoor-Baltork I, Khosropour AR (2011) Inorg Chem Commun 14:1489
130. Kruper WJ, Dellar DD (1995) J Org Chem 60:725
131. Bai D, Duan S, Hai L, Jing H (2012) ChemCatChem 4:1752
132. Ema T, Miyazaki Y, Shimonishi J, Maeda C, Hasegawa J-y (2014) J Am Chem Soc 136:15270
133. Hasegawa J-y, Miyazaki R, Maeda C, Ema T (2016) Chem Rec 16:2260
134. Dai Z, Sun Q, Liu X, Bian C, Wu Q, Pan S, Wang L, Meng X, Deng F, Xiao F-S (2016) J Catal 338:202
135. Cozzi PG (2004) Chem Soc Rev 33:410
136. Paddock RL, Nguyen ST (2001) J Am Chem Soc 123:11498
137. Zhang X, Jia Y-B, Lu X-B, Li B, Wang H, Sun L-C (2008) Tetrahedron Lett 49:6589
138. Castro-Osma JA, Lamb KJ, North M (2016) ACS Catal 6:5012
139. Castro-Osma JA, North M, Wu X (2016) Chem Eur J 22:2100
140. Paddock RL, Nguyen ST (2004) Chem Commun 40:1622
141. Lu X-B, Liang B, Zhang Y-J, Tian Y-Z, Wang Y-M, Bai C-X, Wang H, Zhang R (2004) J Am Chem Soc 126:3732
142. Zhang S, Huang Y, Jing H, Yao W, Yan P (2009) Green Chem 11:935
143. Decortes A, Martinez Belmonte M, Benet-Buchholz J, Kleij AW (2010) Chem Commun 46:4580
144. Taherimehr M, Decortes A, Al-Amsyar SM, Lueangchaichaweng W, Whiteoak CJ, Escudero-Adan EC, Kleij AW, Pescarmona PP (2012) Catal Sci Technol 2:2231
145. Decortes A, Kleij AW (2011) ChemCatChem 3:831
146. Castro-Gómez F, Salassa G, Kleij AW, Bo C (2013) Chem Eur J 19:6289
147. Martin C, Whiteoak CJ, Martin E, Martinez Belmonte M, Escudero-Adan EC, Kleij AW (2014) Catal Sci Technol 4:1615
148. He S, Wang F, Tong W-L, Yiu S-M, Chan MCW (2016) Chem Commun 52:1017
149. Xie Y, Wang T-T, Yang R-X, Huang N-Y, Zou K, Deng W-Q (2014) ChemSusChem 7:2110
150. Lu X-B, Zhang Y-J, Liang B, Wang H, He R (2003) Chin J Catal 24:317
151. Lu X-B, Zhang Y-J, Liang B, Li X, Wang H (2004) J Mol Catal A Chem 210:31
152. Lu X-B, Zhang Y-J, Jin K, Luo L-M, Wang H (2004) J Catal 227:537
153. Ren W-M, Liu Y, Lu X-B (2014) J Org Chem 79:9771
154. Cuesta-Aluja L, Castilla J, Masdeu-Bulto AM (2016) Dalton Trans 45:14658
155. Supasitmongkol S, Styring P (2014) Catal Sci Technol 4:1622
156. Luo R, Zhou X, Chen S, Li Y, Zhou L, Ji H (2014) Green Chem 16:1496
157. Meléndez J, North M, Pasquale R (2007) Eur J Inorg Chem 21:3323
158. Beattie C, North M, Villuendas P, Young C (2013) J Org Chem 78:419
159. Melendez J, North M, Villuendas P (2009) Chem Commun 45:2577
160. Melendez J, North M, Villuendas P, Young C (2011) Dalton Trans 40:3885
161. North M, Villuendas P, Young C (2012) Tetrahedron Lett 53:2736
162. Wu X, North M (2017) ChemSusChem 10:74
163. North M, Young C (2011) Catal Sci Technol 1:93
164. Castro-Osma JA, North M, Wu X (2014) Chem Eur J 20:15005
165. North M, Pasquale R (2009) Angew Chem Int Ed 48:2946
166. Clegg W, Harrington RW, North M, Pasquale R (2010) Chem Eur J 16:6828
167. North M, Villuendas P (2012) ChemCatChem 4:789
168. North M, Wang B, Young C (2011) Energy Environ Sci 4:4163
169. Castro-Osma JA, North M, Offermans WK, Leitner W, Müller TE (2016) ChemSusChem 9:791
170. Licini G, Mba M, Zonta C (2009) Dalton Trans 38:5265

171. Whiteoak CJ, Martin E, Belmonte MM, Benet-Buchholz J, Kleij AW (2012) Adv Synth Catal 354:469
172. Whiteoak CJ, Kielland N, Laserna V, Escudero-Adán EC, Martin E, Kleij AW (2013) J Am Chem Soc 135:1228
173. Xu B, Wang P, Lv M, Yuan D, Yao Y (2016) ChemCatChem 8:2466
174. Qin J, Wang P, Li Q, Zhang Y, Yuan D, Yao Y (2014) Chem Commun 50:10952
175. Gao P, Zhao Z, Chen L, Yuan D, Yao Y (2016) Organometallics 35:1707
176. Zhao D, Liu X-H, Shi Z-Z, Zhu C-D, Zhao Y, Wang P, Sun W-Y (2016) Dalton Trans 45:14184
177. Whiteoak CJ, Martin E, Escudero-Adán E, Kleij AW (2013) Adv Synth Catal 355:2233
178. Laserna V, Fiorani G, Whiteoak CJ, Martin E, Escudero-Adan E, Kleij AW (2014) Angew Chem Int Ed 53:10416
179. Whiteoak CJ, Kielland N, Laserna V, Castro-Gómez F, Martin E, Escudero-Adán EC, Bo C, Kleij AW (2014) Chem Eur J 20:2264
180. Fiorani G, Stuck M, Martín C, Belmonte MM, Martin E, Escudero-Adán EC, Kleij AW (2016) ChemSusChem 9:1304
181. Rokicki A, Kuran W, Marcinick BP (1984) Monatsh Chem 115:205
182. Desens W, Kohrt C, Frank M, Werner T (2015) ChemSusChem 8:3815
183. Song Y, Cheng C, Jing H (2014) Chem Eur J 20:12894
184. Kihara N, Hara N, Endo T (1993) J Org Chem 58:6198
185. Iwasaki T, Kihara N, Endo T (2000) Bull Chem Soc Jpn 73:713
186. Ren Y, Guo C-H, Jia J-F, Wu H-S (2011) J Phys Chem A 115:2258
187. Ramidi P, Munshi P, Gartia Y, Pulla S, Biris AS, Paul A, Ghosh A (2011) Chem Phys Lett 512:273
188. Ma J, Liu J, Zhang Z, Han B (2012) Green Chem 14:2410
189. Tharun J, Mathai G, Kathalikkattil AC, Roshan R, Kwak J-Y, Park D-W (2013) Green Chem 15:1673
190. Roshan KR, Kathalikkattil AC, Tharun J, Kim DW, Won YS, Park DW (2014) Dalton Trans 43:2023
191. Yang Z, Sun J, Cheng W, Wang J, Li Q, Zhang S (2014) Catal Commun 44:6
192. Werner T, Tenhumberg N (2014) J CO2 Util 7:39
193. Xiao B, Sun J, Wang J, Liu C, Cheng W (2013) Synth Commun 43:2985
194. Werner T, Tenhumberg N, Büttner H (2014) ChemCatChem 6:3493
195. Ren Y, Shim J-J (2013) ChemCatChem 5:1344
196. Liu X, Zhang S, Song Q-W, Liu X-F, Ma R, He L-N (2016) Green Chem 18:2871
197. Song J, Zhang Z, Han B, Hu S, Li W, Xie Y (2008) Green Chem 10:1337
198. Liang S, Liu H, Jiang T, Song J, Yang G, Han B (2011) Chem Commun 47:2131
199. Sun J, Cheng W, Yang Z, Wang J, Xu T, Xin J, Zhang S (2014) Green Chem 16:3071
200. Wu Z, Xie H, Yu X, Liu E (2013) ChemCatChem 5:1328
201. Chen W, Zhong L-x, Peng X-w, Sun R-c, Lu F-c (2015) ACS Sustain Chem Eng 3:147
202. Song J, Zhang B, Zhang P, Ma J, Liu J, Fan H, Jiang T, Han B (2012) Catal Today 183:130
203. Ravi S, Kang DH, Roshan R, Tharun J, Kathalikkattil AC, Park DW (2015) Catal Sci Technol 5:1580
204. Yang Z, Sun J, Liu X, Su Q, Liu Y, Li Q, Zhang S (2014) Tetrahedron Lett 55:3239
205. Castro-Osma JA, Lara-Sanchez A, North M, Otero A, Villuendas P (2012) Catal Sci Technol 2:1021
206. Castro-Osma JA, Alonso-Moreno C, Lara-Sanchez A, Martinez J, North M, Otero A (2014) Catal Sci Technol 4:1674
207. Martínez J, Castro-Osma JA, Earlam A, Alonso-Moreno C, Otero A, Lara-Sánchez A, North M, Rodríguez-Diéguez A (2015) Chem Eur J 21:9850
208. Kim SH, Han SY, Kim JH, Kang YY, Lee J, Kim Y (2015) Eur J Inorg Chem 2015:2323
209. Kim SH, Ahn D, Go MJ, Park MH, Kim M, Lee J, Kim Y (2014) Organometallics 33:2770
210. Shibata I, Mitani I, Imakuni A, Baba A (2011) Tetrahedron Lett 52:721
211. Bandar JS, Tanaset A, Lambert TH (2015) Chem Eur J 21:7365
212. Jing H, Nguyen ST (2007) J Mol Catal A Chem 261:12
213. Baba A, Nozaki T, Matsuda H (1987) Bull Chem Soc Jpn 60:1552
214. Guillerm V, Weseliński ŁJ, Belmabkhout Y, Cairns AJ, D'Elia V, Wojtas Ł, Adil K, Eddaoudi M (2014) Nat Chem 6:673
215. Barthel A, Saih Y, Gimenez M, Pelletier JDA, Kuhn FE, D'Elia V, Basset J-M (2016) Green Chem 18:3116

216. Go MJ, Lee KM, Oh CH, Kang YY, Kim SH, Park HR, Kim Y, Lee J (2013) Organometallics 32:4452
217. Kim SH, Ahn D, Kang YY, Kim M, Lee K-S, Lee J, Park MH, Kim Y (2014) Eur J Inorg Chem 2014:5107
218. Bok T, Noh EK, Lee BY (2006) Bull Korean Chem Soc 27:1171
219. Coletti A, Whiteoak CJ, Conte V, Kleij AW (2012) ChemCatChem 4:1190
220. Monassier A, D'Elia V, Cokoja M, Dong H, Pelletier JDA, Basset J-M, Kühn FE (2013) ChemCatChem 5:1321
221. Wilhelm ME, Anthofer MH, Reich RM, D'Elia V, Basset J-M, Herrmann WA, Cokoja M, Kühn FE (2014) Catal Sci Technol 4:1638
222. Dutta B, Sofack-Kreutzer J, Ghani AA, D'Elia V, Pelletier JDA, Cokoja M, Kühn FE, Basset J-M (2014) Catal Sci Technol 4:1534
223. D'Elia V, Ghani AA, Monassier A, Sofack-Kreutzer J, Pelletier JDA, Drees M, Vummaleti SVC, Poater A, Cavallo L, Cokoja M, Basset J-M, Kühn FE (2014) Chem Eur J 20:11870
224. Wang J-Q, Dong K, Cheng W-G, Sun J, Zhang S-J (2012) Catal Sci Technol 2:1480
225. Ratzenhofer M, Kisch H (1980) Angew Chem Int Ed Engl 19:317
226. Wong W-L, Cheung K-C, Chan P-H, Zhou Z-Y, Lee K-H, Wong K-Y (2007) Chem Commun 43:2175
227. Bu Z, Qin G, Cao S (2007) J Mol Catal A Chem 277:35
228. Bu Z, Wang Z, Yang L, Cao S (2010) Appl Organomet Chem 24:813
229. Buonerba A, De Nisi A, Grassi A, Milione S, Capacchione C, Vagin S, Rieger B (2015) Catal Sci Technol 5:118
230. Fuchs MA, Zevaco TA, Ember E, Walter O, Held I, Dinjus E, Döring M (2013) Dalton Trans 42:5322
231. Wang J, Wu J, Tang N (2007) Inorg Chem Commun 10:1493
232. Adolph M, Zevaco TA, Altesleben C, Walter O, Dinjus E (2014) Dalton Trans 43:3285
233. Rulev YA, Larionov VA, Lokutova AV, Moskalenko MA, Lependina OGL, Maleev VI, North M, Belokon YN (2016) ChemSusChem 9:216
234. Inoue S, Koinuma H, Tsuruta T (1969) J Polym Sci Part B 7:287
235. Fuchs MA, Staudt S, Altesleben C, Walter O, Zevaco TA, Dinjus E (2014) Dalton Trans 43:2344
236. Fuchs MA, Altesleben C, Staudt SC, Walter O, Zevaco TA, Dinjus E (2014) Catal Sci Technol 4:1658
237. Adolph M, Zevaco TA, Altesleben C, Staudt S, Dinjus E (2015) J Mol Catal A Chem 400:104
238. Ma R, He L-N, Zhou Y-B (2016) Green Chem 18:226
239. Yang Y, Hayashi Y, Fujii Y, Nagano T, Kita Y, Ohshima T, Okuda J, Mashima K (2012) Catal Sci Technol 2:509
240. Mercadé E, Zangrando E, Claver C, Godard C (2016) ChemCatChem 8:234
241. Cuesta-Aluja L, Campos-Carrasco A, Castilla J, Reguero M, Masdeu-Bultó AM, Aghmiz A (2016) J CO2 Util 14:10
242. Chen T-Y, Li C-Y, Tsai C-Y, Li C-H, Chang C-H, Ko B-T, Chang C-Y, Lin C-H, Huang H-Y (2014) J Organomet Chem 754:16
243. Kim HS, Kim JJ, Lee BG, Jung OS, Jang HG, Kang SO (2000) Angew Chem Int Ed 39:4096
244. Kim HS, Kim JJ, Kwon HN, Chung MJ, Lee BG, Jang HG (2002) J Catal 205:226
245. Kisch H, Millini R, Wang I-J (1986) Chem Ber 119:1090
246. Sun J, Fujita S-I, Zhao F, Arai M (2005) Appl Catal A 287:221
247. Wu S-S, Zhang X-W, Dai W-L, Yin S-F, Li W-S, Ren Y-Q, Au C-T (2008) Appl Catal A 341:106
248. Ono F, Qiao K, Tomida D, Yokoyama C (2007) J Mol Catal A Chem 263:223
249. Kim HS, Kim JJ, Kim H, Jang HG (2003) J Catal 220:44
250. Sun J, Fujita S-i, Zhao F, Arai M (2004) Green Chem 6:613
251. Li F, Xiao L, Xia C, Hu B (2004) Tetrahedron Lett 45:8307
252. Liu M, Liang L, Liang T, Lin X, Shi L, Wang F, Sun J (2015) J Mol Catal A Chem 408:242
253. Seo UR, Chung YK (2014) Adv Synth Catal 356:1955
254. Palgunadi J, Kwon OS, Lee H, Bae JY, Ahn BS, Min N-Y, Kim HS (2004) Catal Today 98:511

Top Curr Chem (Z) (2017) 375:21
DOI 10.1007/s41061-017-0108-9

REVIEW

Synthesis of Lactones and Other Heterocycles

Xi Liu[1] · Liang-Nian He[1]

Received: 19 September 2016 / Accepted: 17 January 2017 / Published online: 6 February 2017
© Springer International Publishing Switzerland 2017

Abstract Chemical fixation of CO_2 into value-added chemicals represents a promising field in view of sustainable development and green synthesis. In this aspect, the construction of heterocyclic compounds from CO_2 and readily available starting materials is particularly appealing in both organic and pharmaceutical fields since CO_2 can be regarded as carbon and oxygen resource with advantages of abundance, renewability, non-toxicity, and non-flammability. In this chapter, we have summarized elegant protocols with elaborately designed substrates for the direct incorporation of entire CO_2 molecule or "CO" or "C" fragments into lactones and other heterocycles such as oxazolidinones, cyclic carbonates, quinazoline-2,4(1H,3H)-diones, etc., through the formation of carbon–carbon, carbon–nitrogen and/or carbon–oxygen bonds promoted by homogeneous catalysts.

Keywords Carbon dioxide · Catalysis · Heterocycle · Lactone · Sustainable chemistry · Synthetic methods

1 Introduction: CO_2 in Heterocycles Synthesis

Since the Industrial Revolution, the concentration of CO_2 in the atmosphere has risen continuously, which is acknowledged as the dominant factor resulting in global warming. In this context, CO_2 capture and storage (CCS) has been proposed as an

---

Chapter 4 was originally published as Liu, X. & He, L-N. Top Curr Chem (Z) (2017) 375: 21. DOI 10.1007/s41061-017-0108-9.

✉ Liang-Nian He
heln@nankai.edu.cn

[1] State Key Laboratory and Institute of Elemento-Organic Chemistry, Collaborative Innovation Center of Chemical Science and Engineering, Nankai University, Tianjin 300071, People's Republic of China

alternative strategy for mitigating carbon accumulation. On the other hand, CO_2 can be regarded as a carbon and oxygen resource with advantages of abundance, renewability, non-toxicity, and non-flammability. In this context, transformation of CO_2 into value-added products has received considerable interest and presents a promising field in organic synthesis [1–6]. The construction of heterocyclic compounds from readily available starting materials is particularly appealing in both organic and pharmaceutical fields. CO_2 as an alternative and sustainable building block has been employed for the purpose of heterocycle synthesis [7–10].

Generally, the carboxylation is involved in CO_2 capture process by adopting carbon, nitrogen, or oxygen-nucleophile and subsequent cyclization is realized with an additional electrophile. With this strategy, CO_2 can be fixed and further incorporated into various heterocycles through the formation of carbon–carbon, carbon–nitrogen, and/or carbon–oxygen bonds. In this chapter, we have summarized selected works on incorporating entire CO_2 molecule or “CO” or “C” fragments into heterocyclic compounds. The subject has been roughly divided into two parts, incorporation of CO_2 into lactones and other heterocycles such as oxazolidinones, cyclic carbonates, quinazoline-2,4(*1H*,*3H*)-diones. With respect to the synthesis of lactones, the general protocol is to couple unsaturated hydrocarbons with CO_2 or through carboxylative cyclization of carbon nucleophiles with CO_2. In regards to other heterocycle construction, CO_2 can be trapped by nitrogen or oxygen nucleophiles, followed by intramolecular cyclization, resulting in the formation of oxazolidinones, cyclic carbonates, and quinazoline-2,4(*1H*,*3H*)-diones etc.

2 Incorporation of CO_2 into Lactones

2.1 Coupling Unsaturated Hydrocarbons with CO_2

The construction of heterocyclic compounds by adopting CO_2 as carboxylation or carbonylation reagent is particularly appealing since CO_2 can be regarded as a sustainable, abundant, and ubiquitous C1 resource. In this respect, incorporation of CO_2 into lactones provides a promising molecular assembly protocol involving simultaneous carbon–carbon and carbon–oxygen bond formation. The synthesis of lactones via coupling CO_2 with unsaturated hydrocarbons such as 1,3-butadiene, diynes, and allenes have been successively reported based on transition-metal catalytic systems (Scheme 1). From a mechanistic perspective, the insertion of CO_2 into carbon–metal bond is generally involved in the reaction pathway, thus resulting in the formation of a carbon–carbon bond. The subsequent reductive elimination process releases the metal catalyst with forming a carbon–oxygen bond.

As early as 1976, a seminal work was reported by Inoue and coworkers about the catalytic addition of CO_2 to 1,3-butadiene in the presence of the palladium–phosphine complex as listed in Table 1 [11]. Solvent-screening implies that polar aprotic solvents such as DMF and DMSO are favorable and $Pd(diphos)_2$ is more effective than $Pd(PPh_3)_4$, leading to the formation of a small amount of the five-membered δ-lactone **1** and butadiene oligomers such as **2**, **3**, **4**.

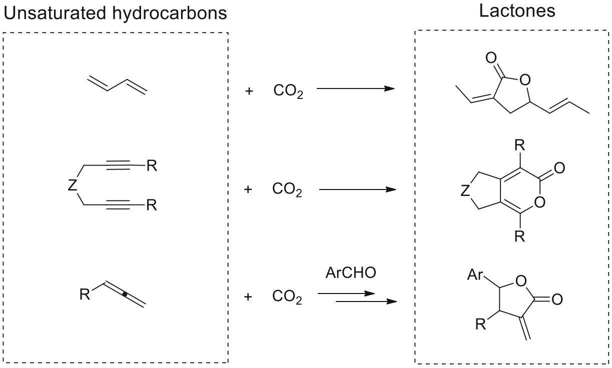

Scheme 1 Lactones synthesis via coupling CO_2 with unsaturated hydrocarbons

Further studies focus on improving the selectivity of lactone **1**. Musco et al. then found that the distribution of the products mainly depends on the phosphine ligands [12]. In particular, the employment of basic phosphine ligand e.g., tricyclohexyl phosphine (PCy_3) is beneficial to the formation of the lactone **1**, that is, the electronic control arising from phosphine ligand is crucial for the selectivity control.

More interestingly, the selective formation of δ-lactone has been realized by using "reversible CO_2-carrier palladium complex" without additional ligand, which is the Pd(II) complex containing a cyclometalated ligand and a functional phosphine (Scheme 2). Another catalytic system composed of the cationic Pd(II) precursor $[Pd(MeCN)_4][BF_4]_2$, phosphine ligand such as PPh_3, *p*-hydroquinone, and trimethylamine is also demonstrated to be effective [13].

With respect to the reaction mechanism, the oxidative coupling of the two butadiene units is assumed to coordinate to the palladium complex, resulting in the formation of the π-allylic complex **7**. Subsequently, CO_2 is inserted into the palladium-carbon bond to give a palladium carboxylate complex **8**. Intramolecular hydrogen transfer and subsequent isomerization affords the carboxylic acid **9**, which then undergoes intramolecular 1,4-addition to produce the five-membered lactone product as depicted in Scheme 3.

α-Pyrones are versatile building blocks in organic synthesis and important heterocyclic structures commonly existing in biological active natural products. In 1988, Tsuda's group disclosed $Ni(COD)_2$/trialkylphosphine as an efficient catalytic system for cycloaddition of terminally dialkyl-substituted diynes and CO_2 to construct the bicycle α-pyrones (Scheme 4, R=Alkyl) [14]. Remarkably, the structures of diynes intensively influence the reaction outcome. As a consequence, each diyne containing different alkyl substituent requires its specific phosphine ligand. For terminally unsubstituted diynes (Scheme 4, R=H), functionalized phosphine ligands (**12a**, **12b**) containing pyridyl groups are applied as efficient ligands for the conversion of **10**, whereas ordinary trialkylphosphine ligands are confirmed to be ineffective [15].

The cycloaddition of the silyl-substituted diynes **13** and CO_2 affords the corresponding α-pyrone bearing a trimethylsilyl group [16]. The silyl substituent

Table 1 Cyclization of 1,3-butadiene with CO_2 catalyzed by palladium-phosphine complex

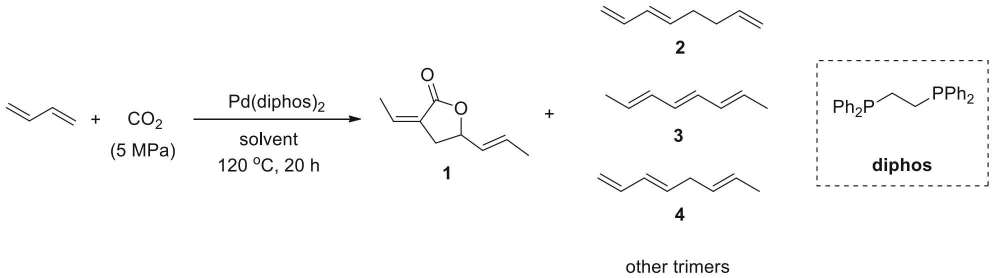

Solvent	Yield (%)[a]				
	Lactone (**1**)	**2**	**3**	**4**	Other trimers
–	Trace	2.4	3.6	58.0	18.5
DMF	4.0	26.8	21.9	13.9	15.1
DMF[b]	12.3	32.8	20.5	7.2	9.3
DMF[c]	0.7	47.5	20.3	4.5	14.5
DMSO	4.2	55.7	12.3	4.5	9.3
*t*BuOH	0.5	44.3	17.9	6.6	15.0
Benzene	0.4	35.7	21.8	17.7	18.1

Reaction conditions: Solvent (10 ml), 1,3-butadiene (7.3 g, 135 mmol), $Pd(diphos)_2$ (0.2 mmol), 120 °C, 20 h

[a] Determined by liquid chromatogram analysis

[b] DMF (20 ml); 84 °C for 20 h, then 120 °C for 20 h

[c] $Pd(PPh_3)_4$ (0.2 mmol)

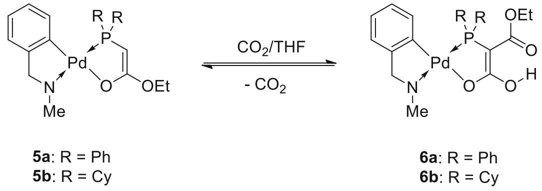

Scheme 2 Reversible CO_2-carrier Pd complex

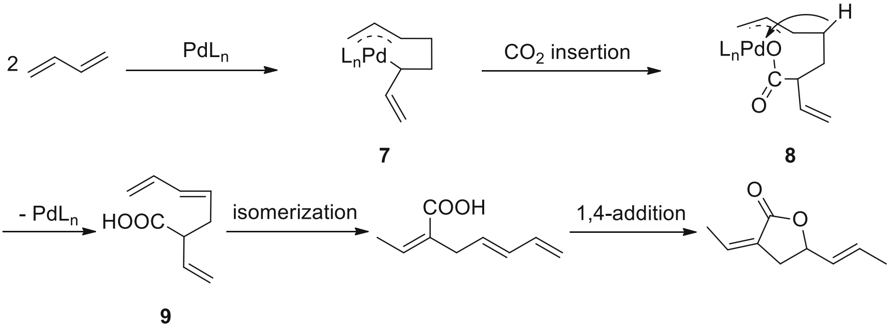

Scheme 3 A plausible mechanism for the palladium-catalyzed incorporating CO_2 into δ-lactone

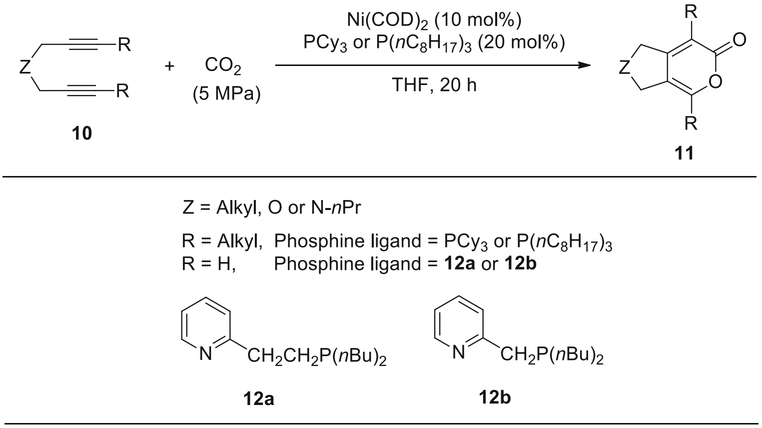

Scheme 4 $Ni(COD)_2$/trialkylphosphine-catalyzed cycloaddition of diynes with CO_2

attached to sp^2 carbon can be easily converted into a variety of functional groups such as hydroxyl, acyl, and halogen. Alternatively, simple protodesilylation of **14** assisted by fluoride can deliver α-pyrone **15** with a quantitative yield as shown in Scheme 5.

As reported by Louie et al. when the *N*-heterocyclic carbene such as 1,3-bis-(2,6-diisopropylphenyl)-imidazol-2-ylidene) (IPr) is employed as a ligand in cooperation with $Ni(COD)_2$, the cycloaddition of diynes and CO_2 can proceed smoothly under

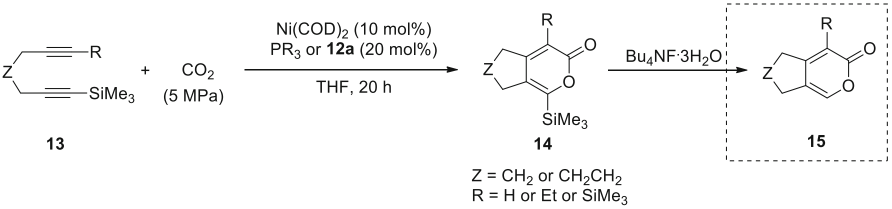

Scheme 5 Synthesis of silyl-substituted α-pyrones through the cycloaddition of the silyl-substituted diynes with CO_2

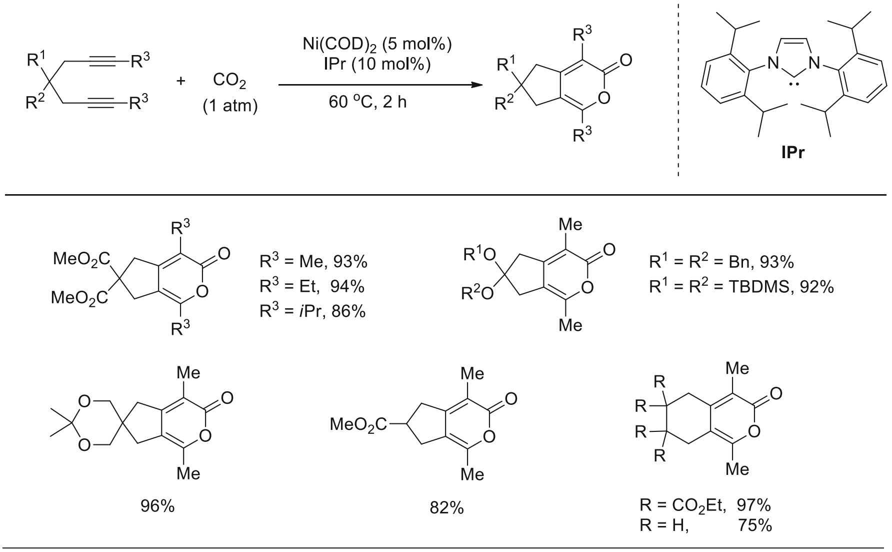

Scheme 6 $Ni(COD)_2$/IPr-promoted cycloaddition of diynes with atmospheric pressure of CO_2

atmospheric pressure (Scheme 6) [17]. Notably, in the case of the isolated, well-defined complex $Ni(IPr)_2$, the catalyst loading can be decreased to 1 mol%, although high substrate concentration is necessary.

The reaction mechanism of Ni(0)/PR_3 or Ni(0)/IPr-catalyzed cycloaddition of diynes with CO_2 is supposed to involve an initial [2 + 2] cycloaddition through coordinating CO_2 to Ni(0) to afford the oxanickelacycle species **16**. Subsequent insertion of another alkynyl delivers the intermediate **17**. The α-pyrone can be obtained through further reductive elimination process, with regeneration of Ni(0) catalyst as depicted in Scheme 7.

In 2003, Mori et al. developed a one-pot multi-step procedure for the regio- and stereoselective synthesis of α-methylene-γ-lactone **19** through the nickel-mediated sequential addition of CO_2 and aryl aldehydes into terminal allenes [18]. As illustrated in Scheme 8, oxidative addition of **18** and CO_2 to the Ni(0) provides the oxanickelacycles **20** or **21**. The oxanickelacycle species is vulnerable to

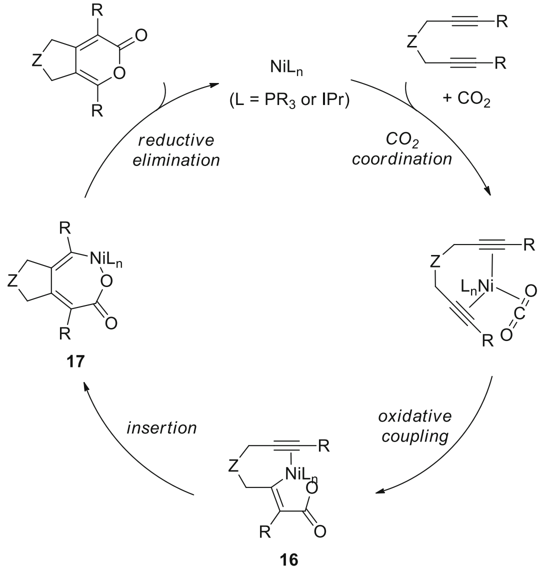

Scheme 7 Possible reaction pathway for the formation of α-pyrone

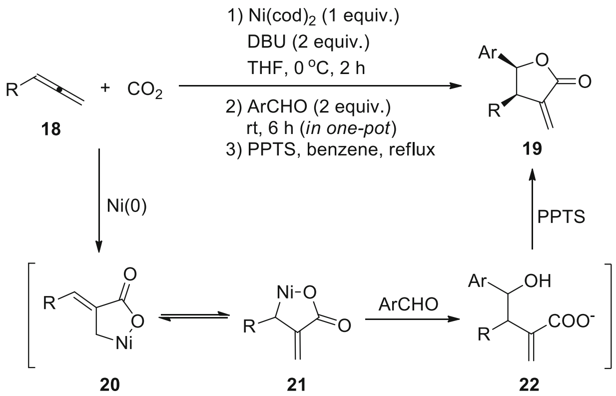

Scheme 8 Nickel-mediated sequential addition of CO_2 and aryl aldehydes into terminal allenes

electrophiles such as aryl aldehydes, resulting in the formation of γ-hydroxy carboxylate derivative **22**. Final dehydration cyclization affords the desired α-methylene-γ-lactone **19**.

2.2 Carboxylative Cyclization of Carbon Nucleophiles with CO_2

Trapping CO_2 by a carbon nucleophile delivers a carboxylate species with the formation of a carbon–carbon bond. If the well-designed substrate contains an additional electrophile such as an alkynyl group, subsequent intramolecular

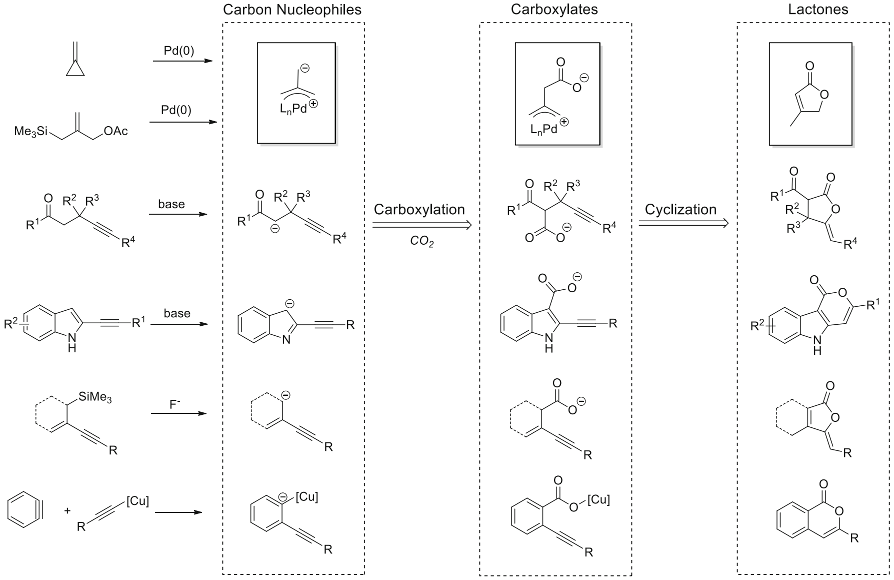

Scheme 9 Synthesis of lactones via cascade carboxylation and cyclization with carbon nucleophiles

cyclization can smoothly occur between the carboxylate and electrophile, thus providing the lactone via forming a carbon–oxygen bond. With this cascade carboxylation and cyclization strategy, lactone derivatives can be produced by capturing CO_2 with an appropriate substrate, that is, an elaborately designed molecule bearing potential nucleophilic site (for CO_2 capture) and electrophilic site (for intramolecular cyclization).

In this part, we focus on the protocols based on an well-designed substrate that can in situ generate a nucleophilic site to trap CO_2 into a carboxylate species, and subsequent intramolecular cyclization with an adjacent electrophilic group affords the desired lactone as summarized in Scheme 9.

The preparation of γ-butyrolactone, an important lactone product, was initially reported by Inoue in 1979 through the Pd-catalyzed [3 + 2] cycloaddition of methylenecyclopropane with CO_2 [19]. Palladium(0) combined with various phosphine ligands is examined for catalyzing this ring-expansion reaction under 4 MPa CO_2 with a reaction temperature greater than 130 °C (Table 2). Less basic phosphine ligands such as PPh_3 and $P(OEt)_3$ exhibit a tendency to produce the lactone **24** rather than **25**. The cycloaddition reaction has been further investigated but a relatively high CO_2 pressure and reaction temperature is still inevitable [20].

Another predominant procedure for the γ-butyrolactone synthesis is described by Greco and coworkers, that is, a Pd-catalyzed [3 + 2] cycloaddition reaction between CO_2 and 2-2-trimethylsilylmethyl-2-propenyl acetates **26** [21]. It is believed that an η^3-Pd trimethylenemethane (Pd-TMM) complex is in situ generated via an oxidative addition of Pd(0) to **26**, which is also supposed to be the catalytic

Table 2 Pd-catalyzed [3 + 2] cycloaddition of methylenecyclopropane with CO_2

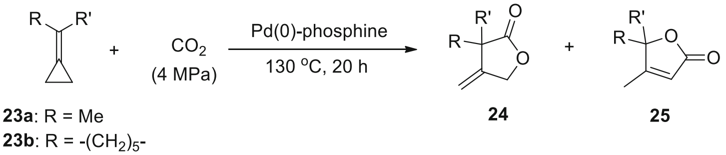

Substrate	Catalyst[a]	Conversion (%)	Yield (%)[c]	
			24	**25**
23a (17 mmol)	Pd(dba)$_2$–PPh$_3$	97	69	8
(17 mmol)	Pd(diphos)$_2$	93	Trace	48
(16 mmol)	Pd(dba)$_2$–P(OEt)$_3$	26	8	Trace
(9 mmol)	Pd(dba)$_2$–P(*n*Bu)$_3$	–[d]	1	5
(17 mmol)	Pd(dba)$_2$–Me$_2$PCH$_2$CH$_2$PMe$_2$[b]	32	4	7
23b (29 mmol)	Pd(dba)$_2$–PPh$_3$	71	32	Trace
(30 mmol)	Pd(diphos)$_2$	74	5	21

[a] Catalyst (0.4 mmol), Pd(0)–phosphine (1:4)

[b] Pd(0)–phosphine (1:2)

[c] Determined by liquid chromatogram analysis

[d] Not determined

species of aforementioned cycloaddition of methylenecyclopropane with CO_2. Subsequently, the electron-rich carbon of Pd-TMM species can capture CO_2 to afford a carboxylate intermediate with formation of a carbon–carbon bond. Then intramolecular ring-closure could readily accomplish through a carbon–oxygen bond formation. With this strategy, the cycloaddition reaction could proceed under quite mild conditions with rapid reaction rate (Scheme 10).

The carboxylative cyclization of β-alkynylketones with CO_2 is able to afford a series of aromatic or aliphatic ketone-substituted γ-lactones **29** in the presence of AgOBz and 7-methyl-1,5,7-triazabicyclo-[4.4.0]dec-5-ene (MTBD) under mild conditions [22]. As shown in Scheme 11, the ketone substrate **28** containing an alkyne group in the β-position, can generate an enolate **30** through deprotonation by strong bases such as MTBD, which is expected to further trap CO_2 to afford β-ketocarboxylate intermediate **32**. With the activation of carbon–carbon triple bond by silver salt, the subsequent cyclization smoothly occurs to give the γ-lactone.

Recently, Skrydstrup's group have reported that the reaction of alkynyl indoles with CO_2 in the presence of 1,5,7-triazabicyclo[4.4.0]dec-5-ene (TBD) furnishes the tricyclic indole-containing heterocyclic compounds through the cascade carboxylation and cyclization process (Scheme 12) [23]. The well-designed indoles derivative, bearing an alkynyl group in the C2-position, the C3-position of which is a potential nucleophilic site. TBD is assumed to activate CO_2 by forming a zwitterionic TBD-CO_2 adduct **35**. The carbon–carbon bond is formed by nucleophilic addition of the C3 of indole onto the TBD-CO_2 adduct, and subsequent

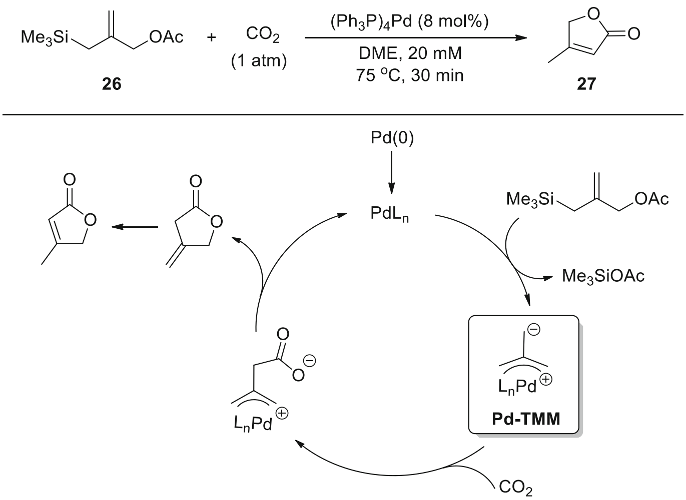

Scheme 10 Formation of catalytic species Pd-TMM complex and further conversion into γ-butyrolactone

re-aromatization furnishes carboxylate intermediate **36**. Further cyclization on the alkyne provides the tricyclic heterocycle **34** containing the indole and lactone scaffold.

Yamada's group then disclosed the silver/CsF-promoted carboxylative cyclization of trimethyl(2-methylenebut-3-yn-1-yl)silane derivatives **38** with CO_2 to afford the corresponding five or six-membered lactone derivatives **39** or **40** (Scheme 13) [24]. With the activation of CsF, carbanion **41** is generated via the cleavage of C–Si bond and formation of Si–F bond. Then nucleophilic addition of **41** to CO_2 furnishes carboxylate intermediate **42**. Silver(I) catalyst serves as an activator of carbon–carbon triple bond, thus facilitating the subsequent cyclization to deliver the 2-furanone **39** and 2-pyrone **40** derivative via path a and b, respectively.

Arynes are highly reactive species to be applied as intermediates in multicomponent coupling reactions for the construction of new carbon–carbon bonds as well as carbon-heteroatom bonds. In this context, Kobayashi et al. have disclosed an NHC-copper-catalyzed three-component coupling reaction between the *ortho*-arynes in situ generated, terminal alkynes and CO_2 to access a wide range of substituted isocoumarins in good to high yields (Scheme 14) [25]. The proposed mechanism is illustrated in Scheme 14. Initially, a copper acetylide intermediate **43** is generated by the base-promoted deprotonation of alkyne. Simultaneously, fluoride-induced silyl elimination of 2-(trimethylsilyl)aryl triflates takes place to afford the *ortho*-benzyne **44**. The copper acetylide **43** then nucleophilic addition to **44** to produce the *ortho*-alkynyl copper complex **45**. The transient intermediate **45** can be rapidly intercepted by CO_2 to generate the copper carboxylate **46**, which further goes through cyclization and protonation process to finally furnish the isocoumarins.

A Pd-catalyzed carboxylation of alkenyl C–H bond of 2-hydroxystyrenes with CO_2 has been achieved by Iwasawa's group [26]. Such a protocol results in the

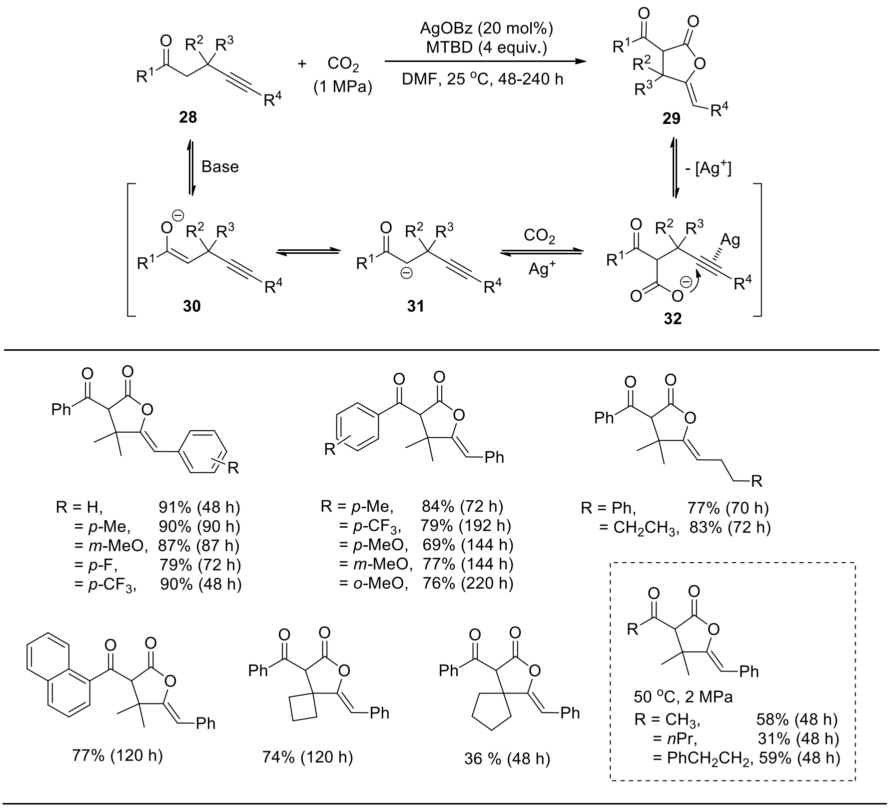

Scheme 11 Carboxylative cyclization of *β*-alkynylketones with CO_2 catalyzed by AgOBz/MTBD

formation of coumarin derivatives in good-to-high yields via carboxylation and lactonization. The hydroxy group in the substrate behaves as a directing group for C–H activation as depicted in Scheme 15.

Recently, a transition-metal free example for the synthesis of lactones has been reported by Zhang et al. [27]. Carboxylative cyclization of the substituted 1-propenyl ketones with CO_2 provides a straightforward access to various α-pyrone compounds promoted by CsF.

3 Heterocycles Synthesis Through Trapping CO_2 with Nitrogen or Oxygen Nucleophiles

3.1 Cyclization of Nitrogen Nucleophiles with CO_2

Trapping CO_2 with a nucleophile centered at nitrogen, generally amino group, leads to the generation of a carbamic species ($R^1R^2NCOO^-$) through the formation of C–N bond. If the substrate molecule contains an unsaturated C–C or C–N bond, the

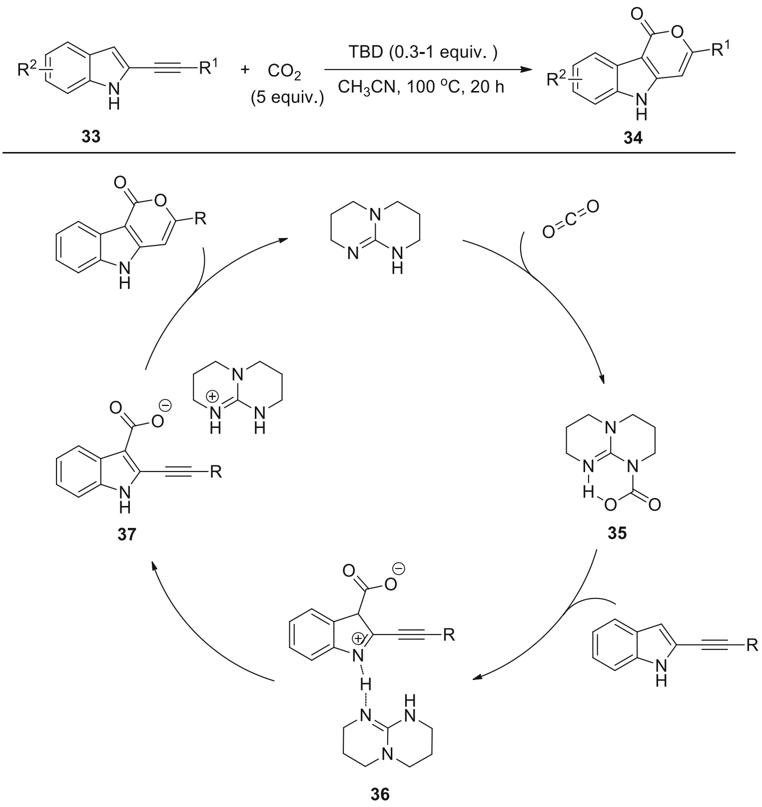

Scheme 12 TBD-catalyzed trapping of CO_2 by 2-alkynyl indoles

carbamic species can further react with such unsaturated function groups thus resulting in intramolecular cyclization to provide various heterocycles. Based on this design pattern, well-designed substrates such as propargylic amines, allyl amines, α-allenyl amines, *o*-alkynylanilines, and 2-aminobenzonitrile perform a carboxylative cyclization with CO_2.

The carboxylative cyclization of propargylic amines with CO_2 is a thermodynamically favored and atom-economic reaction for the synthesis of pharmaceutically significant heterocycles, i.e., oxazolidinones. Superbases such as TBD, 1,8-diazabicyclo[5.4.0]undec-7-ene (DBU), alkylguanidines, and phosphazene bases as shown in Scheme 16 can serve as organocatalysts for this purpose [28]. In the presence of MTBD, 2-oxazolidinones **48** can be obtained from propargylic amines **47** and CO_2 in excellent yields by employing aprotic polar solvent such as CH_3CN under ambient conditions. Catalyst screening indicates that both the basicity and steric hindrance of the superbase have a significant influence on the catalytic performance.

tert-Butyl hypoiodite (*t*BuOI) has been demonstrated as an efficient organocatalyst to promote the cyclization of propargylic amines with CO_2 under atmospheric

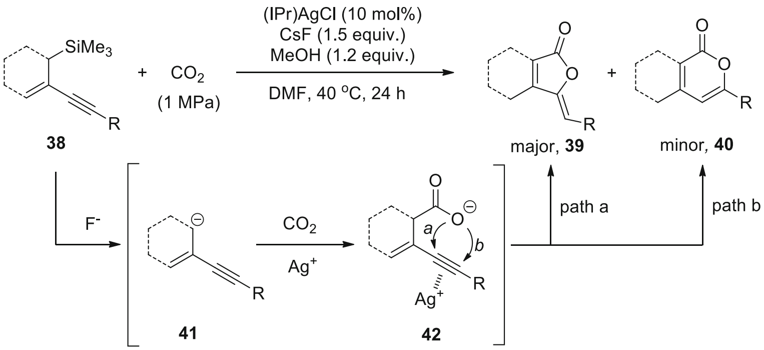

Scheme 13 Silver/CsF-promoted carboxylative cyclization of trimethyl(2-methylenebut-3-yn-1-yl)silanes with CO_2

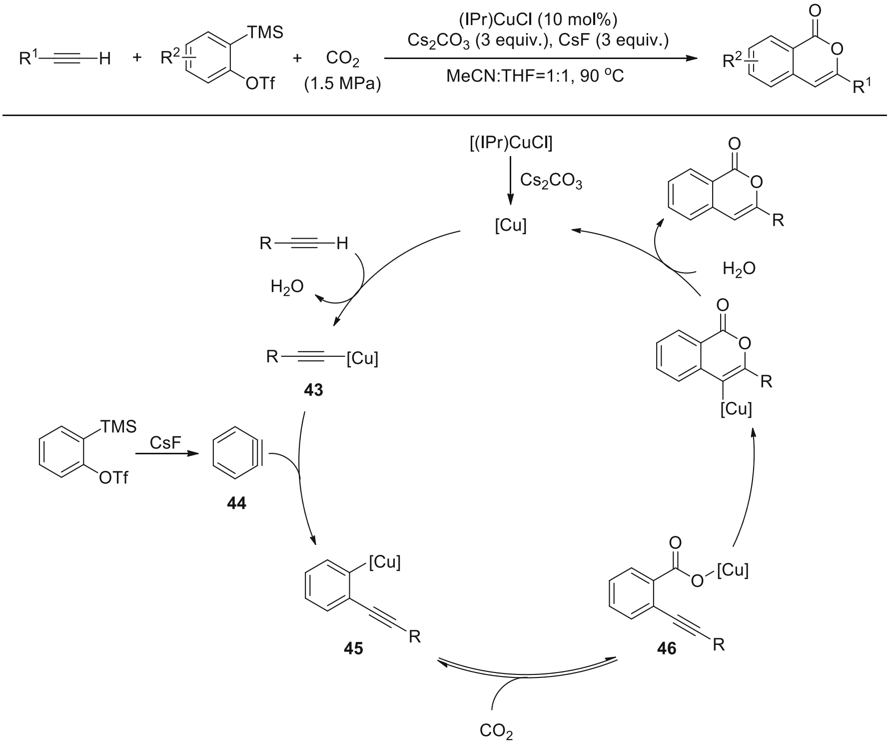

Scheme 14 (IPr)CuCl-catalyzed three-component coupling reaction of 2-(trimethylsilyl)aryl triflates, terminal alkynes and CO_2

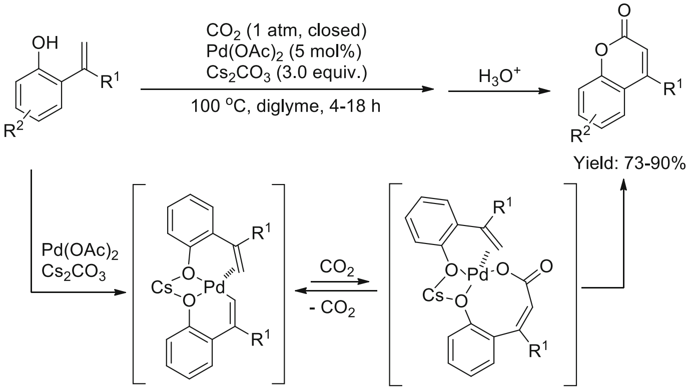

Scheme 15 Pd-catalyzed carboxylation of 2-hydroxystyrenes with CO_2

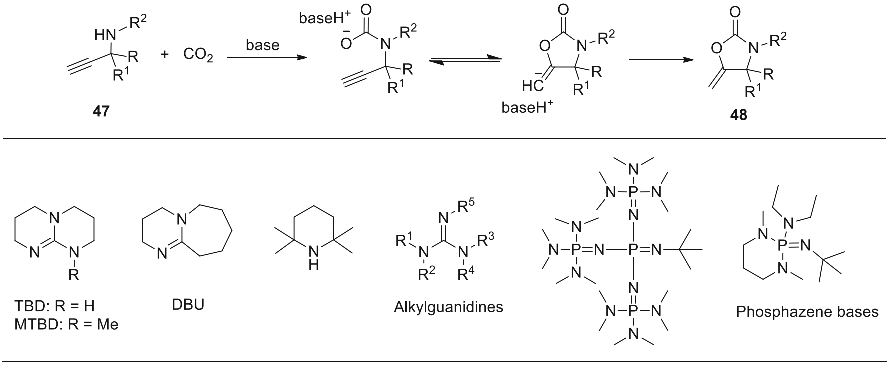

Scheme 16 Superbase-catalyzed carboxylative cyclization of propargylic amines with CO_2

pressure at −20 °C, leading to oxazolidinones bearing an idomethyl group [29]. Noticeably, allyl amines substrates are also tolerated with this protocol.

Recently, Han's group has developed protic ionic liquids (PILs), such as 1,8-diazabicyclo-[5.4.0]-7-undecenium 2-methylimidazolide [DBUH][MIm] to catalyze the reaction of CO_2 with a broad range of propargylic amines to obtain 2-oxazolidinones under mild conditions [30]. Such PILs can be easily reused at least five times without a decrease in catalytic activity. DFT studies reveal that both the cation and anion are crucial in promoting CO_2 electrophilic addition step and intramolecular cyclization step by capturing and providing proton, respectively.

Due to the activation effect on the carbon–carbon triple bond of propargylic amines, transition-metal catalytic systems such as [Ru(COD)-(COT)]/tertiary phosphine, [31] $Pd(OAc)_2$, [32] AgOAc [33] and NHC-Au(I) complexes [34] are demonstrated to be efficient in accelerating this carboxylative cyclization.

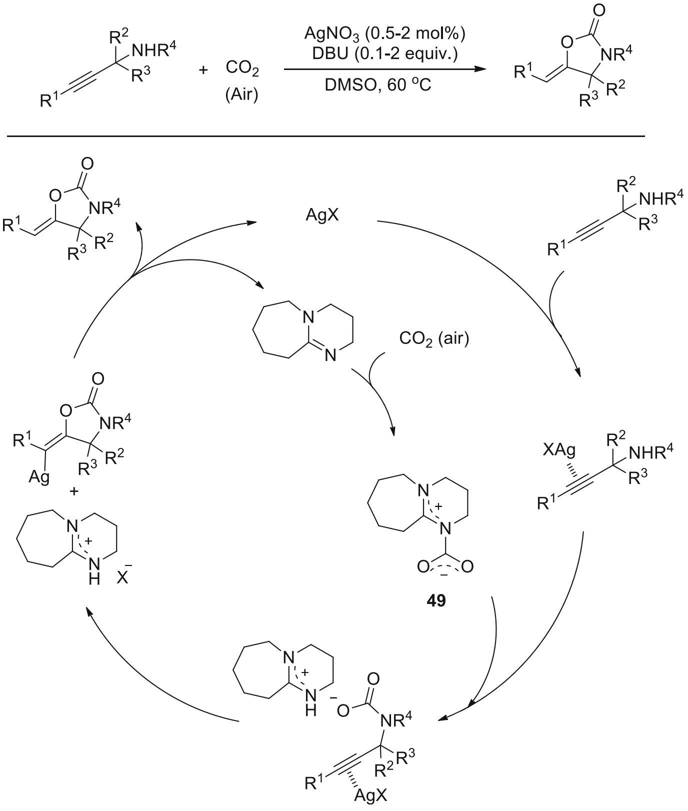

Scheme 17 The cooperative $AgNO_3$/DBU promoted carboxylative cyclization of propargylamines with atmospheric CO_2

Particularly, the dual-component system composed of $AgNO_3$ and DBU has been disclosed to promote this cyclization with the use of air as CO_2 source [35]. With this protocol, various oxazolidinones can be smoothly obtained from propargylic amines under open-air conditions. As shown in Scheme 17, the DBU-CO_2 adduct **49**, a zwitterionic carbamate species comes from the reaction of DBU and CO_2, can be deemed to be an activated form of CO_2. On the other hand, the silver salt is recognized as an efficient activator of carbon–carbon triple bond of propargylic amine. The synergistic effect of the two components renders the reaction to perform under mild conditions with fixation of CO_2 from air.

Our group has described copper(II)-substituted polyoxometalate-based ionic liquids, e.g., $[(nC_7H_{15})_4N]_6[\alpha\text{-}SiW_{11}O_{39}Cu]$ as bifunctional catalysts for the carboxylative cyclization of propargylic amines with CO_2 [36]. The dual activation of the anion of the $[(nC_7H_{15})_4N]_6$ $[\alpha\text{-}SiW_{11}O_{39}Cu]$ towards both propargylic amines and CO_2 has been shown by NMR investigations. Very recently, we have also reported the zinc complex $ZnCl_2(TBD)_2$, which can be in situ generated from $ZnCl_2$ and TBD, as a robust catalyst for such a cyclization reaction under atmospheric pressure and mild temperature [37].

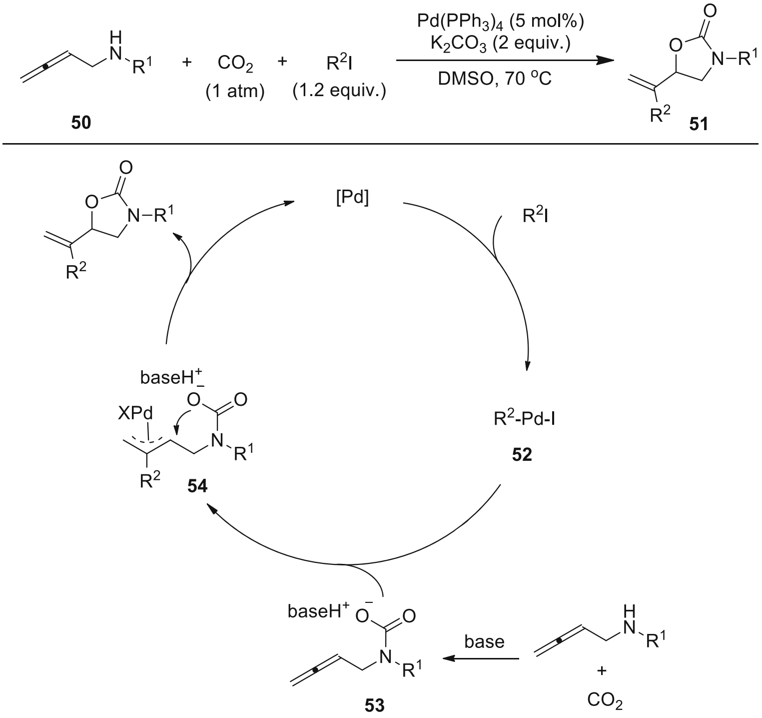

Scheme 18 Pd-catalyzed three-component coupling reaction of α-allenyl amines, aryl halides, and CO_2

α-Allenyl amines, an analogical class of substrates, can work in the same way as propargylic amines to incorporate CO_2 into oxazolidinones. In 2009, Ikariya et al. disclosed that carboxylative cyclization of α-allenyl amines with CO_2 could be promoted by $Pd(OAc)_2$ under supercritical conditions [38]. Then, Ma's group reported a mild procedure of the Pd-catalyzed three-component coupling reaction of α-allenyl amines **50**, aryl halides and CO_2 in the presence of a stoichiometric amount of base (Scheme 18) [39]. The intermediate **52**, which is generated by oxidative addition of R^2I to Pd(0), presumably reacts with the carbamate **53** to yield π-allylic palladium species **54**. Then the subsequent intramolecular cyclization affords the oxazolidinone with release of the palladium catalyst.

More recently, Ikariya et al. have demonstrated that the NHC-Ag(I) carboxylate complexes can serve as an efficient catalyst for the synthesis of oxazolidinone derivatives from allenylmethylamines and CO_2 under mild conditions with excellent selectivities (Scheme 19) [40].

The propargylic amines can be readily prepared through the three-component coupling reaction between alkynes, aldehydes, and amines, so-called A^3-coupling reaction. In this context, Li et al. have combined the A^3-coupling reaction and carboxylative cyclization into one-pot process to synthesize oxazolidinones directly from terminal alkynes, aldehydes, primary amines, and CO_2 (Scheme 20) [41]. In this copper-catalyzed tandem A^3-coupling/carboxylative cyclization reaction, CO_2

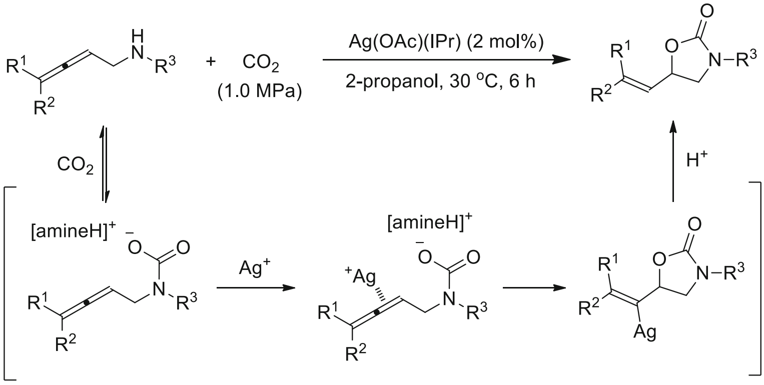

Scheme 19 The carboxylative cyclization of α-allenyl amines with CO_2 promoted by NHC-Ag(I) complex

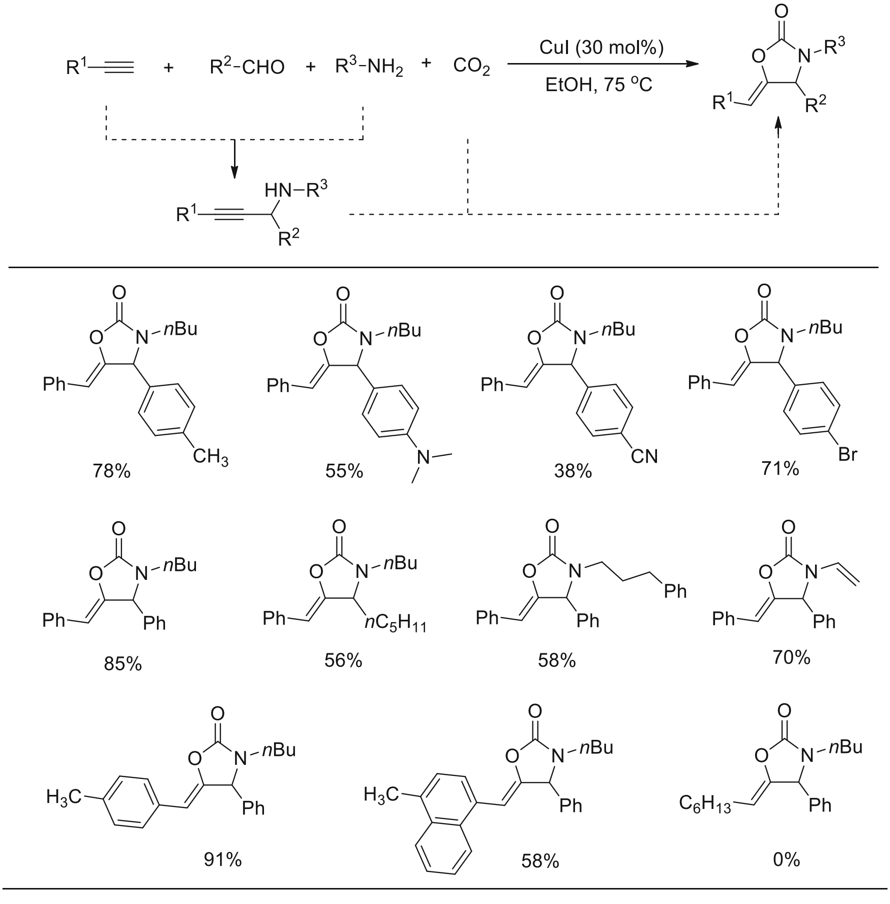

Scheme 20 Copper-catalyzed tandem A^3-coupling/carboxylative cyclization reaction access to oxazolidinones

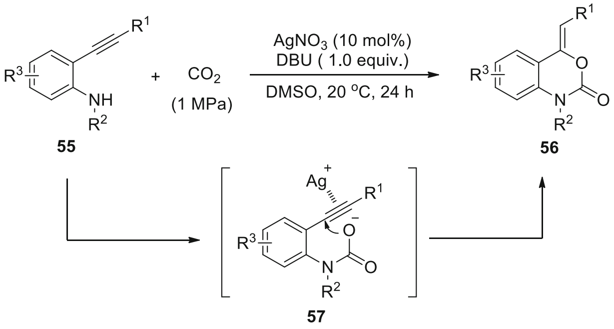

Scheme 21 Incorporation of CO_2 into benzoxazine-2-ones from secondary *o*-alkynylanilines catalyzed by $AgNO_3$/DBU system

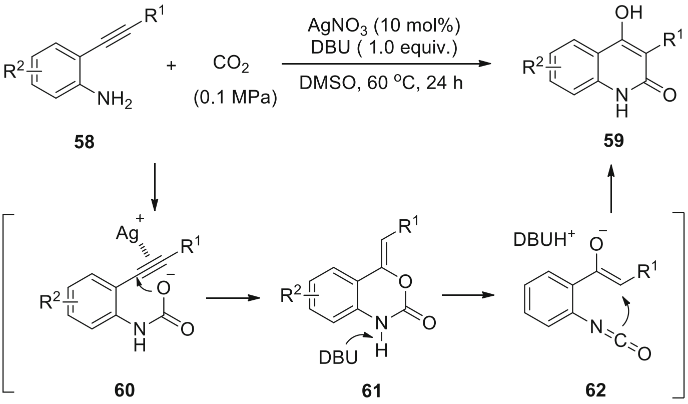

Scheme 22 Carboxylative cyclization of primary *o*-alkynylanilines with CO_2 to yield 4-hydroxyquinolin-2-ones

serve as not only a reagent but also a promoter, that is, to react with primary amines to prevent the amines from poisoning the copper catalyst.

The carboxylative cyclization protocol can be also applied to construct benzoheterocycles like benzoxazine-2-one and 4-hydroxyquinolin-2-one derivatives by employing *o*-alkynylanilines as substrates.

Yamada's group has disclosed that in the presence of catalytic amount of silver salts such as $AgNO_3$ or AgOAc and equivalent DBU, the incorporation of CO_2 into benzoxazine-2-one **56** could be achieved by employing secondary *o*-alkynylanilines **55** as reactants under mild conditions (Scheme 21) [42]. The carboxylative cyclization is suggested to proceed via a silver-activated carbamate intermediate **57**.

Interestingly, when primary *o*-alkynylanilines **58** are selected as substrates, 4-hydroxyquinolin-2-one derivatives **59** are obtained rather than benzoxazine-2-ones under the same $AgNO_3$/DBU catalytic system albeit requirement of higher temperature (Scheme 22) [43]. Similarly, the carbamate species is generated

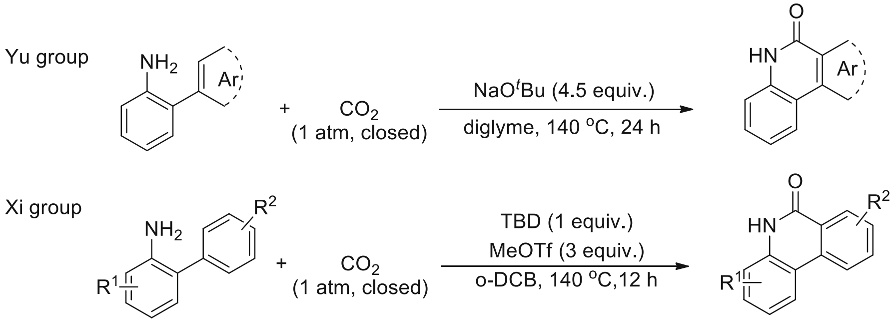

Scheme 23 Lactamization of sp [2] C–H bond access to lactams with CO_2

initially by the reaction of **58** with CO_2. Then subsequent rearrangement occurs with deprotonation by DBU to produce an isocyanate intermediate **62**. Further intermolecular cyclization of **62** affords the 4-hydroxyquinolin-2-one **59**.

Recently, the lactam product, e.g., 2-quinolinones were obtained by lactamization of alkenyl C–H bond with CO_2. Other polyheterocycles containing a lactam moiety were also successfully synthesized via this base-promoted protocol [44]. As depicted in Scheme 23, Xi et al. reported another metal-free method for carbonylation of *o*-arylanilines with CO_2 to afford phenanthridinones as an important class of lactam heterocycles [45]. The isocynate was proposed as a possible intermediate generated at high temperature, following by formation of the carbamate initially.

2-Aminobenzonitriles are a class of readily available substrates containing both nucleophilic sites (amino group) for trapping CO_2 and carbon–nitrogen triple bond (cyano group) for subsequent intramolecular cyclization. Inorganic or organic bases such as Cs_2CO_3, [46] DBU, [47] 1,1,3,3-tetramethylguayyniaine (TMG) [48], and *N*-methyltetrahydropyrimidine (MTHP) [49] have been employed for catalyzing the carbonylative cyclization of 2-aminobenzonitrile with CO_2 to produce biologically and pharmaceutically valuable heterocyles, viz. quinazoline-2,4(*1H*,*3H*)-diones. The mechanism of this cyclization reaction is illustrated as Scheme 24. Carbamate species **63** is readily generated from the amino group and CO_2 with the assistance of a base. Then the carbamate **63** can be converted into the desired product through nucleophilic cyclization and subsequent rearrangement via the isocyanate intermediate **65**.

Monomeric tungstate, i.e., $TBA_2[WO_4]$ (TBA = tetra-*n*-butylammonium) exhibits more excellent catalytic efficiency for the reaction of 2-aminobenzonitrile and CO_2 with higher turnover number (TON) than above base-mediated systems, probably being attributed to the specific interactions between the tungsten-oxo moiety with both CO_2 and 2-aminobenzonitrile as depicted in Scheme 25 [50, 51].

Ionic liquids have also been developed as green and recyclable catalysts for the carbonylative cyclization of 2-aminobenzonitrile with CO_2, as well as acting as reaction medium to replace polar solvents such as DMF and DMSO (Scheme 26). Basic ionic liquids, 1-butyl-3-methyl imidazolium hydroxide ([Bmim]OH) [52] and 1-butyl-3-methylimidazolium acetate ([Bmim]Ac) [53], reversible ionic liquids [54]

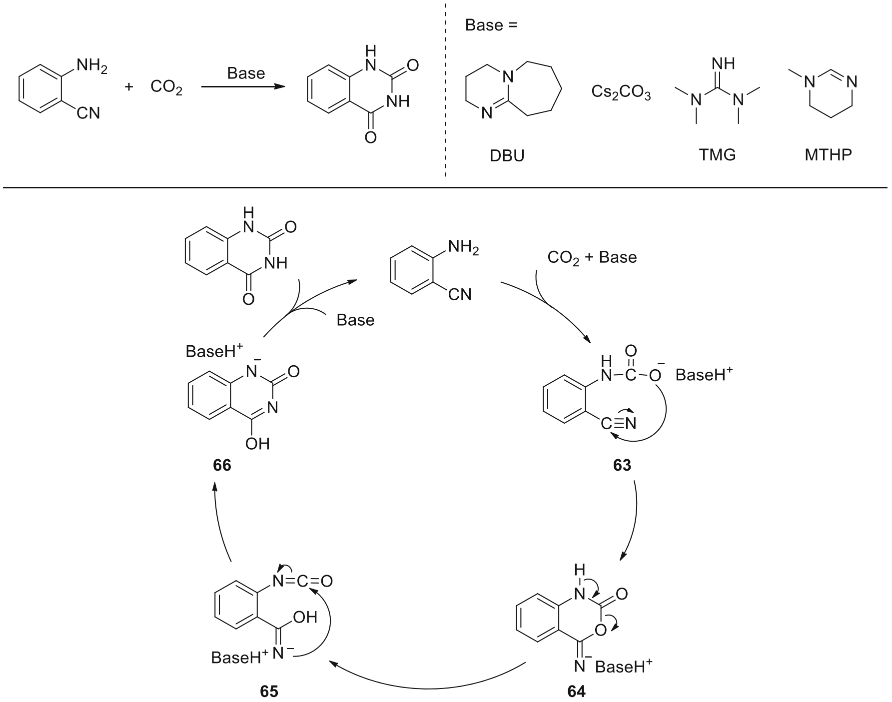

Scheme 24 Base-mediated cyclization f 2-aminobenzonitrile with CO_2

and protic ionic liquids such as [DBUH][TFE] [55] (TFE = trifluoroethanol) are consecutively reported to be effective for this cyclization reaction under atmospheric pressure. Their superior catalytic performance may arise from the basic anions of ILs for activating amino group of 2-aminobenzonitrile. In particular, [DBUH][TFE] could facilitate the reaction to proceed under ambient conditions, which may be ascribed to the simultaneous activation effect to both CO_2 and the substrate.

Interestingly, the reaction of 2-aminobenzonitriles and CO_2 can be realized in water without any catalyst under relatively high CO_2 pressure and reaction temperature (14 MPa and 160 °C) [56]. Density functional theory (DFT) calculation reveals that initially CO_2 may in situ generate carbonic acid in the presence of water, rather than react with the 2-aminobenzonitrile directly. Moreover, carbonic acid was confirmed to react with 2-aminobenzonitrile more easily than CO_2 itself presumably owing to the synergistic action of carbon oxygen atom and one of the hydroxyl oxygen atom towards cyano group (Scheme 27) [57].

The carbonylative cyclization of *o*-phenylenediamines with CO_2 presents an accessible route to benzimidazolones. $TBA_2[WO_4]$ is demonstrated as an efficient catalyst for this cyclization reaction benefiting from the simultaneous activation of the tungsten-oxo moiety towards both CO_2 and *o*-phenylenediamine [58]. Liu's group then disclosed that the carbonylation of *o*-phenylenediamines with CO_2 can

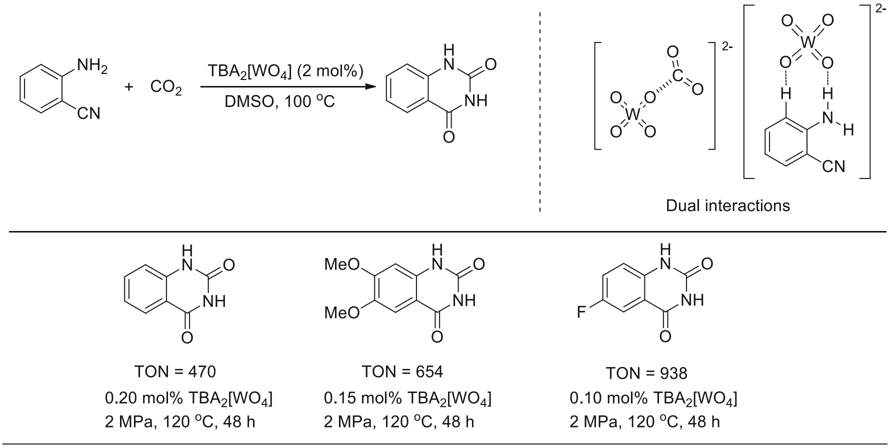

Scheme 25 TBA$_2$[WO$_4$]-promoted cyclization of 2-aminobenzonitrile with CO$_2$ by dual activation effects

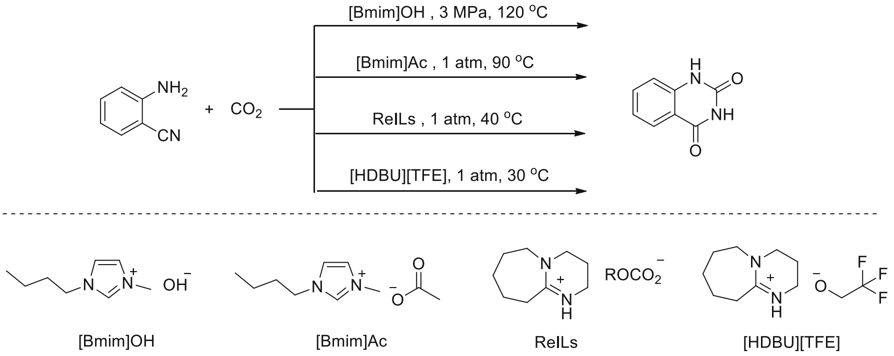

Scheme 26 Catalytic systems based on ionic liquids for the cyclization of 2-aminobenzonitrile with CO$_2$

be promoted by ionic liquid [DBUH][OAc]), which serves as a bifunctional catalyst with the capacity of activating CO$_2$ and *o*-phenylenediamines by the cation and anion of the ILs, respectively [59]. With this protocol, various benzimidazolones are produced in good-to-high yields under 9 MPa CO$_2$ at 120 °C as shown in Scheme 28.

3.2 Trapping CO$_2$ with Oxygen Nucleophiles

Similar to the strategy of trapping CO$_2$ with nitrogen nucleophiles, the reaction of oxygen nucleophile with CO$_2$ furnishes a carbonic acid species (R^{1}OCO$_2$$^-$). In the presence of unsaturated carbon–carbon bond, subsequent intramolecular cyclization can be achieved through the nucleophilic addition of carbonic acid species to

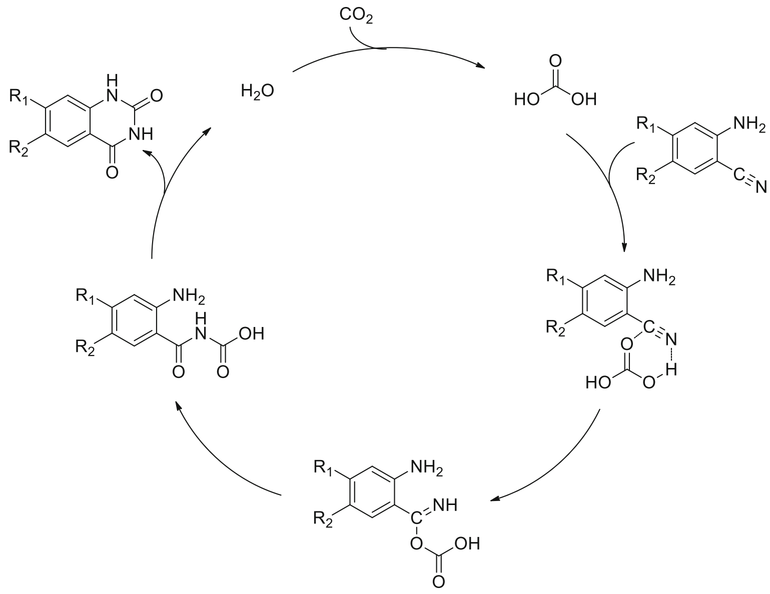

Scheme 27 Possible mechanism for carbonylative cyclization of 2-aminobenzonitrile and CO_2 in water

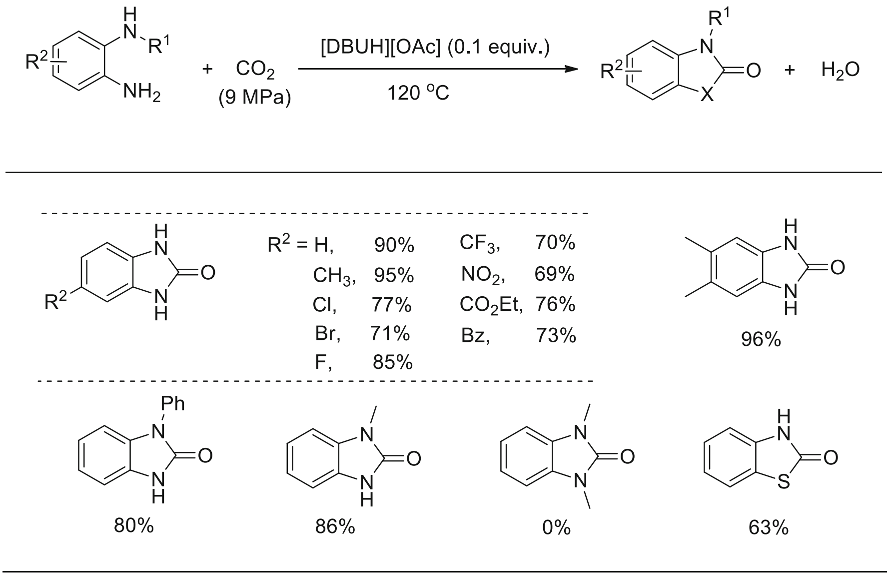

Scheme 28 [DBUH][OAc]-catalyzed carbonylative cyclization of *o*-phenylenediamines with CO_2

unsaturated carbon–carbon bond, delivering cyclic carbonate or other heterocycles via further transformation.

The carboxylative cyclization of propargylic alcohols with CO_2 presents a promising approach to access α-alkylidene cyclic carbonates, which are applied as important intermediates in organic synthesis. In this context, catalytic systems based on organocatalysts or transition-metals have been established. Organocatalysts, for example, tertiary phosphine [60], guanidines [61], *N*-heterocyclic carbene (NHC)-CO_2 adduct [62], *N*-heterocyclic olefin (NHO)-CO_2 adduct [63], and alkoxide-functionalized imidazolium betaines (AFIBs)-CO_2 adduct [64], have been developed for the preparation of α-alkylidene cyclic carbonates with demand of pressurized conditions. Since Co [65], Fe [66], Cu [67, 68], Pd [69], Ag [70–75], and Zn [76] are recognized to be capable of activating carbon–carbon triple bond of propargylic alcohol, catalytic activities can be further enhanced by designing catalysts based on these transition-metals. Besides, inorganic base, e.g., K_2CO_3 in combination with crown ether, is reported as an efficient dual-component catalyst [77].

Ikariya's group has reported the nBu$_3$P-catalyzed carboxylative cyclization of propargylic alcohols in supercritical CO_2 conditions but the catalytic role of the tertiary phosphine remains undefined [60]. A putative zwitterionic phosphane-CO_2 adduct is proposed, in which CO_2 is an activated form, thus promoting nucleophilic addition of the CO_2 to the unsaturated alcohol. As shown in Scheme 29, NHC-CO_2 adduct has also been demonstrated as an efficient catalyst for the reaction of propargylic alcohol with CO_2 [62]. Recently, NHO with high electronegativity at the terminal carbon atom has been found to easily react with CO_2, forming the corresponding NHO-CO_2 adduct [63]. The NHO-CO_2 adduct exhibits a much higher catalytic activity than the corresponding NHC-CO_2 adduct under the same conditions. Lu's group has also developed AFIBs, which bear an alkoxide anion and an imidazolium cation, to be effective catalysts for the cyclization of propargylic alcohols with CO_2 under mild conditions [64].

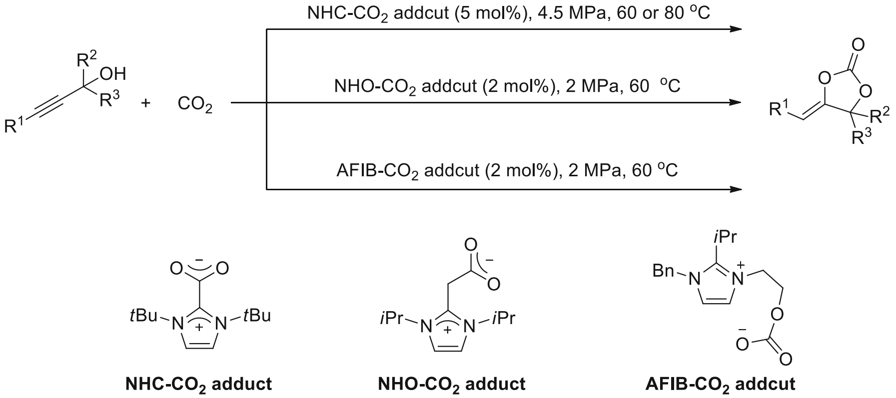

Scheme 29 Carboxylative cyclization of propargylic alcohols with CO_2 promoted by CO_2-zwitterionic adducts

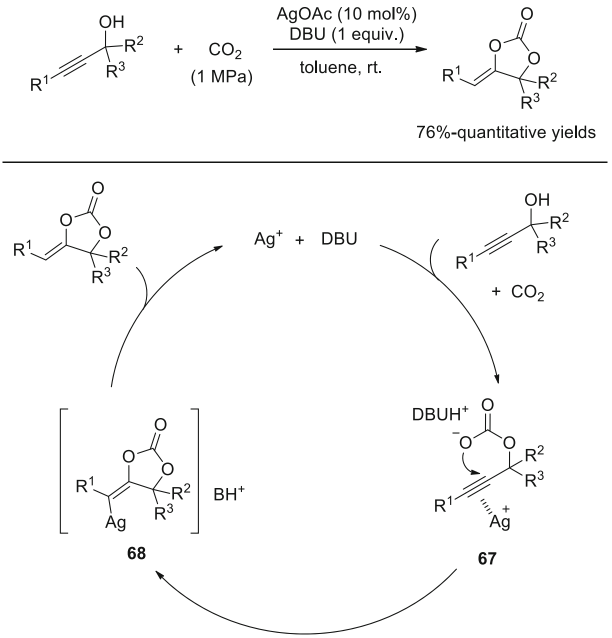

Scheme 30 AgOAc/DBU dual catalysis-promoted cyclization reaction of tertiary propargylic alcohols with CO_2

Among the catalytic systems based on transition-metals, silver has been intensively studied due to its significant capacity of activating carbon–carbon triple bond. In this respect, AgOAc cooperating with DBU has been developed for promoting the incorporation of CO_2 into cyclic carbonates [70]. Initially, the carbonic aid intermediate **67** is generated from the base-induced reaction of alcohol and CO_2. Then intramolecular cyclization is facilitated by a silver salt, which plays an activation role on the alkyne. Finally, the protonation of alkenyl-silver intermediate **68** gives the desired product and releases the silver catalyst (Scheme 30).

Our group has developed silver salts/phosphine catalytic system to avoid the use of equivalent organic base. The binary system Ag_2WO_4/PPh_3 shows dual activation effects towards both propargylic alcohol and CO_2, that is, the silver cation is able to activate carbon–carbon triple bond and the tungstate anion could activate both CO_2 and the O–H bond of propargylic alcohol [71]. We have also discovered that bifunctional silver complex i.e., $[(PPh_3)_2Ag]_2CO_3$, in situ generated form Ag_2CO_3 and PPh_3, exhibits excellent catalytic activity thus facilitating the reaction to proceed under ambient conditions [72]. The bulkier $[(Ph_3P)_2Ag^I]^+$ is supposed to be capable of activating carbon–carbon triple bond and enhancing *O*-nucleophilicity of the alkylcarbonic anion, thereby promote the intramolecular nucleophilic cyclization as shown in Scheme 31. Very recently, we have disclosed that AgOAc, in conjunction with tetraheptylammonium bromide, serves as a robust catalyst for this carboxylative cyclization reaction with TON up to 6024 [74].

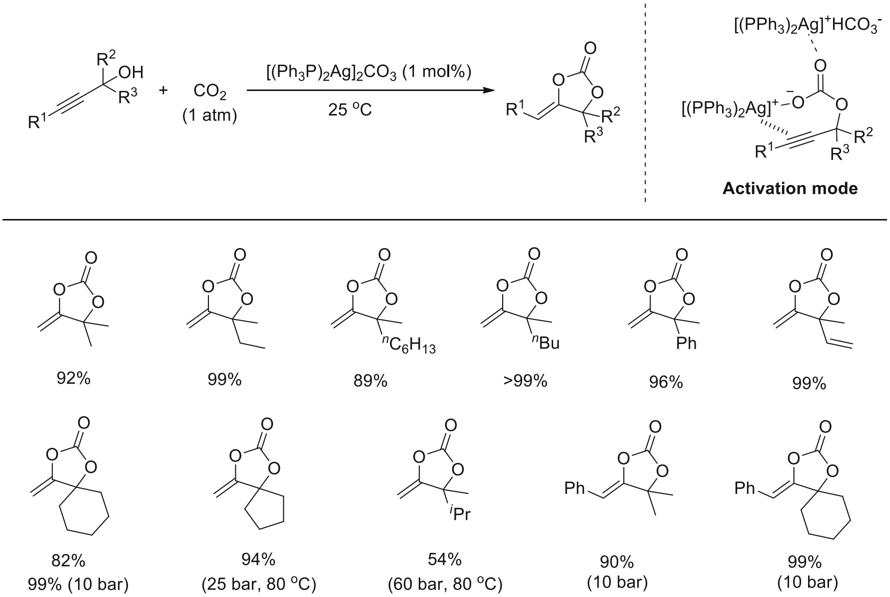

Scheme 31 Bifunctional $[(PPh_3)_2Ag]_2CO_3$-catalyzed CO_2 incorporation into α-methylene cyclic carbonates

The asymmetric incorporation of CO_2 into bispropargylic alcohols **69** can be achieved by the employment of AgOAc and chiral Schiff base ligand, as depicted in Scheme 32 [73].

In addition, the iodo-substituted cyclic carbonates **73** or **74** can be obtained from the mild reaction of olefinic or acetylenic alcohols (**71** or **72**) with CO_2 using *t*BuOI as an organocatalyst [78]. As shown in Scheme 33, the olefinic alcohol can reversibly react with CO_2 to produce the alkylcarbonic acid **75**. This weak acid can be trapped by *t*BuOI to generate an *O*-iodinated species **76** and cyclic carbonate can be formed via further intramolecular ring-closure.

Similarly, enantioselective synthesis of six-member cyclic carbonates has been achieved by using dual Brønsted acid/base catalyst system from homoallylic alcohols and CO_2 [79].

In 2011, Jiang's group reported the copper-catalyzed domino reaction for the preparation of substituted 3(*2H*)-furanones from propargylic alcohols, nitriles, and CO_2 [80]. As illustrated in Scheme 34, α-alkylidene cyclic carbonates **77** is generated from the reaction of propargylic alcohols and CO_2 in the presence of CuI and DBU, further hydrolysis of which affords α-hydroxyketone intermediate **78**. Then, the copper-promoted nucleophilic addition of **78** onto nitrile occurs to form the intermediate **79**. Consecutive intramolecular Claisen condensation and further dehydration produces the desired 3(*2H*)-furanones.

A novel "CO_2-recycling" process involving a palladium-catalyzed cascade reaction between 4-methoxycarbonyloxy-2-butyn-1-ols **80** and phenols to produce the phenoxy-substituted cyclic carbonates **81** has been well demonstrated by

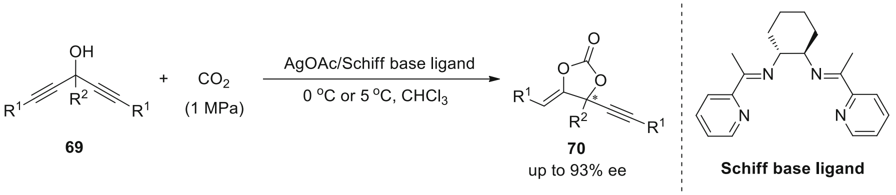

Scheme 32 AgOAc/Schiff base-catalyzed asymmetric incorporation of CO_2 into bispropargylic alcohols

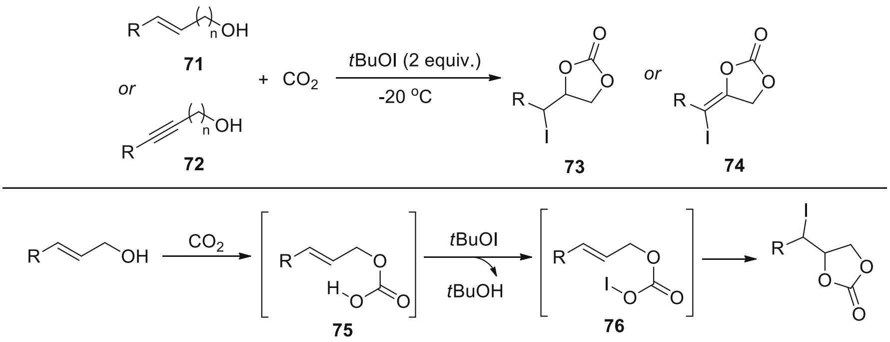

Scheme 33 *t*BuOI-mediated iodinative carboxylative cyclization of unsaturated alcohols and CO_2

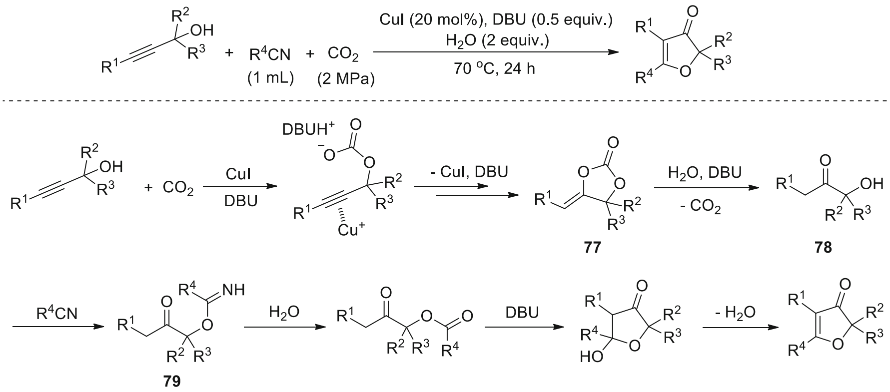

Scheme 34 CO_2-participated copper-catalyzed domino reaction for the construction of 3(2*H*)-furanones

Yoshida et al. [81]. The elaborately designed substrate **80**, initially goes through decarboxylation to eliminate one CO_2 molecule in the presence of palladium catalyst, providing an allenylpalladium methoxide intermediate **83**. Then, the released CO_2 is trapped by oxygen anion and further incorporated into phenoxy-substituted cyclic carbonates through the π-allylpalladium intermediate **85** (Scheme 35).

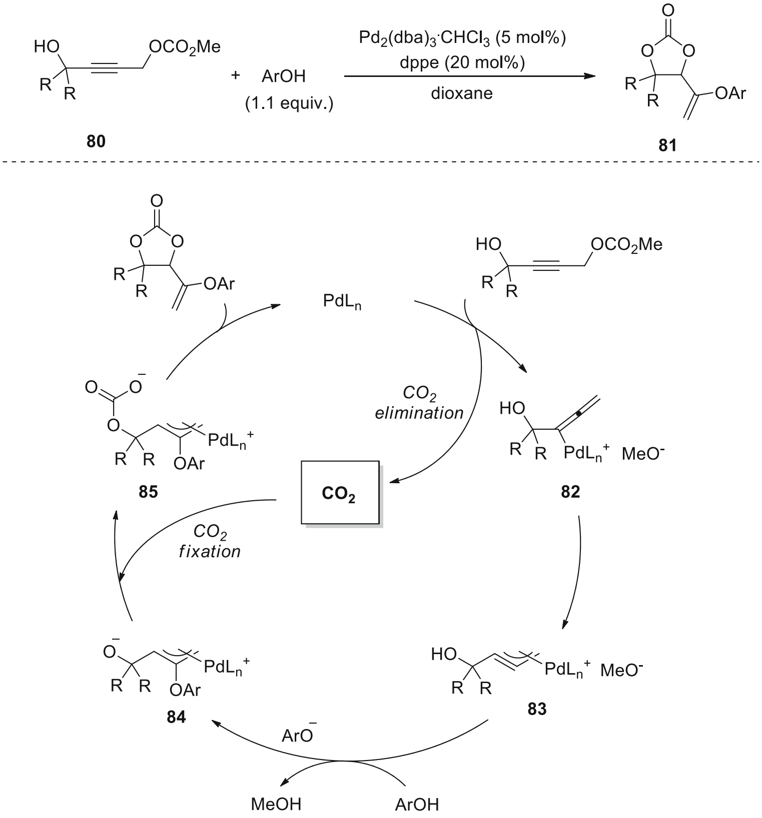

Scheme 35 Palladium-catalyzed CO_2 elimination–fixation reaction

4 Perspectives

Incorporating of CO_2 or “C=O”, “C” fragment into heterocyclic compounds such as lactones, oxazolidinones, cyclic carbonates, quinazoline-2,4(*1H*,*3H*)-diones have been achieved by elegant protocols with rationally designed substrates. Generally, the applied reactant contains potential carbon-nucleophile, nitrogen-nucleophile, or oxygen-nucleophile that can be in situ generated. In this respect, activation of C–H bond and C–Si bond by base and fluoride, respectively, is the key for generating carbon-nucleophile. The activation of N–H bond and O–H bond by base or hydrogen-bond interaction would facilitate the formation of nitrogen-nucleophile or oxygen-nucleophile. Such nucleophiles further trap CO_2 to furnish the corresponding carboxylate, carbamate, or alkylcarbonate intermediate, respectively. Subsequent intramolecular cyclization or/and isomerization provides various heterocyclic products, concomitant with the formation of new carbon–carbon, carbon–nitrogen or/and carbon–oxygen bond. Unsaturated functional groups, for instance, alkynyl, vinyl, and nitrile group are introduced at appropriate positions serving as electrophiles to accomplish intramolecular cyclization process. In this respect, transition-metal catalysts have been designed for the purpose of activating such unsaturated groups, leading to the intramolecular nucleophilic addition proceeding smoothly under mild conditions, particularly low pressure. Moreover, well-defined organocatalysts are also demonstrated as potential alternatives with excellent catalytic performances in promoting insertion of CO_2 into heterocyclic compounds in a cost-effective and environmentally benign manner. Though significant progresses have been made in catalytic transformation of CO_2 for heterocycles construction over the past decades, continuous interest is concentrating on establishing efficient procedures for upgrading CO_2 into value-added products. In this context, we envision that the following aspects would provide new prospects for the development of CO_2 chemistry:

1. Development of metal catalysts with high catalytic activities, non-noble metal catalysts instead of noble metal catalysts, biocompatible metal catalysts in place of toxic metal catalysts;
2. Design of bifunctional or cooperative catalysts for simultaneously activating both the substrate and CO_2, or simultaneously activating multiple functional groups in the substrate;
3. Design of substrates bearing potential nucleophilic and/or electrophilic sites, or adopting highly reactive reagents with high free energy as reactants;
4. Design of thermodynamically favorable reactions;
5. Carbon dioxide capture and utilization (CCU) strategy [8, 82–84]: adopting captured CO_2, for instance the ammonium carbamate, which is derived from absorption of CO_2 by an amine, as a “CO_2-measurable” reagent to perform subsequent conversion.

Acknowledgements This work was financially supported by National key research and development project (2016YFA0602900), the National Natural Science Foundation of China, the Natural Science Foundation of Tianjin Municipality (16JCZDJC39900), Specialized Research Fund for the Doctoral Program of Higher Education (project 20130031110013), and MOE Innovation Team (IRT13022) of China.

References

1. Aresta M, Dibenedetto A, Angelini A (2014) Catalysis for the valorization of exhaust carbon: from CO_2 to chemicals, materials, and fuels. technological use of CO_2. Chem Rev 114:1709–1742
2. He LN (2013) Carbon dioxide chemistry. Chinese Science Press, Beijing
3. Cokoja M, Bruckmeier C, Rieger B, Herrmann WA, Kühn FE (2011) Transformation of carbon dioxide with homogeneous transition-metal catalysts: a molecular solution to a global challenge? Angew Chem Int Ed 50:8510–8537
4. He LN, Yang ZZ, Liu AH, Gao J (2010) CO^2 chemistry at Nankai group: catalytic conversion of CO_2 into value-added chemicals (2010) ACS series book “Advances in CO_2 conversion and utilization”, Chapter 6. pp 77–101
5. He LN, Wang JQ, Wang JL (2009) Carbon dioxide chemistry: examples and challenges in chemical utilization of carbon dioxide. Pure Appl Chem 81:2069–2080

6. Sakakura T, Choi JC, Yasuda H (2007) Transformation of carbon dioxide. Chem Rev 107:2365–2387
7. Yu B, He LN (2015) Upgrading Carbon dioxide by incorporation into heterocycles. Chem Sus Chem 8:52–62
8. Yang Z-Z, He L-N, Gao J, Liu A-H, Yu B (2012) Carbon dioxide utilization with C–N bond formation: carbon dioxide capture and subsequent conversion. Energy Environ Sci 5:6602–6639
9. Wang JL, Miao CX, Dou XY, Gao J, He LN (2011) Carbon dioxide in heterocyclic synthesis. Curr Org Chem 15:621–646
10. Liu Q, Wu L, Jackstell R, Beller M (2015) Using carbon dioxide as a building block in organic synthesis. Nat Commun 2015(6):5933–5947
11. Sasaki Y, Inoue Y, Hashimoto H (1979) Reaction of carbon dioxide with butadiene catalysed by palladium complexes. Synthesis of 2-ethylidenehept-5-en-4-olide. J Chem Soc Chem Commun 1979:605–606
12. Inoue Y, Sasaki Y, Hashimoto H (1978) Incorporation of CO_2 in butadiene dimerization catalyzed by palladium complexes. Formation of 2-ethylidene-5-hepten-4-olide. Bull Chem Soc Jpn 51:2375–2378
13. Braunstein P, Matt D, Nobel D (1988) Carbon dioxide activation and catalytic lactone synthesis by telomerization of butadiene and carbon dioxide. J Am Chem Soc 110:3207–3212
14. Tsuda T, Morikawa S, Sumiya R, Saegusa T (1988) Nickel(0)-catalyzed cycloaddition of diynes and carbon dioxide to give bicyclic α-pyrones. J Org Chem 53:3140–3145
15. Tsuda T, Morikawa S, Sumiya R (1989) Functionalized phosphine ligands in transition metal-catalysed organic synthesis. Nickel(0)-catalysed cycloaddition of terminally unsubstituted diynes and carbon dioxide to bicyclic 2-pyrones. J Chem Soc Chem Commun 1989:9–10
16. Tsuda T, Morikawa S, Hasegawa N, Sumiya R (1990) Nickel(0)-catalyzed cycloaddition of silyl diynes with carbon dioxide to silyl bicyclic α-pyrones. J Org Chem 55:2978–2981
17. Louie J, Gibby JE, Farnworth MV, Tekavec TN (2002) Efficient nickel-catalyzed [2+2+2] cycloaddition of CO_2 and diynes. J Am Chem Soc 124:15188–15189
18. Takimoto M, Kawamura M, Mori M (2003) Nickel(0)-mediated sequential addition of carbon dioxide and aryl aldehydes into terminal allenes. Org Lett 5:2599–2601
19. Inoue Y, Hibi T, Satake M, Hashimoto H (1979) Reaction of methylenecyclopropanes with carbon dioxide catalysed by palladium(0) complexes. Synthesis of five-membered lactones. J Chem Soc Chem Commun 1979:982–982
20. Binger P, Weintz H-J (1984) Palladium(0)-catalyzed preparation of γ-lactone from methylenecyclopropanes and carbon dioxide. Eur J Inorg Chem 117:654–665
21. Greco GE, Gleason BL, Lowery TA, Kier MJ, Hollander LB, Gibbs SA, Worthy AD (2007) Palladium-catalyzed [3 + 2] cycloaddition of carbon dioxide and trimethylenemethane under mild conditions. Org Lett 9:3817–3820
22. Kikuchi S, Sekine K, Ishida T, Yamada T (2012) C–C bond formation with carbon dioxide promoted by a silver catalyst. Angew Chem Int Ed 51:6989–6992
23. Xin Z, Lescot C, Friis SD, Daasbjerg K, Skrydstrup T (2015) Organocatalyzed CO_2 trapping using alkynyl indoles. Angew Chem Int Ed 54:6862–6866
24. Sekine K, Sadamitsu Y, Yamada T (2015) Silvercatalyzed cascade carboxylation and cyclization of trimethyl(2-methylenebut-3-yn-1-yl)silane derivatives. Org Lett 17:5706–5709
25. Yoo WJ, Nguyen TVQ, Kobayashi S (2014) Synthesis of isocoumarins through three-component couplings of arynes, terminal alkynes, and carbon dioxide catalyzed by an NHC-copper complex. Angew Chem Int Ed 53:10213–10217
26. Sasano K, Takaya J, Iwasawa N (2013) Palladium(II)-catalyzed direct carboxylation of alkenyl C–H bonds with CO_2. J Am Chem Soc 135:10954–10957
27. Zhang WZ, Yang MW, Lu XB (2016) Carboxylative cyclization of substituted propenyl ketones using CO_2: transition-metal-free synthesis of α-pyrones. Green Chem 18:4181–4184
28. Costa M, Chiusoli GP, Rizzardi M (1996) Base-catalysed direct introduction of carbon dioxide into acetylenic amines. Chem Commun 1699–1700
29. Takeda Y, Okumura S, Tone S, Sasaki I, Minakata S (2012) Cyclizative atmospheric CO_2 fixation by unsaturated amines with t-BuOI leading to cyclic carbamates. Org Lett 14:4874–4877
30. Hu J, Ma J, Zhu Q, Zhang Z, Wu C, Han B (2015) Transformation of atmospheric CO_2 catalyzed by protic ionic liquids: efficient synthesis of 2-oxazolidinones. Angew Chem Int Ed 54:5399–5403
31. Mitsudo T, Hori Y, Yamakawa Y, Watanabe Y (1987) Ruthenium catalyzed selective synthesis of enol carbamates by fixation of carbon dioxide. Tetrahedron Lett 28:4417–4418

32. Shi M, Shen YM (2002) Transition-metal-catalyzed reactions of propargylamine with carbon dioxide and carbon disulfide. J Org Chem 67:16–21
33. Yoshida S, Fukui K, Kikuchi S, Yamada T (2009) Silver-catalyzed preparation of oxazolidinones from carbon dioxide and propargylic amines. Chem Lett 38:786–787
34. Hase S, Kayaki Y, Ikariya T (2013) NHC–gold(I) complexes as effective catalysts for the carboxylative cyclization of propargylamines with carbon dioxide. Organometallics 32:5285–5288
35. Yoshida M, Mizuguchi T, Shishido K (2012) Synthesis of oxazolidinones by efficient fixation of atmospheric CO_2 with propargylic amines by using a silver/1,8-diazabicyclo[5.4.0]undec-7-ene (DBU) dual-catalyst system. Chem Eur J 18:15578–15581
36. Wang M-Y, Song Q-W, Ma R, Xie J-N, He L-N (2016) Efficient conversion of carbon dioxide at atmospheric pressure to 2-oxazolidinones promoted by bifunctional Cu(II)-substituted polyoxometalate-based ionic liquids. Green Chem 18:282–287
37. Liu X, Wang M-Y, Wang S-Y, Wang Q, He L-N (2016) In situ generated zinc(II) catalyst for incorporation of CO_2 into 2-oxazolidinones with propargylic amines at atmospheric pressure. ChemSusChem. doi:10.1002/cssc.201601469
38. Kayaki Y, Mori N, Ikariya T (2009) Palladium-catalyzed carboxylative cyclization of α-allenyl amines in dense carbon dioxide. Tetrahedron Lett 50:6491–6493
39. Li S, Ye J, Yuan W, Ma S (2013) Highly regioselective three-component palladium-catalyzed synthesis of 5-vinyloxazolidin-2-ones from 2,3-allenyl amines, organic iodides, and carbon dioxide. Tetrahedron 69:10450–10456
40. Yamashita K, Hase S, Kayaki Y, Ikariya T (2015) Highly selective carboxylative cyclization of allenylmethylamines with carbon dioxide using *N*-heterocyclic carbene-silver(I) catalysts. Org Lett 17:2334–2337
41. Yoo WJ, Li CJ (2008) Copper-catalyzed four-component coupling between aldehydes, amines, alkynes and carbon dioxide. Adv Synth Catal 350:1503–1506
42. Ishida T, Kikuchi S, Tsubo T, Yamada T (2013) Silver-catalyzed incorporation of carbon dioxide into o-alkynylaniline derivatives. Org Lett 15:848–851
43. Ishida T, Kikuchi S, Yamada T (2013) Efficient preparation of 4-hydroxyquinolin-2(1H)-one derivatives with silver-catalyzed carbon dioxide incorporation and intramolecular rearrangement. Org Lett 15:3710–3713
44. Zhang Z, Liao L-L, Yan S-S, Wang L, He Y-Q, Ye J-H, Li J, Zhi Y-G, Yu D-G (2016) Lactamization of sp^2 C–H bonds with CO_2: transition-metal-free and redox-neutral. Angew Chem Int Ed 55:7068–7072
45. Wang S, Shao P, Du G, Xi C (2016) MeOTf- and TBD-Mediated carbonylation of ortho-arylanilines with CO_2 leading to phenanthridinones. J Org Chem 81:6672–6676
46. Patil YP, Tambade PJ, Jagtap SR, Bhanage BM (2008) Cesium carbonate catalyzed efficient synthesis of quinazoline-2,4(1H,3H)-diones using carbon dioxide and 2-aminobenzonitriles. Green Chem Lett Rev 1:127–132
47. Mizuno T, Okamoto N, Ito T, Miyata T (2000) Synthesis of 2,4-dihydroxyquinazolines using carbon dioxide in the presence of DBU under mild conditions. Tetrahedron Lett 41:1051–1053
48. Gao J, He L-N, Miao C-X, Chanfreau S (2010) Chemical fixation of CO_2: efficient synthesis of quinazoline-2,4(1H,3H)-diones catalyzed by guanidines under solvent-free conditions. Tetrahedron 66:4063–4067
49. Nagai D, Endo T (2009) Synthesis of 1H-quinazoline-2,4-diones from 2-aminobenzonitriles by fixation of carbon dioxide with amidine moiety supported polymer at atmospheric pressure. J Polym Sci Part A: Polym Chem 47:653–657
50. Kimura T, Kamata K, Mizuno N (2012) A bifunctional tungstate catalyst for chemical fixation of CO_2 at atmospheric pressure. Angew Chem Int Ed 51:6700–6703
51. Kimura T, Sunaba H, Kamata K, Mizuno N (2012) Efficient $[WO_4]^{2-}$-catalyzed chemical fixation of carbon dioxide with 2-aminobenzonitriles to quinazoline-2,4(1H,3H)-diones. Inorg Chem 51:13001–13008
52. Patil YP, Tambade PJ, Deshmukh KM, Bhanage BM (2009) Synthesis of quinazoline-2,4(1H,3H)-diones from carbon dioxide and 2-aminobenzonitriles using [Bmim]OH as a homogeneous recyclable catalyst. Catal Today 148:355–360
53. Lu W, Ma J, Hu J, Song J, Zhang Z, Yang G, Han B (2014) Efficient synthesis of quinazoline-2,4(1H,3H)-diones from CO_2 using ionic liquids as a dual solvent–catalyst at atmospheric pressure. Green Chem 16:221–225

54. Zheng H, Cao X, Du K, Xu J, Zhang P (2014) A highly efficient way to capture CX_2 (O, S) mildly in reusable ReILs at atmospheric pressure. Green Chem 16:3142–3148
55. Zhao Y, Yu B, Yang Z, Zhang H, Hao L, Gao X, Liu Z (2014) A protic ionic liquid catalyzes CO_2 conversion at atmospheric pressure and room temperature: synthesis of quinazoline-2,4(1H,3H)-diones. Angew Chem Int Ed 53:5922–5925
56. Ma J, Han B, Song J, Hu J, Lu W, Yang D, Zhang Z, Jiang T, Hou M (2013) Efficient synthesis of quinazoline-2,4(1H,3H)-diones from CO_2 and 2-aminobenzonitriles in water without any catalyst. Green Chem 15:1485–1489
57. Ma J, Hu J, Lu W, Zhang Z, Han B (2013) Theoretical study on the reaction of CO_2 and 2-aminobenzonitrile to form quinazoline-2,4(1H,3H)-dione in water without any catalyst. Phys Chem Chem Phys 15:17333–17341
58. Kamata K, Kimura T, Sunaba H, Mizuno N (2014) Scope of chemical fixation of carbon dioxide catalyzed by a bifunctional monomeric tungstate. Catal Today 226:160–166
59. Yu B, Zhang H, Zhao Y, Chen S, Xu J, Hao L, Liu Z (2013) DBU-based ionic-liquid-catalyzed carbonylation of o-phenylenediamines with CO_2 to 2-benzimidazolones under solvent-free conditions. ACS Catal 3:2076–2082
60. Kayaki Y, Yamamoto M, Ikariya T (2007) Stereoselective formation of α-alkylidene cyclic carbonates via carboxylative cyclization of propargyl alcohols in supercritical carbon dioxide. J Org Chem 72:647–649
61. Cà ND, Gabriele B, Ruffolo G, Veltri L, Zanetta T, Costa M (2011) Effective guanidine-catalyzed synthesis of carbonate and carbamate derivatives from propargyl alcohols in supercritical carbon dioxide. Adv Synth Catal 353:133–146
62. Kayaki Y, Yamamoto M, Ikariya T (2009) N-heterocyclic carbenes as efficient organocatalysts for CO_2 fixation reactions. Angew Chem Int Ed 48:4194–4197
63. Wang YB, Wang YM, Zhang WZ, Lu XB (2013) Fast CO_2 sequestration, activation, and catalytic transformation using N-heterocyclic olefins. J Am Chem Soc 135:11996–12003
64. Wang Y-B, Sun D-S, Zhou H, Zhang W-Z, Lu X-B (2014) Alkoxide-functionalized imidazolium betaines for CO_2 activation and catalytic transformation. Green Chem 16:2266–2272
65. Inoue Y, Ishikawa J, Taniguchi M, Hashimoto H (1987) Cobalt-catalyzed reaction of carbon dioxide with propargyl alcohol. Bull Chem Soc Jpn 60:1204–1206
66. Kim T-J, Kwon K-H, Kwon S-C, Baeg J-O, Shim S-C, Lee D-H (1990) Iron complexes of 1,1′-bis(diphenylphosphino)ferrocene (BPPF) as efficient catalysts in the synthesis of carbamates. X-ray crystal structure of $(BPPF)Fe(CO)_3$. J Organomet Chem 389:205–217
67. Gu Y, Shi F, Deng Y (2004) Ionic liquid as an efficient promoting medium for fixation of CO_2: clean synthesis of α-methylene cyclic carbonates from CO_2 and propargyl alcohols catalyzed by metal salts under mild conditions. J Org Chem 69:391–394
68. Ouyang L, Tang X, He H, Qi C, Xiong W, Ren Y, Jiang H (2015) Copper-promoted coupling of carbon dioxide and propargylic alcohols: expansion of substrate scope and trapping of vinyl copper intermediate. Adv Synth Catal 357:2556–2565
69. Iritani K, Yanagihara N, Utimoto K (1986) Carboxylative coupling of propargylic alcohols with allyl chloride. J Org Chem 51:5499–5501
70. Yamada W, Sugawara Y, Cheng HM, Ikeno T, Yamada T (2007) Silver-catalyzed incorporation of carbon dioxide into propargylic alcohols. Eur J Org Chem 2007:2604–2607
71. Song QW, Yu B, Li XD, Ma R, Diao ZF, Li RG, Li W, He LN (2014) Efficient chemical fixation of CO_2 promoted by a bifunctional Ag_2WO_4/Ph_3P system. Green Chem 16:1633–1638
72. Song QW, Chen WQ, Ma R, Yu A, Li QY, Chang Y, He LN (2015) Bifunctional silver(I) complex-catalyzed CO_2 conversion at ambient conditions: synthesis of α-methylene cyclic carbonates and derivatives. ChemSusChem 8:821–827
73. Yoshida S, Fukui K, Kikuchi S, Yamada T (2010) Silver-catalyzed enantioselective carbon dioxide incorporation into bispropargylic alcohols. J Am Chem Soc 132:4072–4073
74. Song QW, He LN (2016) Robust silver(I) catalyst for the carboxylative cyclization of propargylic alcohols with carbon dioxide under ambient conditions. Adv Synth Catal 358:1251–1258
75. Yamada T, Ugajin R, Kikuchi S (2014) Silver-catalyzed efficient synthesis of vinylene carbonate derivatives from carbon dioxide. Synlett 25:1178–1180
76. Hu J, Ma J, Zhu Q, Qian Q, Han H, Mei Q, Han B (2016) Zinc(II)-catalyzed reactions of carbon dioxide and propargylic alcohols to carbonates at room temperature. Green Chem 18:382–385
77. Uemura K, Kawaguchi T, Takayama H, Nakamura A, Inoue Y (1999) Preparation of alkylidene cyclic carbonates via cyclization of propargylic carbonates. J Mol Catal A Chem 139:1–9

78. Minakata S, Sasaki I, Ide T (2010) Atmospheric CO_2 fixation by unsaturated alcohols using tBuOI under neutral conditions. Angew Chem Int Ed 49:1309–1311
79. Vara BA, Struble TJ, Wang W, Dobish MC, Johnston J (2015) Enantioselective small molecule synthesis by carbon dioxide fixation using a dual Brønsted acid/base organocatalyst. J Am Chem Soc 137:7302–7305
80. Qi C, Jiang H, Huang L, Yuan G, Ren Y (2011) Carbon dioxide triggered and copper-catalyzed domino reaction: efficient construction of highly substituted 3(2H)-furanones from nitriles and propargylic alcohols. Org Lett 13:5520–5523
81. Yoshida M, Fujita M, Ishii T, Ihara M (2003) A novel methodology for the synthesis of cyclic carbonates based on the palladium-catalyzed cascade reaction of 4-methoxycarbonyloxy-2-butyn-1-ols with phenols, involving a novel carbon dioxide elimination-fixation process. J Am Chem Soc 125:4874–4881
82. Li YN, He LN, Lang XD, Liu XF, Zhang S (2014) An integrated process of CO_2 capture and in situ hydrogenation to formate using a tunable ethoxyl-functionalized amidine and Rh/bisphosphine system. RSC Adv 4:49995–50002
83. Liu AH, Ma R, Song C, Yang ZZ, Yu A, Cai Y, He LN, Zhao YN, Yu B, Song QW (2012) Equimolar CO_2 capture by N-substituted amino acid salts and subsequent conversion. Angew Chem Int Ed 51:11306–11310
84. Song QW, Zhou ZH, Yin H, He LN (2015) Silver(I)-catalyzed synthesis of β-oxopropylcarbamates from propargylic alcohols and CO_2 surrogate: a gas-free process. ChemSusChem 8:3967–3972

Top Curr Chem (Z) (2017) 375:49
DOI 10.1007/s41061-017-0137-4

REVIEW

Synthesis of Ureas from CO_2

Hua Wang[1] · Zhuo Xin[1] · Yuehui Li[1]

Received: 31 December 2016 / Accepted: 27 March 2017 / Published online: 10 April 2017
© Springer International Publishing Switzerland 2017

Abstract Ureas are an important class of bioactive organic compounds in organic chemistry and exist widely in natural products, agricultural pesticides, uron herbicides, pharmaceuticals. Even though urea itself has been synthesized from CO_2 and ammonia for a long time, the selective and efficient synthesis of substituted ureas is still challenging due to the difficulty of dehydration processes. Efficient and economic fixation of CO_2 is of great importance in solving the problems of resource shortages, environmental issues, global warming, etc. During recent decades, chemists have developed different catalytic systems to synthesize ureas from CO_2 and amines. Herein, we focus on catalytic synthesis of ureas using CO_2 and amines.

Keywords Carbon dioxide · Synthesis of ureas · Catalysis · Dehydration · Carbamates

1 Introduction

Ureas are an important class of bioactive organic compounds in organic chemistry and exist widely in natural products, agricultural pesticides, uron herbicides, pharmaceuticals, etc. (Scheme 1). Consequently, a diverse range of synthetic routes leading to ureas have been developed. Nowadays, urea itself is produced from synthetic ammonia and carbon dioxide in industry, which is based on the Bosch–Meiser urea process developed in 1922. In this reaction, the overall conversion of

---

Chapter 5 was originally published as Wang, H., Xin, Z. & Li, Y. Top Curr Chem (Z) (2017) 375: 49. DOI 10.1007/s41061-017-0137-4.

✉ Yuehui Li
yhli@licp.cas.cn

[1] State Key Laboratory for Oxo Synthesis and Selective Oxidation, Suzhou Research Institute of LICP, Lanzhou Institute of Chemical Physics (LICP), Chinese Academy of Sciences, Lanzhou 730000, People's Republic of China

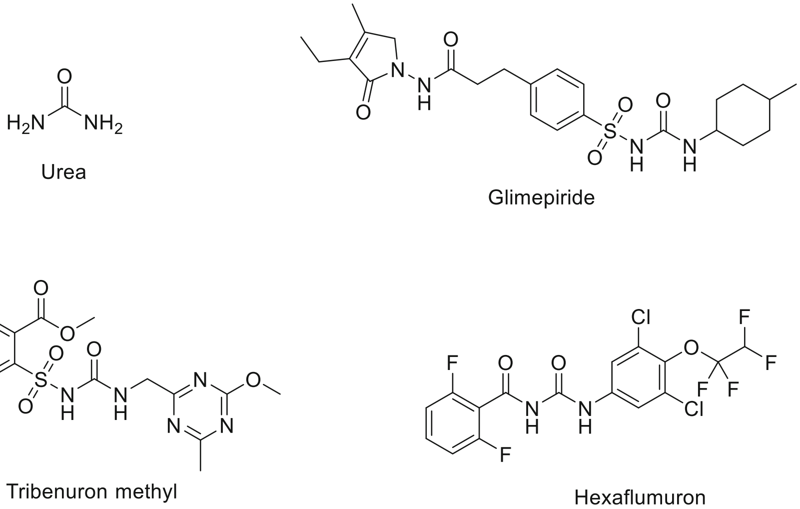

Scheme 1 Selected urea compounds with bioactivity

NH_3 and CO_2 to urea is exothermic and generally the process needs conditions at 150–250 °C with pressures as 5–25 MPa [1]. In fact, to synthesize substituted ureas, careful design of the process and catalysts is needed to make the synthetic methods efficient and practical. Since the 1960s, much effort has been made for this purpose, and methods making use of carbonyl precursors such as phosgene, isocyanates, or carbon monoxide to synthesize ureas were developed. However, to make synthesis in chemical industry more sustainable and environmentally friendly, new catalytic methods other than these traditional ones are required.

Efficient and economic fixation of CO_2 is of great importance in solving the problems of resources shortage, environmental issues, global warming, etc. Synthesis of ureas from CO_2 and amines has attracted chemists' broad interests since Bazarov's discovery on synthesis of urea from ammonia and CO_2 in 1870 [2–6].

Considering the weak acidity of CO_2, it is well known that treating CO_2 with amines will lead to carbamate acid **1** or carbamate anion **2** and **3** even at room temperature and low CO_2 pressure. One key factor to successful urea synthesis from CO_2 and amines is the efficient removal of H_2O. Under catalytic conditions, the starting material undergoes subsequent dehydration of carbamate **3** to generate urea products (Scheme 2). However, the transformations between CO_2 and **1**, **2,** and **3** are reversible [7]. Hence, the efficient conversion of carbamic acids or carbamate anions into ureas is still challenging.

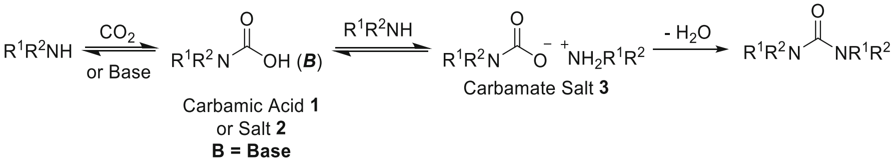

Scheme 2 General process of the preparation of urea from CO_2

There were interesting works since the 1970s developed on the use of dehydration agents such as *N*,*N*′-dicyclohexylcarbodiimide, *N*-phosphonium salt derivatives or diarylphosphite/bases [8]. In 1974, Yamazaki et al. have demonstrated a novel and simple way for the synthesis of ureas and thioureas from CO_2 and CS_2 under low pressure (e.g. through bubbling CO_2 into the solution) and at 40 °C in the presence of diphenyl (or triaryl) phosphites and tertiary amines (Scheme 3) [9]. Co-existence of tertiary amines and phosphites is crucial in the formation of products. The carbamate-substituted *N*-phosphonium salt (**4**), which reacts with another aniline to yield the urea, might be the key intermediate in this reaction. Interestingly, this intermediate is similar to the carbamyl phosphate, which is involved in urea cycle in living cells.

Ogura and co-workers used dry ice to react with amines using carbodiimides as the alternative dehydrating agents at −75 °C to produce disubstituted ureas. Otherwise, the high pressure CO_2 condition must be provided for different primary amines to give ureas in moderate to superior yield with triaryl amines at room temperature. Nevertheless, when aromatic amines were employed as substrate, reactions were relatively sluggish [10].

Another example used unusual $Me_3N{\cdot}SO_3$ complex as dehydration reagent for synthesis of phenyl ureas from CO_2 and amines in the presence of DBU [(1,8-Diazabicyclo(5.4.0)undec-7-ene] as base [11]. In this work, organic base has important influence on the formation of ureas. It is noteworthy that both electron-deficient and electron-rich anilines can be transformed into the corresponding ureas with moderate yields. Attempts to synthesize alkylureas and alkylcarbonates using this protocol were not successful. It was deduced that this failure was ascribed to the addition–elimination mechanism instead of the isocyanate-involving mechanism.

In 2004, Marsura et al. described the use of modified "phosphine-imide" [12] as a valuable and safe alternative reagent to hazardous phosgene or triphosgene for the synthesis of ureas (Scheme 4) [13]. The key factor of this strategy is the formation of iminophosphorane species from amine using $PPh_3/CCl_4/Et_3N$ combination followed by dechlorination with the aid of base. This formed in situ an iminophosphorane intermediate that could react with carbon dioxide and the other molecule of the amine

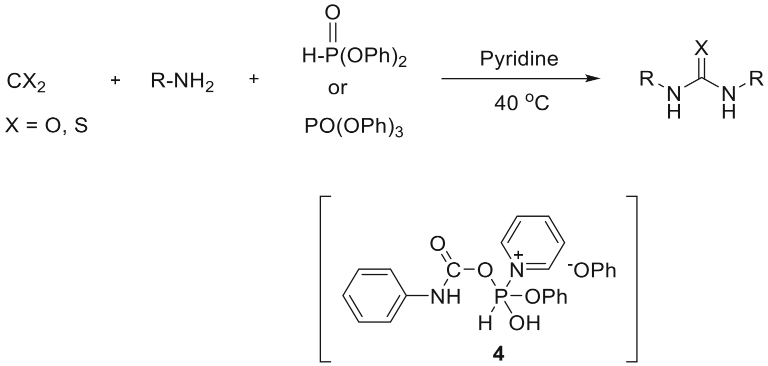

Scheme 3 Urea synthesis from aniline and CO_2 and CS_2

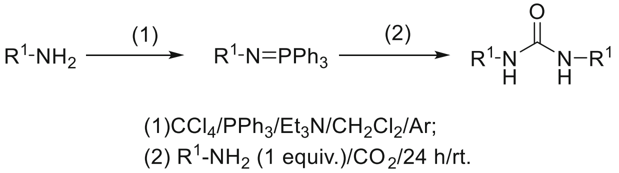

Scheme 4 Urea synthesis via "phosphine-imide" pathway

substrate to produce urea products efficiently. By using this protocol, dialkyl ureas are produced in good yields under mild conditions. Notably, asymmetric configuration of L-amino acid esters could be retained during the reaction.

Another mild route to symmetrical and unsymmetrical ureas was based on the use of Mitsunobu's reagent [14]. This protocol features its broad substrates scope and good yields using a combination of PPh_3/DEAD (diethylazodicarboxylate) at mild reaction conditions (room temperature, bubbling CO_2). The mechanism is depicted in Scheme 5. Carbamate acid from the treatment of amine with CO_2 reacts with PPh_3-derived zwitterion to form the stabilized zwitterion species (**5**), which reacts with another molecule of amine to give highly active intermediate (**6**), followed by a rearrangement step to give the substituted urea products.

Recently, Gee et al. extended Mitsunobu's reagent-based chemistry to transform the short-lived $^{11}CO_2$ into ^{11}C-labelled symmetrical ureas [15]. However, the authors proposed a different phosphine oxonium ion as the intermediate instead of the highly reactive zwitterionic species. Similarly, this system showed broad substrate scope and excellent yields under mild condition providing a practical way to the synthesis of potentially valuable ureas.

In these systems, the condensations could occur efficiently at mild conditions (e.g. at 40 °C, 4 h reaction time). However, the substrate scope was quite limited either to aniline derivatives or aliphatic amines. During recent decades, chemists have developed different catalytic systems on more efficient and powerful

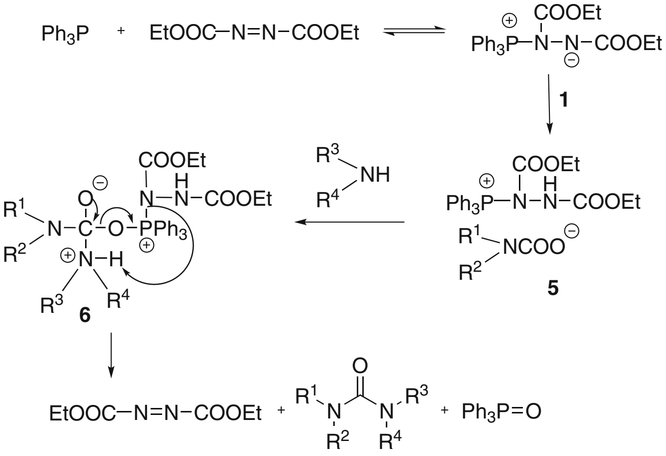

Scheme 5 The mechanism of the Mitsunobu's reagent-involved synthesis of ureas

methodologies to produce ureas from CO_2 and amines. In this chapter, we could not cover all the recent works on synthesis of ureas. Accordingly, a brief discussion focusing on catalytic synthesis of ureas using CO_2 and amines will be given.

2 Catalytic Synthesis of Ureas from Amines and CO_2

In the last decades, many catalytic methods were developed for synthesis of ureas from amines and CO_2 based on the use of Lewis bases, transition metals, ionic liquids, etc.

In 1987, triphenylstibine oxide (Ph_3SbO) was found to be effective to catalyze the conversion of diamines and CO_2 to cyclic ureas in the presence of molecular sieve as a dehydrating agent [16]. Obviously, such reactions of diamines can be attributed to the strategy of substrate-assisted carbon dioxide activation for heterocyclic synthesis [3, 17]. Notably, cyclic ureas are found as important motifs in biologically active molecules with antineoplastic and anti-viral activity [18]. Later, the same group reported the promotion effect of tetraphosphorus decasulfide (P_4S_{10}) for Ph_3SbO-catalyzed synthesis of ureas showing a much broader substrate scope. In the presence of 2.5 mol% of Ph_3SbO and 5 mol% of P_4S_{10}, 1,3-dialkylureas (RNHCONHR, where R = Bu, *i*Bu, *s*Bu, *t*Bu, allyl, Ph) and tetramethylurea were obtained with acceptable reactivity at 80 °C under an initial CO_2 pressure of 4.9 MPa, from the corresponding amines and carbon dioxide. Here, P_4S_{10} was used as not only a dehydration agent, but also a chemical activator via thiolation reactions. It was revealed that two successive steps happened: thiolation of carbamic acid to an intermediate antimony carbamate species followed by aminolysis of the carbamothioic acid (Scheme 6). ^{13}C NMR studies were done for butylamine at 2 atm CO_2. Quantitative formation of butylammonium *N*-butylcarbamate (**7**) was detected. After heating the solution to 30 °C in C_6D_6 in the presence of Ph_3SbO/P_4S_{10}, signals of triphenylantimony bis(butylcarbamate) (**8**) appeared, which was more active toward thiolation by P_4S_{10} to form butylammonium *N*-butylcarbamothioate (**10**) under higher temperatures (step 3). Finally, the mixture was heated at 80 °C, and the amounts of 1,3-dibutylurea started to increase (step 4). Under similar conditions at 80 °C for 48 h, no change was detected in the reaction without the use of catalyst.

In 1986, Fujiwara and co-workers reported the pioneering $PdCl_2(CH_3CN)_2$ catalyzed synthesis of ureas from the reaction of CO_2 and dialkylamines in the presence of PPh_3 in CCl_4/MeCN co-solvent [19]. In this system, formamides could also be obtained selectively by using HCOONa as the additive in 2-methoxyethanol. Among all the tested catalysts such as $PdCl_2$, $PdCl_2(PhCN)_2$, $PdCl_2(Et_2NH)_2$, $PdCl_2(dppe)_2$, $Pd(OAc)_2$, $Pd(OAc)_2(bpy)$, $Pd_2(dba)_3$, $Pd(acac)_2$, and $Rh(CO)(PPh_3)_2Br$, $RuH_2(PPh_3)_4$, $RuCl_2(PPh_3)_2$, only $PdCl_2(CH_3CN)_2$ gives the best results. Here, the use of CCl_4 as the solvent may promote the formation of the $[HNEt_2(CCl_3)]^+Cl^-$. The activated N–H bond will be inserted by the Pd(0) species to form the key $HPdNEt_2$ intermediate. Then CO_2 could insert into a Pd–N bond. The salt intermediate might be well solved in acetonitrile, which is the beneficial factor to use such polar solvent. The highest yield for *N*,*N*,*N*′,*N*′-tetraethylurea was 36% and *N*,*N*-diethylformamide was 9%.

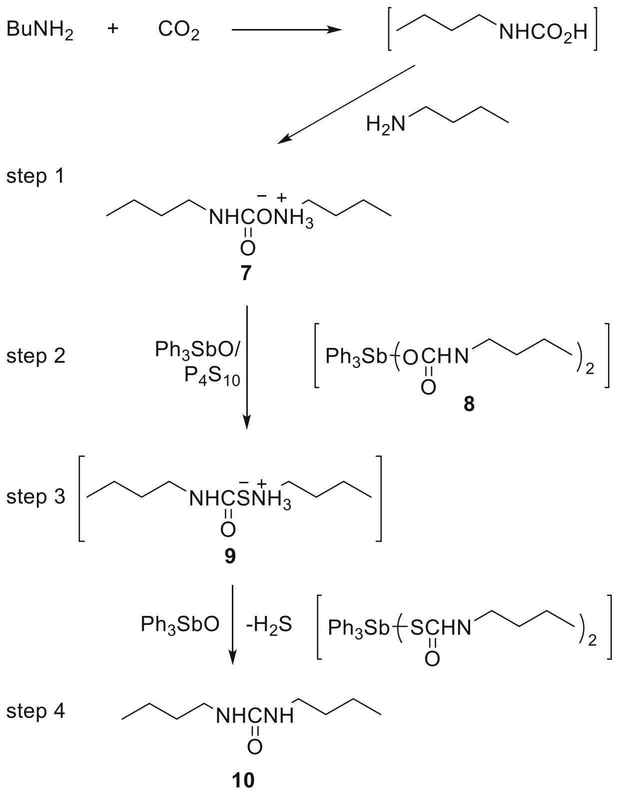

Scheme 6 Proposed mechanism on Ph_3SbO-catalyzed urea synthesis

During the study on the synthesis of carbamates from the reaction of CO_2 and secondary amines with terminal alkynes in the presence of ruthenium catalysts, Dixneuf and co-workers found that straightforward synthesis of *N*,*N*′-disubstituted symmetrical ureas could be achieved when using aliphatic primary amines as the substrates [20]. In this work, under heating conditions, ruthenium complexes reacted with terminal alkynes such as propargyl alcohol to afford alkyne ruthenium species acting as an efficient dehydrating reagent (Eq. 1).

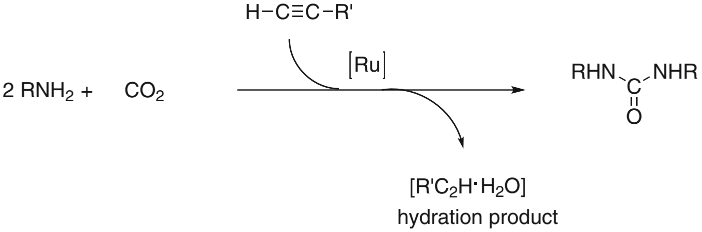

(1)

Thus, the presence of stoichiometric amounts of an alkyne (e.g. 2-methylbut-3-yn-2-ol) was required. However, the organophosphine-promoted reaction of amine and CO_2 with such alkyne compound is a competing side reaction and oxazolidinone **11** was formed as the main by-product. It became to be the major product when higher ratio of Bu_3P/Ru was used, even with formation of urea product being fully retarded (Eq. 2). The best ratio for $PBu_3/RuCl_3 \cdot 3H_2O$ was two and the highest yield was achieved for the reaction of *n*-decylamine giving 68% yield of *N*,*N*′-di-*n*-decylurea.

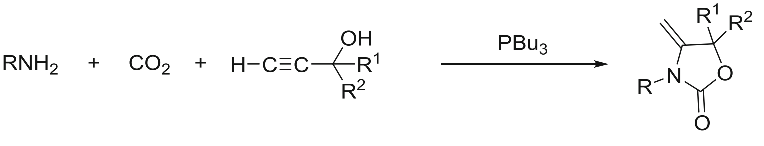

(2)

11

R= cyclohexyl, R^1=R^2= Me

Carbamates were proposed as the key intermediate. In the mechanism, it was proposed that the first step is coordination of the alkyne with the Ru center (**I**) to activate the alkyne; then the nucleophilic addition of the ammonium carbamate to the carbon–carbon triple bond of **I** giving a vinyl ruthenium intermediate **II**; substitutive addition of amine substrate to **II** will lead to the urea product and a ruthenium-coordinated enol (**III**) following with protonation to an organic molecule (e.g. hydroxyl ketone **IV** being in situ consumed up) and regeneration of the active catalytic species **I** (Scheme 7).

In the Ni-catalyzed *N*-methylation of amines with CO_2 and hydrosilanes in the presence of phosphine ligands, production of monomethylated ureas in good yields were achieved by using lower amounts of $PhSiH_3$ for both aliphatic and aromatic primary amines [21]. The best ligands are dippe [(1,2-bisdiisopropylphosphino)ethane] and dcype [(1,2-bis-dicyclohexylphosphino)ethane]. For different amines, the corresponding monomethylated ureas were obtained in 31–82% yields (Scheme 8). This result is consistent with the mechanistic proposal that ureas are the intermediates to the corresponding methylated products.

Based on the product distribution and experimental observations, it was proposed that electrophilic isocyanates are key reaction intermediates. In the presence of hydrosilanes as dehydrants, the carbamic acid would be dehydrated to isocyanate, which could also be generated via dehydration of formamide. The reduction of formamides will lead to the methylated amines, which along with the free primary amines react with isocyanates to give the *N*-methylated tri-substituted target products or di-substituted by-products (Scheme 9).

As famous acid and oxidation catalysts, the basicity of polyoxometalates (POMs) has been less explored for catalysis [22–24]. In fact, highly charged POMs (especially lacunary POMs) have electron-rich oxygen atoms on their surfaces, which can function as basic active sites. Based on density functional theory (DFT) calculations, Mizuno et al. found that a simple monomeric tungstate, $TBA_2[WO_4]$ (**12**, TBA=$[(n\text{-}C_4H_9)_4N]^+$) possessed the highest basicity among these tested tungstates, and thus acted as a promising homogeneous catalyst for chemical

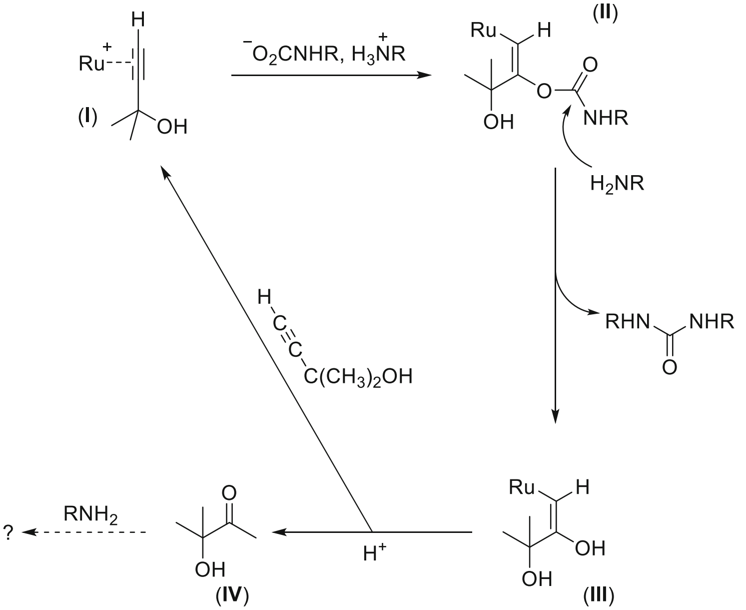

Scheme 7 Proposed mechanism on urea synthesis with alkyne as dehydrant

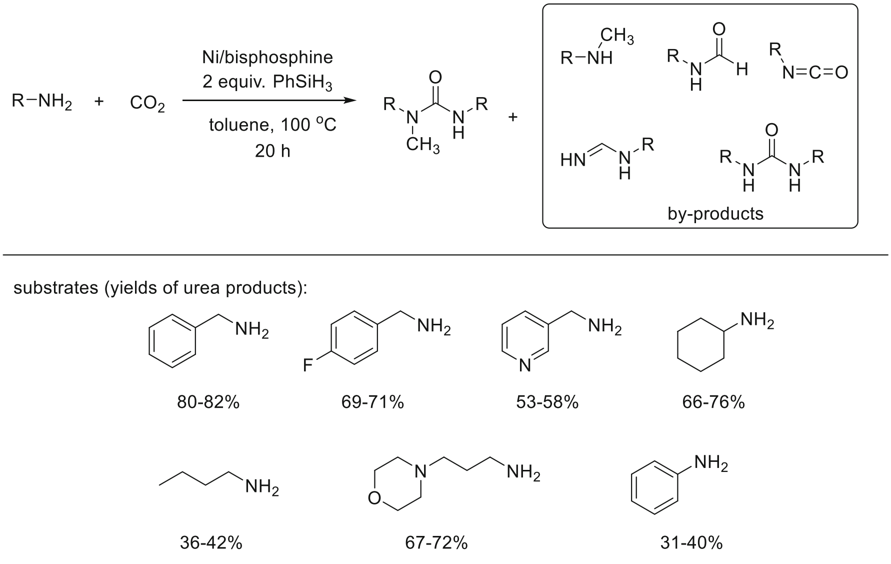

Scheme 8 Ni-catalyzed synthesis of ureas in the presence of phenylsilane

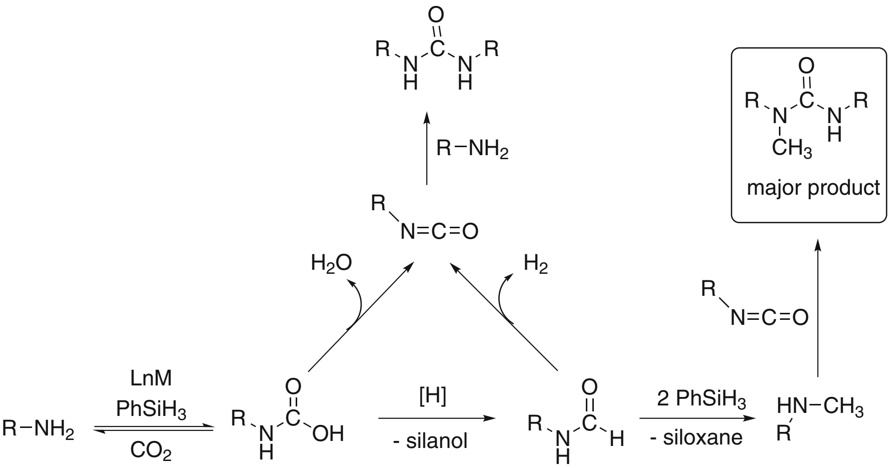

Scheme 9 Proposed pathway for Ni-catalyzed synthesis of ureas in the presence of phenylsilane

fixation of CO_2 with amines to give urea derivatives [25]. Remarkably, in this system formation of urea from *o*-phenylenediamine (**13**) and CO_2 occurred at atmospheric pressure and 413 K. In the presence of such tungstates as the catalysts, efficient synthesis of cyclic ureas (e.g., **14**) from aryl diamines were achieved (Eq. 3). The bifunctionality of for simultaneous activation CO_2 and the substrate was proved by the ^{1}H and ^{13}C NMR spectra. Notably, in the presence of transition metal complexes such $RuCl_2(dppe)_2$ [dppe = 1,2-bis(diphenylphosphino)-ethane], cyclic ureas could also be formed with 20% yield from the reaction of *o*-phenylenediamine with CO_2 [26].

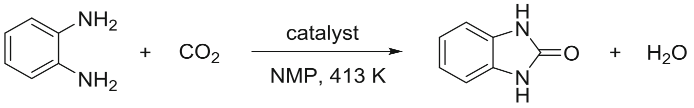

13 **14** (3)

As another benchmark reaction for CO_2 use in synthesis of heterocyclic structures, the reaction of 2-amino-benzonitriles (**15**) with CO_2 can be promoted by tungstate salts such as $TBA_2[WO_4]$ (**12**) [27]. Various of quinazoline-2,4(1*H*,3*H*)-diones (**16**) were obtained in high yields (69–96%) under mild conditions and the turnover number reached up to 938. NMR studies showed that carbamic acid **17** was formed as the key intermediate through the simultaneous activation of both 2-aminobenzonitirile and CO_2 by **12** (Eq. 4).

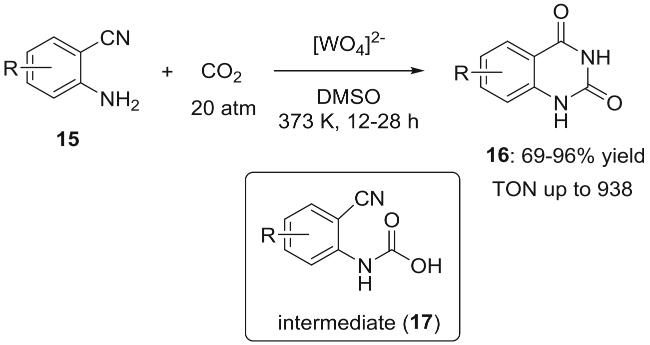

(4)

Later, The effects of POMs and bases on reactions by tungstate $TBA_2[WO_4]$ were further studied and a broad substrate scope was achieved and cyclic urea derivatives as long as 1,3-disubstituted urea derivatives were obtained with medium to good yields, respectively [28].

Very recently, Chao and co-workers described the use of metal salts of oxalates as catalysts for the synthesis of *N*,*N*′-dialkylureas from CO_2 and amines [29]. Among the metal salts of oxalates (metal = Na, Ni, Mn, Y, Ce, and Zr) and other yttrium salts of borate, carbonate and citrate, and yttrium oxide, $Y_2(C_2O_4)_3$ was found to provide the best catalytic performance. Under the optimized conditions, aliphatic primary amines were converted to the corresponding *N*,*N*′-dialkylureas with moderate to high conversions of amines (71–86%) and isolated yields of ureas (57–75%) and very high selectivity (95–97%). However, secondary and aromatic amines proved incompatible with the carbonylation reaction. Notably, besides the targeted product, by-products *N*,*N*′-dialkyloxamide (**18**), *N*-alkyl isocyanate (**19**), and *N*,*N*′-dialkyl carbodiimide (**20**) were also identified in the product mixture (Scheme 10).

Sun and co-workers reported the use of [urea–Zn]I_2 eutectic-based ionic liquid for conversion of carbon dioxide to cyclic carbonates. In the catalyst [urea-Zn]I_2, urea molecule was coordinated to Zn^{2+} ion via forming Zn–O–C=N and/or Zn–O=C–N. The NH_2 groups of urea played a role in activating CO_2 through the

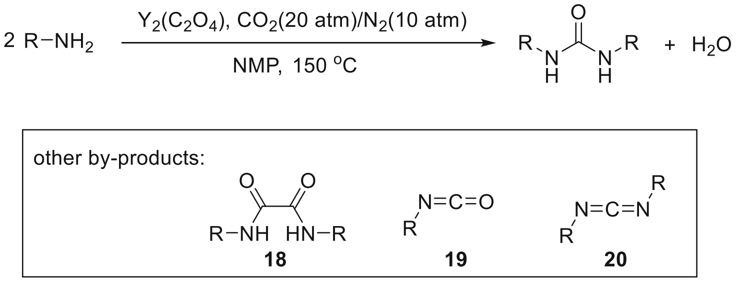

Scheme 10 Yb-catalyzed synthesis of ureas

generation of carbamate salt and could participate in forming hydrogen bond with epoxides [30].

Heterogeneous catalysis for the synthesis of diphenylurea (DPU) from aniline and CO_2 was investigated in the presence of bimetallic Cu–Fe/ZrO_2 materials [31]. Cu–Fe/ZrO_2 was prepared by wetness impregnation of cupric nitrate and ferric nitrate on the ZrO_2 support followed by calcination at 450 °C for 6 h and reduction at 300 °C for 3 h. In this reaction system, metallic copper and cupric oxide are the main active species, while metallic iron and ferric oxide are the promoters. Meanwhile, the Lewis acid sites and Lewis base sites on the surface of ZrO_2 play important roles for activity. The best material has the metal loading based on metal oxide as 10 wt% with molar ratio of Cu to Fe as 3:1. With a weight ratio of catalyst to aniline as 1:10, at 160 °C and 1 MPa of CO_2, yield of DPU lower than 6% with high selectivity (>95%) were obtained after 7 h.

Garcia et al. [32] and Tomishige et al. [33] showed independently that cerium oxide could act as effective and reusable heterogeneous catalyst for direct synthesis of cyclic ureas from CO_2 and diamines. From kinetic and FTIR studies, a mechanism with four sequential stages was proposed as follows: (1) the absorbed amine reacted with CO_2 on CeO_2 to afford carbamic acid and carbamates species, (2) decomposition of the carbamic acid to an amine group and CO_2, (3) nucleophilic addition of a free amino group to the carbamate, which is the rate-determining step, (4) desorption of cyclic urea product and regeneration of CeO_2 catalyst (Scheme 11). Note that severe deactivation occurred upon reuse and attempts to reactivate used catalysts were not completely successful. On the used CeO_2 catalyst,

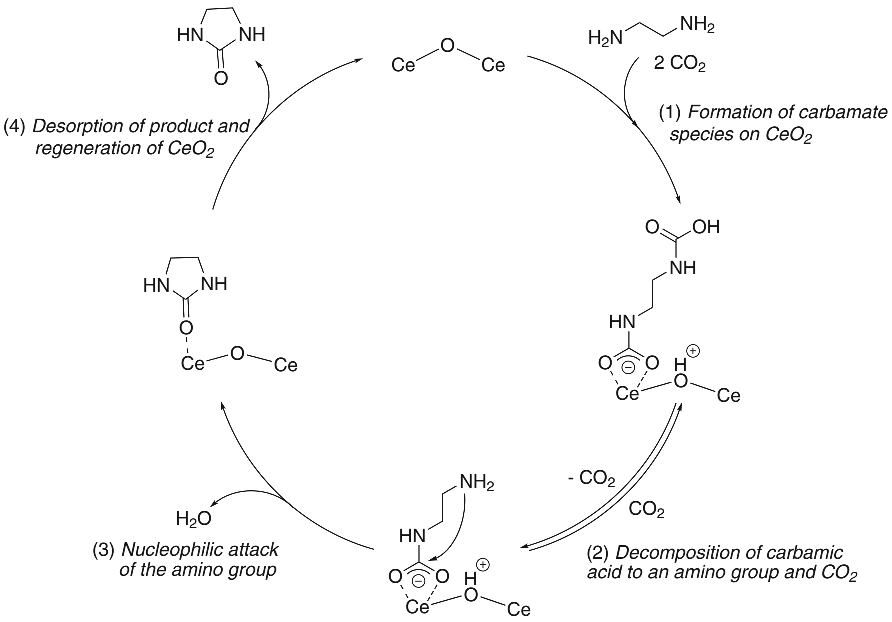

Scheme 11 CeO_2-catalyzed synthesis of ureas from CO_2 and diamines

IR spectroscopic analysis showed the presence of inorganic carbonates, which might block the active sites on the surface.

Although various catalytic systems to form ureas from amine and CO_2 have been developed, further explorations of heterogeneous catalytic strategies would be valuable and attractive in industry. Several heterogeneous catalytic methodologies have been explored. In 2010, KOH/PEG_{1000} was reported by He and co-workers to be capable of promoting carboxylation of amines and CO_2 [34]. PEG has been regarded as CO_2-philic material owing to the existence of "CO_2-expansion effect" could lead to the physical property changes of reaction mixture and it can increase the basicity of KOH through complexation with K^+. On the other hand, PEG can act as the physical dehydrating reagent because of its hydrophilic property. Using catalytic amount of KOH/PEG_{1000}, aliphatic primary amines were transformed into ureas fluently. Nevertheless, aromatic amine is not proper substrate. The catalyst bears excellent recycling ability, maintained its' catalytic activity even after five times.

Later on, the same group demonstrated a similar catalytic system using PEG/superbase binary system for CO_2 uptake, captured CO_2 was stored in the form of amidinium carbonate salt (Scheme 12). Reacting the liquid amidinium carbonate salt with amines including primary amines, even secondary aliphatic amines and diamines at 110 °C could lead to ureas in superior yields [35]. The formation and application of this novel amidinium carbonate salt provided an efficient and elegant pathway to use CO_2 as carbon block in chemical synthesis.

Dehydrant-free strategies represent a greener route to ureas when using amine and CO_2 as substrate, which leads to less by-products comparing with the dehydrating reagent-based systems. DBU was reported to promote the reaction of aniline under high pressure CO_2 atmosphere at 100 °C, giving diphenylurea in 46% yield. Further application of this reaction system to aliphatic amines resulted in mixture of urea and unidentified products [36]. Unlike the dehydrant-based strategy, high temperature and pressure are postulated as key factors to realize the dehydration step.

In 2002, Jessop and co-workers reported the synthesis of tetra-alkylureas from the reaction of dialkylamines with CO_2 at 60 °C without participation of transition metals [37]. In the presence of CCl_4, the reaction was weakly promoted by DMAN (1,8-dimethylaminonaphthalene) or PPh_3. A two-step procedure is beneficial comparing with the one-step reaction. For the reaction of dibutylamine (2 mmol)

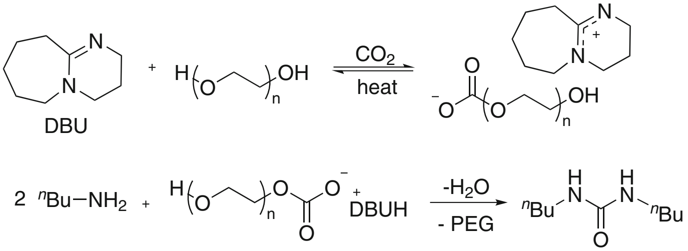

Scheme 12 Organic base/PEG-promoted synthesis of ureas

and CO_2 (1 bar), quantitative yield of the corresponding urea was obtained through this two-step process, and 1 mmol of DMAN, 1 mL of CCl_4 , and 10 mL of THF were used. In this system, dialkylammonium dialkylcarbamate was produced in situ followed by the reaction with CCl_4 and the free dialkylamine to give the final urea product (Eq. 5).

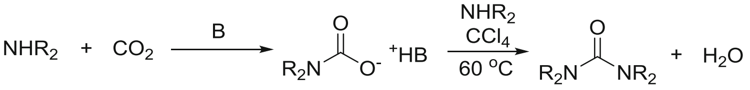

(5)

Interestingly, compared with the use of cesium bases, the simple use of K_3PO_4 as the catalyst in the reaction of CO_2 with aliphatic primary amines leads to 1,3-disubstituted ureas with higher efficiency [38]. In the presence of 1 mol% of K_3PO_4, at 5 MPa of CO_2 the best results (up to 87% yield) for the reaction of *n*-butylamine was achieved at 170 °C in NMP for 4 h. No reactivity was observed for the reaction of aniline, possibly due to its low nucleophilicity. In the presence of K_3PO_4, the first step is the formation of the carbamate salt. (Eq. 6).

$$RNH_2 + CO_2 + B \rightleftharpoons BH^+ RNHCO_2^- \qquad (6)$$

After the reaction, K_3PO_4 was completely transformed into KH_2PO_4 and $KHCO_3$. The reactivity partially attributed to the synergy effect exerted by the co-presence of $KHCO_3$ and KH_2PO_4. The polar solvent was believed to be able to stabilize the intermediate ionic species and to promote the dehydration process.

It was reported that the reactions of aniline with CO_2 or CS_2 could be promoted by $AlCl_3$ [39]. The resulting *N*,*N*′-diphenylurea and *N*,*N*′-diphenyl thiourea were obtained with high yield and selectivity, respectively. In the reaction of aniline with CO_2, phenyl isocyanate was detected as the intermediate by GC/MS. In the case of catalysis by calcined Mg–Al layered double hydroxide, however, the catalyst can be recycled several times with only slight loss of activity. Using *N*-methyl-2-pyrrolidone as solvent, a series of organic amines were converted into 1,3-disubstituted urea smoothly [40].

Ionic liquids (ILs) are generally composed of organic cations and inorganic/organic anions. The combination of different ion components could lead to tailored functions for wide applications. It is known that CO_2 exihibits superior solubility in the ionic liquid [41]. The combination of bases and ionic liquid such as CsOH/[BMIm]Cl was found useful in the synthesis of ureas from CO_2 and amines (Scheme 13) [42]. Under the optimized condition (170 °C, 60 atm CO_2), a broad

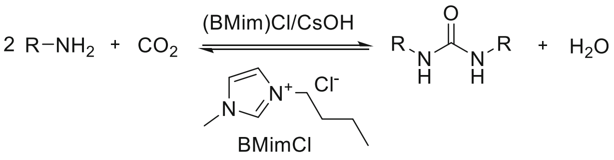

Scheme 13 CsOH/ionic liquid promoted synthesis of ureas

substrate scope (both aliphatic and aromatic amines) and convenient purification makes the method highly attractive and practical. As to less active anilines, ureas were obtained in lower yields although longer reaction time needed. Electron-deficient *m*-nitroaniline failed to produce ureas probably owing to its inertness. It is worth mentioning the catalytic CsOH/BMImCl system could be reused after removing water even after three times without obvious loss of catalytic activity.

Another interersting synthetic pathway to disubstituted ureas from amines and CO_2 has been developed by Han et al. involving use of catalytic amount basic functionalized IL 1-*n*-butyl-3-methyl imidazolium hydroxide ([BMIm]OH) under solvent-free condition [43]. Under the optimal conditions with catalytic amounts (15 mol%) of [BMIm]OH at 170 °C, urea yield for reaction of aliphatic primary amines could reach 55% while branched amines led to lower yields. And no products were obtained when aniline and secondary amines employed. Putative pathway includes the following steps (Scheme 14): (a) combination of nucleophilic amine with CO_2 gives carbamate salt easily and this process could explain the failure that uses less basic aniline as reactant; (b) ionic change between carbamate salt and [BMIm]OH; (c) carbamate anions are activated by $BMIm^+$ through intermolecular interaction, combination of RNH_3^+ and OH^- gives water and free amine; (d) free amine interacts with carbamate leads to urea and the regeneration of catalyst to complete the cycle.

In 2010, Shi and Deng et al. studied the use of $Co(acac)_3$/BMMImCl (BMMImCl = 1-butyl-2,3-dimethylimidazolium chloride) for synthesis of N,N′-disubstituted ureas from amines and CO_2 in the absence of bases [44]. In this system, the use of bases or chemical dehydrants were avoided. Many different metal sources such as Zn-, Cu-, Fe-, and Ni-based salts, showed some reactivity. Among these results, $Co(acac)_3$ showed a little better activity. For the reaction of different substrates (20 mmol scale), 0.2 mmol of $Co(acac)_3$ and 20 mmol of BMMImCl were used at 160 °C for 10 h' reaction, 45–81% isolated yields for *N*,*N*′-dialkylureas and 6–23% isolated yields for *N*,*N*'-diarylureas were obtained. The catalyst system could be recycled without significant loss in activity.

Later, Kim et al. reported a detailed mechanism investigation (including experimental, as well as calculation studies) into the mechanism of urea synthesis from amine and CO_2 assisted by ILs [45]. Reaction parameters in the carboxylation of *n*-butylamine (BA) with CO_2 have been investigated in detail. Notably, the interaction of cation and anion plays crucial roles in the reaction.

Scheme 14 Ionic liquid-promoted synthesis of ureas

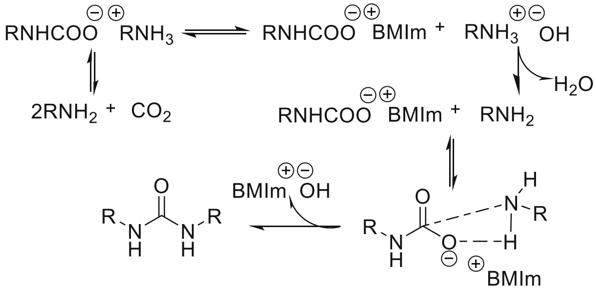

Deprotonation of imidazole by 1,1,3,3-tetramethylguanidine in ethanol leads to the protic ionic liquid 1,1,3,3-tetramethylguanidinium imidazolide [HTMG][Im] (**21**), which promotes efficient synthesis of quinazolines from 2-aminobenzonitriles and CO_2 at ambient conditions (Scheme 15) [46]. Under solvent-free conditions, this method is suitable for various 2-aminobenzonitriles bearing electron-withdrawing or electron-donating substituents to afford the corresponding quinazoline-2,4(1*H*,3*H*)-diones in moderate to excellent yields (up to 94%). Again, this IL is also recyclable for five cycles with almost consistent activity.

Ionic liquid DBU ([DBUH][OAc], **22**) was found active in catalyzing the carbonylation of *o*-phenylenediamines with CO_2 to 2-benzimidazolones under solvent-free conditions [47]. A variety of diamines were transformed to the desired product in 69–96% yield. 2-Aminothiophenol was also tested and benzothiazolone was prepared in 63% yield (Eq. 7). It was proposed that [DBUH][OAc] served as a bifunctional catalyst for reactions with the iminium cation activating CO_2 and the acetate anion activating *o*-phenylenediamines. Control experiments implied that the reaction proceeded via isocyanate intermediates. Interestingly, the catalyst [DBUH][OAc] can be recycled five times without any decrease of reactivity. Similarly, another protic IL [DBU][TFE], which was obtained by the neutralization of DBU with trifluoroethanol (TFE), was successfully applied to transformation of CO_2 and 2-aminobenzonitriles to quinazoline-2,4(1*H*,3*H*)-dione under atmospheric conditions [48].

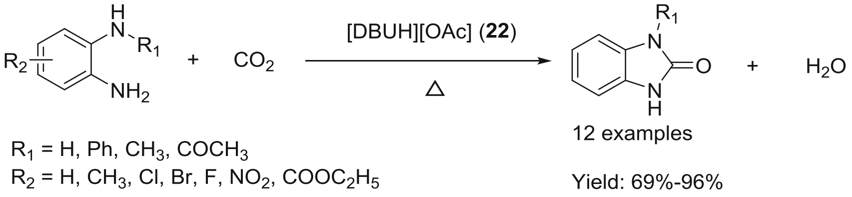

(7)

Except for protic IL catalysis in CO_2 transformation, aprotic ILs based on azole anions were also capable of activating CO_2. Azole-anion-based aprotic ionic liquid $[Bu_4P][2\text{-MIm}]$ (**23**) was synthesized by the deprotonation of weak proton donors (e.g., 2-methylimidazole) with tetrabutylphosphonium hydroxide, $[Bu_4P][OH]$ [49].

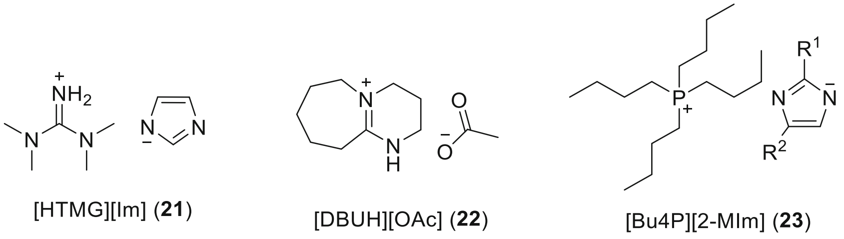

Scheme 15 Ionic liquids used in urea synthesis from amines and CO_2

This adduct [Bu_4P][2-MIm] could activate atmospheric CO_2 through the formation of carbamates as key intermediates (Eq. 8).

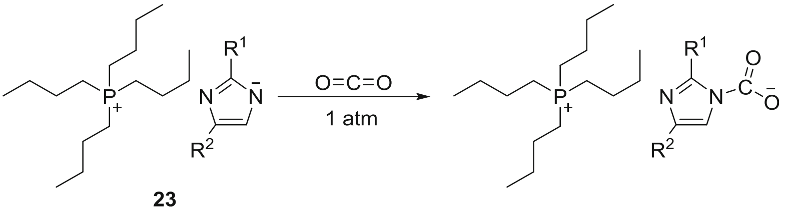

23

(8)

In general, with 50 mol % loading of [Bu_4P][2-MIm] (**23**), catalytic carbonylation of *ortho*-phenylenediamines with CO_2 to produce benzimidazolones in moderate-to-good yields at atmospheric pressure (Scheme 16). Remarkably, the activity in this reaction catalyzed by aprotic IL is comparable to the catalysis by $[TBA]_2WO_4$.

The so-called reversible ionic liquid (ReIL) can be converted back into free neutral compounds by bubbling N_2 or argon through them and/or applying heat. The pioneer work by the Jessop group showed that their smart switchability to influence the chemical reactions and processes providing facile separation techniques [50]. After bubbling CO_2 at atmospheric pressure through the mixture of DBU and ethanol (0.5 mol of each) for 2 h, the mixture was cooled to 0 °C to get the desired reversible ionic liquid **24** as solid. **24** was used for efficient transformation of CO_2 and 2-aminobenzonitriles into quinazoline derivatives at atmospheric pressure and 40 °C without the use of solvent. The catalyst could be reused at least six times without considerable loss in reactivity [51]. Notably, the reaction could also be catalyzed by simple DBU, albeit with lower reactivity (ca. 40% yield). For the substrate scope, seven examples were shown and the corresponding products were obtained with high yields (75–96%) for 15–48 h (Scheme 17).

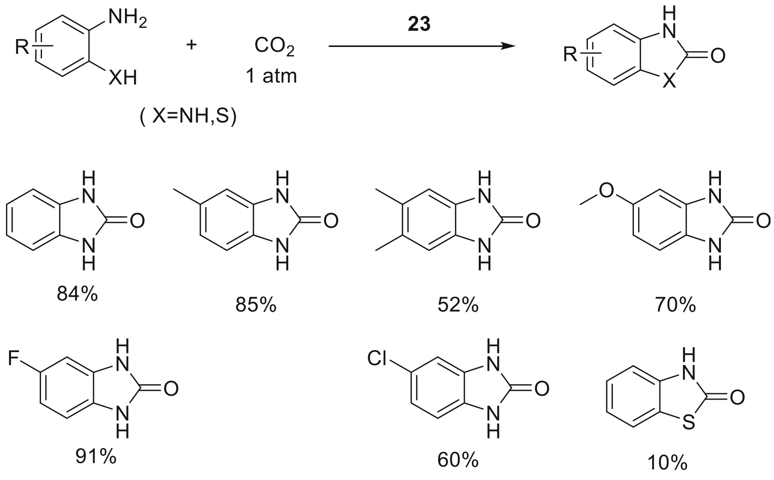

Scheme 16 [Bu_4P][2-MIm] promoted urea synthesis

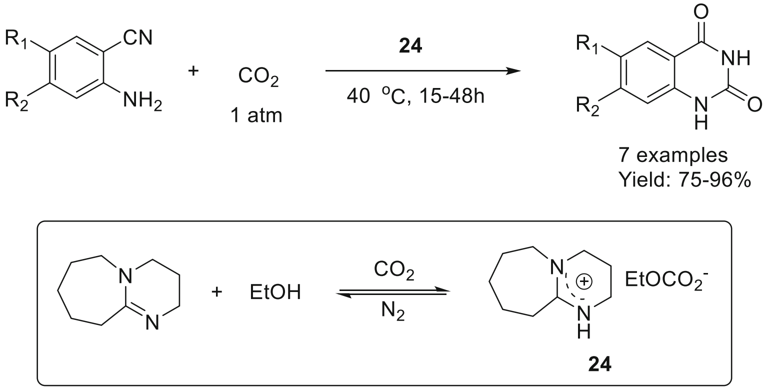

Scheme 17 Reversible ionic liquid promoted transformation of CO_2

Heterogenisation of ionic liquids using polystyrene was shown as a successful strategy for the synthesis of symmetric disubstituted ureas from CO_2 and amines [52]. A three-step procedure was used to prepare the active supported ionic liquid catalyst Poly-2. In detail, the reaction of Merrifield's resin (1% crosslinked, 3.5–4.5 mmol Cl/g) with bis(2-chloroethyl)amine in acetonitrile under heating conditions was followed by treatment with 1-methylimidazole to give a solid intermediate. Anion exchange by mixing the solid intermediate and sodium bicarbonate in anhydrous methanol gave the final basic ionic liquid product (Scheme 18). Effect of different anionic species, such as Cl^-, MsO^-, TsO^-, AcO^-, OH^-, etc. on the activity of dicyclohexylurea synthesis was investigated and the use of basic bicarbonate ion gave the best results (78% yield).

Using Poly-2 as the catalyst, a variety of aliphatic mono- and diamines were transformed to the corresponding diureas in good yields (59–83% yields) at 170 °C with 90 atm CO_2 for 4 h. As weaker nucleophiles, aromatic amines (e.g. aniline) are not suitable substrates showing no reactivity. It was proposed that the catalytic behavior of Poly-2 is enhanced by interactions of bicarbonate anion to both substrates and CO_2. In addition, the flexibility of the aliphatic linker moiety of the cationic part was also suggested to be beneficial. Notably, the catalyst can be recyclable seven times.

It is noteworthy that transition metal imido complexes could react with CO_2 giving ureas or ureate complexes. In 2012, Anderson et al. reported the synthesis of ureas from titanium imido complexes using CO_2 at ambient temperature and

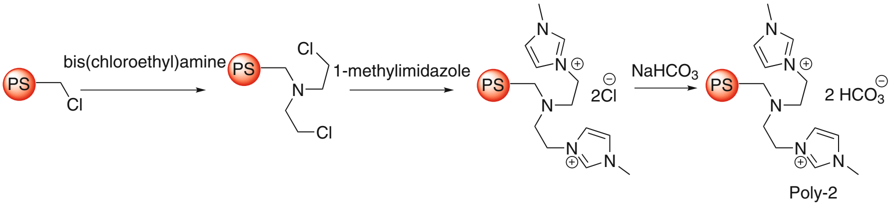

Scheme 18 Preparation of polystyrene supported Poly-2 (PS = polystyrene)

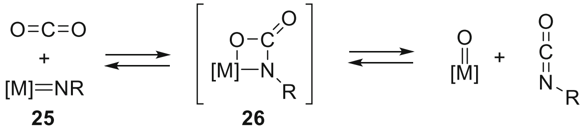

Scheme 19 The formation of a carbamate metallocycle by [2 + 2] reactions

pressure [53]. In this work, the coordinatively unsaturated 12-electron complex dichloro *t*butylimido bispyridine titanium (**25**) reacted with CO$_2$ to produce *N*,*N*′-di-*t*butyl urea. The reactivity of **25** with CO$_2$ in the presence of acid or amine was investigated systematically. It was proposed that the metallocarbamate **26** will be formed from the insertion of M=N bond into C=O bond of CO$_2$ (Scheme 19).

It was believed that the formation of the thermodynamically stable titanium oxo complex is the driving force for the forward reaction of **28** to form isocyanate **29** (Scheme 20). The heterocumulene metathesis reactions of **29** with the other molecule of **27** either form metallocycles **31** via [2 + 2] cycloaddition across RN=C of **29** or form **32** via [2 + 2] cycloaddition across C=O of **29**. Hydrolysis workup of **31** or **32** leads to the formation of symmetrical urea **34**, which could be also generated through carbodiimide **33** from metallocycle **32**.

A terminal imide complex [(O$_3$)–Nb=NMe(Py)$_2$] (**35**) was synthesized from a nitride complex, which was an intermediate in the transformation of dinitrogen to ammonia. Similar with the reactivity of titanium imido complex **27**, imide monomer **35** reacted with CO$_2$ to give metallocycles ureate complex [(O$_3$)–Nb^1(py)] (**36**) via isocyanate intermediate (Scheme 21) [54].

Even though a variety of catalytic systems have been explored, extra base or other additives are required for the successful transformations. In the absence of catalysts, diamines react smoothly with CO$_2$ to give the corresponding cyclic ureas [55]. A recent method to produce ureas has been described by Zhao et al. employing

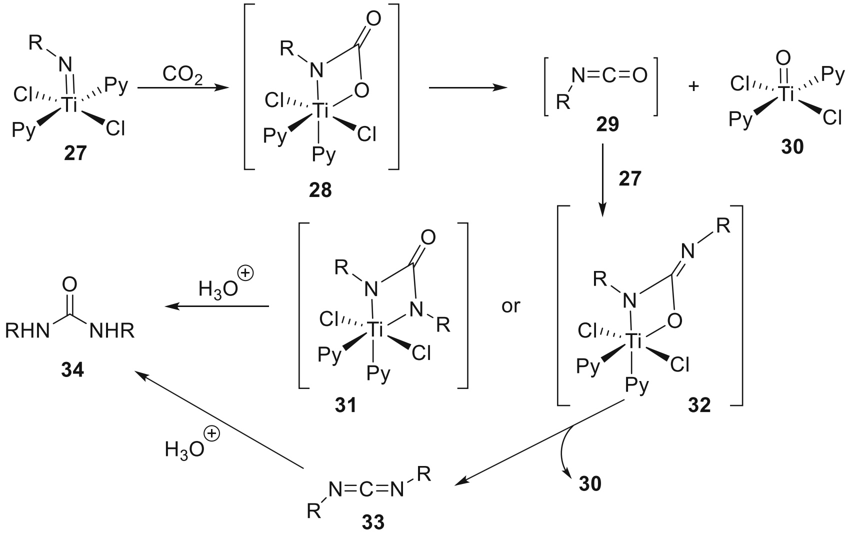

Scheme 20 Possible mechanisms for the conversion of CO$_2$ with Ti-imido complexes to ureas

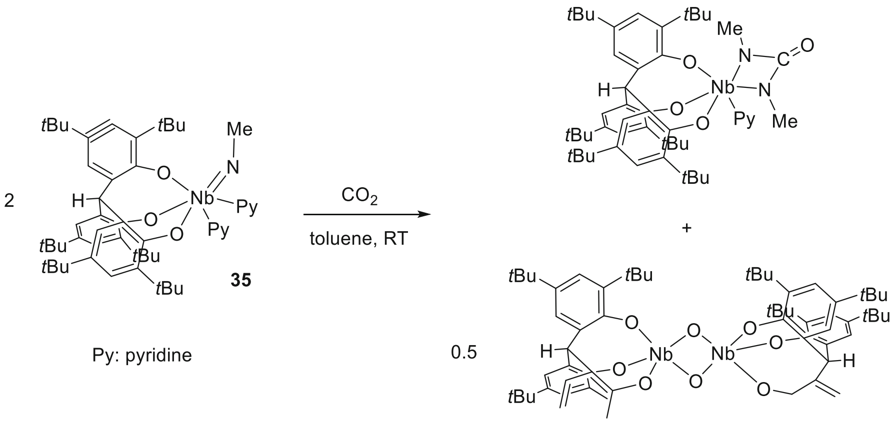

Scheme 21 Synthesis of metallocycles ureate complexes from Nb-imido complexes and CO_2

primary amines and CO_2 in the absence of additives and solvent [56]. Screening about the temperature and pressure revealed that the existence of a balance point of both the factors. Temperature higher than 180 °C decreased the yield gradually could be ascribed to the reversibility of reaction. Addition of extra additives into the system could not improve the yield considerably. Under the optimal reaction condition, aliphatic primary amines react smoothly with CO_2 to give ureas of different type. However, again, secondary and aromatic amines have been proven to be unsuitable substrates to give symmetrical ureas. It is worth mentioning that reacting a primary amine with another secondary one could yield the unsymmetrical urea using this method. By reacting a cyclohexylisocyanate with amines, the formation of relevant ureas proceeds drastically indicated the existence of isocyanates in this reaction process (Scheme 22).

3 Catalytic Transformations of CO_2 Involving Urea Intermediates

In 2013, the Beller group described a general catalytic methylation of amines from CO_2, in which ureas were proposed as the intermediates resulting from dehydration of ammonium carbamates [57]. Notably, under catalytic conditions, relatively bulky aromatic diamine **38** gave 13% of *N*,*N*′-diphenylethyleneurea (**39**), apart from 76% of 1,3-diphenylimidazolidine (**40**) and 10% of the dimethylated product (**41**) (Eq. 9).

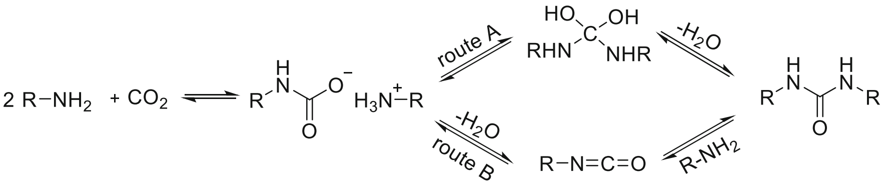

Scheme 22 Synthesis of ureas without the use of catalysts or solvent

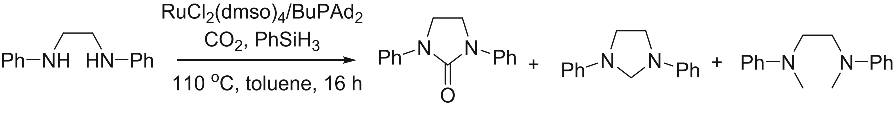

38 **39**(13%) **40** (76%) **41** (10%)

(9)

While an inadequate amount of $PhSiH_3$ was used, Liu et al. also detected the tetra-substituted urea intermediate by employing $B(C_6F_5)_3$ as an metal-free catalyst for the methylation of amines using CO_2 as a C1 building block in the presence of hydrosilanes [58]. In a recent work by Sun and co-workers, $B(C_6F_5)_3$ was used to promote the synthesis of benzimidazoles via cyclization of *o*-phenylenediamines with CO_2 in the presence of $PhSiH_3$ with 2-benzimidazolones as possible key reaction intermediates [59].

4 Related Synthetic Methods (e.g. Production of Carbamates)

In 1986, Inoue's group developed a novel catalyst aluminum porphyrin to activate and fix CO_2 in the presence of a secondary amine and epoxide to afford carbamates under mild reaction conditions [60]. When the reaction was performed at room temperature with a CO_2 balloon, the major product was amino alcohol instead of carbamates. Raising the temperature and the pressure of CO_2, the reaction chemoselectivity was improved obviously (Scheme 23). It is worth noting that the development of catalytic system was based on the organometallic research of aluminum porphyrin. And the reaction intermediates were characterized by NMR systematically.

In the same year, Sasaki and Dixneuf published the first example of one-step synthesis of vinyl carbamates from CO_2, diethylamine and terminal alkynes using $Ru_3(CO)_{12}$ as catalyst [61]. Unfortunately, the yield of the reaction was relatively low (up to 36%) and the chemo- and regioselectivities were poor. Dixneuf et al. improved aforementioned method by using mononuclear ruthenium(II) as catalytic precursors. And the yield of reaction was successfully increased to 67% [62]. A

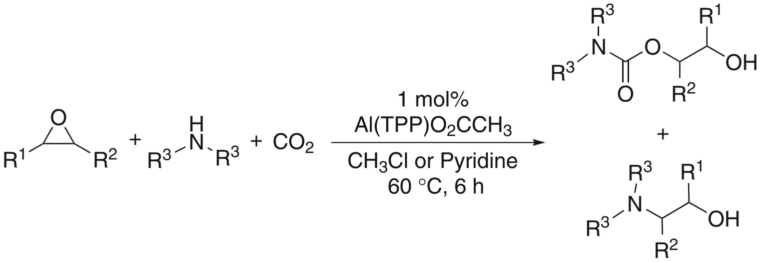

Scheme 23 Aluminum porphyrin catalyzed carbamates synthesis

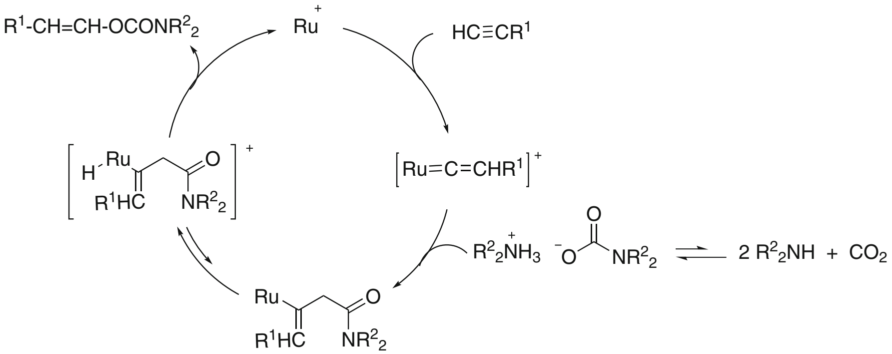

Scheme 24 Proposed mechanism for Ru-catalyzed reaction of ammonium carbamates to terminal alkynes

variety of mononuclear ruthenium(II) precursors can be employed under this reaction condition. They declared that the ammonium carbamate was formed in situ first and suggested that the addition of carbamate to the alkyne may access through a ruthenium-vinylidene intermediate (Scheme 24). In 1987, Sasaki and Dixneuf have discovered that $RuCl_3{\cdot}3H_2O$ have similar reactivity for this reaction [63].

In 1987, the same group developed a method to synthesize oxoalkyl *N*,*N*-diethylcarbamates in one step with CO_2, secondary amine, and acetylenic alcohols catalyzed by $Ru_3(CO)_{12}$ in moderate yield [64]. They also discovered that oxazolidones can be exclusively obtained by exocycloaddition under similar reaction conditions when primary amine *n*-propylamine was used (Scheme 25).

As a type of important intermediates and chemical products, carbamates were often used in organic synthesis. As early as in 1981, Laas et al. developed a methodology to synthesize 3*H*-indole in three steps [65]. First, the cyclic carbonate was formed in the reaction of CO_2 and acetylenic alcohol in the present of triethylamine and CuI. Then the oxazolidone was obtained efficiently by the nucleophilic addition of aniline followed by dehydration afterwards in second step. The 3*H*-indole was ultimately obtained by decarboxylation (Scheme 26).

Under solvent-free conditions, the combination of Ag_2WO_4/Ph_3P was used to promote the three-component reaction of amines, CO_2 and propargyl alcohols [66]. Various of α-alkylidene cyclic carbamates bearing exocyclic alkenes and carbamates were obtained in moderate to high yields in the one-pot reaction of primary or secondary amines, 5 bar of CO_2 with propargyl alcohols at 50 °C for 12 h. It was proposed that the reaction went through a tandem aminolysis of α-alkylidene cyclic carbonates/intramolecular cyclization/tautomerization sequence and the dual activation capacity of Ag_2WO_4 relies on the role of both the silver cation and the tungstate anion.

As we know that ureas can be synthesized via the carbonylation of amines with CO_2, carbamates can be formed similarly by carbonyaltion of amines and alcohols with CO_2. In 2007, De Vos et al. reported the methodology of synthesis of urea compounds from CO_2 employing Cs(I) base catalysts [67]. Both symmetrical and unsymmetrical ureas were synthesized in moderate to superior yields. Screening

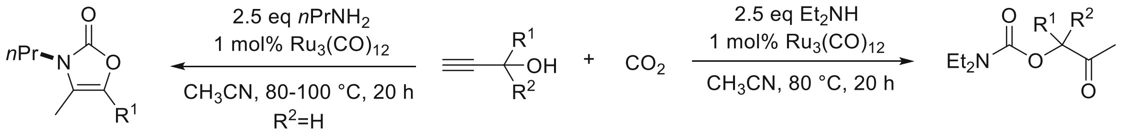

Scheme 25 Reaction of CO_2, amine and acetylenic alcohol

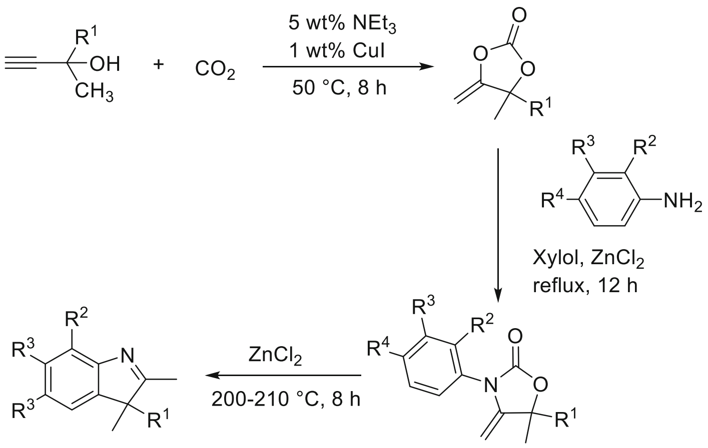

Scheme 26 The synthetic procedure of 3*H*-indole from acetylenic alcohols via oxazolidones

inorganic bases with different anions and cations indicated that suitable combinations can lead to good reactivity. Suitable temperature is indispensable for the high conversion within a set of reaction time period. Operating reaction at higher temperature resulted in the decreased yields, which could probably resulted from reversibility of the reaction as mentioned above. NMP is rather important for the successful transformation as it is capable of absorbing CO_2 and stabilizing the probable ionic intermediate. Anilines and secondary amines failed to give symmetrical ureas under the same reaction. Comparing with primary amines, lower basicity of anilines and steric hindrance could explain this observation. When using a primary amine and a secondary amine as substrates, unsymmetrical ureas were obtained in satisfying yields (67–95%).

De Vos and co-workers developed the method further to access carbamates with CO_2, amines, and alcohols [68]. They discovered that the selectivity to carbamate increases from K_2CO_3 to Cs_2CO_3 in the series of alkali carbonates. A large amount of alcohols (usually over 10 times) was necessary to suppress the side product urea. Mechanistic investigations suggested that two main pathways, most probably parallel routes, may be involved in carbamate formation, either via ureas or via isocyanates (Scheme 27). Sakakura's group also developed Sn [69] and Ni [70] catalytic systems on direct synthesis of carbamates from CO_2, amines, and alcohols, respectively.

In 2010, Muñoz et al. reported the synthesis of cyclic carbamates and cyclic ureas using CO_2 as carbonylating agent via an activated carbamate generated by treating carbamate anion (generated in situ from amines and CO_2) with electrophiles such as DPPA (diphenylphosphoryl azide), DPPCl (diphenyl chlorophosphate), $SOCl_2$, etc.

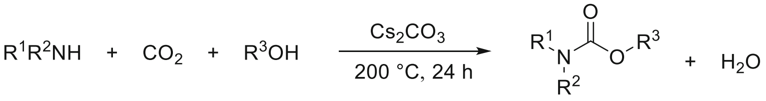

Scheme 27 Cs_2CO_3 catalyzed synthesis carbamates from amines, alcohols and CO_2

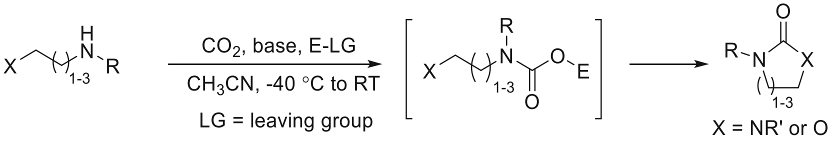

Scheme 28 Synthesis of cyclic carbamates and cyclic ureas via activated carbamates

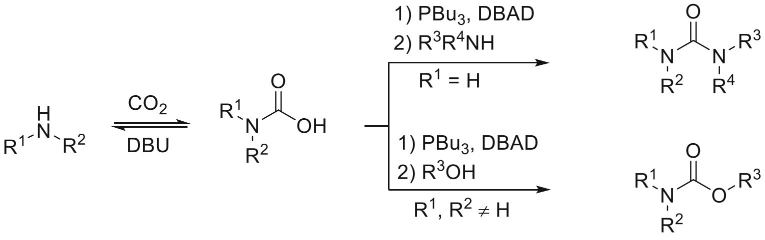

Scheme 29 Synthesize ureas and carbamates with Mitsunobu reagents

Then the intramolecular trapping of the activated carbamate processed either by a hydroxyl group or an amino group to form of cyclic carbamates or cyclic ureas in good to excellent yields (Scheme 28) [71]. The authors discovered that the electrophiles had the effects on carbamate anion generation and product configuration.

Almost at the same time, Dinsmore et al. used the similar strategy to synthesize ureas and carbamates with Mitsunobu reagents (Scheme 29) [72]. For the primary amine carbamic acid, unlike the aforementioned intramolecular reaction of S_N2 mechanism, the author suggested that the reaction underwent isocyanates as the intermediate via dehydration of the carbamic acid by Mitsunobu reagent.

5 Conclusion

In recent decades, catalytic synthesis of ureas from CO_2 and amines have gained increasing interests. In fact, this topic is also closely related with the concept of chemical CO_2 fixation. Generally, in these systems no much energy is needed and the formation of the stable urea products makes this type of transformation thermodynamically favoured. There were many in situ-generated or defined catalyst systems developed for this transformation to make the final carbonyl group contained urea products. Notably, it is quite interesting to see that many different types of catalysts are effective for activation of CO_2, amine, or carbamate intermediates. Notably, it is clear that efficient removal of water (dehydration process) is the key factor for the synthesis of ureas from CO_2/amine and often (over)stoichiometric amounts of dehydrants are required. Consequently, large volumes of wastes are generated. This is for sure not friendly to the requirement of sustainable chemical industries. Apart from dehydration efficiency, chemoselective catalytic systems are also highly desired, considering the often involved isocyanate intermediates. Besides, the substrate scope is sometimes quite limited to either aliphatic or aromatic amines.

Hence, from the viewpoint of cost-effectiveness and green chemistry the use of a cheap, stable and recyclable catalyst without stoichiometric excess of dehydrants in urea synthesis is very attractive. Obviously, this means chemists still need to look for new dehydration concepts and technologies for urea synthesis, especially based on new activation mode for CO_2, amines, or carbamates.

Acknowledgements We are grateful for the financial support from National Program for Thousand Young Talents of China, NSFC (Grant 21602228), and the Special Innovation Funding of LICP.

References

1. Forlani P, Paris I, Zardi V (1968) Ger. Patent 1962882
2. Fiorani G, Guo W, Kleij AW (2015) Green Chem 17:1375–1389
3. Yang Z, Liu Z (2016) Scientia Sinica Chimica 46(10):973–993
4. Alexander O, Grube T, Schiebahn S, Stolten D (2015) Energy Environ Sci 8:3283–3297
5. Tamura M, Honda M, Nakagawa Y, Tomishige K (2014) J Chem Technol Biotechnol 89:19–33
6. Yu B, He LN (2015) Chemsuschem 8:52–62
7. Hampe EM, Rudkevich DM (2003) Tetrahedron 59:9619–9625
8. Yamazaki N, Iguchi T, Higashi F (1976) Tetrahedron 31:3031–3039
9. Yamazaki N, Higashi F, Iguchi T (1974) Tetrahedron Lett 15:1191–1194
10. Ogura H, Takeda K, Tokue R, Kobayashi T (1978) Synthesis 1978:394–396
11. Cooper CF, Falcone SJ (1995) Synth Commun 25:2467–2474
12. Appel R (1975) Angew Chem Int Ed 14:801–811
13. Porwanski S, Menuel S, Marsura X, Marsura A (2004) Tetrahedron Lett 45:5027–5029
14. Chaturvedi D, Mishra N, Mishra V (2008) Mon Chem 139:267–270
15. Dheere AKH, Bongarzone S, Taddei C, Yan R, Gee AD (2015) Synlett 26:2257–2260
16. Nomura R, Yamamoto M, Matsuda H (1987) Ind Eng Chem Res 26:1056–1059
17. Rintjema J, Kleij AW (2016) Synthesis 48:3863–3878
18. Katritzky AR, Oliferenko A, Lomaka A, Karelson M (2002) BioorgMed Chem Lett 12:3454
19. Morimoto Y, Fujiwara Y, Taniguchi H, Hori Y, Nagano Y (1986) Tetrahedron Lett 27:1809–1812
20. Fournier J, Bruneau C, Dixneus PH, Lécolier S (1991) J Org Chem 56:4456–4458
21. Lucero GS, Marcos FA, García JJ (2015) Organometallics 34:763–769
22. Zhou Y, Chen G, Long Z, Wang J (2014) RSC Adv 4:42092–42113
23. Kamata Keigo (2015) Bull Chem Soc Jpn 88:1017–1028
24. Wang MY, Ma R, He LN (2016) Sci China Chem 59:507–516
25. Kimura T, Kamata K, Mizuno N (2012) Angew Chem Int Ed 51:6700–6703
26. Yu B, Zhang H, Zhao Y, Chen S, Xu J, Huang C, Liu Z (2013) Green Chem 15:95–99
27. Kimura T, Sunaba H, Kamata K, Mizuno N (2012) Inorg Chem 51:13001–13008
28. Kamata K, Kimura T, Sunaba H, Mizuno N (2014) Catal Today 226:160–166
29. Sun DL, Ye JH, Fang YX, Chao ZS (2016) Ind Eng Chem Res 55:64–70
30. Liu M, Li X, Lin X, Liang L, Gao X, Sun J (2016) J Mol Catal A Chem 412:20–26
31. An H, Zhang L, Zhao X, Wang Y (2014) Chem Eng J 225:266–270
32. Primo A, Aguado E, García H (2013) ChemCatChem 5:1020–1023
33. Tamura M, Noro K, Honda M, Nakagawa Y, Tomishige K (2013) Green Chem 15:1567–1577
34. Kong DL, He LN, Wang JQ (2010) Synlett 2010:1276–1280
35. Yang ZZ, He LN, Zhao YN, Li B, Yu B (2011) Energy Environ Sci 4:3971–3975
36. Munshi P, Heldebrant DJ, McKoon EP, Kelly PA, Tai CC, Jessop PG (2003) Tetrahedron Lett 44:2725–2727
37. Tai CC, Huck MJ, McKoon EP, Woo T, Jessop PG (2002) J Org Chem 67:9070–9072
38. Choi YS, Kim H, Shin SH, Cheong M, Kim YJ, Jang HG, Kim HS, Lee JS (2014) Appl Catal B Environ 144:317–324
39. Xu H, Yuan X (2013) Key Eng Mater 575–576:531–534

40. Zhang R, Hua L, Guo L, Song B, Chen J, Hou Z (2013) Chin J Chem 31:381–387
41. Dupont J, Souza RF, Suarez PA (2002) Chem Rev 102:3667–3692
42. Shi F, Deng Y, SiMa T, Peng J, Gu Y, Qiao B (2003) Angew Chem Int Ed 42:3257–3260
43. Jiang T, Ma X, Zhou Y, Liang S, Zhang J, Han B (2008) Green Chem 10:465–469
44. Li J, Guo X, Wang L, Ma X, Zhang Q, Shi F, Deng Y (2010) Sci China Chem 53:1534–1539
45. Shim YN, Lee JK, Im JK, Mukherjee DK, Nguyen DQ, Cheong M, Kim HS (2011) Phys Chem Chem Phys 13:6197–6204
46. Lang XD, Yu YC, Li ZM, He LN (2016) J CO_2 Util 15:115–122
47. Yu B, Zhang H, Zhao Y, Chen S, Xu J, Hao L, Liu Z (2013) ACS Catal 3:2076–2082
48. Zhao YF, Yu B, Yang ZZ, Zhang HY, Hao LD, Gao X, Liu ZM (2014) Angew Chem Int Ed 53:5922–5925
49. Zhao Y, Wu Y, Yuan G, Hao L, Gao X, Yang Z, Yu B, Zhang H, Liu Z (2016) Chem Asian J 11:2735–2740
50. Jessop PG, Heldebrant DJ, Li XW, Eckert CA, Liotta CL (2005) Nature 436:1102
51. Zheng H, Cao X, Du K, Xu J, Zhang P (2014) Green Chem 16:3142–3148
52. Nguyen DS, Cho JK, Shin SH, Mishra DK, Kim YJ (2016) ACS Sustain Chem Eng 4:451–460
53. Anderson JC, Moreno RB (2012) Org Biomol Chem 10:1334–1338
54. Akagi F, Suzuki S, Ishida Y, Hatanaka T, Matsuo T, Kawaguchi H (2013) Eur J Inorg Chem 2013:3930–3937
55. Bhanage BM, Fujita S, Ikushima Y, Arai M (2003) Green Chem 5:340–342
56. Wu C, Cheng H, Liu R, Wang Q, Hao Y, Yu Y, Zhao F (2010) Green Chem 12:1811–1816
57. Li Y, Fang X, Junge K, Beller M (2013) Angew Chem Int Ed 52:9568–9571
58. Yang Z, Yu B, Zhang H, Zhao Y, Ji G, Ma Z, Gao X, Liu Z (2015) Green Chem 17:4189–4193
59. Zhang Z, Sun Q, Xia C, Sun W (2016) Org Lett 18:6316–6319
60. Fumitoshi K, Aida T, Inoue S (1986) J Am Chem Soc 108:391–395
61. Sasaki Y, Dixneuf PH (1986) J Chem Soc Chem Commun 790–791
62. Mahé R, Dixneuf PH, Lécolier S (1986) Tetrahedron Lett 27:6333–6336
63. Sasaki Y, Dixneuf PH (1987) J Org Chem 52:314–315
64. Sasaki Y, Dixneuf PH (1987) J Org Chem 52:4389–4391
65. Laas H, Nissen A, Nürrenbach A (1981) Synthesis 12:958–959
66. Song QW, Yu B, Li XD, Ma R, Diao ZF, Li RG, Li W, He LN (2014) Green Chem 16:1633–1638
67. Ion A, Parvulescu V, Jacobs P, De Vos D (2007) Green Chem 9:158–161
68. Ion A, Doorslaer CV, Parvulescu V, Jacobs P, De VD (2008) Green Chem 10:111–116
69. Abla M, Choi JC, Sakakura T (2001) Chem Commun 21:2238–2239
70. Abla M, Choi JC, Sakakura T (2004) Green Chem 6:524–525
71. Paz J, Pérez-Balado C, Iglesias B, Muñoz L (2010) J Org Chem 75:3037–3046
72. Peterson SL, Stucka SM, Dinsmore CJ (2010) Org Lett 12:1340–1343

Top Curr Chem (Z) (2017) 375:23
DOI 10.1007/s41061-017-0107-x

REVIEW

Homogeneous Reduction of Carbon Dioxide with Hydrogen

Kaiwu Dong[1,2] · **Rauf Razzaq**[2,3] · **Yuya Hu**[2] · **Kuiling Ding**[1]

Received: 3 November 2016 / Accepted: 12 January 2017 / Published online: 6 February 2017
© Springer International Publishing Switzerland 2017

Abstract Carbon dioxide (CO_2), a key greenhouse gas produced from both anthropogenic and natural sources, has been recently considered to be an important C1 building-block for the synthesis of many industrial fuels and chemicals. Catalytic hydrogenation of CO_2 using a homogeneous system is regarded as an efficient process for CO_2 valorization. This approach leads to the direct products including formic acid (HCOOH), carbon monoxide (CO), methanol (MeOH), and methane (CH_4). The hydrogenation of CO_2 to CO followed by alkene carbonylation provides value-added compounds, which also avoids the tedious separation and transportation of toxic CO. Moreover, the reduction of CO_2 with H_2 in the presence of amines is of significance to attain fine chemicals through catalytic formylation and methylation reactions. The synthesis of higher alcohols and dialkoxymethane from CO_2 and H_2 has been demonstrated recently, which opens access to new molecular structures using CO_2 as an important C1 source.

Keywords Homogeneous catalysis · Carbon dioxide · Hydrogen · Formic acid · Methanol · Methylation

---

Chapter 6 was originally published as Dong, K., Razzaq, R., Hu, Y. & Ding, K. Top Curr Chem (Z) (2017) 375: 23. DOI 10.1007/s41061-017-0107-x.

✉ Kuiling Ding
kding@mail.sioc.ac.cn

[1] State Key Laboratory of Organometallic Chemistry, Shanghai Institute of Organic Chemistry, Chinese Academy of Sciences, 345 Lingling Road, Shanghai 200032, People's Republic of China

[2] Leibniz-Institut für Katalyse e.V. an der Universität Rostock, Albert-Einstein Straße 29a, 18059 Rostock, Germany

[3] Department of Chemical Engineering, University of Engineering and Technology Lahore, City Campus, GT Road, Lahore, Pakistan

1 Introduction

Carbon dioxide (CO_2) constitutes an important by-product during fossil fuel use and has been accumulating significantly over the past few decades due to rapid industrialization and urban population growth. Consequently, two major CO_2-related problems confront the world today. Firstly, the concentration of atmospheric CO_2 has reached record levels and continues to increase, which is a huge concern in climate change, rising sea levels, and ocean acidification [1, 2]. Secondly, the increasing worldwide concern for gradually depleting fossil fuel reserves might lead to higher energy- and chemical-costs [3].

Nowadays, CO_2 is of great interest as a C1 feedstock due to its high availability, low toxicity, and recyclability. The sequestration and use of CO_2 to manufacture fuels and value-added chemicals with renewable energy will not only mitigate the net amount of CO_2, but also contribute substantially to the sustainable growth of the global economy. On the other hand, CO_2 is a highly oxidized and thermodynamically stable form of carbon, hence its chemical use usually requires high energy input through thermal-, photo-, and/or electro-reductive processes. Photo- and/or electrochemical reduction of CO_2 would most likely operate on a smaller scale, and extensive reports regarding this area can be found elsewhere [4, 5]. Thermal reduction of CO_2, according to the nature of the catalyst, can be divided into homogeneous and heterogeneous processes. The latter is outside the scope of this chapter, and many relevant works can be found in the literature [6, 7]. There are also several reviews [3, 8–12] concerning the fixation of CO_2 in homogeneous hydrogenation.

Among the reagents used for a homogeneous CO_2 reduction process, hydrogen (H_2) is probably the most promising reductant, which can also be produced from non-fossil resources, such as photochemical water splitting. Common products from direct CO_2 hydrogenation can be formic acid (HCOOH), carbon monoxide (CO), methanol (MeOH), and/or methane (CH_4), depending on the number of reductive electrons involved in the process. The thermodynamic quantities in such transformations, including the relevant changes in the Gibbs free energies and enthalpies, are shown in Eqs. (1)–(4) [8, 13].

$$CO_2(g) + H_2(g) \rightarrow HCOOH(I) \quad \Delta G^o = 32.8\,kJ\,mol^{-1};\ \Delta H^o = -31.5\,kJ\,mol^{-1} \tag{1}$$

$$CO_2(g) + H_2(g) \rightarrow CO(g) + H_2O(g) \quad \Delta G^o = 28.6\,kJ\,mol^{-1};\ \Delta H^o = 41.2\,kJ\,mol^{-1} \tag{2}$$

$$CO_2(g) + 3H_2(g) \rightarrow MeOH(I) + H_2O(I) \quad \Delta G^o = -9.5\,kJ\,mol^{-1};\ \Delta H^o = -131.2\,kJ\,mol^{-1} \tag{3}$$

$$CO_2(g) + 4H_2(g) \rightarrow CH_4(g) + 2H_2O(I) \quad \Delta G^o = -130.6\,kJ\,mol^{-1};\ \Delta H^o = -253.0\,kJ\,mol^{-1} \tag{4}$$

The reduction of CO_2 with H_2 in the presence of a nucleophile, such as amines, is of great significance to attain value-added chemicals. In this chapter, relevant

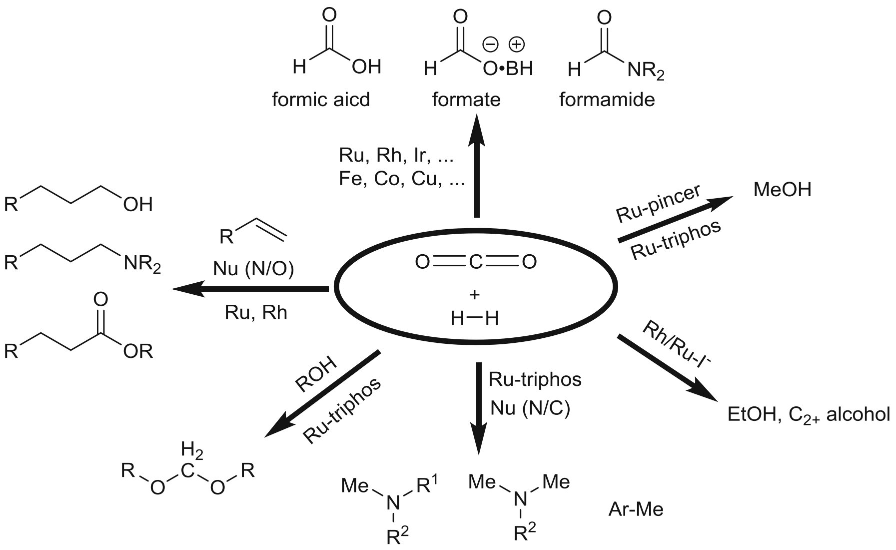

Fig. 1 CO_2 valorization via homogeneous reduction with H_2

discussions will also include the formylation and methylation of amines using CO_2 and H_2, as well as reverse water–gas shift (RWGS) reaction followed by the carbonylation of alkenes (Fig. 1).

2 Hydrogenation of CO_2 to Formic Acid and Its Derivatives

2.1 Hydrogenation of CO_2 to Formate

Formic acid is widely used in the leather and tanning industry, as animal feed additives, as well as in the preparation of silage. Compared to the established process for formic acid production, which is based on the use of MeOH and CO, the hydrogenation of CO_2 provides a promising alternative. However, the change in Gibbs free energy (ΔG) for such transformation in the gas phase is positive (Eq. 1). In order to drive the equilibrium towards the thermodynamically unfavorable direction, normally the reaction is carried out in the presence of a base (Eq. 5).

$$CO_2(g) + H_2(g) + \text{base} \rightarrow HCOO^- + \text{H-base}^+ \quad \Delta G^o < 0;\ \Delta H^o < 0 \qquad (5)$$

2.1.1 In Organic Solvent

Pioneered by the group of Inoue, in 1976 the homogeneous hydrogenation of CO_2 to formate using transition metal complexes of Ru, Rh, or Ir as catalysts in the presence of trimethylamine (Et_3N) was described [14]. In later studies, intensive efforts were devoted to the development of catalytic systems that can improve the turnover number (TON) and frequency (TOF) for such transformation [13, 15], and representative systems are summarized in Table 1. Early results of CO_2 to formate

Table 1 Ru-, Rh-, and Ir-catalyzed hydrogenation of CO_2 to formate

Catalyst precursor	Ligand	Solvent	Additive	*P*/MPa (H_2/CO_2)	T /°C	TON	TOF /h^{-1}
$[RuH_2(PPh_3)_4]$[7] $[RhCl(PPh_3)_3]$[7] $[IrH_3(PPh_3)_3]$[7] $[Pd(PPh_3)_4]$[7]	PPh_3	C_6H_6	Et_3N	2.5/2.5	rt	87 22 15 3	4 0.5 0.7 0.1
$[RuH_2(PMe_3)_4]$[9]	PMe_3	$scCO_2$	Et_3N	8.5/12	50	3700	1400^a
$[RuCl(OAc)(PMe_3)_4]$[29]	PMe_3	$scCO_2$	Et_3N, C_6F_5OH	7/12	50	32,000	95,000
$[Ru(Cl)(PMe_3)_3($**NN1**$)]$[30]	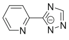 **NN1**	$scCO_2$	DBU	7/10	100	4800	1200
$[RuCl_2[P(OMe)_3]_4]$[31]	$P(OMe)_3$	$scCO_2$	DBU	7/10	100	6630	1655
$[Ru(bpy)_2(H_2O)_2](OTf)_2]$[32]	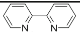 bpy	EtOH	Et_3N	3/3	150	5000	625
$[RuH(HCO_2)(CO)($**PNN1**$)]$[12]	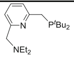 **PNN1**	diglyme	K_2CO_3	3/1	200	23,000	2200^a
$[RuH(Cl)(CO)($**PNP1**$)]$[13]	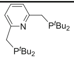 **PNP1**	DMF	DBU	3/1	120	--	1,100,000
$[RuH(Cl)(CO)($**CNC1**$)]$[14-15]	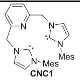 **CNC1**	DMF	DBU	3.9/0.1	84	17,500	99100^a
$[RuH(BH_4)(CO)($**PNP2**$)]$[16]	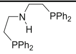 **PNP2**	2-MTHF/ H_2O	DABCO	5/--	55	7000^b	--
$[Rh(cod)Cl]_2$/dppb[17a]	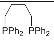 dppb	DMSO	Et_3N	2/2	rt	1150	52
$[RhCl_3 \cdot 3H_2O]/CyPPh_2$[17d]	$CyPPh_2$	MeOH	PEI_{600}	4/4	60	542	34
$[Rh($**PNP3**$)_2OTf]$[17e]	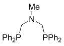 **PNP3**	THF	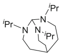 Verkade's base	2/2	21	280	920
$[IrH_3($**PNP4**$)]$[19a, 19b]	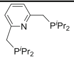 **PNP4**	THF	KOH	2.5/2.5	120 200	300,000 3,500,000	150,000 73,000
$[IrH_3($**PNP5**$)]$[20]	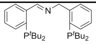 **PNP5**	THF	KOH	4/2	140	450,000	22,500
$[RhCl(m\text{tppts})_3]$[21]	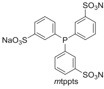 *m*tppts 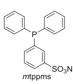 *m*tppms  PTA	H_2O	$NHMe_2$	2/2	rt	3439	286
$[RhCl(m\text{tppms})_3]$[23a] $[RuCl_2(m\text{tppms})_2]_2$[23a, 23c] $[HRu(ac)(\ m\text{tppms})_3]$[23a] $[RuCl_2(PTA)_4]$[23a, 23b] $[Cp{*}Ir(PTA)_2Cl]^+$ [33]		H_2O	$NaHCO_3$	3.5/0.5 6/0 1/0 6/0 10/0	24 54 50 54 100	524 289 284 358 --	262 1.4 16 0.78 23^a
$[RuCl_2(tppms)_2]_2$[23c]		H_2O	$NaHCO_3$	6/3.5	80	--	9600
$[RuCl_2(C_6H_6)]$/dppm[25]	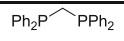 dppm	H_2O	$NaHCO_3$	5/3.5	70	2520	1260
$[Cp{*}RhCl(DHPT)]^{+,}$ [26a] $[C_6Me_6RuCl(DHPT)]^{+,}$ [26a] $[Cp{*}IrCl(DHPT)]^{+,}$ [26a, 26c]	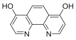 DHPT	H_2O	KOH	3/3 2/2 3/3	120 80 120	15,400 2400 222,000	3360^a 270^a 33,000^a
$[Cp{*}RhCl(4DHBP)]^{+,}$ [26b] $[C_6Me_6RuCl(4DHBP)]^{+,}$ [26b] $[Cp{*}IrCl(4DHBP)]^{+,}$ [26c] $[Cp{*}Ir(OH_2)(3DHBP)]^{2+,}$ [26e] $[Cp{*}Ir(OH_2)(5DHBP)]^{2+,}$ [26e] $[Cp{*}Ir(OH_2)(6DHBP)]^{2+,}$ [26d]	3DHBP 4DHBP 5DHBP 6DHBP 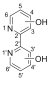	H_2O	KOH KOH KOH $KHCO_3$ $KHCO_3$ $KHCO_3$	0.5/0.5 0.5/0.5 3/3 0.5/0.5 0.5/0.5 0.5/0.5	80 80 120 50 50 120	1200 5400 190,000 0.3 1.1 12,500	160^a 92^a 42,000^a 0.3 1.1 25,200^a

Table 1 continued

Catalyst precursor	Ligand	Solvent	Additive	*P*/MPa (H_2/CO_2)	T /°C	TON	TOF /h^{-1}
[(Cp*IrCl)$_2$(THBPM)]$^{+}$, [26f]	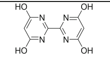 THBPM	H_2O	$KHCO_3$	2/2 2.5/2.5	50 80	153,000 79,000 34,000	15,700 53,800
[Cp*Ir(**NN2**)(OH$_2$)]$^{2+}$, [26g]	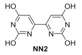 NN2	H_2O	$KHCO_3$	1.5/1.5	80	34,000	33,000[a]
[IrH$_2$(HCOO)(**PNP6**)][34]	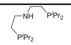 PNP6	H_2O	KOH	2.8/2.8	185	348,000	14,500[a]
[IrI$_2$(AcO)(**NHC1**)][27]	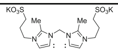 NHC1	H_2O	KOH	3/3	200	190,000	2500
[Cp*RhCl(**NHC2**)]$^{-}$, [28]	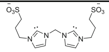 NHC2	H_2O	$KHCO_3$	5/--	100	3600	50

TON turnover number, *TOF* turnover frequency, *DBU* 1,8-diazabicyclo[5.4.0]undec-7-ene, *DABCO* 1,4-diazabicyclo[2.2.2]octane, *Cp** pentamethylcyclopentadienyl

[a] Initial reaction TOF

[b] The catalyst was recycled for five consecutive times

revealed Ru-phosphine complexes to be the most active. In 1994, Noyori et al. reported the high activity of $[RuH_2(PMe_3)_4]$ for CO_2 to formate transformation in supercritical carbon dioxide ($scCO_2$), with a TOF of 1400 h^{-1} [16]. In 2001, Jessop and co-workers improved the activity (TOF of 95,000 h^{-1}) using $[RuCl(OAc)(PMe_3)_4]$ as the catalyst by survey of a variety of amines and alcohols in $scCO_2$. There are several advantages in using $scCO_2$ both as the reactant and solvent, such as efficient mass and heat transport, as well as high miscibility of H_2. Besides monodentate and bidentate phosphines [17], tridentate compounds can also be employed as anchoring ligands in the Ru-catalyzed hydrogenation of CO_2. In the last decade, a variety of pincer-type ligands have gained considerable attentions in reduction reactions. In the context of CO_2 reduction, the group of Milstein reported in 2012 the structural studies of a Ru-pincer complex [RuH(CO)(^{t}BuCOO)(**PNP1**)], which was proposed to activate CO_2 through an aromatization/dearomatization mechanism [18]. One year later, [RuH(HCOO)(CO)(**PNN1**)], the crucial intermediate, was characterized through X-ray diffraction studies by Sanford et al., and high TON and TOF of 23,000 and 2200 h^{-1} were achieved with the Ru-pincer complex [19]. In 2014, Pidko et al. improved the activity to a TOF of 1,100,000 h^{-1} using [RuH(CO)(Cl)(**PNP1**)] as the catalyst and DBU as the base in DMF [20]. In the same year, they prepared lutidine-derived bis-*N*-heterocyclic carbene ruthenium CNC–pincer complexes and applied them in CO_2 hydrogenation [21]. Later on, the activity of a representative Ru–CNC pincer catalyst [RuH(Cl)(CO)(**CNC1**)] was improved and a TOF of 99,100 h^{-1} was achieved [22]. In 2016, Olah and Prakash et al. combined the CO_2 capture and hydrogenation steps to generate to ammonium formate. The amines used in the process were proposed to serve dual purpose of capturing CO_2 and stabilizing the formate product. The in situ formed ammonium carbamate/bicarbonate/carbonate from the captured CO_2 was selectively converted to formate in high yield with the Ru-pincer complex [RuH(BH_4)(CO)(**PNP2**)] under moderate reaction conditions. The catalyst was recycled for five consecutive cycles and a TON of >7000 was obtained by performing a biphasic reaction [23]. Usually, ruthenium complexes have shown better performance than rhodium catalysts in the hydrogenation of CO_2 to formate. Although various phosphine and pincer ligands have been investigated in the Rh-catalyzed reduction of CO_2, generally only moderate activity has been achieved [24–29]. Moreover, phosphine ligands have also been used in the Ir-catalyzed hydrogenation of CO_2. However, the activity was somehow lower than that of Ir with nitrogen-containing or pincer ligands [14, 30]. Nozaki et al. in 2009 reported a state-of-the-art catalyst system based on the pincer-type complex [IrH_3(**PNP4**)], which converted CO_2 to HCOOK with very high TON and TOF of 3,500,000 and 73,000 h^{-1} at 200 °C [31–33]. In 2015, the group of Zhou reported the development of a new Ir-pincer catalyst, which was demonstrated to be highly efficient for hydrogenation of CO_2 to formate in THF, with a TON and TOF of 450,000 and 22,500 h^{-1}, respectively [34].

2.1.2 In H_2O Solution

In the context of the sustainable chemistry, reactions carried out in water have attracted much interest. The first water-soluble rhodium-phosphine complex effective for the hydrogenation of CO_2 to formate in water was reported by Leitner et al. in 1993, and high TON of 3,440 at room temperature was achieved while using [RhCl(*m*tppts)$_3$] as the catalyst and $HNMe_2$ as the base [35]. Later, Joó and Laurenczy et al. investigated several water-soluble Rh- and Ru-complexes [36–38] such as [RhCl(*m*tppms)$_3$], [$RuCl_2$(*m*tppms)$_2$]$_2$, and [$RuCl_2$(PTA)$_4$] for the hydrogenation of CO_2 in aqueous $NaHCO_3$ solution [39–41] or $CaCO_3$ suspension [42], and TON of several hundreds was achieved. In 2010, Beller and Laurenczy et al. investigated the hydrogenation of CO_2 in aqueous $NaHCO_3$ solution by screening of Ru complexes generated by reaction of [$RuCl_2(C_6H_6)_4$] with phosphine ligands such as PPh_3, bis(diphenylphosphino)methane (dppm), bis(dicyclohexylphosphino)methane (dcpm), bis(diphenylphosphino)ethane (dppe) [43, 44]. High TON and TOF of 2520 and 1260 h^{-1} were achieved when dppm was employed as the ligand, but a loss of activity was observed for the catalyst after the first few hours. Recently, Himeda et al. developed a series of half-sandwich Ir complexes with proton responsive ligands, which contained pendant base moieties in the second coordination sphere [8, 15]. These catalysts exhibited high activity in the hydrogenation of CO_2 to formate salt, some even at ambient temperature and pressure [45–51]. In particular, their half-sandwich Ir complexes with 4,4′-dihydroxy-2,2′-bipyridine (4DHBP) or 4,7-dihydroxy-1,10-phenanthroline ligands (DHPT) have successfully been applied to the hydrogenation of CO_2, with TONs up to 222,000 and 190,000. *N*-Heterocyclic carbenes (NHCs) have also been demonstrated by Peris et al. to be effective ligands in the Ir-catalyzed hydrogenation of CO_2 to formate, with TON of 190,000 being achieved using [IrI_2(OAc)(**NHC1**)] as the catalyst [52]. In 2016, The group of Kühn recently prepared water-soluble bis-heterocyclic carbene complexes and found that the rhodium catalyst [Cp*RhCl(**NHC2**)]$^-$ was more active compared with the corresponding iridium derivative in the hydrogenation of bicarbonate to formate [53].

Table 2 Fe-, Co-, and Cu-catalyzed hydrogenation of CO_2 to formate

Catalyst precursor	Ligand	Solvent	Additive	*P*/MPa (H_2/CO_2)	T /°C	TON	TOF /h^{-1}
$[N(PPh_3)_2][Fe_3H(CO)_{11}]$[35]	$[N(PPh_3)_2]^+$	MeOH	--	2.07/2.07	175	6	0.06
$[FeCl_3]$/dcpe[36] $[NiCl_2]$/dcpe[36]	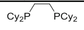 dcpe	DMSO	DBU	4/6	50	113 117	15 16
$[Fe(BF_4)_2{\cdot}6H_2O/$**PP$_3$1**$]$[37] $[Co(BF_4)_2{\cdot}6H_2O/$**PP$_3$1**$]$[39]	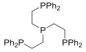 **PP$_3$1**	MeOH	$NaHCO_3$	6/0	80 120	610 3877	30 194
$[Fe(BF_4)_2{\cdot}6H_2O/$**PP$_3$2**$]$[38]	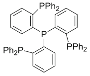 **PP$_3$2**	MeOH	$NaHCO_3$	6/0	60	7546	770[a]
$[FeH_2(CO)($**PNP1**$)]$[40a]	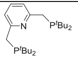 **PNP1**	THF	NaOH	0.66/0.33	80	788	156
$[FeH(CO)(BH_4)($**PNP7**$)]$[40b]	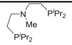 **PNP7**	THF	DBU, LiOTf	3.5/3.5	80	58,990	2458
$[FeHCl(CO)($**PNP8**$)]$[40d]	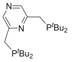 **PNP8**	THF	NaOH	0.63/0.33	55	388	24
Knölker's iron complex[41]	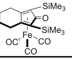	H_2O/ EtOH	$NaHCO_3$	3/--	120	447	19
$[Fe(BF_4)_2($**P$_4$1**$)]$[42]	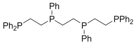 **P$_4$1**	MeOH	$NaHCO_3$	6/--	80	1229	51
$[FeHBr(CO)($**PNP9**$)]$[43]	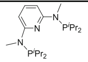 **PNP9**	EtOH	DBU	0.42/0.42	80	10,275	489
$[Cp^*Co(OH_2)(4DHBP)]^{2+,}$ [48]	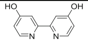 4DHBP	H_2O	$NaHCO_3$	2/2	100	39	39
$[CoH(dmpe)_2]$[44]	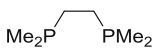 dmpe	THF	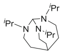 Verkade's base	1/1	21	9400	74,000[a]
$[Cu(OAc)_2]$[45]	--	dioxane	DBU	4/4	100	165	8
$[Cu(triphos)(CH_3CN)PF_6]$[46-47]	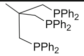 triphos	CH_3CN	DBU	2/2	140	500	25

TON turnover number, *TOF* turnover frequency, *DBU* 1,8-diazabicyclo[5.4.0]undec-7-ene

[a] Initial reaction TOF

Owing to the ready availability, low-cost, as well as eco-friendliness, the use of non-precious metals to replace noble metals in catalysis is an important long-term goal in chemistry. As shown in Table 2, early studies on the hydrogenation of CO_2 to methyl formate based on $[Fe_3H(CO)_{11}]^-$ catalyst system were reported by the group of Evans and Newell in 1978, but only very low TON and TOF of 6 and 0.06 h^{-1} were observed [60]. In 2003, Jessop and co-workers described the combined use of Fe and Ni with phosphine ligands as catalysts for the hydrogenation of CO_2, and reasonable activity was achieved when using DBU as the base in DMSO (TON of 113 and 117 for $[FeCl_3]$/dcpe and $[NiCl_2(dcpe)]$, respectively) [61]. In 2010 Beller and co-workers presented a well-defined $[Fe(BF_4)_2/$**PP$_3$1**$]$ catalyst for the reduction of bicarbonates to formate with TON of 610 [62]. Later, the same group improved the activity of such transformation, with TON of up to 7546 and 1897 using $[Fe(BF_4)_2/$**PP$_3$2**$]$

as the catalyst [63]. Interestingly, the tetradentate ligand **$PP_3$1** has also been found effective in Co-catalyzed hydrogenation of CO_2 to formate, with TON and TOF of 3877 and 194 h^{-1} [64]. Fe complexes with pincer-type ligands have been demonstrated highly efficient in the hydrogenation of CO_2 to formate [65–68]. Pioneering work in this context was reported in 2011 by Milstein et al. with [FeH_2(CO)(**PNP1**)] as the catalyst, and moderate TON and TOF of 788 and 156 h^{-1} were achieved [65]. Recently, the group of Hazari and Bernskoetter et al. described an enhancement of the activity by Lewis acid in Fe-pincer catalyzed CO_2 hydrogenation, which might originate from cation assisted substitution of formate for dihydrogen during the slow step [66]. Knölker's iron complex was also demonstrated to be active on the hydrogenation of bicarbonate and carbon dioxide with a TON of up to 447 [69]. In 2015, the group of Gonsalvi synthesized molecularly defined iron complexes including [$Fe(BF_4)_2$(-**$P_4$1**)] and moderate to good activities were observed in bicarbonate hydrogenation to formate [70]. One year later, they found iron complexes [FeHBr(CO)(**PNP9**)] with PNP pincer ligands based on the 2,6-diaminopyridine scaffold promoted the catalytic hydrogenation of CO_2 and $NaHCO_3$ to formate, reaching a high TON of up to 10,275 [71].

For Co-based catalysts, Linehan et al. reported the hydrogenation of CO_2 under ambient conditions using [CoH(dmpe)$_2$] in aqueous media [72–74]. High TON and TOF of 9400 and 74,000 h^{-1} were obtained when Verkade's base was used in the reaction. In addition to Fe and Co, some Cu-phosphine complexes have also been demonstrated as effective catalysts in the reduction of CO_2 to formate. In 2015, Ikariya and Watari et al. reported the catalytic ability of some Cu complexes in the presence of strong organic bases, and TON of up to 165 was observed [75]. In 2016, the group of Appel described the use of triphos in the Cu-catalyzed CO_2 hydrogenation, with an improved TON value of 500 [76]. Further studies including the measurement of the thermodynamic hydride donor ability, or hydricity, of $[(triphos)(Cu)_2H]^+$ demonstrated the thermodynamic favorability using copper hydrides for CO_2 hydrogenation [77].

2.2 Hydrogenation of CO_2 to Formamide

Formamides have been widely applied as versatile building blocks in organic synthesis. Perhaps the most important chemical in this class is of *N*,*N*-dimethylformamide (DMF), which is extensively used as a polar solvent and an important chemical reagent. Nowadays, DMF is industrially produced by carbonylation of dimethylamine (DMA) with CO. When the hydrogenation of CO_2 is carried out in the presence of primary/secondary amines such as DMA, the resulting formate would be transformed into the corresponding formamide. The latter route, based on the use of CO_2 instead of the toxic CO, has been shown very promising for the synthesis of formamides [79].

In 1970, Haynes et al. reported the first homogeneous catalysts for the synthesis of DMF from CO_2/H_2, including several well-defined complexes such as [CoH(dppe)$_2$], [CuCl(PPh$_3$)$_3$], [RhCl(PPh$_3$)$_3$], and [IrCl(CO)(PPh$_3$)$_2$], and TON of up to 1200 was achieved (Table 3) [80]. Studies by the group of Vaska on the

Table 3 Catalytic hydrogenation of CO_2 to formamides

Catalyst precursor	Ligand	Solvent	amine	*P*/MPa (H_2/CO_2)	T/°C	TON	TOF/h^{-1}
$[CoH(dppe)_2]$[50] $[CuCl(PPh_3)_3]$[50]	PPh_3	C_6H_6	$NHMe_2$	2.7/2.7	125	1000 900	59 53
$[RhCl(PPh_3)_3]$[50] $[IrCl(CO)(PPh_3)_2]$[50] $[RuCl_2(PPh_3)_3]$[50]	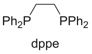	C_6H_6	$NHMe_2$	2.7/2.7	125 125 120	170 1200 8120	10 70 0.5
$[Pd(PPh_3)_2(CO_3)\ ]$[50]							7
$[RuCl_2(PPh_3)_3]$[51] $[Pt_2(dppm)_3]$[51]	PPh_3 dppm	toluene	$NHMe_2$	9/1	125 75	201 1460	8 60
$[RuC1_2(PMe_3)_4]$[52a]	PMe_3	$scCO_2$	$NHMe_2$	8/13	100	370,000	19,470
$[RuC1_2(PMe_3)_4]$[52b]	PMe_3	$scCO_2$	$NHEt_2$ $NH_2{}^iPr$	8/13 8/13	100 100	420,000 260	6000 52
$[RuCl_2(dppm)_2]$[53a] $[RuCl_2(dppe)_2]$[53a] $[RuCl_2(dppp)_2]$[53a]	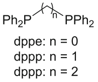	$scCO_2$ $scCO_2$ $scCO_2$	$NHMe_2$	8.5/13	100	95,000 740,000 10,700	190,000 360,000 2650
$[RuCl_2(dppe)_2]$[54]	dppe	$scCO_2$	morpholine	8.7/12.8	100	210,000	68,400
$[RuH(Cl)(CO)(\mathbf{PNP2})]$[55]	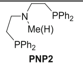	THF	morpholine $NHMe_2$	3.5/3.5 3.5/3.5	120 120	194,0000 599,000	202,000 5400
$[MoH_3(\mathbf{P_2SiP_2})]$[56]	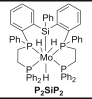	toluene	$NHMe_2$	3.5/2.5	110	115	--
$[Fe(BF_4)_2{\cdot}6H_2O/\mathbf{PP_31}]$[37]	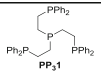 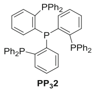	NEt_3	$NHMe_2$	6/3	100	727	36
$[Fe(BF_4)_2{\cdot}6H_2O/\mathbf{PP_32}]$[38]		THF	$NHMe_2$ $NHEt_2$	7/3 3/3	100 100	5104 2114	255 110
$[Co(BF_4)_2{\cdot}6H_2O/\mathbf{PP_31}]$[39]		Et_3N	$NHMe_2$	6/3	100	1308	65

TON turnover number, *TOF* turnover frequency

complexes of Ru, Os, Rh, Ir, and Pt revealed that the most active platinum based catalyst $[Pt_2(dppm)_3]$ gave a TON of 1460 [81, 82]. In the 1990s, Noyori et al. reported a highly active catalyst system, $[RuC1_2(PMe_3)_4]$, for the synthesis of DMF in $scCO_2$, with TON of up to 370,000 and TOF of up to 19,470 h^{-1} [83, 84]. It is noteworthy that with the liquid dimethylammonium dimethylcarbamate as the source of DMA, the same results were obtained under similar reaction conditions. The same group demonstrated that diethylamine and *n*-propylamine could also be transformed into the corresponding formamides with decreased activity using the same catalyst [84]. Inspired by these results, Baiker et al. studied a series of Ru complexes with biphosphine ligands such as dppm, dppe and dppp in the synthesis of DMF from CO_2 under supercritical conditions. High TON and TOF of up to 740,000 and 360,000 h^{-1} were observed when using $[RuCl_2(dppe)_2]$ as the catalyst [85, 86]. Under similar conditions, morpholine was also successfully converted to the desired product in high activity [87]. The state-of-the-art catalytic system using Ru-pincer complex [RuH(Cl)(CO)(**PNP2**)] for the formylation of DMA and morpholine with CO_2 was reported by Ding et al. [88] in 2015. Under relatively mild conditions (120 °C, $CO_2/H_2 = 35/35$ atm), the catalyst showed very high

Table 4 Catalytic hydrogenation of CO_2 to free HCOOH

Catalyst precursor	Ligand	Solvent	*P*/MPa (H_2/CO_2)	T/°C	TON	TOF/h^{-1}	FA/M
$[Rh(NBD)(PMe_2Ph)]BF_4$[57]	PMe_2Ph	THF	4.8/4.8	40	128	2.6	--
[Cp*Ru(**NN3**)$(OH_2)]SO_4$[58]	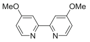 **NN3**	H_2O	5.5/2.5	40	55	0.8	--
[RhCl(*m*tppms)$_3$][59]	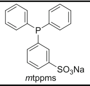 *m*tppms	H_2O	5/5	50	--	--	0.13
$[RuCl_2(PTA)_4]$[60]	 PTA	DMSO	5/5	60	749	6	1.9
[Cp*IrCl(**NN4**)]Cl[61]	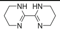 **NN4**	H_2O	3.8/3.8	40	10,000	--	0.12
$[RuCl(PhCO_2)$(**PNP10**)$(PPh_3)]$[62]	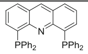 **PNP10**	DMSO/H_2O	8/4	60	4200	260	0.33

TON turnover number, *TOF* turnover frequency

TON and TOF values for formylation of morpholine (1,940,000 and 20,2000 h^{-1}) and DMA (599,000 and 5400 h^{-1}), respectively.

Remarkable progress has also been made in the development of catalytic systems based on non-precious metals for the formylation of amines with CO_2 (Table 3). Ito et al. reported in 2001 a class of well-defined molybdenum catalysts for DMF synthesis from CO_2 with a TON of 115. An efficient Fe-based catalyst with tetraphosphine ligand **$PP_3$1** was developed by Beller and co-workers in 2010, and DMF was obtained in high turnover (TON 727) [62]. In further studies, they improved the Fe catalyst with **$PP_3$2** instead of **$PP_3$1** as the ligand for the hydrogenation of CO_2 to DMF and diethylformamide with high TONs of 5104 and 2114, respectively [63]. Interestingly, the same group also developed a novel Co catalyst with **$PP_3$1** which exhibited an improved catalytic activity with a TON of 1308 for the production of DMF [64].

2.3 Hydrogenation of CO_2 to Free Formic Acid

The metal complex-catalyzed hydrogenation of CO_2 to formates or formamides has been intensively studied for a long time. The stoichiometric base can shift the equilibrium of CO_2 hydrogenation to the reduction direction due to the stabilization of the product (Eq. 5). However, the added base for formate has to be removed from the reaction solution by neutralisation to yield free HCOOH, which complicates the overall operation. For CO_2 hydrogenation, the nature of the solvent can also have a significant effect on the catalytic performance, through stabilizing the catalytic intermediate or influencing the entropy difference between reactants and products. Probably by virtue of hydrogen bonding stabilization of formic acid, polar solvents such as dimethylsulfoxide (DMSO) and water have been identified as favorable solvents for CO_2 hydrogenation to free HCOOH.

Early studies revealed that the hydrogenation of CO_2 to free HCOOH in THF with a Rh-monophosphine complex was inefficient (TON of 128 after 2 days,

Table 4) [90]. The CO_2 hydrogenation to free HCOOH in H_2O catalyzed by a bipyridine-containing Ru-complex was also not satisfactory, and TON of 55 was achieved after 70 h [91]. In 2011, Joó et al. reported the use of [RhCl(*m*tppms)$_3$] for such transformation in aqueous sodium formate, and 0.13 mol L^{-1} HCOOH was achieved [92]. When the reaction was carried out in the absence of sodium formate, almost no formic acid was observed. An efficient catalytic system for producing high concentration of free HCOOH, in the absence of a base or other additives, was firstly reported by the group of Laurenczy in 2014. TON of up to 749 after 120 h was achieved with the complex [$RuCl_2$(PTA)$_4$], which provided 1.9 mol L^{-1} HCOOH in DMSO [93]. Soon after Li et al. reported the base-free direct hydrogenation of CO_2 to formic acid in water with [Cp*IrCl(**NN3**)]$^+$, an Ir-*N*,*N*′-diimine complex, affording HCOOH with concentration up to 0.12 mol L^{-1} [94]. Very recently, Leitner and co-workers developed a new catalytic system for CO_2 hydrogenation, which yields 0.33 mol L^{-1} of HCOOH under base-free conditions [95]. With a Ru-pincer complex [RuCl($PhCO_2$)(**PNP10**)(PPh_3)] as the catalyst, the reaction was carried out in mixed solvent (DMSO/H_2O) at 60 °C, to give the product with very high TON and TOF of 4200 and 260 h^{-1}.

3 Hydrogenation of CO_2 to CO Followed by Alkene Carbonylation

The hydrogenation of CO_2 to CO (RWGS) is usually performed under heterogeneous catalysis and/or by photo-/electrochemical methods. The generated CO can be used in various industrially important processes, including methanol synthesis, carbonylation reactions and Fischer–Tropsch reactions. Herein, we describe the developments in the carbonylation reaction of alkenes using CO_2 as CO surrogate in homogeneous catalysis.

In 2000, Sasaki et al. reported the hydroformylation/reduction of cyclohexene with CO_2 and H_2 using the ruthenium catalyst derived from [$H_4Ru_4(CO)_{12}$] and LiCl, to give hydroxymethylcyclohexane in 88% yield [96]. Following studies by the group of Haukka revealed that such transformation was promoted by the presence of halides and suitable counter ions, such as alkali metal cations or alkaline earth cations [97]. Tominaga and co-workers studied alkene carbonylation with CO_2/H_2 catalyzed by some ruthenium cluster complexes and halide salts, and found that under identical reaction conditions, the same products were formed in similar or even better yields as compared to the conventional carbonylation with CO [98]. In 2004, the group of Tominaga and Sasaki applied a biphasic ionic liquid–toluene system in Ru-catalyzed hydroformylation/reduction of 1-hexene with CO_2, to give heptanol in high yield and moderate chemoselectivity [98]. A halide salt was used as the promoter to suppress the hydrogenation of alkene to alkane. In this system, the ruthenium complexes effectively catalyzed the RWGS reaction, alkene hydroformylation, and aldehyde hydrogenation, leading to the ultimate formation of alcohols. Recently, the group of Beller disclosed that the combination of a bulky phosphite ligand and [$Ru_3(CO)_{12}$] gave a more efficient catalyst than the known ruthenium/chloride system for hydrohydroxymethylation of terminal and internal olefins with CO_2 at lower temperature (Scheme 1) [99].

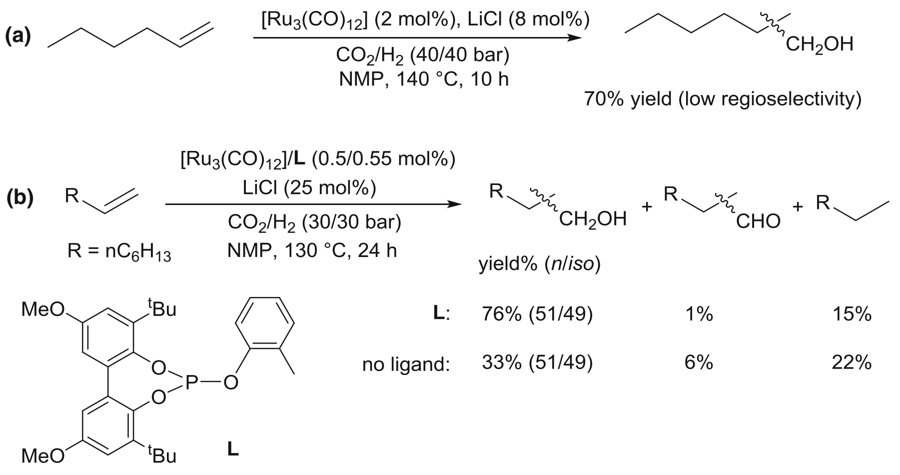

Scheme 1 Ru-catalyzed hydrohydroxymethylation of alkenes with CO_2/H_2

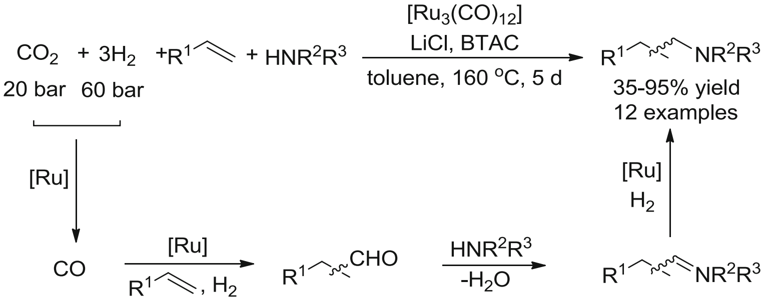

Scheme 2 Ru-catalyzed hydroaminomethylation of alkenes with CO_2/H_2 and amines

In 2009, Eilbracht et al. reported Ru-catalyzed one-pot RWGS/hydroformylation/reductive amination of alkenes using CO_2 as the C1 source, furnishing a variety of amines in moderate to high yields [100]. LiCl and benzyl triethyl ammonium chloride (BTAC) were used as additives to suppress the formation of side products such as alkanes, alcohols, and formamides (Scheme 2).

Later on, Leitner et al. disclosed a catalytic protocol for the synthesis of free carboxylic acids directly from CO_2/H_2 and olefins (Scheme 3) [101]. With $[RhCl(CO)_2]_2$ as the catalyst and CH_3I and *p*-toluenesulfonic acid (PTSA) as additives, terminal and internal olefins were converted to the corresponding one-carbon-elongated carboxylic acids in high conversion, but with moderate regioselectivity. Using PTSA as the co-catalyst, an enhancement of the hydrocarboxylation was observed. Mechanistic studies suggested that the overall transformation might be accomplished via a Rh-catalyzed RWGS reaction followed by hydroxycarbonylation cycles.

In 2014, Beller and co-workers developed an unprecedented alkene alkoxycarbonylation with CO generated in situ from CO_2 reduction by alcohols. The direct

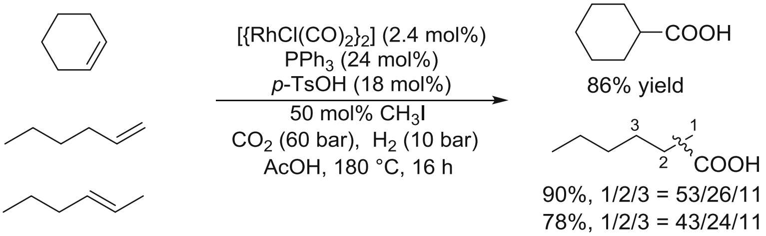

Scheme 3 Rh-catalyzed hydroxycarbonylation of alkenes with CO_2/H_2

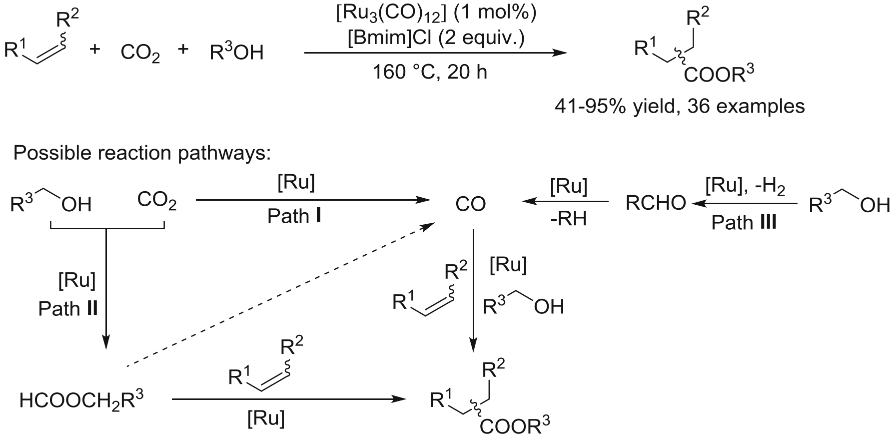

Scheme 4 Ru-catalyzed alkoxycarbonylation of alkenes with CO_2 and alcohols

$[Ru_3(CO)_{12}]$-catalyzed alkoxycarbonylation of alkenes was carried out in the presence of halide source at 160 °C to give the esters in high yield (Scheme 4) [102]. Several possible pathways were proposed for the process, which might involve aldehyde and/or formate intermediates.

4 Hydrogenation of CO_2 to MeOH

Methanol is used as a fuel for our daily life, and a versatile building block for the manufacture of many bulk chemicals. Nowadays, MeOH is industrially produced from syngas (CO/H_2) at high temperatures (250–300 °C) and high pressures (50–100 atm) using a copper-zinc-based oxide catalyst. The hydrogenation of CO_2 to MeOH provides a promising way for its valorization. Although the direct hydrogenation of CO_2 to MeOH is thermodynamically a downhill reaction, it is difficult to be realized in real-world via an energy-efficient and cost-effective way. On the other hand, catalytic hydrogenation of some CO_2 derivatives, e.g., formic acid, formates, carbonates, carbamates, or urea, is of significant current interest, which provides an alternative and mild approach for the indirect hydrogenation of CO_2 to MeOH. It is worth to note that the transformations of CO_2 to its derivatives

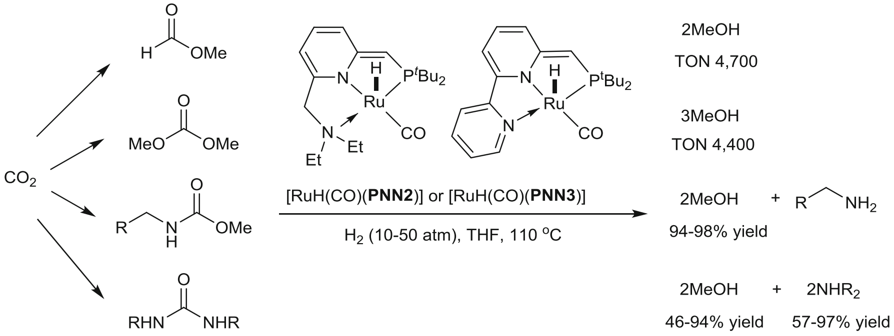

Scheme 5 Catalytic hydrogenation of methyl formate, dimethyl carbonate, carbamates, and urea derivatives

have been widely used in CO_2 fixation, and some have been well developed in industrial processes.

4.1 Hydrogenation of CO_2 Derivatives to MeOH

Although the hydrogenation of ketones and aldehydes to alcohols has been well developed, so far the reduction of CO_2 derivatives, e.g. carbonates and carbamates to MeOH proves much more challenging and has been less explored. A seminal study for indirect catalytic hydrogenation of CO_2 to MeOH was reported by Milstein et al. in 2011 using some Ru-pincer complexes [103]. As shown in Scheme 5, for the hydrogenation of methyl formate and dimethyl carbonate to MeOH with [RuH(CO)(**PNN3**)], high TONs of 4400 and 4700 were attained respectively under 50 atm H_2 at 110 °C after 14 h. In the catalytic reduction of carbamate, the corresponding amines and MeOH were produced in high yield with the same catalyst under 10 atm H_2. These remarkable results revealed that the catalysts are effective in breaking C–N or C–O bonds of these CO_2 derivatives, along with a simultaneous reduction of a carbonyl group. When the same complex was used as the catalyst in the hydrogenation of methyl formate, an even higher activity with TON of 4700 was observed under identical reaction conditions. Simultaneously, the same group also communicated the catalytic hydrogenation of urea derivatives with [RuH(CO)(**PNN3**)], affording the corresponding amines and MeOH in high yields under relatively mild conditions (13 atm H_2, 110 °C) [104].

On the basis of the experimental investigations by Milstein and DFT studies by Yang [105], a metal–ligand cooperative catalysis mechanism involving aromatization–dearomatization of the pincer ligand has been proposed. As shown in Fig. 2, for the hydrogenation of dimethyl carbonate heterolytic cleavage of H_2 by complex **1** resulted in the formation of *trans*-dihydride complex **2**. Subsequently, the hydride from the complex was transferred to the carbonyl group of coordinated carbonate to form intermediate **3**. In this step, the temporary dissociation of the Et_2N group was essential to provide a free site for substrate coordination. The benzylic arm in the complex **3** was deprotonated by the adjacent methoxy group, which gave one molecule of MeOH and the dearomatized species **4** with coordinated formate.

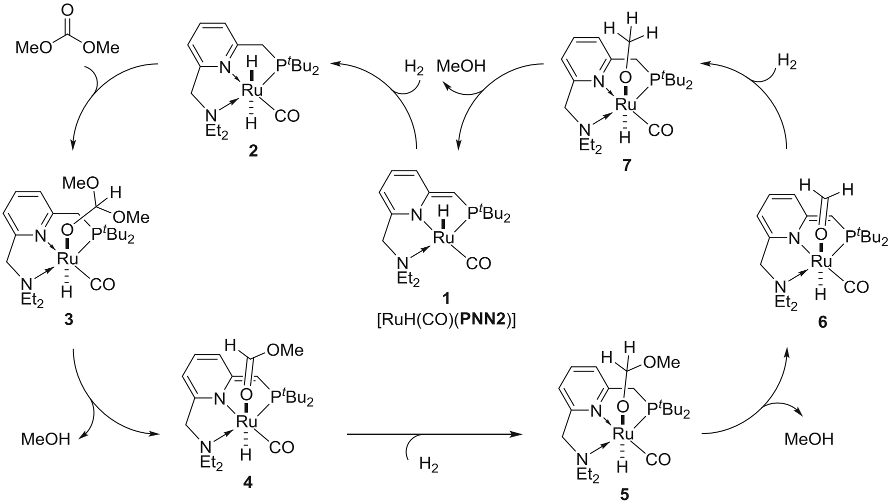

Fig. 2 Postulated mechanism for the hydrogenation of dimethyl carbonate to MeOH catalysed by [RuH(CO)(**PNN2**)]

Similarly, the addition of H_2 to **4** followed by the hydride transformation to formate lead to the intermediate **5**. After the deprotonation of the benzylic arm by the methoxy group, MeOH and a dearomatized complex **6** with formaldehyde were formed. Finally, catalyst **1** was regenerated through the dihydrogen addition to **6**, and the deprotonation by the methoxy group in the complex **7**. The formation of the second molecular of MeOH involving breaking of a C–OCH_3 bond of formate was suggested to be the rate-determining step.

In 2012, Ding and co-workers reported the hydrogenation of ethylene carbonate to give MeOH and ethylene glycol (EG), both are important bulk chemicals (Scheme 6) [106]. High activity with TON of 84,000 for MeOH and 87,000 for EG were achieved with Ru-pincer complex [RuHCl(CO)(**PNP2**)] as the catalyst under 50 atm H_2 at 140 °C in THF. Notably, coupling of this present catalytic system with the ethylene carbonate production in OMEGA process is expected to establish a new bridge from CO_2 and ethylene oxide to MeOH and EG. The catalyst has also been used for the hydrogenation of polycarbonates to afford 1,2-propylene glycol and MeOH. A mechanism was proposed based on deuterium-labeling studies and some control experiments. The catalytic precursor [RuHCl(CO)(**PNP2**)] would undergo an elimination of HCl by reaction with KO^{t}Bu, leading to the formation of amido Ru complex **1**. The following-up heterolysis of H_2 on complex **1** was expected to furnish the Ru-dihydride complex **2**. Repetitive outer-sphere attacks of Ru-dihydride/NH on the carbonyl group of the substrate or its reduced intermediate would finally give the corresponding alcohol products with regeneration of amido complex **1**.

Usually, the decomposition of formic acid releases H_2 and CO_2 by dehydrogenation or produces CO and H_2O by dehydration [107]. The disproportionation of formic acid to methanol was communicated by Miller and Goldberg et al. in 2013 using [Cp*Ir(bpy)(OH_2)](OTf)$_2$] as a catalyst [108]. Under optimized conditions,

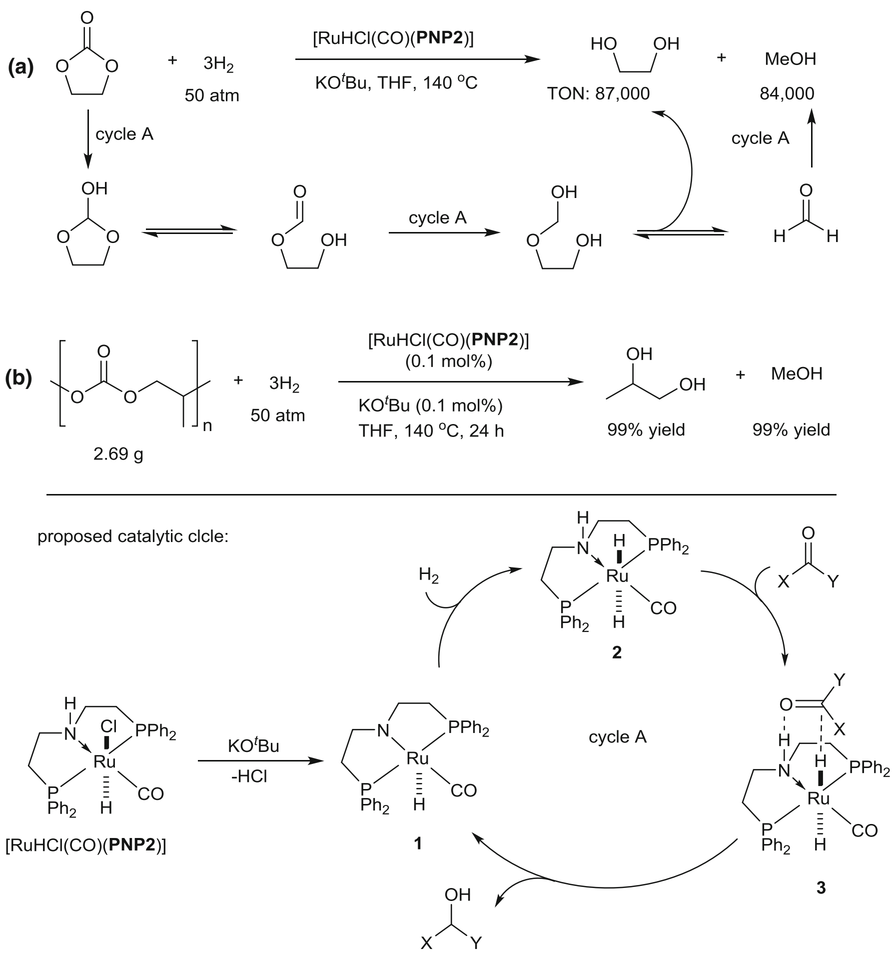

Scheme 6 Catalytic hydrogenation of ethylene carbonate to MeOH and EG with Ru-pincer complex

they obtained MeOH selectivity of 12% corresponding to a TON of 70. The author proposed that formic acid was first converted to formaldehyde, which was further reduced to methanol based on isotope labeling experiments. One year later, Cantat et al. significantly improved the yield of FA disproportionation to MeOH using ruthenium catalysts containing of [Ru(cod)(methylallyl)$_2$], triphos ($CH_3C(CH_2PPh_2)_3$) ligand and methanesulfonic acid. They achieved the highest selectivity of 27% for formic acid disproportionation to MeOH in THF solution at 150 °C [109]. Their experiments showed that MeOH was generated by transfer hydrogenation of formic acid other than the hydrogenation of CO_2. Compared with the Ir complex, the Ru complex was less reactive, but it showed high selectivity for methanol production. In 2015, Cantat et al. found the nonprecious metal complex, [CpMo(CO)$_3$H], was active for the catalytic formation of methanol and methyl formate from formic acid and achieved a selectivity of 21% relative to decarboxylation [110]. Interestingly, Himeda and Laurenczy et al. demonstrated that with an iridium catalyst [(Cp*)Ir(4DHBP)(OH_2)][SO_4] (structure of 4DHBP, see Table 1) both the hydrogenation of carbon dioxide to formic acid and the disproportionation of formic acid into methanol can be realized in one-pot reaction. The first step was carried out in aqueous acidic media without additives. The resulting formic acid can undergo complete disproportionation into MeOH with unprecedented selectivities of 96% with the same catalyst in the presence of H_2SO_4, with FA conversions of 98% [111].

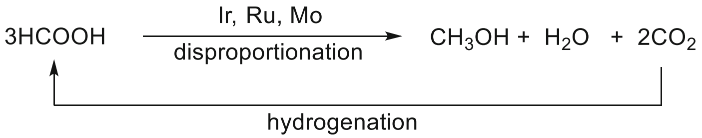

(6)

4.2 Direct Hydrogenation of CO_2 to MeOH

Direct CO_2 hydrogenation to MeOH proves extremely challenging for homogeneous catalysis, and so far there are only a few reports in the literature [112–117]. Recently, the group of Sanford described the use of a cascade approach for the hydrogenation of CO_2 to MeOH [118]. As depicted in Scheme 7, this strategy involved a three-step sequence mediated independently by several catalysts: (1) CO_2 hydrogenation to HCOOH catalyzed by a Ru-phosphine complex cat**A**, (2) a Lewis acid-promoted esterification to generate methyl formate, (3) MeOH production by the hydrogenation of ester using a Ru-pincer complex cat**C**. To access the compatibility of each step, the catalysts and reaction conditions were carefully investigated and a vapor transfer method was used to prevent the deactivation of cat**C** by Sc(OTf)$_3$: cat**A** and cat**B** were placed in a vial in the center of the vessel, while cat**C** was placed in the outer well of the Parr reactor. Under optimized reaction conditions, TON of 2.5 for MeOH was observed in the one-pot reaction, while TON was increased to 21 using transfer approach for CO_2 hydrogenation.

Additionally, the same group reported the tandem hydrogenation of CO_2 to MeOH catalyzed Ru-pincer complexes in the presence of amine. MeOH was obtained with TON of up to 550 using [RuH(BH_4)(CO)(**PNP2**)] as the catalyst. The amine was proposed to capture CO_2 to produce dimethylammonium dimethylcarbamate (DMC) and convert formic acid to DMF. Independently, Ding et al. also developed a one-pot two-step procedure for the hydrogenation of CO_2 to MeOH via the intermediacy of formamide [88]. With Ru-pincer complex

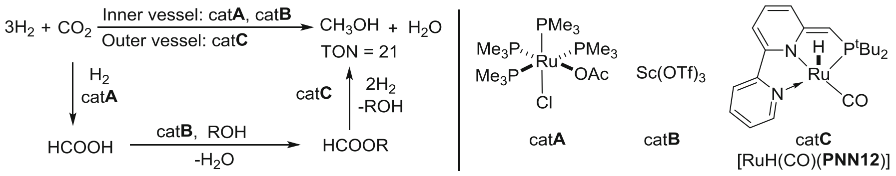

Scheme 7 Cascade catalysis for the hydrogenation of CO_2 to MeOH

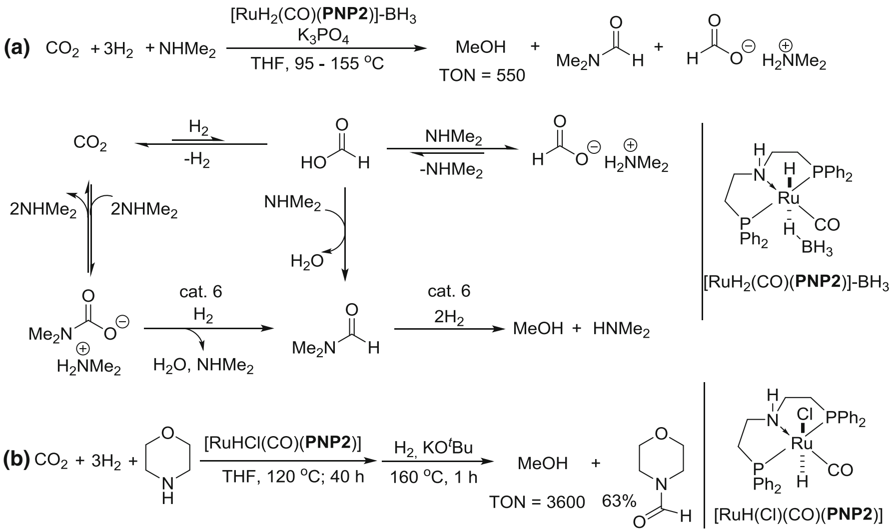

Scheme 8 Tandem Ru-catalyzed hydrogenation of CO_2 to MeOH

[RuH(Cl)(CO)(**PNP2**)] as the catalyst, high TON of up to 3600 for MeOH was achieved in the presence of morpholine (Scheme 8).

The first CO_2 capture from air and direct reduction to MeOH in one-pot was demonstrated by the group Olah and Prakash in 2015 [119]. As presented in Scheme 9, pentaethylenehexamine (PEHA) was used to capture CO_2 by bubbling air in the aqueous solution to form carbamate and bicarbonate/carbonate. The resulting mixture was in situ hydrogenated by Ru-pincer complex [RuH(BH_4)(-CO)(**PNP2**)], to give MeOH with TON of up to 215. In the same year, Milstein et al. reported an aminoethanol-mediated approach for CO_2 hydrogenation to MeOH [120]. CO_2 was captured by (2-methylamino)ethanol and valinol with catalytic Cs_2CO_3 to give the corresponding oxazolidinone in moderate to high yield. Efficient hydrogenation of the captured product was realized using Ru-pincer complex to give the corresponding aminoethanol and MeOH in high yield.

The direct hydrogenation of CO_2 to MeOH without use of amines was presented in 2012 by the group of Leitner et al. (Scheme 10) [121]. With [Ru(tmm)(triphos)] and bis(trifluoromethane)sulfonimide as the catalyst, TON of up to 221 for MeOH was achieved under 20/60 bar of CO_2/H_2 at 140 °C in THF within 24 h. Based on mechanistic studies, a biphasic system consisting of H_2O and 2-methyltetrahydrofuran (2-MTHF) was further developed, and methanol was synthesized with an improved TON of up to 603 using re-pressurisation [122].

5 Reduction of CO_2 to Higher Alcohols and Dialkoxymethane Ethers

When MeOH and CO are both produced from the hydrogenation of CO_2, the carbonylation of MeOH in the presence of halide salts can result in the formation of acetic acid, which could be further hydrogenated to ethanol (EtOH). Repeating the

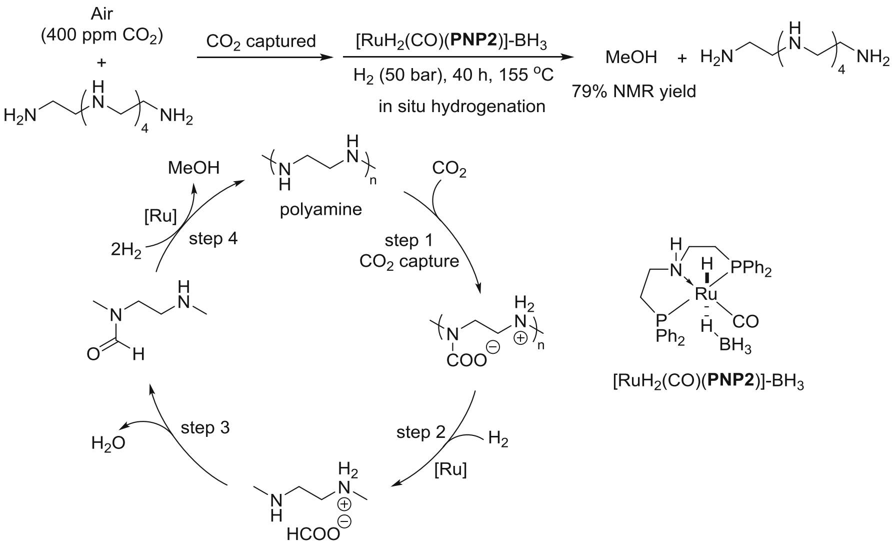

Scheme 9 CO_2 capture from air using a polyamine and in situ hydrogenation to MeOH

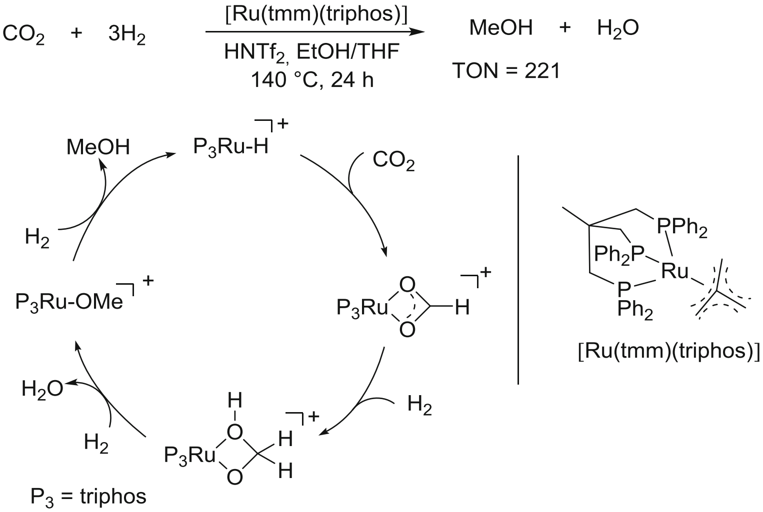

Scheme 10 Direct hydrogenation of CO_2 to MeOH with Ru-triphos system

carbonylation and hydrogenation of ethanol, C_{2+} alcohols could in principle be obtained. Early studies from the group of Sasaki described the Ru–Co bimetallic catalysis for the hydrogenation of CO_2 to CO, MeOH, EtOH, and methyl formate (Scheme 11) [114]. The reaction was carried out at 200 °C using $[Ru_3(CO)_{12}]$ and $[Co_2(CO)_8]$ as the catalysts and KI as the additive, to give EtOH in poor activity and selectivity. In 2015, Qian and Han et al. reported the hydrogenation of CO_2 to C_{2+} alcohols with a $[Ru_3(CO)_{12}]/[Rh_2(CO)_4Cl_2]$–LiI system [123]. The reaction was

$$CO_2 + H_2 \xrightarrow[\text{Iodide salt}]{\text{bimetallic catalysis}} CO + MeOH + C_{2+}\ \text{alcohols}$$

(a) $[Ru_3(CO)_{12}]/[Co_2(CO)_8]$-KI, H_2/CO_2 (2/10 MPa), 200 °C, NMP
EtOH: 26% selectivity

(b) $[Ru_3(CO)_{12}]/[Rh_2(CO)_4Cl_2]$-LiI, H_2/CO_2 (4/4 MPa), 160 °C, DMI
C_{2+} alcohols: 96% selectivity

Scheme 11 Catalytic hydrogenation of CO_2 to higher alcohols

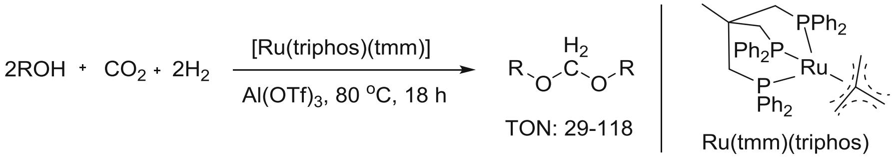

Scheme 12 Catalytic hydrogenation of CO_2 to dialkoxymethane

carried out at 160 °C, which was the lowest temperature reported so far, and the selectivity for C_{2+} alcohols was as high as 96%.

Very recently, the group of Leitner reported for the first time the synthesis of dimethoxymethane (DMM) by a multistep reaction of methanol with CO_2 (Scheme 12) [124]. Using [Ru(tmm)(triphos)] in combination with the Lewis acid $Al(OTf)_3$, various dialkoxymethane ethers were afforded with TON of 29-118. This new catalytic reaction provides the first synthetic example for the selective conversion of CO_2/H_2 into a formaldehyde oxidation level, thus opening access to new molecular structures using CO_2 as an important C1 source.

6 Methylation Reaction Using CO_2 and H_2

Methylation reaction has been frequently used for the synthesis of bio-active compounds and important chemicals. The most common methylation method in industry makes use of toxic formaldehyde, whereas in organic synthesis less benign reagents such as methyl iodide and dimethyl sulfate prevail. Catalytic methylation using CO_2 and H_2 represents an elegant and viable method with H_2O as the only by-product. A breakthrough in the methylation of amines using CO_2/H_2 has been reported in 2013 by the group of Klankermayer and Leitner [125] and the group of Beller, respectively [126]. The two methodologies both used Ru-triphos complex as the catalyst and required similar reaction conditions ((H_2/CO_2: 60/20 bar, temperatures: 140 or 150 °C), which afforded the respective mono- or bis-methylation of primary and secondary anilines in high yields. In both catalytic systems, a catalytic amount of acid ($HNTf_2$ = trifluoromethanesulfonimide or MSA = methanesulfonic acid) was found to play a crucial role for the generation of the Ru–H active species. While exploring the substrate scope, they both found aliphatic amines to be the least

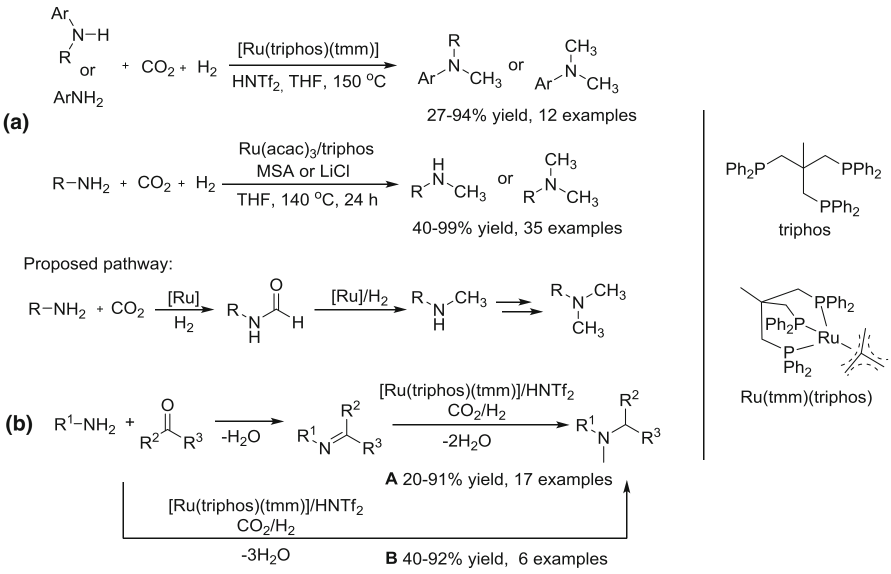

Scheme 13 Ru-catalyzed *N*-methylation using CO_2/H_2: **a** methylation of amines, **b** tandem condensation/reductive methylation of amines with aldehydes

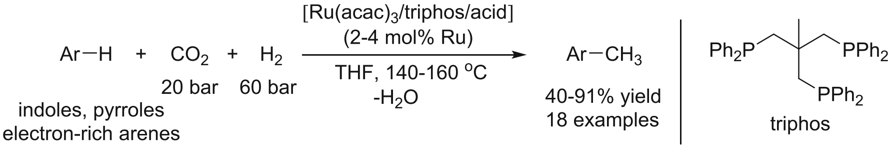

Scheme 14 Catalytic methylation of C–H Bonds with CO_2 and H_2

reactive substrates, probably due to the reduction of the corresponding formamide intermediate, which is more difficult in the absence of an aromatic substitute. To solve this problem, Beller et al. used LiCl instead of MSA as the promoter, and increased the catalyst loading, which resulted in the bismethylation of aliphatic primary amines in high yields. In parallel, the group of Klankermayer employed acetanilides as the substrate in the hydrogenation/*N*-methylation to give unsymmetric methyl/alkyl anilines. Further studies by Klankermayer et al. revealed that the combination of the complex [Ru(triphos)(tmm)] and an acid promoter also enabled the reductive methylation of isolated imines, as well as the direct coupling of amines with aldehydes followed by reductive methylation of the in situ formed amines [127]. Interestingly, the practical utility of the protocol which resulted in the corresponding *N*-methyl amines was demonstrated with the preparation of butenafine as a model pharmaceutical product in high yield (Scheme 13).

Beller et al. reported the first example for the catalytic methylation of C–H bonds using CO_2 and H_2 (Scheme 14). The key to realize such transformation is the combination of an in situ formed Ru-triphos catalyst and some Lewis acids. The efficient methylation of carbon nucleophiles, for example, indoles, pyrroles, and electron-rich arenes, was performed in THF at 140–160 °C to give the corresponding methylarenes in high yields [128].

7 Future Perspective and Outlook

The capture and valorization of CO_2 are highly energy intensive processes, which results in additional CO_2 emissions. To realize these transformations in a more benign and sustainable manner, efficient catalytic systems that are effective under mild conditions have to be developed in the future. The production of H_2 accounts for a significant part of the overall economics of the CO_2 reduction process. Non-fossil fuel-based renewable H_2 production methods, including photo- and/or electrochemical splitting of water and biomass pyrolysis, should be explored.

Although very high activity has been achieved in the reduction of CO_2 to formate, the separation of the product to free acid still complicates the process. On the other hand, the hydrogenation of CO_2 to free formic acid provides an ideal way to valorized CO_2, but the activity of this transformation is still far away from practical application. The catalytic reductive formylation and methylation of amines represent important alternatives in the activation and chemical use of CO_2. In such transformations, the reductive deoxygenation energy is significantly compensated by the coordination of amines to CO_2, and the formation of N–C bonds facilitating the reduction of CO_2. These protocols represent a diagonal approach for CO_2 use, which effectively combine both the reduction of CO_2 and C-N bond formation in a single transformation. RWGS reaction for producing CO has recently been considered an ideal approach for efficient CO_2 activation/reduction. Development of RWGS systems effective under mild conditions is required, and photo-/electrochemical promoted RWGS reaction provides an alternative method for this reaction. When CO is produced from CO_2 hydrogenation, a better way is to use CO in situ for follow-up reactions such as Fischer–Tropsch reaction, MeOH synthesis, and MeOH/alkene carbonylation, which could avoid the tedious separation and transportation.

The hydrogenation of CO_2 to MeOH provides an ideal way to transform CO_2 to value-added fuels and chemicals. Nowadays, the only industrial process utilizes heterogeneous catalyst with $Cu/Zn/Al_2O_3$ under harsh conditions. In homogeneous hydrogenation of CO_2 to MeOH, there are only two catalytic systems (Ru-triphos and Ru-pincer complexes). Nevertheless, the activity still needs to be improved further. Hence, the development of efficient homogeneous catalyst for the hydrogenation of CO_2 to MeOH is highly desired. The reduction of CO_2 to value-added fine chemicals such as higher alcohols and dialkoxymethane ethers present an alternative method for the use of CO_2.

Currently, most of the homogeneous catalytic systems are based on precious metals (Rh, Ru, Pd, Ir), which are not readily available and expensive. With respect to process sustainability and eco-friendliness, the development of catalytic systems based on non-noble metals is highly preferred. Although high pressure system is required for the use of $scCO_2$ both as reactant and solvent, it could enhance the solubility and mass transfer of the reactant resulting in superior activity and also eliminate the need of additional solvents. In this regard, the CO_2 varolization in its supercritical state should be explored further.

References

1. Doney SC, Fabry VJ, Feely RA, Kleypas JA (2009) Ann Rev Mar Sci 1:169–192
2. Aresta M, Dibenedetto A (2007) Dalton Trans 28:2975–2992
3. Alberico E, Nielsen M (2015) Chem Commun 51:6714–6725
4. Kuhl KP, Cave ER, Abram DN, Jaramillo TF (2012) Energy Environ Sci 5:7050–7059
5. Lu Q, Rosen J, Zhou Y, Hutchings GS, Kimmel YC, Chen JG, Jiao F (2014) Nat Commun 5:3242–3247
6. Porosoff MD, Yan BH, Chen JGG (2016) Energy Environ Sci 9:62–73
7. Wang W, Wang S, Ma X, Gong J (2011) Chem Soc Rev 40:3703–3727
8. Wang W-H, Himeda Y, Muckerman JT, Manbeck GF, Fujita E (2015) Chem Rev 115:12936–12973
9. Appel AM, Bercaw JE, Bocarsly AB, Dobbek H, DuBois DL, Dupuis M, Ferry JG, Fujita E, Hille R, Kenis PJA, Kerfeld CA, Morris RH, Peden CHF, Portis AR, Ragsdale SW, Rauchfuss TB, Reek JNH, Seefeldt LC, Thauer RK, Waldrop GL (2013) Chem Rev 113:6621–6658
10. Aresta M, Dibenedetto A, Angelini A (2014) Chem Rev 114:1709–1742
11. Jessop PG, Ikariya T, Noyori R (1995) Chem Rev 95:259–272
12. Arakawa H, Aresta M, Armor JN, Barteau MA, Beckman EJ, Bell AT, Bercaw JE, Creutz C, Dinjus E, Dixon DA, Domen K, DuBois DL, Eckert J, Fujita E, Gibson DH, Goddard WA, Goodman DW, Keller J, Kubas GJ, Kung HH, Lyons JE, Manzer LE, Marks TJ, Morokuma K, Nicholas KM, Periana R, Que L, Rostrup-Nielson J, Sachtler WMH, Schmidt LD, Sen A, Somorjai GA, Stair PC, Stults BR, Tumas W (2001) Chem Rev 101:953–996
13. Leitner W (1995) Angew Chem Int Ed 34:2207–2221
14. Inoue Y, Izumida H, Sasaki Y, Hashimoto H (1976) Chem Lett 5:863–864
15. Himeda Y (2007) Eur J Inorg Chem 2007:3927–3941
16. Jessop PG, Ikariya T, Noyori R (1994) Nature 368:231–233
17. Tai C-C, Pitts J, Linehan JC, Main AD, Munshi P, Jessop PG (2002) Inorg Chem 41:1606–1614
18. Vogt M, Gargir M, Iron MA, Diskin-Posner Y, Ben-David Y, Milstein D (2012) Chem Eur J 18:9194–9197
19. Huff CA, Sanford MS (2013) ACS Catal 3:2412–2416
20. Filonenko GA, van Putten R, Schulpen EN, Hensen EJM, Pidko EA (2014) ChemCatChem 6:1526–1530
21. Filonenko GA, Cosimi E, Lefort L, Conley MP, Copéret C, Lutz M, Hensen EJM, Pidko EA (2014) ACS Catal 4:2667–2671
22. Filonenko GA, Smykowski D, Szyja BM, Li G, Szczygieł J, Hensen EJM, Pidko EA (2015) ACS Catal 5:1145–1154
23. Kothandaraman J, Goeppert A, Czaun M, Olah GA, Surya GK (2016) Prakash. Green Chem 18:5831–5838
24. Graf E, Leitner W (1992) J Chem Soc Chem Commun 8:623–624
25. Angermund K, Baumann W, Dinjus E, Fornika R, Görls H, Kessler M, Krüger C, Leitner W, Lutz F (1997) Chem Eur J 3:755–764
26. Ezhova NN, Kolesnichenko NV, Bulygin AV, Slivinskii EV, Han S (2002) Russ Chem Bull 51:2165–2169
27. Li Y-N, He L-N, Liu A-H, Lang X-D, Yang Z-Z, Yu B, Luan C-R (2013) Green Chem 15:2825–2829
28. Bays JT, Priyadarshani N, Jeletic MS, Hulley EB, Miller DL, Linehan JC, Shaw WJ (2014) ACS Catal 4:3663–3670
29. Burgemeister T, Kastner F, Leitner W (1993) Angew Chem Int Ed 32:739–741
30. Fernández-Alvarez FJ, Iglesias M, Oro LA, Polo V (2013) ChemCatChem 5:3481–3494
31. Tanaka R, Yamashita M, Nozaki K (2009) J Am Chem Soc 131:14168–14169
32. Tanaka R, Yamashita M, Chung LW, Morokuma K, Nozaki K (2011) Organometallics 30:6742–6750

33. Federsel C, Jackstell R, Beller M (2010) Angew Chem Int Ed 49:6254–6257
34. Liu C, Xie J-H, Tian G-L, Li W, Zhou Q-L (2015) Chem Sci 6:2928–2931
35. Gassner F, Leitner W (1993) J Chem Soc Chem Commun 19:1465–1466
36. Horváth H, Laurenczy G, Kathó Á (2004) J Organomet Chem 689:1036–1045
37. Kathó Á, Opre Z, Laurenczy G, Joó F (2003) J Mol Catal A: Chem 204–205:143–148
38. Joó F, Laurenczy G, Karády P, Elek J, Nádasdi L, Roulet R (2000) Appl Organomet Chem 14:857–859
39. Joo F, Joo F, Nadasdi L, Elek J, Laurenczy G, Nadasdi L (1999) Chem Commun 11:971–972
40. Laurenczy G, Joó F, Nádasdi L (2000) Inorg Chem 39:5083–5088
41. Elek J, Nádasdi L, Papp G, Laurenczy G, Joó F (2003) Appl Catal A 255:59–67
42. Jószai I, Joó F (2004) J Mol Catal A: Chem 224:87–91
43. Federsel C, Jackstell R, Boddien A, Laurenczy G, Beller M (2010) ChemSusChem 3:1048–1050
44. Boddien A, Gärtner F, Federsel C, Sponholz P, Mellmann D, Jackstell R, Junge H, Beller M (2011) Angew Chem Int Ed 50:6411–6414
45. Himeda Y, Onozawa-Komatsuzaki N, Sugihara H, Arakawa H, Kasuga K (2004) Organometallics 23:1480–1483
46. Himeda Y, Miyazawa S, Hirose T (2011) ChemSusChem 4:487–493
47. Himeda Y, Onozawa-Komatsuzaki N, Sugihara H, Kasuga K (2007) Organometallics 26:702–712
48. Wang W-H, Hull JF, Muckerman JT, Fujita E, Himeda Y (2012) Energy Environ Sci 5:7923–7926
49. Suna Y, Ertem MZ, Wang W-H, Kambayashi H, Manaka Y, Muckerman JT, Fujita E, Himeda Y (2014) Organometallics 33:6519–6530
50. Hull JF, Himeda Y, Wang W-H, Hashiguchi B, Periana R, Szalda DJ, Muckerman JT, Fujita E (2012) Nat Chem 4:383–388
51. Wang W-H, Muckerman JT, Fujita E, Himeda Y (2013) ACS Catal 3:856–860
52. Azua A, Sanz S, Peris E (2011) Chem Eur J 17:3963–3967
53. Jantke D, Pardatscher L, Drees M, Cokoja M, Herrmann WA, Kühn FE (2016) ChemSusChem 9:2849–2854
54. Munshi P, Main AD, Linehan JC, Tai C-C, Jessop PG (2002) J Am Chem Soc 124:7963–7971
55. Muller K, Sun Y, Heimermann A, Menges F, Niedner-Schatteburg G, van Wüllen C, Thiel WR (2013) Chem Eur J 19:7825–7834
56. Muller K, Sun Y, Thiel WR (2013) ChemCatChem 5:1340–1343
57. Lau CP, Chen YZ (1995) J Mol Catal A: Chem 101:33–36
58. Erlandsson M, Landaeta VR, Gonsalvi L, Peruzzini M, Phillips AD, Dyson PJ, Laurenczy G (2008) Eur J Inorg Chem 2008:620–627
59. Schmeier TJ, Dobereiner GE, Crabtree RH, Hazari N (2011) J Am Chem Soc 133:9274–9277
60. Evans GO, Newell CJ (1978) Inorg Chim Acta 31:L387–L389
61. Tai C-C, Chang T, Roller B, Jessop PG (2003) Inorg Chem 42:7340–7341
62. Federsel C, Boddien A, Jackstell R, Jennerjahn R, Dyson PJ, Scopelliti R, Laurenczy G, Beller M (2010) Angew Chem Int Ed 49:9777–9780
63. Ziebart C, Federsel C, Anbarasan P, Jackstell R, Baumann W, Spannenberg A, Beller M (2012) J Am Chem Soc 134:20701–20704
64. Federsel C, Ziebart C, Jackstell R, Baumann W, Beller M (2012) Chem Eur J 18:72–75
65. Langer R, Diskin-Posner Y, Leitus G, Shimon LJW, Ben-David Y, Milstein D (2011) Angew Chem Int Ed 50:9948–9952
66. Zhang Y, MacIntosh AD, Wong JL, Bielinski EA, Williard PG, Mercado BQ, Hazari N, Bernskoetter WH (2015) Chem Sci 6:4291–4299
67. Fong H, Peters JC (2015) Inorg Chem 54:5124–5135
68. Rivada-Wheelaghan O, Dauth A, Leitus G, Diskin-Posner Y, Milstein D (2015) Inorg Chem 54:4526–4538
69. Zhu F, Zhu-Ge L, Yang G, Zhou S (2015) ChemSusChem 8:609–612
70. Bertini F, Mellone I, Ienco A, Peruzzini M, Gonsalvi L (2015) ACS Catal 5:1254–1265
71. Bertini F, Gorgas N, Stöger B, Peruzzini M, Veiros LF, Kirchner K, Gonsalvi L (2016) ACS Catal 6:2889–2893
72. Jeletic MS, Mock MT, Appel AM, Linehan JC (2013) J Am Chem Soc 135:11533–11536
73. Jeletic MS, Helm ML, Hulley EB, Mock MT, Appel AM, Linehan JC (2014) ACS Catal 4:3755–3762
74. Kumar N, Camaioni DM, Dupuis M, Raugei S, Appel AM (2014) Dalton Trans 43:11803–11806
75. Watari R, Kayaki Y, Hirano S-I, Matsumoto N, Ikariya T (2015) Adv Synth Catal 357:1369–1373

76. Zall CM, Linehan JC, Appel AM (2015) ACS Catal 5:5301–5305
77. Zall CM, Linehan JC, Appel AM (2016) J Am Chem Soc 138:9968–9977
78. Badiei YM, Wang W-H, Hull JF, Szalda DJ, Muckerman JT, Himeda Y, Fujita E (2013) Inorg Chem 52:12576–12586
79. Tlili A, Blondiaux E, Frogneux X, Cantat T (2015) Green Chem 17:157–168
80. Haynes P, Slaugh LH, Kohnle JF (1970) Tetrahedron Lett 11:365–368
81. Schreiner S, Yu JY, Vaska L (1988) Inorg Chim Acta 147:139–141
82. Schreiner S, Yu JY, Vaska L (1988) J Chem Soc Chem Commun 9:602–603
83. Jessop PG, Hsiao Y, Ikariya T, Noyori R (1994) J Am Chem Soc 116:8851–8852
84. Jessop PG, Hsiao Y, Ikariya T, Noyori R (1996) J Am Chem Soc 118:344–355
85. Krocher O, Koppel RA, Baiker A (1997) Chem Commun 5:453–454
86. Schmid L, Canonica A, Baiker A (2003) Appl Catal A 255:23–33
87. Schmid L, Schneider M, Engel D, Baiker A (2003) Catal Lett 88:105–113
88. Zhang L, Han Z, Zhao X, Wang Z, Ding K (2015) Angew Chem Int Ed 54:6186–6189
89. Minato M, Zhou D-Y, Sumiura K-I, Hirabayashi R, Yamaguchi Y, Ito T (2001) Chem Commun 24:2654–2655
90. Tsai JC, Nicholas KM (1992) J Am Chem Soc 114:5117–5124
91. Hayashi H, Ogo S, Fukuzumi S (2004) Chem Commun 23:2714–2715
92. Zhao G, Joó F (2011) Catal Commun 14:74–76
93. Moret S, Dyson PJ, Laurenczy G (2014) Nat Commun 5:4017–4023
94. Lu S-M, Wang Z, Li J, Xiao J, Li C (2016) Green Chem 18:4553–4558
95. Rohmann K, Kothe J, Haenel MW, Englert U, Hölscher M, Leitner W (2016) Angew Chem Int Ed 55:8966–8969
96. Tominaga K-I, Sasaki Y (2000) Catal Commun 1:1–3
97. Jääskeläinen S, Haukka M (2003) Appl Catal A 247:95–100
98. Kontkanen M-L, Oresmaa L, Moreno MA, Jänis J, Laurila E, Haukka M (2009) Appl Catal A 365:130–134
99. Liu Q, Wu L, Fleischer I, Selent D, Franke R, Jackstell R, Beller M (2014) Chem Eur J 20:6888–6894
100. Srivastava VK, Eilbracht P (2009) Catal Commun 10:1791–1795
101. Ostapowicz TG, Schmitz M, Krystof M, Klankermayer J, Leitner W (2013) Angew Chem Int Ed 52:12119–12123
102. Wu L, Liu Q, Fleischer I, Jackstell R, Beller M (2014) Nat Commun 5:3091–3096
103. Balaraman E, Gunanathan C, Zhang J, Shimon LJW, Milstein D (2011) Nat Chem 3:609–614
104. Balaraman E, Ben-David Y, Milstein D (2011) Angew Chem Int Ed 50:11702–11705
105. Yang X (2012) ACS Catal 2:964–970
106. Han Z, Rong L, Wu J, Zhang L, Wang Z, Ding K (2012) Angew Chem Int Ed 51:13041–13045
107. Mellmann D, Sponholz P, Junge H, Beller M (2016) Chem Soc Rev 45:3954–3988
108. Miller AJM, Heinekey DM, Mayer JM, Goldberg KI (2013) Angew Chem Int Ed 52:3981–3984
109. Savourey S, Lefèvre G, Berthet J-C, Thuéry P, Genre C, Cantat T (2014) Angew Chem Int Ed 53:10466–10470
110. Neary MC, Parkin G (2015) Chem Sci 6:1859–1865
111. Sordakis K, Tsurusaki A, Iguchi M, Kawanami H, Himeda Y, Laurenczy G (2016) Chem Eur J 22:15605–15608
112. Tominaga K-I, Sasaki Y, Watanabe T, Saito M (1995) Bull Chem Soc Jpn 68:2837–2842
113. K. Tominaga, Y. Sasaki, M. Kawai, T. Watanabe, M. Saito, *Chem. Commun.* **1993**, 629-631
114. Tominaga K, Sasaki Y, Saito M, Hagihara K, Watanabe T (1994) J Mol Catal 89:51–56
115. Tominaga KI, Sasaki Y, Hagihara K, Watanabe T, Saito M (1994) Chem Lett 8:1391–1394
116. Li Y-N, Ma R, He L-N, Diao Z-F (2014) Catal Sci Technol 4:1498–1512
117. Choudhury J (2012) ChemCatChem 4:609–611
118. Huff CA, Sanford MS (2011) J Am Chem Soc 133:18122–18125
119. Kothandaraman J, Goeppert A, Czaun M, Olah GA, Prakash GKS (2013) J Am Chem Soc 138:778–781
120. Khusnutdinova JR, Garg JA, Milstein D (2015) ACS Catal 5:2416–2422
121. Wesselbaum S, vom Stein T, Klankermayer J, Leitner W (2012) Angew Chem Int Ed 51:7499–7502
122. Wesselbaum S, Moha V, Meuresch M, Brosinski S, Thenert KM, Kothe J, vom Stein T, Englert U, Holscher M, Klankermayer J, Leitner W (2015) Chem Sci 6:693–704

123. Qian Q, Cui M, He Z, Wu C, Zhu Q, Zhang Z, Ma J, Yang G, Zhang J, Han B (2015) Chem Sci 6:5685–5689
124. Thenert K, Beydoun K, Wiesenthal J, Leitner W, Klankermayer J (2016) Angew Chem Int Ed 55:12266–12269
125. Beydoun K, vom Stein T, Klankermayer J, Leitner W (2013) Angew Chem Int Ed 52:9554–9557
126. Li Y, Sorribes I, Yan T, Junge K, Beller M (2013) Angew Chem Int Ed 52:12156–12160
127. Beydoun K, Ghattas G, Thenert K, Klankermayer J, Leitner W (2014) Angew Chem Int Ed 53:11010–11014
128. Li Y, Yan T, Junge K, Beller M (2014) Angew Chem Int Ed 53:10476–10480

Top Curr Chem (Z) (2018) 376:1
https://doi.org/10.1007/s41061-017-0179-7

REVIEW

Photo- and Electrochemical Valorization of Carbon Dioxide Using Earth-Abundant Molecular Catalysts

Alonso Rosas-Hernández[1] · Christoph Steinlechner[1] · Henrik Junge[1] · Matthias Beller[1]

Received: 10 October 2017 / Accepted: 15 November 2017 / Published online: 6 December 2017
© Springer International Publishing AG, part of Springer Nature 2017

Abstract The dramatic increase in anthropogenic carbon dioxide emissions in recent decades has forced us to look for alternative carbon-neutral processes for the production of energy vectors and commodity chemicals. Photo- and electrochemical reduction of CO_2 are appealing strategies for the storage of sustainable and intermittent energies in the form of chemical bonds of synthetic fuels and value-added molecules. In these approaches, carbon dioxide is converted to products such as CO, HCOOH and MeOH through proton-coupled electron transfer reactions. The use of earth-abundant elements as components of the catalytic materials is crucial for the large-scale applicability of this technology. This review summarizes the most recent advances related to this issue, with particular focus on studies where molecular metal complexes are used as catalysts. In addition, with the aim of aiding in the design of more robust and efficient non-noble metal-based catalysts, we discuss the lessons learned from the corresponding mechanistic studies.

Keywords CO_2 reduction · Molecular catalysts · Earth-abundant metals · Photocatalysis · Electrocatalysis

---

Chapter 7 was originally published as Rosas-Hernández, A., Steinlechner, C., Junge, H. & Beller, M. Top Curr Chem (Z) (2018) 376: 1. https://doi.org/10.1007/s41061-017-0179-7.

✉ Matthias Beller
Matthias.Beller@catalysis.de

[1] Leibniz-Institute for Catalysis at the University of Rostock, Albert-Einstein-Straße 29a, 18059 Rostock, Germany

1 Introduction

Over the past 150 years, societal development has been largely powered by the combustion of non-renewable fossil fuels, and our current standard of living is clearly a result of numerous innovations driven by the energy obtained from these fuels. However, the global supply of such resources is not limitless, and with the ever-expanding global population, the world energy demand continues to increase [1]. In 2015, total world energy consumption was 13,147 Mtoe (million tonnes of oil equivalent), or 5.50×10^{20} J, equal to average power consumption of 17.5 TW [2]. Energy demands are projected to increase by 37% between 2013 and 2035, with average growth of 1.4% per year [3]. Approximately 86% of this energy is obtained from oil, coal, and natural gas in roughly equal parts. In addition, due to the excessive consumption of such fossil fuels, the concentration of atmospheric carbon dioxide (CO_2) has increased, with values now exceeding 400 ppm, which contributes to the ongoing changes in our planet's climate. It is clear, therefore, that in order to stop the continued accumulation of CO_2 in the atmosphere and to realize world energy goals, a shift towards carbon-neutral, secure, and renewable energy sources is crucial [4].

On a global scale, sunlight is one of the few energy sources that can meet the projected human energy demands in an environmentally and socially responsible manner. Solar energy reaches the surface of the earth at a rate of 120,000 TW [5], far exceeding the global rate of human energy consumption. The use of sunlight as an energy source requires systems with the ability to capture, convert, and store such energy. The capacity for storage is a fundamental need, given the temporal mismatch between solar irradiance and human energy demands. Nature provides us with proof that solar energy conversion can be performed on such a large scale. Photosynthesis stores solar energy in reduced carbon compounds at a rate of 120 TW [6], and in the process of cellular respiration, these solar fuels are efficiently oxidized using oxygen as the terminal electron acceptor. The blueprints provided by photosynthesis and cellular respiration have enabled the development of energy infrastructure for the capture of solar energy and its storage in chemical compounds.

In this context, the catalytic conversion of carbon dioxide into fuels and organic materials using either light or electric current as energy input is an important strategy that not only reduces atmospheric CO_2 levels, but also provides a pathway for the replacement of fossil fuels [7]. Energy transportability is a particularly important issue in the development of energy conversion technologies. The fact that liquid products from the photo- or electrochemical reduction of CO_2, such as methanol and formic acid, can be easily transported from the production site to where they are needed is a major advantage of this technology [8–10].

Carbon dioxide is the ultimate product of oxidation of carbon-based compounds, and it is an extremely thermodynamically stable molecule. Thus, the recycling of carbon dioxide to create useful products is a challenging process that requires a large energy input. Despite the linear symmetry and overall nonpolar nature of the molecule, some chemical reactivity may be anticipated, associated with either the presence of the π-electron density of the double bonds, the lone pairs of electrons on the oxygen atoms, or the electrophilic nature of the carbon atom. Thus, one possible means of activating carbon dioxide is through modification of its electronic and geometric properties via direct coordination to a metal center of a molecularly defined catalyst. In this case, the energy barriers for the corresponding proton-coupled electron transfer reactions are lowered, allowing the catalytic reduction of CO_2 (vide infra).

The energy requirements for CO_2 reduction are highly sensitive to pH and to the number of electrons required for the half-reactions, as shown for pH 7 vs. NHE in Fig. 1 [11]. The reduction of CO_2 by one electron to form CO_2^- is an extremely unfavorable process, having a formal reduction potential of −1.90 V (Eq. 1), due at least in part to the kinetic restrictions imposed by the structural difference between linear CO_2 and bent CO_2^- [12]. An alternative and more favorable pathway for reducing CO_2 is through proton-coupled electron transfer (PCET) reactions, since thermodynamically more stable molecules are produced (Eqs. 2–7). Because they involve protons, these reactions are more favorable at low pH [13]. However, it should be noted that according to the redox potentials of reactions in Eqs. (2), (3), (4) and (9), any catalyst that reduces CO_2 to carbon monoxide or formate is also thermodynamically capable of reducing H^+ to H_2. Thus, when reduction of CO_2 is carried out at low pH values, generation of H_2 is favored, and the selectivity for CO_2 reduction is diminished.

One major challenge in proton-assisted multi-electron reduction of CO_2 to liquid fuels is the formation of chemical bonds to transform the simple CO_2 molecule into more complex and energetic molecules such as methanol (Eq. 6) and methane (Eq. 7). Although the synthesis of such molecules from CO_2 is thermodynamically more favorable than the formation of carbon monoxide, the difficulty in transferring multiple electrons to the site of reduction limits the feasibility of the process. Accordingly, $2H^+/2e^-$ reduction products, namely formic acid and carbon monoxide, are generally obtained in the reaction. While CO is a useful chemical

$$CO_2 + e^- \longrightarrow CO_2^- \qquad E^0 = -1.90\ V \qquad (1)$$

$$CO_2 + 2H^+ + 2e^- \longrightarrow CO + H_2O \qquad E^0 = -0.53\ V \qquad (2)$$

$$CO_2 + 2H^+ + 2e^- \longrightarrow HCO_2H \qquad E^0 = -0.61\ V \qquad (3)$$

$$CO_2 + H^+ + 2e^- \longrightarrow HCO_2^- \qquad E^0 = -0.43\ V \qquad (4)$$

$$CO_2 + 4H^+ + 4e^- \longrightarrow HCHO + H_2O \qquad E^0 = -0.48\ V \qquad (5)$$

$$CO_2 + 6H^+ + 6e^- \longrightarrow CH_3OH + H_2O \qquad E^0 = -0.38\ V \qquad (6)$$

$$CO_2 + 8H^+ + 8e^- \longrightarrow CH_4 + 2H_2O \qquad E^0 = -0.24\ V \qquad (7)$$

$$2H_2O \longrightarrow O_2 + 4H^+ + 4e^- \qquad E^0 = 0.82\ V \qquad (8)$$

$$2H^+ + 2e^- \longrightarrow H_2 \qquad E^0 = -0.41\ V \qquad (9)$$

Fig. 1 Energy requirements for reducing carbon dioxide through proton-coupled electron transfer reactions. All potentials are reported vs. NHE at pH 7 and can be converted into liquid hydrocarbons via the Fischer–Tropsch reaction with H_2, formic acid has recently garnered attention as a carrier of H_2 because it is liquid at ambient temperatures and can be converted into H_2 and CO_2 in the presence of catalysts under moderate conditions [14].

In this book work, we review the use of molecularly defined catalysts for the photo- and electrochemical conversion of carbon dioxide to useful products. Considering the obvious advantages in integrating the corresponding molecular catalysts into devices for economically viable applications, we aim to highlight the recent developments in the use of earth-abundant metal complexes as CO_2 reduction catalysts. The first section is devoted to the molecular electrochemical reduction of CO_2, while the second section is focused on photochemical approaches.

2 Electrochemical Reduction of CO_2

Electrochemical systems for the reduction of carbon dioxide to liquid fuels require the application of an external bias or current to supply the electrons for reducing CO_2 [15–17]. Instead of using a sacrificial reductant, as in the case of the photochemical reduction of CO_2 (vide infra), the corresponding oxidation occurs at the counter electrode. In some cases, the cathodic and anodic reactions are separated in a two-compartment cell to avoid reoxidation of the species derived from the reduction of CO_2. Although the use of a sacrificial electron donor is not necessary, the presence of Lewis and Brønsted acids enhances catalysis considerably [18]. In a broad sense, electrocatalysts are electron transfer molecules that ideally operate near the thermodynamic potential of the reaction to be driven (e.g. reduction of CO_2 to CO). Direct electrochemical reduction on most electrode surfaces requires a large overpotential (η), which reduces conversion efficiency. The overpotential can be considered as the difference between the applied electrode potential, V_{applied}, and the potential of the chemical reaction, E^0 (products/substrates), at a given current density.

The use of an electrocatalyst is essential to achieving efficient reactivity and selectivity. Such a molecule is involved in the electron transfer process at the cathode and also accelerates the chemical reaction. Fast kinetics for both processes are a necessary condition for an efficient electrocatalyst. In addition, a thermodynamic match between the redox potential for the electron transfer at the cathode and the chemical reaction that is being catalyzed is crucial for the catalytic efficiency of the system. All these factors can be optimized through chemical tuning of the electrocatalyst by screening different metal centers with the appropriate ligand. Reaction rates for these processes can be estimated from the steady-state limiting current in cyclic voltammetry (CV), or by rotating-disk voltammetry studies of the heterogeneous electron transfer kinetics. The electrocatalytic activity can be easily observed in CV. In a CV under an inert atmosphere, an electrocatalyst should show a wave corresponding to the reversible redox couple $\text{Cat}^{n+/0}$. Upon addition of CO_2, the current of the CV should increase significantly, while the potential shifts anodically, and reversibility in the return oxidation wave is lost due to a reaction between CO_2 and the electrocatalyst. Thus, the use of electrocatalysts as mediators in the electrochemical reduction of CO_2 lowers the overpotential, improves selectivity, and increases the reaction kinetics.

2.1 Mn Complexes

In 1984, Lehn and coworkers first introduced the use of $[Re(bpy)(CO)_3Cl]$-type complexes as catalysts for the electrochemical reduction of carbon dioxide [19]. When bulk electrolysis experiments were performed in DMF-H_2O (10%) at -1.25 V vs. NHE, carbon monoxide was observed as the only product, with faradaic efficiency (FE) of up to 98%. Following on this seminal work, Deronzier and coworkers in 2011 reported the use of $[Mn(bpy)(CO)_3Br]$ **1** (Fig. 2) as electrocatalyst for the selective reduction of CO_2 to CO [20]. On the basis of CV studies using tetrabutylammonium perchlorate (TBAP) in MeCN as the supporting electrolyte and under an Ar atmosphere, it was proposed that after the one-electron reduction of complex **1** and immediate loss of bromide anion Br^-, a dimer species $[Mn(bpy)(CO)_3]_2$ (**2**) was formed. Subsequent reduction of the dimer species resulted in the formation of $[Mn(bpy)(CO)_3]^-$ (**3**). The formation of dimer **2** had already been shown for **1** by IR and UV/Vis spectroelectrochemical experiments in tetrahydrofuran (THF) electrolytes [21].

The electrochemical behavior of **1** in an acetonitrile solution saturated with CO_2 showed no significant differences between the first two reduction events observed under an Ar atmosphere. On the other hand, the presence of 5% v/v H_2O induced a dramatic change, with strong enhancement of the cathodic current at the second reduction event, evidence of the involvement of the reduced Mn dimer **2** as the active species in the electrocatalytic process. Controlled potential electrolysis of a solution containing the complex **1** at a concentration of 1 mM in MeCN/H_2O (95/5) under CO_2 confirmed the catalytic activity of such a complex. Carbon monoxide was observed as the only product of the reaction, with FE $> 99\%$. Compared with its rhenium analogue, electrocatalyst **1** reduced CO_2 at markedly lower overpotential (a gain of 0.40 V), while selectivity and FE for the production of CO were almost identical. This represented a major advantage, since manganese is 1.3 million times as abundant as rhenium in the Earth's crust, at 950 mg Mn/kg crust versus only 7×10^{-4} mg Re/kg crust [22]. This fact becomes important when the cost of scale-up and the environmental ramifications of mining large quantities of raw material are considered.

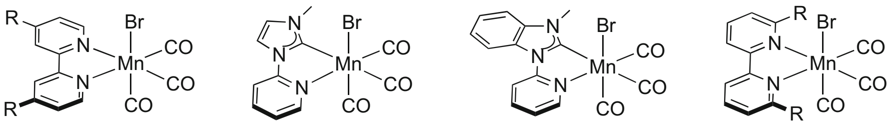

1 R= H
4 R= *t*Bu

7

8

9 R = Mes

Fig. 2 Molecular structures of Mn-based catalysts used in the electrochemical reduction of CO_2

In 2013, and stemming from the work of Deronzier, Kubiak and coworkers modified complex **1** by replacing the bipyridine ligand with 4,4′-di-*tert*-butyl-2,2′-bipyridine (bpy-*t*Bu). The resulting complex Mn(bpy-*t*Bu)$(CO)_3$Br (**4**) was a robust, selective, and efficient catalyst for the reduction of CO_2 to CO [23]. The addition of Brønsted acids to a CO_2-saturated solution of **4** and subsequent reduction of the complex led to the stable and efficient production of CO from CO_2. Three different weak acids were used (H_2O, MeOH, and TFE), and the catalytic current increased in cyclic voltammograms as the acid strength was increased. In particular, when 2,2,2-trifluoroethanol (1 M) was used, current densities of up to 30 mA/cm^2 were observed during bulk electrolysis at -2.2 V vs. SCE using **4** (5 mM) and a glassy carbon working electrode in MeCN. In all cases, carbon monoxide was selectively produced, with no observable production of H_2. The role of the corresponding dimer [Mn(bpy-*t*Bu)$(CO)_3]_2$ (**5**) and anionic [Mn(bpy-*t*Bu)$(CO)_3]^-$ (**6**) species as catalytic intermediates was confirmed with the assistance of infrared spectroelectrochemistry (IR-SEC) and X-ray crystallographic studies.

With the aim of exploring a ligand platform other than the commonly used bipyridine scaffold, Agarwal and coworkers in 2014 introduced the first manganese *N*-heterocyclic carbene complexes as catalysts for the CO_2-to-CO electrochemical conversion [24]. Surprisingly, complexes **7** and **8** mediated the reduction of carbon dioxide following a two-electron reduction step, as observed in the CV and preparative-scale electrolysis experiments. This is in contrast to the previously observed behavior of **1** and **4**, where two sequential single-electron reduction events were necessary prior to the formation of the catalytically active species. In addition, even though the strong σ-donor character of the NHC ligands pushed the reduction potentials cathodic, both species **7** and **8** exhibited catalytic current enhancement under a CO_2 atmosphere at voltages comparable to **1**. As previously observed with other Mn-based catalysts, carbon monoxide was selectively produced, with rather low FE of 35%, during bulk electrolysis experiments using TBAP and MeCN/H_2O (95/5) as supporting electrolyte.

With the goal of improving the aforementioned manganese electrocatalysts in terms of increased activity and reduced overpotential, Kubiak and coworkers designed and synthesized complex **9**, where a sterically demanding bipyridine ligand, 6,6′-dimesityl-2,2′-bipyridine (mesbpy), was utilized to eliminate dimerization during the catalytic cycle [25]. As expected, complex **9** displayed a single two-electron reduction wave under nitrogen, with no evidence of dimerization. The corresponding anionic [Mn(mesbpy)$(CO)_3]^-$ (**10**) species was formed at -1.6 V vs. Fc^+/Fc, which corresponds to 300 mV more positive potential than in the case of catalyst **1**. IR-SEC experiments and chemical reduction experiments with KC_8 unambiguously corroborate the role of **10** as a catalytic intermediate. Controlled potential electrolysis at -2.2 V vs. Fc^+/Fc with 0.3 M TFE resulted in the selective production of CO from CO_2 with FE of $> 98\%$. Unfortunately, when the anionic complex **10** binds CO_2 with H^+, catalytic activity does not occur until a ca. 400 mV more negative potential, which results in no decrease in catalytic overpotential when compared to complex **1**.

It was recently reported that the use of Lewis acids, specifically Mg^{2+} cations, significantly reduces the required overpotential for the electrochemical reduction of

CO_2 to CO when complex **9** is used as catalyst [18]. In fact, carbon dioxide reduction proceeded at the same potential as CO_2 binding (ca. -1.6 V vs. Fc^+/Fc), which translates to one of the lowest overpotentials ever reported for a molecular electrocatalyst ($\eta = 0.3$–0.45 V). Based on variable-concentration CV studies, IR-SEC experiments, and controlled potential electrolysis, it was proposed that catalysis with added $Mg(OTf)_2$ proceeds via a reductive disproportionation mechanism of $2CO_2 + 2e^- \rightarrow CO + CO_3^{2-}$.

An important strategy in the development of molecular electrocatalysts for energy storage is the incorporation of functional groups in the second coordination sphere of the catalyst that can directly interact with substrates bound to the metal during a catalytic cycle, which facilitates crucial reaction steps such as H–H bond heterolysis and hetero-formation, intra- and intermolecular proton transfer, and coupling of proton and electron transfer [26]. In this regard, the research groups of Gobetto and Bocarsly independently reported the synthesis of a Mn complex featuring a pendant phenolic group in the second coordination sphere, with the intention of directly stabilizing the O atom of the CO_2 molecule through hydrogen bonding (Fig. 3) [27, 28]. In the case of Gobetto and coworkers, a Mn(I) tricarbonyl complex containing two hydroxyl groups (**10**) was synthesized, and its electrochemical behavior towards CO_2 reduction was tested. In contrast to the catalytic behavior of the aforementioned Mn-based catalysts, complex **10** was able to drive the electrochemical reduction of CO_2 to CO in the absence of Brønsted acid additives [27]. This is explained by the proximity of protons to the active site rather than their bulk concentration in solution. An unusual selectivity for manganese electrocatalysts was observed when bulk electrolysis experiments at -1.8 V vs. SCE were performed with **10** in anhydrous MeCN, giving a mixture of CO (70%) and HCOOH (22%).

Bocarsly and coworkers designed and prepared a manganese complex with the ligand 6-(2-hydroxyphenyl)-bpy, containing only one pendant hydroxyl group (**11**) [28]. Although the catalytic behavior in the absence of added Brønsted acids was not tested, production of CO from CO_2 with FE of 76% was observed during electrolysis experiments using **11** (1 mM) at -1.5 V vs. SCE in $MeCN/H_2O$ (95/5). Based on the results of CV studies, it was reported that catalyst **11** exhibited over seven times the catalytic current density of $MnBr(bpy)(CO)_3$ (**1**) at roughly the same overpotential. Theoretical computations suggest that the origin of the increased

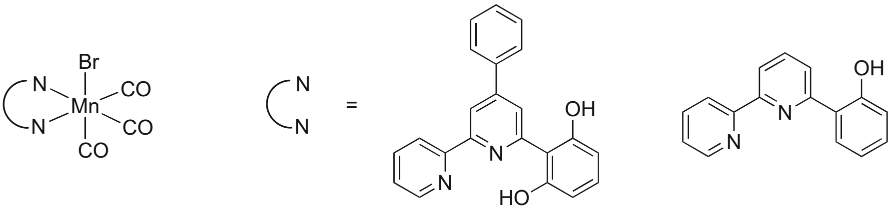

10

11

Fig. 3 Manganese electrocatalysts featuring pendant hydroxyl functional groups in the second coordination sphere activity is the result of an intramolecular mechanism for the corresponding proton-assisted dehydration of the catalytic intermediate [Mn(6-(2-hydroxyphenyl)-bpy)$(CO)_3$COOH] (**12**). Since the addition of pendant hydroxyl groups in the second coordination sphere of Mn-based complexes **10** and **11** did not render catalytic systems capable of operating at lower overpotentials than [Mn(bpy)$(CO)_3$-Br] (**1**), additional research is still needed in this area.

2.2 Fe Complexes

Iron-based molecular electrocatalysts for the conversion of CO_2 to CO rely almost exclusively on porphyrin-based ligand platforms [18]. In terms of catalytic activity, selectivity, and overpotential, iron(0) porphyrin complexes represent the state of the art in the homogeneous electrocatalytic reduction of CO_2 [8, 29]. The first report in this area was in 1991 by Savéant and coworkers, who claimed that iron(0) porphyrin **12** (Fig. 4) was able to drive the electrochemical conversion of CO_2 to CO at −1.8 V vs. SCE in DMF [30]. In 1996, the same research group reported that electrocatalysis was significantly improved in terms of both efficiency and lifetime in the presence of weak Brønsted acids [31]. The reported system did, however, require reduction potentials that were still too negative for practical use (ca. −1.5 V vs. SCE). More importantly, these seminal contributions paved the way for future developments within the framework of iron-based molecular electrocatalysts.

In 2012, Savéant and coworkers reported a breakthrough in the area of molecular catalysts for CO_2 electroreduction [32]. They found that iron complex **13**, featuring phenolic groups in all ortho and ortho' positions of the phenyl groups, was considerably more active than electrocatalyst **12** for the conversion of carbon dioxide to CO. For instance, when CV experiments were carried out using complex **13** (1 mM) with a CO_2-saturated DMF solution containing 2 M H_2O, a 60-fold increase in catalytic current at −1.33 V vs. NHE was observed relative to the corresponding experiments under an Ar atmosphere. This is indicative of a fast

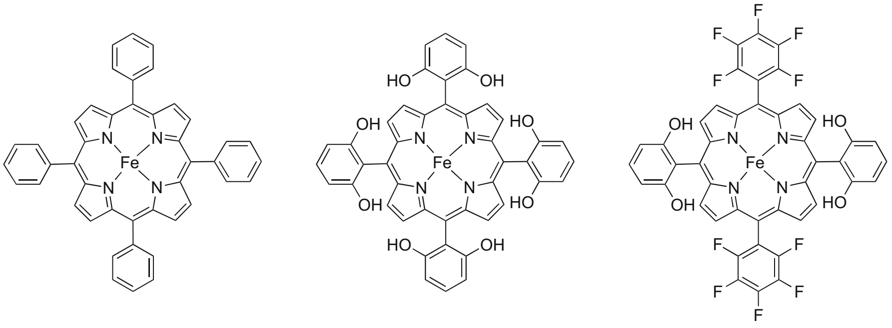

12 **13** **14**

Fig. 4 Molecular structures of iron tetraphenylporphyrin complexes used as molecular catalysts in the electrochemical reduction of CO_2

catalytic reaction. In fact, preparative-scale CO_2 electrolysis at -1.16 V vs. NHE resulted in the formation of CO with FE of 94% and average current density of 0.31 mA/cm^2, which corresponds to logTOF $= 3.5$ [33]. The catalyst also displayed remarkably robustness: no degradation of the iron complex was observed after 50 million turnovers at low overpotential (465 mV), which were achieved in only 4 h of electrolysis. Based on mechanistic investigations, it was unambiguously shown that the basis for the enhanced activity was the high local concentration of protons associated with the phenolic hydroxyl substituents around the iron center [34].

In a further development, Savéant and coworkers prepared an iron porphyrin complex by substituting two of the opposite phenyl rings of tetraphenylporphyrin with ortho-, ortho'-phenol groups while replacing the other two phenyl groups with perfluorinated arenes (**14**) [35]. This complex proved to be an excellent catalyst with respect to selectivity, overpotential, and turnover frequency for the conversion of CO_2 to CO. For instance, CV experiments using **14** (1 mM) in a CO_2-saturated DMF solution containing 1 M PhOH resulted in a 120-fold increase in catalytic current at -1.28 V vs. NHE relative to the corresponding experiments under an Ar atmosphere. Fixed-potential electrolysis at -1.08 V vs. NHE with 1 mM **14** under CO_2 in the presence of 3 M PhOH was marked by stable CO production over 3 h, with faradaic yields $> 99\%$ and no visible degradation of the iron complex. Fluorine substitution upon switching from **13** to **14** proved to be a successful strategy, with improved catalytic efficiency and overpotential, thanks to the inductive effect of the fluorine substituents.

In 2015, Naruta and coworkers reported the use of a cofacial iron tetraphenylporphyrin dimer **15** for the selective electrochemical reduction of carbon dioxide to CO (Fig. 5) [36]. This electrocatalyst was inspired by the metalloenzyme carbon monoxide dehydrogenase (CODH), which features a Ni–Fe dinuclear complex at its active center and cooperatively promotes the selective interconversion of CO_2 and CO at extremely low overpotentials [37]. CV experiments showed a strong catalytic current at -1.46 V vs. NHE in the presence of CO_2 when a solution of **15** (0.5 mM)

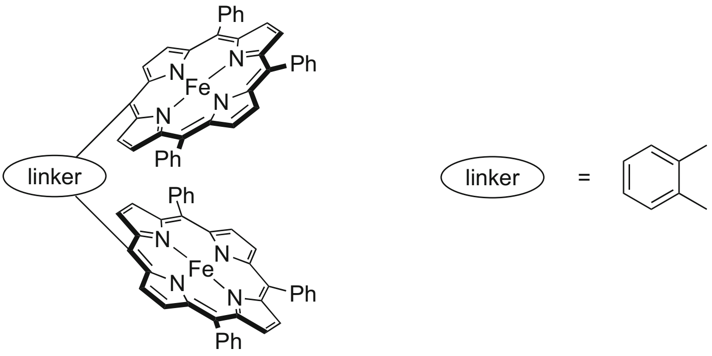

15

Fig. 5 Chemical structure of the iron porphyrin dimer used in the electrocatalytic reduction of carbon dioxide in DMF/H_2O (10%) was employed with the cofacial iron tetraphenylporphyrin dimer **15**. This indicated a catalytic process once the Fe^{+}–Fe^{0} porphyrin species was electro-generated. Bulk electrolysis experiments at −1.35 V vs. NHE confirmed the catalytic activity of the iron dimer. In this case, after 10 h of electrolysis reaction, carbon monoxide was obtained with FE of 88%, and hydrogen with 12%. The high activity, selectivity, and stability of **15** can be plausibly attributed to the resulting cavity between the two iron centers, where a molecule of CO_2 can be easily embedded. The double interaction of the CO_2 molecule with the metallic active centers facilitates a push–pull mechanism, where one Fe center acts as a Lewis base to push an electron pair to the coordinated CO_2, and the second Fe center acts as a Lewis acid to promote C–O bond cleavage and the formation of CO.

Most of the iron-based molecular catalysts employed in the electrochemical reduction of CO_2 produce CO as product. However, in terms of energy vectors, HCOOH is by far a more interesting product [14]. In this context, Berben and coworkers showed that the iron carbonyl cluster $[Fe_4N(CO)_{12}]^-$ (**16**, Fig. 6) was a selective electrocatalyst for the reduction of CO_2 to formate in aqueous solutions [38, 39]. During controlled potential electrolysis at −1.2 V vs. SCE and pH 7, electrocatalyst **16** produced formate with a high current density of 4 mA cm^{-2} for over 24 h, and FE of 96%. According to thermochemical measurements performed using IR-SEC, the difference between the hydride donor ability of the catalytic intermediate $[HFe_4N(CO)_{12}]^-$ in MeCN and aqueous buffered solutions is key to explaining the high and rather unusual selectivity for the electroreduction of CO_2 in water when complex **16** is used. An attempt to increase the catalytic activity of iron cluster **16** by adding a pendant hydroxyl group in the second coordination sphere of the catalyst was reported in 2016 [40]. Unfortunately, the resulting iron cluster **17** was no longer active for the electrocatalytic reduction of CO_2, and in this case, protons were selectively reduced to H_2 even in the presence of CO_2.

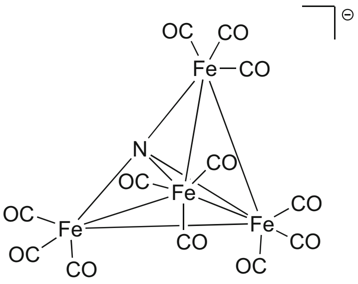

16

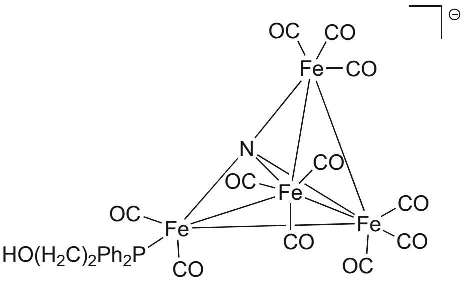

17

Fig. 6 Molecular structures of iron carbonyl clusters used as electrocatalysts for the conversion of CO_2 to formate in water

2.3 Ni and Co Complexes

Based on the seminal work of Sauvage and colleagues with $[Ni(cyclam)]^{2+}$ (cyclam = 1,4,8,11-tetraazacyclotetradecane) and related macrocyclic complexes showing high selectivity for the activation of CO_2 over H_2O under reductive electrocatalytic conditions [41], several Ni-based catalysts have recently been developed [42]. For instance, Chang and coworkers reported the synthesis of a series of nickel(II) complexes supported by *N*-heterocyclic carbene–pyridine ligands (**18**–**20**, Fig. 7) and their ability to drive the CO_2-to-CO electrochemical conversion with high selectivity for the activation of CO_2 over H_2O [43]. However, CV studies under a CO_2 atmosphere using mixtures of MeCN/H_2O clearly showed rather low efficiency for the reduction of CO_2.

In a work by Fujita and coworkers, a series of molecular complexes similar in structure to $[Ni(cyclam)]^{2+}$ were reported as efficient electrocatalysts for the selective reduction of CO_2 to CO in aqueous solutions [44]. For instance, complex **21** produced CO with FE of 88% at −0.96 V vs. NHE and pH 5. As expected, when the pH of the supporting electrolyte was lowered to values less than 2, the electrochemical reduction of CO_2 was no longer selective, and a 1:1 mixture of CO:H_2 was produced during controlled potential experiments, although the FE remained unchanged, at 88%.

In 2015, Sun and coworkers reported the synthesis of a planar nickel complex coordinated with a pincer-type carbene–pyridine–carbene ligand (**22**) and its use as electrocatalyst for the generation of CO from carbon dioxide [45]. According to long-term controlled potential electrolysis of **22** at −1.773 V vs. Fc^+/Fc for 2 h in CO_2-saturated MeCN with 0.4 mM H_2O, only CO was produced as the major product, and no detectable H_2 was obtained via gas chromatographic analysis. As in the case of nickel complexes **18**–**20**, the catalytic efficiency of **22** was moderated, as observed in the CV studies under a CO_2 atmosphere.

Peters and coworkers explored electrochemical CO_2 reduction using a cobalt complex supported by a redox-active pyridyldiimine ligand platform (**23**, Fig. 5) [46]. Specifically, the authors showed that when H_2O was employed as the proton source (10 M in MeCN), CO was produced with FE of 45% near the $Co^{I/0}$ redox couple for **23** ($E_{1/2} = -1.88$ V vs. Fc^+/Fc) and simultaneous H_2 evolution (FE = 30%). X-ray photoelectron spectroscopy (XPS) measurements of glassy

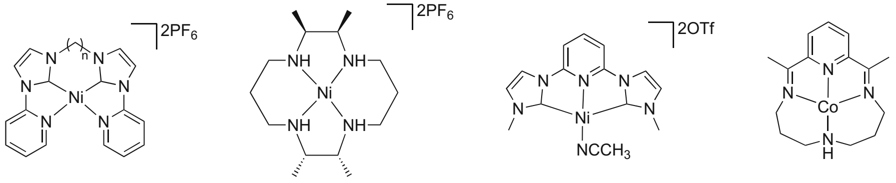

18 n = 1
19 n = 2
20 n = 3

21

22

23

Fig. 7 Chemical structures of Ni- and Co-based electrocatalysts for electrochemical CO_2-to-CO conversion carbon electrodes after controlled potential electrolysis experiments supported the assertion of the molecular nature of the cobalt active species rather than an electrodeposited film. The ability to store electrons in the structure of the pyridyldiimine ligand of **23** during electrocatalysis was confirmed by X-ray crystallography and theoretical studies.

3 Photochemical Reduction of CO_2

Systems applied for light-driven CO_2 reduction usually include a catalyst (CAT), responsible for CO_2 coordination and its subsequent reduction; a sacrificial electron donor (SD), which is consumed stoichiometrically; and a photosensitizer (PS) that mediates the electron transfer from the SD to the CAT (Fig. 8). Two mechanisms by which the excited PS is quenched are known. In oxidative quenching, an electron from the PS* is transferred directly to the catalyst, whereby the PS is oxidized, and the active, reduced form of the catalyst is generated. In the second step, the original PS is regained by donation of an electron from the SD to the PS^+. In the reductive mechanism, the excited PS is first reduced by an SD molecule to form PS^- and SD^+. This electron is then transported to the neutral catalyst to generate the active CAT^-. The preference for one mechanism over the other is strongly dependent on the redox potentials of the particular species of the CAT, PS and SD.

Ruthenium complexes ($Ru(N^\wedge N)_3$) bearing diimine ligands such as 2,2′-bipyridine (bpy) or phenanthroline, along with cyclometalated iridium complexes $Ir(C^\wedge N)_3$) such as $Ir(ppy)_3$ (ppy = 2-phenylpyridine) and their derivatives, are widely used as light-harvesting components (Fig. 9). Due to their absorption in the visible light range and their strong internal heavy atom effect (triplet MLCT), high quantum efficiency in photocatalysis will be achieved [47]. To find fully earth-abundant systems employing a CAT and a PS containing non-precious metal

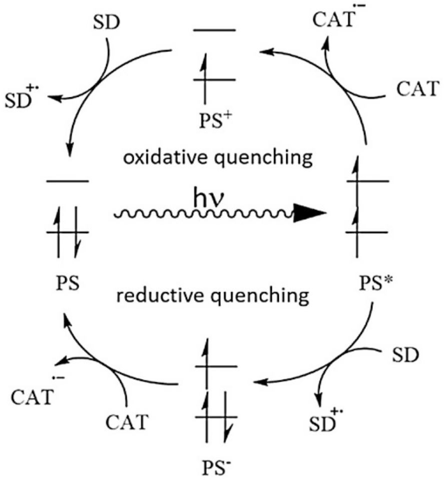

Fig. 8 Oxidative and reductive quenching mechanisms during the photochemical reduction of CO_2

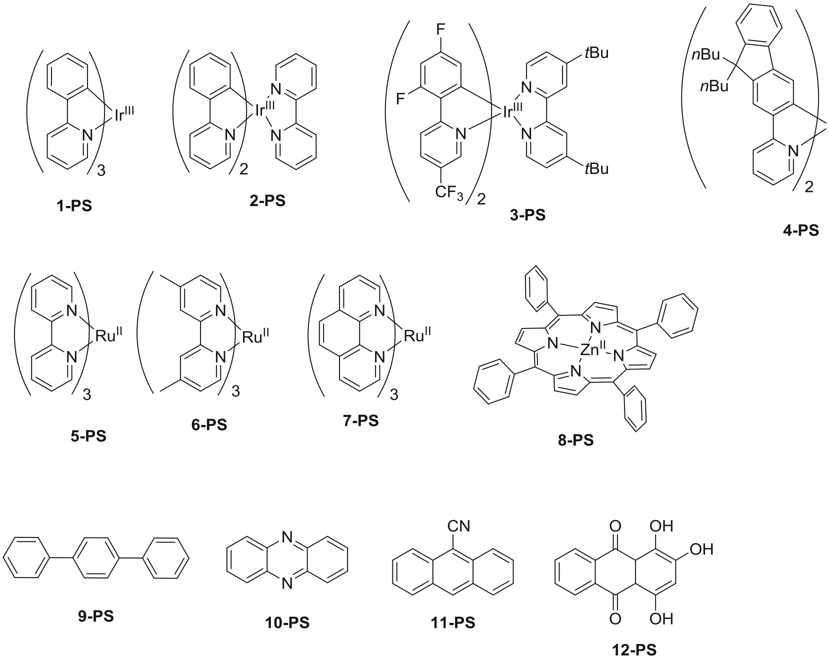

Fig. 9 Molecular structures of transition metal complexes and organic dyes used as photosensitizers in the photochemical reduction of CO_2

centers, heteroleptic emissive copper(I) complexes ligated by a diphosphine (e.g. xantphos) and a diimine (phenanthroline derivatives) applied as PS were developed by Beller, originally for proton reduction [48, 49], and by Ishitani (Fig. 10) [50].

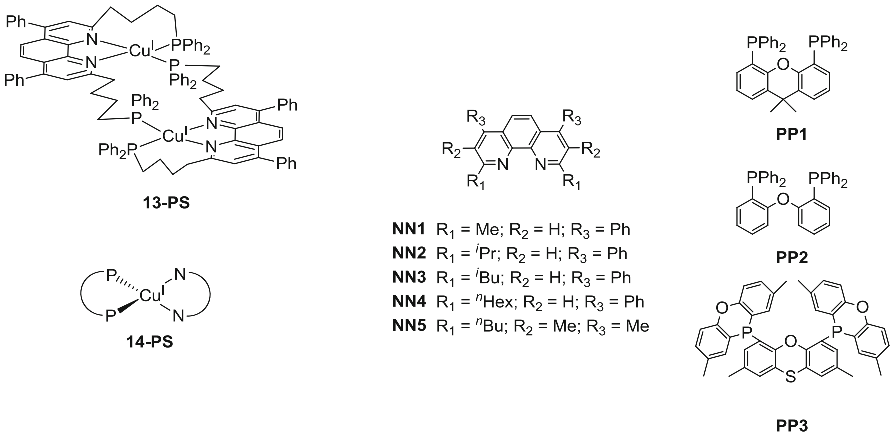

Fig. 10 Molecular structures of Cu-based complexes used as photosensitizers in the photochemical reduction of CO_2

For the conversion of carbon dioxide into highly valuable molecules (CO, HCOOH), the application of an SD is imperative (Fig. 11). It provides either the PS (reductive quenching) or the catalyst (oxidative quenching) with an electron. Amines and ascorbic acid continue to be used in homogeneous CO_2 reduction. Researchers have reported ongoing challenges in employing water as a simple and green electron donor and combining CO_2 reduction with water oxidation in an effort to mimic photosynthesis [51].

3.1 Mn Complexes

The first photochemical reduction of carbon dioxide with a homogeneous manganese catalyst was reported in 2014 by Ishitani's group using a system consisting of a solution of DMF/TEOA or MeCN/TEOA (25% v) containing fac-$Mn(bpy)(CO)_3Br$ (**1**) as CAT (0.05 mM), **6-PS** (0.05 mM) as PS, and BIH as SD (0.1 M). After irradiation for 12 h with monochromatic light (480 nm), formate was formed as the main product ($TON_{HCOOH} = 157$), along with carbon monoxide ($TON_{CO} = 12$) and hydrogen ($TON_{H_2} = 8$) as by-products. The product that was preferentially produced was dependent on the solvent. In the case of acetonitrile, the formation of formate was drastically reduced ($TON_{HCOOH} = 78$), while the quantity of carbon monoxide and hydrogen ($TON_{CO} = 40$; $TON_{H_2} = 17$) increased. Thus, it is obvious that the solvent has a strong influence on the selectivity of the system [52]. During irradiation, dimerization takes place after reductive quenching of $RuPS^-$. Dimerization of the one-electron-reduced species was previously reported for electrocatalytic CO_2 reduction with **1-Mn** as catalyst [20] (Fig. 12).

In 2015, Kubiak et al. reported a heterogeneous manganese-bipyridine system (**26**) for the photocatalytic reduction of CO_2. Instead of employing a common bipyridine as a ligand, a 5,5′-dicarboxylate-2,2′-bipyridine was used, which ligated Zr(IV) ions to form a stable metal–organic framework (UiO-67; University of Oslo) which was doped with $Mn(bpy)(CO)_3Br$ (Fig. 13). After 18 h of irradiation with monochromatic light (470 nm; $2.51*10^{-7}$ einstein s^{-1}), formate was the main product ($TON_{HCOO} = 110$), with selectivity of 99%, while carbon monoxide ($TON_{CO} = 14.5$) and hydrogen ($TON_{H2} = 1$) were by-products. An overall quantum yield of 13.8% was calculated. The photocatalytic reaction took place in a mixture of DMF/TEOA (4:1 v/v) with 0.5 mM CAT, 0.5 mM **6-PS** as PS, and 0.2 M BNAH as SD. After the reaction, the catalyst was recovered from the solution and reused in a subsequent experiment (TON_{HCOO} after 4 cycles = 170). This

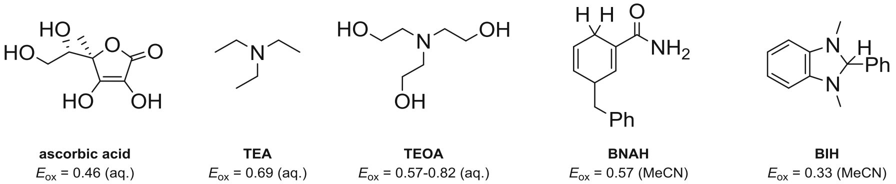

Fig. 11 Chemical structures of sacrificial electron donors used in the photochemical reduction of CO_2

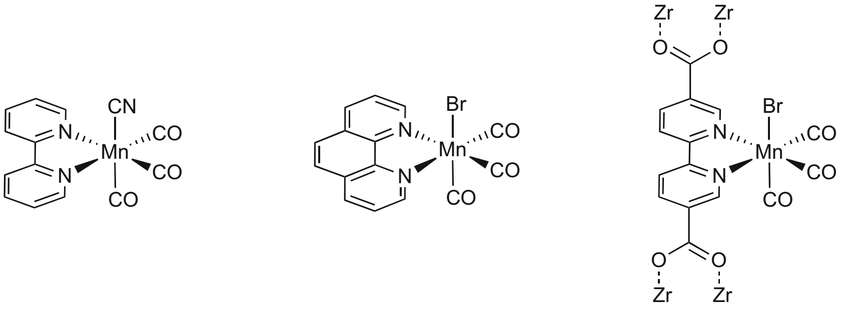

24 **25** **26**

Fig. 12 Molecular structures of Mn-based catalysts used in the photochemical reduction of CO_2

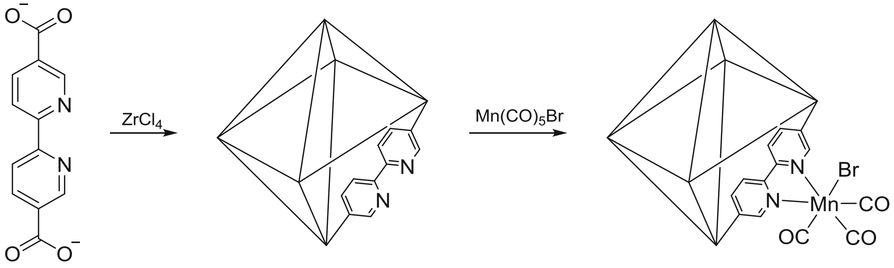

Fig. 13 MOF-based photocatalyst used in the photochemical reduction of CO_2

concept involves fixing the Mn center into a stable framework to stabilize the catalyst by avoiding the dimerization process during photocatalysis [53] (Fig. 14).

A system similar to the Mn(bpy)$(CO)_3$Br was reported by Kubiak et al., in which the exchange of bromide with cyanide should lead to a more efficient catalyst (**24**). Ishitani et al. reported that dimerization of the one-electron-reduced Mn-species occurs in conjunction with the loss of the bromide ligand. As a ligand, cyanide binds much more strongly than bromide to the metal center, due to π-backbonding, which should prevent the loss of ligand and consequent diminished dimerization. The authors proposed that, instead of dimer formation following one-electron reduction, a disproportion of two one-electron-reduced species to the initial complex **24** and the two-electron-reduced active intermediate $[Mn(bpy)(CO)_3]^-$. The experiments were performed in DMF/TEOA (4:1 v/v) or MeCN/TEOA (4:1 v/v) with varying ratios of CAT to PS. Two different products were formed, while the distribution of the products was strongly influenced by the solvent used (see above). In DMF/TEOA (0.1 mM CAT; 0.5 mM PS), the main product was formate ($TON_{HCOO} = 130$). Carbon monoxide ($TON_{CO} = 7.1$) and hydrogen ($TON_{H_2} = 1.6$) were also formed after 15 h of irradiation with monochromatic light (470 nm) in the presence of **6-PS** as PS and BNAH as SD. In acetonitrile, carbon monoxide became the favored product ($\mathrm{TON_{CO}} = 21$), followed by formate ($\mathrm{TON_{HCOO}} = 9$) and hydrogen ($\mathrm{TON_{H_2}} = 1.3$) [54].

In all previously described systems, ruthenium was used as a light-harvesting unit. In 2016, Bian et al. reported the first fully earth-abundant manganese-based photocatalytic system, applying **8-PS** as PS and **25** as CAT. CO was the major product ($\mathrm{TON_{CO}} = 119$) accompanied by formate ($\mathrm{TON_{HCOO}} = 19$) as a by-product in wet acetonitrile (20:1 v/v) when a CAT concentration of 2 mM was employed in conjunction with TEA as SD and a fourfold increase in the concentration of PS [55].

3.2 Fe Complexes

The first iron catalyst for carbon dioxide reduction was reported in 1997 by Grodkowski et al., who employed a tetraphenylporphyrin iron(III) (Fe(III)TTP) complex with a chloride as ligand in the axial position. Those porphyrin complexes have been established as efficient catalysts in electrocatalytic CO_2 reduction. Irradiation of a solution containing Fe(III)TTP and TEA or TEOA as SD in DMF caused the loss of the Cl^- ligand and a multistep reduction of the iron center to Fe(0), which acted as the active species for a nucleophilic attack of CO_2 to form the corresponding formyl adduct that was subsequently reduced to CO. The main product was CO ($\mathrm{TON_{CO}} = 70$), and hydrogen was formed as a by-product. In that system, no PS was involved, and the porphyrin served as the light-harvesting unit via ligand-to-metal charge transfer. The photoexcitation of FeTTP was inefficient. Upon light excitation, the porphyrin was reduced to the corresponding chlorine structure and was subject to photolysis [56]. To mitigate photo-decomposition of the

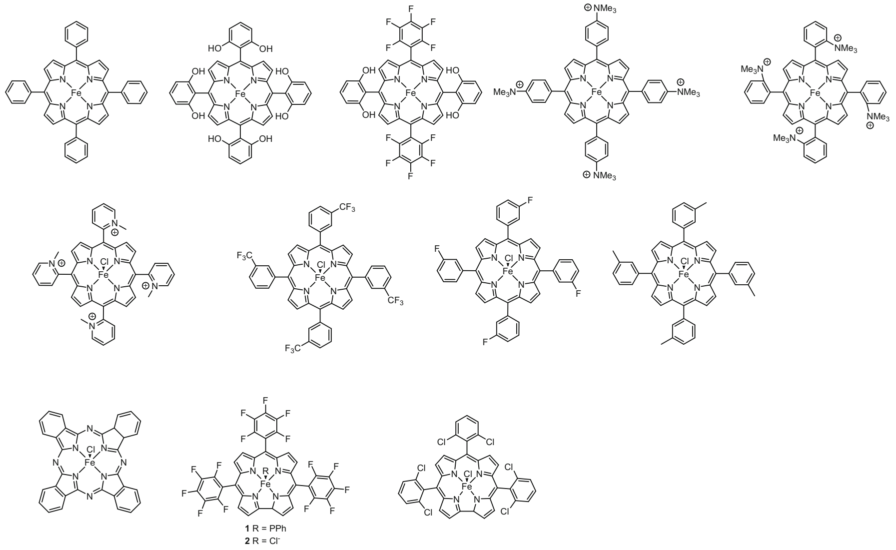

Fig. 14 Molecular structures of iron tetraphenylporphyrin, phthalocyanine, and corrole complexes used as molecular catalysts in photochemical reduction of CO_2

porphyrin ligand, **9-PS** was added as PS, which, owing to its reduction power, was able to generate the active Fe(0) species. The efficiency of a system containing both CAT and PS increased approximately by a factor of 10 [57].

In addition to porphyrins, phthalocyanines and corroles have been employed as macrocyclic ligands for Fe(III) in CO_2 reduction. The photoexcitation and the mechanism of reduction leading to the active species and CO_2-to-CO conversion were analogous to those of the porphyrins. Also, the photocatalytic activity, the amount of carbon monoxide formed in the presence or absence of **9-PS**, was comparable to the that of the porphyrins [58, 59].

Substitution of iron porphyrins with simple iron salts ($Fe(ClO_4)_2$) as CAT in conjunction with an organic dye (**9-PS**) in an acetonitrile solution containing TEA or TEOA (5% v/v) as SD also led to activity in proton-coupled reduction of CO_2. After irradiation with visible light, a TON_{CO} of 18.4 was obtained, with selectivity of 21%. Compared to tetra-*m*-tolylporphyrin ($Fe^{III}TTP$), $Fe(ClO_4)_2$ led to lower CO formation and diminished selectivity ($TON_{CO}(Fe^{III}TTP) = 61.8$, select. = 38%) [60].

Bonin et al. investigated an FeTTP with two hydroxyl moieties in the ortho position of each phenyl ring. A solution containing the CAT and TEA as SD was irradiated with UV light (280 nm). The favored product was CO, with a TON_{CO} of 28 and selectivity of ~ 80%. The activity was in the range of the parent FeTTP, but the hydroxyl groups stabilized the resulting iron-formyl complex after coordinating CO_2 to Fe(0) via hydrogen bonding. The phenolic protons acted as an internal proton source and accelerated C–O bond cleavage. Adding either **1-PS** or an organic dye **11-PS** allowed the system to operate under visible light irradiation and increased the activity of this CAT to a TON_{CO} of 140 (organic dye: $TON_{CO} = 40$–60; selectivity ~ 100%) with selectivity for CO of 93% in acetonitrile using TEA as SD [61].

Robert and coworkers introduced an Fe-*p*-TMA bearing tertiary tri-methylammonium moieties on all four phenyl rings as a CAT for 100% CO formation in the absence of a PS. In this case, the TMA groups served as the light-harvesting unit in the visible light range. In a solution of acetonitrile containing BIH as SD and TFE as a proton source, which enhanced the activity of the system, a turnover number of 101 with respect to CO was obtained after 102 h of visible light (420 nm) irradiation. At 102 h, the CO production reflected the high stability and robustness of the CAT. The mechanism is very similar to all other porphyrin derivatives [62].

Beller's group published a method for CO_2 reduction via photocatalysis using $Fe_3(CO)_9$ **27** as CAT, TEOA as SD, and either **2-PS** or **5-PS** as PS in NMP. With the addition of excess bipyridine as a ligand (**L1**), the activity of the system improved with respect to the formation of CO. All other ligands (**L2**–**L11**) had no significant effect on selectivity or productivity. Both the ligand and the PS employed influenced the selectivity of the catalytic system (**L1**–**11**, depicted in Fig. 15). After 5 h of visible light irradiation, an overall TON_{CO/H_2} of 291 of a mixture consisting of CO and H_2 was reached, with a decent quantum yield of 15.1% ($TON_{CO} = 36$, select. = 47%; $TON_{CO} = 42$, select. = 53 using **L1**). Using operando FTIR, $Fe(bpy)(CO)_3$ **28** was proposed as an "in situ"-formed active intermediate in CO_2 reduction [63].

In the 1990s, Knölker et al. reported an iron cyclopentadienone complex which was first used in organic synthesis. These iron complexes (**30**–**33**) have been

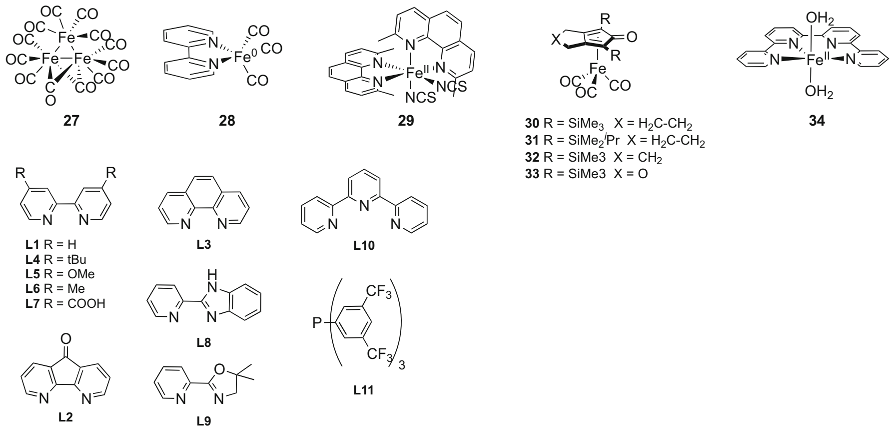

Fig. 15 Molecular structures of iron catalysts used in the photochemical reduction of CO_2

successfully applied as CO_2reduction CATs in combination with **3-PS**. The active species is a hydrido iron carbonyl complex. The carbonyl group in the ligand was reduced to a hydroxyl moiety and acted as an internal proton source to facilitate C–O bond cleavage and stabilize the intermediate iron-formyl complex. A mixture of NMP/TEOA (5:1) containing CAT **30** and **3-PS** irradiated with monochromatic light (400–700 nm; 5 h; light power output = 2.5 W) led to the formation of CO ($TON_{CO} = 421$), formate ($TON_{HCOO} = 40$), and trace amounts of hydrogen. For quantum yield determination, the solution was irradiated with 440 nm, and a quantum yield of 68% was calculated for CO. The activity and selectivity was heavily influenced by the steric and electronic properties of the cyclopentadienone ligand. TEOA was used as SD and proton source. The active species, the iron hydrido complex, was detected with operando IR [64].

A plethora of systems using non-noble metal complexes as CAT have been reported, but stable and efficient PS containing non-precious metals are still rare, as it is very difficult to compete with the high efficiency of triplet harvesting complexes containing Ru or Ir. Heteroleptic emissive Cu(I) PS developed by the Beller group for photocatalytic proton reduction are also suitable for CO_2 reduction in the visible light range when combined with iron catalysts. Ishitani et al. reported the first Fe/Cu system for the effective reduction of CO_2 by employing a dimeric macromolecular heteroleptic CuPS (**13-PS**) with one diimine and one diphosphine ligand, together with an iron complex **29** as CAT. Visible light irradiation of an acetonitrile/TEOA solution containing PS, CAT, and BIH as SD produced only CO ($TON_{CO} > 270$) and H_2, with selectivity of 78% with respect to CO. Quantum yields of 6.7% (mononuclear) and 2.6% with a $TON_{CO} > 54$ (dimeric) were reached [50].

To establish a fully non-noble-metal system, Fe-CAT (**30**, Fig. 15) was combined with in situ-generated heteroleptic CuPS. Numerous phenanthrolines and diphosphines have been applied as ligands for the CuPS (**NN1**–**NN5**, **PP1**–**PP3**, Fig. 10). An array of ligands with sterically demanding groups were tested to avoid flattening of the excited state of the PS and subsequent exciplex quenching by a solvent molecule. The best system consisted of Cu(Bathocuproine)(Xantphos) and CAT **30**, and showed activity of $TON_{CO} = 487$, selectivity of 99%, and a quantum yield of 13.3% after 5 h of irradiation with visible light in a solution of NMP/TEOA and BIH as SD. Key advantages of in situ formation include the ability to bypass the synthesis of the PS, the simple screening of ligands, and the use of an excess of diphosphine ligand to force the equilibrium between heteroleptic and homoleptic bathocuproine complexes towards the more active heteroleptic species [49] (Fig. 16).

Applying an iron quaterpyridine **34** complex together with **5-PS** in acetonitrile/TEOA (4:1) using BIH as SD, remarkable activity for iron catalysts was reached, with a TON_{CO} of 1879 and selectivity of 97%. The substitution of Ru PS with an organic dye as light-harvesting unit enabled the selective conversion of CO_2 to CO with a TON_{CO} of 1365, an exceptionally high quantum yield for a single metal complex system at a loading of 1.1% [65].

3.3 Co Complexes

In 1982, Lehn et al. reported the first application of $CoCl_2$*6 H_2O as photocatalyst for CO_2 reduction using either MeCN or DMF containing 20% water as solvent, TEA or TEOA as electron source as well as proton donor, and **5-PS** as PS. With the addition of aromatic redox-active diimine ligands such as bpy or phen, the activity increased significantly. A TON_{CO} of 0.7 with selectivity of 88% in MeCN/H_2O (4:1), and a TON_{CO} of 8.5 in DMF with dmp as additional ligand, with selectivity of 33%, was achieved with respect to CO in a CO/H_2 mixture. In DMF, quantum yields of 1.2% for CO and 6.5% H_2 were calculated [66–68] (Fig. 17).

To avoid the use of precious transition metals not only in the CAT but also in the PS, Yanagida et al. reported a combination of an earth-abundant Co-cyclam CAT and *p*-terphenyl **9-PS** as the light-harvesting unit. UV light (> 290 nm) irradiation of a MeCN/MeOH (2:1) solution containing **35**, **36**, or **37** and TEA or TEOA as SD, CO and $HCOO^-$ formed preferentially, with trace amounts of H_2. CO was preferentially generated over formate by a factor of 2. Co-cyclam together with p-terphenyl **9-PS** gave rise to good selectivity and a high quantum yield of 25%. Upon substituting Co-cyclam with $CoCl_2$*6 H_2O, no activity was observed [69, 70]. Interestingly, when phenazine **10-PS** was used in place of **9-PS**, $HCOO^-$ was formed as product, with selectivity of 99%. In addition to an electron, phenazine transferred an additional proton to the cobalt metal center to form a cobalt hydride complex, which facilitated the insertion of CO_2 to form a formyl ligand [71].

Lau et al. investigated a Co^{II} complex **38** using a pentadentate macrocyclic ligand based on pyridine, together with a cyclometalated Ir(ppy)$_3$ **1-PS** PS and TEA as SD. Irradiation of an acetonitrile solution with light (> 440 nm) led to a TON_{CO} of < 270 and selectivity of 97% with respect to CO. Supported by electrochemical investigations, a $Co^{I}(L^{\cdot -})$ intermediate was observed which allowed activation of CO_2 to form the adduct $(LCo^{II}CO_2^{\,-})$. The electron-withdrawing π-backdonation, which weakened the C–O bond and facilitated the consequent cleavage, provides a plausible explanation for the significant formation of CO [72].

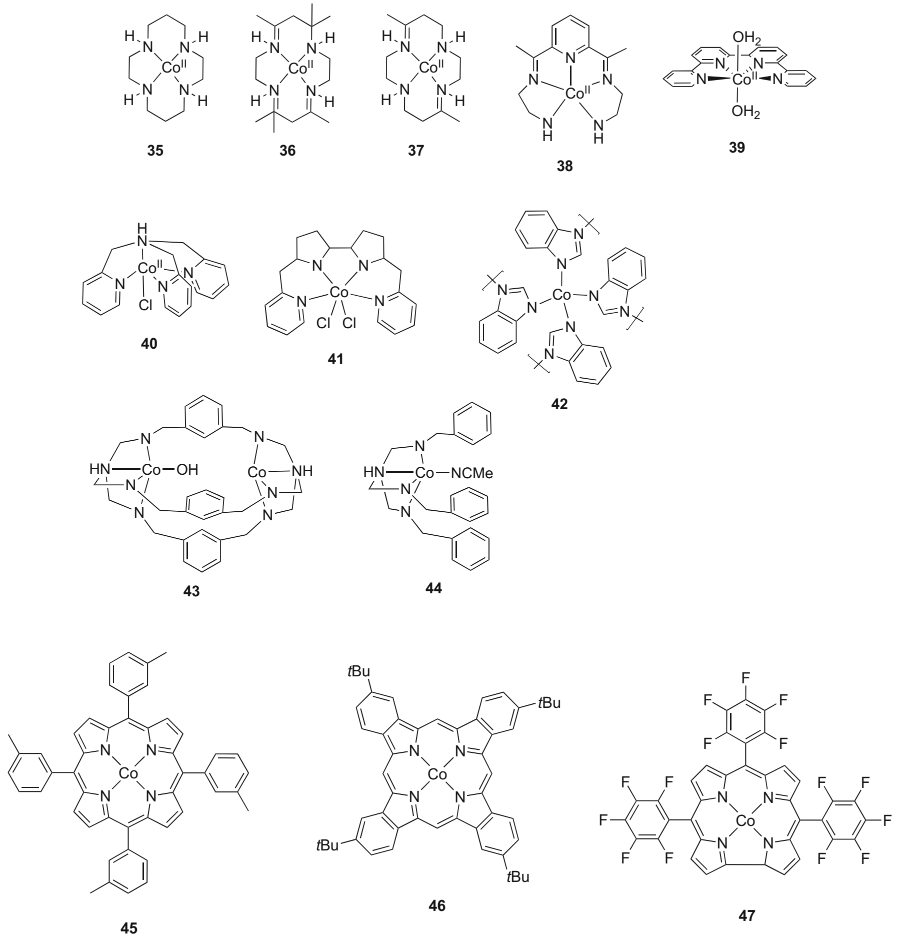

Fig. 16 Molecular structures of cobalt catalysts used in the photochemical reduction of CO_2

The same group reported a quaterpyridine cobalt complex **39** bearing two H_2O molecules as ligands. This complex, in combination with a Ru(bpy)$_3$ **5-PS** as PS and BIH as SD in MeCN/TEOA (5:1), led to highly selective (98%) CO_2-to-CO conversion, with a TON_{CO} of 497 (0.05 mM CAT) up to 2660 (0.005 mM CAT). The catalyst loading was inversely proportional to the turnover number. A quantum yield of 2.8% was calculated for CO. Applying an organic dye **12-PS** instead of **5-PS**, a TON_{CO} of 790 and a quantum yield of 0.8% was achieved by irradiation at 460 nm in DMF [65].

Chan et al. reported a Co^{II} complex with a tetradentate tripodal nitrogen ligand used in photocatalytic CO_2 reduction as CAT **40** (5 μM) in combination with **1-PS** (0.4 mM) as PS and TEA as SD in MeCN. The major product was CO (hydrogen was the only by-product), with selectivity of 85% and a maximum TON_{CO} of 953 after irradiation for 70 h with blue LEDs (460 nm) [73]. The selectivity of CO formation (> 95%) and the TON_{CO} were significantly improved by applying **4-PS** instead of **1-PS**. The compound **4-PS** displayed enhanced emission properties and better long-term stability during irradiation [74]. The introduction of a new Co^{II} complex **41** bearing a less rigid tetradentate ligand based on 2,2′-bipyrrolidine gave rise to even higher selectivity (95%) and a turnover number of 368 for CO [75].

Co^{II} implemented in metal organic frameworks (MOFs) with incorporated benzimidazole moieties **42** have been investigated as CATs. A suspension of microporous zeolites with topically applied MOFs was irradiated (420 nm) in $MeCN/H_2O$ (4:1) containing **5-PS** as PS and TEOA as SD. A mixture of CO and H_2 was produced after irradiation, with selectivity of 58% with respect to CO and a quantum yield of 1.48%. The CAT was recycled and used for five further catalytic reactions. The CO_2-capturing properties of the MOF improved the performance of the CAT [76].

Ouyang et al. recently reported a dinuclear cobalt cryptate complex for light-driven CO_2 reduction. Irradiation of a solution of $MeCN/H_2O$ (4:1) containing **43** (0.025 μM) as CAT, **7-PS** as PS, and TEOA as SD at a wavelength of 450 nm gave rise to high selectivity with respect to CO (98%) and a TON_{CO} up to 16,896 ($TOF = 0.47\ s^{-1}$) after 10 h. A quantum yield of 0.04% was calculated. When the mononuclear complex **44** was applied instead of **43**, the system showed no activity. The authors proposed that the high efficiency was attributable to the synergistic effect of two Co metal centers, which was supported by DFT calculations [77].

Cobalt porphyrins **45**, phthalocyanines **46**, and corroles **47** have also been applied as photocatalysts, with activity and reactivity analogous to that of iron porphyrins [58, 78].

3.4 Ni Complexes

In 1987, inspired by the electrocatalytic CO_2 reduction with Ni^{II}-cyclam reported by Beley et al. and the light-driven CO_2 reduction with Co-cyclam as a homogeneous catalyst reported by Tinnemans et al., Spreer et al. and Otvos et al. introduced a photocatalytic system for CO_2-to-CO-conversion employing **48** as catalyst, **5-PS** as PS, ascorbate buffer as the electron source, and water as solvent. The TON for CO was very low at certain pH values, and selectivity of 78% with respect to the produced hydrogen was observed [$TON_{CO} = 0.1$ (0.052), select. = 13 (78); pH 4 (6)] [79, 80].

Nearly 10 years later, Mochizuki et al. reported a Ni^{II}-cyclam-dimer (**49**). Using the same conditions and PS (**5-PS**) as Spreer et al., the authors found that the dimer showed increased activity and higher selectivity in CO_2 reduction than the corresponding monomer ($TON_{CO} = 4.4$, select. = 94%) [81].

Girault et al. reported a biphasic system of water and supercritical CO_2 for the conversion of carbon dioxide to CO using **1-Ni** as CAT, **5-PS** as PS, and ascorbic acid or TEOA as sacrificial agent. The proposed mechanism assumes that the reduction of the catalyst by the PS and the subsequent reduction of the bound CO_2 occurs in the aqueous phase, contrary to the binding of CO_2 to the active CAT, which occurs at the phase interface between water and $scCO_2$. Even the applied pressure has an influence on the quantity of products formed. Higher pressure leads

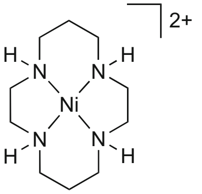

48

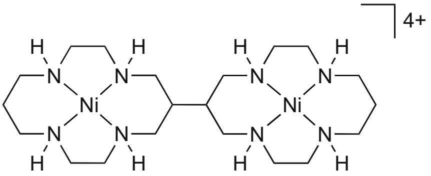

49

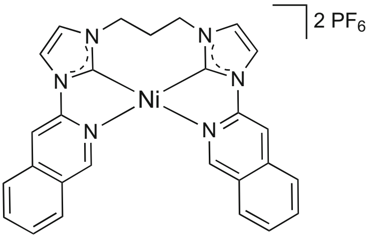

50

Fig. 17 Chemical structures of Ni-based catalysts for the photochemical CO_2-to-CO conversion

to a higher TON of CO ($TON_{CO} = 2.2$ in $H_2O/scCO_2$, pH 5.1, select. of 88%, quantum yield = 0.14) [82].

In 2013, Chang et al. reported a very active system using **50** with an NHC-isoquinoline ligand. The CAT showed high activity in electrocatalytic CO_2 reduction at very low overpotentials ($E = -1.20$ V vs. SCE). Therefore, this complex was employed in a photocatalytic system using **1-PS** as PS and TEA as SD in acetonitrile. After irradiation for 7 h in the visible light range (400–700 nm), a TON of 98,000 with selectivity of ~ 100% was reached, with catalyst loading of 2 nM. Similar to some Mn-systems, the catalyst loading was inversely proportional to the turnover number. In this system, Chang et al. proposed an oxidative quenching mechanism between PS, CAT, and SD for CO_2 reduction [83].

4 Outlook

As discussed in this review, tremendous advances have taken place in the electro- and photochemical reduction of carbon dioxide using earth-abundant molecular catalysts, in terms of both activity and selectivity. With the proper design of a redox-active ligand, catalysts based on low-cost metals such as Fe, Mn, and Co are able to selectively reduce CO_2 to CO or HCOOH as primary products. However, one of the main drawbacks of these catalytic systems is their low stability under operating conditions. Most of the catalysts reviewed here decompose after a few hours of reaction, which is a serious impediment to their implementation on a large scale. Accordingly, future research efforts in this area should focus on developing strategies to extend the lifetime of such molecular catalysts. In addition, initial steps should be taken towards the integration of these earth-abundant catalysts in tandem cells, where the electrons and protons for the reduction of carbon dioxide are provided by the oxidation of H_2O, to demonstrate the sustainability of this promising technology.

References

1. Smil V (2003) Energy at the crossroads: global perspectives and uncertainties. MIT Press, Cambridge
2. (2016) BP Statistical review of energy
3. United Nations Development Programme (2003) World energy assessment report: energy and the challenge of sustainability
4. Nocera DG (2009) Chem Soc Rev 38:13
5. Lewis NS, Nocera DG (2006) Proc Natl Acad Sci USA 103:15729
6. Barber J, Archer MD (2004) In: Archer MD, Barber J (eds) Molecular to global photosynthesis. Imperial College Press, London, pp 1–44
7. Gray HB (2009) Nat Chem 1:7
8. Costentin C, Robert M, Saveant J-M (2013) Chem Soc Rev 42:2423
9. Windle CD, Perutz RN (2012) Coord Chem Rev 256:2562
10. Cole EB, Bocarsly AB (2010) In: Aresta M (ed) Carbon dioxide as chemical feedstock. Wiley-VCH, Weinheim, pp 291–316
11. Sutin N, Creutz C, Fujita E (1997) Comments Inorg Chem 19:67–92
12. Frese KW (1993) In: Sullivan BP, Krist K, Guard HE (eds) Electrochemical and electrocatalytic reactions of carbon dioxide. Elsevier, Amsterdam, pp 145–216
13. Rosen BA, Salehi-Khojin A, Rorson M, Zhu W, Whipple DT, Kenis PJA, Masel RI (2011) Science 334:643
14. Johnson TC, Morris DJ, Wills M (2010) Chem Soc Rev 39:81
15. Benson EE, Kubiak CP, Sathrum AJ, Smieja JM (2008) Chem Soc Rev 38:89
16. Dubois MR, Dubois DL (2009) Acc Chem Res 42:1974–1982
17. Saveant J-M (2008) Chem Rev 108:2348–2378
18. Sampson MD, Kubiak CP (2016) J Am Chem Soc 138:1386
19. Hawecker J, Lehn J-M, Ziessel R (1984) J Chem Soc Chem Commun 328
20. Bourrez M, Molton F, Chardon-Noblat S, Deronzier A (2011) Angew Chem Int Ed 50:9903
21. Hartl F, Rossenaar BD, Stor GJ, Stufkens DJ (1995) Recl Trav Chim Pays-Bas 114:565
22. (2011–2012) Haynes WM (ed) CRC handbook of chemistry and physics, 92nd edn. CRC Press, Boca Raton
23. Smieja JM, Sampson MD, Grice KA, Benson EE, Froehlich JD, Kubiak CP (2013) Inorg Chem 52:2484
24. Agarwal J, Shaw TW, Stanton CJ III, Majetich GF, Bocarsly AB, Schaefer HF III (2014) Angew Chem Int Ed 53:5152
25. Sampson MD, Nguyen AD, Grice KA, Moore CE, Rheingold AL, Kubiak CP (2014) J Am Chem Soc 136:5460
26. DuBois DL (2014) Inorg Chem 53:3935–3960
27. Franco F, Cometto C, Ferrero Vallana F, Sordello F, Priola E, Minero C, Nervi C, Gobetto R (2014) Chem Commun 50:14670
28. Agarwal J, Shaw TW, Schaefer HF III, Bocarsly AB (2015) Inorg Chem 54:5285
29. Finn C, Schnittger S, Yellowlees LJ, Love JB (2012) Chem Commun 48:1392
30. Qiao J, Liu Y, Hong F, Zhang J (2014) Chem Soc Rev 43:631
31. Hammouche M, Lexa D, Momenteau M, Saveant JM (1991) J Am Chem Soc 113:8455
32. Bhugun I, Lexa D, Saveant JM (1996) J Am Chem Soc 118:1769
33. Costentin C, Drouet S, Robert M, Savéant J-M (2012) Science 338:90
34. Costentin C, Drouet S, Robert M, Savéant J-M (2012) J Am Chem Soc 134:11235
35. Costentin C, Passard G, Robert M, Savéant J-M (2014) J Am Chem Soc 136:11821
36. Costentin C, Passard G, Robert M, Savéant J-M (2014) Proc Natl Acad Sci USA 11:14990

37. Mohamed EA, Zahran ZN, Naruta Y (2015) Chem Commun 51:16900
38. Jeoung J-H, Dobbek H (2007) Science 318:1461
39. Shin W, Lee SH, Shin JW, Lee SP, Kim Y (2003) J Am Chem Soc 125:14688
40. Taheri A, Thompson EJ, Fettinger JC, Berben LA (2015) ACS Catal 5:7140
41. Loewen ND, Thompson EJ, Kagan M, Banales CL, Myers TW, Fettinger JC, Berben LA (2016) Chem Sci 7:2728
42. Costamagna J, Ferraudi G, Canales J, Vargas J (1996) Coord Chem Rev 148:221
43. Thoi VS, Chang CJ (2011) Chem Commun 47:6578
44. Schneider J, Jia H, Kobiro K, Cabelli DE, Muckermana JT, Fujita E (2012) Energy Environ Sci 5:9502
45. Sheng M, Jiang N, Gustafson S, You B, Ess DH, Sun Y (2015) Dalton Trans 44:16247
46. Lacy DC, McCrory CCL, Peters JC (2014) Inorg Chem 53:4980
47. Koike T, Akita M (2014) Inorg Chem Front 1:562
48. Luo S-P, Mejía E, Friedrich A, Pazidis A, Junge H, Surkus A-E, Jackstell R, Denurra S, Gladiali S, Lochbrunner S, Beller M (2013) Angew Chem Int Ed 52:419–423
49. Rosas-Hernández A, Steinlechner C, Junge H, Beller M (2017) Green Chem 19:2356
50. Takeda H, Ohashi K, Sekine A, Ishitani O (2016) J Am Chem Soc 138:4354
51. Pellegrin Y, Odobel F (2017) C R Chim 20:283
52. Takeda H, Koizumi H, Okamotoa K, Ishitani O (2014) Chem Commun 50:1491
53. Fei H, Sampson MD, Lee Y, Kubiak CP, Cohen SM (2015) Inorg Chem 54:6821
54. Cheung PL, Machan CW, Malkhasian AYS, Agarwal J, Kubiak CP (2016) Inorg Chem 55:3192
55. Zhang J-X, Hu C-Y, Wang W, Wang H, Bian Z-Y (2016) Appl Catal A 522:145
56. Grodkowski J, Behar D, Neta P, Hambright P (1997) J Phys Chem A 101:248
57. Dhanasekaran T, Grodkowski J, Neta P, Hambright P, Fujita E (1999) J Phys Chem A 103:7742
58. Grodkowski J, Dhanasekaran T, Neta P, Hambright P, Brunschwig BS, Shinozaki K, Fujita E (2000) J Phys Chem A 104:11332 **11339**
59. Grodkowski J, Neta P, Fujita E, Mahammed A, Simkhovich L, Gross ZJ (2002) Phys Chem A 106:4772
60. Grodkowski J, Neta P (2000) J Phys Chem A 104:4475
61. Bonin J, Robert M, Routier M (2014) J Am Chem Soc 136:16768
62. Rao H, Bonin J, Robert M (2017) Chem Commun 53:2830
63. Alsabeh PG, Rosas-Hernández A, Barsch E, Junge H, Ludwig R, Beller M (2016) Catal Sci Technol 6:3623
64. Rosas A, Alsabeh PG, Barsch E, Junge H, Ludwig R, Beller M (2016) Chem Commun 52:8393
65. Guo Z, Cheng S, Cometto C, Anxolabéhère-Mallart E, Ng S-M, Ko C-C, Liu G, Chen L, Robert M, Lau T-C (2016) J Am Chem Soc 138:9413
66. Lehn J-M, Ziessel R (1982) Proc Natl Acad Sci 79:701
67. Hawecker J, Lehn J-M, Ziessel R (1983) J Chem Soc Chem Commun 536
68. Ziessel R, Hawecker J, Lehn J-M (1986) Helv Chim Acta 69:1065
69. Matsuoka S, Yamamoto K, Pac C, Yanagida S (1991) Chem Lett 20:2099
70. Matsuoka S, Yamamoto K, Ogata T, Kusaba M, Nakashima N, Fujita E, Yanagida S (1993) J Am Chem Soc 115:601
71. Ogata T, Yamamoto Y, Wada Y, Murakoshi K, Kusaba M, Nakashima N, Ishida A, Takamuku S, Yanagida S (1995) J Phys Chem 99:11916
72. Chen L, Guo Z, Wei X-G, Gallenkamp C, Bonin J, Anxolabéhère-Mallart E, Lau K-C, Lau T-C, Robert M (2015) J Am Chem Soc 137:10918
73. Chan SL-F, Lam TL, Yang C, Yan S-C, Cheng NM (2015) Chem Commun 51:7799
74. Yang C, Mehmood F, Lam TL, Chan SL-F, Wu Y, Yeung C-S, Guan X, Li K, Chung CYS, Zhou C, Zou T, Che C-M (2016) Chem Sci 7:3123
75. Wang F, Cao B, To W-P, Tse C-W, Li K, Chang X-Y, Zang C, Chan SL-F, Che C-M (2016) Catal Sci Technol 6:7408
76. Wang S, Yao W, Lin J, Ding Z, Wang X (1034) Angew Chem Int Ed 2014:53
77. Ouyang T, Huang H-H, Wang J-W, Zhong D-C, Lu T-B (2017) Angew Chem Int Ed 56:738
78. Grodkowski J, Neta P (2002) J Phys Chem A 106:4772
79. Grant JL, Goswami K, Spreer LO, Otvos JW, Calvin M (1987) J Chem Soc Dalton Trans 2105

80. Craig CA, Spreer LO, Otvos JW, Calvin M (1990) J Phys Chem 94:7957
81. Mochizuki K, Manaka S, Takeda I, Kondo T (1996) Inorg Chem 35:5132
82. Méndez MA, Voyame P, Girault HH (2011) Angew Chem Int Ed 50:7391
83. Thoi VS, Kornienko N, Margarit CG, Yang P, Chang CJ (2013) J Am Chem Soc 135:14413